Humboldt–Universität zu Berlin

The Early Evolution of Synapsida (Vertebrata, Amniota) and the Quality of their Fossil Record

Neil Brocklehurst

2015

Titel der Arbeit:
The Early Evolution of Synapsida (Vertebrata, Amniota) and the Quality of their Fossil Record

DISSERTATION
zur Erlangung des akademischen Grades

Doctor rerum naturalium
(Dr. rer. nat.)
im Paleontology

eingereicht an der Lebenswissenschaftlichen Fakultät der Humboldt-Universität zu Berlin

von
Neil Brocklehurst, Msci

Präsident der Humboldt-Universität zu Berlin

Prof. Dr. Jan-Hendrik Olbertz

Dekanin/Dekan der Lebenswissenschaftlichen Fakultät
der Humboldt-Universität zu Berlin

Prof. Dr. Richard Lucius

Gutachter/innen

1. Prof. Dr Jörg Fröbisch

2. Prof. Dr. Johannes Müller

3. Dr Kenneth Angielczyk

Tag der mündlichen Prüfung: 8/9/2015

Erklärung

Hiermit versichere ich, dass ich diese Dissertation eigenständig und nur unter Verwendung der angegebenen Quellen und Hilfsmittel angefertigt habe.

Berlin, den 30. March 2015

Neil Brocklehurst

Acknowledgements

First and foremost I must acknowledge the guidance of my supervisor, Prof. Jörg Fröbisch, who has offered me aid and comfort throughout this project and was willing to risk his hard-earned grant money on me. The members of the Fröbisch Working Group, both past and present, have provided company, diverting conversation and excellent discussions on issues both pertinent and irrelevant to my work. I have greatly enjoyed my time at the Museum für Naturkunde in Berlin, and it is my colleagues who have helped make this period so entertaining and academically productive. On that note I would like to offer my thanks to Christian Kammerer, Soizic Le Fur, Maren Jansen, Marcus Walther, Antoine Verrière, Lena Nehls, Leda Piculjan and Tina Aschenbach.

Others outside of my immediate colleagues are owed a debt of gratitude. I would not be where I am today without the guidance offered to me early in my career by Paul Upchurch, Philip Mannion, Susan Evans and Marc Jones, all of whom aided my first experiences of research and continued to make their expertise available to me even after I left their institution. The instructors on the Paleobiology Database Workshop in Quantitative Palaeontology should be thanked for giving me many of the tools necessary to complete this thesis: John Alroy, David Polly, Michel Kowaleski, Alistair Evans and Graeme Lloyd. Graeme Lloyd is deserving of special thanks, as is Johan Renaudie, for putting up with my incessant requests for assistance with R. Also providing helpful comments, discussion and assistance with the German language have been Johannes Müller, Marcello Ruta, Robert Reisz, Roger Benson, David Button, Stephanie Smith, Emily Orzechowski and Serjoscha Evers.

The Museum für Naturkunde in Berlin, the Palaeontological Institute of Moscow, the Geological Survey of Freiberg, The Muséum National d'Histoire Naturelle of Paris, The American Museum of Natural History in New York, the Museum of Comparative Zoology at Harvard and the Field Museum of Chicago allowed access to specimens. I am grateful to Marten Schöle, Valery Bulanov, Frederik Spindler, Ronan Allain, Jocelyn Falconnet, Carl Mehling, Jessica Cundiff, Mark Renczkowski, William Simpson and Kenneth Angielczyk for giving up their valuable time to organise visits to collections and provide me with assistance during these visits. Carola Radke and Elke Siebert, of the Museum für Naturkunde, also took the time to provide technical support in the making of images of specimens.

Finally I would like to thank those outside the academic realm who have been no less important during the last three years. My parents have offered never-ending support, both

moral and financial. My partner and the Bane of my Life, Emma Humphries, has also gone out of her way to back me in my endeavours here and has been particularly tolerant of me leaving to work in a different country. I can never thank my family and Emma enough for the help they have given (I hope they think this thesis is worth it).

The work in this thesis was financially supported by a Sofja Kovalevskaja Award to Jörg Fröbisch, which is awarded by the Alexander von Humboldt Foundation and donated by the German Federal Ministry for Education and Research.

Contents

List of Figures and Tables

List of Figures

List of Tables

Abstracts

Abstract in English

Synapsids (the clade containing mammals and all taxa more closely related to them than to other vertebrates) first appear in the fossil record during the late Pennsylvanian, and dominated the terrestrial realm until the end of the Palaeozoic. Their early evolution includes some of the first amniotes to evolve large size, herbivory, and macrocarnivory. However, much of the research into their macroevolutionary patterns during the Palaeozoic has focussed on therapsids, the clade containing mammals. Very little work has been done on the more basal pelycosaurian-grade synapsids, a paraphyletic assemblage of six families which were particularly diverse and abundant during the Late Carboniferous and Early Permian. This thesis provides the first detailed examination of the earliest evolution of synapsids. First, new material is incorporated into a phylogenetic analysis of basal synapsids, including the eothyridid *"Mycterosaurus" smithae*, re-described herein. The phylogeny produced is integrated into an examination of the completeness of the fossil record of pelycosaurian-grade synapsids. Modifications of previously published metrics are used to assess the completeness of their specimens, and a variety of methods are employed to measure the fit of the fossil record to the phylogeny. An assessment of species richness is undertaken, with multiple sampling correction methods used to provide a detailed picture of how the diversity of pelycosaurian-grade synapsids has changed through time. Finally, analysis of tree topology is used to investigate the timing and location within the phylogeny of significant shifts in the rate of diversification, and to investigate the link between these shifts and potential "key" morphological innovations. The analysis into the completeness of pelycosaurian-grade specimens reveals a negative correlation between diversity and the Skeletal Completeness Metric, assessing the bulk of material preserved, suggesting a tendency to name many species based on poor material. The lack of correlation between the Character Completeness Metric (assessing the proportion of phylogenetic characters that can be scored) and diversity is attributed to the history of discovery in the group: the majority of pelycosaurian-grade species were named between the 1930s and 1960s, when assignments were often based on size, location and stratigraphy rather than morphological characters. A strong correspondence between the phylogeny and stratigraphy implies a reliable phylogenetic hypothesis, but the low Relative Completeness Index score suggests that a great deal of the fossil record is missing. Despite this, and evidence of anthropogenic sampling bias affecting richness estimates throughout history, the different methods of assessing diversity provide very similar results. The initial diversification of synapsids in the Late Pennsylvanian and early Cisuralian was followed by an extinction event during the Sakmarian. A second extinction event occurred across the Kungurian/Roadian boundary. Despite the large number of morphological innovations occurring in early synapsids, the tree topology analysis found no significant increases in diversification rate occurring in pelycosaurian-grade taxa relative to their contemporaries. A broader examination of diversification patterns in Palaeozoic and Triassic amniotes reveals a possible explanation; diversification rate shifts within early amniotes tend to occur during periods of elevated extinction. While there are diversification rate shifts coinciding with the evolution of innovations, the elevation of origination rates occur during times of elevated extinction, rather than at the first appearance of such novelties. The fact that pelycosaurian-grade synapsids were so innovative did not translate into great increases in their diversification rate.

Abstract in German

Synapsiden, Vertreter die Evolutionslinie der Säugetiere, erscheinen erstmals im Fossilbericht im Oberkarbon (späten Pennsylvanium) und dominierten terrestrische Ökosysteme bis zum Ende des Paläozoikums. Zur frühen Evolutionsgeschichte der Synapsiden gehören unter anderem die ersten Amnioten mit großen Körpermaßen sowie herbivoren beziehungsweise makrocarnivoren Nahrungsanpassungen. Makroevolutive Forschung an paläozoischen Synapsiden war bisher jedoch zumeist auf Therapsiden fokussiert, das abgeleitete Monophylum zu dem auch die Säugetiere gehören. Wenig Augenmerk wurde bisher auf die basaler klassifizierten Pelycosaurier gerichtet, eine paraphyletische Gruppe bestehend aus sechs Familien, die während des Oberkarbon und unterem Perm besonders divers und abundant waren. Diese Arbeit ist die erste detaillierte Betrachtung der frühen Evolution der Synapsiden. Zunächst wird neues Material in eine phylogenetische Analyse der basalen Synapsiden eingebaut. Dazu gehört der eothyridide Synapside „*Mycterosaurus*“ *smithae*, der innerhalb dieser Arbeit neu bewertet und beschrieben wird. Die resultierende Phylogenie wird für eine Untersuchung der Vollständigkeit des Fossilberichts der Pelycosaurier verwendet. Modifizierte Versionen zuvor publizierter Vollständigkeitsmaße werden benutzt, um die Vollständigkeit von Pelycosaurier Fossilien einzuschätzen. Zudem wird eine Reihe unterschiedlicher Methoden genutzt, um die Übereinstimmung von Fossilbericht und Phylogenese zu messen. Um ein unverzerrtes Bild der Diversitätsdynamik der Pelycosaurier über die Zeit zu bekommen, wird der Artenreichtum mittels unterschiedlicher Methoden hinsichtlich der Datenerfassung korrigiert. Letzlich wird durch eine Topologie-Analyse festgestellt, zu welchen Zeiten und an welchen Knotenpunkten der Phylogenie es signifikante Veränderungen in der Diversifikationsrate gegeben hat, und ob eine Verbindung zwischen diesen Veränderlichkeiten und potentiellen morphologischen „Schlüsselinnovationen“ besteht. Die Vollständigkeitsanalyse der Pelycosaurier zeigt eine negative Korrelation zwischen Diversität und dem Maß der Merkmalsvollständigkeit, was darauf hindeutet, dass viele Spezies auf unvollständig erhaltenem Material basieren. Die fehlende Korrelation zwischen dem Maß zur Merkmalsvollständigkeit (basierend auf Abschätzung der Proportion phylogenetisch erfassbarer Merkmale) und der Diversität wird auf die Entdeckungsgeschichte der Gruppe zurück geführt: Die Mehrheit der Pelycosaurier-Arten wurden zwischen den 1930er und 1960er Jahren benannt, als taxonomische Zuordnungen häufig auf Körpergrösse, Fundort und Stratigraphie anstatt auf morphologischen Merkmalen basierten. Eine starke Korrespondenz zwischen Phylogenese und Stratigraphie impliziert eine zuverlässige phylogenetische Hypothese, während aber der geringe Wert des relativen Vollständigkeitsindex suggeriert, dass der Fossilbericht zu großen Teilen unvollständig vorliegt. Trotz dieser Feststellung, sowie Anzeichen von anthropogener Stichprobenverzerrung, welche Schätzungen der Artenzahl über die Erdgeschichte beinflussen, produzieren die unterschiedlichen Methoden zur Diversitätsrekonstruktion sehr ähnliche Ergebnisse. Der initialen Diversifikation der Synapsiden im Oberkarbon und Unterperm (frühes Cisuralium) folgte ein Aussterbeereignis während des Sakmariums. Ein zweites Aussterben ereignete sich an der Grenze vom Kungurium zum Roadium. Trotz des Auftretens einer großen Zahl von morphologischen Innovationen in frühen Synapsiden ergab die phylogenetisch Topologie-Analyse keine signifikanten Steigerungen der Diversitätsrate der Pelycosaurier relativ zu zeitgleich lebenden Taxa. Eine breiter angelegte Auswertung der Diversitätsentwicklung paläozoischer und triassischer Amnioten liefert ein mögliches Erklärungsmodell; Veränderungen der Diversitätsraten früher Amnioten tendieren dazu, zu Zeiten erhöhter Aussterberaten aufzutreten. Während Veränderungen der Diversitätsrate durchaus mit dem evolutiven Auftreten von Innovationen zusammenfallen, treten Steigerungen der Speziationsraten zeitgleich mit erhöhtem Aussterben auf, anstatt mit dem ersten Vorkommen der morphologischen Neuerungen zu koinzidieren. Das Auftreten zahlreicher Innovationen bei Pelycosauriern ist daher nicht in eine Erhöhung der Diversifikationsrate zu übersetzen.

Chapter 1

Introduction and Literature Reviews

Introduction to the Pelycosaurian-grade Synapsids

Synapsida is the clade including mammals and all taxa more closely related to them than to other modern vertebrates. The earliest unambiguous members of this clade appear in the fossil record during the Moscovian (Middle Pennsylvanian) after which they rapidly diversified, dominating terrestrial ecosystems during the Late Carboniferous and Permian. Their early evolution includes some of the earliest amniotes to show large body size, high-fibre herbivory, macro-carnivory, evidence of group-living, and possibly a return to a semi-aquatic lifestyle. They are defined by the following synapomorphies: presence of a lower temporal fenestra (Romer and Price, 1940); five or more cervical vertebrae (Benson, 2012); posterior shaft of the humerus convex around the exit of the entepicondylar foramen (Benson, 2012); postparietals fused to form an interparietal (Hill, 2005); craniomandibular joint positioned posterior to the occiput (Hill, 2005).

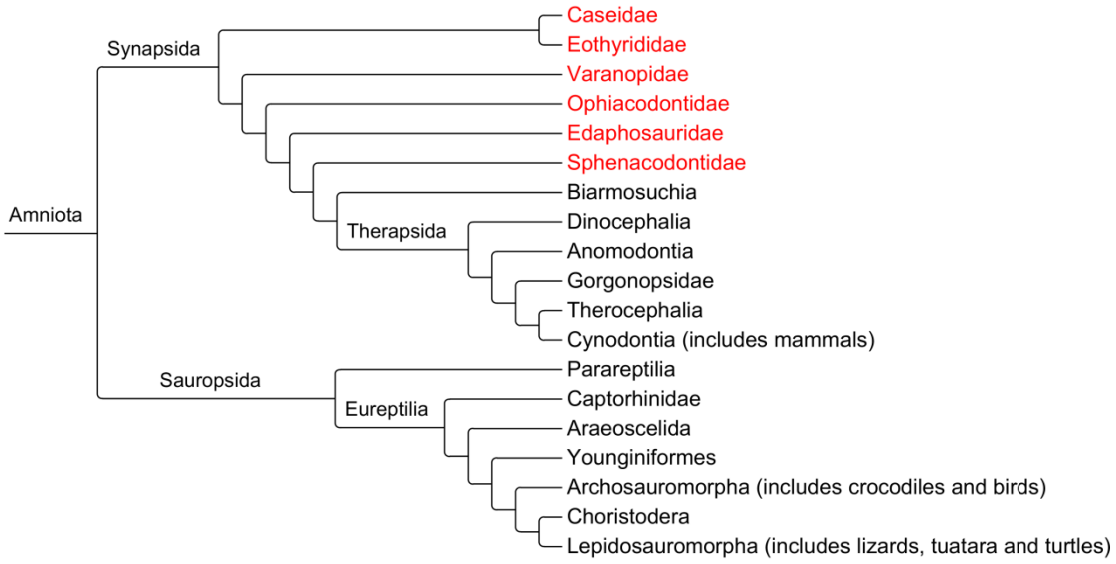

Figure 1: Composite phylogeny showing relationships of major amniote clades. Synapsid relationships based on Reisz and Fröbisch (2014) and Sidor and Hopson (1998). Sauropsid relationships based on Bickelmann et al. (2009). Pelycosaurian-grade synapsids are highlighted in red.

Synapsids belong to the clade Amniota, the fully terrestrial vertebrates which possess the amniotic egg, giving their reproduction independence from water (Reisz, 1997). The amniotes are split into two clades (Figure 1): Synapsida (including extant mammals) and Sauropsida (including extant reptiles and birds). The earliest examples of amniotes in the fossil record are found in the Joggins Formation of Canada, of late Bashkirian age (Benton and Donoghue, 2007). This formation also includes the earliest putative synapsid,

Protoclepsydrops haplous (Carroll, 1964; Reisz, 1972), although this assignment is debated; the characters previously linking it to synapsids have now been observed in basal sauropsids (Reisz, 1980; 1986). The earliest undisputed synapsids are *Archaeothyris florensis* and *Echinerpeton intermedium*, both from the Morien Group of Nova Scotia, of late Moscovian age (Reisz, 1972).

During the Late Carboniferous and Early Permian, six synapsid families were particularly diverse and abundant in the terrestrial realm: Ophiacodontidae, Edaphosauridae, Varanopidae, Sphenacodontidae, Caseidae and Eothyrididae (shown in order of their appearance in the fossil record). These families have historically been united into a group known as "Pelycosauria" (Cope, 1878a; Case, 1907; Romer and Price, 1940; Reisz, 1986). Pelycosaurs are now known to be a paraphyletic grade (Figure 1) including all synapsids not belonging to the monophyletic clade Therapsida, the clade from which mammals originate.

Palaeozoic Synapsids

Ophiacodontidae

The earliest synapsid family to appear in the fossil record is Ophiacodontidae. *Archaeothyris florensis*, one of the earliest synapsids from the Morien group (see above) was assigned to this family (Reisz, 1972), an assignment supported by numerous phylogenetic analyses (Berman et al., 1995; Maddin et al., 2006; Reisz et al., 2009; Reisz et al., 2010; Benson, 2012). Ophiacodontidae is defined by a dorsally projecting pubic tubercle anteroventral to the acetabulum (Berman, 1995) and a dorsoventrally narrow temporal fenestra with a deep temporal bar (Benson, 2012). Their skulls are elongated and narrow, particularly in the facial region (Romer and Price, 1940). All species for which dentition is preserved are inferred to be carnivorous. Their teeth are numerous, but the caniniform region is weakly developed (Romer and Price 1940). Ophiacodontidae are known from North America and western Europe from the Middle Pennsylvanian until the end of the Early Permian.

One genus of this family, *Ophiacodon*, has been interpreted as a semi-aquatic piscivore. This was first suggested by Case (1907) in his review of pelycosaurian-grade synapsids, although this monograph provided no evidence. The hypothesis was challenged by Williston and Case (1913), citing the slender tail as poorly adapted for swimming. However, other anatomical features have provided support for an aquatic lifestyle, including flattened unguals (Romer and Price 1940), longer hind limbs than forelimbs (Romer and Price, 1940;

Kemp, 1982), and the poorly ossified appendicular skeleton, slow ossification being widespread among secondarily aquatic tetrapods (Reisz, 1986). The skull morphology has also been cited as being indicative of a piscivorous diet. The tall, narrow skull with slender jaws and thin bone would be mechanically weak, unsuited for large terrestrial prey (Romer and Price, 1940). The small, numerous, unserrated conical teeth are also suggestive of a fish-based diet (Romer and Price, 1940). Conversely, Thomson and Russell (1986) argued against the mechanical weakness of the skull, pointing out that the large palatines would brace the snout against bending and torsion. The significance of the flat unguals has also been challenged, having been found in other terrestrial amniotes (Maddin and Reisz, 2007). Felice and Angielczyk (2014) argued the morphology of the manus and pes is mostly inconsistent with other secondarily aquatic amniotes. They also used morphometrics to show the morphology of the vertebrae was closer to that of a terrestrial animal. Analysis of bone microstructure has proven inconclusive: the high bone density of *Ophiacodon*, whilst suggesting an aquatic lifestyle, is outside the range of any extant species, aquatic or otherwise (Germain and Laurin, 2005).

Varanopidae

Varanopidae is a clade of small to medium-sized carnivores. As their name suggests, their skulls strongly resemble those of varanid lizards, with a long, narrow rostrum and strongly recurved and serrated teeth (Romer and Price, 1940). Other defining features include an elongated external naris (Reisz and Dilkes, 2003), a large, sheet-like septomaxilla (Reisz and Dilkes, 2003), absence of the supraglenoid foramen (Maddin et al., 2006), reduction of the occipital flange of the squamosal (Maddin et al., 2006), a short anterior process of the jugal (Benson, 2012), separation of the atlantal and axial intercentra (Benson, 2012), anterior orientation of posterior dorsal neural spines (Benson, 2012), a strongly concave ventral surface of the pubic apron (Benson, 2012) and a straight anterior margin of the interclavicle (Benson, 2012). Most known varanopid species are small carnivores, but three species, *Varanodon agilis* (Olson 1965) and *Watongia meieri* (Olson, 1974; Reisz and Laurin, 2004) from the Chickasha Formation of Oklahoma, and *Tambacarnifex unguifalcatus* from the Tambach Formation of Germany (Berman et al., 2014), reached lengths of over 1.2 meters, possibly approaching two meters (Reisz and Laurin, 2004). The large macro-carnivores in most Lower Permian terrestrial ecosystems are sphenacodontid synapsids (see below). However, the Tambach Formation has yielded only small sphenacodontid specimens (Berman et al., 2001; Berman et al., 2004), whilst the Chickasha Formation has yielded none. Berman

et al. (2014) theorised that in the dry upland areas represented by these formations, large varanopids replaced sphenacodontids as the dominant carnivores.

The earliest and most basal member of Varanopidae, *Archaeovenator hamiltonensis*, appears in the Virgilian (late Kazimovian-Gzhelian) aged Hamilton Quarry of Kansas (Reisz and Dilkes, 2003). *Milosaurus mccordi*, from the earlier Missourian (Kazimovian) sediments of Illinois, was originally described as a varanopid (DeMar 1970), but the fragmentary nature of this specimen makes a reliable assignment difficult (Reisz, 1986). The varanopids are the longest-lived and geographically most widespread clade of pelycosaurian-grade synapsids, having been found in North America, western Europe, European Russia and South Africa as late as the Middle Permian. The youngest known pelycosaur is an unnamed varanopid from the *Pristerognathus* Assemblage Zone (late Capitanian-early Wuchiapingian) of South Africa (Modesto et al., 2011). The South African varanopid *Heleosaurus scholtzi* has provided the earliest evidence of group-living and parental care in amniotes. A group assemblage of specimens includes an adult and four juveniles possibly living together in a burrow (Botha-Brink and Modesto, 2007; 2009).

Edaphosauridae

Edaphosauridae are ecologically an extremely important clade. The genus *Edaphosaurus* represents one of the earliest terrestrial herbivores to appear in the fossil record, along with diadectid amphibians which appeared at a similar time (Vaughn, 1968; Kissel, 2010). Prior to the appearance of *Edaphosaurus* in the Gzhelian (Williston and Case, 1913; Lucas et al., 2005), and possibly earlier in the Kazimovian of Kansas and the Czech Republic (Fritsch, 1895; Peabody, 1957), most primary consumers in terrestrial ecosystems were arthropod detritivores (Shear and Sheldon 2001). *Edaphosaurus* and the diadectid amphibians are the earliest examples of vertebrates feeding directly on living plants. *Edaphosaurus* itself possesses several adaptations related to its dietary specialisation. Its palatal and dentary teeth form occluding tooth plates which, combined with a propalineal motion of the lower jaw, allow it to grind vegetation (Modesto, 1995). They also possess a large, barrel-shaped trunk presumably housing the large digestive system required to digest plants (Romer and Price, 1940).

Edaphosaurids other than *Edaphosaurus* have varied diets. The basalmost member of the clade, *Ianthosaurus hardestiourm* from the late Kazimovian Garnett Quarry of Kansas, is a small insectivore (Modesto and Reisz, 1990; Mazierski and Reisz, 2010). Two other species appear in the later Early Permian in the USA: *Glaucosaurus megalops* (Williston, 1915;

Modesto, 1994) and *Lupeosaurus kayi* (Romer, 1936; Sumida, 1989). Both of these species are problematic. *Lupeosaurus* does not preserve a skull or dentition, so no reliable inferences about its diet may be made. However the large size and morphology of the ribs (recalling the barrel-like trunk of *Edaphosaurus*) do suggest an herbivorous animal (Sumida, 1989). *Glaucosaurus*, meanwhile, is only represented by juveniles, and is therefore difficult to interpret. Although the conical teeth suggest an insectivorous or omnivorous diet, other features thought to correlate with herbivory are present, such as isodonty, loss of the transverse flange of the pterygoid, and the shortened snout (Modesto, 1994). It is possible that its diet varied through ontogeny; the consumption of herbivorous insects as a juvenile may have provided amniotes with the bacteria necessary for fermentation of plant material in adulthood (Sues and Reisz, 1998).

Edaphosaurids are characterised by spatulate, slightly bulbous teeth which lack recurvature (Modesto, 1994), a long and broad postfrontal (Modesto, 1994), dorsal neural spines being subcircular and rod-like for most of the spine's length (Modesto, 1994), strongly posteriorly inclined posterior dorsal neural spines (Modesto, 1994), the quadrate condyles being confluent rather than distinctly separate (Modesto, 1995), a short frontal process (Benson, 2012), anterior inclination of the axial neural spine (Benson, 2012) and dorsal transverse processes located anterior to the midlength of the neural arch (Benson, 2012). All members of Edaphosauridae for which postcranial information is available possess elongated neural spines (Romer and Price, 1940; Reisz and Berman, 1986). These structures, sometimes up to three times the height of the animal, have also appeared numerous times in sphenacodontid synapsids (Romer and Price, 1940; Hook and Hotton, 1991), as well as in dinosaurs (Benton, 1979; Sereno et al., 1996), crurotarsan archosaurs (Butler et al., 2011b) and amphibians (Lewis and Vaughn, 1965; Vaughn, 1971). Most workers believe them to have supported a sail formed from skin webbing, although defensive spines (Jaekel, 1910) or a fatty hump as found in bison (Bailey, 1997) have also been suggested. With the exception of *Lupeosaurus*, the spines of edaphosaurids possess lateral tubercles which would have protruded from the sail (Romer and Price, 1940; Reisz and Berman, 1986).

The function of such sails is debated, with sexual display (Bakker, 1986) and thermoregulation (Romer and Price, 1940) having been suggested. Under the thermoregulatory hypothesis, large animals such as *Dimetrodon* and edaphosaurids would use the sails to increase their surface area, allowing them to heat up more quickly in the sun and become active faster than their predators or prey. Experiments on airflow and heat flow over a model edaphosaurid (Bennett, 1996) suggest that the turbulent airflow over the sail caused by

the lateral tubercles causes the sail to be a more efficient radiator. On the other hand, Tomkins et al. (2010) opposed a thermoregulatory function. These authors argued that if sails had such a purpose, then they should scale allometrically with size, since smaller animals heat up more rapidly and have less need of a large heating surface. This is not seen in *Dimetrodon*, and several small species of synapsids such as the enigmatic *Xyrospondylus eocordi* and the edaphosaurid *Ianthasaurus* carry sails larger than they would need for thermoregulation. This, as well as evidence of sexual dimorphism in sail height (Romer and Price, 1940) lead Tomkins et al. (2010) to support display as their function.

Sphenacodontidae

Sphenacodontidae, as mentioned above, were the most abundant large carnivores during the Early Permian, and represent the earliest evolution of macro-carnivory (feeding on large vertebrate prey) in amniotes. Sphenacodontids have a morphology ideally suited for feeding on large animals. The skulls of most species are tall and strongly built, with the exception of *Secodontosaurus*, which has a long, narrow rostrum (Romer and Price, 1940). The teeth are laterally compressed and serrated. The genera *Dimetrodon* and *Secodontosaurus* demonstrate the earliest known example of serrations possessing denticles with a dentine core, a condition known as ziphodonty (Brink and Reisz, 2014). The dentition is strongly heterodont, with enlarged anterior teeth. There is a step in the upper jaw into which the anterior teeth of the lower jaw fit, presumably to grip prey (Romer and Price, 1940). Other defining characters include extreme elongation of the frontal (Benson 2012) and the lateral centrale proximally overlapping the third distal carpal (Benson 2012).

Sphenacodontidae first appears in fossil record in the late Pennsylvanian. A number of possible sphenacodontid specimens have been identified from the Kazimovian aged Rakonitz Coal Basin of the Czech Republic (Romer, 1945), but all are highly fragmentary and their affinity cannot be determined with confidence. The earliest unambiguous species are of Gzhelian age: *Sphenacodon ferox* from the El Cobre Canyon Formation of New Mexico (Case, 1907), and *Cryptovenator hirschbergeri* from the Remiguisberg Formation of Germany (Fröbisch et al., 2010). Many species appear in the Early Permian, most of which are assigned to the genus *Dimetrodon* (although this genus has not undergone substantial revision since the comprehensive review of Romer and Price in 1940). Only one species is known from the Middle Permian: *Dimetrodon angelensis* from the San Angelo Formation of Oklahoma, of early Roadian age (Olson, 1962).

Caseidae

Caseids reflect the second independent evolution of herbivory in synapsids. Their morphology is very different to that of *Edaphosaurus*; instead of the grinding tooth plates, caseid teeth are leaf-shaped with serrated tips, presumably for the shredding of plant material (Olson, 1968). The fore-limbs are robust, with large claws suitable for digging (Sues and Reisz, 1998). Similar to *Edaphosaurus*, the rostrum is short and the ribs form a barrel-shaped trunk, again presumably to house a large gut (Olson, 1968). Other defining features include a large external naris (Maddin et al., 2008), a maxillary tooth count of less than 15 (Maddin et al., 2008) and a deep depression on the anterior process of the lacrimal (Maddin et al., 2008). There is considerable size variation within caseids, but extremely large sizes were obtained, including the largest known pelycosaur-grade synapsid at 6.5 meters: *Cotylorhynchus romeri* (Romer and Price, 1940; Olson, 1968).

Until very recently, caseids were known only from the Permian. The earliest caseids identified before 2014 were from the Richard's Spur locality of Oklahoma (Reisz, 2005) and the Bromacker Quarry of Germany (Sumida et al., 2002; Berman et al., 2004). Richard's Spur has been dated radiometrically to 289 Ma (Woodhead et al., 2010) and a similar Artinskian age has been suggested for Bromacker (Lucas et al., 2005). It was not until description of *Eocasea martini* from the Late Pennsylvanian Hamilton Quarry (Reisz and Fröbisch, 2014) that a record for the early evolution of this clade was available. This specimen shows that early caseids were small insectivores with sharp conical teeth (Reisz and Fröbisch, 2014).

Like varanopids, caseids were a long-lived and geographically widespread clade. During the Early Permian they are known from the USA, France and Germany (Olson, 1968; Sumida et al., 2002; Berman et al., 2004). Middle Permian deposits in the Russian Mezen Group have produced the species *Ennatosaurus tecton* (Efremov, 1956; Maddin et al., 2008). Specimens thought to belong to *Cotylorhynchus* are known from the Lodève group of France (Lucas et al., 2006) and a specimen recently named *Alierasaurus ronchii* has been found at the Cala del Vino Formation of Sardinia (Ronchi et al., 2011, Romano & Nocosia, 2014). Both of these last formation are of uncertain age but are thought to be Middle Permian.

Eothyrididae

For a long time after this family was erected by Romer and Price (1940), Eothyrididae was treated very much as a "wastebasket taxon", containing any small, carnivorous, primitive-looking pelycosaur-grade synapsids that could not be assigned to any other clades. Nine genera were included within the family in the review of Langston (1965), but with the

introduction of a classification based on cladistics, Reisz (1986) assigned most of these taxa to other families, either within Synapsida or in some cases more distant clades. Only two species were retained in the Eothyrididae: *Eothyris parkeyi* and *Oedaleops campi*. The monophyletic grouping of these two species was later confirmed by phylogenetic analysis (Maddin et al., 2008; Reisz et al., 2009; Benson, 2012). These species share a secondary canniniform region posterior to the primary caniniform teeth (Maddin et al., 2008), nasals shorter than the frontals (Reisz et al., 2009) and an elongated subnarial process of the premaxilla (Reisz et al., 2009).

A number of authors have commented on the seemingly primitive morphology of Eothyrididae (Romer, 1937; Romer and Price, 1940; Langston, 1965; Sumida et al., 2014). However, despite the highly plesiomorphic skulls, Eothyrididae appears in the fossil record comparatively late. The oldest species, *Oedaleops campi* (Langston, 1965), was found in the Camp Quarry of the upper El Cobre Canyon Formation. This formation spans the Pennsylvanian-Permian boundary, and the internal biostratigraphy is uncertain, but the upper part of the formation is likely to represent the earliest Permian, possibly Asselian-early Sakmarian (Lucas et al., 2005), leaving Eothyrididae with no Carboniferous representatives. *Eothyris parkeyi* (Romer, 1937) appears in the younger Belle Plains Formation, of early Kungurian age.

Therapsida

Therapsids are the more derived synapsids that survive to the present day as mammals (Kemp, 1982). The Palaeozoic therapsids include an increased number of mammal-like features of the anatomy, such as the loss of several skull elements (Sidor, 2001) and the acquisition of a femoral head, which allows a more upright posture (Kemp, 1978). The heterodont dentition that first appeared in pelycosaurian-grade synapsids has further advanced. Carnivorous clades like Biarmosuchia, Therocephalia and Gorgonopsia have greatly enlarged canine teeth in the upper and lower jaws (Rubidge and Sidor, 2001). The Dinocephalia (a clade containing both carnivorous and herbivorous species) possess intermeshing incisors with a lingual heel forming a grinding surface (King, 1988). The herbivorous clade Anomodontia and their diverse subclade Dicynodontia show reduction and eventual loss of teeth, replacing them with a keratinous beak (King, 1988). Therapsids also possess an elongated choana and later develop a secondary palate independently in multiple lineages (Sidor, 2003), allowing more efficient ventilation. The more effective food processing and ventilation allowed a higher metabolic rate, permitting greater environmental

tolerance and a more active foraging mode (Kemp, 2006; Hopson, 2012). Therapsids replaced the pelycosaurian-grade synapsids in their ecological roles during the earliest Middle Permian, and were particularly diverse and abundant during the Middle and Late Permian. Their diversity was greatly reduced by the end-Permian mass extinction, although anomodonts, therocephalians and cynodonts survived into the Triassic (Fröbisch, 2008; Sahney and Benton, 2008; Fröbisch, 2013; Irmis et al., 2013; Fröbisch, 2014).

Some studies have suggested *Tetraceratops insignis*, from the late Kungurian Arroyo Formation of Texas, is the earliest and basalmost therapsid (Laurin and Reisz, 1990; 1996; Amson and Laurin, 2011). Unfortunately there is only one poorly preserved specimen of this species, and its assignment to Therapsida is disputed (Conrad and Sidor, 2001; Liu et al., 2009a). The earliest unambiguous therapsids appear in the fossil record during the Roadian in the Golyusherma Group of Russia (Ivakhnenko, 1995; Benton, 2012). Olson (1962) described a large number of putative therapsid species from the San Angelo formation in Oklahoma, of similar age to the Russian material, but all were extremely fragmentary and most have been reinterpreted as sphenacodontid or caseid synapsids (Sidor and Hopson, 1995; Battail, 2000; Kammerer, 2011).

Introduction to the Study of Diversity

The investigation of diversity patterns through time is an important aspect of the study of macroevolutionary processes occurring in organisms. It enables palaeontologists to deduce the major events in the history of the group under study and is also relevant to broader questions, such as the impact and recovery from mass extinctions, the processes underlying evolutionary radiations and the importance of competition and co-evolution.

As would be expected for such an important aspect of palaeontological research, there has been considerable debate throughout its history regarding suitable methods. Much of this debate has concerned the completeness of the fossil record and its adequacy for inferring biological signals (Raup, 1975; Sepkoski et al., 1981; Maxwell and Benton, 1990; Sepkoski, 1993; Benton, 1999; Benton et al., 2000; Fara and Benton, 2000; Alroy et al., 2001; Fountaine et al., 2005; Dyke et al., 2007; Smith and McGowan, 2007; Alroy et al., 2008; Fröbisch, 2008; Barrett et al., 2009; Alroy, 2010b; Benton et al., 2011b; Mannion et al., 2011; Benton, 2012; Brocklehurst et al., 2012; Benson and Upchurch, 2013; Fröbisch, 2013; Pearson et al., 2013; Fröbisch, 2014). Other debates have concerned suitable methods to estimate species richness

and correct for sampling biases (Alroy et al., 2001; Lane et al., 2005; Smith and McGowan, 2007; Alroy et al., 2008; Alroy, 2010b; Benton and Ruta, 2011; Mannion et al., 2011).

Biases in the Fossil Record

The incompleteness of the fossil record has long been acknowledged, but it wasn't until the seminal paper of Raup (1972) that consideration was given towards how the incompleteness of the fossil record may be impacting on our interpretations of it in a systematic and, more importantly, correctable manner. Raup identified seven sources of error which may be influencing estimates of species richness:

1: Range charts. Early estimates of diversity were based on compendia giving range data of the taxa rather than details of specific occurrences. For example, if a species is listed as being present from the Asselian until the Artinskian, its range will pass through the Sakmarian stage, even if no specimens of that species have been discovered in Sakmarian strata. Such counting methods lead to phenomena known as edge effects, resulting from the fact that the first and last appearances of a taxon in the fossil record are unlikely to be the true first and last appearances; the ranges will actually be truncated at either end (Raup, 1972). This leads to diversity being artificially lowered during the earliest time slices, as taxa which were actually present in these time slices may not have their ranges extended back into them. If the time period under study does not extend to the recent, then the latest time slices will also have lowered diversity.

Mass extinctions can produce a specific edge effect for the same reason (Signor and Lipps, 1982); many taxa may have died out in a single event, but not all their ranges will be observed as extending to this event. Therefore, many taxa (particularly rare taxa with a lower probability of preservation and discovery) will appear to have died out before the event, and the mass extinction will appear to be a gradual decline (Signor and Lipps, 1982). This effect has been dubbed the Signor-Lipps effect.

2: Influence of extant records. Since our knowledge of extant taxa is better than that of the fossil record, fossil taxa with living representatives will most probably have their ranges extended to the recent (Cutbill and Funnel, 1967). As such the truncation of ranges mentioned above is considerably less likely for taxa surviving to the present. This leads to a specific edge effect dubbed "The Pull of the Recent" (Raup, 1972): since a higher number if late Mesozoic

and Cenozoic taxa have living representatives and will have their ranges extended to the recent, estimates of diversity during the late Mesozoic and Cenozoic will be raised relative to the Palaeozoic.

Alroy et al. (2008) demonstrated that the Pull of the Recent has a large effect on global diversity patterns. Two curves were produced, the ranges of recent taxa in one extended to the recent, and ranges in the other extended only to the last fossil occurrence. There was little difference between the two curves during the Palaeozoic, since few Palaeozoic species have survived until the present day. However, during the Late Jurassic and Cretaceous the curve not including recent occurrences is noticeably lower than the other (Figure 2). During the Palaeogene and the Neogene, the curve incorporating recent occurrences shows a considerable increase in diversity from less than 1000 to almost 2500 genera. However, the curve only based on fossil occurrences shows a much more modest increase to less than 1500. Alroy et al. (2008) argued that the Cenozoic increase which has been supported in previous diversity curves of Valentine (1970) and Sepkoski (1982; 1993) was in fact an artefact of the Pull of the Recent.

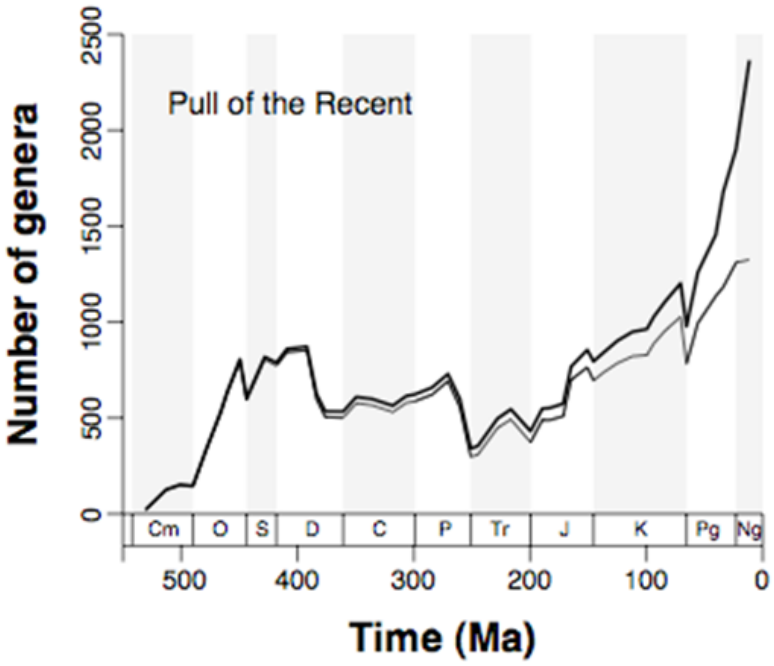

Figure 2: Diversity curves illustrating the impact of the Pull of the Recent, from Alroy et al. (2008). The thick line represents the diversity estimate when the ranges of genera are extended to the recent. The thin line represents the diversity estimate when the ranges of genera are extended to the last fossil occurrence.

3: Duration of geological time units. The time bins employed in diversity studies are usually the geological time units, whether stages, epochs or periods. Raup (1972) argued that this is problematic, since longer time intervals will show a higher diversity. Foote (1994)

supported this opinion, arguing that more taxa would come and go during a long interval, raising that interval's diversity. Miller and Foote (1996) added that during a longer time interval, there would be more sedimentation, leading to a higher probability of preservation. On the other hand, Fastovsky et al. (2004), in their study on dinosaur diversity, found no correlation between generic richness and the length of the stages and argued that the richness patterns they observed were not related to stage length. It is important to note that the geological time units are based on biostratigraphy, and the length of these units is therefore not independent of species turnover through time.

4: Monographic effects. Raup (1972) suggested that the level of interest in a particular group or geographic area will affect diversity estimates, as will the quality of the taxonomic research into a group. As an example of this, Raup cited a single monograph (Cooper, 1958) which alone shifted a diversity peak in brachiopods from the Devonian to the Ordovician. The tendency for workers to examine particular areas more thoroughly is well documented (e.g. Fastovsky et al., 2004; Brocklehurst et al., 2012; Cleary et al., 2015), with many groups showing a bias towards North America, Europe and Asia and the southern landmasses being considerably less well sampled. Interest in particular clades, either for reasons of popularity e.g. dinosaurs, or usefulness e.g. ammonites for biostratigraphy, will lead to substantially more work being done on those clades and potentially more species being named (Raup, 1972). A time dependant aspect was also noted by Raup: if a fossil clade has living representative, more complete morphological information is available for that clade, which will affect taxonomic revisions.

5: Lagerstätten. Areas of exceptional preservation, such as the Burgess Shale, Solnhofen, and the Messel Shale, produce large numbers of nearly complete fossils. The quantity of material will obviously produce a high diversity, and the quality of the preservation will increase the amount of information available for taxonomic revisions. This correlation between Lagerstätten and peaks in diversity has been noted in multiple studies (e.g. Brocklehurst et al., 2012; Friedman and Sallan, 2012; Cleary et al, 2015). Raup (1972) pointed out that Lagerstätten appear to be more common in younger rocks, possibly raising recent diversity estimates. At the very least, they add noise to the data (Raup, 1972).

6: Area-diversity relationships. Taxa tend to be geographically restricted due to barriers to their dispersal. As such, when a new area is explored, a high rate of discovery of new taxa

inevitably follows (Raup, 1972). Raup suggested that this problem should be particularly severe in the marine realm; only a small fraction of the ocean area at any point in the geological past is available for study since, with the exception of deep ocean cores, palaeontologists are limited to studying rocks on continents and islands. Therefore the apparent diversity of any group is limited to the taxa restricted to the areas available for sampling. This problem is exacerbated by the fact that diversity has been shown to be area dependant (Preston, 1962). Our diversity estimates depend not only on outcrop exposure, but also on the distribution of the exposure. Moreover if geographic coverage improves towards the recent, as Raup (1972) suggests, this is yet another bias towards higher diversity in younger rocks.

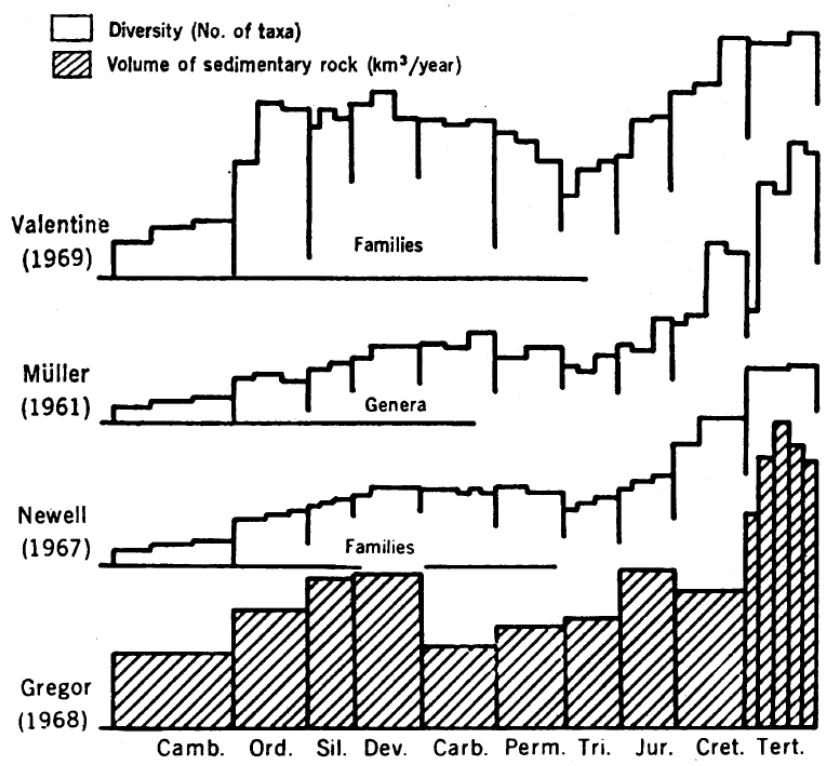

Figure 3: The relationship between estimates of diversity and the volume of sedimentary rock. From Raup (1972)

7: Sediment volume. Raup (1972) was the first to note a correlation between sediment volume and diversity estimates (Figure 3). Since then such a correlation, as well correlations with similar proxies such as number of formations in each time interval and rock outcrop area, has been verified both globally and within individual clades and areas (Smith, 2001; Crampton et al., 2003; Fröbisch, 2008; Smith and McGowan, 2008; Wall et al., 2009; Benson et al., 2010; Mannion et al., 2011; Benson and Upchurch, 2013; Fröbisch, 2013; 2014). It is

intuitive that a higher availability of rock of a particular age would lead to a higher observed diversity in that particular time bin. Unfortunately the strength of the correlations between observed diversity and proxies for rock availability seem to be suggesting that our diversity estimates are merely showing how much rock is available from each time bin rather than diversity. Rocks are continuously being destroyed by erosion or subduction, or overlain by other layers. Moreover, rates of sedimentation have varied through time, and a higher rate of sedimentation increases the probability of preservation (Raup, 1972).

Since this leading paper, other influences have been shown to affect the quality of the fossil record. The impact of the size of the organisms, for example, has been shown to be important but also complicated. It is natural to think that smaller animals, more easily destroyed by taphonomic processes, would have a worse fossil record than larger, more robust species. Indeed, it has been shown in studies of dinosaurs in the Dinosaur Park Formation (Brown et al., 2013) and in comparing sauropod dinosaurs to Mesozoic birds (Brocklehurst et al., 2012) that smaller animals tend to leave more incomplete skeletons. However, Fara and Benton (2000), assessing the proportion of Lazarus taxa relative to observed lineages in Cretaceous tetrapods, found the fossil record of small bodied animals is no less complete than that of larger ones. Cleary et al. (2015), in their study on ichthyosaurs, found an unusual result: both small and large ichthyosaurs were poorly preserved relative to those of intermediate size. Complicating factors may include the influence of Lagerstätten; smaller animals may be easier to destroy, but are also easier to rapidly bury and preserve whole (Brocklehurst et al., 2012). Historical factors are also important; during the early days of palaeontological collection, a desire for large articulated specimens for museum displays may create the impression that smaller animals are less likely to be preserved (Brown et al., 2013).

The environment in which an organism lived unsurprisingly has a great effect on the probability of its preservation, as well as the quality of the fossil preserved. For example, Brocklehurst et al. (2012) showed that Mesozoic birds from fluvial and lacustrine localities were better preserved than those from marine localities (where the high energy would destroy skeletons) or terrestrial localities (in which sedimentation rates are lower). Cleary et al. (2015), meanwhile, found ichthyosaurs to be better preserved in marine muds and sands than carbonates. They suggested this is due to the larger number of benthic scavengers in marine carbonates. However, again, this issue is shown to be more complicated by further study. Benson and Butler (2010) showed that the influences of sampling biases on the record of marine tetrapods differ in shallow marine and open ocean formations; the open ocean record

is heavily influenced by the quantity of rock known from each time interval, suggesting a strong influence of bias due to temporal heterogeneity of fossil sampling. The shallow marine record, meanwhile, showed a stronger relationship with continental flooding, demonstrating that it was the environment directly influencing diversity: the Common Cause hypothesis (Benson and Butler, 2010). Uneven sampling of different lithologies will affect the fossil record: taxa limited in the proportion of environments in which they live will not be sampled if their preferred environment is not sampled (Rook et al., 2013). This biases the marine and non-marine realms differently; marine vertebrate diversity correlates strongly with the evenness of sampling of different lithologies, but marine invertebrates and continental taxa do not (Rook et al. 2013).

The influence of lithification (consolidation of sediments) on the fossil record has recently begun to receive attention. Lithified rock units produce about half of the diversity of unlithified units (Alroy et al., 2008; Hendy, 2009) since fossils are more likely to be destroyed during lithification or during the mechanical breaking required to examine such sediments (Kowaleski et al., 2006). Small specimens are particularly vulnerable to being destroyed, or simply overlooked (Kowaleski et al., 2006). Meanwhile, unlithified rocks may be examined by sieving, increasing the likelihood of finding smaller specimens undamaged (Kowaleski et al., 2006). Unlithified sediments are more common in more recent sediments (Hendy 2009), yet another bias towards higher observed diversity in the Cenozoic. For invertebrate workers, there is a bias towards organisms with calcite shells in lithified sediments, since aragonite is more easily destroyed during diagenesis (Hendy, 2009).

With these complications surrounding the interaction between diversity and sampling biases, it is unsurprising that debate exists concerning the quality of the fossil record, and whether the signal of our diversity curves represents biases or an actual biological signal. As might be predicted, investigation into the completeness of the fossil record of different clades produces different results. Tarver et al. (2011) suggested that systematic datasets of palaeontological data should be investigated individually for the quality of their record if they are to be used to derive macroevolutionary patterns.

Creation of Diversity Curves

The simplest method of producing curves of species richness through time is the taxic diversity estimate. This is a raw count of the number of species in each time bin. Whilst this method is simple and requires minimal information, it is, as discussed above, heavily

influenced by the vagaries of sampling and other sources of error in the fossil record, and may not accurately reflect the true palaeodiversity. As such, several methods have been proposed in order to create diversity estimates which more closely represent actual historical trends.

The Use of Compendia and Databases in Diversity Estimates

Early estimates of diversity (species richness) were produced using extremely basic methods. In fact the earliest published curve (Philips, 1860), based on a compendium of British fossil data, was a hand drawn estimate of diversity, with no scale or indications of time binning. Later studies (e.g. Valentine, 1969; Sepkoski et al., 1981; Raup and Sepkoski, 1982) used the more objective method of assigning taxa to bins and creating a curve representing the changing diversity between bins to produce family-level curves. These diversity estimates showed many of the signals found in later diversity estimates, such as the "Big Five" mass extinctions (Raup and Sepkoski, 1982), the three evolutionary faunas (Sepkoski, 1981) and the large increase in diversity during the Cenozoic (Valentine, 1969). All of these early studies were based on compendia of marine taxa detailing first and last appearances in the fossil record, several updates of which were published by Sepkoski, along with diversity curves and extinction estimates over the following years (Sepkoski, 1984; 1993; 1996; 2002). However, diversity estimates based on compendia are problematic. These supply age range data for taxa, but little or no information on collections, localities, geography, environment, or collection method. As such, the possible counting methods available to researchers are limited, as well as the possibility of correcting for sample size or examining local patterns or biases. The need for such information has led to the introduction of databases into diversity studies

The Paleobiology Database (hereafter PBDB, recently renamed Fossilworks) was created to address these issues. This database not only lists taxa at the genus and species level, but also collections, references, localities, formations, and information on lithology and ecology. Such data allows not only the generation of diversity curves at both global and local levels, but furthermore allows investigation into ecological changes through time and space in in the fossil record and also into sample size. The PBDB is a user-updated database, and as such is not fully complete and may contain errors due to failure to update changes in taxonomy or the ages of formations. However, for a well-sampled, numerous, and comprehensively updated clade, such rare errors in the database should not have a large effect on diversity estimates. The PBDB has been used to investigate global diversity through time by Alroy et al. (2001; 2008) as well as in other investigations into local and clade-specific

diversity patterns, sampling biases and ecological changes through geological time (see PBDB official publication list)

Because datasets in the terrestrial fossil record tend to be smaller than those in the marine realm, the impact of missing or incorrect data becomes greater. Many studies of terrestrial clades have therefore not taken data from the PBDB, but instead used up-to-date databases generated specifically for their chosen time and clade. One such database is the Early Tetrapod Database, used in several studies on the diversity of tetrapods from the Middle Devonian until the Early Jurassic (Sahney and Benton, 2008; Sahney et al., 2010; Benton, 2012; Benton et al., 2013). A local database details the contents of localities belonging to the Beaufort Group of the Karoo Supergroup of South Africa, spanning the Middle Permian until the Early Triassic (Nicolas & Rubidge, 2009; 2010). This has been instrumental in investigations of diversity and sampling bias in South Africa across the Permian-Triassic boundary (Fröbisch, 2013; Irmis et al., 2013; Fröbisch, 2014).

Counting Methods

Simple modifications to counting methods may produce more accurate diversity estimates. The earliest diversity estimates, based on range data of species (e.g. Valentine, 1969; Raup and Sepkoski, 1982) are afflicted by edge effects (Figure 4A). Foote (1999; 2000) suggested that one should only count taxa sampled in the time bin and ignoring Lazarus taxa (taxa sampled before and after a particular time bin, and so inferred to be present within the bin). This so-called "sampled in bin" diversity estimate reduces issues such as edge effects, but does not remove another set of biases known as rate effects. Periods of high species turnover would lead to many species being present for only a short period of time. This reduces the probability of their preservation and discovery in the present day (Foote, 1999; Alroy, 2010a). As such our diversity estimates would be lower for times of high species turnover, particularly in time bins where sampling is poor. Alternatively, if turnover rates are high within a long, well-sampled time bin, the number of species counted within that time bin will be considerably higher than the standing diversity (the actual diversity at any one point in time) (Foote, 1999). It has been suggested that a possible solution to rate effects might be to remove taxa known only from a single interval (singletons) from diversity estimates (Harper, 1996). To do so would also reduce the effect of Lagerstätten by eliminating taxa only found in areas of exceptional preservation. However, removing singletons artificially reduces the diversity estimated for the most recent time bins (Figure 4B): any species which first appears in the latest time bin can only be a singleton (Foote, 2000).

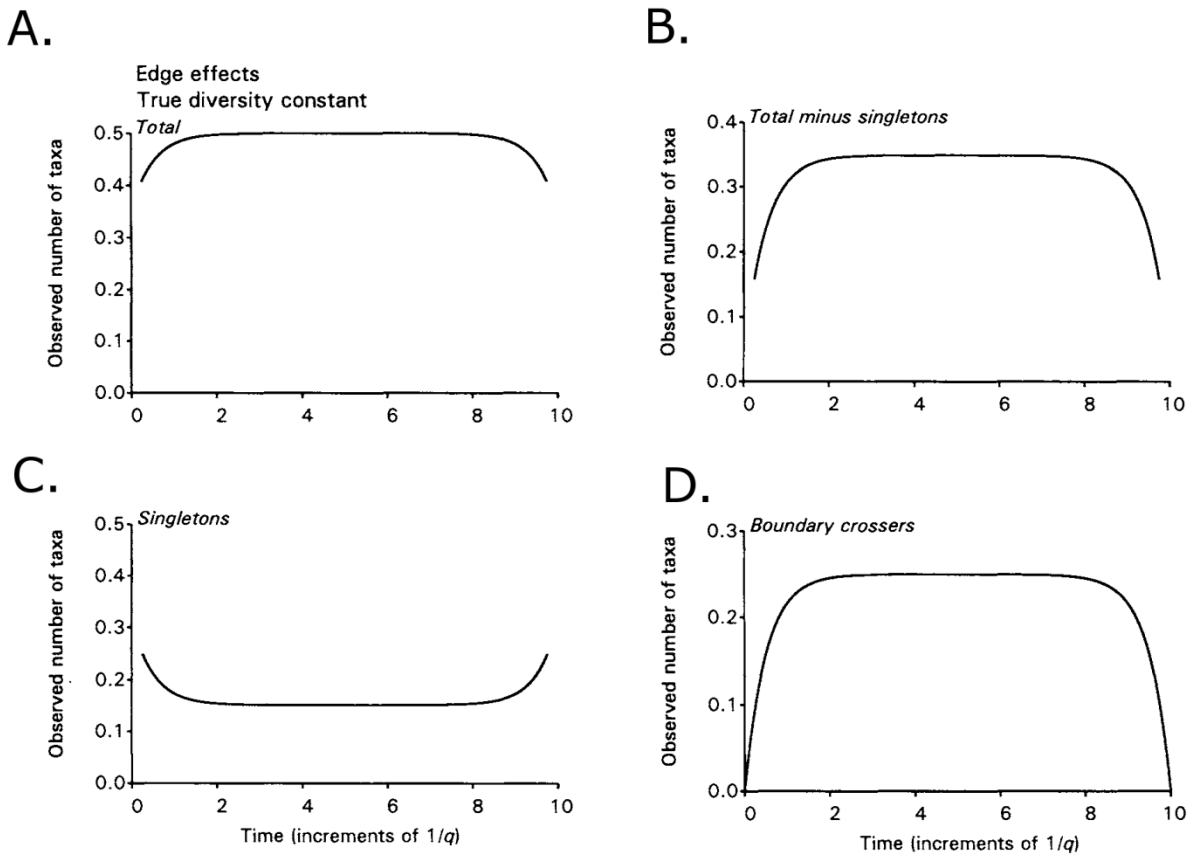

Figure 4: Illustration of the impact of different counting methods on a time period of constant diversity. From Foote (2000). A) All observed species counted; B) All observed species except singletons (taxa known only from one time bin) counted; C) Singletons only counted; D) Taxa which cross the boundaries between time bins counted.

Alroy (1996) and Alroy et al. (2001) suggested counting taxa at the boundaries between time bins, including only the taxa which crossed the boundary. This method automatically eliminates singletons, which by definition do not cross the boundaries, and is independent of interval length. The smoothness of the diversity curve was interpreted as the curve containing less "noise" (Alroy et al., 2001). However, Foote (2000) suggests that this method is heavily biased by edge effects (Figure 4D). Alroy (2010a) argued that, although sampled in bin diversity estimates are not completely reliable due to rate effects, the heavy impact of edge effects on boundary crosser and range through diversity estimates makes it the best method to use.

Sampling proxies

One of the most frequently used methods to investigate the impact of sampling biases on the fossil record is to investigate the strength of the correlation between diversity estimates and various proxies for biases. Such proxies endeavour to quantify a particular aspect of the

bias through geological time. For example, one can use the area of sedimentary rock outcrop available from each time bin as a proxy for geological biases (Smith, 2001; Crampton et al., 2003; Smith and McGowan, 2007; 2008; Wall et al., 2009; Fröbisch, 2013; 2014). An alternative quantification of rock availability is the number of fossil-bearing rock formations (Fröbisch, 2008; Barrett et al., 2009; Butler et al., 2009; Benson et al., 2010; Mannion et al., 2011; Benton, 2012; Benson and Upchurch, 2013). Quantification of human sampling effort is more difficult, but the development of the PBDB allows the use of fossil-bearing collections. Each of these collections represents an event in which a fossil-bearing locality of a particular age was sampled, and so can provide a quantification of the amount of effort workers have put into sampling rocks of a different ages. Some studies have used the number of fossil-bearing collections as a proxy for anthropogenic sampling biases (Crampton et al., 2003; Butler et al., 2011a; Brocklehurst et al., 2012).

Many of the above studies have cited a significant correlation between such sampling proxies and the diversity estimates of the clades under study as evidence that the signal from the diversity curves is predominantly that of sampling rather than a biological signal. However, such inferences have been criticised. Benton et al. (2011) argued that the sampling proxies used may well be redundant with the diversity signal; if the diversity of a particular clade decreases, one would expect the number of formations or collections bearing fossils of that clade to decrease as well. It was also argued that using the number of formations or collections bearing fossils of a particular clade as a sampling proxy for that clade does not take into account times when workers have studied rocks of a particular age, but have not found fossils of the clade of interest (Benton et al., 2011). Benson and colleagues (Benson et al., 2010; Benson and Mannion, 2012) supported the use of such proxies, but argued against the simplistic view that presence of a significant correlation indicates a strong influence of sampling biases and absence of a significant correlation indicates the fossil record is good. The observed fossil record is a product of both the biological signal and sampling, and one should only expect a perfect correlation between sampling and observed diversity if the actual diversity was constant through time (Benson and Mannion, 2012). It was shown that multivariate models incorporating both sampling bias and an underlying biological signal fit marine reptile data (Benson et al., 2010) and sauropodomorph data (Benson and Mannion, 2012) best.

As well as these more general issues, problems with specific proxies have been identified. Formation counts have been criticised as being extremely arbitrarily defined, with formations varying by up to eight orders of magnitude in volume (Peters, 2006; Peters and

Heim, 2010; Dunhill, 2012). Crampton et al. (2003) demonstrated that the number of formations poorly represents sedimentary outcrop area. In fact, rock outcrop area measured from geological maps may not necessarily correlate with the area of rock that is exposed and available for study due to factors such as soil coverage (Dunhill, 2012). Benton et al. (2013) provided a detailed comparison of various proxies for the quality of the rock record, including formation counts from various sources, rock outcrop area, and counts of rock units from the Macrostrat database (units representing hiatus bound sedimentary rock packages [Peters and Heim, 2010]). These different proxies, supposedly assessing similar biases, showed great variation in the strength of their correlation to each other and to tetrapod diversity.

Another extensively-discussed issue with the use of such proxies is the possibility that both diversity and proxies such as rock outcrop area or number of formations may be under the control of an external factor: the Common Cause hypothesis. The most frequently cited external cause is sea-level change, the impact of which is complex and has received much attention in the literature. It is logical that fluctuations in sea level will affect the preservation potential in certain environments. Positive correlations have been found between sea level and the raw diversity of marine organisms, suggesting that increased formation and preservation of coastal deposits have resulted in a higher quality fossil record (e.g. Benson and Butler, 2010; Rook et al., 2013). It has also been suggested that increased sea level increases preservation potential for terrestrial organisms, as more will be washed into environments with high preservation quality such as deltas, estuaries and lagoons (Haubold, 1990). Conversely, a negative correlation between sea level and the quality of the terrestrial fossil record has been found (Mannion and Upchurch, 2010; Upchurch et al., 2011), as higher sea level reduces the amount of terrestrial sedimentary rock (Smith, 2001; Smith and McGowan, 2007). The Common Cause hypothesis further complicates the relationship between sea level and diversity. In the marine realm, it has been argued that rises in sea level not only increase the quantity of coastal deposits, but also marine diversity itself due to the expansion of near shore environments (Benton and Emerson, 2007; Butler et al., 2009; Benson and Butler, 2010; Hannisdal and Peters, 2011). On land it is possible that rises in sea level result in fragmentation of terrestrial land areas, promoting an increase in speciation rates (Bakker, 1977; Upchurch and Barrett, 2005; Benton, 2009). Conversely, higher sea level reduces available land area, maybe resulting in decreases in the diversity of terrestrial clades (Weishampel and Horner, 1987; Dodson, 1990; Benton and Emerson, 2007). A final alternative is that sea level may have little impact on either preservation potential or diversity

in the terrestrial fossil record. Butler et al. (2009) demonstrated that sea level does not show significant positive or negative correlation with the diversity of dinosaurs.

Sampling correction

While different counting methods are able to reduce the impact of certain errors such as edge effects, they do not solve the problems of heterogeneous sampling by palaeontologist, or variations in rock availability. Raup (1972) suggested two methods to deal with this issue: modelling and subsampling. Later a third method was introduced: the phylogenetic diversity estimate (Norrell, 1992; Smith, 1994).

Diversity analyses, both in palaeontology and neontology, depend heavily on sample size (Sanders, 1968; Raup, 1972). If only one specimen from a locality is sampled, the dataset will contain only one species. Increasing the number of specimens will increase the number of species, although the amount by which the number of species increases depends upon the relative abundances of individual species. If the locality is dominated by a few very abundant species and all other species are rare, sampling more specimens will lead to a very slow increase in the number of species since most new specimens sampled are more likely to belong to the abundant species rather than a new species.

Subsampling standardises the size of all samples to the size of the smallest sample. The method which has been most commonly used in palaeontology is rarefaction (Sanders, 1968). The technique, originally proposed for ecological study, was to draw specimens from a locality at random until the number of specimens reached the chosen sample size, and to count the number of species present in the subsample. This would be repeated multiple times in order to converge on a mean expected number of species. When applied to palaeodiversity, one wishes to standardise the sample size of each time bin instead of each locality. As such, instead of drawing specimens from each locality at random, one may draw either individual taxonomic occurrences (Miller and Foote, 1996) or entire collections (Smith et al., 1985; Alroy et al., 2001) at random from each time bin. The former weights each taxonomic occurrence equally, assuming that the number of occurrences is directly proportional to the number of species (Alroy et al., 2001). This is a problematic assumption to make, as the relationship between occurrences and taxa will vary depending on how widespread individual taxa are: widespread taxa are found in more localities, and so will be represented by more occurrences. On the other hand, to draw collections assumes that the number of species is proportional to the number of collections. This is again a problematic assumption if different collections within a single time period have produced very different numbers of species.

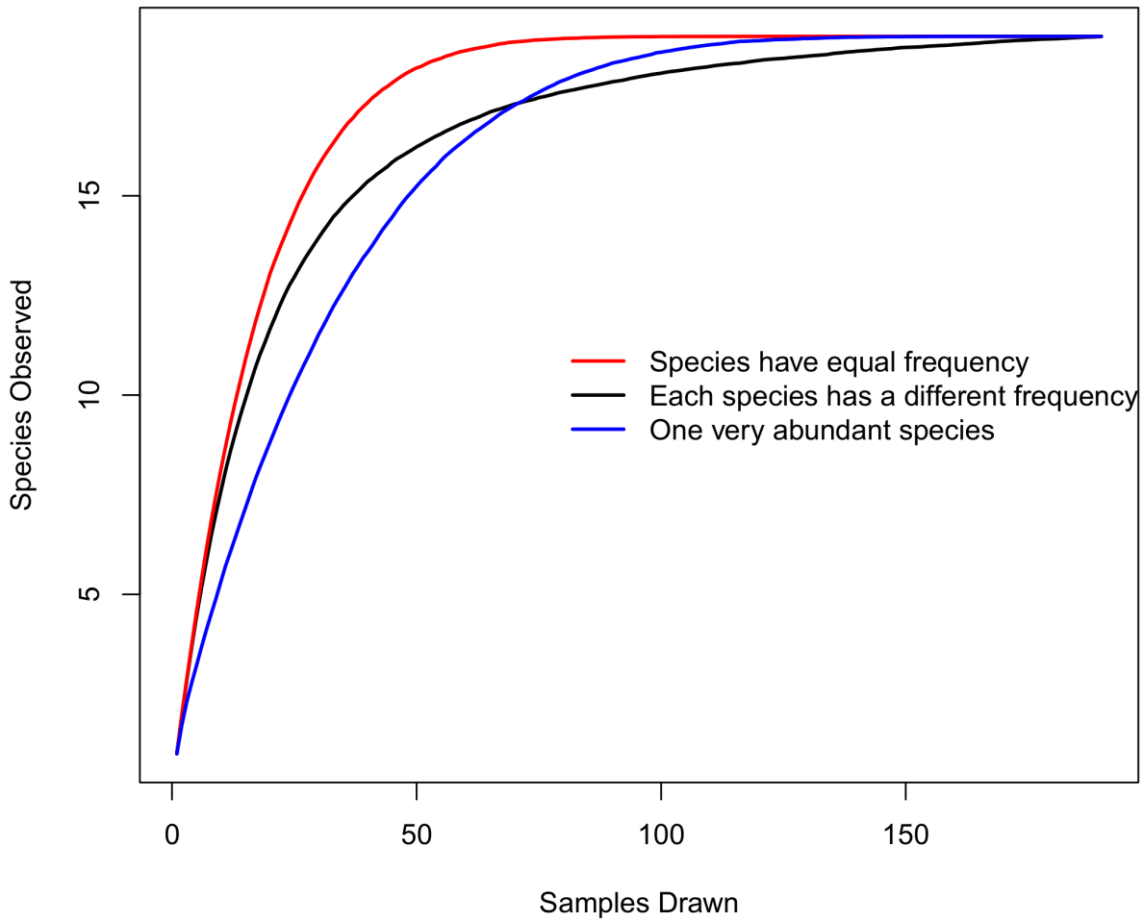

Figure 5: Three species accumulation curves representing the mean number of species observed over 1000 random sets samplings from three collections of specimens. Each collection has identical numbers of species and identical numbers of individuals, but different relative abundances of species. The red curve represents a collection in which all species have the same frequency; the black curve represents a collection in which all species have a different frequency; the blue curve represents a collection in which one species has a high abundance, and all other species have equal lower abundance.

In short, rarefaction makes assumptions that are only valid if taxon abundance and distribution do not vary. The consequences of these assumptions of rarefaction may be seen when one examines taxon accumulation curves (Figure 5). These curves represent the relationship between the number of samples drawn (either occurrences or collections) and the mean number of species sampled. Such curves show a rapid initial increase as each new draw has a large potential to uncover a new species, before reaching a plateau when most of the species have been found and drawing a new sample is less likely to add a new taxon. For rarefaction to give an accurate representation of the relative diversity difference between two time bins, the rarefaction curve for both time bins should be identical if they contain the same number of species. However this is not always the case: the curves may vary because of different relative abundances and range sizes of different species. If one were to subsample

the three time bins represented by the rarefaction curves in Figure 5, drawing for example 50 samples from each, one would obtain different diversity values despite the fact that the actual number of species in all three collections is the same.

Alroy (2010b) presents an alternative subsampling method as a solution to this problem: Shareholder Quorum Subsampling (SQS). The name comes from the fact that each taxon is treated as a "shareholder", whose share is its number of occurrences. As in rarefaction, occurrences are sampled at random. A taxon's full share is considered represented if it is sampled at least once. Unlike rarefaction, the sampling does not continue until a specific number of occurrences have been drawn, but instead continues until a certain proportion of shares (the "quorum") are represented (Alroy, 2010b). Alroy (2010a) provided a hypothetical example demonstrating the advantages of the SQS method over rarefaction. One time bin contains 10 species, each of equal frequency making up 0.1 of occurrences. If two samples are drawn, on average 1.9 species will be observed, since the second sample will be a different species from the first 90% of the time. A second time bin has 20 species again of equal frequency, so each species will have a frequency of 0.05. Thus, if two samples are drawn again, the mean number of species counted will be 1.95. Rarefaction has failed to show that the second time bin is twice as diverse as the first. If, however, SQS is used with a quorum of 0.2, the correct relative diversity is recovered. Since every species in the first time bin has a frequency of 0.1, the quorum is reached when two species have been drawn. In the second time bin, in which each species has a frequency of 0.05, the quorum is reached when four species have been drawn. SQS therefore shows that the second time bin is twice as diverse as the first.

Subsampling methods are only appropriate when the sample sizes in all time bins are reasonably large. One ideally would not reduce the sample size to the point on the species accumulation curve before the plateau (Hammer and Harper, 2006). When the curve is beginning to plateau, this implies that the subsample contains all but the rarest taxa. However, if one time bin contains a particularly small sample, then one is faced with two options: either reducing the sample size of all time bins to a point where subsampling becomes unreliable, or removing this bin from the analysis and potentially missing a key event. Neither of these options is ideal, and so researchers working on clades or time periods where sample sizes are small are forced to use different methods to correct for sampling bias.

Raup (1972) suggested modelling as an alternative to subsampling, but this was not explored in great detail until Smith and McGowan (2007) introduced the residual diversity estimate. This approach requires a proxy for sampling bias such as number of collections or

formations or outcrop area in each time bin. A model diversity estimate, based on a perfect linear relationship between diversity and the chosen sampling proxy, is produced by sorting both diversity and proxy data from low to high and fitting a linear model. The model diversity estimate is then subtracted from the observed diversity, leaving the residual diversity estimate. The thinking behind this method is that the observed diversity estimate is a signal of both sampling and the actual diversity. Subtracting the model diversity estimate in theory removes the signal from sampling, leaving only the biological signal (Smith and McGowan, 2007). This method has proven popular, particularly in analyses of terrestrial datasets where sample sizes are often small (Smith and McGowan, 2008; Barrett et al., 2009; Butler et al., 2009; Wall et al., 2009; Benson et al., 2010; Butler et al., 2011a; Benson and Upchurch, 2013; Fröbisch, 2013; Pearson et al., 2013; Fröbisch, 2014).

There have been controversies surrounding this method. Benton et al. (2011) has subjected it to the same criticism of using proxies to test for sampling bias: the problem of redundancy. It should also be noted that it only takes into account a single sampling bias, and assumes sampling has a perfect linear relationship with diversity, an assumption only true if diversity never varied (Benson and Mannion, 2012). Lloyd (2012) refined the method, allowing for non-linear relationships between the sampling proxy and diversity, and also introducing confidence intervals to show which peaks and troughs are significant. However, Pearson et al. (2013) argued against using this method, finding no reason why there would be a polynomial relationship between sampling and diversity.

The final method of sampling correction is the phylogenetic diversity estimate (Smith, 1994). This method incorporates ghost lineages into a diversity estimate: lineages not sampled from the fossil record but inferred from a phylogeny under the assumption that two sister taxa must have split from their common ancestor at the same time (Norrell, 1992). Incorporating these lineages into a phylogeny allows the inclusion of as-yet unsampled portions of the fossil record. Use of this method is obviously limited to clades for which a comprehensive phylogeny exists, and as such it has been most widely applied to vertebrates (Upchurch and Barrett, 2005; Barrett et al., 2009; Benson et al., 2010; Mannion et al., 2011; Ruta et al., 2011; Walther and Fröbisch, 2013).

As with all other sampling correction methods, flaws have been identified with the phylogenetic diversity estimate. The sampling correction is one-directional: lineages may only be extended back in time, not forward, causing higher diversity earlier in time (Wagner, 2000; Lane et al., 2005) and exaggerating the Signor-Lipps effect (Lane et al., 2005). Polytomies in the phylogeny will also create an error, biasing towards higher diversity as all

taxa in the polytomy will have ghost lineages extending back as far as the oldest taxon (Upchurch and Barrett, 2005). Another issue surrounds ancestor-descendant relationships. The cladograms produced by current cladistic methods assume bifurcating speciation from hypothetical ancestors (Norrell, 1992; Smith; 1994; Wagner and Erwin, 1995). If ancestors are sampled in the fossil record, cladistic analysis will resolve them either in a polytomy with or as the sister to the descendants (Lane et al., 2005; Bapst, 2013). While previous studies have tried to sidestep this issue by assuming that the probability of sampling an ancestor is low enough to be negligible (e.g. Norrell, 1993), it has been shown that such assumptions are invalid (Funk and Omland, 2003). If ancestors are included in a phylogeny and are not identified as such, they will lead to the inference of an incorrect ghost lineage and raise the phylogenetic diversity estimate (Lane et al., 2005). Despite these issues, the simulations of Lane et al. (2005) suggest that the phylogenetic diversity estimate is more accurate than the raw data, although these simulations assumed a correct phylogeny.

No method of estimating species richness through time is without flaws or biases. While some methods are more appropriate for certain datasets than others, none may be considered perfect. As such it is advisable to use multiple methods to estimate species diversity. Where the methods agree, one may assume that the estimated diversity trends are reflecting an accurate biological signal. Where they disagree, one must examine the biases affecting each method and deduce which diversity estimate is most reliable in the particular instance.

New Research Areas

Studies into the diversity and the completeness of the fossil record during the time period occupied by pelycosaurian-grade synapsids have been extremely limited. There have been no studies dedicated to the detailed examination of the changes in species richness in synapsids during the Late Carboniferous and Early Permian. Examinations of the wider tetrapod and amniote clades have produced differing opinions, for example regarding the diversification of herbivores, Olson's extinction and the impact of sampling biases on the fossil record. The use of sampling correction has been patchy, and restricted to the use of the residual diversity estimate. Investigations onto the quality of the fossil record have included correlation tests with sampling proxies and an examination of the completeness of specimens using the arbitrary and coarse grading system, but little else.

This thesis will present a thorough evaluation of the evolution of basal synapsids. The investigation will begin with a study of the phylogeny of pelycosaurian-grade synapsids, which will form the basis of further analyses. This part of the thesis also includes the redescription of the poorly-known basal synapsid *"Mycterosaurs" smithae*. In addition, an examination of the quality of the fossil record of pelycosaur-grade synapsids will be undertaken, including the completeness of their specimens using both the character and skeletal completeness metrics, the fit of the fossil record to phylogeny, and also examination of the history of discovery in order to ascertain whether the influence of biases has changed through time and how the taxonomic practices may affect diversity estimates. Synapsid diversity will be investigated at both the genus and the species level. Global diversity curves will be generated, as well as diversity curves for each family of pelycosaurian-grade synapsids in order to examine the changes in faunal composition occurring at this time. Sampling correction will be carried out using the phylogenetic and residual diversity estimates.

Morever, since synapsids represent the earliest appearance of many morphological innovations, such as herbivory, macro-carnivory and possibly a semi-aquatic lifestyle, the impact of such innovations on the patterns of cladogenesis, origination and extinction will be studied. This examination will be extended to all amniotes until the end of the Triassic, in order that the more general patterns can be identified and compared to those found in pelycosaurian-grade synapsids. Tree topology analysis will be used to identify areas in the amniote phylogeny in which significant shifts in the rate of cladogenesis occur. These shifts will be examined for correlation with events such as mass extinctions and the evolution of "key innovations". To further test the impact of innovations such as herbivory and an aquatic lifestyle, origination rates of those with such innovations will be compared to those without, to see if the timing of increases in origination rate of those with "key innovations" coincides with the timing of diversification shifts identified by tree topology analysis.

Chapter 2

Phylogenetic Analysis of Pelycosaurian-Grade Synapsids

Hypotheses of the Relationships of Pelycosaurian-grade Synapsids

Romer and Price (1940) provided the first review of relationships of pelycosaurian-grade synapsids incorporating information from all specimens known at the time. This review proposed that basal synapsids were divided into three suborders: Ophiacodontia, Edaphosauria and Sphenacodontia (Figure 6). Ophiacodontia were considered the basalmost group from which the other clades evolved, and contained Ophiacodontidae and Eothyrididae. Edaphosauria was a grouping of the two herbivorous clades, Edaphosauridae and Caseidae. The Sphenacodontia contained Varanopidae (supposedly basal within this clade), Sphenacodontidae and Therapsida. Since this review by Romer and Price (1940), the sister-group relationship between sphenacodontids and therapsids has been largely accepted, whereas the relationships of all other basal synapsid clades have undergone many revisions.

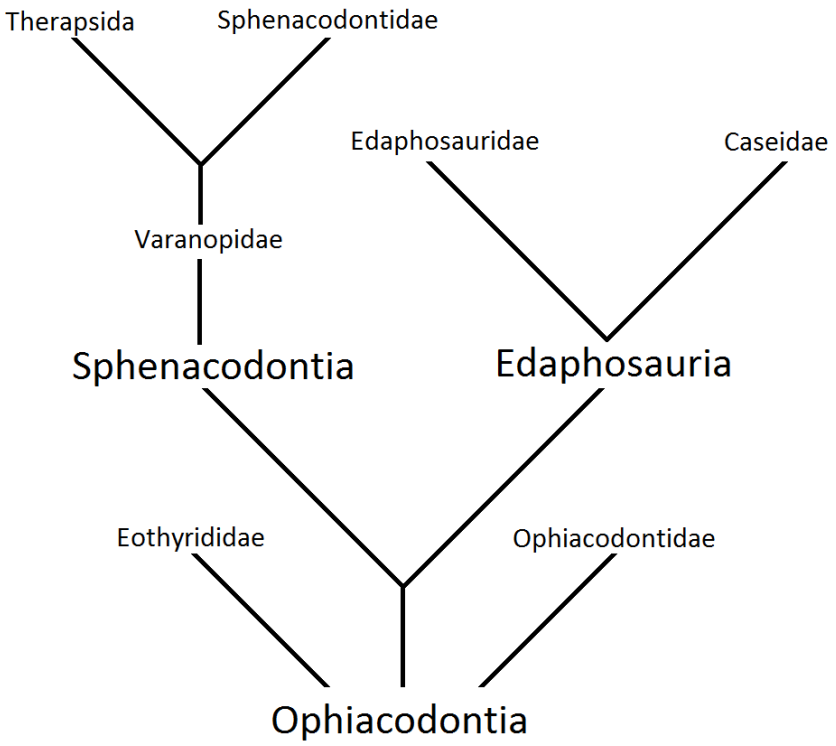

Figure 6: The relationships of pelycosaurian-grade synapsids suggested by Romer and Price (1940)

Reisz (1980) was the first to employ phylogenetic treatment of characters to decipher the relationships of pelycosaurian-grade synapsids. Unlike Romer and Price (1940), who focused mostly on the postcranium, 20 out of the 24 characters used by Reisz (1980) were cranial characters. This analysis supported a basal split between the Caseasauria (a clade containing caseids and eothyrids) and Eupelycosauria (all other synapsids). Romer and

Price's Sphenacodontia was still supported, with Varanopidae, Edaphosauridae, Ophiacodontidae, and Caseasauria as successive outgroups (Figure 7A). Brinkman and Eberth (1983) also used a phylogenetic approach, but employed a different character list compiled through study of six well-known species representing the major clades. For the first time a sister-group relationship between Edaphosauridae and the clade containing sphenacodontids and therapids was suggested, a grouping named Sphenacomorpha (Ivakhnenko, 2003; Spindler et al., 2015), that is also considered valid in the most recent phylogenetic analyses of basal synapsids. Ophiacodontidae was suggested to represent the sister taxon to Sphenacomorpha, whereas Varanopidae were found to be the sister to Caseidae (Figure 7B).

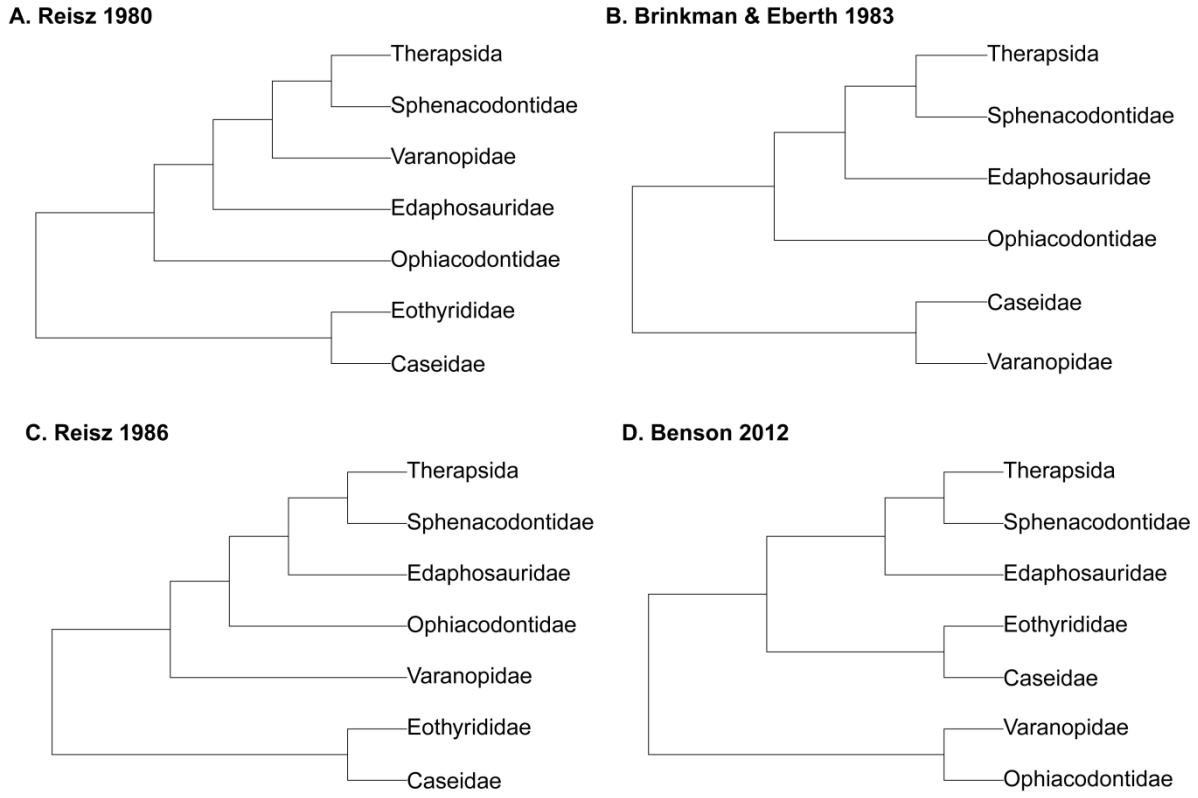

Figure 7: Four hypotheses of the phylogenetic relationships of pelycosaurian-grade synapsids. A) Reisz (1980); B) Brinkman and Eberth (1983); C) Reisz (1986); D) Benson (2012)

Reisz (1986), in the volume of the Handbook of Paleoherpetology dedicated to Pelycosauria, used a set of 26 characters to infer the relationships that have since become the widely accepted consensus (Figure 7C). The basal split between Caseasauria and Eupelycosauria was supported and Edaphosauridae, Ophiacodontidae and Varanopidae were found to be successive outgroups to Sphenacodontia (the clade containing sphenacodontids and therapsids). These relationships have been sustained by the introduction of computer

algorithms for phylogenetic analysis (Gauthier et al., 1988; Modesto, 1994; Berman et al., 1995; DeBraga and Rieppel, 1997; Reisz and Fröbisch, 2014).

Most recent phylogenetic analyses of pelycosaurian-grade synapsids have examined the relationships within clades. Varanopidae has been a particular focus, not only with the description of new taxa and specimens (Reisz and Dilkes, 2003; Anderson and Reisz, 2004; Maddin et al., 2006; Campione and Reisz, 2010; Modesto et al., 2011; Berman et al., 2014) but also the reassignment to this clade of several species previously thought to be diapsids or therapsids (Reisz et al., 1998; Reisz and Laurin, 2004; Reisz and Modesto, 2007; Reisz et al., 2010). Sphenacodontidae has also come under scrutiny (Reisz et al., 1992; Laurin, 1993; Kissel and Reisz, 2004; Fröbisch et al., 2011; Spindler et al., 2015), leading to the realisation that one of the subfamilies traditionally included within this clade, the Haptodontinae (Romer and Price, 1940), are in fact a paraphyletic grade outside Sphenacodontidae. Other analyses have examined the relationships within Ophicaodontidae (Berman et al., 1995), Caseidae (Maddin et al., 2008; Reisz and Fröbisch, 2014), and Edaphosauridae (Modesto, 1994; 1995; Mazierski and Reisz, 2010).

Recently, Benson (2012) reviewed the relationships of pelycosaurian-grade synapsids with a global phylogenetic analysis of 53 taxa. This analysis included evaluation of all characters from analyses published prior to that date, as well as the addition of new characters. Recognising that the majority of phylogenetic analyses thus far had been heavily biased towards the cranium, Benson (2012) added large numbers of new postcranial characters. The relationships obtained by this analysis did not recover the basal split between Caseasauria and Eupelycosauria. Instead, Caseasauria was found to be the sister to Sphenacomorpha, while Ophiacodontidae and Varanopidae formed a monophyletic grouping that was the sister to all other synapsids (Figure 7D). It was the postcranial characters which forced this set of relationships; when these characters are removed, Caseasauria is returned to a basal position. However, Benson (2012) acknowledged that the lack of information on the early evolution of both caseids and eothyridids was a problem. At that time, no postcranial information was available on either *Eothyris* or *Oedaleops*, and caseids earlier than the latter part of the Early Permian were unknown. The discovery of the Late Carboniferous caseid *Eocasea* provided fresh information on the postcranial anatomy of caseids early in their evolution (Reisz and Fröbisch, 2014) and re-analysis of Benson's matrix with *Eocasea* included found Caseasauria in their more "traditional" position as the sister to all other synapsid clades (Reisz and Fröbisch, 2014).

Expanding Phylogenetic Analysis of Pelycosaurian-grade Synapsids

Institutional Abbreviations

MCZ – Museum of Comparitive Zoology, Harvard.

FMNH – Field Museum of Natural History, Chicago

USNM – National Museum of Natural History, Washington DC

Many of the analyses undertaken in this thesis required an up-to-date and comprehensive phylogeny of pelycosaurian-grade synapsids. As such, the data matrix of Benson (2012) was expanded by the addition both of new material and new characters. The new material includes four previously described species as well as the postcranial material of *Oedaleops campi* (Sumida et al., 2014), unpublished at the time of Benson's original analysis. The four species newly added to the matrix are:

1: *Apsisaurus witteri* (MCZ 1474) includes a partial skull and lower jaw, a string of vertebrae from the posterior cervicals to the anterior caudals, several ribs and parts of both limbs. This specimen from Archer City Formation of Texas was first described as a diapsid by Laurin (1991), and so was not included in most subsequent phylogenetic analyses of pelycosaurian-grade synapsids. However, in more recent years, knowledge of basal synapsid morphology and relationships, in particular that of varanopids (Reisz and Dilkes, 2003; Anderson and Reisz, 2004; Maddin et al., 2006), has increased. With the benefit of this knowledge, Reisz et al. (2010) re-assigned *Apsisaurus* to Varanopidae, an assignment supported by a phylogenetic analysis including both varanopids and eureptiles. Reisz et al. (2010) noted that several of the previously considered synapomorphies of diapsids were in fact present in varanopids, such as the short quadratojugal. *Apsisaurus* did lack the recurved, laterally compressed teeth thought characteristic of varanopids, but the discovery of *Archaeovenator* (Reisz and Dilkes, 2003) showed that conical teeth are the primitive condition for varanopids. The presence of a tubercle on the jugal and similarities of the mandible to that of *Archaeovenator* confirmed the varanopid affinities of *Apsisaurus*. However, this specimen was not included in the global analysis of Benson (2012). Due to its importance as a basal member of the varanopids it was added to the analysis presented herein.

2: *Casea nicholsi* is a large caseid represented by two specimens (FMNH UR 85 and 86) from the late Kungurian Upper Vale Formation of Texas (Olson, 1954). The specimens

include partial vertebral columns, fragments of the skull roof, partial pelvic girdles, a forelimb, a pes, and a distal femur. The specimen was re-examined by Olson in his review of the family Caseidae (Olson, 1968), but has never been included in a phylogenetic analysis. Such an analysis is required to confirm the monophyly of the genus *Casea*. Four species were included in this genus in the review of Reisz (1986), but the analyses of Maddin et al. (2006) and Benson (2012) confirmed that "*Casea*" *rutena* did not form a monophyletic clade with the type, *Casea broilii*; this species has since been assigned to a new genus, *Euromycter* (Reisz et al., 2011). Further examination of this genus is required in order to produce reliable estimates of diversity. For this purpose, *Casea nicholsi* was included in the analysis presented here.

3: *Eocasea martini* is currently the earliest known caseid, represented by a fairly complete skeleton found in the Upper Pennsylvanian Hamilton Quarry (Reisz and Fröbisch, 2014). This is a crucial species for understanding the earliest evolution of caseids. Not only is it the earliest, and also the most basal member of the clade (Reisz and Fröbisch, 2014), but it is also not a medium-large sized herbivore, as are the other members of Caseidae. Instead, it is small, and was thought to be an insectivore (although unfortunately the sharp conical teeth were lost in preparation) (Reisz and Fröbisch, 2014). Moreover, a phylogenetic analysis presented in the supplementary materials of the description suggested that this specimen lacked many of the characters which Benson (2012) had used to unite Caseasauria with the clade containing Sphenacodontidae and Edaphosauridae, returning Caseasauria to their basal position within synapsids. It is necessary to examine this material alongside the eothyridid postcranial material now available in order to confirm or reject this hypothesis.

4: *Mycterosaurus smithae* was described very briefly in a catalogue of the vertebrate fauna found at the Placerville Localities of southwestern Colorado (Lewis and Vaughn, 1965). Two specimens were assigned to this species. The holotype MCZ 2985 (Figure 8) consisted of a partial skull, five vertebrae and ribs and a proximal femur and tibia, while the referred specimen USNM 22098 was a partial femur and a string of seven vertebrae. The type species of *Mycterosaurus*, *M. longiceps* (Williston, 1915), has been included in numerous cladistic analyses which have supported its assignment to the varanopid subfamily Mycterosaurinae (Maddin et al., 2006; Botha-Brink and Modesto, 2009; Campione and Reisz, 2010; Benson, 2012). However *Mycterosaurus smithae* has received comparatively little attention since its original description. In order to incorporate it into the phylogeny presented herein, the holotype underwent further preparation to reveal more details of its morphology. The new

material exposed, as well as the improved knowledge of basal synapsid anatomy since its original description, allowed the re-assignment of this species to Eothyrididae. This makes "*Mycterosaurus" smithae* an extremely important taxon. It is only the third known eothyridid species, and the second with postcranial material. It is also one of the earliest members of this family (see geological setting below), and as such can potentially provide a great deal of information on the earliest evolution of Caseasauria. The new information obtained from this specimen is presented here in a re-description of the type specimen, MCZ 2985.

Geological Setting

The Cutler Group spans the late Pennsylvanian and most of the Early Permian (Lucas, 2006), outcropping across New Mexico, Utah and Colorado. The Placerville Area, from which MCZ 2985 originates, is a locality where the sediments of the Cutler Group are exposed in the San Miguel Canyon (Lewis and Vaughn, 1964). Unfortunately, the biostratigraphy of the Cutler Group in Colorado is not so well established as in other areas. Lewis and Vaughn (1964) considered the localities to represent the upper portion of the Cutler Group, equivalent to the late Sakmarian-Artinskian aged Moran, Putnam and Admiral Formations (Lucas, 2006). However, they also drew comparisons with the Dunkard Group of Ohio. Most of the taxa from Placerville which are shared with the Dunkard Group are found in the lower layers of the latter: the lower Washington Formation (Lucas, 2013), implying an earlier age, possibly Asselian-Sakmarian. Baars (1962; 1974) also supported an earlier age of the Cutler Group in southwest Colorado, suggesting equivalence with the Halgaito Tongue and lower Supai Formation of Utah and lower Abo Formation of New Mexico. These formations are considered earliest Early Permian (Asselian-Sakmarian) or possibly latest Carboniferous in the case of the Halgaito Tongue (Lucas, 2006). Since MCZ 2985 was found in the uppermost 200ms of the section, an Asselian-Sakmarian age seems best supported.

List of Abbreviations in Figures

ac – anterior coronoid; an – angular; d – dentary; dv – dorsal vertebra; f – frontal; fe – femur; j – jugal; l – lacrimal; m – maxilla; p – parietal; pa – prearticular; pc – posterior coronoid; pf – postfrontal; ph – phalanx; pm – premaxilla; po – postorbital; prf – prefrontal; pt – pterygoid; qj – quadratojugal; sa – surangular; sp – splenial; sq – squamosal; st – supratemporal; ti – tibia; u – ulna.

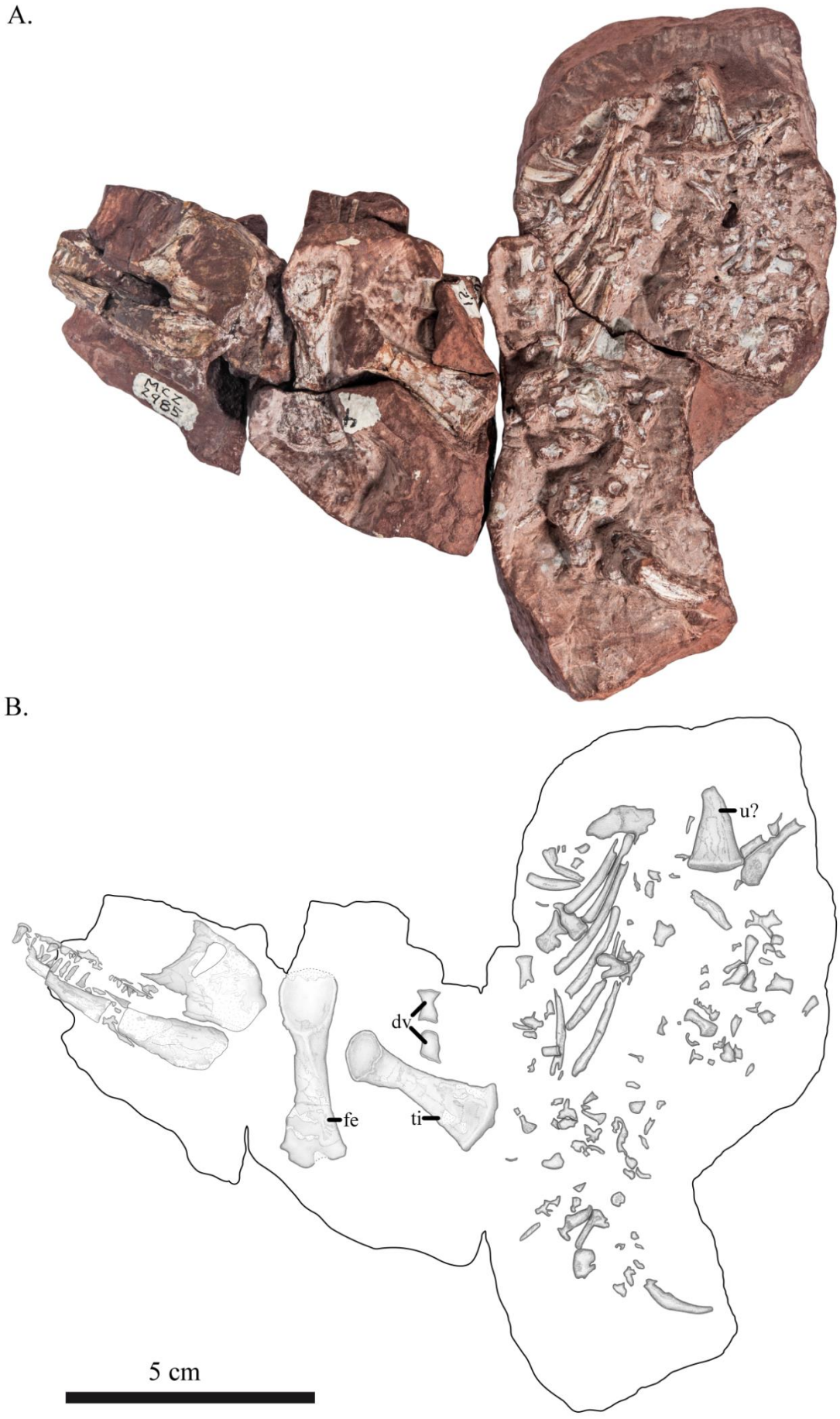

Figure 8: MCZ 2985, after preparation.

Systematic Palaeontology

Synapsida (Osborn, 1903)
Caseasauria (Wiliston, 1912)
Eothyrididae (Romer and Price, 1940)
"Mycterosaurus" smithae (Lewis and Vaughn, 1965)

Diagnosis: Distinguished from other members of Eothyrididae by the unusually small temporal fenestra and the large posttemporal region. Distinguished from other pelycosaurian-grade synapsids by the extension of the posterior ramus of the maxilla beyond the posterior margin of the temporal fenestra.

Holotype: MCZ 2985 (Museum of Comparative Zoology, University of Harvard), a partial skull; a string of six dorsal vertebrae; several ribs; a left femur and tibia; other fragments.

Locality and Horizon: Placerville Localities 11-13, San Miguel County, Colorado (38.0° N, 108.0° W). Cutler Group, Asselian-Sakmarian.

Description

The specimen MCZ 2985 consists of a previously articulated block bearing a skull and several postcranial fragments, including five vertebrae, ribs and a proximal femur and tibia (Figure 8). During the course of preparation, the skull has been separated from the block bearing postcranial material, and the postcranial block has been separated into multiple blocks in order to better expose the postcranial material, although these fragments still articulate.

Skull

The skull (Figures 9-11) is laterally compressed and slightly distorted, but preserved in three dimensions. The preservation quality of the skull roof makes defining sutures problematic. The sutures on the lateral sides of the skull are considerably clearer, particularly on the right (Figure 9). Most of the occiput and palate is not exposed. The orbit is relatively large, but the temporal fenestra is extremely small compared to other pelycosaurian-grade taxa, less than a quarter of the length of the orbit. Its dorsoventral height is greater than the anteroposterior length. The fenestra is oblong in shape, rather than being narrower ventrally

as in ophiacodontids or dorsally as in most other pelycosaurian-grade synapsids, including *Oedaleops*. Its shape is instead more similar to that of *Eothyris* and some mycterosaurine varanopids.

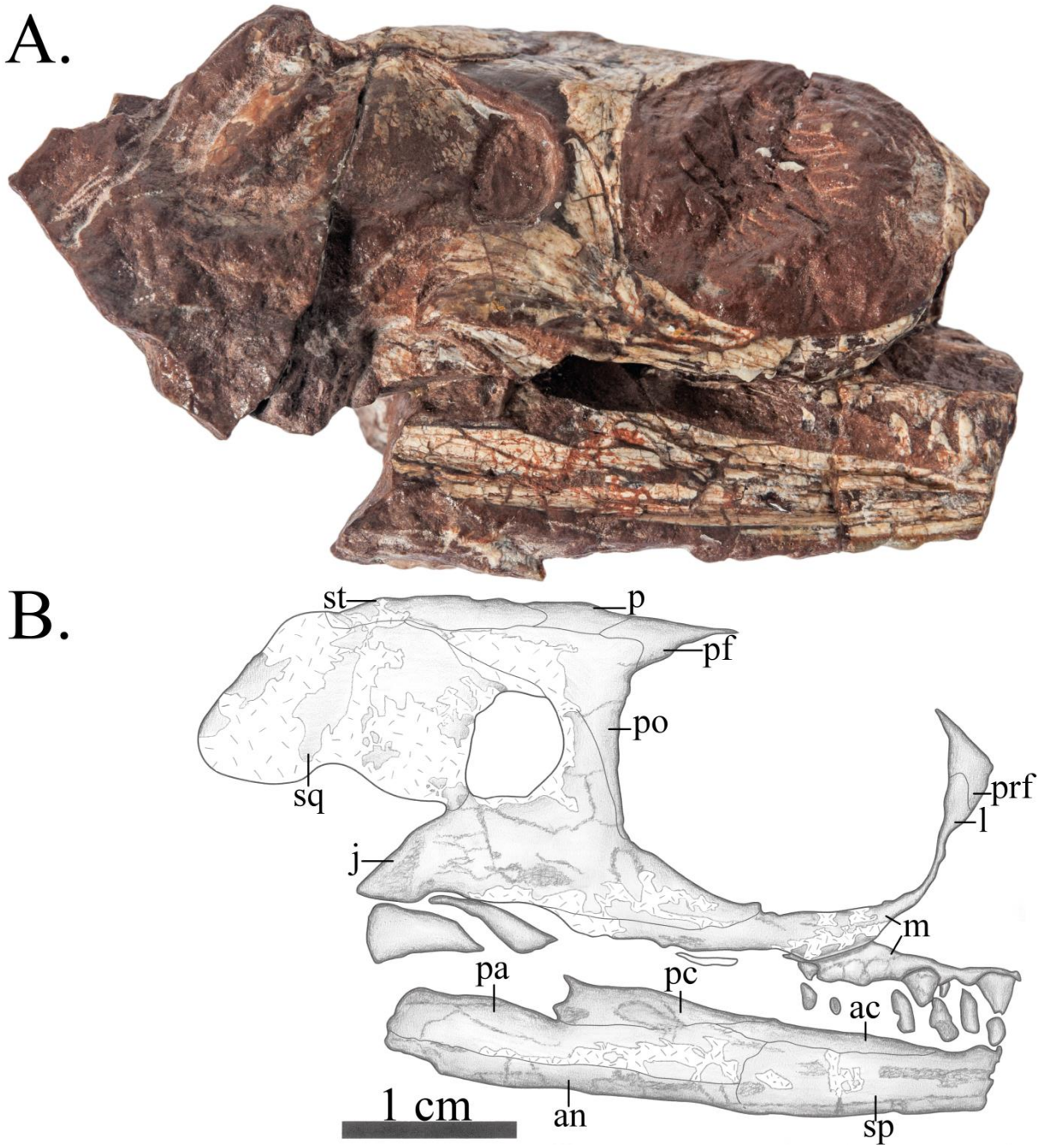

Figure 9: Skull and lower jaw of MCZ 2985 in right lateral view

The antorbital region is missing except for a separate fragment, representing a counterpart and preserving a part of the left maxilla and premaxilla with teeth as well an internal view of the tip of the right mandible (Figure 10).

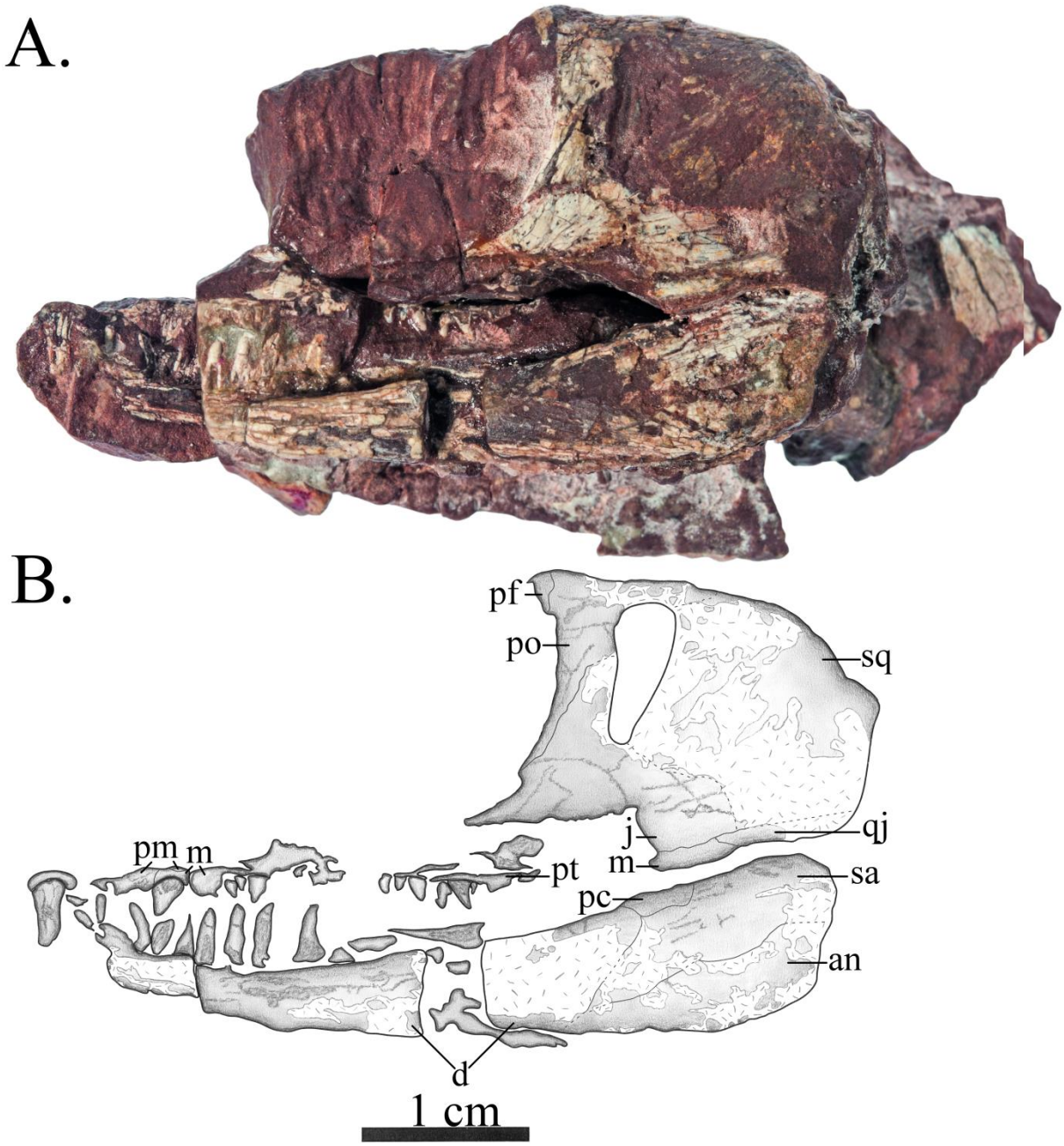

Figure 10: Skull and lower jaw of MCZ 2985 in left lateral view. The premaxilla, maxilla and tip of the dentary is a separate fragment articulating with the skull, and represents an internal view of the right upper and lower jaw fragments preserved on a counterpart.

Only a small part of the premaxilla is preserved in medial view on the small separate fragment, which fits as a counterpart and extends the anteriormost preserved part of the skull. Nothing can be said about the anatomy of the premaxilla, except for details about its teeth (see Dentition below). The septomaxillae and the nasals are not present.

The frontal is the anteriormost preserved element of the skull roof. Its anterior margin is not preserved, so it is impossible to ascertain its length. The bones around the dorsal margin of the orbits are damaged, so it is unclear whether there is a lateral lappet of the frontal

contacting the orbit. If there is one it would have to be extremely narrow, as seen in caseasaurs. The posterior process of the frontal is only visible on the right hand side. It is a short triangle of bone intruding between the parietal and the postfrontal but still leaving a substantial contact between the two, unlike in varanopids and ophiacodontids where the contact is limited.

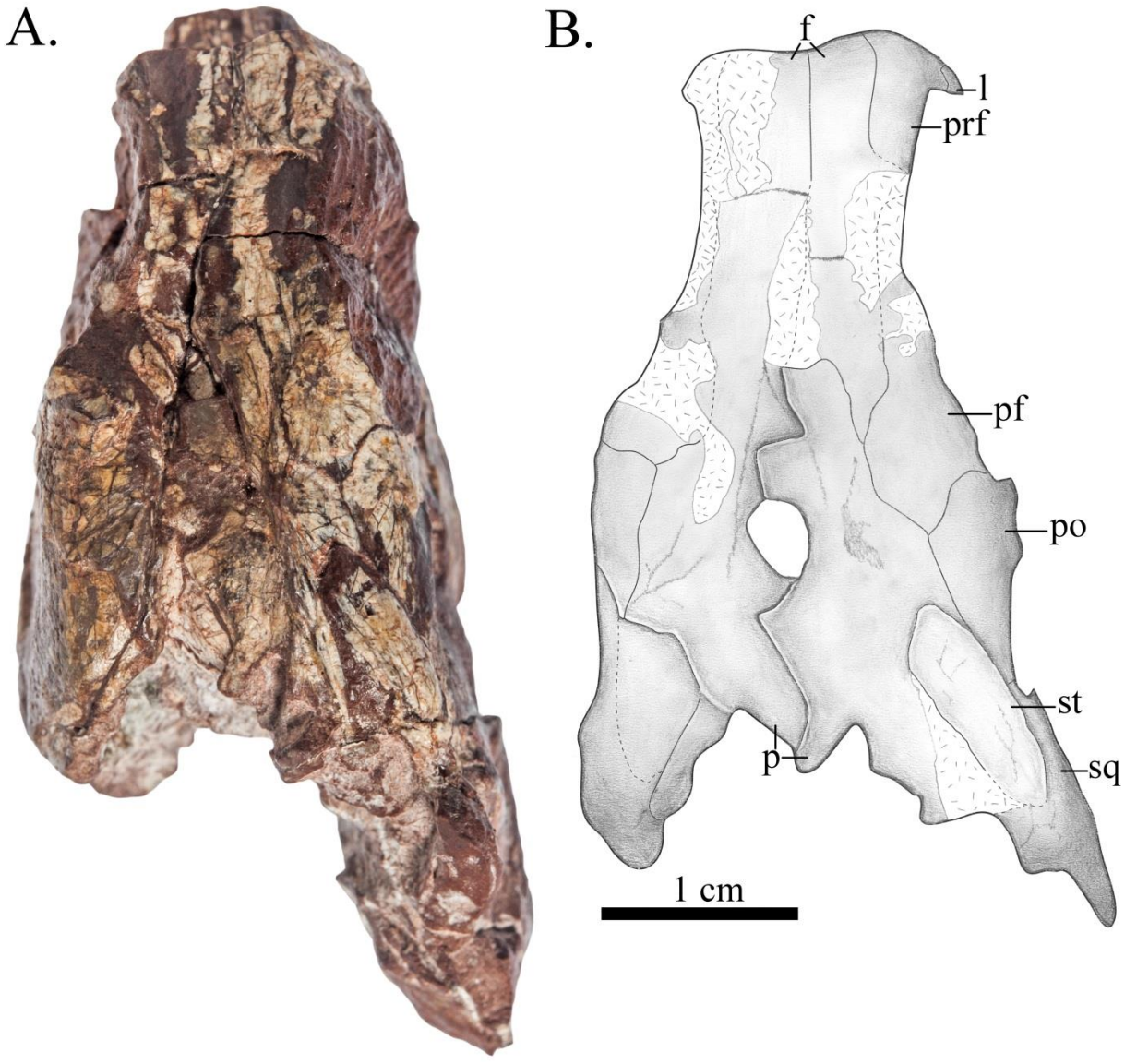

Figure 11: Skull of MCZ 2985 in dorsal view

The parietals have been displaced so that the posterior end of the right one overlies that of the left. Despite this, one can see that the pineal foramen is large and positioned at about midlength of the parietal, as in eothyridids.

The maxilla is only fragmentarily preserved, but better on the right than the left side. The posterior process of the maxilla is a narrow splint extending beyond the level of the temporal fenestra, and contributes to the lower orbital margin.

A fragment of the lacrimal is preserved at the anterior edge of the right orbit. A ventral process of the prefrontal incises the lacrimal and limits its contribution to the orbital margin in lateral view, a feature of eothyridids, sphenacodontids and some varanopids. A lacrimal foramen cannot be identified.

The lateral surface of the prefrontal is flat, lacking the concavity observed in sphenacodontids and ophiacodontids. In dorsal view the prefrontal has a long, narrow posterior process forming about a third of the upper margin of the orbit.

The postfrontal, best preserved on the right side, is a transversely narrow triangular element with a flat surface. It contacts the parietal posteriorly but is separated from it anteriorly by the posterior process of the frontal. The posterior margin of the postfrontal is incised by an anterior protrusion of the postorbital, a feature shared with *Eothyris* and sphenacodontids.

The postorbital is a robust element with a broad posterior process. It has a posterior contact with a squamosal, but this contact does not extend far back over the temporal region as in some sphenacodontids and mycterosaurine varanopids. The ventral process of the postorbital and the dorsal process of the jugal form a thick postorbital bar, similar to those of *Eothyris* and *Eocasea*.

The jugals are also robust elements: both the anterior and posterior rami are dorsoventrally thick. The anterior ramus is short, not reaching beyond the orbital midline, but the posterior ramus extends well beyond the posterior margin of the temporal fenestra reaching at least halfway along the posttemporal region (the erosion of the lateral surface of this region makes identifying the full extent impossible).

The supratemporal is preserved on the right, but eroded away on the left. It is a large element set in the parietal, more similar in proportions to that of caseasaurs than to the splint of bone seen in varanopids and sphenacodontids. It is oblong in shape.

The squamosal is broad, flat and has a lateral exposure similar to that seen in ophiacodontids: the length of the postemporal region is considerably greater than the breadth of the temporal fenestra. The temporal fenestra itself is bordered anteriorly by the jugal and dorsally by the postorbital and squamosal; there is no anterior process of the squamosal contacting the jugal dorsally.

On both sides of the skull a narrow splint of bone excludes the jugal from the ventral margin of the skull, formed from both the posterior process of the maxilla and the anterior process of the quadratojugal. The contribution of the quadratojugal to the exclusion of the jugal to the ventral margin of the skull, visible on the left side (Figure 11) is reduced relative to other caseasaurs, wherein the anterior ramus reached anteriorly beyond the temporal fenestra. *"Mycterosaurus" smithae* shows the condition found in mycterosaurine and varanodontine varanopids with the posterior ramus of the maxilla having the greatest contribution. In *"Mycterosaurus" smithae*, in fact, the posterior ramus of the maxilla extends further posteriorly than in any other pelycosaurian-grade synapsid, reaching beyond the posterior margin of the temporal fenestra.

The occipital and ventral sides of the skull of MCZ 2985 are almost entirely covered my matrix. However, a small portion of the pterygoid is exposed in left lateral view between the left maxilla and mandible. Not much can be said about the morphology of the pterygoid, but it bears a few teeth. Unfortunately not enough is exposed to say anything about their arrangement and distribution, although they are obviously large.

Mandible

Both left and right mandibles are preserved, the right as a counterpart showing the lingual sutures. The left mandible is preserved throughout most of its length, although the tip is missing. The counterpart of the right mandible is preserved throughout its entire length, although the tip is on the separate fragment also bearing the premaxilla. The mandible is a gracile element with slight curvature, narrowing distally. The coronoid eminence is only a slight prominence, positioned more posteriorly than that of *Eothyris*. It is formed laterally by the posterior coronoid.

The dentary is the largest element in lateral view, although it does not quite reach two thirds of the length of the mandible. The splenial does not appear to have lateral exposure seen in caseids, edaphosaurids and sphenacodontids. On the lingual surface, the splenial covers about half the length of the mandible, not reaching posteriorly enough to contact the posterior coronoid. The angular is visible in both labial and lingual views. On the lingual side it extends anteriorly about halfway along the length of the mandible. There is no keel on its ventral surface. The prearticular covers a similar length.

Dentition

One premaxillary tooth is preserved with space for two more behind it. This tooth is enlarged relative to the maxillary teeth, implying that it is the anteriormost tooth (this tooth is also enlarged in *Eothyris*).

Four maxillary teeth are preserved on each side of the skull. Two of those preserved on the right side are larger and more robust than the others. From their position (under the anterior margin of the orbit) it might be suggested that these represent the secondary caniniform region seen in *Eothyris* and *Oedaleops*. The maxillary teeth are conical, with no serrations and only slight recurvature.

Four teeth are preserved on the right dentary and two on the left. Some poorly preserved teeth are visible in the dentary tip on the separate fragment. These are identical in morphology to the maxillary teeth: conical and only slightly recurved. Those preserved are uniform in size.

Axial skeleton

Preparation has exposed a series of six dorsal vertebrae in dorsal view (Figure 12), three of which are mostly uninformative. Two of these vertebrae are also exposed ventrally (Figure 13). The vertebrae are plesiomorphic in anatomy, very similar to those described for *Oedaleops*. The ventral surface is rounded, without the keel present in varanopids and sphenacodontids, and no longitudinal troughs as in ophiacodontids. The neural spines have been slightly eroded dorsally so that no information is available on their exact height, but the bases indicate a blade-like morphology. The neural arches are again plesiomorphic, with no swelling or buttressing. The prezygapophyses show a flat morphology, without the concave surface seen in some caseids. The postzygapophyses are widely spaced with no hyposphene visible. The transverse processes are positioned far anteriorly on the vertebrae, a feature seen in some caseids and edaphosaurids. They are broad and flat and project slightly anteriorly; whether this is distortion or a feature of their morphology is unclear.

Fragments of at least 14 dorsal ribs are preserved on various postcranial blocks (Figures 14-15). The ribs are curved only proximally, in contrast to those of herbivorous pelycosaurian-grade synapsids, which are curved throughout their length to form a barrel-like chest. In proportions, however, they are very thick compared to the vertebrae, more similar to derived caseids than those of *Oedaleops* and *Eocasea*.

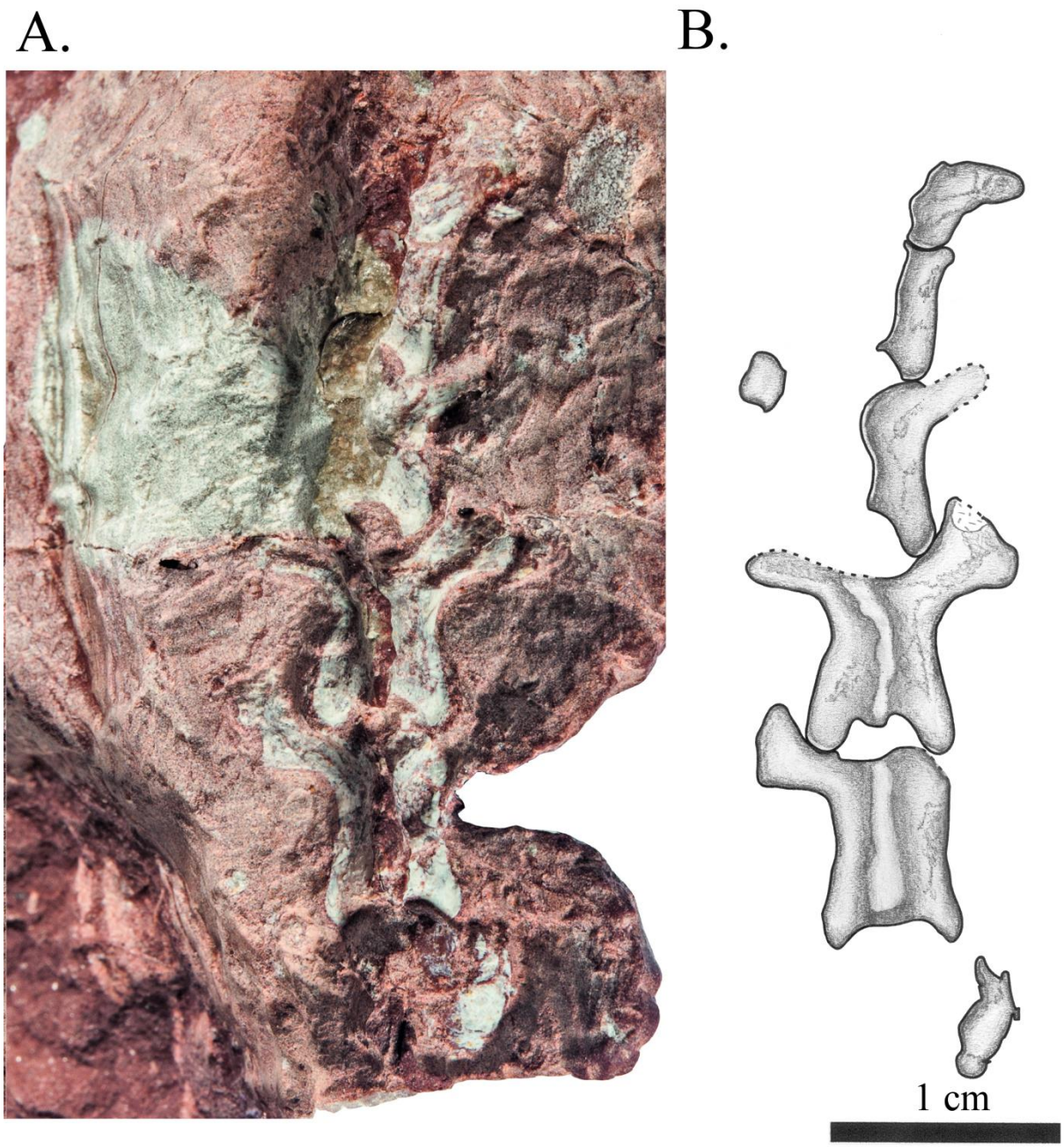

Figure 12: Dorsal vertebrae of MCZ 2985 in dorsal view.

Appendicular skeleton

Preparation has revealed the right femur fully in dorsal (Figure 14) and ventral (Figure 13) views. It is very plesiomorphic in its anatomy and agrees in most details with that of *Oedaleops*. However, the femoral shaft of MCZ 2985 is considerably more robust, the proportions being more similar to those of sphenacodontids. The head of the femur is short relative to its total length. The shaft is almost straight, and is oval rather than circular in cross section. The internal trochanter has been eroded away, but the prominent fourth trochanter is preserved. The internal fossa is enclosed posteriorly by a ventral ridge, the plesiomorphic

condition absent in caseids and *Dimetrodon*. A low longitudinal ridge extends proximodistally across the ventral surface of the femur. There is no longitudinal mound on the proximodorsal surface, a condition independently evolved in several clades, but unfortunately not visible in *Oedaleops*. The distal end of the femur is damaged, so less information can be derived. The condyles are separated with virtually no difference in distal expansion, as in *Oedaleops* and *Eocasea* but unlike in more derived caseids. Also similar to *Oedaleops* and *Eocasea* but different to more derived caseids is the lack of compression of the anterior condyle. The dorsal surface of the posterior condyle is not concave as in some varanopids.

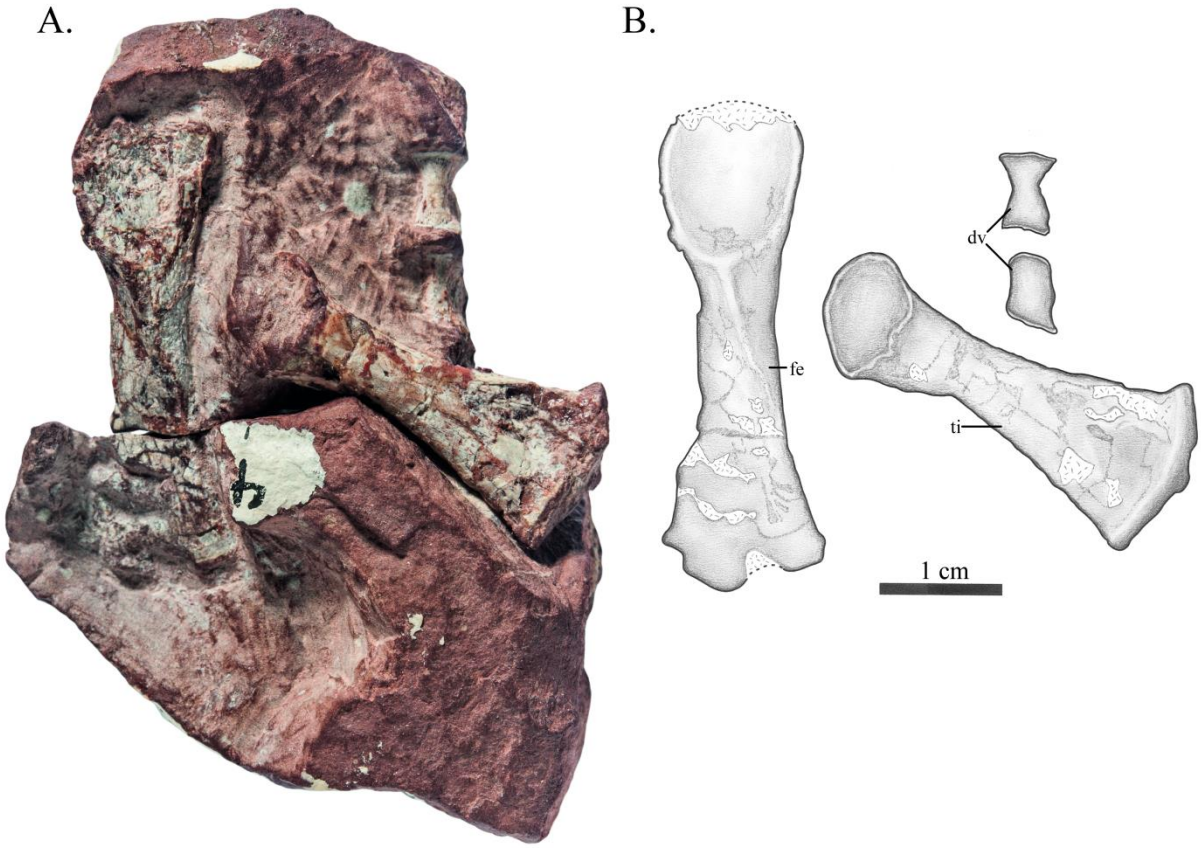

Figure 13: Postcranial material of MCZ 2985, including two dorsal vertebrae, left femur and left tibia, all in ventral view

The right tibia has been exposed completely in ventral view (Figure 13), whereas only the proximal part is visible in dorsal view (Figure 14A). Like the femur, its morphology is very similar to *Oedaleops* in its characteristics. It is almost straight with a low ridge along the ventral surface and a prominent cnemial crest. However, again, the proportions of the tibia of *"Mycterosaurus" smithae* are different to that of *Oedaleops* in that it is shorter but considerably thicker throughout.

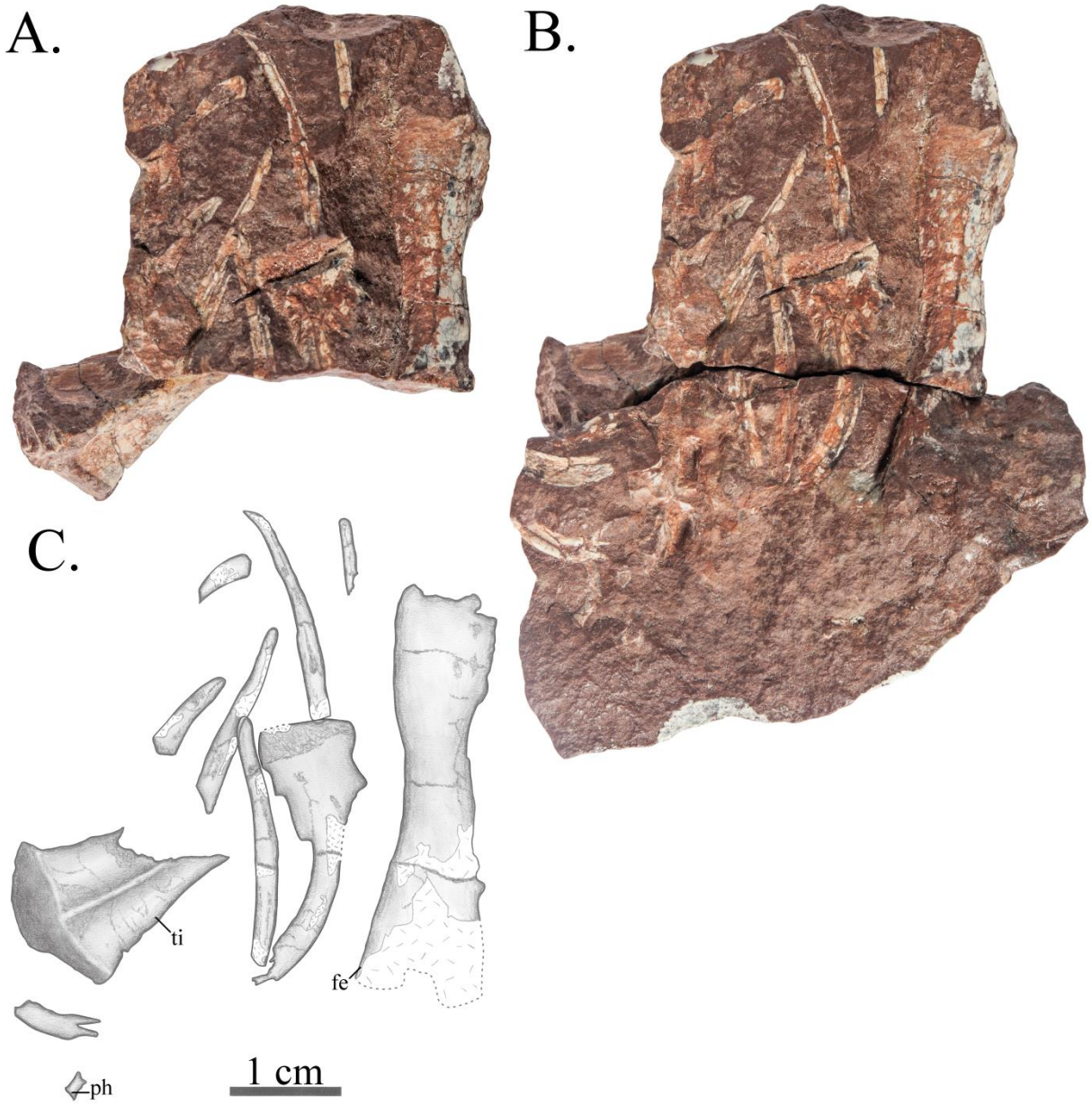

Figure 14: Two articulating rock fragments bearing postcranial material of MCZ 2985, including a left femur and tibia in dorsal view, a phalanx of unclear origin and rib fragments. A) The first of these fragments, fully exposing the proximal part of the left tibia in dorsal view; B) The two fragments in articulation, covering part of the proximal part of the tibia but showing the almost complete right femur in dorsal view; C) drawing incorporating information from both of these views.

Another element is preserved which could be the distal end of the ulna or fibula; it is a flattened concave fragment of bone with part of a cylindrical shaft visible (Figure 15).

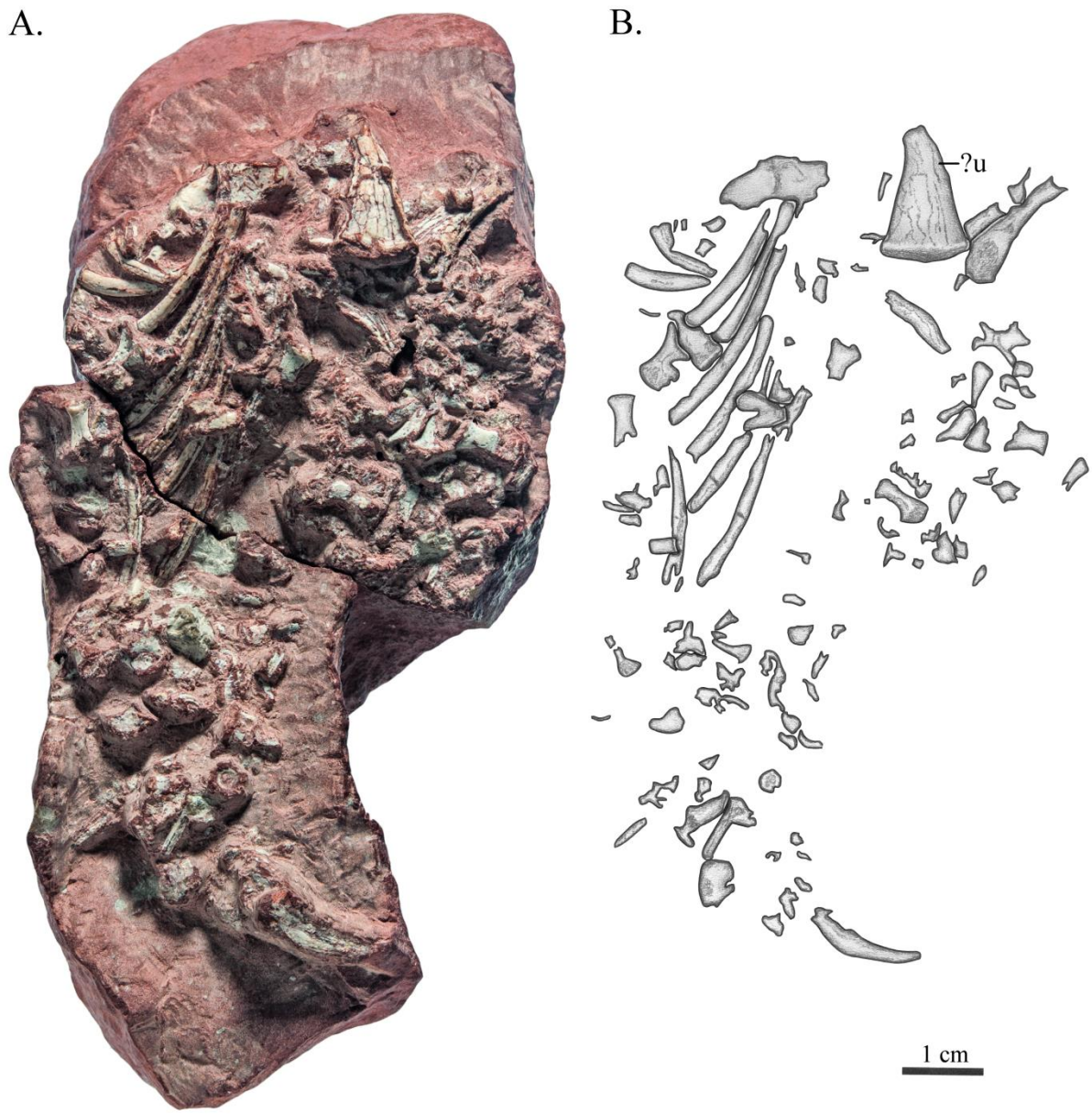

Figure 15: Block with postcranial material of MCZ 2985, including ribs and possible distal ulna

Eothyridid Affinities of MCZ 2985

Since its original description, the type specimen of *"Mycterosaurus" smithae* has received only limited attention in the literature. Berman and Reisz (1982), in their re-descriptopn of *M. longiceps*, tentatively kept this species assigned to the genus *Mycterosaurus* within Varanopidae, though noting that no characters of either were visible. Reisz (1986), in his thorough review of pelycosaurian-grade synapsid species undertaken for the Handbook of Paleoherpetology, also noted the lack of varanopid synapomorphies in *"Mycterosaurus" smithae*, and suggested the assignment should be considered provisional.

This detailed re-examination of MCZ 2985 and new features revealed in preparation allow the rejection of an affinity with *Mycterosaurus*, Mycterosaurinae and Varanopidae. *"Mycterosaurus" smithae* has a ventral ridge system on the femur, the lack of which was considered an autapomorphy of *Mycterosaurus* (Berman and Reisz, 1982). Most unambiguous varanopid and mycterosaurine synapomorphies that could be compared reject a varanopid affinity for MCZ 2985: the femur is not slender, the teeth are not serrated and there is no lateral boss on the postorbital. The long posterior ramus of the jugal is a feature of Mycterosaurinae, but this is a variable character within pelycosaurian-grade synapsids and is also present in eothyridids. Other characters that *"Mycterosaurus" smithae* shares with varanopids are those that are extremely variable within basal synapsids, such as the short anterior process of the jugal (also seen in caseasaurs) and the reduced lacrimal contribution to the orbital margin (also in eothyridids and sphenacodontids).

The large supratemporal is set in the parietal and in contact with the postorbital, supporting the assignment of *"Mycterosaurus" smithae* to Caseasauria, the clade containing the families Caseidae and Eothyrididae. Further evidence includes the short dentary relative to the rest of the lower jaw and the large size of the pineal foramen. An affinity with Eothyrididae is suggested based on the reduced contribution of the lacrimal to the orbital margin, the extension of the posterior ramus of the jugal beyond the temporal fenestra and the position of the pineal foramen midway along the midline of the parietal. Eothyrididae thus far contains only two other species of small carnivorous basal synapsids: *Eothyris parkeyi* and *Oedaleops campi*. Of the two, *"Mycterosaurus" smithae* is most similar to *Eothyris*, sharing with this species the thick postorbital bar, the incision of the postfrontal by the postorbital and the small temporal fenestra with an oblong rather than trapezoid or triangular shape. The separate fragment bearing the dentary tip, premaxilla and maxilla indicate a large overbite, another similarity with *Eothyris*.

It is unlikely that *Eothyris parkeyi* and *"Mycterosaurus" smithae* represent two specimens of the same species; *"Mycterosaurus" smithae* has a shorter posterior process of the postorbital, a more posteriorly placed coronoid eminence, a smaller temporal fenestra and a greatly expanded lateral surface of the squamosal (more similar in extent to Ophiacodontidae). There could, meanwhile, be justification for assigning them to the same genus. *"Mycterosaurus" smithae* shares with *Eothyris* the contribution of the maxilla to the margin of the orbit, a character Reisz et al. (2009) considered definitive of *Eothyris*. However, this is an extremely variable character, also seen in some derived caseids and varanopids. Other autapomorphies of *Eothyris* could not be compared with the less complete skull of

"Mycterosaurus" smithae. Therefore, in this study it is considered more conservative to regard them as separate genera, implying the need for a new generic name for *"Mycterosaurus" smithae*, which will be given elsewhere.

Eothyrididae is widely considered to consist of small, agile carnivores or insectivores (Romer and Price 1940, Langston 1965, Benton 2005, Reisz et al. 2009). The recent description of new material of *Oedaleops campi* (Sumida et al., 2014), including the first postcranium, supports this ecological hypothesis, illustrating generalised tooth structure, long gracile limbs and ribs with only proximal curvature unlike those of herbivorous caseids. The lower dentition of *"Mycterosaurus" smithae* is of the same conical shape, with little recurvature and no visible serrations, possibly indicating a similar diet. Unfortunately very little information is available on the upper dentition; the robust caniniform teeth seen in *Oedaleops* and *Eothyris* are not preserved, and the presence of a secondary caniniform region cannot be confirmed with certainty. An important difference between *Oedaleops* and *"Mycterosaurus" smithae* is in the robusticity of the limbs and the skull; although *Oedaleops* has a longer femur and tibia, those of *"Mycterosaurus" smithae* are considerably broader, both at the distal ends and at the mid-shaft. The postorbital and subtemporal bars are also thicker than their equivalents in *Oedaleops*. It appears that *"Mycterosaurus" smithae* may not have led the lifestyle of an agile insectivore that is inferred for *Oedaleops*, but may have been a more robust carnivore. Alternatively, it is possible that the differences in proportions were ontogenetic; the small size and large orbit of *"Mycterosaurus" smithae* could indicate a young individual. However the state of ossification of the limb bones suggests otherwise; all condyles and trochanters of the femur and the cnemial crest of the tibia are well ossified. Alternative explanations must be sought for the unusual morphology of *"Mycterosaurus" smithae*. It is clear from this specimen that there was a greater morphological diversity and potentially greater ecological diversity within eothyridids than has previously been suspected.

Comparison with USNM 22098

USNM 22098 is another specimen found at Placerville, although much lower in the section than MCZ 2985, the holotype of *"Mycterosaurus" smithae* (Lewis and Vaughn, 1965). This specimen consists of seven poorly preserved dorsal vertebrae, a proximal right femur and shaft, and other rather undiagnostic fragments. Lewis and Vaughn (1965) concluded that this was a second specimen of *"Mycterosaurus" smithae*, although they acknowledged that the preservation was too poor to properly compare it with the type. Their

justification for assigning the two specimens to the same species was the similar size of the vertebrae and the occurrence in the same formation and area. They also favourably compared the proportions of the femur of USNM 22098 with that of "*Mycterosaurus" longiceps*.
The additional preparation of MCZ 2985 in the framework of this study has revealed a complete femur, permitting comparison between these two specimens. Based on this it is clear that they cannot be assigned to the same species. The femur of "*Mycterosaurus*" *smithae* is considerably more robust, with a much thicker shaft than that of USNM 22098. Moreover, the femoral head of USNM 22098 is proportionately much longer relative to its width than that of "*Mycterosaurus*" *smithae*. The gracile nature of the USNM 22098 femur hints at a varanopid affinity, although the preservation and current state of preparation of this specimen prevent reliable assignment. Unfortunately no diagnostic characters are visible on the vertebrae.

Phylogenetic Analysis

The four species noted above, as well as the postcranial material of *Oedaleops campi* were added to the matrix of Benson (2012). Also added were two extra characters. The first of these represents the shape of the temporal fenestra and has three character states: 0 – temporal fenestra is narrower dorsally than ventrally; 1 – temporal fenestra is narrower ventrally than dorsally; 2 – temporal fenestra is oblong, dorsal and ventral margins are of similar length. While most pelycosaurian-grade synapsids have a temporal fenestra narrower dorsally than ventrally, the eothyridids *Eothyris parkeyi* and *"Mycterosaurus"* smithae both share an oblong temporal fenestra, with a dorsal margin of a similar length to the ventral margin. This feature is also seen in the varanopids *Mycterosaurus longiceps* and *Mesenosaurus romeri*. Meanwhile, the ventrally narrow temporal fenestra has been noted for the members of Ophiacodontidae which preserve skulls (Romer and Price, 1940; Berman, 1995). The second character added refers to the webbing under the transverse processes of the vertebrae, and also has three character states: 0 – Webbing absent; 1 – webbing slight, does not extend further ventrally than the tip of the transverse process; 3 – webbing extensive, reaches ventrally beyond the transverse process. This character was introduced in the hope of resolving the relationships of *Echinerpeton intermedium*, which was found to be a wildcard taxon in the analysis of Benson (2012), but shares the extensive webbing with some members of Ophiacodontidae. The character scores of these new characters for all taxa, the character scores for the new specimens added to the matrix, and details of all changes made to the codings of Benson (2012), are available in Appendix A.

The matrix was analysed with parsimony in the Willi Hennig Society edition of TNT version 1.1 (Goloboff et al., 2008). The new technology driven search at level 100 was used, incorporating the drift, sectorial search and fusion algorithms. The minimum tree length was searched for 100 times. *Limnoscelis* was set as the outgroup. 756 most parsimonious trees (MPTs) were identified, with a length of 759, a retention index of 0.74 and a consistency index of 0.43. Support values for individual nodes were calculated using bootstrap resampling (10,000 replicates) and relative fit difference (Goloboff and Farris, 2001), again calculated in TNT.

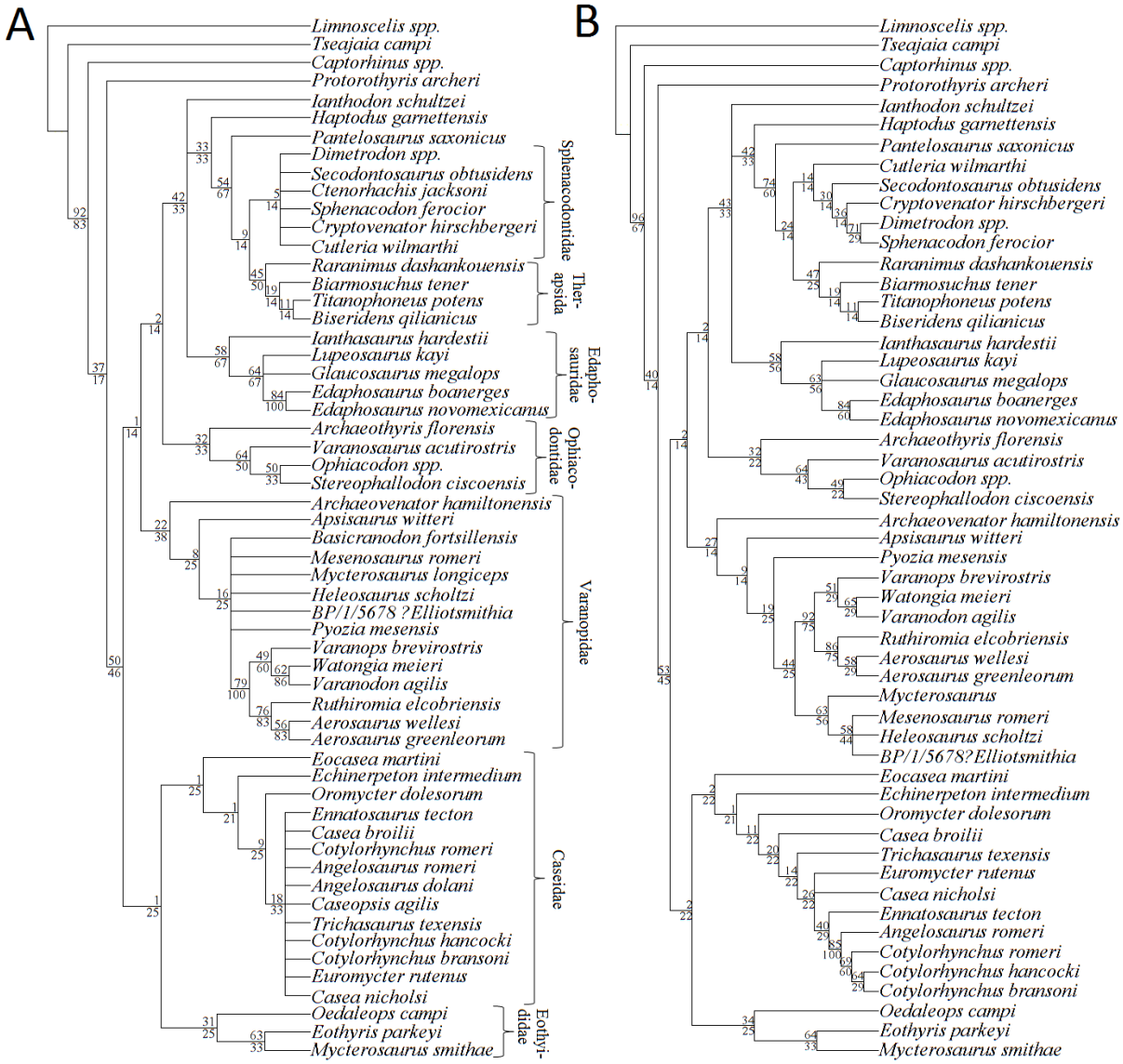

Figure 16: Strict consensus phylogenies produced by parsimony analyses A) All taxa included; B) The wildcard taxa *Angelosaurus dolani, Caseopsis agilis, Ctenorhachis jacksoni* and *Basicranodon fortsillensis* excluded.

In all most parsimonious trees (Figure 16A), *"Mycterosaurus" smithae* was found to be the sister to *Eothyris parkeyi*, with *Oedaleops campi* the sister to these two eothyridids. The monophyly of Eothyrididae is fairly poorly supported, but the sister-taxon relationship between *"Mycterosaurus" smithae* and *Eothyris* receives better support. The position of *Eocasea* as the basalmost caseid and that of *Apsisaurus* as a basal varanopid were confirmed. *"Casea" nicholsi* was not found to form a monophyletic grouping with *Casea broilii*, but was instead found in a polytomy with *Euromycter rutenus* and the clade containing *Ennatosaurus*, *Cotylorhynchus* and *Angelosaurus*. Relationships elsewhere in the phylogeny were identical to those found in the original analysis by Benson (2012), with two exceptions. In the original analysis *Echinerpeton intermedium* was found in three equally parsimonious positions: as basalmost synapsid, as ophiacodontid and as sister taxon to a clade containing caseasaurs, edaphosaurids and sphenacodontians. In this analysis it is found to be a caseid. This position has never before been suggested in previous examinations of this taxon (Reisz, 1972; Reisz, 1986; Benson 2012), and is only supported here by three characters: the short anteroposterior length of the dorsal centra, the lack of recurvature of the teeth, and the flattened medial surface of the ilium. Both the monophyly of and the relationships within Caseidae are extremely poorly supported, particularly near the base where *Echinerpeton* is found.

The second difference between the results presented here and those found by Benson (2012) is the position of Caseasauria (the clade containing Eothyrididae and Caseidae). Since the review of Reisz (1986), caseasaurs have been considered the sister clade to all other synapsids (the Eupelycosauria), a position based primarily on cranial characters. Benson (2012) introduced a larger number of postcranial characters into the analysis and found caseasaurs to be more derived, as sister group to Sphenacomorpha. However, Benson (2012) did note the lack of postcranial material available for eothyridids, and predicted that the discovery of such material could return caseasaurs to their position as sister to all other synapsids.

After the modifications to the original matrix presented here, the prediction of Benson is borne out. As argued by Reisz and Fröbisch (2014), it is here suggested that the result observed by Benson (2012) was due to the lack at the time of postcranial material of eothyridids and of a well-preserved basal caseid, provided by *Eocasea*. Many of the characters that were put forward by Benson (2012) as synapomorphies of a clade containing Caseasauria, Edaphosauridae and Sphenacodontia are found to be absent in *Eocasea* and the new eothyridid material (Table 1). However, once again the monophyly of Eupelycosauria is extremely poorly supported both by bootstrapping and relative fit.

Characters used by Benson to unite Caseasauria, Edaphosauridae and Sphenacodontia	New information from *Eocasea*, *Oedaleops* and *"Mycterosaurus" smithae*
Character 92, state 1 – presence of a prominent lateral process of supraoccipital	Absent in *Eocasea*
Character 131, state 1 – coronoid eminence formed laterally by the dentary	Formed laterally by the coronoid in *Eocasea* and *"Mycterosaurus" smithae*
Character 158, state 1 – dorsal transverse processes extend far laterally	Not seen in *Eocasea* or *"Mycterosaurus" smithae*
Character 172, state 1 – three or more sacral vertebrae	Only two in *Eocasea*
Character 173, state 1 – first sacral rib of similar size to posterior sacral ribs	First sacral rib much broader in *Eocasea*
Character 191, state 1 – posterior margin of interclavicle head grades gradually into the shaft	Interclavicle head emarginated posterolaterally in *Oedaleops*
Character 215, state 0 – medial surface of ilium flat or weakly concave	Prominent ridge is present in *Eocasea*
Character 233, state 0 – anterior condyle of femur dorsoventrally compressed	Condyle is thick in *Eocasea*, *Oedaleops* and *"Mycterosaurus" smithae*
Character 239, state 1 – Calcaneum length conspicuously greater than width	Length approximately equal to width in *Eocasea*

Table 1: Nine characters used by Benson (2012) to support the relationship between Caseasauria, Edaphosauridae and Sphenacodontia, and the new information on these characters provided by *Eocasea*, *Oedaleops* and *"Mycterosaurus" smithae*.

Lack of resolution within the strict consensus cladogram is found within Caseidae, Sphenacodontidae and Varanopidae. The iterative reduced positional congruence method (Pol and Escapa, 2009), implemented in TNT, was used to identify the four wildcard taxa: *Caseopsis agilis*, *Basicranodon fortsillensis*, *Ctenorhachis jacksoni* and *Angelosaurus dolani*. After pruning these taxa, four MPTs remained (Figure 16B). These four wildcard taxa were subjected to the analyses proposed by Pol and Escapa (2009) to ascertain the reason for their lack of stability: inability to score potentially relevant characters due to the incompleteness of the fossils, or conflicting characters. The ancestral condition of unscored characters in the unstable taxa was examined in each MPT; if the optimisation of an unscored character is different in different MPTs, then the missing information in this character could have

provided greater resolution. Meanwhile, scored characters may be examined by comparing the length of the character when the score for the unstable taxon is replaced by a missing entry. If the change in length differs between different MPTs, this character is supporting conflicting positions for that taxon. These analyses were carried out in TNT.

Wildcard Taxon	Unscored characters which could better resolve its position	Characters supporting conflicting topologies
Caseopsis agilis	1, 2, 5, 9, 23, 24, 25, 29, 34, 57, 73, 85, 92, 93, 98, 101, 110, 111, 115, 119, 122, 126, 129, 131, 139, 142, 148, 151, 157, 158, 159, 160, 161, 162, 166, 172, 173, 176, 179, 182, 187, 189, 190, 191, 193, 194, 195, 197, 198, 201, 205, 206, 208, 209, 210, 213, 238, 239 **(Total = 58)**	171, 233
Basicranodon fortsillensis	4, 17, 22, 25, 29, 30, 32, 34, 36, 40, 41, 42, 43, 51, 52, 53, 65, 67, 69, 75, 81, 84, 87, 92, 114, 119, 132, 152, 153, 156, 164, 198, 199, 207, 217, 219, 224, 227, 228, 234, 187, 189, 190, 191, 193, 194, 195, 197, 198, 201, 205, 206, 208, 209, 210, 213, 238, 239 **(Total = 40)**	None
Ctenorhachis jacksoni	2, 7, 8, 17, 18, 19, 22, 27, 28, 32, 33, 35, 43, 51, 56, 58, 59, 63, 65, 66, 68, 69, 75, 85, 98, 104, 106, 123, 125, 126, 127, 131, 135, 136, 138, 140, 151, 152, 162, 180, 185, 187, 200, 202, 230, 194, 195, 197, 198, 201, 205, 206, 208, 209, 210, 213, 238, 239 **(Total = 40)**	None
Angelosaurus dolani	25, 29, 44, 102, 110, 148, 171, 176, 182, 189, 205 **(Total = 11)**	None

Table 2: Characters with missing scores which could provide better resolution in the wildcard taxa, and characters supporting conflicting topologies in the wildcard taxa.

It was found that missing data is mostly responsible for the instability of the wildcard taxa (Table 2). In *Basicranodon*, *Angelosaurus dolani* and *Ctenorhachis*, no character conflict was found, while multiple unscored characters were found to be potentially relevant missing entries (40 characters for *Basicranodon*, 11 for *A. dolani* and 40 for *Ctenorhachis*. Two

scored characters in *Caseopsis* were found to support conflicting topologies, but 58 unscored characters were found to be important missing data. The character conflict in *Caseopsis* is between character 171 and 233. The cup-like articular facet of the dorsal rib tuberculum of *Caseopsis* (Character 171, state 2) is characteristic of the caseid clade containing the genera *Angelosaurus* and *Cotylorhynchus*. However, the anterior condyle of the femur of *Caseopsis* is not compressed (character 233, state 0), which supports a more basal position within Caseidae; all caseids more derived than *Casea* have a compressed anterior condyle.

Due to the poorly supported relationships and lack of resolution provided by parsimony analysis, alternative methods were used to assess phylogenetic relationships in order to compare the results. The first was Bayesian analysis, a model based approach that has been widely used in analyses of molecular data as it can incorporate information on the probabilities of different mutations (Lanave et al., 1984; Tavaré, 1986). Its use in analyses of morphology is controversial (Spencer and Wilberg, 2013), but some morphological systematists have suggested its use should be preferred over parsimony (Lee and Worthy, 2010; Wright and Hillis, 2014). One reason cited is that Bayesian analysis, which takes into account branch lengths, is less affected by issues such as long-branch attraction (Felsenstein, 1978); longer branches are more likely to convergently evolve characters and therefore cluster together under parsimony.

The second alternative method used was an implied weights analysis (Goloboff, 1993). This method is a modification of maximum parsimony: after a single round of tree searches, characters found to be homoplasies are downweighted for a subsequent round of searches. Again, the use of this method has been controversial, mainly due to a sentiment that the weighting of characters is unparsimonious (Kluge, 1997 a; b; 2005; Källersjö et al., 1999). Nevertheless, it has been shown that using such weighting schemes produces better supported relationships (Goloboff et al., 2008).

The Bayesian analysis was carried out in MrBayes version 3.2.2 (Ronquist et al., 2012) using the Markov model (Lewis, 2001) with a gamma distributed rate parameter. Two analyses were carried out: the first with the same matrix used in the parsimony analysis, and the second including 109 autapomorphous characters; since Bayesian analysis takes into account branch lengths, autapomorphies are necessary information (Müller and Reisz, 2006). The autapomorphies are available in Appendix B. For both analyses a majority rule consensus was constructed from the probability distribution of trees. The Implied Weights analysis was undertaken in TNT, using the same settings as in the parsimony analysis. Homoplasious

characters were downweighted with a concavity constant of 3.0. 18 most parsimonious trees were found by the implied weights analysis (Figure 17B).

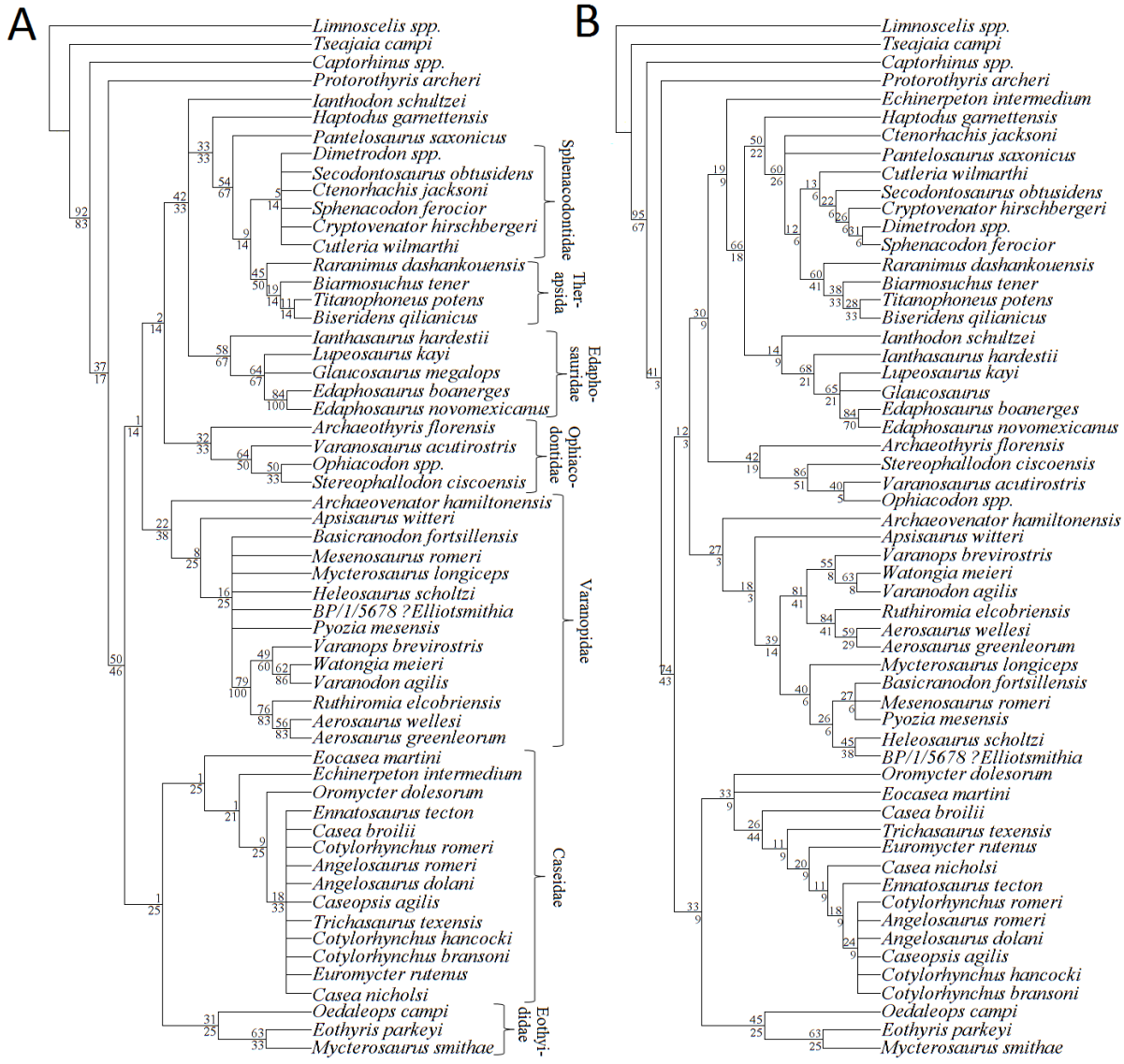

Figure 17: Comparison of the results of the phylogenetic analysis using A) Parsimony, and B) Implied Weights.

The implied weights and Bayesian analyses (Figures 17-18) show broadly similar results to the parsimony analysis. The biggest difference is that in both *Echinerpeton* is found to be the sister taxon to the clade containing Edaphosauridae and Sphenacodontia rather than as a caseid, a position supported by the increased number of precanine maxillary teeth, the elongation of neural spines and the flattened medial surface of the ilium. The support values for the phylogeny produced by implied weights analysis are higher than those found in the parsimony analysis, although still low. The clade credibility values found in the Bayesian analyses are considerably higher, with most being over 80% and many being over 90%.

The positions of the wildcard taxa are better resolved in both the implied weights and Bayesian analyses; *Basicranodon* is found to be a mycterosaurine varanopid, *Caseopsis* is resolved within the clade containing *Cotylorhynchus* and *Angelosaurus*, and *Ctenorhachis* is found in a basal position within Sphenacodontidae. However, in some areas resolution is worsened. The relationships of basal varanopids are not so well resolved in both Bayesian analyses. Moreover, when autapomorphies are not included in the Bayesian analysis, the monophyly of Eothyrididae could also not be resolved; *Oedaleops* is found in a polytomy with Caseidae and the clade containing *Eothyris* and *"Mycterosaurus" smithae*.

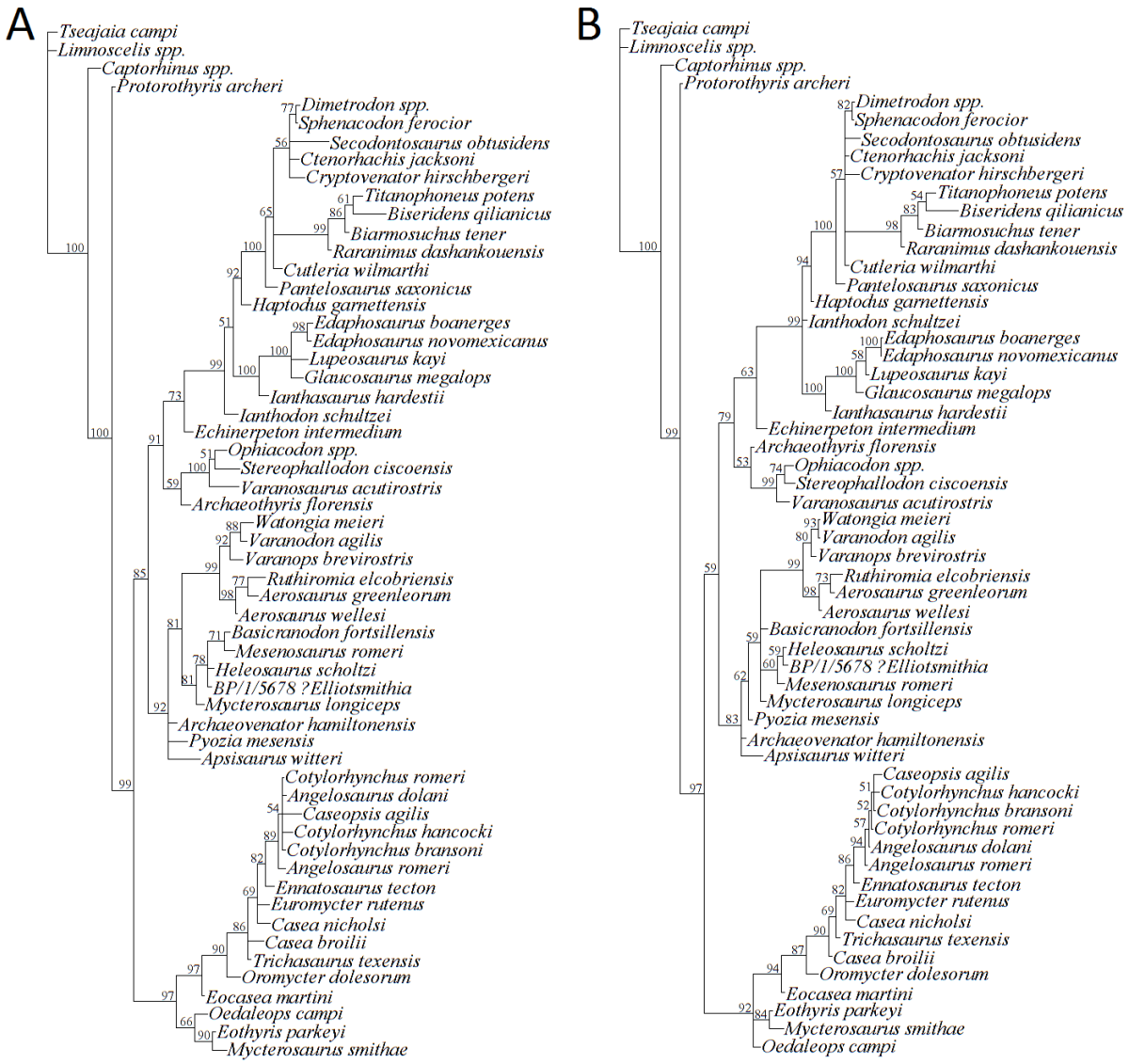

Figure 18: Phylogenies produced by the Bayesian analyses. Numbers at nodes represent clade credibility values. A) Autapomorphies included; B) Autapomorphies not included.

While these analyses and comparisons provide much to consider in future phylogenetic examinations of pelycosaurian-grade synapsids, it is encouraging that, with the exception of the placement of *Echinerpeton*, the relationships obtained with the different methods are remarkably stable. The eothyridid affinity of *"Mycterosaurus" smithae* is consistent in all analyses. However, low resolution and poor support for relationships within caseasaurs are also consistent. Considerably more work is needed before firm conclusions may be drawn about caseasaurian relationships. It is regrettable that the lack of resolution in the parsimony analyses is due to missing data rather than conflicting characters. The issue of conflicting characters may be resolved by the addition of more characters or species to provide further information on character polarities. There is unfortunately little that can be done to resolve the issue of incomplete data, at least until more specimens are found. However, the increased resolution provided by the implied weights and Bayesian analyses provide working hypotheses which may be kept in mind during future examinations of these taxa.

Chapter 3

Data

Database

A comprehensive database of synapsid taxa, both pelycosaurian-grade and therapsid, from their earliest occurrence in the late Westphalian of Nova Scotia (Reisz 1972) until the latest occurrence of pelycosaurian-grade taxa named to species level from the *Tapinocephalus* Assemblage Zone of South Africa (Dilkes and Reisz, 1996; Reisz and Modesto, 2007; Botha-Brink and Modesto, 2009), was assembled for this study. This list was scrutinised for synonyms and nomina dubia. *Protoclepsydrops haplous* (Carroll, 1964), from earlier in time but of dubious synapsid affinity (Reisz, 1986), was not included. The youngest record of pelycosaurian-grade synapsids, a varanopid from the middle Permian *Pristerognathus* Assemblage Zone of South Africa (Modesto et al., 2011) was excluded, as this specimen is only identifiable to subfamily level. The database may be regarded as complete until April 2014, and is available in Appendix C, indicating the age range of the species and the country of origin. The time scale was obtained by splitting the international stages into two equal substages (early and late), which were used as time bins. The boundary between each substage was set as the middle of the international stage. The timescale used was that of Gradstein et al. (2012). The time interval under study stretched from the late Moscovian until the late Capitanian.

If a taxon's age could not be constrained, it was included in the full range of possible time bins. While this method does lead to less resolution i.e. certain taxa known from a single specimen or locality will be found in more than one time bin, it has been demonstrated that, as long as the stratigraphic uncertainties are randomly distributed, the diversity signal will not be false, but merely "dampened" (peaks and troughs become less extreme) (Raup, 1991; Smith, 2001). This is preferable over attempting to provide resolution to the data and potentially crating a false signal. In order to assess the impact of stratigraphic uncertainty, a more resolved dataset was created, in which each locality is constrained to no more than two substages.

As part of the analysis into the completeness of the fossil record of pelycosaurian-grade synapsids, further data was added to the taxonomic entries in this database. A list of all specimens recorded in the published literature was created and details of these specimens, including number and material preserved, were added. The data from the published literature was supplemented by personal observations in museum collections. This database includes details of the locality from which each specimen is known and may be found in Appendix D.

Supertree

A Review of Supertree Methods and Uses

Although macroevolutionary studies require phylogenies to be as inclusive as possible, such phylogenies are not always available. Workers very rarely include all known species in a phylogenetic analysis, either because poor specimens lead to a lack of resolution, because they do not feel a species is relevant to the study they are undertaking, or in some cases simply because a specimen was not available for study at the time of their analysis. Continual updating of molecular phylogenetic analyses is easier, since sequence data may be constantly added to databases such as Genbank. Morphological characters, on the other hand, are subject to constant revision and disagreement. The practical difficulties of examining first-hand the necessary specimens limit the possible scope of morphological analyses. At the moment of writing, the largest trees produced using morphological data are limited to 192 taxa (Gauthier et al., 2014) and 4541 characters (O'Leary et al., 2013). Palaeozoic synapsids provide an excellent example of the dearth of comprehensive phylogenies. The vast majority of phylogenetic analyses focus on a single family or clade. There are not analyses that include large samples of taxa from both pelycosaurian-grade and therapsid synapsids; even the more comprehensive studies focus on one or the other (Liu et al., 2009a; Cisneros et al., 2011; Benson, 2012). As a result, in order to elucidate the evolutionary history of a clade, one must attempt to combine these hypotheses. Some workers have created composite trees by simply 'grafting' trees together and adding missing species in their preferred position, and have used these trees in studies of macroevolutionary patterns (e.g. Laurin, 2004; Ruta et al., 2011). However, such methods of tree building are highly subjective, and the author feels that they should not be used in quantitative macroevolutionary analyses.

Supertree and supermatrix methods allow one to combine phylogenetic hypotheses into a more quantitative way. These are two very different concepts. Supermatrix methods use the primary character data; data matrices from the phylogenetic hypotheses are combined into one supermatrix with taxa coded as missing for all characters in the matrices in which they are not present. The supermatrix may be analysed using parsimony, as in morphological analyses.

Supertree methods instead use the tree topologies rather than the characters as the source data, with a variety of methods available for combining these topologies. If all trees are compatible, with no conflict suggested, the procedure is simple: a 'backbone' tree may be constructed from the shared taxa, and then each branch of the backbone tree may be compared

to corresponding branches in the source trees to ascertain if any taxa unique to any source tree should be added. Steel (1992) has provided an algorithm suitable for this task. More usually, some phylogenetic hypotheses will conflict, and more complex methods are needed to reconcile them. The earliest suggested, and most commonly used, is 'Matrix Representation with Parsimony' (MRP), independently proposed by Baum (1992) and Regan (1992). This method combines source trees in such a way that no tree has the power of veto over another; where conflict occurs, the most commonly occurring topology will be chosen, or a polytomy will be formed from the conflicting taxa. The method (Figure 19) constructs a matrix in which characters refer to the nodes within source trees rather than morphology. Each node on each source tree is represented by one character. Each taxon descended from that node is scored '1'. Taxa present in the source tree but not descended from that node are scored '0'. Taxa not present in that particular source tree are scored '?'. The resulting matrix may be analysed using parsimony, rooted on a hypothetical outgroup taxon with all 'characters' scored as '0'.

A

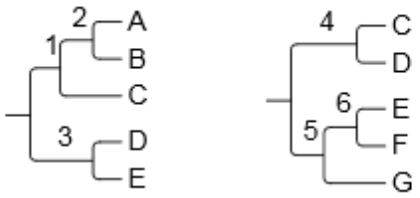

B

	1	2	3	4	5	6
Outgroup	0	0	0	0	0	0
A	1	1	0	?	?	?
B	1	1	0	?	?	?
C	1	0	0	1	0	0
D	0	0	1	1	0	0
E	0	0	1	0	1	1
F	?	?	?	0	1	1
G	?	?	?	0	1	0

C

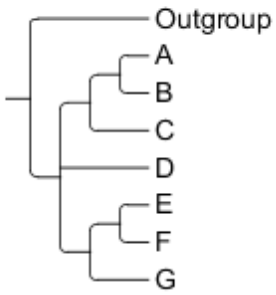

Figure 19: A hypothetical example illustrating the Matrix Representation with Parsimony method. A) Two source trees with nodes numbered. Conflict is present regarding the position of taxon D. B) The MRP matrix representing the presence or absence of each taxon within each node. C) The supertree produced from the MRP matrix.

Purvis (1995) suggested a modification to the Baum and Ragan method. He pointed out that their method is biased in favour of the topologies of larger source trees, since these trees will contain more nodes and therefore be represented by more characters, a bias later confirmed in simulations (Beninda-Emonds and Bryant, 1998). The modification suggested was to base the coding on sister group relationships rather than inclusion within clades. In the Purvis method, each node is again represented by a character, and taxa descended from that node are scored '1'. However, it is only the sister taxa to that node which are scored '0'. All other taxa, whether included in the source tree or not, are scored '?'. The performance of the Purvis method compared to the Baum and Ragan method has been examined (Purvis and Webster, 1998), using primates as an example. It was found that of 160 resolved nodes obtained using the Purvis method, only 12 conflicted with the tree produced using the Baum and Ragan method (Purvis and Webster 1998). The Baum and Ragan tree was also better resolved (Purvis and Webster, 1998). It was suggested that greater conflict between the source trees would lead to greater conflict between the two methods (Purvis and Webster, 1998).

The Purvis method has been criticised in that it fails to weight the source trees equally, since larger trees now contribute more missing data (Ronquist, 1996), but a further criticism is warranted. The reasoning behind the modification suggested by Purvis (1995) was that the Baum and Ragan method provides greater weight to larger source trees. However, it could be argued that it is right that this should occur. More inclusive phylogenetic analyses are more reliable (Gauthier et al., 1988; Pollock et al., 2002; Zwickl and Hillis, 2002; Conrad, 2008) since the addition of more taxa can provide information on the polarity of characters and will thus affect tree topology. As such, the additional weight given towards larger trees in the Baum and Ragan method is providing additional weight towards more reliable trees. In any case, the bias appears to be minimal (Beninda-Emonds et al., 2002). Another criticism against MRP was put forward by Wilkinson et al. (2001; 2005a), who analysed tree-shape related biases and found MRP would favour topologies suggested by an unbalanced tree. Moreover, it has been demonstrated that unsupported clades, not suggested by any of the input source trees, can be recovered by the MRP method (Beninda-Emonds and Bryant, 1998). This is obviously undesirable; the supertree is supposed to summarise existing hypotheses, not suggest new relationships. However, such clades are extremely rare (Beninda-Emonds and Bryant, 1998; Pisani et al., 2002; Beninda-Emonds, 2003).

Other methods have been proposed to produce supertrees. The BUILD algorithm (similar to the Adam's consensus) organises taxa into clusters, excluding each cluster's outgroup taxa one at a time (Aho et al., 1981). This method often produces more resolution,

but at the cost of ignoring certain possible relationship combinations (Beninda-Emonds et al., 2002). It is also not able to include incompatible source trees. The MinCut algorithm (Semple and Steel, 2000) expanded on this method, allowing incompatible trees to be included. When clusters cannot be separated due to conflicting source trees, the minimum number of branches needed to create an agreed outgroup are removed. The MinFlip method (Chen et al., 2003) uses a similar matrix representation method to MRP, but resolves conflict by 'flipping' matrix cells from 0 to 1 or 1 to 0. The supertree with the minimum number of flips necessary is selected. MRP has a large advantage over these methods, in that it has been extensively tested with regard to various biases and potential methodological problems. There are also practical advantages: it is simple, computationally easy and there are a large number of computer programs capable of performing the analysis quickly.

Some workers (e.g. Gatesy et al., 2002; Gatesy et al., 2004; Gatesy and Springer, 2004) have criticised the use of supertrees over supermatrices as they are removed from the primary data i.e. the morphological or molecular character list. These authors have suggested that using the character data in a supermatrix is more reliable than using the trees themselves as a source. Gatesy et al. (2004) also argued that the supermatrix may produce novel clades, supported by 'hidden character support'; two sets of characters on their own may indicate two different relationships, but together they may favour one or the other, or even suggest entirely new relationships. However, supermatrix methods do have their drawbacks. Firstly, supermatrices contain a large amount of missing data, which can lead to poorly resolved phylogenies (Beninda-Emonds, 2004). While one should most certainly not choose a method purely because it provides more resolution, taxa that have been included in only one phylogenetic analysis may become 'wildcard taxa', even if the original analysis was able to constrain their position. This problem is exacerbated if fewer taxa are shared between analyses (Sanderson et al., 1998). Simulations have shown that supertree methods can produce no less accurate representations of the source trees than supermatrix methods (Beninda-Edmonds and Sanderson, 2001; Chen et al., 2003; Levasseur and Lapointe, 2003; Piaggio-Talice et al., 2004). Supermatrix methods are also computationally demanding and time consuming. A further issue with supermatrix methods mentioned by Beninda-Emonds (2004) is that data of different sorts e.g. molecular and morphological, cannot be combined. This concern is irrelevant to this particular study, limited to morphological data as it is, but is still worth noting. For these reasons, supertree methods have been used in this study.

There are a number of supertree analyses that have included phylogenies based on fossils. Some have been used to investigate the topologies recovered when source trees are

combined (Pisani et al., 2002; Ruta et al., 2003; Bronzati et al., 2012). Others have also been produced to compare methods of supertree formation or to compare supertree methods to supermatrix methods (Gatesy et al., 2004; Lefebvre, 2005; Hone and Benton, 2008). More recently they have been applied to analytical palaeontology: supertrees have been used by Marjanović and Laurin (2007) to investigate the fit of fossils to stratigraphy and molecular clock dates, by Ruta et al. (2007) and Lloyd et al. (2008) to investigate shifts in rates of diversification, and by Ruta et al. (2008; 2011) to create phylogenetic diversity estimates.

Supertree Generation

The results of phylogenetic analysis of pelycosaurian-grade synapsids produced in the previous chapter were not entirely satisfactory for the further analyses intended for this thesis. Since the different analyses found *Echinerpeton* to be in greatly different positions, one cannot use the consensus of all trees produced in subsequent analyses; the lack of resolution would greatly affect the results. Moreover, the analyses of diversity through time requires phylogenies not only of pelycosaurian-grade synapsids, but also of therapsids in order to compare the diversity curves. Currently a combined phylogeny of pelycosaurian-grade and therapsid synapsids does not exist, and such an analysis is beyond the scope of this study. In order to alleviate these issues a supertree of all synapsids from their first appearance in the late Moscovian until the end of the Capitanian (the last appearance of all named pelycosaurian-grade synapsids) was generated using MRP. All hypotheses of phylogenetic relationships published before April 2014, produced using computer algorithms, rather than manually generated, and containing three or more taxa from the time period under study were considered as source trees. The phylogenies produced in Chapter 2 were also included.

In order that the supertree input data was "accountable" (a concern raised by Gatesy et al., 2002), publications that did not include full details of their method e.g. not including a character matrix, details of algorithms or outgroups used, were rejected. In order to reduce instances of tree non-independence (another issue raised by Gatesy et al., 2002; including many trees based on the same character list would bias the supertree towards topologies suggested by those characters) the following procedure was followed (modified from Beninda-Emonds et al., 2004): (1) if one study uses a character list and a taxon list that is identical to or a subset of another analysis, then only the more inclusive study was included as a source tree; (2) if one study uses a character list which is identical to, or a subset of, another analysis, but the taxon lists are not identical nor is one a subset of the other, then a mini

supertree (using the MRP method) was constructed from the two or more trees. This mini supertree was included as a source tree; (3) if a study uses different methods to analyse the same dataset e.g. analysing the dataset using both parsimony and Bayesian methods, a mini-supertree was constructed from the results of each analysis to be used as a source tree.

After pruning the list of published phylogenetic analyses in this way, 29 phylogenetic hypotheses and four mini supertrees remained (Appendix E). These trees then needed to be standardised with respect to the taxonomic level. Different phylogenetic analyses study phylogeny at different levels: the family, genus or species level. This is a problem when combining trees, and has in the past led to a supertree with, for example, Lepidosauromorpha, Squamata and two rhynchocephalian species included as terminal taxa (Hone and Benton, 2008) despite the fact that squamates and rhynchocephalians are contained within Lepidosauromorpha. The following procedures were carried out to standardise the level of the source trees: (1) If a taxon is not studied at species level in any included analysis, then it is included at the genus level in all source trees e.g., *Sphenacodon* spp. (2) If the paper specifies that their coding for a higher level taxon above the level of species is based primarily on a particular species, then that species is used to replace the higher-level taxon in the source tree. (3) If a taxon is included at the genus level or higher in one or more studies, and one or more different studies use more than one different species of that taxon, then a single representative of the higher taxon is chosen to replace it (the type if possible) e.g. if Ophiacodontidae is used as a terminal taxon in a source tree, it is replaced in this analysis with *Ophiacodon mirus*. The taxon specified as the outgroup in the original analyses were removed, as their position is assumed rather than tested. The MRP matrix was generated from the source trees using the program Supertree0.85b (Salamin et al., 2002). The Baum and Regan method was applied. All trees and nodes within trees were given equal weight. The matrix was input into the Willi Hennig Society edition of TNT (Goloboff et al., 2008). A new technology search was applied, using the tree fusing, drift and sectorial search algorithms.

Time Calibration

Time calibration of a phylogeny can be a complex issue with many potential problems. For example, if a taxon is only known from a single occurrence and its sister taxon is younger, the younger taxon will have a ghost lineage extended only as far back as the older. The length of the branch representing the older taxon will be zero e.g. taxa V and W in Figure 20C. This would imply instantaneous character evolution from the states of the common

ancestor to those of the older taxon. Zero-length branches may also imply instantaneous speciation events; if three taxa X, Y and Z (Z being the oldest), have relationships (X,(Y,Z)), then the ghost lineages of X and Y will only be extended as far back as Z (Figure 20C). This would imply that the cladogenic event splitting X and (Y,Z), and the cladogenic event splitting Y and Z, occurred simultaneously. These implications of zero-length branches are unrealistic, and will affect analyses of diversification and morphological evolution.

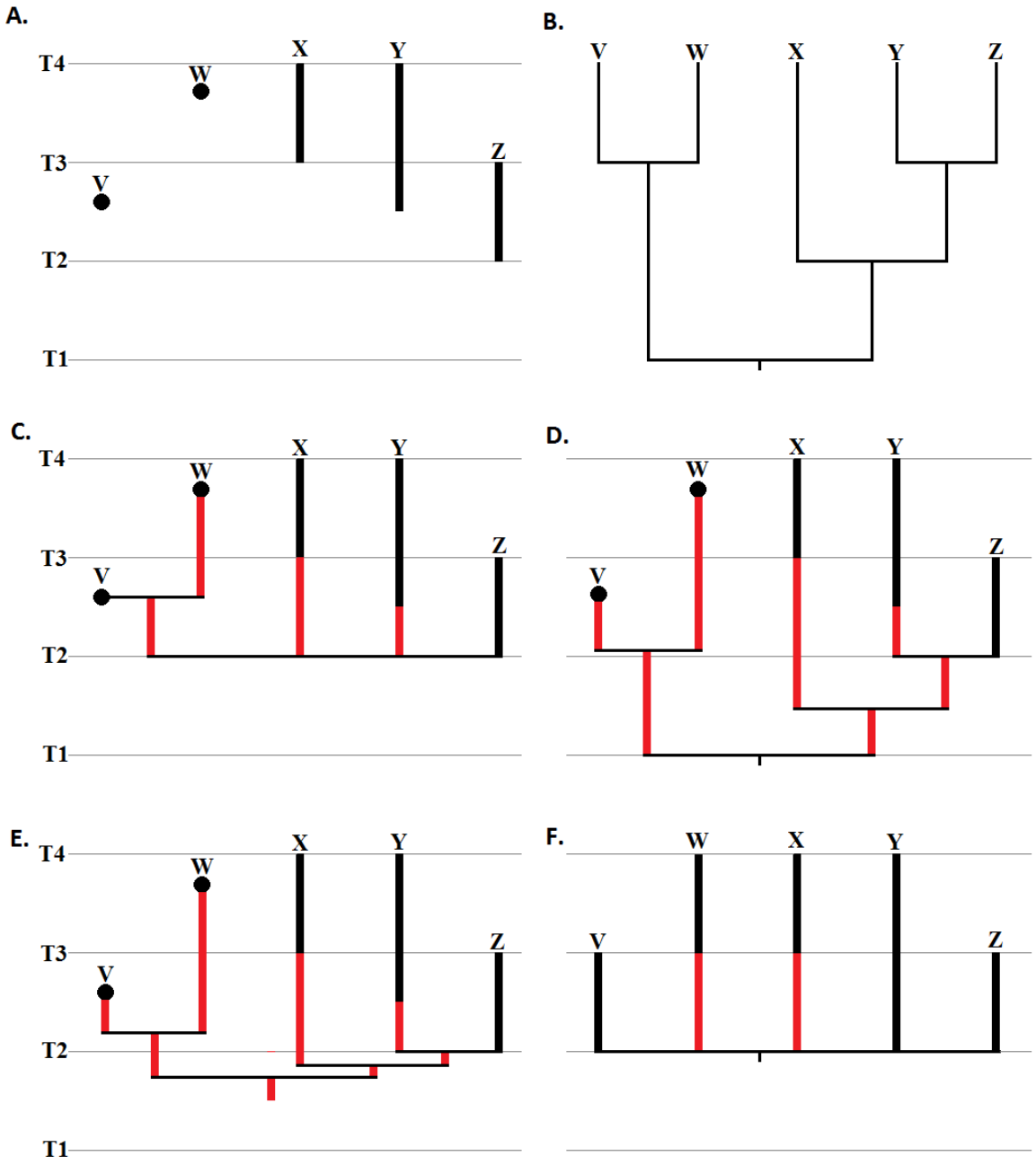

Figure 20: Time calibration of phylogenies using different methods. A) The observed fossil record of five taxa. Black dots indicate single occurrences, black lines indicate ranges. B) The uncalibrated phylogeny of the five taxa. C) The most basic time calibration of the phylogeny, with no correction for zero-length branches. Ghost lineages in red. D) Time calibration of the phylogeny, with a minimum branch length of T0.5 enforced, as in Laurin (2004). E) Time calibration of the phylogeny using the branch-sharing method of Brusatte et al. (2008). F) Time calibration using the method proposed herein.

A variety of methods exist to eliminate these zero-length branches. The majority involve selecting an arbitrary length of time, and adding this to all branches (Ruta et al., 2011) or to zero-length branches only (Hunt and Carrano, 2010), or extending the length of branches until all reach an arbitrary minimum length (Laurin, 2004), the latter illustrated in Figure 20D. These methods suffer from being highly subjective, with the results of phylogeny-based analyses depending greatly on the length of time selected. Two less arbitrary methods have been proposed. Both involve extending zero-length branches back in time along the non-zero-length branch immediately ancestral to them, sharing this ancestral branch's length among the zero-length branches descended from it. The zero-length branches may be shared equally among the ancestral branch (Brusatte et al., 2008) as illustrated in Figure 20E or, if a morphological character matrix exists, adjusting branch lengths to represent the proportion of morphological change occurring along each branch (Ruta et al., 2006). While these methods are more objective, they do make assumptions: Brusatte et al.'s method assumes equal speciation rate, while Ruta et al.'s method assumes equal rates of morphological change. Since this thesis is investigating patterns of diversification and species richness, employing a method that biases towards equal rates of speciation is circular and inappropriate. Ruta et al.'s method is more appropriate (its bias towards equal rates of character change is irrelevant to the analyses herein) but since it is a supertree being analysed, there is no matrix of morphological characters to deduce character evolution along any branch.

In this study, a new method of time calibration is used, working on the assumption that the majority of speciation and extinction occurs at the boundaries between the geological time intervals, an assumption that is both supported by previous studies (Foote, 1994; Alroy et al., 2008; Alroy, 2010a) and intuitive (the geological timescale is based on biostratigraphy). The range of each terminal taxon is extended to include the entirety of any substage in which it has been found (Figure 20F), concentrating speciation and extinction events at the boundaries between substages. The zero-length branches are regarded as zero-length; adding values, whether arbitrarily determined or not, will push the origination rates away from the boundaries. Instead it is assumed that the length of time between the speciation events concentrated at the boundaries between substages is short enough to become negligible. This produces similar results to the basic time calibration shown in Figure 20C, but one important difference is that the hypothetical ancestors of nodes implied by the phylogeny (ghost taxa) are never present in the same time bin as their descendants. Under the basic time calibration method these would be counted as separate taxa in a phylogenetic diversity estimate, pushing the in-bin diversity higher than the maximum standing-diversity (the diversity counted from

the record at a single point in time rather than in the whole bin). For example in Figure 20C, the most recent common ancestor of V and W would be counted as an additional taxon in the same time bin as X and the ghost lineage of W. Under the new time calibration method presented here, ghost taxa are only counted in time bins not shared with their descendants (Figure 20F), and so in-bin diversity is never pushed above maximum standing diversity.

Relationships suggested by the Supertree

It should be emphasised that the supertree does not incorporate any new information, and the raw data are previously-proposed phylogenetic relationships rather than characters. As such the supertree should not suggest any relationships that have not been previously suggested. However, the relationships of basal synapsids are still not fully resolved, and conflicting topologies have been produced in cladistic analysis. The selection of a particular topology by the supertree can provide insights into the characteristics of the method used. It is worth examining some of the relationships produced by the supertree analysis.

Caseasauria

As discussed in Chapter 2, since the review by Reisz (1986), Synapsida has been thought to be split into two clades: Caseasauria (Eothyrididae and Caseidae) and Eupelycosauria. This relationship was supported by the cladistic analyses that examined phylogenetic relationships between amniote clades (e.g. Gauthier et al. 1988, Hill 2005), although these analyses were characterised by poor within-clade sampling. Phylogenetic analyses of pelycosaurian-grade synapsid clades have used caseasaurs as outgroups, assuming rather than testing a basal position (e.g. Modesto, 1994; Berman et al., 1995; Reisz et al., 1998; Modesto et al., 2001; Anderson and Reisz, 2004; Maddin et al., 2006; Maddin et al., 2008; Botha-Brink and Modesto, 2009; Reisz et al., 2009; Campione and Reisz, 2010).

The first global analysis by Benson (2012) in fact challenged the basal position of Caseasauria. In this analysis, Caseasauria were found to be the sister to the clade containing Edaphosauridae and Sphenacodontia, while Ophiacodontidae and Varanopidae formed a clade, which was the sister taxon to all other synapsids. These relationships are supported by the fact that Ophiacodontidae are the earliest clade to appear in the fossil record (Reisz, 1972) while Caseasauria does not appear until the latest Carboniferous (Reisz and Fröbisch, 2014). If the relationships advocated by Reisz (1986) are correct, they would imply a long ghost lineage of Caseasauria.

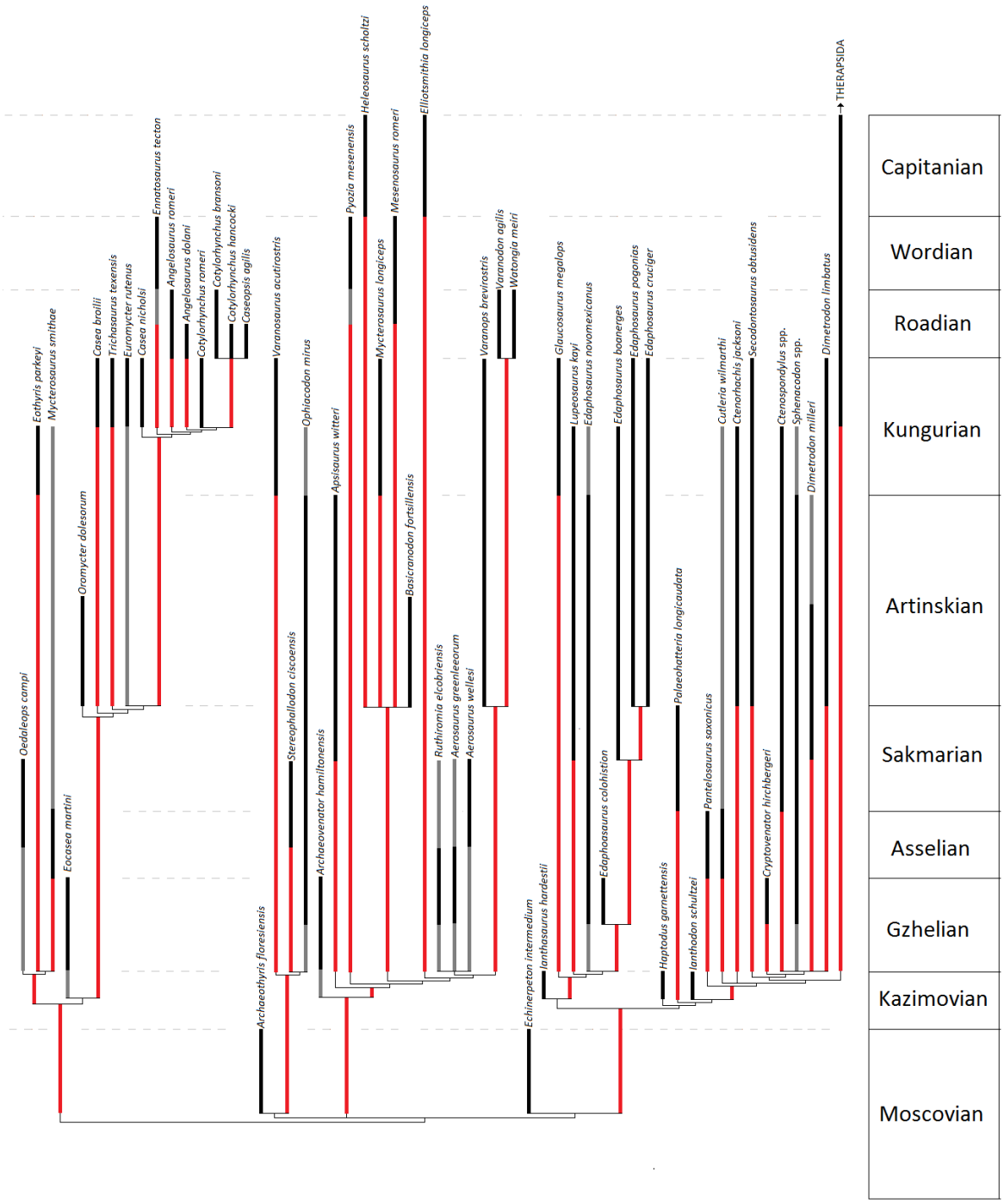

Figure 21: The portion of the time calibrated supertree showing the relationships of pelycosaurian-grade synapsids. Black lineages indicate best supported observed range, grey lineages indicate uncertainty surrounding the age ranges, red lineages indicate ghost lineages

The supertree, however, does not include the analysis of Benson (2012) as a source tree, since this analysis was expanded in Chapter 2. Therefore the supertree recovered Caseasauria as the sister to other synapsids (Figure 21). The other source trees supporting this relationship included Modesto (1994) and Hill (2005), although it should be noted that these latter analyses have extremely poor within-clade taxon sampling. Despite this and the poor

support for the split between Caseasauria and Eupelycosauria found in Chapter 2, the basal position of Caseasauria is assumed in all subsequent analyses of this thesis.

Elliotsmithia longiceps

Elliotsmithia is a varanopid from the Abrahamskraal Farm in South Africa. It is an important species in studying the later evolution of pelycosaurian-grade synapsids. Along with *Heleosaurus scholtzi* it is the youngest pelycosaurian-grade synapsid named to species level (both species are known from the *Tapinocephalus* Assemblage zone of South Africa), and one of the two varanopid species known from South Africa. The holotype, some fragmentary skull material and cervical vertebrae, was originally described as a therapsid (Broom, 1937), but was reassessed as a pelycosaurian-grade synapsid (Romer and Price, 1940) and later a varanopid (Olson, 1965; Langston and Reisz, 1981). Reisz et al. (1998) provided the first cladistic analysis of *Elliotsmithia*, which was shown to belong to the varanodontine subfamily. Modesto et al. (2001) described a second specimen, supposedly of *Elliotsmithia*, which was incorporated into cladistic analysis and suggested *Elliotsmithia* was a mycterosaurine varanopid. This debate has great implications for varanopid evolution. A varanodontine affinity for *Elliotsmithia* would imply that two invasions of South Africa were made by varanopids since the other South African genus, *Heleosaurus*, is unquestionably a mycterosaurine (Botha-Brink and Modesto, 2009; Benson, 2012). A mycterosaurine affinity of *Elliotsmithia*, however, would not only imply a single invasion of South Africa, but also that only the mycterosaurine varanopids survived until the Capitanian; the Varanodontinae would have died out in Olson's Extinction (See Chapter 5).

The interpretation of *Elliotsmithia* as a mycterosaurine is based on the assumption that the second specimen (BP/1/5678) does in fact belong to this genus. This assignment has been questioned (Reisz and Dilkes, 2003). Later analyses not using this specimen in coding *Elliotsmithia* (Maddin et al., 2006; Reisz et al 2010) supported varanodontine affinities, while that of Botha-Brink and Modesto (2009), adding two characters to the Maddin et al. matrix shows *Elliotsmithia* to be a mycterosaurine. Campione and Reisz (2010) found that the morphological data alone supported varanodontine relationships, but a stratocladistic analysis found *Elliotsmithia* to be a mycterosaurine. This analysis added an ordered character representing the stratigraphic position of each taxon. The most parsimonious tree implied by the stratigraphic character is that which minimises the length of ghost lineages (each time bin covered by a ghost lineage is represented by a character state change).

That the supertree supports varanodontine affinities of *Elliotismithia* (Figure 21) is due to the procedure used to select which phylogenetic hypotheses to include. Two of the source trees include *Elliotsmithia*: Reisz et al. (2010) and mini supertree 1. Both show varanodontine relationships. The Modesto et al. (2001) analysis was not included as its character and taxon list is a subset of the Botha-Brink and Modesto (2009) analysis. The Botha-Brink and Modesto analysis, which also supported mycterosaurine affinities, was included in mini supertree 1 along with the Maddin et al. analysis and the Campione and Reisz analysis. Since these latter two analyses support varanodontine relationships, the mini supertree does also. Some might criticise the inclusion of the Maddin et al. (2006) analysis in the mini supertree. Its character list is a subset of that of Botha-Brink and Modesto (2009), but Maddin et al. includes *Archaothyris* and *Ophiacodon*, while Botha-Brink and Modesto score Ophiacodontidae as a single terminal taxon (replaced with *Ophiacodon mirus* when forming the supertree; see above). Thus the taxon list of Maddin et al. is not a subset of that of Botha-Brink and Modesto, and it is included in the mini supertree. One might argue that the inclusion of *Archaeothyris* should not force the inclusion of the Maddin et al. phylogeny, since it is not a species, which belongs to the group that was under focus in the analysis (Varanopidae). Such questions as these do indicate that the guidelines of Bininda-Emonds et al. (2004), though refined for this study, are still worth further examination.

It should also be noted that the stratocladistic analysis of Campione and Reisz (2010) was not included as a source tree. The reason is that the supertree is used to investigate the fit of the fossil record to stratigraphy in Chapter 4; to incorporate a source tree produced using stratigraphic data would be circular. Nevertheless it has been suggested that the combination of stratigraphy and morphology should be preferred over morphology alone (Clyde and Fisher, 1997; Fox et al., 1999). While the analysis based solely on morphology supported a varanodontine affinity of *Elliotsmithia*, the stratocladistic analysis found it to be the sister of the contemporary *Heleosaurus*, a mycterosaurine (Campione and Reisz, 2010). Both specimens referred to *Elliotsmithia* require redescription to resolve such inconsistencies.

Tetraceratops insignis

Tetraceratops is an enigmatic synapsid represented by a single, incomplete and severely crushed skull from the Big Witchita locality of Texas. When first described, it was thought to be closely related to *Dimetrodon* (Matthew, 1908). However, in their Review of the Pelycosauria, Romer and Price (1940) argued that it belonged to Eothyrididae, at that time a wastebasket group containing several small carnivores now known to be unrelated

(Langston, 1965; Reisz, 1986; Reisz et al., 2009). More recently, arguments have been put forward that *Tetraceratops* is in fact the basalmost therapsid (Laurin and Reisz 1990, 1996), a hypothesis supported by phylogenetic analysis (Laurin and Reisz 1990, Amson and Laurin 2011, Cisneros et al. 2011). However, this association has been disputed; Conrad and Sidor (2001) argued that *Tetraceratops* is actually a sphenacodontid. Liu et al. (2009a) were unable to resolve the position of *Tetraceratops* in their cladistic analysis (it formed a polytomy with therapsids and sphenacodontids) but the authors considered sphenactodontid affinities more likely. Amson and Laurin (2011) reassessed the Liu et al. analysis. By adding seven characters and modifying the coding of three others, Amson and Laurin were able to resolve this polytomy, and again demonstrated therapsid affinities for *Tetraceratops*.

The supertree shows *Tetraceratops* to be the basalmost therapsid (Figure 22). Although arguments have been put forward for its sphenacodontid affinities, no published phylogenetic analyses have demonstrated this relationship. The only cladistic analysis that has cast doubt on the therapsid affinities is that of Liu et al (2009), which was not included as a source tree as the character list is a subset of that of Amson and Laurin (2011). Two of the three analyses containing *Tetraceratops* were included as source trees (Amson and Laurin, 2011; Cisneros et al., 2011) and all support its position as a basal therapsid. The third, that of Laurin and Reisz (1990) also supports a therapsid affinity, but was not included as a source tree due to the fact that a character list and matrix were not published along with the analysis. This does highlight one issue with the supertree; the position of an uncertain taxon will depend on what taxa it has been tested against. Thus far, no one has tested the relationships of *Tetraceratops* against a comprehensive set of pelycosaurian-grade synapsids. Benson (2012) unfortunately did not include it in their wide-ranging analysis due to the material not being available for study. The poor quality of the single specimen is also unfortunate. The fact that one poor specimen has been found at a heavily sampled locality lead to the suggestion that it might be allochtonous (Amson and Laurin 2011). This is regrettable, as it would make the discovery of more material unlikely.

Therapsid relationships

Although this study is primarily concerned with pelycosaurian-grade synapsids, the relationships of therapsids will strongly influence the phylogenetic diversity curve of synapsids during the Guadalupian. As such it is worth discussing the phylogeny of therapsids used in this diversity estimate.

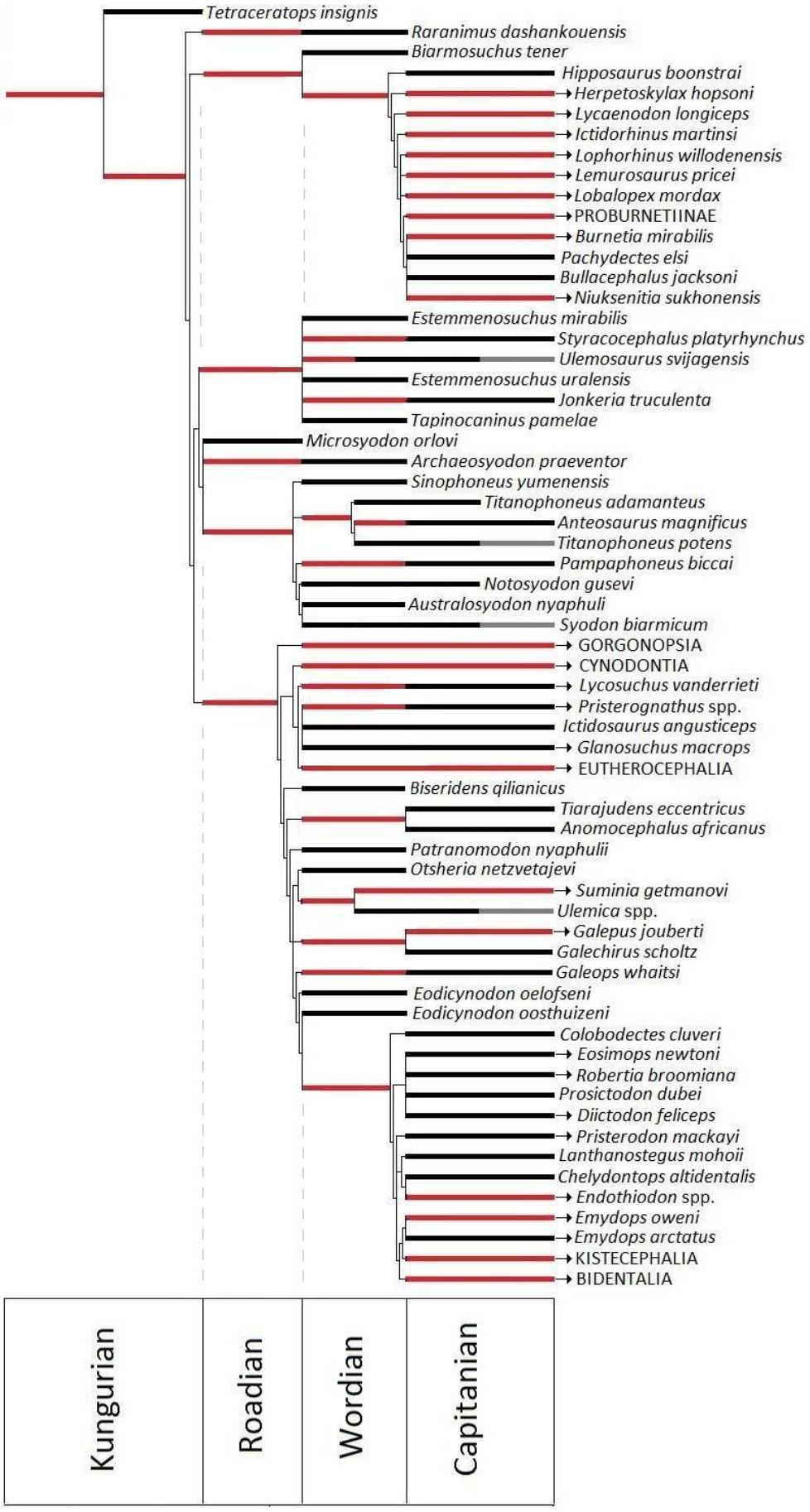

Figure 22: The portion of the time calibrated supertree showing the relationships of therapsids.

The ‘traditional’ view of therapsid relationships, put forth by Romer (1956) was that they were split into two clades: 1) Anomodontia, which contained the taxa currently refered to as anomodonts, and also those belonging to Dinocephalia; 2) Theriodontia containing Biarmosuchia, Gorgonopsia, Therocephalia and Cynodontia. More recent cladistic analyses have overturned these ideas, although there is still considerable disagreement. Many analyses have suggested that Biarmosuchia are the sister to all other therapsid clades (Hopson and Barghusen, 1986; Rowe, 1986; Gauthier et al., 1988; Sidor and Hopson, 1998). However, the analysis of Liu et al. (2009) and its subsequent modification by Amson and Laurin (2012) found Biarmosuchia to be more closely related to Gorgonopsia (a return to the traditional relationship), while Dinocephalia were the basalmost therapsid clade. It has also been suggested that Biarmosuchia are paraphyletic (Kemp, 2009; Cisneros et al., 2011). Dinocephalia are usually not found to be more closely related to Anomodonts than to other therapsid taxa (Hopson and Barghusen, 1986; Rowe, 1986; Gauthier et al., 1988; Laurin and Reisz, 1990; Liu et al 2009a; Amson and Laurin, 2011; but see Liu et al, 2009b; Cisneros et al., 2011). The placement of Gorgonopsia is controversial; they have been variously placed within Theriodontia as the sister to Therocephalia and Cynodontia (Hopson and Barghusen, 1986; Sidor and Hopson, 1998), the sister to Biarmosuchia (Liu et al, 2009b; Amson and Laurin, 2011), and the sister to a clade containing Anomodontia, Therocephalia and Cynodontia (Rowe, 1986; Gauthier et al., 1988; Laurin and Reisz, 1990).

A final controversy is found in the relationships between Therocephalia and Cynodontia. While there has been little doubt that these taxa form a clade to the exclusion of other therapsids (Kemp, 1978; Kemp, 1982; Hopson and Barghusen, 1986; Sidor and Hopson, 1998), the exact nature of their relationship is unclear. Some cladistic analyses have suggested that Therocephalia are in fact paraphyletic, with Cynodontia nested within (Abdala, 2007; Botha et al., 2007; Oliveira et al., 2010), while others suggest that Therocephalia is the monophyletic sister taxon of Cynodontia (Huttenlocker, 2009; Huttenlocker et al., 2011).

The supertree supports Biarmosuchia and Dinocephalia being successive outgroups to other therapsid clades (Figure 22). This is unsurprising; it is the most commonly suggested topology among the source trees (Sidor and Hopson, 1998; Sidor and Welman, 2003; Hill, 2005; Sidor and Rubidge, 2006). Gorgonopsia are not well represented; only three species are present. No published analyses of gorgonopsian relationships have been undertaken, and usually a single taxon (typically *Gorgonops*) is used as an outgroup to studies of other taxa (e.g. that of Fröbisch and Reisz, 2011 on Anomodontia; Huttlenlocker et al., 2011 on Therocephalia; Sidor and Rubidge, 2006 on Biamosuchia). Only two studies have tested the

relationships of multiple gorgonopsians against the other therapsid clades: Liu et al. (2009a) and the modification by Amson and Laurin (2011). Amson and Laurin (2011), included as a source tree, showed Gorgonopsia to be the sister to Biarmosuchia. However this relationship is not recovered in the supertree. Instead, Gorgonopsia occupy a position as the sister to Anomodontia, Therocephalia and Cynodontia (Figure 22), as supported by the analysis of Hill (2005). However it should be noted that this analysis only included a composite coding of Gorgonopsia (replaced by *Gorgonops torvus* when forming the supertree). The clade containing anomodonts, therocephalians and cynodonts to the exclusion of Gorgonopsia and other therapsids is not well supported, demonstrating the urgent need for work on gorgonopsian relationships. Preliminary work on a global phylogeny of early therapsids, including a greater sampling of gorgonopsians and a number of new early dinocephalians, is in fact suggesting a topology similar to that proposed by Romer in 1956: dinocephalians were found to be the sister to the anomodonts, while gorgonopsians, therocephalians and cynodonts were found within a paraphyletic Biarmosuchia (Kammerer et al., 2014). However, this analysis is as yet unpublished and so was not included in the supertree.

The supertree suggests that Therocephalia is the monophyletic sister taxon to Cynodontia (Figure 22). Why this relationship is supported over a paraphyletic Therocephalia becomes apparent when one examines the source trees. Those analyses that suggest cynodonts are a clade within therocephalians are mostly analyses focussing of cynodont relationships (Abdala, 2007; Botha et al., 2007; Oliveira et al., 2010). They contain few therocephalians, and as cynodonts are only known from the latest Permian, none of these studies contain the four taxa from the time period under study. As such none were included as source trees. The two analyses that support a monophyletic Therocephalia (Huttenlocker, 2009; Huttenlocker et al., 2011) focus on Therocephalian relationships, and contain several taxa from the time period under study, although only three cynodonts. The more inclusive study of Huttenlocker et al. (2011) was included as a source tree, and the sister group relationship between Cynodontia and Therocephalia is the one recovered in the supertree and is well supported. This implies a ghost lineage of Cynodontia extending back into the Guadalupian

This particular controversy demonstrates the need for an inclusive phylogeny containing large samples of taxa from both Cynodontia and Therocephalia. The existing studies focus on one or the other, and as such vital information on character polarities may be missed. This also highlights the dangers of being too selective when choosing source trees; when a wider selection of trees is included (those containing three or more taxa from the late Moscovian until the end of the Triassic), a paraphyletic Therocephalia is recovered, and no

cynodont ghost lineage extends into the Guadalupian (see Chapter 6). One can justify restricting the number of source trees; the more inclusive analyses may confuse the relationships of the taxa present during the time period under study. The most obvious example of this is the analysis of Abdala (2007), which included *Prorubidgea*. This taxon is not used in any other analysis, and even the analysis of Abdala (2007) shows little about its relationships other than it being outside Therocephalia. As such becomes a wildcard taxon in the supertree, obscuring the relationships of other clades. Finally, if one chooses to include as source trees phylogenetic analyses containing no taxa within the time period under study one has to ask where one should stop. What effect would including analyses containing three or more taxa from just the Permian, but including the Lopingian, have? What would be the effect of including only those phylogenies containing five or more taxa from the time period under study instead of just four? Such questions are beyond the scope of this thesis, but are worth bearing in mind.

Chapter 4

The Completeness of the Fossil Record of Pelycosaurian-Grade Synapsids

Quantifying the Completeness of the Fossil Record

When one considers the multitude of issues which can affect the fossil record, the difficulty of assessing its quality becomes apparent. An enormous variety of metrics and methods have been proposed, each using different raw data and investigating a different aspect of the completeness of a clade's fossil record.

Fit of Phylogenies to Stratigraphy

A widely-explored branch of methods used to examine the quality of the fossil record incorporates stratigraphic ranges of species and phylogenetic hypotheses of their relationships. Phylogenies are usually produced using data independent of stratigraphy, and so stratigraphy can be used to test these phylogenetic hypotheses, or a phylogenetic hypothesis can be used to test for gaps in the fossil record. In theory, given a complete record and a correct phylogeny, taxa should appear in the stratigraphic column in the order implied by the splitting of the nodes in the phylogeny, and ghost lineages (lineages not observed in the fossil record but inferred from the phylogeny on the assumption that sister taxa should diverge from their common ancestor at the same time) should be absent. If species appear in the fossil record at a time which defies the sequence suggested by the phylogeny, one may infer either there are gaps in the record or the phylogenetic hypothesis is erroneous.

There exist a large number of methods to show to what extent a phylogeny fits the stratigraphic ranges of the taxa. Many of these have been examined in simulations or in case studies, investigating biases such as tree balance (Siddall, 1996; Hitchin and Benton, 1997a; b; Siddall, 1997; 1998; Wills, 1998; 1999; Pol et al., 2004; Wills et al., 2008), tree size (Benton and Storrs, 1994; Hitchin and Benton, 1997a) and the length of time represented by the phylogenetic analysis (Benton and Storrs, 1994; Hitchin and Benton, 1997a; b; Finarelli and Clyde, 2002; Pol et al., 2004), as well as studying the completeness of the record and the reliability of phylogenies of various clades (Gauthier et al., 1988; Norrell and Novacek, 1992; Benton and Storrs, 1994; Huelsenbeck, 1994; Smith and Littlewood, 1994; Hitchin and Benton, 1997a; Benton et al., 2000; Angielczyk, 2002).

Stratigraphic Rank Correlation

The Stratigraphic Rank Correlation (SRC) measures the correlation between two sets of ranks applied to each species in the phylogeny: a stratigraphic rank based on their relative

position in the stratigraphic column, and a phylogenetic rank based on the number of nodes the taxa are removed from the root. These two ranks can be subjected to tests for correlation. The first study of this sort used the Product Moment Correlation Coefficient (Gauthier et al., 1988), although later it was suggested that the Spearman's Rank is more appropriate (Norrell and Novacek, 1992). The latter authors also pointed out that, while stratigraphic data is linear, the phylogenetic data are not unless a fully pectinate tree is used. It was suggested that the phylogenies should be reduced to all possible fully pectinate topologies, each of which should be subjected to separate examination (Norrell and Novacek, 1992). This creates a second problem: how to combine tests on different pectinate trajectories; simply averaging the Spearman's rho value is problematic as the nodes within separate analyses are not independent (Siddall, 1998). Furthermore, the rank correlation tends to increase in larger (Benton and Storrs, 1994) and more resolved (Hitchin and Benton, 1997a) trees. Another concern is that this metric does not account for the length of the gaps implied by the phylogeny, instead only measuring the clade rank (Norrell and Novacek, 1992). In fact, simulations suggest that the SRC shows little relationship with sampling, and is more strongly affected by the accuracy and resolution of the phylogeny (Wagner and Sidor, 2000).

Stratigraphic Consistency Index

The Stratigraphic Consistency Index (SCI) counts the number of stratigraphically consistent nodes relative to the total number of nodes in a phylogeny (Siddall, 1997). A node is considered consistent if it appears in the same or a later time bin than its sister (Figure 23A). This method has been criticised most frequently for tree-shape related biases (Siddall, 1996; 1997; 1998). In any tree that is not fully pectinate, there will be at least one node inconsistent by virtue of the fact that its sister is consistent (Siddall, 1998). This also leads to the phenomenon that in a completely balanced tree the minimum score is 50%, not 0. The exact nature of the bias of tree balance on results is debateable. Hitchin and Benton (1997 a; b) argued that it has no effect, finding no correlation with metrics of balance and the SCI. However, their analysis included cladograms containing recent taxa, biased towards higher SCI scores; all nodes containing only modern taxa are consistent (Siddall, 1997). Simulations suggest that there is a correlation between SCI and tree balance, but both positive (Siddall, 1997) and negative (Pol et al., 2004) relationships have been supported. Another problem is that one taxon can have a large effect on the result (Hitchin and Benton, 1997a); a single long lived derived taxon can render many nodes inconsistent. Despite these issues, simulations suggest that an accurate phylogeny should score reasonably well (Wagner and Sidor, 2000).

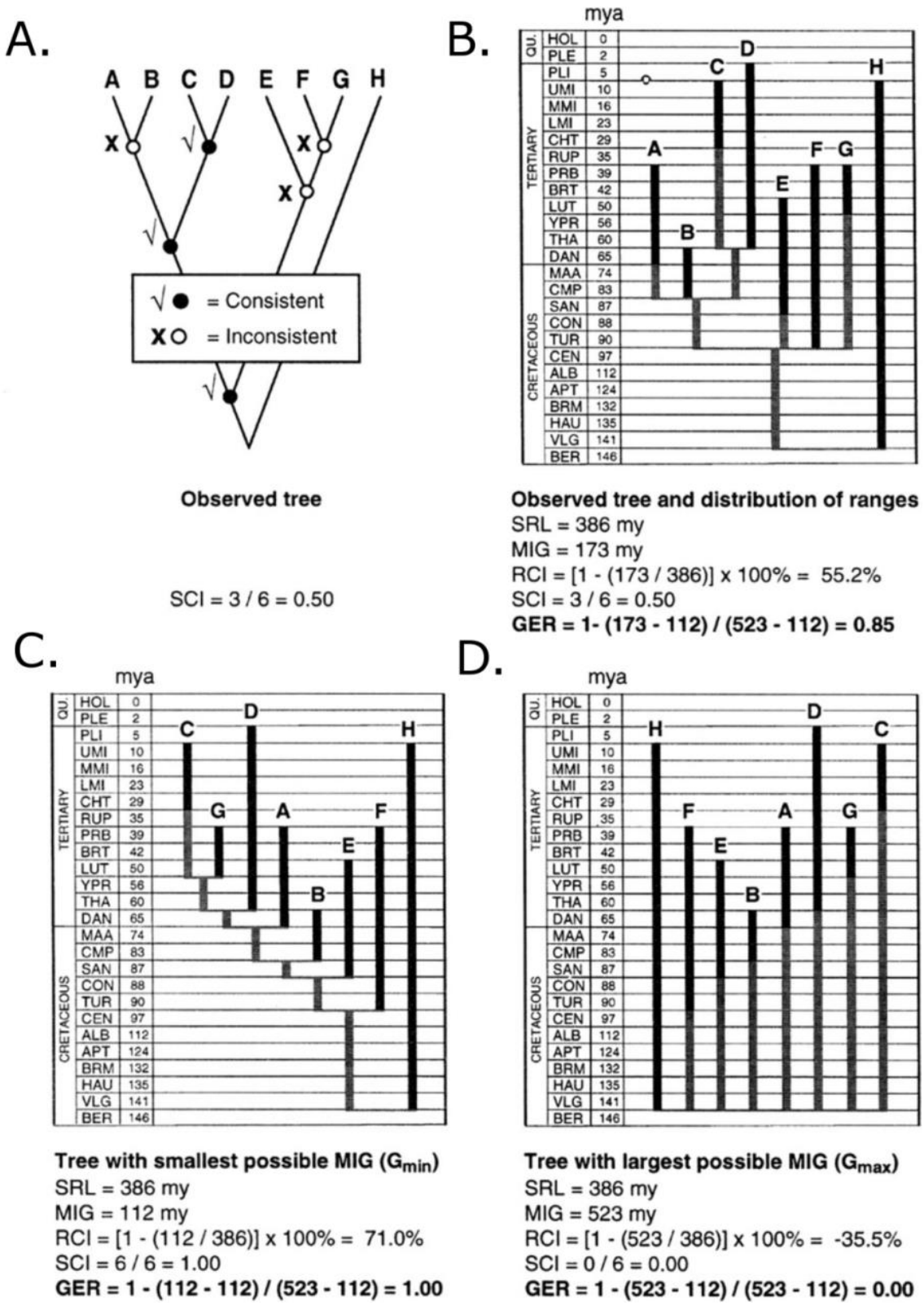

Figure 23: Methods of comparing the consistency of a phylogeny to the fossil record. From Wills (1999). A) Stratigraphic consistency index (SCI); B) Observed tree and stratigraphic ranges. Relative completeness index (RCI calculated by dividing the minimum implied gap (MIG; length of inferred ghost lineages) by the simple range length (SRL; observed ranges). Gap excess ratio (GER) is derived from the MIG, normalised for the maximum and minimum possible gap inferred in C and D. Observed lineages in black, ghost lineages in grey; C) tree with the smallest possible MIG; D) tree with the largest possible MIG.

Gap Excess Ratio

The Gap Excess Ratio (GER) was introduced by Wills (1999) to correct for problems with the SCI such as tree balance and size bias. This metric compares the length of the "gaps" (ghost lineages) implied by the phylogeny (Figure 23B) to the maximum and minimum gap possible with the stratigraphic ranges observed (Figure 23C, D). Like the SCI, it ranges from 0 to 100%. As well as correcting for problems with balance, this method takes into account the length of the implied gaps, rather than just the stratigraphic rank as in the SRC, or whether a node is consistent as in the SCI. There is still a tree shape bias (simulations suggest the GER is higher in balanced trees), but it is less pronounced than in the SCI (Pol et al., 2004). However, the same simulations also suggested that a higher GER would be seen when the length of time observed was higher.

Relative Completeness Index

The above three metrics all measure the fit of a phylogeny to the fossil record. Although they may be affected by both inaccuracy of the phylogeny and an incomplete fossil record, if all taxa appear in the fossil record in the order implied by the phylogeny, the phylogeny should receive a perfect score (notwithstanding the issues of tree balance affecting the SCI). On the other hand, the Relative Completeness index (RCI) is more a measure of completeness than of fit (Benton and Storrs, 1994). It will be affected by inaccuracies in the cladogram (Wagner, 2000), but it is possible for a phylogeny to have perfect consistency with the stratigraphy, and thus perfect SRC, SCI and GER scores, but to have a poor RCI score. The RCI measures the gap implied by the phylogeny relative to the length of observed lineages but, unlike the GER, does not normalise for the maximum and minimum possible gap implied by the stratigraphic ranges presented (Figure 23B). Thus the score has a maximum value of 100% (no gaps implied), but a theoretically infinite lower limit; values can be negative if the ghost lineages implied by the phylogeny cover more time than observed lineages (Benton and Storrs, 1994). This metric does not appear to be affected by the same tree balance biases as the other metrics discussed (Hitchin and Benton, 1997 a; b), but different problems have been identified. Firstly, the taxonomic level of the cladograms under study will have an effect: high level groups e.g. families, with long stratigraphic ranges will mask gaps within the families (Benton and Storrs, 1994). Secondly, unless ancestors are included in phylogenetic hypotheses, the maximum score of 100% may never be reached.

Other Methods

The four metrics described above have been used most extensively in studying the fit of the fossil record, having been applied to many clades from multiple time periods. Other methods do exist, but have been less widely applied either due to methodological concerns or practical issues e.g. lack of readily available automation. These will therefore be discussed only briefly.

The Stratigraphic Retention Index (Clyde and Fischer, 1997) quantifies how well a matrix of stratigraphic characters (wherein each character refers to a time interval crossed by a taxon) fits a phylogeny. Although the performance and assumptions of this method have been examined (Clyde and Fischer, 1997; Finarelli and Clyde, 2002), this has never been applied to empirical data. Problems identified with this method include the fact that the stratigraphic character matrix includes no way of taking into account periods where no fossils at all are found (Finarelli and Clyde, 2002). The method also only takes into account the length of ghost lineages in an indirect way: the number of stratigraphic character changes rather than the actual length of time (Clyde and Fischer, 1997). The Implied Gap (Smith and Littlewood, 1994) is similar to the RCI, but simply divides the length of ghost lineages by the total length (observed and ghost). This method is subject to similar biases to the RCI, but has a lower and upper limit (0-1). It has been applied to empirical data only once to compare phylogenies of echinoids (Smith and Littlewood, 1994). Finally, the Character Consistency Ratio (Angielczyk, 2002) employs a character list to examine how consistent with stratigraphy the character changes inferred from the phylogeny are. A character change is inconsistent if the more derived state appears in the record before the plesiomorphic state. This method was tested on the therapsid clade Anomodontia (Angielczyk, 2002), but several issues were raised: different character optimisations and different character lists can produce different results for the same phylogeny. A lack of readily available automation has also limited its application.

Completeness of Specimens

An aspect of the completeness of the fossil record which received little attention during early discussions of sampling bias, but has been considered more in recent years, is the completeness of the specimens themselves. This may provide information not only on the impact of taphonomic processes on our interpretations of the fossil record, but also on how reliable our taxonomic assignments may be; their accuracy depends on enough of the

organism being preserved to display the relevant characters. Early investigations into the completeness of fossil specimens were based on grading specimens. For example, in their study on Mesozoic birds, Fountaine et al. (2005) assigned each bird species a grade from 1-4 whereby a species given a grade of 1 was represented by a single bone, 2 by more than one bone, 3 by a single nearly complete specimen and 4 by more than one nearly complete specimen. Similar systems have been used in studies on early tetrapods (Benton et al., 2004), echinoids (Smith, 2007) and dinosaurs (Benton, 2008). Such studies are subjective and provide only coarse quantifications of specimen quality. For example, where exactly is the boundary between a collection of associated skeletal elements (scored as '2' in Fountaine et al.'s scheme) and a nearly complete skeleton (scored as '3')? Different workers may assign different completeness scores to the same specimens, making it difficult to reproduce the results of the analyses. Also, the coarse nature of completeness metrics based on just four or five categories means that important fluctuations in fossil record quality might be obscured.

Mannion and Upchurch (2010), in their study on Sauropodomorpha, attempted to remedy these issues with two new completeness metrics: the Skeletal Completeness Metric (SCM) and the Character Completeness Metric (CCM). Both these metrics assign a percentage completeness score to each species. In the SCM, the percentage is based on the relative bulk and number of elements preserved, while in the CCM it is based on the portion of phylogenetic characters that may be scored. As well as the initial study on sauropodomorph dinosaurs, the Character Completeness Metric has also been applied to Mesozoic birds (Brocklehurst et al., 2012), anomodont therapsids (Walther and Fröbisch, 2013) and expanded to include all dinosaurs (Bell et al., 2013). The Skeletal Completeness Metric has been used globally in the original study on sauropodomorphs and most recently ichthyosaurs (Cleary et al., 2015), but also at a more local level to examine body size bias in the Dinosaur Park Formation (Brown et al., 2013).

A variety of methods have been used to implement the CCM. In the original study, Mannion and Upchurch (2010) examined four published character lists from phylogenetic analyses of sauropodomorphs and counted what percentage of characters from each referred to each bone. A score for each bone was assigned to each bone by finding the average percentage across the four character lists. If a species preserves a particular bone, it receives the relevant percentage score. Brocklehurst et al. (2012) modified this method, assembling a single list of over 500 characters, and calculating what proportion of the characters related to each bone. This method has two advantages over other implementations. Firstly, it allows the inclusion of all species; the methods discussed below only allow the inclusion of species,

which have been incorporated into phylogenetic analysis. Moreover, different specimens of the same species may be scored separately e.g. if appearing in different time bins or in different localities. However it does have one flaw in that it over-estimates the completeness of specimens. It assumes that if a bone is preserved, all characters referring to the bone may be coded and that the specimens should receive the full percentage score for that bone; it does not take into account issues such as surface weathering or damage which may obscure characters.

Walther and Fröbisch (2013) took a different approach, using what was then the most comprehensive phylogenetic analysis of anomodonts and calculating what percentage of characters that had been scored for each species within. This method can calculate completeness only for specimens included in that phylogeny, and so is only appropriate when applied to a clade for which such a comprehensive phylogeny exists. Bell et al. (2013), in a study of dinosaurs, expanded this method so that all phylogenetic analyses of the clade in question would be taken into account. Again, this method does not include species which have not been included in phylogenetic analyses, but it allows the analysis of clades for which a single comprehensive phylogeny does not exist. Unlike the Brocklehurst et al. method, both the Walther and Fröbisch and the Bell et al. methods are based directly on the character scorings rather than the presence or absence of bones and are therefore less likely to over-estimate completeness. In fact, it is possible that completeness may be underestimated since characters referring to a portion of the anatomy not possessed by a particular species are scored as unknown and so are deducted from the completeness score. However, since individual specimens are not scored separately in phylogenetic analyses, the Walther and Fröbisch and Bell et al. methods do not allow different specimens from the same taxon found in different time bins or environments to be scored separately.

The Completeness of the Fossil Record of Palaeozoic Synapsids

Thus far, there has never been a dedicated study examining the completeness of the fossil record of pelycosaurian-grade synapsids. Such studies on contemporary organisms have been more general, focusing on wider groups like amniotes and tetrapods. In this chapter, I present the first examination of the quality of the basal synapsid record as a precursor to the examinations of diversity and diversification patterns in the following chapters. Completeness metrics are used to examine the record through geological time, including modifications of previously proposed methods to examine the completeness of the fossil specimens (Mannion

and Upchurch, 2010). Four methods are used to examine the fit of the fossil record to phylogeny to investigate the reliability of cladistic hypotheses and the possibility that large portions of the record may be missing. Finally a historic approach is used to examine whether new discoveries are altering our interpretations of the evolution of pelycosaurian-grade synapsids.

Materials and Methods

Completeness Metrics

An investigation into the completeness of basal synapsid specimens was undertaken using the Character and Skeletal completeness metrics of Mannion and Upchurch (2010). The Character Completeness Metric (CCM) was undertaken using the method applied by Brocklehurst et al. (2012) to the avian fossil record. This method was selected over those proposed by Walther and Fröbisch (2014) and Bell et al. (2013) due to its ability to score all species, not just those included in phylogenetic analyses. The specimens incorporated into this analysis were those included in the database described in Chapter 3, based on the published literature prior to April 2014 and personal observations from museum specimens.

The Character Completeness Metric requires a list of phylogenetic characters relevant to the group under study. Five character lists were selected for the present study: one of amniotes (Reisz et al., 2010), two of pelycosaurian-grade synapsids (Mazierski and Reisz, 2010; Benson, 2012), and two of therapsids (Huttenlocker, 2009; Amson and Laurin, 2011), relevant as therapsids overlap in time with pelycosaurian-grade synapsids and so it is necessary to include characters which may distinguish them. These character lists were combined, and duplicate characters were removed, creating a list of 503 characters (see Appendix F). Scores were then assigned to each region of the skeleton based on the number of characters pertaining to that region. If a species preserves a particular region of the skeleton, then it received the relevant CCM percentage score. The percentage scores assigned to each region of the skeleton may be viewed in Appendix G.

For the Skeletal Completeness Metric (SCM), Mannion and Upchurch (2010) did not propose a quantitative way to assess the bulk of particular regions of the skeleton and assign a percentage score to each region. In this study we propose that if the various regions of the skeleton were modelled as cones, cylinders and prisms, percentage scores for each bone may be derived from the volume of each region. While such a model is clearly not a perfect

measure of the volume of the bones, it does allow a more objective measure of the bulk of skeletal elements than the estimates provided by Mannion and Upchurch (2010). Obviously the proportions of the various bones in a skeleton vary from species to species. As such, four specimens, each from a different family of pelycosaurian-grade synapsids, were selected as representatives, and the final percentages assigned to each region were based on the mean volume of each element from each species. The specimens used were AMNH FARB 7517 (*Cotylorhynchus romeri*), MCZ 1365 (*Dimetrodon milleri*), MCZ 1366 (*Ophiacodon uniformis*) and FMNH UR 34 (*Varanops brevirostris*). Edaphosaurids and eothyridids were represented due to a lack of nearly complete specimens. *Eothyris*, *Oedaleops* and *"Mycterosaurus" smithae* are known from limited material; the former from a skull and the latter two by partial skulls and few postcranial elements. There are more complete edaphosaurid specimens, but the most complete skeletons are mostly composites. The percentage scores assigned to each region of the skeleton, and details of the shapes used to model the skeleton for the SCM may be viewed in Appendix H, and a condensed overview of the percentages assigned to the CCM and SCM is shown in Table 3.

	Character Completeness Metric	**Skeletal Completeness Metric**
Skull	69.98%	18.13%
Pectoral girdle	4.37%	7.19%
Forelimb	6.19%	10.94%
Pelvic girdle	3.20%	3.26%
Hindlimb	5.37%	18.30%
Vertebral column	9.58%	42.18%

Table 3: A comparison of the percentage scores assigned to different regions of the skeleton (see Appendices G and H for the more detailed breakdown of the scores)

As in the CCM, a species preserving a particular element received the relevant percentage score for that element. A species for which only part of an element is preserved will receive only a part of the relevant score e.g. a single femur will receive an SCM score of 4.08%, while if only proximal end of a femur is preserved it will receive a one third of this score: 1.36%. For a region of the vertebral column, the completeness of a specimen is based on the number of vertebrae preserved compared to the number of vertebrae the species is thought to have had e.g. the dorsal column is worth 7.67%. If a species had 22 dorsal

vertebrae, but one specimen preserves only 11 of these, that specimen will receive only half the SCM score: 3.84%. Where the total number of vertebrae of a species is not known for certain, it is inferred from closely related species. The same system is used for digits; the SCM score is based on then number of phalanges preserved relative to the number the species is thought to have had.

A CCM and SCM score is calculated for each time bin by assigning a score to each species present within that bin, and then calculating the mean score of all species (see Appendix I). If different specimens of the same species were known from different time bins, they were scored separately. Where there is uncertainty over the age of a specimen, it is assigned to the full range of possible ages. These mean scores were plotted through time to create CCM and SCM curves. The correlation between these two curves, and between each curve and the taxic diversity, was tested using Kendall's Tau and Spearman's Rank correlation coefficients, implemented using R version 3.0.0 (R Core Team, 2013) after applying generalised differencing to correct for autocorrelation (McKinney, 1990).

It should be noted that Mannion and Upchurch (2010) proposed two methods to implement both of these metrics. SCM1 and CCM1 estimate the completeness of the most complete specimen of each species, while SCM2 and CCM2 assess the completeness based on the combined information from all known specimens. Mannion and Upchurch (2010) and Brocklehurst et al. (2012) considered the second of these metrics to be more meaningful, not only because it includes all available information, but also because the SCM1 and CCM1 both require some species to be omitted from an analysis in cases where associations of disarticulated bones make it difficult to recognise 'the most complete individual'. As such, in this study only the SCM2 and CCM2 are applied.

Fit of the Phylogeny to the Fossil Record

The fit of the phylogeny of pelycosaurian-grade synapsids to the stratigraphic record was assessed to examine both the completeness of the fossil record and to provide an independent test of the accuracy of the phylogeny. The metrics used were the Stratigraphic Rank Correlation (SRC), the Stratigraphic Consistency Index (SCI), the Gap Excess Ratio (GER) and the Relative Completeness Index (RCI). These have been used widely, including on contemporary taxa closely related to pelycosaurian-grade synapsids, e.g. Palaeozoic amniotes and other synapsid clades (Norrell and Novacek, 1992; Benton and Storrs, 1994; Hitchin and Benton 1997; Benton 2000, Angielczyk, 2001). It is important that this be the

case: the completeness of the fossil record is a relative concept, and so the results of this study need to be compared to previous analyses. The Character Consistency Index (Angielczyk, 2002), despite having been applied to the closely related Palaeozoic synapsid group Anomodontia, was not used due to methodological concerns. This index assesses whether the time of character transitions implied by the phylogeny agrees with the appearance of a particular character state in the fossil record. However, this method introduces further uncertainties into the study. A poor result could mean a poor phylogeny or an incomplete record, as in other metrics, but could also mean a poor choice of characters or incorrect character optimization.

The four metrics were applied to a time calibrated version of the supertree produced in chapter 3. Only the portion representing pelycosaurian-grade synapsids was included. Therapsids were collapsed into a single lineage. In implementing the SRC the tree was reduced to all possible fully pectinate phylogenies, following the recommendations of Norrell and Novacek (1992). All phylogenies containing four or less taxa were removed from the analysis, since it is impossible for such small phylogenies to show a significant correlation (Hitchin and Benton, 1997a). Stratigraphic and clade ranks were inferred from all others and were subjected to the Spearman's Rank Correlation Coefficient using R (R Core team, 2013). The SCI, GER and RCI were all implemented using R (R Core team, 2013) using custom scripts based on functions in the Paleotree package (Bapst, 2013). In order to test the significance of the obtained values, R was also used to generate 10,000 random tree topologies, onto which the observed age ranges were overlain. The resultant values were compared to the values observed, in order to assess the probability of obtaining the observed results by chance.

Collector Curves

Collector curves (Cain, 1938) show changes in the rate of discovery through historical time and allow examination of the pattern of knowledge accumulation. The numbers of taxa known can be plotted against any measure of effort, in palaeontology usually the number of years of study. One use of such curves is to investigate whether the number of species found from a certain taxonomic group is reaching saturation, or whether there are likely to be many more yet to be discovered. In a clade in which discovery is approaching saturation, one expects a sigmoid-shaped curve, with low initial rates of discovery, followed by a rapid acceleration in the number of species found per year, and then eventually a slowing in the rate

of discovery, as the curve approaches an asymptote representing the maximum 'knowable' record (Benton et al., 2011). Collector curves formed for different clades have shown different signals, with some e.g., mammals (Alroy, 2002), birds (Fountaine et al., 2005) dinosaurs (Benton, 2008) and amphibians (Bernard et al., 2010) showing no sign of having reached an asymptote, while others e.g., tetrapods as a whole (Maxwell and Benton, 1990), echinoderms (Smith, 2007) and trilobites (Tarver et al., 2007) indicate that the rate of discovery is slowing.

A collector curve was formed to illustrate discoveries of pelycosaurian-grade synapsids since 1854, when *Bathygnathus borealis* (Leidy, 1854), was described. New discoveries were added in annual intervals until 2014. This curve represents "now valid" species, as opposed to "then valid", as distinguished by Alroy (2002), meaning that the curve represents when species considered valid in the present dataset were discovered, whether or not they were originally recognised as pelycosaurian-grade synapsids, and does not include taxa which after their original description were synonymised, declared *nomina dubia* or assigned to other clades. The 'now valid' curve is considered more relevant to this study on the current state of the record.

The polynomial model function in Past (Hammer et al., 2001) was applied to the collectors curve. The function fits several polynomial curves to the data, and the best-fitting model was chosen based on the Akaike Information Criterion. This reveals the long-term trends in the curve, enabling identification of the point at which the stepwise increase in the number of species shows a genuine rather than temporary slowing of the rate of discovery.

Investigating the Influence of New Discoveries

A taxic (raw, without sampling correction) diversity estimate of pelycosaurian-grade synapsids was used for an examination of the degree to which new discoveries change the shape of diversity curves and our interpretations of major events within the evolution of pelycosaurian-grade synapsids. A "current" diversity curve, representing the state of knowledge in 2014, was produced by counting the number of basal synapsid species known in each substage. Taxa were pruned from the diversity curve going back in time in decade-long intervals from 2014. A new diversity curve was formed only from the taxa remaining in the dataset after the pruning. This was done as far back as 1864, at which point only one taxon (*Bathygnathus borealis*) was present in the dataset. The correlation between the past diversity curves and the 2014 diversity curve was tested with the Kendall's Tau and Spearman's Rank

Correlation Coefficients using R, after transforming the data with generalised differencing to correct for autocorrelation.

This study did not take into account changing opinions on the stratigraphic ages of formations. It is difficult to ascertain what the 'widely-held opinion' of the age of a particular formation was during history, particularly when the age of sediments are even now subject of debate. Previous databases could give an idea of how these opinions have changed, but the two previously published databases of pelycosaurian-grade synapsids (Romer and Price, 1940; Reisz, 1986) do not provide ages giving enough temporal resolution to form diversity curves. As such, the ages assigned to species in the past diversity curves are the same as those assigned to the species in the 2014 diversity curve. However changes in the known stratigraphic ranges of species are taken into account. If a species was named one year, but a specimen was discovered later which extended the range, the full range will only be used in the more recent diversity curve.

The Relative Completeness Index was used to investigate how the completeness of the fossil record has changed through history, and to answer the question: are new discoveries filling gaps or creating more? The RCI of the basal synapsid record was calculated for the supertree to give a value for 2014. Values for each preceding year were calculated by pruning taxa not named before that year. The tree topology of the remaining taxa was retained after the pruning. The RCI was calculated for each year back in time until 1878, when the first pelycosaurian-grade species since subjected to phylogenetic analysis were described. As described above, changes in the opinion on the age of formations was not taken into account, but new discoveries which changed the stratigraphic range of a species were.

Results

Completeness Metrics

The Character Completeness Metric (Figure 24A) starts on a peak in the late Moscovian of 42.52%, higher than in any other Carboniferous time bin, before falling to its lowest trough (17.94%) in the Kasimovian. After this initial fluctuation, the CCM curve remains extremely stable for the next ten time bins with only small variations between 28.00 and 36.12%. This consistency lasts until the late Kungurian, when there is a peak CCM score of 45.79%, and then another trough in the early Roadian of 29.05%. The score then rises to an overall peak in the Wordian of 67.16%, before dropping slightly to 60.38% in the Capitanian.

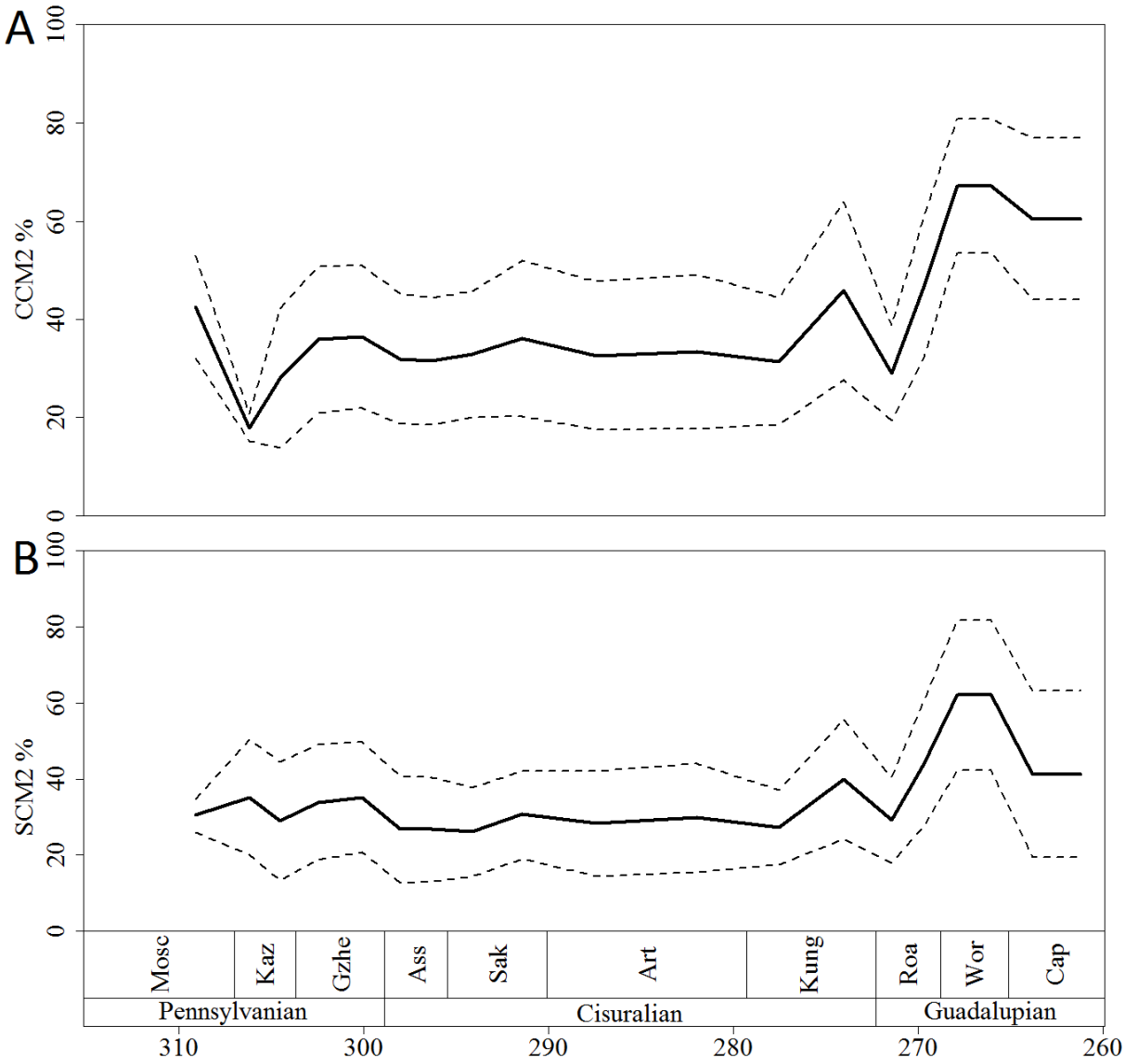

Figure 24: A) Character Completeness Metric Curve (solid line) and one standard deviation either side (dashed line). B) Skeletal Completeness Metric curve (solid line) and one standard deviation either side (dashed line). Timescale representing millions of years ago shown at the bottom.

The Skeletal Completeness Metric (Figure 24B) shows a significant positive correlation with the Character Completeness Metric (Table 4). The same trends and peaks appearing in the CCM curve are mostly visible in the SCM curve as well. The biggest difference between the two appears in the first two substages. Whereas the CCM curve indicates a fall from a late Moscovian peak to an early Kasimovian trough, the SCM scores increase from 30.35 to 35.15% between these substages. Between the late Kasimovian and early Kungurian, the SCM shows the same stability as the CCM, although the SCM values are consistently lower (ranging from 26.11 to 35.29%). As in the CCM, the SCM curve shows a late Kungurian peak, an early Roadian trough, and a Wordian overall peak.

	Kendall's tau	Spearmann's rank
CCM vs SCM	0.503268 (p=0.002986)*	0.6594427 (p=0.093701)*
CCM vs TDE	-0.254902 (p=0.1519)	-0.3828689 (p=0.1177)
SCM vs TDE	-0.3856209 (p=0.02643)*	-0.504544 (p=0.03456)*

Table 4: The correlations between the Character Completeness Metric curve (CCM), the Skeletal Completeness Metric curve (SCM) and the taxic diversity curve (TDE) of pelycosaurian-grade synapsids. Significant correlations ($p<0.05$) are highlighted with an asterix.

Both the CCM and the SCM show a negative relationship with the diversity of the pelycosaurian-grade synapsids (Figure 25), according to the Spearman's rank and Kendall's tau correlation coefficients. Only the correlation with the SCM is significant (Table 4).

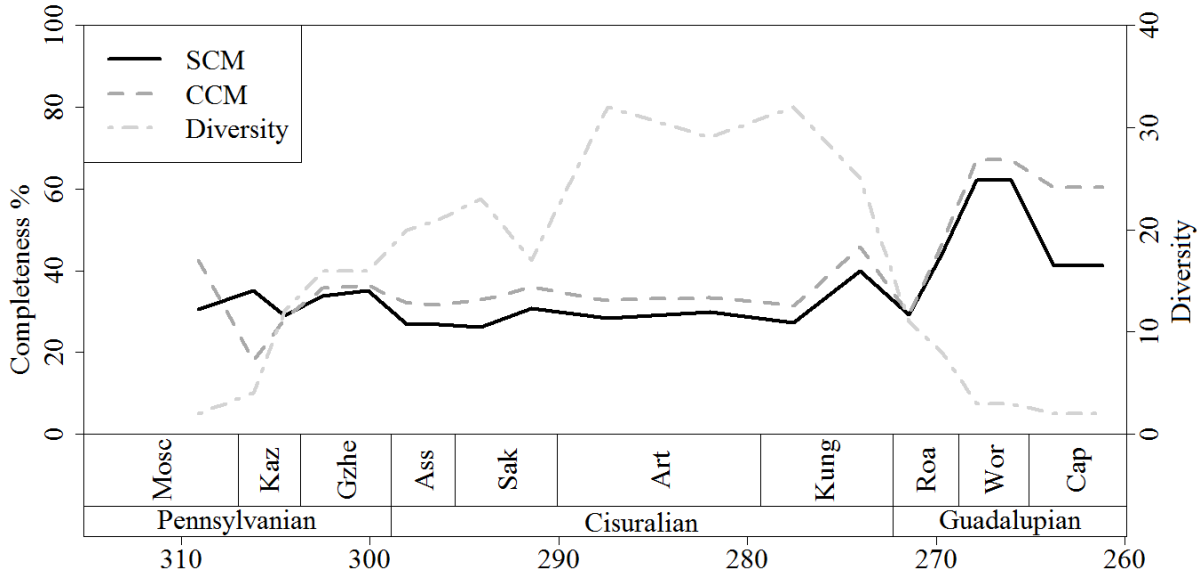

Figure 25: A comparison of the Character Completeness Metric curve, the Skeletal Completeness Metric curve and the taxic diversity curve of pelycosaurian-grade synapsids. Timescale representing millions of years ago shown at the bottom.

Fit of the Phylogeny to the Fossil Record

When the supertree is reduced to all its fully pectinate component trees, and all those containing four or less taxa were removed, 107 trees remained. Of these, 36% showed a significant ($p<0.05$) Spearmann's rank correlation between the phylogenetic rank and stratigraphic rank of the taxa. The mean Spearmann's rank score was 0.57. The largest fully pectinate trees (13 terminal taxa) all show significant correlation, with values ranging from 0.56 to 0.74 ($p= 0.031936–0.0038814$).

The other three metrics of fit were applied to the entire supertree and so produced one value each: the Stratigraphic Consistency Index = 54%; the Gap Excess Ratio = 58% (P-value obtained from random permutations = 0.0169); the Relative Completeness Index = 2% (P-value = 0.0159).

Collector's Curve

The collector's curve (Figure 26) shows that the rate of discovery of pelycosaurian-grade synapsids remained low between 1854 and 1877, during which only 5 species were described. There was a brief and rapid increase in the number of known species to 11 in 1878, following five papers by Cope (Cope, 1877b; a; 1878a; b; c). After this year the gradual increase in the rate of discovery continued, with 9 new species named between 1879 and 1906. During the 1900s and 1910s, the rate of discovery again intensified. The Revision of the Pelycosauria of North America by Case (1907) and the papers of Williston (Williston, 1910; 1911; 1913; Williston and Case, 1913; Williston, 1915), among others, contributed to the naming of 11 new species in an interval of 7 years.

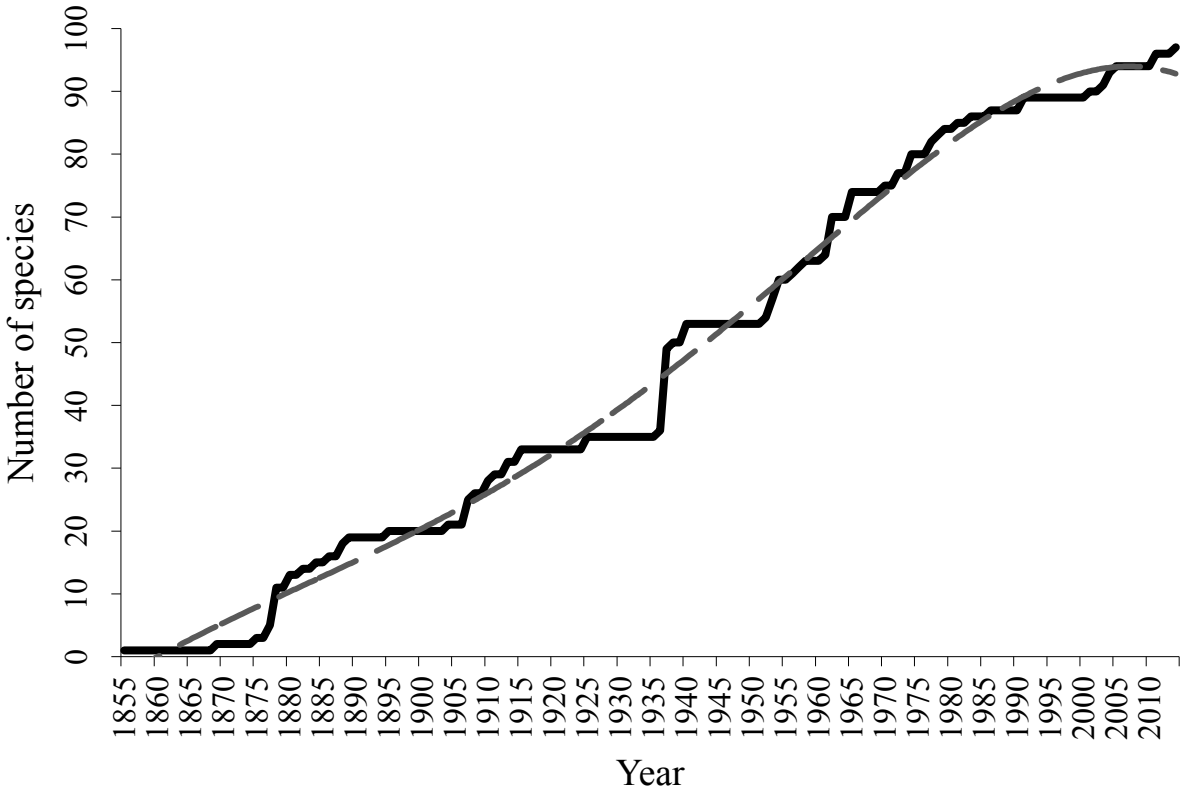

Figure 26: The collectors curve representing descriptions of pelycosaurian-grade synapsid taxa through historical time (solid line) and the polynomial model fitted using Past (dashed line).

The biggest leap in the number of known species occurred in 1937, when 13 new species were described, 11 erected by Romer (1937). A further 4 species were named over the next four years, but after 1940, no new descriptions were made until 1952. It is unclear why there was such a long period without discovery. Benton (2008) observed a slower rate of discovery of dinosaurs at a similar time and attributed it to the Second World War.

Discoveries since 1952 do not follow the stepwise pattern described for the preceding years. Instead there is a consistent rate of increase in known species until 1991. During these 39 years, 35 species were named. Many of those found in the 1950s and 1960s were named in papers by Olson (Olson and Beerbower, 1953; Olson, 1954; 1962; Olson and Barghusen, 1962; Olson, 1965). After 1991, there was again a plateau which has lasted until the present day, with no new species named for the next 10 years, and only 7 named in the 20 years between 1991 and 2011.

The polynomial model function in Past suggests that, according to the Akaike information criterion, a fifth order model best fits the collector's curve. This model indicates the sigmoid pattern expected for a clade whose discovery is reaching saturation. After a low initial rate of discovery, the rate accelerates between the 1920s and 1980s. During the 1980s, the rate of discovery slows, reaching a plateau after the year 2000.

Historical RCI Analysis

The Relative Completeness Index has fluctuated greatly through historical time (Figure 27). It was at its highest during the early years of discovery; when the supertree is pruned to include only taxa known in 1878, the RCI is 30% (although it should be noted that this value is based on a supertree pruned to only 3 pelycosaurian-grade taxa and a lineage representing Therapsida). Early discoveries caused large changes in the RCI; as there were so few taxa, a single discovery can have a large effect. Most of the changes are decreases. The discovery of *Varanosaurus acutirostris* (Broili, 1904) produced a long ghost lineage from the Kungurian to the Sakmarian, and the RCI decreased from 32 to 15%. Further discoveries in 1907 and 1908 led to additional gaps in the record, causing the RCI to fall to its lowest point: -57%.

After this trough, the RCI rose following the descriptions of Williston (Williston, 1910, 1911, 1913; Williston and Case, 1913; Williston, 1915) to a peak of -6% in 1913. It fell again to -13% in 1915, and remained between -13 and -11% for the next 21 years. Between 1936 and 1938, 9 species now included in the supertree were described, 5 of them in Romer

(1937). These discoveries again created more gaps than they filled, causing the RCI to fall to -38%. This trough lasted only until 1940, when the new taxa described in Romer and Price (1940), and the expansion of ranges of known species by the identification of new specimens in the same volume, pushed the RCI up to -24%.

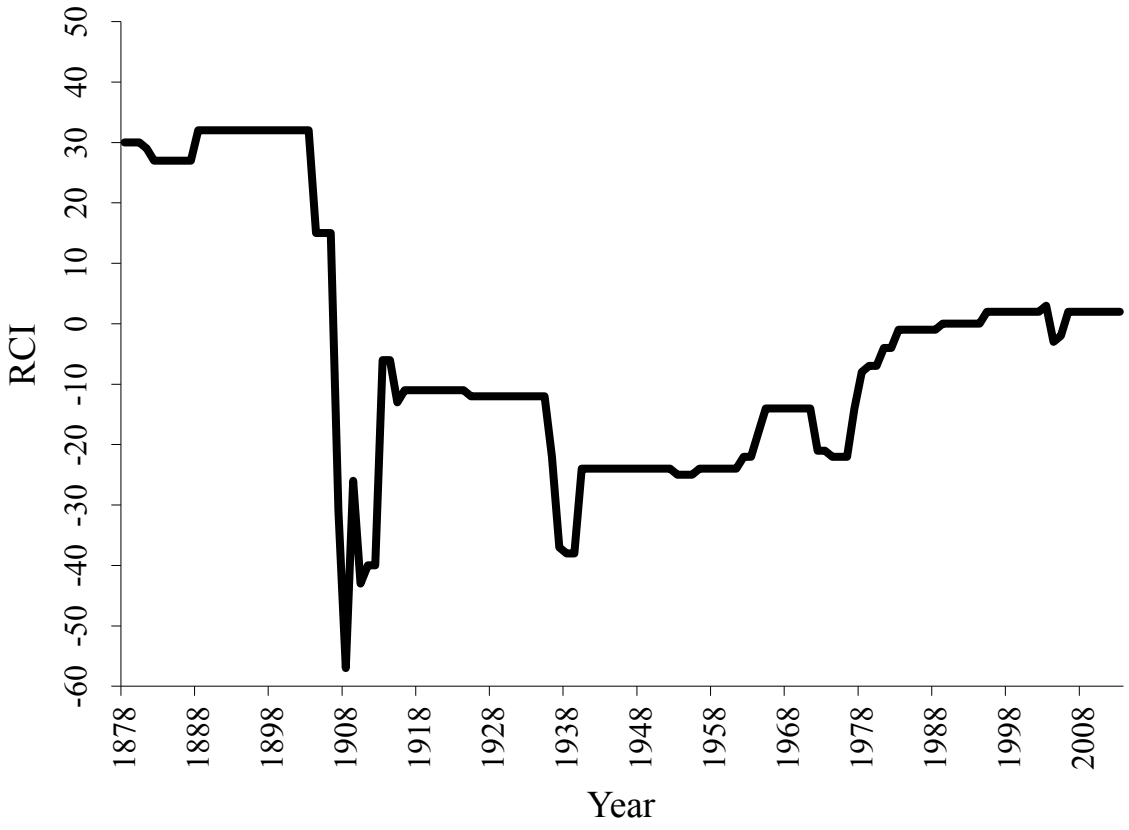

Figure 27: The changes in Relative Completeness Index through historical time.

Discoveries between the early 1940s and early 1960s have very little impact on the RCI, which remains between -24 and -22%. It is not until 1965 that there is a noticeable increase to -14%. This increase is in part due to the discovery of *Oedaleops campi* (Langston, 1965), which partially fills a caseasaur ghost lineage stretching from the Kungurian to the late Carboniferous. In 1972 the earliest known synapsid, *Archaeothyris floresiensis* (Reisz, 1972) was described. This late Moscovian ophiacodontid caused ghost lineages from Caseasauria, Varanopidae, and the clade containing Edaphosauridae and Sphenacodontia to be drawn back into the late Moscovian, decreasing the RCI to -21%. During the late 1970s and early 1980s the RCI rose again, reaching -1% in 1983. Thereafter, the RCI fluctuates between -3% and 3% with no large excursions, either positive or negative.

Historical Diversity Curves

The current diversity curve of pelycosaurian-grade synapsids correlates significantly with each of the historical diversity curves as far back as 1914 (Table 5). Unsurprisingly, the correlation becomes weaker further back in time. The 1874 curve shows a significant correlation when Spearman's rank is used, but not Kendall's tau. However, in 1874 only two taxa were known, so it is likely that this significant correlation is an artefact of this.

	Kendall's tau	**Spearmann's rank**
2014 vs 2004	0.8823529 ($p=8.282x10^{-10}$)*	0.9628483 ($p=6.54x10^{-6}$) *
2014 vs 1994	0.8823529 ($p=8.282x10^{-10}$) *	0.9690402 ($p=7.434x10^{-6}$) *
2014 vs 1984	0.8300654 ($p=2.713x10^{-8}$) *	0.9484004 ($p=3.235x10^{-6}$) *
2014 vs 1974	0.7908497 ($p=2.295x10^{-7}$) *	0.9360165 ($p=2.2x10^{-16}$) *
2014 vs 1964	0.7385621 ($p=2.522x10^{-6}$) *	0.9029928 ($p=2.2x10^{-16}$) *
2014 vs 1954	0.5947712 (p=0.0003246) *	0.7121063 (p=0.001265) *
2014 vs 1944	0.503268 (p=0.002986) *	0.5768834 (p=0.01374) *
2014 vs 1934	0.5163399 (p=0.002244) *	0.5727554 (p=0.01455) *
2014 vs 1924	0.4901961 (p=0.003935) *	0.5438596 (p=0.0214) *
2014 vs 1914	0.503268 (p=0.002986) *	0.5706914 (p=0.01497) *
2014 vs 1904	0.254902 (p=0.1519)	0.3601651 (p=0.1425)
2014 vs 1894	0.254902 (p=0.1519)	0.370485 (p=0.1308)
2014 vs 1884	0.2287582 (p=0.2008)	0.3168215 (p=0.1999)
2014 vs 1874	0.3333333 (p=0.05736)	0.4901961 (p=0.04076) *
2014 vs 1864	-0.1111111 (p=0.5498)	-0.124871 (p=6.208)

Table 5: The correlations between the current (2014) taxic diversity curve of pelycosaurian-grade synapsids and pruned diversity curves, with taxa described after the specified year removed. Significant correlations ($p<0.05$) highlighted with an asterix.

The Quality of the Fossil Record of Pelycosaurian-Grade Synapsids – Current Perspectives

Completeness of Specimens Through Geological Time

The two methods employed for assessing the completeness of pelycosaurian-grade synapsid specimens, the Character Completeness Metric (CCM) and the Skeletal

Completeness Metric (SCM), are assessing different aspects of the fossil record. The CCM is a measure of how much information may be obtained from the fossils, since it is based on phylogenetically relevant characters. However, it should not be considered a representation of taphonomic bias, since it is possible for a species to receive a complete CCM score with less than half the skeleton preserved; each paired bone can be scored if only one is present, and only one vertebra and neural spine from each region of the column is needed. The SCM, however, requires all regions to be preserved to achieve a perfect score. For example, if two femora are preserved, the SCM score will be 8.15%, but if only one is preserved, the score will be 4.08%. The SCM more closely represents the amount of material, rather than information, that is preserved and so is a better proxy for taphonomic biases.

With all that said, Mannion and Upchurch (2010) found a significant correlation between the two metrics, implying that the choice of metric may not have been important. However, the SCM and CCM percentage scores assigned to each region, when applied to Sauropodomorpha, were reasonably similar. When applied to pelycosaurian-grade synapsids, they are very different (Table 3). The CCM shows a great emphasis towards the skull, which is the basis for 69.98% of characters. In the SCM, however, the skull is responsible for only 18.13% of the skeleton by volume. The SCM instead shows a large emphasis on the axial skeleton (vertebrae, neural spines and ribs): 42.18%.

Given these differences, it is surprising that there is a significant correlation between the two metrics (Figure 25, Table 4). The two curves show extremely similar scores and trends, including a peak in the late Kungurian and an overall peak in the Wordian (Figure 25). The only noticeable difference is found in the early Kazimovian, in which four species are represented by mostly postcranial material and only poor skulls. As such, the CCM of this period is extremely low, while the SCM is similar to the following substages. The SCM curve shows lower values for most substages (Figure 25). This should not be surprising; as mentioned, a species needs considerably less of its skeleton preserved to achieve the same CCM score. The same can be observed in the curves of Mannion and Upchurch (2010: Fig 2).

For most of the period under study, both the mean SCM and CCM vary between about 25 and 35%, although the confidence intervals are wide, indicating a great range of individual values for species (Figure 24). As mentioned, the completeness of the fossil record is a relative concept, and it is necessary to compare these results to others in order to judge whether the fossil record of pelycosaurian-grade synapsids can be called “good” or “bad”. Unfortunately, these recently proposed methods have been applied to very few clades, and so comparison is difficult. The range of values is similar to those observed in Sauropodomorpha

(Mannion and Upchurch, 2010), but a much larger range of values was observed in the mean CCM of Mesozoic birds, which ranged from 1.53% to 75.72% (Brocklehurst et al., 2012). This was thought to result from the effect of Lagerstätten, which would more strongly influence the record of small delicate animals as they can be more easily buried and preserved whole than large animals, but also can more easily be completely destroyed (Brocklehurst et al., 2012). There are no Carboniferous and Lower Permian formations containing pelycosaurian-grade synapsids that could be described as areas of exceptional preservation. However during the Middle Permian the Mezen faunal assemblage produces abundant fossils, although with varying degrees of articulation and preservation (Efremov, 1940; Olson, 1957). The overall peak of both the SCM and CCM is in the Wordian (Middle Permian), during which time all known pelycosaurian-grade synapsid species are from this assemblage. There are only three species known from this area, but two of them (*Mesenosaurus romeri* and *Ennatosaurus tecton*) are represented by numerous, in some cases fully articulated specimens. These species are also smaller than many of their relatives in the Early Permian. It is possible that the Wordian peak in the SCM and CCM is due to a similar Lagerstätten effect to that which caused peaks in the CCM curve of Mesozoic birds.

The only attempt to apply the CCM to a group from a similar time period to that occupied by the pelycosaurian-grade synapsids is the study of Walther and Fröbisch (2013) on anomodont therapsids. The mean CCM of Anomodontia in all but one time bin is consistently higher than 60%, considerably higher than the values obtained for pelycosaurian-grade synapsids. However, it should be noted that the periods in which the pelycosaurian CCM is at its highest are in the latest time slices, during which they overlapped temporarily and spatially with anomodonts. Walther and Fröbisch (2013) suggested that the exceptional completeness of known anomodonts may be the result of the unrivalled fossil record of Permian–Triassic terrestrial tetrapods in the South African Karoo Basin. One might therefore suggest that the Mid–Late Permian record is better than that of the Early Permian and Pennsylvanian. However, as noted, very few studies using these metrics have been undertaken, and further work is necessary before such conclusions can be firmly supported.

Completeness Metrics and Diversity

It has been suggested that the completeness of specimens may have an influence on diversity estimates (Benton et al., 2004; Mannion and Upchurch, 2010; Benton et al., 2011a; Brocklehurst et al., 2012; Walther and Fröbisch, 2013). A time period containing many poorly

preserved specimens may have a lower number of taxa named to species level, as it is more difficult to identify diagnostic characters. Such a mechanism has been proposed to explain the significant positive correlation observed between various completeness metrics and taxic diversity of sauropodomorphs (Mannion and Upchurch, 2010), Permian tetrapods (Benton et al., 2011) and Mesozoic birds (Brocklehurst et al., 2012). It has even been suggested that the CCM and the SCM could be used as sampling proxies in order to implement sampling correction on diversity curves (Mannion and Upchurch, 2010). Alternative reasons for a strong positive correlation between diversity and completeness score might be that an absolutely greater number of fossil discoveries in a particular time period leads not only to more species being discovered, but also more taxa being represented by more specimens and receiving a higher completeness score. A final possibility suggested by Brocklehurst et al. (2012) is that in a time period in which the clade was more abundant and diverse, there is a higher probability of specimens being preserved.

Surprisingly, the SCM of pelycosaurian-grade synapsids show a significant negative correlation with the taxic diversity curve (Figure 25, Table 4). In contrast to previous studies, it seems that as the quality of the preserved specimens gets worse, the estimates of diversity increase. Such a result has never been observed in previous studies although the possibility has been discussed (Mannion and Upchurch, 2010; Brocklehurst et al., 2012). The hypothesised scenario is that basal synapsid workers have diagnosed a large number of species based on poorly preserved, non-overlapping material which could potentially have belonged to a single species, thus raising the diversity estimate.

The correlation between diversity and the character completeness metric, while also negative, is not significant. This is again surprising; one might expect it to be the number of characters preserved in a specimen that affects the number of taxa identified, as has been seen in sauropodomorphs and Mesozoic birds (Mannion and Upchurch, 2010; Brocklehurst et al., 2012). Both these studies showed significant correlation between the CCM and taxic diversity. The lack of such a correlation in pelycosaurian-grade synapsids may reflect the history of discovery. The period of greatest discovery in basal synapsids was between the 1930s and 1960s (Figure 26). At this time, classifications were based to a large extent on stratigraphy, location and body size (e.g. Romer and Price, 1940). While there have been some recent taxonomic revisions using phylogenetic methods, this has mostly focussed on a single family: the Varanopidae (Reisz and Dilkes, 2003; Anderson and Reisz, 2004; Maddin et al., 2006; Reisz et al. 2010). Meanwhile, the rate of discovery of dinosaur (including avian) species has increased alongside the introduction and refinement of phylogenetic methods

between the late 80s and the present day (Fountaine et al, 2005; Benton, 2008). As such, phylogenetic methods have been much more important in the classification of dinosaur species. This may be why sauropodomorph and bird diversity is much more closely linked to the CCM, a metric based on phylogenetic characters. Anomodontia, a clade subjected to many recent cladistics analyses (for summary see Kammerer et al., 2011), also show a strong relationship between diversity and the CCM (Walther and Fröbisch, 2013). The classification of pelycosaurian-grade synapsids is not so closely linked to methods based on characters, and correlates more closely to the measure of absolute completeness provided by the SCM.

The Fit of the Phylogeny to Stratigraphy

Previous studies comparing the fossil record to phylogeny have suggested a good fit when examining phylogenies of Palaeozoic organisms. Benton et al. (2000), examining how the quality of the fossil record changes through time, found that the Gap Excess Ratio (GER) and Stratigraphic Consistency Index (SCI) of phylogenies containing Palaeozoic organisms were 52.9% and 61.8 % respectively: the same as, or little worse than, those of more recent time periods. In fact the Relative Completeness Index (RCI) of phylogenies of Palaeozoic organisms was 62.064%, considerably higher than those of other time periods. Benton et al. (2000) concluded that the Palaeozoic record, while incomplete, was adequate for study.

Other results, focussing on amniotes and tetrapods in general (clades containing pelycosaurian-grade synapsids) have again found a strong correspondence between phylogenies and stratigraphy. The first such study, performed by Gauthier et al. (1988) using the Stratigraphic Rank Correlation (SRC) coefficient between a taxon's stratigraphic rank and its clade rank, found a significant correspondence for Amniota: 0.679. When the Speamann's rank correlation coefficient method was applied to the same phylogeny, including a reduction of the phylogeny to its various fully pectinate components, a much lower score was obtained (a mean of 0.376) (Norrell and Novacek, 1992). However, when the analysis is limited to synapsids, this is raised to 0.978 (Norrell and Novacek, 1992), suggesting that synapsids have a much better record than that of other amniotes. The SCI of this same phylogeny was found to be 0.74 (Huelsenbeck, 1994). Hitchin and Benton (1997a) applied the SCI, SRC and RCI to a large number of phylogenies of tetrapods, finding a mean SCI of 0.618, mean SRC of 0.58 and mean RCI of 49.8 %. This RCI value was lower than for echinoderms and fish, implying more of the tetrapod record is missing, but the other two metrics were higher than those of fish, indicating a better fit of phylogeny to stratigraphy (Hitchin and Benton, 1997a).

The GER produced in this study from the supertree of pelycosaurian-grade synapsids is 57%, higher than the mean GER of Palaeozoic organisms (Benton et al., 2000). This result is strongly significant according to the randomisation test, in which only 1.69% of randomly permuted trees achieved a higher GER value. The mean SRC of the pectinate components of the supertree was 0.56, only slightly lower than that of other tetrapod phylogenies (Hitchin and Benton, 1997a). While only 36% out of all 107 fully pectinate trees produced from the supertree showed a significant correlation between the record and stratigraphy, it should also be noted that reducing the supertree to all its pectinate components means a large number of very small phylogenies are included in this analysis, which are less likely to show a significant fit. The largest fully pectinate trees that can be obtained from the supertree produce SRC values ranging from 0.56 ($p=0.046411$) to 0.74 ($p=0.0038814$), implying a highly significant fit. The SCI of pelycosaurian-grade synapsids is 0.54, less than that produced for phylogenies of amniotes, tetrapods, and Palaeozoic organisms (Huelsenbeck, 1994; Hitchin and Benton, 1997a; Benton et al., 2000). However, the difference between the results for basal synapsids produced here and those of Hitchin and Benton (1997a) is not great. One should also note the SRC and SCI can only indicate what proportion of nodes is inconsistent, not how inconsistent they are. That information can only be obtained from the GER, which we consider to be a more reliable measure of fit.

The Relative Completeness Index provides a different view of the fossil record of pelycosaurian-grade synapsids. The RCI of the supertree is only 2%. This value, close to 0, implies that the many ghost lineages inferred from the phylogeny cover almost as much time as observed lineages. Comparing the RCI of these basal synapsids to values obtained by other studies is not encouraging. The mean RCI for phylogenies of Palaeozoic organisms is 62.064% (Benton et al., 2000), while that of tetrapods is 49.8% (Hitchin and Benton, 1997a). Despite this, only 1.59% of the randomly permuted trees had a higher RCI value than the supertree.

One can reconcile the disparity in results by looking at the differences in what each of the metrics measure. The SRC, SCI and GER are measures of congruence between a phylogeny and stratigraphy, while the RCI is a measure of completeness. A low value of the former measures can mean either a poor fossil record or an incorrect phylogeny. The poor fossil record may not even be indicated by the SRC and SCI: the simulations of Wagner and Sidor (2000) suggest that these metrics are inappropriate as measures of sampling and that an accurate phylogeny should score reasonably well even if the fossil record is poor. The RCI, however, measures the amount of missing data compared to the amount of observed data, and

does not normalise the implied gap relative to the maximum and minimum possible gap (as does the GER). It is entirely possible for a tree to be perfectly consistent with the fossil record, to have perfect scores in the SRC, SCI and GER, but to have a low RCI score.

Simulations suggest that a low RCI may be a result of an incorrect phylogeny as well as an incomplete fossil record (Wagner, 2000). However the SRC, SCI and GER all suggest that the congruence of the phylogeny to stratigraphy is no worse than in other tetrapod groups, or other clades from the Palaeozoic. This implies that the result of the phylogeny is of no worse quality than others it has been compared to. Therefore in this case it seems more likely that the gaps in the fossil record are to blame for the low RCI score. The completeness of the record of pelycosaurian-grade synapsids is not only low, it is considerably worse than most of the other clades to which the RCI has been applied. The significant p-value obtained from the RCI should not be taken to indicate a significantly complete fossil record; the random permutations used the same age ranges as the observed data. As such, what they are testing is what happens when a fossil record of similar quality is applied to different tree topologies.

It appears that relationships of pelycosaurian-grade synapsids are reasonably well understood. Their phylogeny shows a good congruence with the stratigraphy, comparable to many other clades that have been tested. However it is obvious that there are large gaps in the record, leading to an extremely low Relative Completeness Index. It has not escaped the notice of previous workers on this taxonomic group that the earliest evolution of synapsids is not clear (Romer and Price, 1940; Benson, 2012). With such gaps in our record, it needs to be asked: is the fossil record improving? Or is this record as good as it is going to get?

The Quality of the Fossil Record of Pelycosaurian-Grade Synapsids – Historical Perspectives

The observation that new discoveries do not appear to change the shape of diversity curves has been made before. Maxwell and Benton (1990) compared six databases of vertebrates formed between 1900 and 1987, and found that all databases showed the same global diversity signal, with most of the major events appearing in all six curves. Sepkoski (1993) compared diversity curves formed from his 1982 compendium of marine fossils to those from the next edition in 1992. Despite the addition of over 800 new families, the deletion of nearly 200 invalid families, and more than 2000 stratigraphic alterations, the two curves correlated significantly. Irmis et al. (2013) examined the effect of using different datasets on diversity estimates in the Karoo, including datasets based on collection records

from museums (likely to contain misidentifications and obsolete taxonomy), and datasets updated by different researchers with different interests. Again, all datasets produced a similar diversity signal (although see Bernard et al., 2010, who found noticeable historical changes when examining early tetrapod datasets, and Lloyd and Friedman, 2013, who found fish datasets show highly variable correlations, with some even being negative).

Such a result is supported in pelycosaurian-grade synapsids. Examining the diversity curve pruned to species known 100 years ago (Figure 28), one can still see the events present in the current diversity curve: the rise to an early Sakmarian peak, the trough in the late Sakmarian, a second peak in the early Kungurian, and a decline during the Roadian. The similarities of the present curve with the diversity curve produced from taxa known 50 years ago are striking, with even minor, short-term changes being picked up, such as the brief Gzhelian plateau during the initial radiation. The present diversity curve correlates significantly with the signal obtained including only the taxa known in 1914, 100 years ago. It is only once the dataset has been reduced to taxa known 110 years ago that the correlation becomes insignificant, and by that time the dataset contains only 19 species (Table 4).

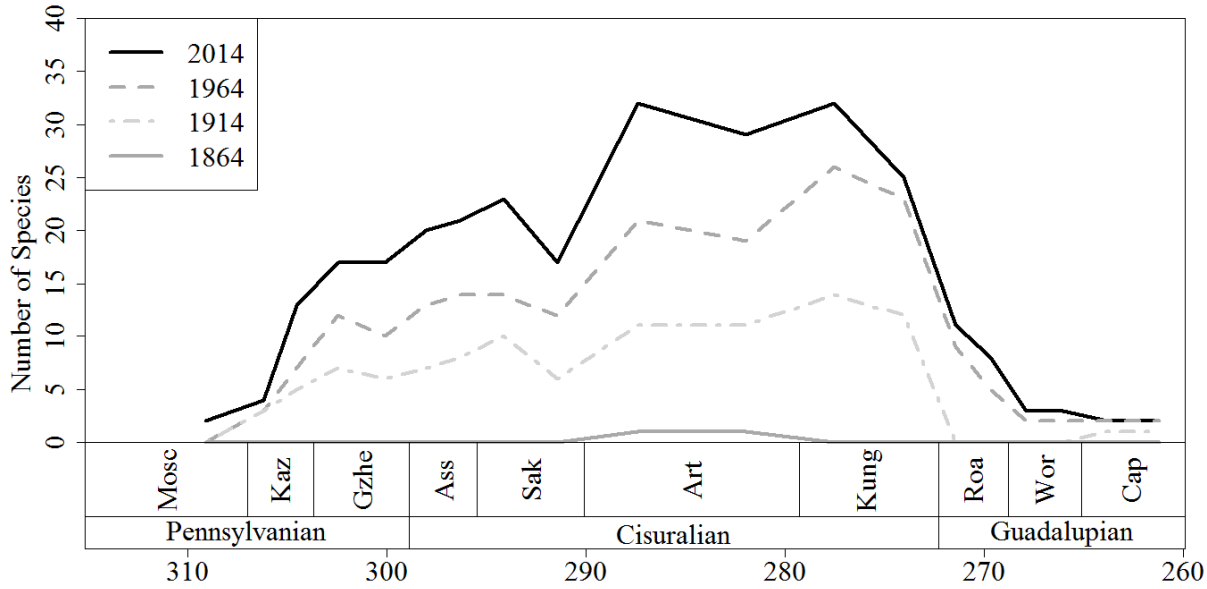

Figure 28: A comparison of the current (2014) taxic diversity curve with pruned taxic diversity curves representing species known in 50-year intervals.

Both Maxwell and Benton (1990) and Sepkoski (1993) concluded that the similarity of the curves produced by databases of different age was an indication that the events shown are genuine; that despite the gaps in our knowledge, real macroevolutionary events are still visible with an incomplete dataset. This cannot be supported when one examines

pelycosaurian-grade synapsids. The extremely low relative completeness index implies an extremely poor record. Moreover evidence for extensive sampling bias, both temporal and geographical, has already been noted for the Early Permian (Benson and Upchurch, 2013). The strong correlation between the number of amniote-bearing formations and diversity (Benson and Upchurch, 2013) suggests that the signal that has been visible for the last 150 years is the signal of sampling biases. There are two explanations for the strong correlation seen between older datasets and the current one: 1) workers have continued to sample well-known collections rather than finding new collections from less well-sampled time periods, or 2) the number of collecting opportunities in the time periods which have, over the decades, continued to produce fewer taxa, are limited by a low number of fossiliferous formations.

While new discoveries may not be altering the shape of diversity curves, it does not necessarily imply new discoveries have no effect on our interpretations of the fossil record. New discoveries can both create and fill gaps in the fossil record. It has been asserted that the fossil record is improving, and that new discoveries are filling gaps, rather than creating them (Benton and Storrs, 1994; Fara and Benton, 2000; but see Tarver et al., 2011). When one examines the RCI curve of pelycosaurian-grade synapsids through historical time, the issue appears to be more complicated. The curve constantly fluctuates, particularly during the earliest years of discovery. The RCI values range from 37% in 1881 to -57% in 1908 (Figure 27).

When making a judgement on whether discoveries are creating or filling gaps, it is unreasonable to include these earliest years of discovery in our examination. While the RCI of the supertree pruned to taxa known in the late 1800s is consistently higher than it is today, and remains so until 1908, this is likely to be an artefact of the low number of known taxa. At the time of peak RCI (1881), only 12 pelycosaurian-grade species were known, of which only 5 have been included in phylogenetic analyses. Moreover, the time period in which these taxa lived was much shorter than the range occupied by taxa known today. As such there was considerably less potential for long ghost lineages, resulting in the much higher RCI values.

It is more sensible to limit the examination to the RCI values since 1914, the time at which enough species were known to produce a diversity curve similar to that of the present day (see above). When one examines the historical RCI curve from this year onward, one can see there has been a trend towards an increase in the RCI from -6% to 2% (Figure 27). Even then, the statement that new discoveries tend to fill gaps in our knowledge should still be considered an oversimplification. Despite the 11 new species discovered in the last 30 years (Figure 28), there has been very little change in the RCI, which has remained between -3 and

3%. This implies that the recent discoveries are creating just as many gaps as they are filling. Periods of great discovery and great increase in the number of species known can fill gaps, such as the discoveries of the late 70s and early 80s which coincide with a rapid increase in RCI. However, such periods of great discovery can also create gaps, such as during the late 1930s, when large increases in the number of species coincide with troughs in the RCI. It should also be noted that it is not only the description of large numbers of species that can cause great change in the RCI; single species can have a large effect. The most obvious example of this is *Archaeothyris florensis*, described in 1972, which extended the age of synapsids back into the Moscovian (Reisz, 1972). This drew back ghost lineages of other clades to this time, causing the RCI to fall from -14 to -21%.

When one considers that the RCI has reached only 2%, it is worrying that the polynomial model applied to the collector's curve appears to suggest that the curve is levelling off, and has been doing so since 1990 (Figure 26). In the past 20 years, only 9 new pelycosaurian-grade synapsid species have been found, compared to 12 in the preceding 20 years and 23 in the 20 before that. The fact that the collector's curve is approaching an asymptote may imply that the limit of what the fossil record has to offer is close to being reached. The RCI indicates that this limit may be extremely low. Alternatively, the asymptote may reflect the current lack of fieldwork in Lower Permian terrestrial sites, limiting most recent discoveries to description of specimens from museum collections (e.g. Reisz and Dilkes, 2003; Reisz 2005; Mazierski and Reisz, 2010; Reisz et al., 2010; Reisz and Fröbisch 2014). It is mostly in the Middle Permian of South Africa, Sardinia and Russia that fieldwork is still producing new specimens of pelycosaurian-grade synapsds (e.g. Botha-Brink and Modesto, 2009; Modesto et al., 2011, Romano & Nicosia, 2014).

Conclusions

While this chapter may present a bleak picture of the basal synapsid fossil record, it is not intended to indicate that the evolutionary history is unknowable. Rather it is meant to highlight the need for sampling correction when examining the patterns of diversity. The results presented in the following chapters need to be examined with the quality of the fossil record kept in mind. The fossil record may be poor, and the events it indicates may be artifacts of bias and incompleteness, but there is a biological signal present in the data. It is simply necessary to apply the required methods to tease out this signal.

Chapter 5

Diversity of Early Synapsids and the Influence of Sampling on their Fossil Record

The identification of diversity patterns through time is an important aspect of the investigation into the macroevolutionary processes occurring in organisms. It enables palaeontologists to determine the major events in the history of the group under study and is also relevant to broader questions, such as the impact and recovery from mass extinctions, the processes underlying evolutionary radiations and the importance of competition and co-evolution. Because of their importance in the establishment of terrestrial ecosystems, several studies have been made of changes in species richness though time in both basal synapsids and other early amniotes. Much of this study has focussed on the later Permian and Triassic, in particular the changes across the Permian-Triassic boundary and the impact of the great mass extinction occurring at this time on amniote evolution (e.g., Sidor and Smith, 2004; Fröbisch, 2008; 2009; Fröbisch et al., 2010; Huttenlocker et al., 2011; Fröbisch, 2013; Irmis et al., 2013). The diversity of tetrapods during the Late Carboniferous and Early Permian has been less well studied, and thus far no study has examined species richness in pelycosaurian-grade synapsids in detail.

Previous Studies into the Diversity of Early Amniotes

The first examination of the changes in diversity of tetrapods including the Early and Middle Permian was by Sahney and Benton (2008). This paper included a diversity curve of tetrapods at the family level from the Artinskian (late Early Permian) until the Early Triassic. No method of sampling correction was used, and there was no examination of the individual clades, although the relative diversity of families of different body sizes and ecologies was examined. While the main focus of this study was the end-Permian mass extinction, there was discussion of the changes in diversity during the late Early Permian and Middle Permian, including the first description of an extinction event at the end of the Early Permian, coinciding with the transition from the pelycosaur-dominated Early Permian fauna to the therapsid-dominated Late Permian fauna (Sahney and Benton, 2008), an event they dubbed Olson's extinction.

The transition between these two faunas has been an issue of some debate. Part of the reason for this has been the argument for a gap in the fossil-bearing rock record of terrestrial vertebrates during the Roadian, dubbed Olson's gap (Lucas and Heckert, 2001; Lucas, 2004; 2006). This gap supposedly separates the pelycosaur-dominated formations in North America from the therapsid-dominated formations in Russia and South Africa, giving very little idea of the timing and causes of the transition. However, this interpretation of the biostratigraphy has

been disputed (Reisz and Laurin, 2001; 2002; Lozovsky, 2005; Liu et al., 2009a; Benton, 2012). Reisz and Laurin (2001) argued that the presence of the parareptile *Macroleter* in both North American and Russian deposits suggested that there was temporal overlap between these formations. These authors argued for a Roadian age for the Chikasha and San Angelo formations in North America, and the Mezen assemblage of Russia. The link between these faunas was supported by Lozovsky (2005), who argued for a "bridge" between Russia and North America at this time, allowing easy dispersal between the two. Liu et al. (2009a) maintained that the presence of basal therapsids in the Xidagou Formation of China supported a Roadian age for this fauna.

Kemp (2006) put forward a biogeographic hypothesis for the transition. He pointed out that the Lower Permian pelycosaur-dominated fauna is known almost entirely from North America and western Europe, then in equatorial positions, while the Middle Permian therapsid-dominated fauna is known almost entirely from the palaeotemperate localities of Russia and South Africa. Attention was also drawn to the climate changes occurring at the time of the transition: the equatorial tropical everwet biome which had sustained the pelycosaur-dominated fauna disappeared, to be replaced with a desert belt (Rees et al., 2002). Kemp (2006) hypothesised that the elimination of the tropical everwet biome forced terrestrial ecosystems to move towards the temperate latitudes, where the therapsids, with their advanced physiology and metabolism, were better able to survive in this more seasonal environment. However, doubt is cast on the idea that the Middle and Upper Permian faunas were restricted to palaeotemperate regions by the recent work on the Moradi Formation of Niger, which has yielded a diverse Upper Permian palaeoequatorial fauna (Sidor et al., 2003; O'Keefe et al., 2005; Sidor et al., 2005; Damiani et al., 2006; Steyer et al., 2006; Smiley et al., 2008; Sidor, 2013; Tsuji et al., 2013).

Sahney and Benton (2008) were the first to recognise that transition between the two faunas may have been a period of mass extinction amongst tetrapods, dubbed Olson's extinction (Figure 29B). During the Artinskian and Kungurian, they found two thirds of families were lost, along with a loss in the number of occupied ecological guilds. Recovery began almost immediately, but was interrupted by a second extinction event at the end of the Middle Permian (Sahney and Benton, 2008). Both these extinctions changed the Permian faunas, both in terms of clades and ecological guilds present, and also the degree of endemism; the Upper Permian and Lower Triassic faunas were considerably more provincial than those at the end of the Early Permian (Sahney and Benton, 2008).

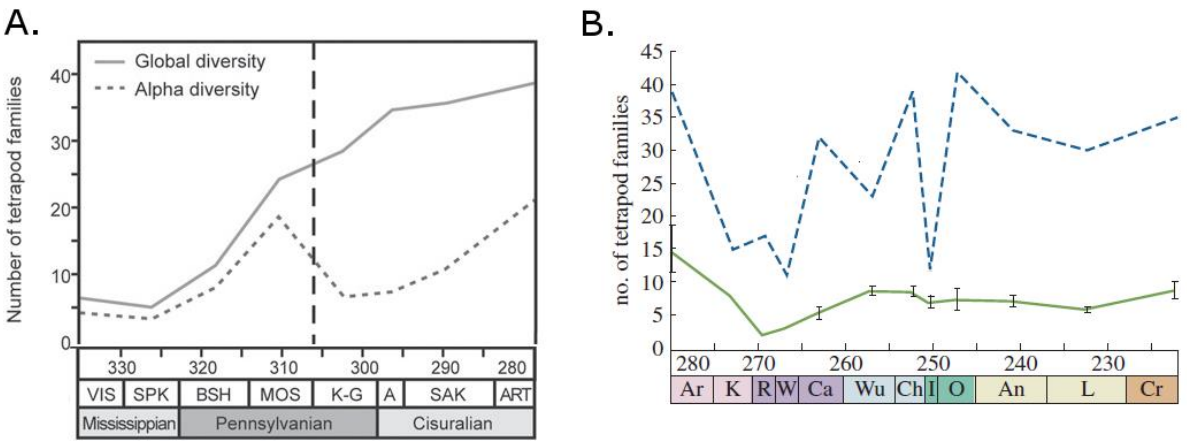

Figure 29: Family level diversity curves of tetrapods. A) Global (solid line) and alpha (dashed line) diversity of tetrapods from the Carboniferous until the earliest Permian, from Sahney et al. (2010); B) Global (dashed line) and alpha (solid line) diversity of tetrapods from the latest Early Permian until the end of the Triassic. From Sahney and Benton. (2008).

Sahney et al. (2010) expanded on this earlier study, examining family-level tetrapod diversity during the Carboniferous and Early Permian (Figure 29A). This study focussed on the impact of the collapse of rainforests on the diversity of tetrapods. During the Pennsylvanian, North American and Europe were positioned at the equator and covered in tropical rainforest (DiMichele et al., 2006). It was in these "Coal Forests" that the earliest amphibians and basal amniotes diversified. However, towards the end of the Carboniferous, the aridification of the climate lead to the decline and fragmentation of these rainforests and the development of more seasonal ecosystem based on ferns and tree-ferns (DiMichele and Philips, 1996; DiMichele et al., 2006). The diversity curve of tetrapod families shows that, while family richness increased gradually during the Late Carboniferous and Early Permian, the diversity within each locality (alpha diversity) drops sharply during the Kazimovian and Gzhelian (Sahney et al., 2010). A drop in alpha diversity, with no substantial change in global diversity (Figure 29A), was interpreted as an increase in endemism following the fragmentation of the rainforest (Sahney et al., 2010). Amphibians suffered widespread extinction, while amniotes, and in particular synapsids, diversified (Sahney et al., 2010). The relative success of amniotes was assumed to result from the amniotic egg and scales, both of which allowed water retention in the drier, more seasonal environment (Sahney et al., 2010).

In 2012, Benton undertook a thorough re-examination of Permian biostratigraphy and geological biases affecting the terrestrial fossil record at this time (Benton 2012). This study also included the first genus-level diversity curve of Permian amphibians and amniotes. Benton (2012) argued that geological biases were not substantially affecting the diversity

estimates of tetrapods during the Permian. No evidence of Olson's gap was found, and no significant correlation was seen between the number of tetrapod-bearing formations and the genus-level diversity. As such, it was argued that the raw data was adequate for inferring diversity patterns. Benson and Upchurch (2013) opposed this interpretation of the record. By fitting multivariate models to the observed diversity data (this time at the species level), it was found that tetrapod diversity was best explained as being a composite of sampling and genuine diversity change. A strong relationship between the sampling proxy and observed diversity was found (Benson and Upchurch, 2013). The lack of a significant correlation between diversity and number of formations found in Benton (2012) was judged to be due to the use of inappropriate measures to correct for autocorrelation.

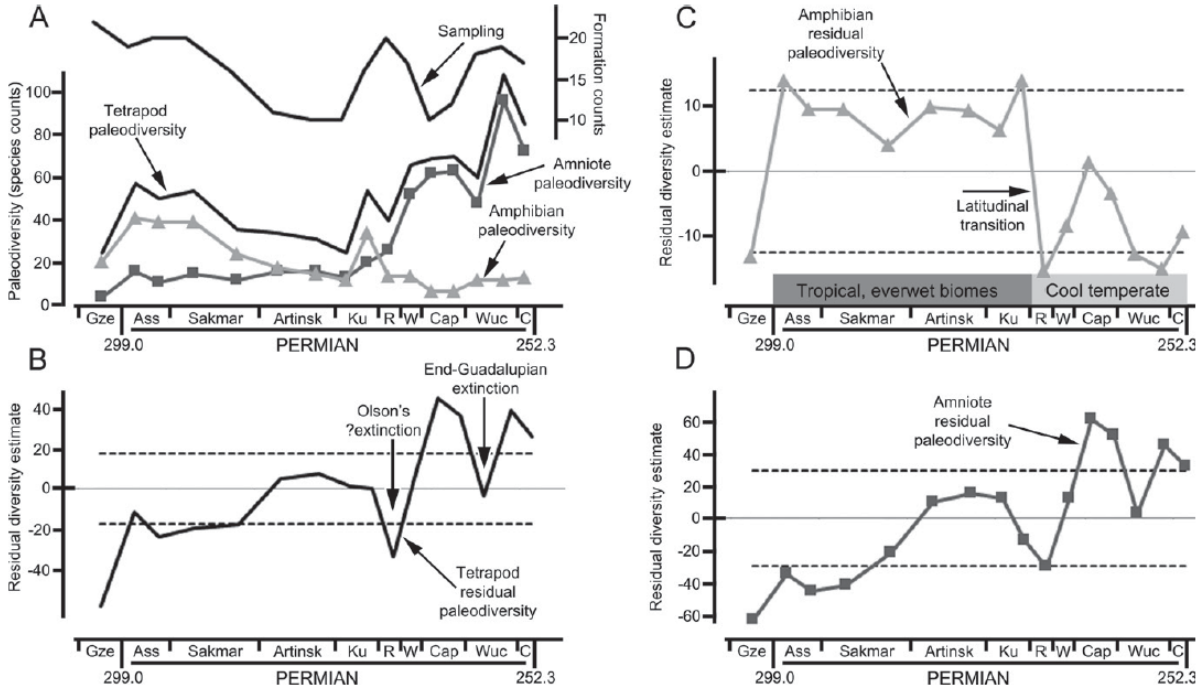

Figure 30: Diversity estimates of tetrapods, from Benson and Upchurch (2013). A) Taxic diversity estimates of tetrapods, amniotes and amphibians, and sampling represented by number of formations; B) Residual diversity estimate of tetrapods; C) Residual diversity estimate of amphibians; D) Residual diversity estimate of amniotes.

The raw diversity data in Benton (2012) and Benson and Upchurch (2013) both show evidence of a diversity decrease across the Kungurian/Roadian boundary (Figure 30A), providing further support for Olson's extinction. When examining the raw data, it is only the amphibians which suffer in the extinction; amniotes in fact increase in diversity throughout the latest Early Permian and Middle Permian. Benson and Upchurch (2013) also presented a sampling-corrected diversity estimate using the residual diversity estimate (see Chapter 1), which supports a significant diversity decrease across the Kunguian/Roadian boundary

affecting both amphibians and amniotes (Figure 30C, D). However, these authors still argued against Olson's extinction being a genuine event, reasoning that the observed decrease in diversity is an artefact of the geographic shift in the fossil-bearing localities. As mentioned above, our knowledge of the terrestrial realm during the Early Permian is restricted to the then equatorial localities in North America and western Europe, while during the Middle Permian, the record abruptly shifts to the palaeotemperate localities of South Africa, South America, Russia, and China. It is possible that the apparent extinction merely reflects a latitudinal biodiversity gradient: prior to the Kungurian/Roadian boundary diverse equatorial faunas are sampled, while after the boundary the more species-poor temperate localities are sampled (Benson and Upchurch, 2013). The residual diversity estimate would not correct for such a bias, as it assumes a linear relationship between sampling and number of species found, an assumption violated by spatial variations in diversity.

The evolution of herbivores during this early stage in amniote evolution has been a point of considerable interest, due to their importance in the establishment of early terrestrial ecosystems and the morphological innovations with which this new diet was explored (Olson, 1966; Sues and Reisz, 1998; Reisz and Sues, 2000). A recent study examined the changes in the global diversity of early herbivores, as well as the changing patterns within individual herbivorous clades (Pearson et al., 2013). Sampling correction was carried out using residuals, with tetrapod bearing formations as a sampling proxy. The earliest appearance of herbivores in the fossil record coincided with the collapse of rainforests described by Sahney et al. (2010). However no massive increase in the diversity of herbivores is found to have occurred at this time in either the raw or sampling corrected diversity curves (Pearson et al., 2013). Sahney et al. (2010) had argued that the fragmentation of the rainforest into isolated "islands" had resulted in the simultaneous independent evolution of herbivory. This hypothesis was rejected by Pearson et al. (2013), who demonstrated that the diversity of herbivores increased gradually during the late Pennsylvanian and Early Permian, with new herbivorous clades appearing throughout this time. This study also found little evidence for Olson's extinction; neither the raw nor sampling corrected diversity estimates show a significant decline in diversity across the Kungurian/Roadian boundary. Following Benson and Upchurch (2013) in arguing that any apparent extinction is an artefact of the latitudinal shift in the record, Pearson et al. (2013) suggested that the hypothesised latitudinal biodiversity gradient was less pronounced in herbivores. Alternatively they suggested that differences in the timescale used might have affected the results. Benson and Upchurch (2013) used substages as the time bins, whilst Pearson et al. (2013) used the Land Vertebrate Faunachrons (time bins defined by

terrestrial vertebrate biostratigraphy). Interestingly, the taxic diversity estimate of herbivorous tetrapods does not correlate significantly with the number of tetrapod-bearing formations (Pearson et al., 2013) leading the authors to suggest that a strong biological signal was present in the dataset. They still argued that sampling correction was necessary; although the signal from the data contains a large "genuine" diversity signal, this did not mean that sampling has had no effect on the fossil record. The differences between the taxic diversity estimate and residual diversity estimate were small but were potentially important (Pearson et al., 2013).

The most recent global examination of changes in species richness among tetrapods during the Late Carboniferous and Early Permian was that of Benton et al. (2013), compiled using the early tetrapod database. Taxic diversity estimates at the genus level were compiled for tetrapods as a whole, as well as for amniotes and amphibians, from their earliest appearance in the Middle Devonian until the Early Jurassic. This study also included extensive discussion into the use of sampling proxies such as number of formations to assess and correct for sampling biases. During the period under study in this thesis (Late Carboniferous-Middle Permian), two major extinction events were identified. The first is a major drop in amphibian diversity at the end of the Moscovian as identified by Sahney et al. (2010), coinciding with the breakdown of rainforests and increased seasonality of the climate. The second, Olson's extinction, was recovered as a gradual decline in diversity throughout the Early Permian rather than the single mass extinction event recovered by previous studies (Sahney and Benton, 2008; Benson and Upchurch, 2013). There was also no evidence of a decline found in amniotes, whose diversity rose gradually to a Wordian peak (Benton et al., 2013). Amphibian diversity remained low and reasonably constant for the rest of the Permian, while the diversity of amniotes fluctuated greatly, with peaks in the Wordian and mid Capitanian separated by a substantial trough.

No attempt was made to correct for sampling biases in this study, although significant correlations were found between the diversity of tetrapods and the number of tetrapod-bearing formations. Investigation was made into the completeness of the tetrapod fossils using a grading system from 1-4: a grade of 1 was represented by a single bone, 2 by more than one bone, 3 by a single nearly complete specimen and 4 by more than one nearly complete specimen. A mean completeness score was calculated for each time bin, and also a ratio of good material (number of taxa graded 2-4) to the total amount of material. The completeness score was found to correlate significantly with amniote diversity but not with tetrapod diversity as a whole or the diversity of amphibians (Benton et al., 2013), possibly indicating that the different environments in which amphibians and amniotes lived affected the quality

of the preservation. On the whole, the mean completeness of tetrapod specimens was high, remaining above 3 for most of the Carboniferous and Permian, with more than 50% of fossils classed as "good" in most time bin throughout this period.

As has been seen, considerable debate surrounds many areas of early amniote evolution. As one of the most diverse and abundant clades during the Late Carboniferous and Early Permian, a detailed examination of the changes in species richness of synapsids during the time period occupied by the pelycosaurian-grade synapsids would be a vital addition to discussions of tetrapod evolution at this time. Moreover, although a few of the previous studies have employed sampling correction, its use has been patchy and limited to the residual diversity estimate. The analyses described in Chapter 4 give clear indications that the fossil record of basal synapsids is incomplete and that correction for sampling bias is necessary. Moreover, as mentioned in the introduction, all methods of sampling correction have their advantages and disadvantages. Here multiple methods are used and compared in order to provide as thorough an assessment of synapsid diversity as possible.

Materials and Methods

Raw Data and the Taxic Diversity Estimate

The comprehensive database of all synapsid species, both pelycosaurian-grade and therapsid, from the late Moscivian until the late Capitanian described in Chapter 3 was employed in this study. A taxic diversity estimate was generated by counting the number of species and genera present in each time bin (including Lazarus taxa). Such diversity curves were compiled for all synapsids, pelycosaurian-grade synapsids, therapsids, Caseasauria, Ophiacodontidae, Sphenacodontidae, Varanopidae and Edaphosauridae. As mentioned in Chapter 3, two sets of ages had been applied to each taxon: one in which, if a taxon's age could not be constrained, it was included in the full range of possible time bins; one in which each locality was restricted to two substages or less. While the former method does lead to less resolution (certain taxa known from a single specimen or locality will be found in more than one time bin), it has been demonstrated that, as long as the stratigraphic uncertainties are randomly distributed, the diversity signal will not be false, but merely "dampened" (peaks and troughs become less extreme) (Raup, 1991; Smith, 2001). A second taxic diversity curve was produced from the second set of ages. However, for the reasons given, this curve is

considered less reliable and, though the differences between the two curves will be noted, the curve that takes into account the uncertainty will form the basis of the discussion.

The Residual Diversity Estimate

The residual diversity estimate, the modelling approach to sampling correction described in Chapter 1, was calculated using the recent update of the method proposed by Lloyd (2012) which allows non-linear relationships between sampling the sampling proxy and the observed diversity to be taken into account, and allows confidence intervals to be placed around the data to indicate which peaks and troughs are significant. The sampling proxy used was the number of amniote-bearing collections (sensu Benton et al., 2011) in each time bin, collections being considered to be a proxy for human sampling effort (Alroy et al., 2001; Crampton et al., 2003; Alroy et al., 2008; Butler et al., 2011a). Data on this proxy was downloaded from the Paleobiology Database (http://paleodb.org) in June 2012 and was supplemented with data from the published literature. The Spearman's rank and Kendall's Tau correlation coefficients, implemented in R, were used to compare the taxic diversity estimate of synapsids to the proxy, to ascertain the impact of biases on the fossil record, after transforming the time series using generalised differencing. Amniote-bearing collections were used instead of synapsid-bearing collections to mitigate the concerns reported by Benton et al (2011): redundancy and non-occurrences (see Chapter 1). This proxy includes instances where searches have been made in rocks producing closely related taxa, but not synapsids have been found, thus taking into account non-occurrences. This method also deals with the issue of redundancy: if the diversity of synapsids decreased, one would expect there to be less synapsid-bearing collection, but not necessarily less amniote-bearing collections.

Residual diversity curves were generated in R, using the functions made available online by Lloyd (2012), for Synapsida, Caseasauria, Varanopidae, Ophiacodontidae, Sphenacodontidae, Edaphosauridae and Therapsida. Geological influences on sampling were not tested; while it is possible that the area of rock outcrop of a particular age may influence opportunities to find fossils (Smith, 2001; Crampton et al., 2003; Smith and McGowan, 2008; Wall et al., 2009), there is little data on this proxy from this time period (but see Fröbisch, 2013; 2014, for a regional perspective on the South African Karoo Basin). An alternative might be to use the number of formations (Fröbisch, 2008; Barrett et al., 2009; Butler et al., 2009; Benson et al., 2010; Mannion et al., 2011; Benson and Upchurch, 2013). However, formations are very much artificial subdivisions, and it is somewhat arbitrary where one

begins and the other ends. The impact of the length of time bin was also examined; in a longer interval, there is more time for sediment to be laid down and a higher probability of preservation (Miller and Foote, 1996). In this case, no significant correlation was found between the length of the substages and the diversity (Table 6), so no correction was made for this.

The Phylogenetic Diversity Estimate

The second method used to correct for sampling bias was the phylogenetic diversity estimate. As described in Chapter 1, this method incorporates ghost lineages inferred from a phylogeny into the diversity estimate in order to take into account missing portions of the fossil record. The supertree produced in Chapter 3 was used to infer a phylogenetic diversity estimate for synapsids as a whole, and also for Caseasauria, Varanopidae and Edaphosauridae (none was constructed for Ophiacodontidae or Sphenacodontidae as too few species from these families have been tested in a phylogenetic context). A second phylogenetic diversity estimate for all synapsids was generated using the second set of ages, where localities of uncertain age were restricted to two or less substages. As noted above, this curve is considered less reliable and the discussion will primarily be based on the curve produced from the set of ages taking into account uncertainty in dating.

One caveat should be noted when generating phylogenetic diversity curves: the presence of unresolved polytomies in the phylogeny can affect these curves. Moreover, the polytomies do not produce a random error, but instead a bias towards higher diversity, since all taxa in the polytomy will have ghost lineages extending back as far as the oldest taxon (Upchurch and Barrett 2005). Several options exist on how to deal with polytomies. The first is to produce separate diversity curves for all possible trees to ascertain if they differ. For this study this is clearly an unrealistic option, as the analysis produced hundreds of most-parsimonious trees. Alternatively one can select a preferred most-parsimonious tree and base the phylogenetic diversity estimate on that. This decision suffers from being highly arbitrary, depending on the personal preferences of the researcher. Finally, one could prune taxa from the tree until a fully resolved tree remains. However, when polytomies contain many taxa or even entire families, removing them will greatly reduce the number of taxa, and therefore the reliability of the phylogenetic diversity estimate. It was decided to keep polytomies in the supertree and include the relevant ghost lineages in the phylogenetic diversity curve. Time intervals where this may have affected the results will be noted.

Results

Sampling Bias in the Early Synapsid Fossil Record

The taxic diversity estimate shows very close correlation with the number of amniote-bearing collections (Table 6). If collections are accepted as a proxy for sampling effort, then there is a clear bias in temporal sampling, which is affecting the taxic diversity curve. For example, the early Capitanian is the most extensively sampled substage (239 amniote-bearing collections), and has produced the most synapsid taxa (63 species in 59 genera). There is also significant spatial bias. Of those species known from the Pennsylvanian and Cisuralian, only 17% were found outside North America, and all of those 17% are from Europe. In the Guadalupian, by contrast, 79% of known species have been found in South Africa and Russia (the remainder from the USA, Brazil and China). These spatial biases indicate huge gaps in our knowledge of synapsid diversity, although whether this is due more to biases in sampling (a preference for looking in rocks where amniotes of a particular age are known to be found) or a lack of fossiliferous rocks of a particular age in a particular area is yet to be seen. Nevertheless, it is clear that correction for sampling is necessary in this study.

Statistical Test	Spearman's ρ	Kendall's τ
Number of synapsid species vs Number of amniote-bearing collections.	0.76667 (p=0.0012867) *	0.60234 (p=0.0031394) *
Number of synapsid species vs Length of time bin.	-0.10526 (p=0.66801)	-0.099415 (p=0.55201)
Number of synapsid species (total dataset) vs Number of synapsid species (pruned dataset containing only taxa present in the supertree).	0.75263 (p=0.00020063) *	0.60234 (p=0.00031394)*

Table 6: The correlations between selected variables, tested by Spearmann's ρ and Kendall's τ. Significant correlations (p=0.05) are highlighted with an asterix

Taxic Diversity Estimates

The earliest synapsid family to appear in the fossil record, and the only family present in the late Moscovian, was Ophiacodontidae, represented by *Archaeothyris florensis* (Reisz

1972). *Echinerpeton intermedium* (Reisz, 1972) is from the same time interval, but cannot be constrained phylogenetically (see Chapter 2). Ophiacodontidae is also the only family present in the early Kasimovian. Varanopidae, Edaphosauridae and Sphenacodontidae appeared in the late Kasimovian (Romer, 1945; Reisz and Dilkes, 2003; Mazierski and Reisz, 2010) and diversified during the early Gzhelian. The earliest caseid caseasaur (*Eocasea martini*) first appears in the fossil record at a similar time, but later members do not appear until later in the Cisuralian, producing a long ghost lineage within this clade. The earliest member of Eothyrididae (one of the two families within Caseasauria) is *"Mycterosaurus" smithae* (see Chapter 2), found in sediments of uncertain age but probably Asselian or Sakmarian.

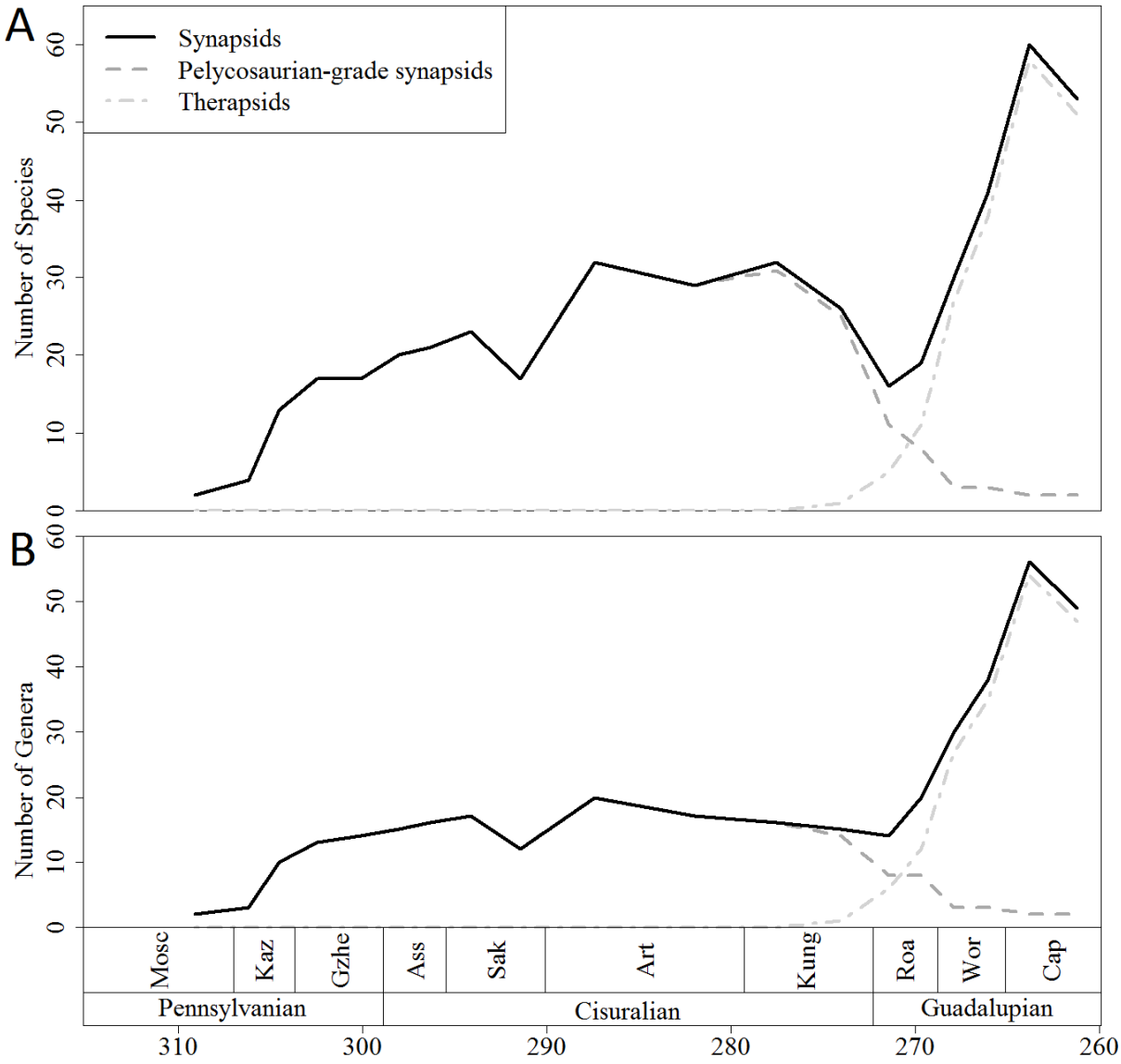

Figure 31: Taxic diversity curves of Synapsida, Therapsida and pelycosaurian-grade synapsids at A) the species level, and B) the genus level.

The taxic diversity estimate (Figure 31) shows these Carboniferous radiations with a continuous rise from two species in the late Moscovian to 16 by the end of the Gzhelian. The most diverse families during the Carboniferous are Ophiacodontidae, with a maximum diversity of four species in as many genera present during the late Gzhelian, and Varanopidae, with four species in three genera in the same substage (Figure 32A, B). Caseasaurs and varanopids both have considerably higher phylogenetic diversity estimates than taxic diversity estimates at this time, indicating many unsampled ghost lineages at this time (Figure 32B, E)

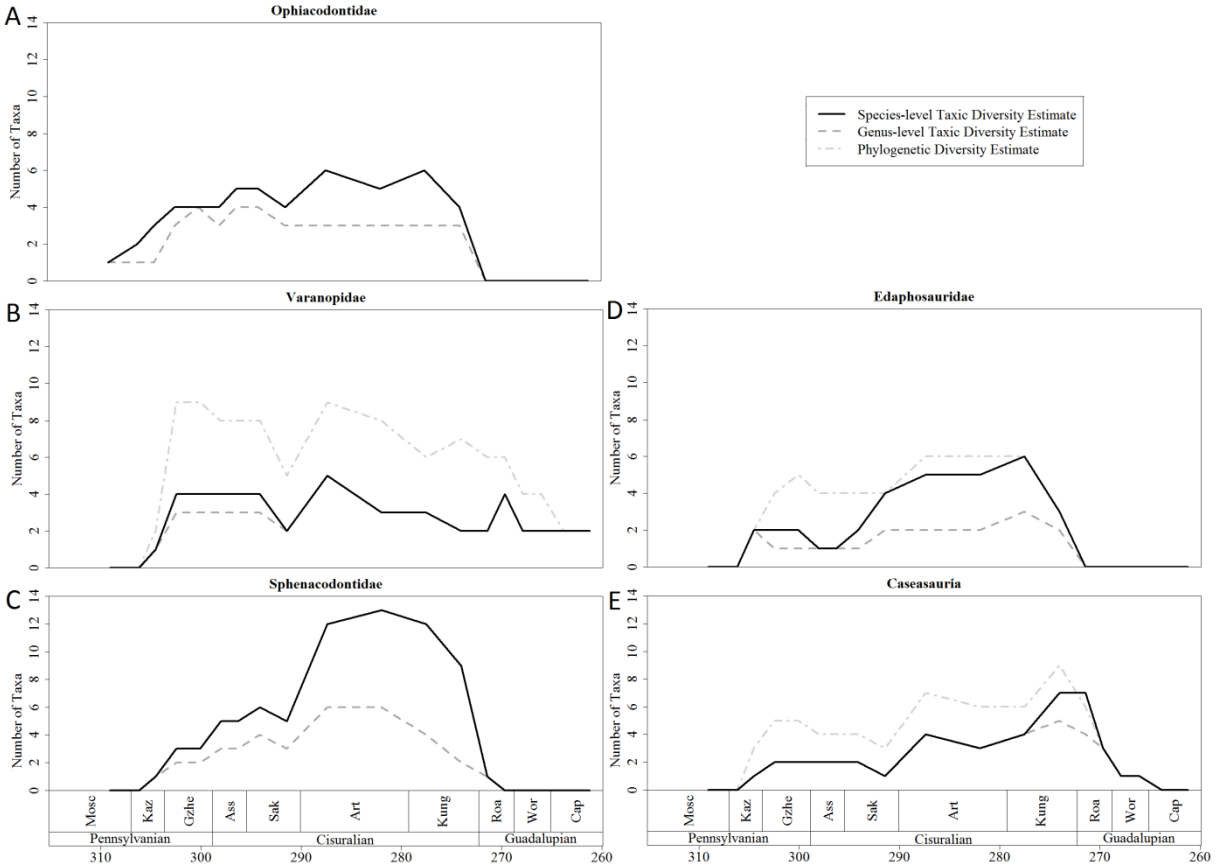

Figure 32: Species and genus-level taxic diversity curves and phylogenetic diversity curves (grey dashed-dotted) of: (A) Ophiacodontidae, (B) Varanopidae, (C) Edaphosauridae, (D) Sphenacodontidae and (E) Caseasauria.

The taxic diversity curve indicates that this radiation continues into the early Cisuralian, reaching a peak in the early Sakmarian of 23 species in 17 genera. Between the early and late Sakmarian, diversity falls to just 13 species in 11 genera. This fall in diversity is visible in all families with the exception of Edaphosauridae, whose diversity actually continues to increase between the two substages (Figure 32C).

The diversity of all clades recovers during the early Artinskian. Sphenacodontidae became considerably more diverse (Figure 32D), particularly with the radiation of the genus

Dimetrodon (five new species of this genus originate in the Artinskian). The herbivorous caseid caseasaurs also appear at this time, with three species known from the Artinskian. *Euromycter rutenus* and *Ruthenosaurus russelorum* (Sigogneau-Russell and Russell, 1974; Reisz et al., 2011) have been found in the Grès Rouge group of France. The age of this group is debated (Rolando et al. 1988), but is thought to be Artinskian-Kungurian. Meanwhile the age of the Richards Spur Locality, Oklahoma, which has produced the basal caseid *Oromycter dolesorum* (Reisz, 2005), has been radiometrically dated to the earliest Artinskian: 289 ± 0.68 Mya (Woodhead et al., 2010).

The taxic diversity of synapsids continues to rise to an early Kungurian peak of 29 species in 16 genera, but the composition of the faunas begins to change. Ophiacodontidae, Edaphosauridae, Varanopidae and Sphenacodontidae begin to decline between the early and late Kungurian, although Sphenacodontidae remain the most diverse synapsid family, with 12 species known from the early Kungurian and nine from the late. The diversity of Caseidae increases to a peak of seven species in the late Kungurian (Figure 32B, E). The earliest therapsid, *Tetraceratops insignis* (Matthew, 1908; Laurin and Reisz, 1990; 1996; Amson and Laurinm 2011), appears in the late Kungurian. It should be mentioned that the youngest species of Eothyrididae, *Eothyris parkeyi* (Romer, 1937), is found in early Kungurian sediments. After this time bin, the diversity curves of Caseasauria relate only to Caseidae.

Across the Kungurian/Roadian boundary, an interval of extinction is visible, and diversity falls from 26 synapsid species in the late Kungurian to 16 in the early Roadian (Figure 31A). Interestingly the number of genera only falls by one (Figure 31B), possibly due to the large number of polyspecific genera from the Kungurian. Ophiacodontidae and Edaphosauridae disappear from the record across this boundary, and the number of sphenacodontid species falls to one (Figure 32B). The number of caseid and varanopid species does not decrease, remaining at seven and two respectively (Figure 32D, E). There is no extinction visible in therapsids, whose diversity increases from one species in the late Kungurian to five in the early Roadian (Figure 31). Between the early and late Roadian, there is further extinction among the pelycosaurian-grade synapsids. Sphenacodontidae die out, and the number of caseid species falls to three. However, Varanopidae show no decline (Figure 32B) and the number of therapsid species continues to increase (Figure 32). The total diversity of synapsids increases to 19 species (Figure 31).

Thereafter, synapsid diversity rises rapidly and continuously to an overall peak in the early Capitanian of 59 species in 55 genera, before the number of species drops to 52 in the late Capitanian. During this period, the number of therapsids increases to a peak of 57 species

in the early Capitanian, but the number of pelycosaurian-grade synapsid species falls to two. No caseids are known after the Wordian, but varanopids survive beyond the study interval.

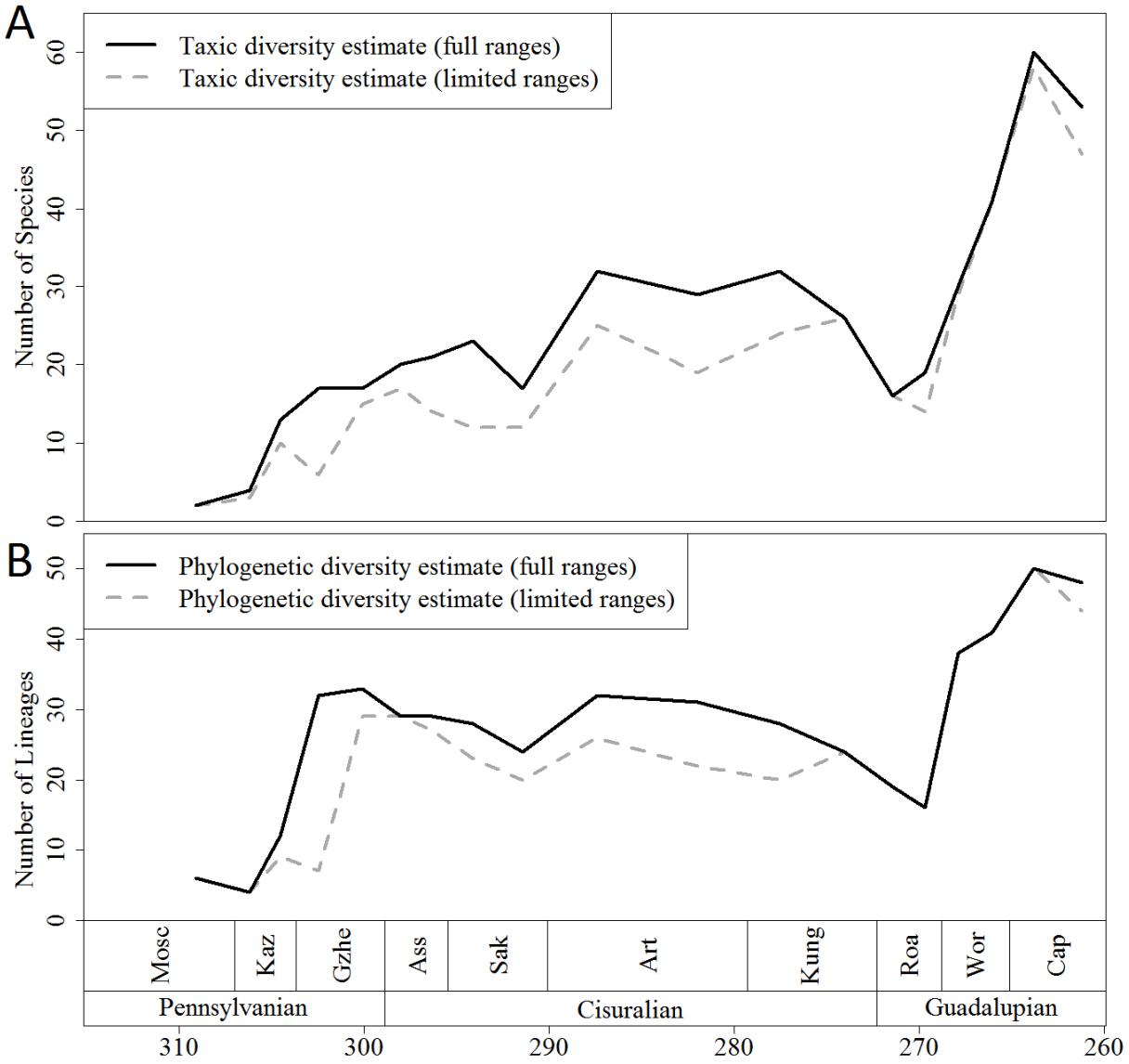

Figure 33: The diversity curves produced when taxa of uncertain age are assigned to the full possible stratigraphic range (dashed-dotted lines) compared to the diversity curves produced when each locality of uncertain ages is restricted to two or less time bins (solid line). A) Taxic diversity curves. B) Phylogenetic diversity curves. Timescale representing millions of years ago appears at the bottom.

The taxic diversity estimate produced using the dataset in which localities of uncertain age are restricted to two or less time bins (Figure 33) shows an extremely similar signal to the curve already discussed, which incorporates the uncertain ages and is thus considered more reliable. Both show a diversity increase during the Late Carboniferous, a trough during the late Sakmarian, recovery from this trough during the Artinskian, a decline across the

Kungurian/Roadian boundary and a peak during the Capitanian. There are, however, noticeable differences. The Late Carboniferous rise occurs in a more step-wise fashion, with a decline in the early Gzhelian (many localities dated as Gzhelian in the dataset incorporating uncertain ages are restricted to the late Gzhelian when the greater temporal resolution is applied). Also the decline to the late Sakmarian trough occurs more gradually when the greater resolution is applied as a number of localities are removed from the late Sakmarian.

Phylogenetic Diversity Estimate

The reliability of the phylogenetic diversity estimate depends on the phylogeny containing a high enough proportion of taxa to be representative of the whole. It also requires that taxa missing from the phylogeny be randomly distributed, rather than concentrated in a particular time bin. In order to test that these requirements are not violated, a pruned taxic diversity estimate was produced, including only taxa present in the supertree. This correlates significantly with the complete taxic diversity estimate (Table 6), indicating that a representative sample of taxa is present in the supertree.

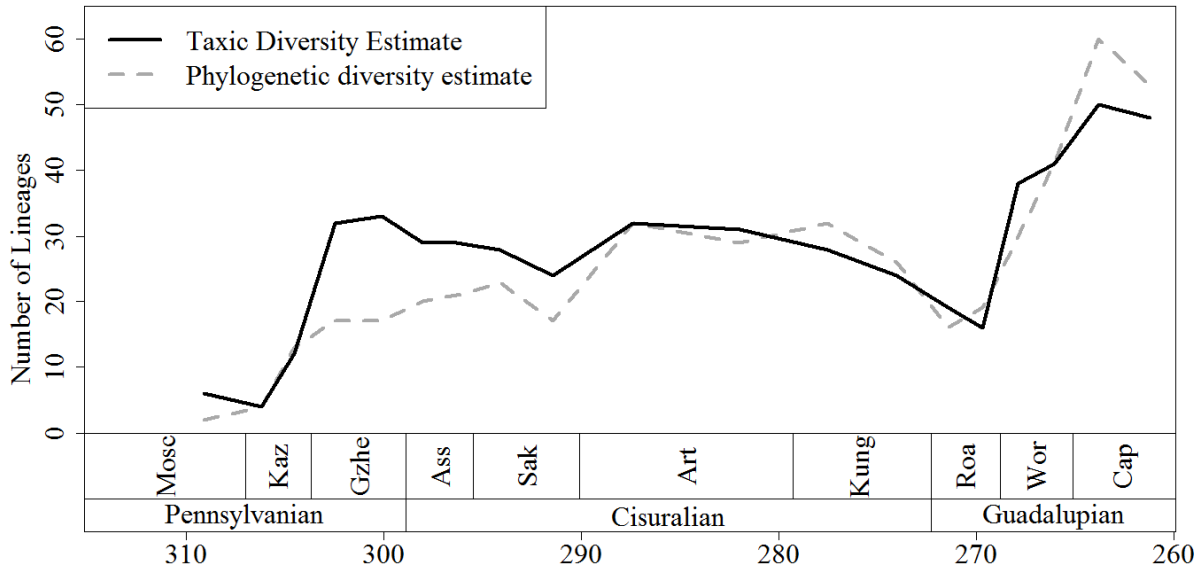

Figure 34: A comparison of the phylogenetic and species-level taxic diversity estimates of Synapsida.

The phylogenetic diversity estimate (Figure 34) begins with a slight decline from five lineages in the late Moscovian to four in the early Kasimovian, due to the lack of phylogenetically tested Kasimovian species, after which there is a rapid rise, reaching 30 lineages in the late Gzhelian. This Gzhelian peak coincides with a peak in the phylogenetic

diversity of Varanopidae (nine lineages) and Edaphosauridae (five lineages) (Figure 32B, C). During the early Cisuralian, the phylogenetic diversity curve indicates a slight but steady decline to a late Sakmarian trough of 20 lineages. As in the taxic diversity estimate, the recovery occurs during the early Artinskian, and for the rest of the Cisuralian diversity remains between 23 and 25 lineages. It is, however, possible that the lack of species-level phylogenies of the two most speciose genera (*Dimetrodon* and *Ophiacodon*) has lowered the phylogenetic diversity during the Artinskian and Kungurian, the time that most of these species are known from. The diversity of Caseasauria increases to six lineages in the early Artinskian (Figure 32E), as the position of *Euromycter rutenus* in the supertree causes several caseid ghost lineages to be drawn back into this bin. Caseidae reach their highest phylogenetic diversity of eight lineages in the Late Kungurian.

Like the taxic diversity curve, the phylogenetic diversity curve indicates that diversity declined across the Kungurian/Roadian boundary from 23 to 18 lineages (Figure 34). Declines in diversity are experienced by Caseidae and Varanopidae, while Edaphosauridae go extinct as indicated by the taxic diversity curve (the phylogenetic diversity estimate cannot extend the ranges of lineages forward from their last occurrence, so the possibility that these families survived beyond their last appearance cannot be tested). Meanwhile, the presence of *Microsyodon orlovi* (Ivakhnenko, 1995) in Roadian sediments draws several therapsid ghost lineages back into the Roadian. However, unlike the taxic diversity curve, the extinction continues into the late Roadian, when the number of lineages falls to 16.

As in the taxic diversity estimate, the phylogenetic diversity estimate rises to a peak in the early Capitanian of 49 lineages, before declining in the late Capitanian to 47 (Figure 34). During this time, both Varanopidae and Caseidae decrease in diversity; Caseidae decline from three lineages in the late Roadian, to one in the Wordian, and none in the Capitanian, while Varanopidae decline from six lineages to four and two in the same intervals (Figure 32B, E).

The phylogenetic diversity curve produced when the ages of localities are restricted to two less time bins (Figure 33) is extremely similar to the estimate in which temporal uncertainty is taken into account. The only noticeable difference between the two is that rapid rise in phylogenetic diversity occurs in the late Gzhelian when greater temporal resolution is applied. As mentioned previously, when greater temporal resolution is applied, localities previously dated as Gzhelian are restricted to the late Gzhelian.

Residual Diversity Estimate

The residual diversity estimate (Figure 35) indicates a rise from an early Kasimovian trough to a significant peak in the late Kasimovian. Ophiacodontidae and Varanopidae both show significant increases (Figure 36A, B). A second peak in the residual diversity curve occurs in the early Sakmarian, immediately followed by a decline to a significant trough in the late Sakmarian. This extinction event affects all clades with the exception of Edaphosauridae, which, as shown in the taxic diversity curve, increase in diversity between the early and late Sakmarian (Figure 36C). Residual diversity recovers during the Artinskian. The variation in residual diversity remains within confidence limits between the late Artinskian and late Kungurian, indicating no substantial changes in diversity of synapsids, although the residual diversity of Caseasauria increases significantly (Figure 36E).

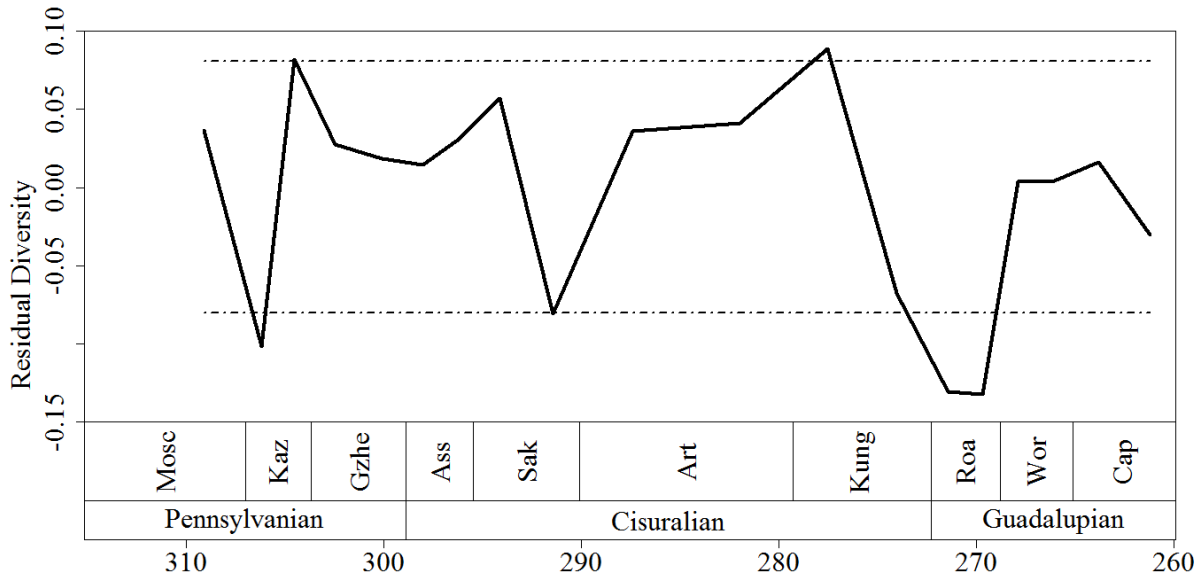

Figure 35: The residual diversity estimate of Synapsida (solid black) with 95% confidence intervals based on the standard deviation of the model (dashed-dotted lines). 3: A comparison of the phylogenetic diversity estimate and species-level taxic diversity estimate of Synapsida.

A significant decrease in residual diversity occurs across the Kungurian and Roadian boundary (Figure 35). The residual diversity of Sphenacodontidae shows a similar decline (Figure 36D), but that of Caseidae and Therapsida reach their peak diversity during the early Roadian (Figure 36E, F). No significant change is seen in the diversity of Varanopidae (Figure 36B). Unlike the taxic diversity, residual diversity does not recover during the late Roadian, instead decreasing to its lowest value in the interval under study (Figure 35). After

this time, the residual diversity estimate contains signals from only therapsids, caseids and varanopids.

The residual diversity of synapsids increases between the Roadian and Wordian (Figure 35), after which no significant change is seen. The diversity of Caseidae falls from their early Roadian peak until their last appearance in the fossil record during the late Wordian, while that of Varanopidae also reaches its lowest point during the Wordian and the Capitanian (Figure 36B, E).

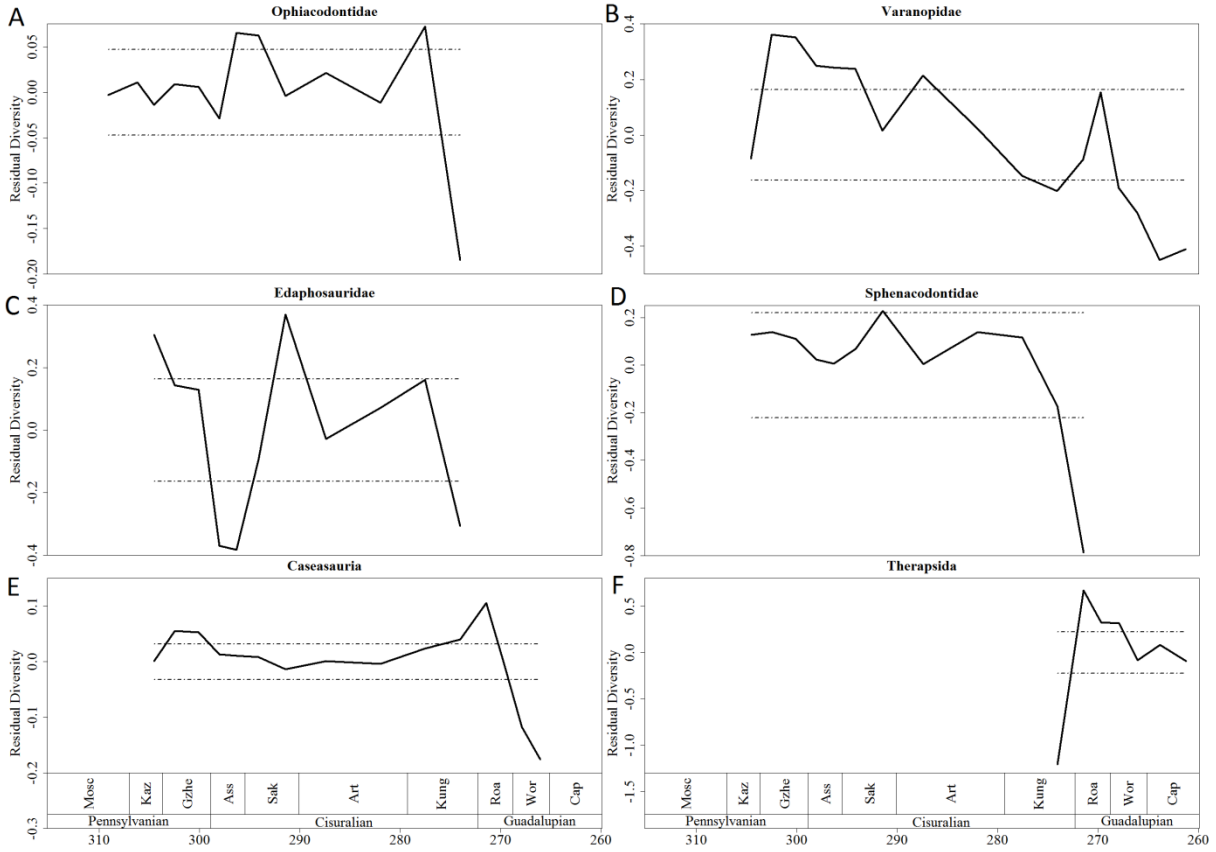

Figure 36: The residual diversity estimates (solid black) of (A) Ophiacodontidae, (B) Varanopidae, (C) Edaphosauridae, (D) Sphenacodontidae, (E) Caseasauria and (F) Therapsida, with 95% confidence intervals based on the standard deviation of the model (dashed-dotted lines).

The Effect of Sampling Bias on Synapsid Diversity

There has been considerable discussion in recent years concerning the quality of the Permian terrestrial fossil record, much of which has focussed on potential geological factors influencing our assessment of diversity. For example, Lucas and Heckert (2001) and Lucas (2004; 2006) have argued for a significant gap in the record during the Roadian, dubbed Olson's gap, but this has been disputed (Reisz and Laurin, 2001; Lozovsky, 2005; Liu et al.,

2009a; Benton, 2012). Other discussions have concerned possible correlations between numbers of fossiliferous formations and diversity. Fröbisch (2008) found that the diversity of Anomodontia correlated strongly with the number of anomodont-bearing formations, and used this correlation to argue for significant sampling bias in the continental Permian. On the other hand Benton (2012) observed no such correlation between formations and family-level diversity of tetrapods during the Permian, and concluded that the Permian fossil record was adequate for macroevolutionary analyses. In fact the studies of Sahney and Benton (2008) and Sahney et al. (2010) assessing tetrapod diversity during the Carboniferous, Permian and Triassic, made no attempt to correct for sampling. Benson and Upchurch (2012) disputed the suggestion that geological biases have not been affecting the terrestrial Permian record. In fact they found a significant correlation between tetrapod diversity and the number of tetrapod formations. The discrepancy between these results and the findings of Benton (2012) were put down to the different methods used to correct for autocorrelation (McKinney, 1990). Significant geological influences on vertebrate diversity were also found at a regional scale in the Karoo Basin of South Africa (Fröbisch, 2013; 2014)

There has, however, been no discussion of potential global anthropogenic bias, caused by workers investigating formations of a particular age more frequently than those of other ages. Such biases have been examined at a regional scale in the later Permian and Triassic of the South African Karoo Basin and the fore-Ural Region of Russia (Irmis et al., 2013; Fröbisch, 2013) and found to be significant. The global study presented here also finds anthropogenic sampling biases to be an important factor affecting the Late Carboniferous and Permian fossil record of Synapsida. The strong correlation between the number of amniote-bearing collections within each time interval and the number of synapsid species indicates that this factor is strongly influencing our interpretations of diversity. As such, one has to treat the taxic diversity estimate with extreme caution, as a large part of the signal may have been overprinted by the sampling bias. There is also a clear geographical bias in the diversity of terrestrial tetrapods during the Carboniferous and Permian. As described above, while the Carboniferous and Cisuralian are dominated by collections from North America and western Europe, the Guadalupian is dominated by those from South Africa and Russia. It is unclear whether this is due to an anthropogenic sampling bias (the relevant formations have not yet been found) or a geological bias (there are no fossil-bearing rocks of relevant age), but whatever the cause, this is an obvious gap in our understanding of the Carboniferous and Permian; data from entire continents is missing from certain time intervals.

It has been suggested that this spatial bias may represent, at least in part, a genuine biogeographic signal. The shift in spatial sampling coincides with an environmental change: the disappearance the palaeoequatorial tropical everwet biome, which had supported the pelycosaur-dominated fauna (Rees et al., 2002). It is possible that these environmental changes restricted Middle Permian tetrapods to the higher palaeolatitudes (Sidor et al., 2005; Kemp, 2006). However the discovery of mid-Late Permian palaeoequatorial localities (Jalil, 1999; Sidor et al., 2005) does indicate that there is an equatorial fauna at this time. This is yet another reason why sampling correction is necessary. For example, the supertree (Figure 21) indicates that several Russian taxa, such as *Pyozia mesenensis* (Anderson and Reisz, 2004), *Mesenosaurus romeri* (Efremov, 1938), and *Ennatosaurus tecton* (Efremov, 1956) have ghost lineages extending into the Cisuralian, and in the case of *Pyozia* into the Carboniferous (although see Maddin et al., 2006, who cast doubt on *Pyozia*'s synapsid affinities; also note that the ghost lineage of *Mesenosaurus* may have been extended by the polytomy present in the mycterosaurine varanopids in the supertree), allowing the inference of a possible Russian fauna not yet sampled. Such inferences are vital for biogeographic studies.

Benton's (2012) assertion that the fossil record is adequate cannot be supported with the available data. While he may have shown a lack of geological bias, there is clearly an anthropogenic bias in sampling, as well as a geographical bias, both of which will affect diversity estimates. Therefore the taxic diversity estimate must be questioned, and the phylogenetic and residual diversity estimates probably represent true diversity more closely.

Diversity Trends in Early Synapsids

The Effect of Environmental Change on Early Synapsid Diversification

The Late Carboniferous and early Cisuralian was a period of considerable environmental change. This is an interval in which significant warming and drying of the climate occurred (Kessler et al., 2001; Rees et al., 2002; Tarbor and Poulsen, 2008; Izart et al., 2012) and the coal swamps and forests in North America and Europe transitioned to a savannah-like biome (Rees et al., 2002; Tarbour and Poulsen, 2008). During the Kasimovian, the coal forests had been reduced to islands of rainforest surrounded by more arid habitats (DiMichele et al., 2006; DiMichele et al., 2009). Later, during the early Cisuralian, alkanes from European sediments indicate that the climate there transitioned to a seasonal tropical climate (Izart et al., 2012). The tropical belt across the equator narrowed, and the arid zones

surrounding it expanded (Rees et al., 2002; Tarbor and Poulsen, 2008). The family-level taxic diversity curve of tetrapods (Sahney and Benton, 2010) indicates a rapid increase in diversity during the Late Carboniferous, coinciding with the aridification and fragmentation of the rainforest habitats. This was explained by the diversification of Amniota, whose amniotic egg allowed them to cope in the drier climate (Sahney and Benton, 2010).

This study supports a Late Carboniferous radiation in synapsids. The taxic, phylogenetic and residual diversity curves all show increases during the Kasimovan and Gzhelian. Varanopidae and Ophiacodontidae were particularly successful during this early radiation; they are the only families that show significant increases in residual diversity (Figure 36A, B). In fact, both the residual and phylogenetic diversity estimates indicate that the Kasimovian was the time of greatest varanopid diversity (Figure 36B, 32B). The first amniote herbivores also appear during the Kasimovian, not only in synapsids (*Edaphosaurus*) but also independently in other tetrapod clades (Sues and Reisz, 1998).

Both the taxic and residual diversity curves presented in this study show an early Sakmarian peak in diversity followed by significant extinction of synapsids (Figure 31, 35). This event had not previously been discussed in studies of Permian tetrapod diversity. The curve of Sahney and Benton (2010) does not show any evidence of increased extinction during the Cisuralian, possibly due to their diversity being calculated at the family level. Species level taxic diversity curves of Permian tetrapods produced by Benson and Upchurch (2013) do indicate a trough in diversity during the late Sakmarian (Figure 29), but when the residual method of sampling correction is applied, the event no longer appears to affect amniotes, although it does affect amphibians (Figure 29). Interestingly the extinction event is still visible in synapsids even after sampling correction is applied (Figure 35). Although the number of synapsid species declines from 23 species to 13, no families become extinct. All synapsid families are affected, however, except for Edaphosauridae, whose taxic, residual and phylogenetic diversity increases between the early and late Sakmarian (Figure 36C, 32C).

It is interesting to note that the phylogenetic diversity curve presented in this study does not show a sudden extinction event during the Sakmarian as seen in the taxic and residual curves. Instead a gradual decline from a late Gzhelian peak is indicated (Figure 34). The disagreement of the phylogenetic diversity curve with the others is probably due to the unidirectional correction of the phylogenetic diversity curve; observed lineages may only be extended backwards in time, not forwards. This has the effect of "smearing" extinction events over a longer period of time, causing a bias towards higher diversity earlier in time and exaggerating the Signor-Lipps effect (Signor and Lipps, 1982; Lane et al., 2005).

The reasons for this Sakmarian extinction can only be speculative at the moment, but it is possible that environmental change may have had an influence. The changes in the Late Carboniferous climate mentioned before continued into the Cisuralian (Rees et al., 2002; Tarbour and Poulsen, 2008; Izart et al., 2012) with further expansion of arid areas. During the Sakmarian, there was a sudden spike in CO_2 levels, an abrupt shift to a higher temperature, and rapid deglaciation occurring at the south pole (Montanez et al., 2007). These environmental changes may have had an adverse effect on synapsids. The recovery from the extinction during the Artinskian and Kungurian included the radiation of large carnivores such as *Ophiacodon major*, *Ctenospondylus casei*, *Secodontosaurus obtusidens* and many of the largest species of *Dimetrodon*, as well as large herbivores such as Caseidae (which include the largest pelycosaurian-grade synapsids known) and the largest species of *Edaphosaurus* (Romer and Price, 1940; Reisz, 1986). It is possible that the evolution of larger animals was a result of the decline of the closed forests and transition to a more open habitat.

The Evolution of Synapsid Herbivores

One of the key innovations that appeared in terrestrial tetrapods during the Late Carboniferous and Permian is the evolution of high-fibre herbivory. This appeared several times independently in clades such as diadectomorphs, captorhinids and several lineages within parareptiles. Among synapsids, two pelycosaurian-grade families have produced herbivorous species. Edaphosauridae include the genus *Edaphosaurus*, possessing large tooth plates on their palate and the lingual surface of their lower jaw which, together with an anteroposterior motion of the lower jaw, allowed it to crush vegetation (Modesto, 1995). Caseidae possess a particularly wide ribcage, robust forelimbs with large claws, possibly for digging, as well as spatulate teeth suitable for shredding plant material (Sues and Reisz, 1998).

It is interesting to compare the trends in diversity of these two families. During the Late Carboniferous and early Cisuralian, the only synapsid herbivores known from the fossil record are several species of *Edaphosaurus*; although the insectivorous *Eocasea* is present in the Carboniferous, herbivorous members of the clade do not appear until the Artinskian. During the Artinskian and the Kungurian, Caseidae increased in diversity (Figure 32E, 36E), while the diversity of Edaphosauridae remained high until the early Kungurian, before declining to extinction in the early Roadian (Figure 32C, 36C).

Reisz (2005) discussed the possibility of competitive exclusion of edaphosaurids from the herbivorous niche by caseids. He came to the tentative conclusion that extinction of edaphosaurids, followed by the occupation of the freed ecospace by caseids, was more likely, since direct competition would require co-existence of the two families. It is true that there has been little evidence found of the two living side-by-side (only three localities have produced both edaphosaurid and caseid specimens). However, both groups were definitely present in southern North America during the Kungurian. The significant increases in taxic, residual and phylogenetic diversity of Caseidae during the late Kungurian occurs while there are still two species of the herbivorous genus *Edaphosaurus*, as well as *Glaucosaurus megalops* (Williston, 1915), which is represented by a juvenile and so is hard to interpret, but may have had a herbivorous component to its diet or a herbivorous ancestor (Modesto, 1994). There is little evidence of a substantial decline in Edaphosauridae prior to the radiation of Caseidae. Instead one sees the increase in the diversity of the caseids occurring contemporaneously with the decline in edaphosaurids (Figure 32, 36). While it is generally difficult to test competitive exclusion in the fossil record (Benton, 2008, Butler et al., 2009) the "inverse wedge" pattern displayed by the diversity curves of these two synapsid clades suggests that this possibility should not be rejected without further investigation.

Olson's Extinction and the Demise of "Pelycosaurs"

The early Guadalupian was an interval of major turnover in terrestrial vertebrate faunas. It is at this time that the earlier Permian faunas, dominated by pelycosaurian-grade synapsids, are replaced by the therapsid-dominated faunas of the Late Permian. This changeover is accompanied by ecological changes, including increased complexity of ecosystems with more trophic levels (Olson, 1966). Unfortunately, our understanding of this turnover is hindered by a fossil record of doubtful quality.

One problem is the patchiness of fossil distribution during this time. As discussed above, the Cisuralian record of amniotes is almost entirely dominated by records from North America and western Europe, while that of the Guadalupian is dominated by records from Russia and South Africa (Lucas, 2006). The San Angelo and Chickasha formations of Texas are probably Roadian in age (Olson, 1962; Reisz and Laurin, 2001; Lozovsky, 2003; 2005; Benton, 2012), but this still leaves little idea of what was occurring in North America for the rest of the Guadalupian. Moreover, Lucas and Heckert (2001) and Lucas (2004; 2006) consider even these formations to be Kungurian rather than Roadian. For the sam reasons,

there is little evidence of what occurred in Africa and Russia during the Cisuralian. As such it is not clear over what timescale the transition takes place and to what extent biogeographic factors play a role.

Another problem is that the Roadian synapsid record includes several species whose therapsid or "pelycosaurian" affinities are uncertain. Several taxa from the San Angelo formation e.g., *Dimacrodon hottoni*, *Driveria ponderosa*, *Steppesaurus gurleyi* (Olson and Beerbower, 1953), *Gorgodon minutus*, *Knoxosaurus niteckii* and *Mastersonia driverensis* (Olson 1962), were assigned to various therapsid groups, but have since been reinterpreted as indeterminate sphenacodontids or caseids (Sidor and Hopson, 1995; Kammerer, 2011). Various Russian taxa based on postcranial elements (e.g., Phreatosuchidae) also require study; although originally described as therapsids (Efremov, 1954), some may represent caseids (Olson, 1962). These taxa create further confusion over the timing and duration of the turnover.

The raw family-level diversity curve of tetrapods indicates an extinction event between the Kungurian and Roadian, dubbed Olson's extinction (Sahney and Benton, 2008). This has since been supported by sampling corrected curves of tetrapods, temnospondyls and parareptiles (Ruta and Benton, 2008; Ruta et al., 2011; Benson and Upchurch, 2012). As such, it is worth assessing whether Olson's extinction is visible in synapsids.

The taxic, residual and phylogenetic diversity curves all support an extinction event across the Kungurian/Roadian boundary. The number of synapsid species falls from the early Kungurian peak of 29 to 26 in the late Kungurian and 16 in the early Roadian. One might be tempted to assume this is a result of sampling bias; more amniote-bearing collections have been sampled from the late Kungurian than any other substage in the Cisuralian, and considerably less have been sampled from the late Roadian. However both methods used to correct for sampling bias have supported this extinction event, which coincides with the disappearance from the fossil record of Ophiacodontidae and Edaphosauridae. The taxic and residual diversity curves of Sphenacodontidae indicate a large decrease in the diversity of this family (Figure 32D, 36D).

The effects of this event are not consistent across clades. The taxic, phylogenetic and residual diversity curves indicate little significant change in the diversity of Varanopidae (Figure 32B, 36B). The phylogenetic diversity curve of Caseidae suggests a decline across the boundary (Figure 32E), but this curve is likely to have been influenced by a polytomy within the supertree, which draws several caseid ghost lineages into the late Kungurian, increasing the phylogenetic diversity of this substage relative to the Roadian. The residual diversity

curve for this clade shows that the early Roadian was actually the peak of their diversity (Figure 36E). Therapsids also increase in diversity across this boundary (Figure 31, 36F); 5 species are known from the early Roadian compared with 1 from the late Kungurian (not including several species of uncertain affinities; see above). The presence of *Microsyodon orlovi* (Ivakhnenko, 1995), an anteosaurian therapsid, in Roadian sediments causes several therapsid ghost lineages to be drawn back into the early Roadian, indicating a large cryptic radiation in therapsids occurred at this time.

It is interesting that only a slight decline in genus-level diversity is observed (Figure 31B). The number of genera falls by only one across the Kungurian/Roadian boundary, from 15 to 14. However, this may be explained by the large number of polyspecific genera in the late Kungurian. Genera like *Dimetrodon*, with eight species known from the Kungurian, and *Casea*, with three, have a much greater impact on the species-level diversity curve. One must treat this genus-level curve with caution; many of the polyspecific pelycosaurian-grade genera are of untested monophyly; as demonstrated in Chapter 2, for example, the genus *Casea* is likely to be non-monophyletic as *"Casea" nicholsi* is more closely related to the genera *Euromycter*, *Cotylorhynchus*, *Angelosaurus* and *Ennatosaurus* than to *Casea broilii*. Even at the genus level, it is clear that a significant event is occurring across the Kungurian/Roadian boundary: the diversity of pelycosaurian-grade synapsids declines from 14 genera to eight, while that of therapsids rises from one genus to six.

The biases relating to the completeness of specimens described in Chapter 4 should be remembered at this point. The results of that analysis indicated that, when an abundance of poor material was present, those who worked on pelycosaurian-grade synapsids have tended to name large numbers of species based on inadequate material. During the early Roadian, at the time of Olson's extinction, there is a sharp drop in the completeness of specimens relative to the late Kungurian (Figure 24). The poor quality of the specimens at this time could have led to an oversplitting of the Roadian taxa. Indeed this has been observed; as mentioned above, large numbers of putative therapsids from the San Angelo Formation have been declared undiagnostic pelycosaurian-grade synapsids (Sidor and Hopson, 1995; Kammerer, 2011). There are, however, numerous poorly preserved taxa from the early Roadian which have not yet been subjected to re-examination. Therefore it is possible that the diversity of the early Roadian has been overestimated, and therefore the severity of the extinction has been underestimated

The taxic diversity curve (Figure 31) indicates the recovery from this extinction event began during the Roadian, as the number of synapsid species increases to 19 in the late

Roadian. Again, however, the influence of sampling bias should be noted. More amniote-bearing collections have been sampled from the late than the early Roadian, and it is possible the apparent recovery visible in the taxic diversity curve is an artefact of the greater effort put into sampling rocks of this age. Both the phylogenetic and residual diversity curves (Figure 33, 35) indicate that the fall in diversity continues throughout the Roadian. Between the early and late Roadian, Sphenacodontidae disappear from the fossil record and Caseidae, which had been unaffected by the Kungurian/Roadian extinction, experience a fall in diversity from seven to three species, a decline supported by the phylogenetic and residual diversity curves (Figure 31E, 36E). Therapsid diversity, however, continues to increase (Figure 31), and again no significant change is visible in the diversity of Varanopidae (Figure 32B, 36B).

It has been suggested that the Roadian, unlike the sphenacodontid-dominated Artinskian and Kungurian and the therapsid-dominated later Permian, was a period with a distinct fauna of its own, dominated by varanopids and caseids (Reisz and Laurin, 2002). This study does indicate that in the early Roadian, pelycosaurian-grade synapsids were still more speciose relative to therapsids (although once again remember the cautionary note above about the affinities of many taxa) (Figure 31). Varanopid species present in North America at this time are larger predatory species such as *Watongia meieri* (Olson, 1974; Reisz and Laurin, 2004) and *Varanodon agilis* (Olson, 1962), possibly replacing the sphenacodontids as apex predators after the latter's decline from an early Kungurian peak. Caseids, although suffering in the second phase of the Roadian extinction, were more speciose than any other synapsid clade during the early Roadian (Figure 32). However, while pelycosaurian-grade synapsids suffer extinctions during the Roadian, therapsids are unaffected, instead increasing in diversity. In the late Roadian, they outnumber pelycosaurian-grade synapsids. The mass extinction during the Roadian while therapsids are still rare does lend support to Sahney and Benton's (2008) hypothesis that the changes between the Lower and Middle Permian communities are a result of Olson's extinction.

The Rise of Therapsids

Taxic, phylogenetic and residual diversity curves support the recovery of synapsids from the Roadian extinction across the Roadian/Wordian boundary, with the radiation of therapsid groups such as anteosaurian dinocephalians and anomodonts. Pelycosaurian-grade synapsids are a very minor part of the fauna, and are extremely rare (Figure 31). There are three species of pelycosaurian-grade synapsid found in the late Roadian-Wordian sediments

of the Russian Mezen group: the varanopids *Mesenosaurus romeri* (Efremov, 1938) and *Pyozia mesenensis* (Anderson and Reisz, 2004), and the caseid *Ennatosaurus tecton* (Efremov, 1956). Ghost lineages of the South African varanopids *Heleosaurus scholtzi* (Botha-Brink and Modesto, 2007; Reisz and Modesto, 2007) and *Elliotsmithia longiceps* (Dilkes and Reisz, 1996) are also present during these intervals. According to the residual and phylogenetic diversity curves, the Wordian is a period of decreasing varanopid and caseid diversity (Figure 36). Although varanopids survive into the Capitanian in South Africa (Dilkes and Reisz, 1996; Botha-Brink and Modesto, 2007), no caseids younger than *Ennatosaurus* are known, with the possible exception of an unnamed specimen from sediments of uncertain age in Lodève, France (Lucas et al., 2006).

While the taxic diversity curve indicates a continuous increase in synapsid diversity from the early Wordian until the early Capitanian, the phylogenetic diversity curve argues for a more stepwise increase (Figure 32). The first radiation, across the Roadian/Wordian boundary, includes Dinocephalia, basal Therocephalia and non-dicynodont Anomodontia. A second radiation occurs across the Wordian/Capitanian boundary. According to both the phylogenetic and taxic diversity estimates, the early Capitanian represents the overall peak in synapsid diversity during the Permian (Figure 31, 34). This is due to a burst of diversification in Dicynodontia (although the earliest members of this clade are known from the Wordian, most species appear during or after the Capitanian) and Biarmosuchia (there are only three species known from the Capitanian, but 9 ghost lineages are also present). Both curves indicate a decline in diversity between the early and late Capitanian. However, no higher level synapsid clades become extinct and the phylogenetic diversity estimate suggests a decrease in diversity of only two lineages.

The residual diversity curve conflicts with the taxic and phylogenetic diversity estimates. This curve indicates a decline between the late Wordian and the end of the Capitanian (Figure 35), due to the model's correction for the enormous number of amniote-bearing collections from South Africa. It is difficult to reconcile this signal with any of the available data. All other indications are that the Wordian and the Capitanian were times of radiation not only of species, but of entire clades, including anomodonts and dinocephalians in the Wordian and dicynodonts and biarmosuchians in the Capitanian. While it is probable that the Capitanian peak from the taxic diversity curve contains a large signal from sampling, the idea of a decline directly conflicts with both the raw data and the supertree. The fact that all the residual values during the Capitanian change within the confidence intervals suggests that the apparent decrease in diversity is not significant. Another issue to note is the length of

the *Tapinocephalus* Assemblage Zone, which covers much of the Capitanian. While efforts are being made to subdivide it (Angielczyk and Rubidge 2012), the lack of radiometric dates is proving a hindrance (but see Rubidge et al., 2013 for radiometric dates of later assemblage zones). It is possible that greater resolution within the *Tapinocephalus* Assemblage Zone would lead to a different signal being observed.

The Capitanian is the last period containing pelycosaurian-grade synapsids named to species level. They are a very minor part of the fauna, with only 2 species present, compared to therapsids, with 60 and 53 species known from the early and late Capitanian respectively (Figure 31). Only Varanopidae survived until the end of the interval under study. A single varanopid specimen is known from after this interval, in the *Pristerognathus* Assemblage Zone of South Africa (Modesto et al., 2011), but this has not been assigned to a species, and so was not included in this analysis.

Unlike the varanopids present in the Roadian, all the Wordian and Capitanian species are small, having been replaced in the macro-predator niche by anteosaurian dinocephalians, biarmosuchians and early therocephalians. Despite their reduction in diversity and their smaller size compared to the Kungurian and Roadian varanodontine species, varanopids retained a role in the Middle Permian ecosystem as small predators until the appearance of small diapsid and eutherocephalian predators in the latest Capitanian. There may only be four species known from the Wordian and Capitanian, but they are present in both the northern and southern hemispheres. Caseids were replaced in the herbivorous niche by the new therapsid and pareiasaurian herbivores. The last caseid is only found in the Mezen group where such herbivores are not known (Reisz and Laurin, 2002).

Conclusions

The present study describes the major trends in early synapsid diversity, including two extinction events that influenced the evolution of pelycosaurian-grade synapsids. An initial radiation occurred during the Kasimovian, particularly among Ophiacodontidae and Varanopidae. An extinction during the Sakmarian interrupted the diversification of synapsids, possibly due to the changing climate at the time and the transition to a more open and arid habitat. This extinction was followed by the radiation of many larger species of synapsid, as well as the diversification of Caseidae. However, Sphenacodontidae, Ophiacodontidae and Edaphosauridae began to decline during the Kungurian, and Eothyrididae went extinct.

An extinction event across the Kungurian/Roadian boundary caused the demise of Ophiacodontidae and Edaphosauridae, whereas Caseidae and Therapsida diversified. The early Roadian fauna was still dominated by pelycosaurian-grade synapsids, but unlike the Artinskian and Kungurian, in which sphenacodontids were most speciose, the early Roadian fauna contained large predatory varanopids and large herbivorous caseids. Further extinctions occurred during the Roadian with Sphenacodontidae disappearing between the early and late Roadian, and Caseidae decreasing in diversity, while therapsids continued to diversify.

Synapsid diversity recovered from this extinction during the Wordian, but it was therapsid clades that radiated; no recovery is visible in the surviving pelycosaurian-grade families. They are a minor component of the Middle Permian fauna, with only 2 small varanopid species present in the Capitanian. Capitanian diversity is ambiguous due to conflicting diversity curves; the taxic and phylogenetic diversity curves indicate that this was the time of greatest diversity during the interval under study, but the residual diversity estimate shows no significant change from the late Wordian.

Debates surrounding the adequacy of the Permian terrestrial record have previously focussed on potential geological biases, with less attention paid to "human" factors, such as the greater effort put into sampling rocks of a particular age. The strong correlation between the number of amniote-bearing collection, as well as the geographically 'patchy' record indicates that the fossil record at this time is clearly inadequate for studying macroevolutionary patterns without correction for sampling.

Chapter 6
Clade Diversification and Key Innovations in Early Amniotes

Clade Diversification

Investigating Uneven Rates of Diversification

Diversification rate is the rate at which the diversity of a clade increases, and is thus a function of both origination and extinction (Foote, 1999). The asymmetric shape of the Tree of Life testifies to the fact that different clades have undergone different rates of diversification throughout their evolutionary history. If a clade is at any point in time more diverse than its sister, this is an indication that this clade has either experienced a higher rate of origination, a lower rate of extinction, or both. Particularly interesting are events in which the rates of diversification in a clade shift significantly relative to its contemporaries. The detection of shifts in diversification rates is central to investigations on clade dynamics and the interaction between originations and extinctions that ultimately shaped the Tree of Life.

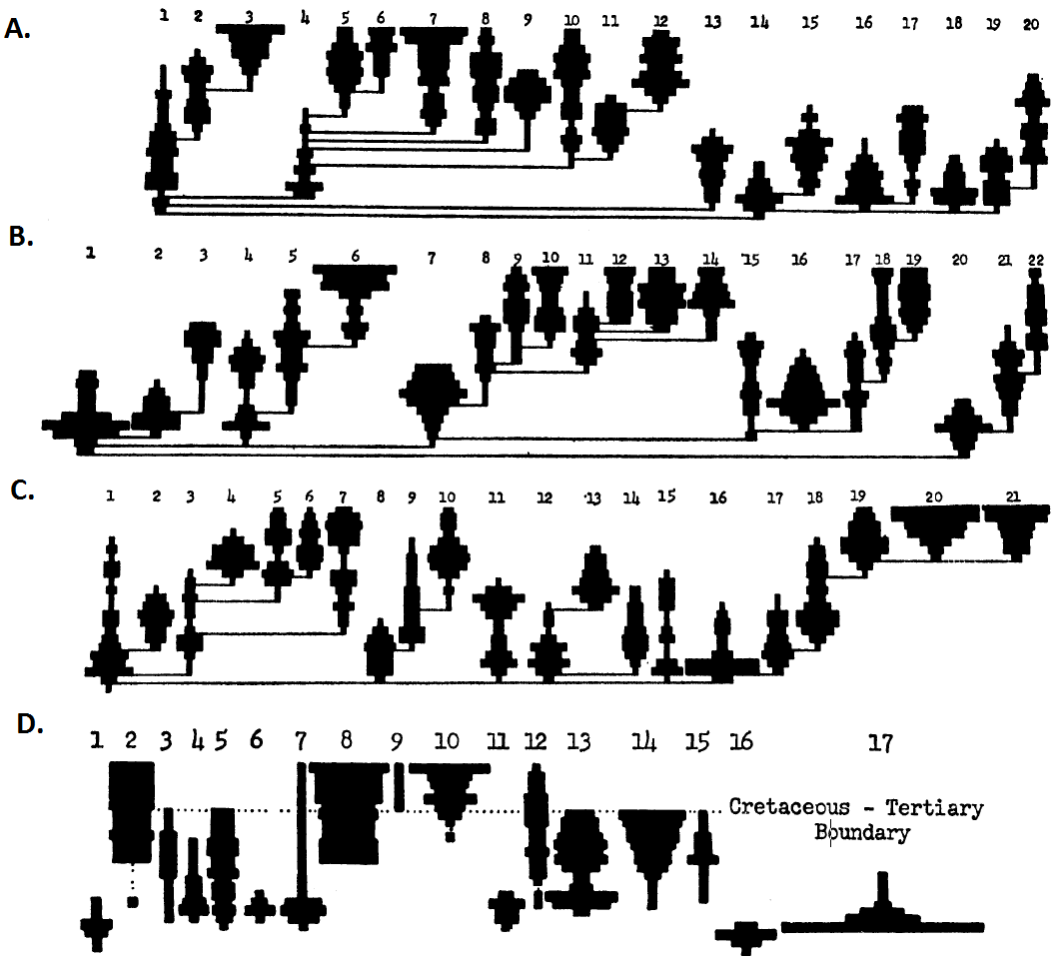

Figure 37: A-C) Examples of phylogenies produced in a stochastic birth-death model, indicating the diversities of clades produced; D) true diversity of reptile clades. (1) Cotylosauria, (2) Chelonia, (3) “latipinnate” ichthyosaurs, (4) “longipinnate” ichthyosaurs, (5) Sauropterygia, (6) Placodontia, (7) "primitive" lepidosaurs, (8) lizards, (9) Amphisbaenia, (10) Serpentes, (11) Thecodontia, (12) Crocodilia, (13) Saurischia, (14) Ornithischia, (15) Pterosauria, (16) “Pelycosauria”, and (17) Therapsida. From Raup et al. (1973).

Numerous methods have been devised to identify uneven rates of cladogenesis and extinction within a clade. One of the earliest studies of this issue (Raup et al., 1973) provided a template for many that have come since: a simple birth-death model was used to randomly generate phylogenies, in which each lineage had at any one time an equal probability of speciation (splitting into two lineages) or extinction. The diversity profiles of clades (Figure 37A-C) within model phylogenies was compared to the observed diversity profiles of reptile clades (Figure 37D), albeit visually rather than statistically. The similarities between the two indicated that the background pattern of diversification in reptiles follows the simple stochastic model. There were a number of time periods and clades which showed variation outside that which is observed in the model phylogenies e.g. the end-Cretaceous extinction, the rapid diversification of therapsids in the Permian, and the consistently low diversity of Rhynchocephalia since the Triassic; these were taken to indicate time periods and clades in which diversification rates were greatly different to background rates. This seminal study introduced much of the theory which underlies the methods used in this section of the thesis: the comparison of observed diversity patterns with the diversity patterns from an equal-rates model. This model, along with an alternative model in which an optimum clade size was specified, was tested against a larger selection of clades by Gould et al. (1977). In this study real clades showed greater fluctuations in diversity than modelled clades, indicating real clades experience variation in rates of origination and extinction beyond what would be expected from an equal-rates model, although the differences were not marked. Heard and Mooers (2002) further modified these models, incorporating parameters to simulate rapid initial radiations, wherein extinction rates were reduced until the clade reached a specific size, and mass extinction events. Although these models were not compared to empirical data, Heard and Mooers (2002) did model selective extinction based on a modelled trait to show that selective extinctions produce greater variation in clade size than random extinction.

Other methods investigating uneven rates of origination and extinction have eschewed a modelling approach. Roy et al. (2009) used matrix correlations to investigate selectivity in extinction between different families of bivalves. Two pairwise matrices of genera were created, one indicating whether each species pair belonged to the same family or not, one indication whether each species pair shares the same extinction fate (survival or extinction) in the time period under study. The matrix correlation between these two matrices provided a measure of whether the extinction is clustered in particular families or is random. The study showed that selectivity of extinction in bivalves varied; in most time bins studied, little

selectivity was observed. However in certain periods such as the Maastrichtian, Aptian and Toarcian, strong phylogenetic clustering of extinctions was observed (Figure 38).

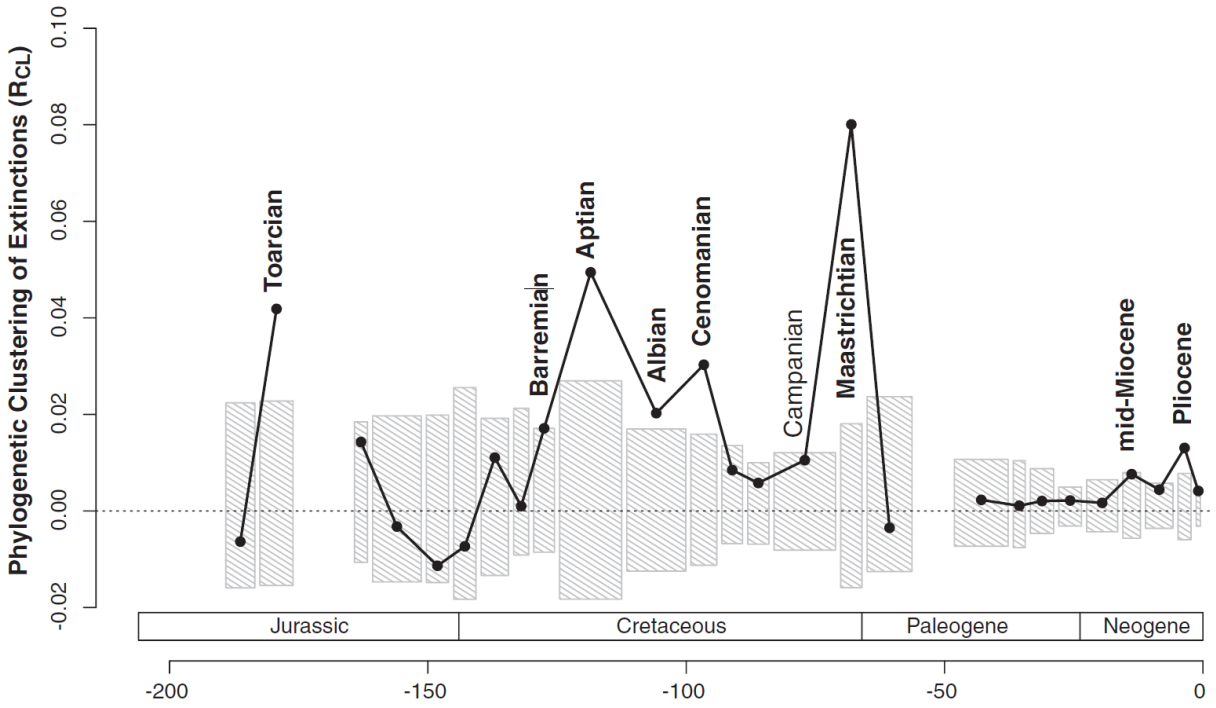

Figure 38: Temporal trend in phylogenetic clustering of extinctions. Shaded bars represent 95% confidence intervals around the expected value of RCL. The intervals showing statistically significant phylogenetic clustering of extinctions are labeled in bold; an additional interval, the Campanian, is marginally significant. From Roy et al. (2009).

Tree Topology and Diversification Rates

The methods described above all employ a higher-level taxonomic framework; that is they are comparing diversification patterns within families or other higher taxa. This presents a problem, particularly when endeavouring to compare observed diversification patters with a birth-death model in the manner of Raup et al. (1973) and Gould et al. (1977). As discussed previously, families are highly subjective groupings, and it is impossible to accurately overlay taxonomic practices over a phylogeny grown by a birth-death model. Raup et al. (1973) and Gould et al. (1977) defined the higher taxa in their model as monophyletic groupings which reached a particular size, but families vary hugely and have even been erected for single species.

Studies of diversification shifts that rely on tree topology have recently attracted much attention as a potential solution to the problem. These were first introduced by Rambaut et al. (1997) in the program End-Epi. This algorithm, and others similar, follows the ideas introduced by Raup et al. (1973): variation in diversity between different clades that is beyond

the variation produced in a stochastic birth-death model is an indication of significant differences in diversification rate. End-Epi compares an ultrametric phylogeny of the clade of interest, with branch lengths scaled to represent divergence times, to those created from stochastic birth-death models in order to indicate points on the tree where diversification events have been concentrated in time relative to what one expects from the models.

The program SymmeTREE (Chan and Moore, 2002) implements a slightly different set of statistics which require no information on branch lengths. Once again, these statistics not only deduce the presence of uneven diversification rates within a phylogeny, but can also show at which nodes in the phylogeny shifts in diversification rate occur. The statistics used in SymmeTREE, the Δ_1 and Δ_2 shift statistics (Moore et al., 2004), assess the likelihood that the observed imbalance between two lineages descended from a particular node could have appeared under two models: an equal rates Markov model (Chan and Moore, 2002) in which speciation rate is constant and a lineage has equal probability of diverging at any time, and a heterogeneous diversification model. Having calculated the difference in likelihoods under the equal-rates and heterogeneous models, one then needs to ascertain whether any shift in diversification rate occurred at the node being investigated, or at a higher node within the more diverse descendant. Therefore, the likelihood of a diversification shift at a particular node must be conditioned by the likelihood of a rate shift within the descendants of that node (Moore et al. 2004). The Δ_1 and Δ_2 shift statistics differ in the way in which they correct for this issue. The Δ_1 simply calculates the difference between the likelihood of a shift occurring at the node in question and the likelihood of a shift occurring within the node immediately descending from its more diverse descendant (Moore et al., 2004). The Δ_2 statistic is more complicated. The diversity of the descendants of the node under study is adjusted by removing tips which can be attributed to a rate shift along an internal node rather than the node under examination (Moore et al., 2004). Under simulation studies, the Δ_2 was found to perform better (Moore et al., 2004).

Diversification Shifts and Key Innovations

Although analyses of rate shifts are primarily designed to assess variation in rates of cladogenesis and extinction at different nodes in phylogenies, they have also been used to link shifts to both extrinsic (e.g. physical) and intrinsic (e.g. biological) causes. For instance, the timing of a shift may happen to coincide with that of a climatic or environmental change (Wiens et al., 2007; Tolley et al., 2008; Steeman et al., 2009), occur in the aftermath of a

large-scale crisis such as a mass extinction (Ruta et al., 2007), or be associated with a "key" morphological, ecological, or behavioural feature (Cook and Lessa, 1998; Vences et al., 2002; Rüber et al., 2003; Kozak et al., 2005; Forest et al., 2007; McLeish et al., 2007; Kazancıoğlu et al., 2009). Potential links between a "key innovation" and a shift in diversification rate have received special interest: a particular innovation might provide access to a new resource or gives a clade a competitive advantage over other species, leading to rapid speciation (Cook and Lessa, 1998; Beninda-Edmonds et al., 1999; Benson and Choiniere, 2013). Innovations that have been correlated with diversification shifts, and a causal relationship suggested, have been morphological e.g. the first appearance of elaiosomes in milkworts (Forest et al., 2007) and the evolution of powered flight in birds (Benson and Choiniere, 2013); behavioural e.g. the change in breeding behaviour in gobies (Rüber et al., 2003) and Malagasy tree frogs (Vences et al., 2002); or ontogenetic e.g. a change in host in acacia thrips (McLeish et al., 2008).

It is obviously tempting to view a diversification shift occurring in a clade that also possesses an obvious evolutionary innovation as being causally linked to the novelty (Cook & Lessa, 1998; Vences et al., 2002; Ruber et al., 2003; Kozak et al., 2005; Forest et al., 2007; McLeish et al., 2008; Kazancıoğlu et al., 2009). This is an adaptive radiation model (Simpson, 1953): a key innovation gives a lineage a selective advantage or allows it to enter a new ecological niche, thus leading to a massive increase in the rate of speciation. However there are problems with viewing a diversification rate increase and an evolutionary novelty as being causally linked. Such inferences are often circumstantial, relying solely on the coincidence of the two events. Moreover, the inference makes an implicit assumption that the diversification shift is the result of an increase in the rate of cladogenesis, an assumption that is not always valid. Diversification is a function of both origination and extinction (Foote, 1999). A diversification rate shift in one clade could imply either that its origination rate has increased or the extinction rate of its sister has increased. Tree topology analyses alone cannot distinguish between these two instances. Finally, the analyses often focus on a limited temporal and taxonomic range. Such limited analyses force the researcher to focus on the small number of shifts occurring in the clade of interest and do not allow investigation into the more general patterns of origination and extinction behind the diversification rate shifts occurring in the larger clade. The analysis of McLeish et al. (2008), for example, suggested that a diversification rate shift at a particular node in a milkwort phylogeny was caused by the evolution of elaiosomes. This analysis, in fact, found several other diversification shifts within milkworts, but the authors did not attempt to find a common factor uniting these shifts

and then look for possible exceptions to the general pattern. Instead the shift coinciding with the supposed "key innovation" was assumed to be an adaptive radiation.

Therefore, in the analysis of diversification rates presented herein, a much broader dataset is used. A supertree of all amniotes from the Pennsylvanian until the end of the Triassic was generated. This supertree maximizes the taxonomic scope and sample size of our investigation, and is used to address three major questions: (1) What portions of the Palaeozoic and early Mesozoic amniote tree underwent significant shifts in diversification? (2) Did shifts coincide with the acquisition of morphological innovations? (3) What is the influence of uneven rates of extinction on diversification rates? In order to address these questions, the supertree was subjected to analysis of tree topology-dependent shifts. Species richness, origination rates, and extinction rates were deduced from the supertree and compared to the timing of the shifts and the appearance of key innovations.

Amniote evolution in the late Palaeozoic and early Mesozoic offers a benchmark for analysing models of diversification and the influence of evolutionary innovation in a diverse and successful vertebrate radiation. Early amniotes evolved a large variety of morphologies and occupied a wide range of niches. They developed numerous ecological adaptations, such as herbivory (Sues and Reisz, 1998), fossoriality (Cox, 1972; Cluver, 1978), arboreality (Renesto, 1994; Spielmann, 2005; Fröbisch and Reisz, 2009), and secondarily aquatic lifestyles (DeBraga and Reisz, 1995; Modesto, 2006; 2010), and went through multiple radiations and extinctions, including the most catastrophic of all biological crises in Earth's history at the Permian-Triassic boundary (Benton, 1989; 2003; Sahney and Benton, 2008; Benton et al., 2013; Fröbisch, 2013). Amniotes are used as a model group to infer general patterns of vertebrate diversification over an extensive time period, which can then be used to make inferences about possible factors responsible for individual shifts within the group on which this thesis focusses: the pelycosaurian-grade synapsids.

Materials and Methods

Expansion of the Supertree

An expanded supertree was generated using the methods described in Chapter 3. For this set of analyses the list of source trees was expanded to include all phylogenies containing three or more amniote taxa from the time period covering the late Moscovian until the end of the Triassic. Once again, the source trees were limited to those which included full details of

the method and data. Those that did not were rejected, as were those which had been superseded by more recent analyses (methods for judging this were identical to those presented in Chapter 3). After pruning the list of published phylogenetic analyses in this way, 177 phylogenies remained (Appendix J), which were standardised with respect to taxonomic level (see Chapter 3). The MRP matrix was again produced using Supertree0.85b (Salamin et al., 2002) and analysed in TNT under identical settings to those presented before. However at this point a modification to the method had to be made since the MRP matrix of all 177 trees could not be analysed using parsimony; more trees were produced in a single round of searches than could be stored in the memory of TNT. In order to deal with this problem, the list of source trees was divided into 8 categories: Synapsida, Parareptilia, Archosauromorpha, Lepidosauriformes, Sauropterygia, Ichthyopterygia, and "Basal" forms. The source trees were divided between these categories based on which clade they were representing the relationships of. Those in the "Basal" category include studies examining the relationships of multiple clades relative to each other and those including diadectomorphs and stem eureptiles. An MRP matrix was produced for each category, and a supertree created for each clade, using the procedure described above. Because of the uncertainty surrounding the position of turtles (either within parareptiles or lepidosauromophs), the categories Parareptilia, Sauropterygia and "Basal" forms were combined, and a single supertree of the taxa in the categories produced in order to test which of these relationships was best supported. The supertrees produced in each of these separate analyses were combined, again with MRP. The final supertree, after collapsing all nodes containing no descendant taxa from the time interval under study and removing *post hoc* several taxa whose position could not be resolved (Appendix K), contained 686 species. The full time calibrated tree may be seen in Appendix L, and a summary version in Figure 39.

It should be noted that the lack of resolution of the position of those taxa was sometimes due to controversy surrounding their relationships, but it could also be due simply to the fact that a species had not been tested against a wide enough sample of taxa for the MRP method to resolve its position e.g. the assignment to *Nothosaurus* of *N. haasi*, *N. jagisteus*, *N. edingerae*, *N. marchicus*, *N. winterswijkensis*, *N. youngi*, *N. juvenilis*, *N. tchernovi*, *N. winkelhorsti*, *N. yangiuanensis* is not controversial and was supported in a recent study (Klein and Albers, 2009). However, since this study employed few outgroup taxa and no other has included any *Nothosaurus* species other than the type and *N. giganteus*, the MRP methods could not resolve the position of these species relative to other sauropterygians.

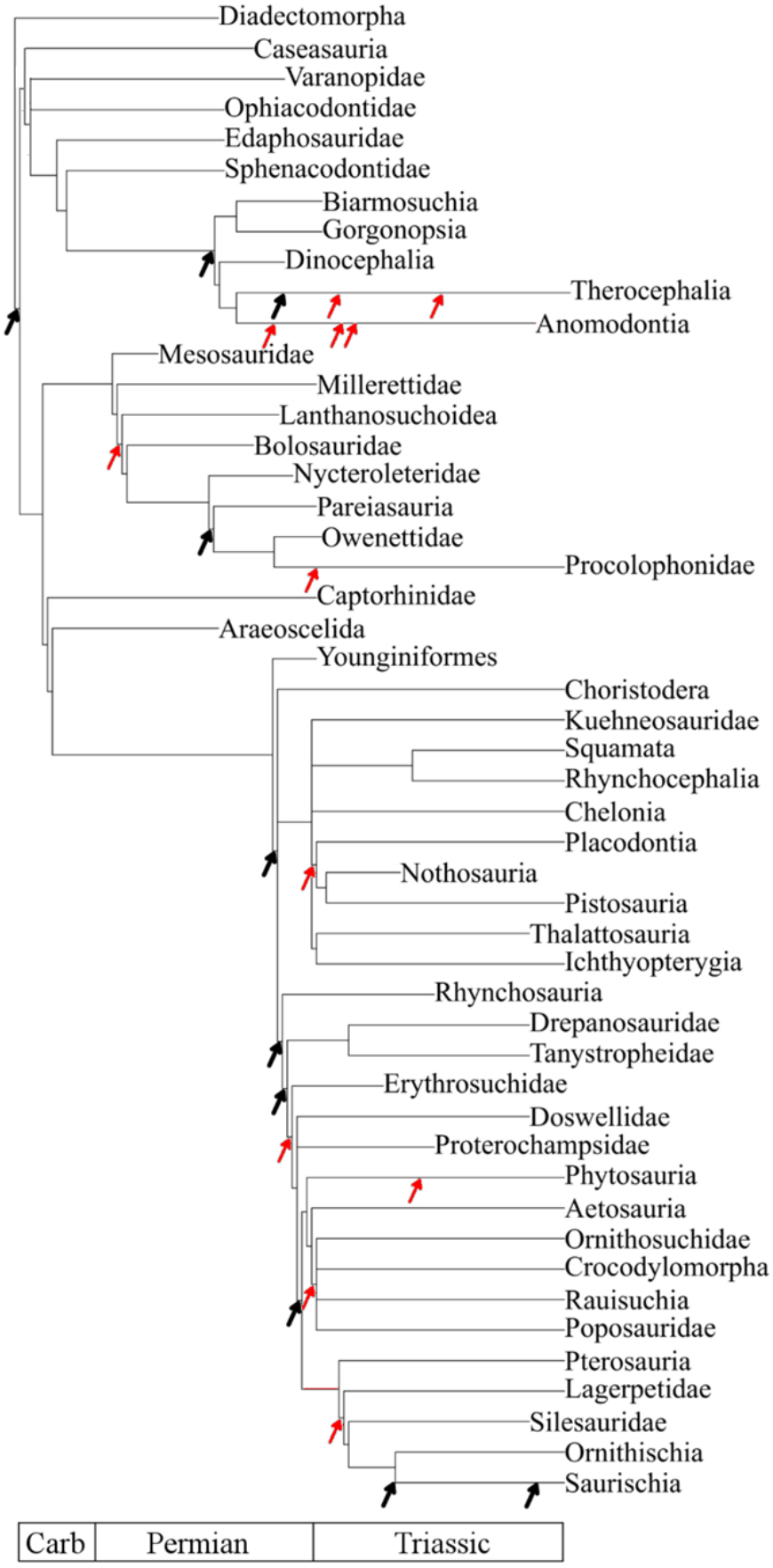

Figure 39: A summary version of the supertree (see Appendix L for the full tree). Red arrows indicate substantial diversification shifts, identified using the Ruta method of time slicing; black arrows indicate statistically significant shifts.

SymmeTREE Analysis

The supertree was subjected to analysis in SymmeTREE v. 1.1 (Chan and Moore, 2002, 2005) to infer diversification shifts. Random resolutions were used to resolve polytomies in the analysis: 10^6 for the whole tree and 10^4 for individual nodes. 10^6 trees were simulated under the equal rates and heterogeneous models: the maximum allowed by SymmeTREE. The program outputs a value of Δ_1 and Δ_2 for each node, as well as a p-value for each indicating whether the departure from the equal rate model for that node is statistically significant. The Δ_2 statistic was used to infer diversification shifts following recommendations in Moore et al. (2004). A p-value of less than 0.05 indicates that a lineage underwent a significant shift, whereas a p-value between 0.05 and 0.1 indicates a substantial shift (Ruta et al., 2007; Lloyd et al., 2008). A diversification shift was inferred to have occurred on the lineage leading to the more diverse of the two descendants of the node with a significant or substantial Δ_2 (Chan and Moore, 2002). The timing and location within the tree of the diversification shifts may be seen in Appendix N. A plot of mean Δ_2 values through time was produced to illustrate temporal trends in magnitude and frequency of shifts.

Sensitivity Analyses

Three analyses were carried out to test the impact of three possible sources of error: poorly supported relationships within the supertree, uncertain ages of specimens, and different methods of time slicing.

Method of time slicing

SymmeTREE does not incorporate any temporal information into the analysis. However the statistics employed assume that descendants of the node under analysis have had equal time to diversify (Ruta et al., 2007). This assumption is not valid if a tree includes fossils; lineages that die out before their sisters had less time to diversify. As such, Ruta et al. (2007) suggested that time slicing be employed for datasets containing extinct taxa. This has a further advantage in that it allows the researcher to ascertain the timing of a diversification shift as well as its location within the phylogeny. The period of time under study is split into bins and the phylogeny is pruned to include only taxa observed in a particular bin, as well as ghost lineages inferred from the phylogeny (Ruta et al., 2007). The phylogenies of each time slice are analysed individually (hereafter, this method is referred to as the "Ruta method").

Tarver and Donoghue (2011) suggested a different method of time slicing (hereafter referred to as the "Tarver method"). They point out that the trees produced by the Ruta method are incomplete and therefore one cannot distinguish between extinction and speciation as causes of the imbalance of nodes. As such, they advocated "growing" the tree through time: every time slice, add in the new lineages which appear in this time interval, but retain those which became extinct (and would therefore be removed under the Ruta method).

Both methods of time slicing were implemented using the *timeSliceTree* function of the paleotree (Bapst, 2012) package in R (R Core Team 2013). For each substage, a phylogeny was derived from the supertree using both the Ruta and the Tarver methods. These phylogenies were analysed in SymmeTREE under the settings described above.

Support for relationships

It is important to remember that a supertree analysis should not be considered a unique morphological analysis. Rather it should be considered a summary of researchers' opinions on the relationships of the clade under study. That the MRP analysis favoured a particular set of relationships does not necessarily mean that those relationships are supported by better morphological data. Moreover, although in theory an MRP supertree should not contain any relationships that have never before been suggested, unsupported relationships can appear, albeit rarely (Beninda-Emonds, 2003). For these reasons, it is necessary to provide a support measure indicating to what extent the source trees support the relationships shown in the supertree. Since the usual support measure for phylogenetic analysis, such as Bremer support and Bootstrapping, are inappropriate for supertrees (the input data of a supertree are source trees rather than characters), several alternative measures have been put forward.

In this study the V measure was used (Wilkinson et al., 2005b). Each node is assigned a value between -1 and 1, representing the proportion of source trees supporting that node relative to the source trees conflicting with it. A V of 1 indicates that all relevant source trees support the node, a V of 0 indicates equal numbers of trees supporting and conflicting with the node, and a V of -1 indicates none of the source trees support the node. Other measures of support for supertrees exist, such as the qualitative support (Beninda-Emonds, 2003) and input tree bootstrapping (Creevey et al., 2004), but these were rejected for the current study. The qualitative support measure has been criticised for being too harsh: Wilkinson et al. (2005b) showed an example of a supertree which did not conflict with any input trees, but the mean QS was only 0.028 (in a measure ranging from -1 to 1). Input tree bootstrapping was rejected, meanwhile, since it is inappropriate for datasets containing many non-overlapping

trees (Moore et al. 2006). In order to ensure that poorly supported relationships do not unduly affect the inferences, the analyses with SymmeTREE were repeated with nodes having negative support collapsed into a polytomy. The nodes collapsed due to low support are marked in Appendix L.

Uncertainty of ages of taxa

As in the investigation of diversity, two sets of ages were assigned to each species. The first took into account uncertainty in the dating of certain formations; if a formation was of uncertain age, species within that formation were assigned to the full range of possible ages. The second set of ages restricted the age of formations of uncertain age to at most two substages based on examination of the recent literature. Data using both sets of ages were subjected to analyses in SymmeTREE to assess the effect of uncertain dates on results. The age ranges assigned to taxa may be viewed in Appendix N

Comparison of Rate Shifts with Diversity, Extinction Rates and Origination Rates

A phylogenetic diversity estimate of amniotes from the late Moscovian until the end of the Triassic was calculated from the time-calibrated supertree. The supertree was also used to infer extinction and origination rates. Per-lineage extinction rates were calculated by dividing the number of lineages terminating in a time bin by the total number of lineages (observed and ghost) present in that bin. Per-lineage origination rates are calculated by dividing the total number of cladogenic events in each time bin by the total number of lineages present in that bin. Since inference of origination rates is affected by polytomies, these were randomly resolved 1000 times in order to provide a mean origination rate.

Origination rates were used to evaluate the impact of morphological innovation on diversification. Two such innovations within early amniotes were examined: herbivory and a secondarily aquatic lifestyle. Two binary characters were created, one representing the presence or absence of each innovation in all taxa in the supertree. These characters were optimised over the tree by deducing ancestral character states for all nodes with parsimony using the ancestral.pml function from the phangorn package in R. A set of per-lineage origination rates within all lineages descended from an herbivorous ancestor, and another for those descended from an aquatic ancestor.

The PDE and rate estimates were calculated from the supertree in R using custom scripts written from functions in paleotree. The origination and extinction rate estimates were

compared to the number of diversification shifts in each time bin using the Spearman's rank and Kendall's tau correlation coefficients, carried out in R, after implementing generalised differencing. Generalised least squares regression (GLS) was also used to investigate the relationship between diversification and origination and extinction rates. This method has an advantage over simple correlation tests in that it allows multivariate models to be compared as well as single variables. The curve of amniote Δ_2 through time was compared using GLS to a null model (random variation around a mean of 0), to origination and extinction rates, and to a multivariate model of both origination and extinction.

Results and Discussions

Sensitivity Analysis

The analyses that tested the impact of uncertainty surrounding the age ranges of species and of poorly supported relationships both found that neither of these issues substantially affect the results. When nodes with negative support are collapsed into a polytomy, the timing and location of the substantial and significant diversification shifts identified by SymmeTree are unchanged from those found using the original supertree (Appendix M). There are minor differences in the analyses employing the two different sets of age ranges, however, this only affect four clades. In two clades the timing of the diversification shift changes: a diversification shift in the clade containing Pareiasauridae and Procolophonoidea is found in the late Wuchiapingian when the restricted ages are used, but when uncertainty of ages is incorporated it is found in the early Wuchiapingian. A diversification shift in anomodonts more derived than *Wadiasaurus* is found in the early Ladinian when uncertainty of ages is taken into account, but is found in the late Anisian when ages are restricted. Two further clades are only found to experience a diversification shift only when using ages which account for uncertainty: Eucynodontia and Kannemeyeriiformes.

The use of different time-slicing methods has a greater effect (Appendix M). The Ruta method identified 21 clades experiencing substantial diversification shifts, while the Tarver method identified 26. Of these clades, only 16 were identified using both methods: Amniota, Ankyromorpha, anomodonts more derived than *Wadiasaurus*, Archosauromorpha, the clade containing Erythrosuchidae and archosauromorphs more derived, the clade containing Leptopleurinae and Proclophoninae, the clade containing Pylaecephalidae and dicynodonts more derived, Dinosauromorpha, Eucynodontia, Eutherocephalia, Paracrocodylomorpha,

Phytosauria, Sauria, Saurischia, Sauropterygia and Therapsida. With two exceptions, the timing of the shifts in these clades was identical: when using the Tarver method of time slicing, a diversification shift in Archosauromorpha occurs in the early Olenekian, but in the late Olenekian when using the Ruta method; when using the Tarver method of time slicing, a diversification shift in Eutherocephalia occurs in the late Ansian, but in the early Wuchiapingian when using the Ruta method. Five clades were found to experience shifts only when using the Ruta method: Archosauria, the clade containing Kayentatheridae and cynodonts more derived, the clades containing Protorosauria and all archosauromorphs more derived, Kannemeyeriiformes and Plateosauria. Ten clades were found to experience shifts only when using the Tarver method: the clade containing Captorhinidae and Diapsida, the clade containing Dinocephalia, Therocephalia and Anomodontia, the clade containing Eutherocephalia and Scylacosauridae, the clade containing Millerettidae and all parareptiles more derived, the clade containing Traversodontidae and Trirachodontidae, the clade containing Venjukovoidea and all anomodonts more derived, Diapsida, Dinosauriformes, Protorosauria and Sphenacodontia.

The results presented in the main text are those using the ages that take into account uncertainties in dating, and time sliced using the Ruta method. The Tarver method, while allowing one to observe the relative effects of both speciation and extinction, does not resolve the issue that Ruta et al. (2007) were trying to solve: under the Tarver method, not all the lineages of the trees input into SymmeTree will have had equal time to diversify.

Extinction and Origination Rates Compared to Diversification Statistics

There is a significant correlation between the number of significant (those with a p value of less than 0.05 using the Δ_2 statistic) and substantial (those with a p value of less than 0.1) shifts in the rate of diversification in each time bin and the per-lineage origination rate (Spearman's $\rho = 0.4275418$, $p = 0.009835$; Kendall's $\tau = 0.3047619$, $p = 0.008596$). Δ_2 values depend both on the number and on the arrangement of taxa on the more speciose of the two branches subtended by a given internal node, such that a substantial shift allows us to infer increased cladogenesis. Interestingly, a significant (albeit weaker) correlation was also found a between number of shifts and per-lineage extinction rate ($\rho = 0.3840412$, $p = 0.0214$; $\tau = 0.2666667$, $p = 0.02215$). This result implies that one cannot only explain shifts in diversification rate as increases in the rate of cladogenesis in the more diverse clades; increased extinction in the less diverse clades must also be considered.

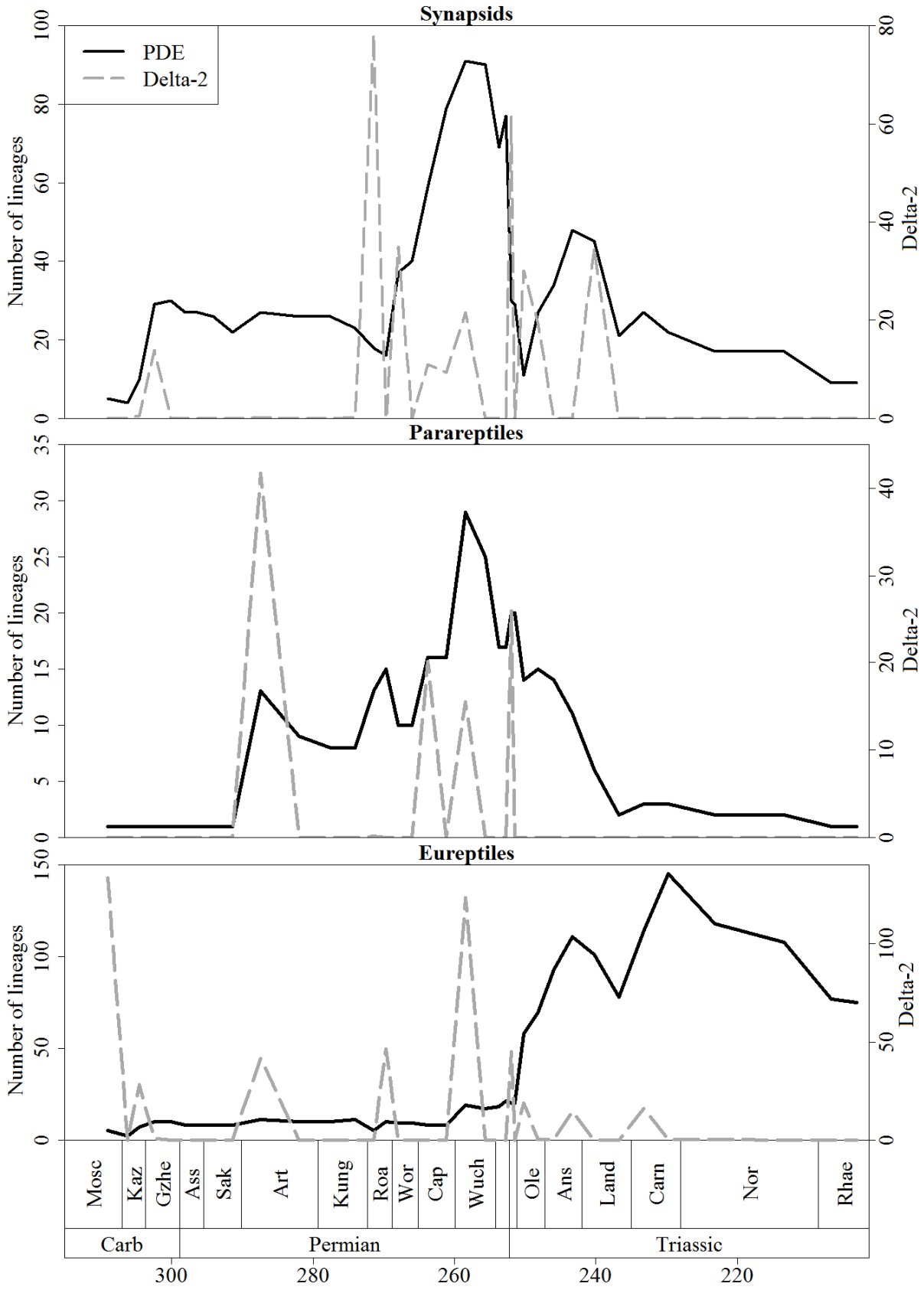

Figure 40: A comparison of the phylogenetic diversity estimate (black solid) and mean Δ2 values (grey dashed) for A) Synapsida; B) Parareptilia and C) Eureptilia.

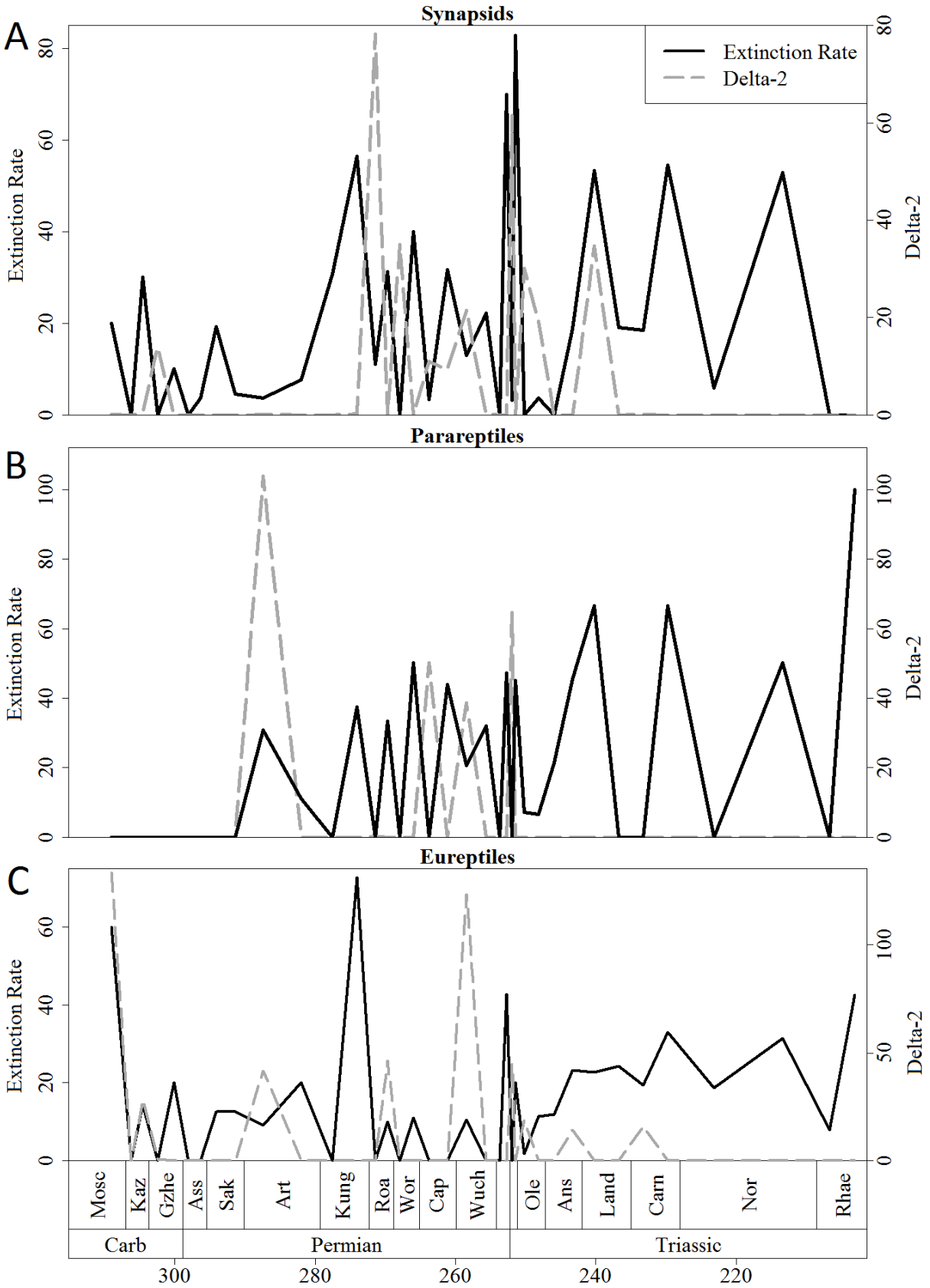

Figure 41: A comparison of per-lineage extinction rate (black solid) and mean Δ2 values (grey dashed) for a) Synapsida; b) Parareptilia and c) Eureptilia.

The coincidence of diversification shifts with periods of high extinction is clearly evident in plots of mean Δ_2 through time (Figures 40, 41). Peaks in mean Δ_2, representing both the magnitude and the number of shifts, tend to coincide with, or follow immediately after, large drops in diversity and peaks in extinction rate, the latter representing mass extinctions. Among synapsids (Figures 40A, 41A), the two largest peaks in mean Δ_2 values occur immediately after two mass extinctions: Olson's Extinction in the Kungurian and Roadian (Sahney and Benton, 2008; Benton 2012, see also Chapter 5) and the end-Permian event (Benton, 1989; 2003; Sahney and Benton, 2008; Benton et al., 2013; Fröbisch, 2013). The former extinction event, as discussed in Chapter 5, included the decline of pelycosaurian-grade synapsids, and was followed immediately by the radiation of therapsids. The extinction rates presented here support the fact that this was a severe extinction event in synapsids; per-lineage extinction rates at the end of the Kungurian are almost as high as those during the end-Permian mass extinction. Immediately following the extinction, there is a diversification shift found at the base of therapsids, which as discussed in Chapter 5 show a dramatic increase in diversity relative to their outgroups within pelycosaurian-grade synapsids. The diversification shift found here is both a product of the massive increase in therapsid diversity following Olson's extinction, but also the high extinction rates within the pelycosaurian-grade outgroups.

The end-Permian mass extinction was the most severe extinction event in early synapsid evolution. The two curves of phylogenetic diversity estimate (PDE) and extinction rates point to a two-phase event, with synapsids showing peaks in extinction rate occurring at the end of the Changhsingian and at the end of the Induan (Figure 40A, 41A). The first peak coincides with the complete extinction of gorgonopsians and biarmosuchians, as well as large loss of diversity within anomodonts and therocephalians. The second phase of the extinction coincided with the extinction of the Induan post-extinction fauna, including the members of the genus *Lystrosaurus*. A further peak in Δ_2 occurs in the early Ladinian, coinciding with another peak in synapsid extinction rate and a diversification shift in the anomodont clade containing *Wadiasaurus* and the more derived Kannemyeriiformes.

In parareptiles, an early Artinskian peak in mean Δ_2 coincides with the sudden appearance of multiple lineages in the fossil record. Mesosauridae are an exclusively early Artinskian clade, and there are also several parareptiles known from the Richard's Spur locality in Oklahoma, also of Early Artinskian age (MacDougal and Reisz, 2012). Finally, several bolosaurid specimens are known from the Artinskian aged Admiral Formation (Sander 1989). The appearance of these clades within a short space of time is represented by a

diversification shift within Ankyromorpha (the clade containing lanthanosuchoids and parareptiles more derived), identified by SymmeTREE at this time. This is a clear example of a diversification shift driven by increased rates of cladogenesis. However, the next two biggest peaks in mean parareptile Δ_2 values follow the two largest extinction rate peaks in the Permian (Figure 41B), one at the end of the Wordian and one at the very end of the Permian. The extinction peak at the end of the Wordian is driven by the disappearance of bolosaurids and the decline of nycteroleterids, and is followed by a substantial shift in diversification rate within the clade containing Pareiasauridae and Procolophonoidea. The end-Permian mass extinction, in which Pareiasauridae, Nycteroleteridae and Millerettidae die out, is followed by a diversification shift within the procolophonid clade containing Leptopleurinae and Procolophininae. As in synapsids, one can observe shifts in diversification rate in parareptiles being driven not only by increased cladogenesis, but also selective extinction.

The largest peak in extinction rate of eureptiles occurs during Olson's extinction; the rate of extinction in eureptiles at the end of the Early Permian is higher than during the end-Permian mass extinction. At this time, Captorhinidae, then the most diverse sauropsid family in the Permian, suffered a massive decline in diversity. A peak in mean Δ_2 follows immediately after Olson's Extinction (Figure 40C, 41C). There is a second peak in extinction rate at the end of the Permian, again followed by a smaller peak in mean Δ_2 (Figure 41C) and a shift in diversification rates in Sauria (the clade containing Lepidosauriformes and Archosauriformes). This shift represents the extinction of the more basal sauropsid clades such as captorhinids and basal diapsids such as Younginiformes, but also cladogenesis within saurians. In the immediate aftermath of the extinction, Lepidosauromorpha such as *Paliguana* (Broom, 1903a), ichthyopterygians such as *Utatsusaurus* and *Grippia* (Shikama et al., 1978; Brinkman et al., 1992) and sauropterygians such as *Placodus* appear in the fossil record, along with Archosauromorpha such as *Koilamasuchus* (Ezcurra et al., 2010), *Proterosuchus* (Broom, 1903b), *Osmolskina* (Borsuk-Bialynicka and Evans, 2003) and the poposauroid *Xilousuchus* (Wu, 1981). This provides a further example of a selective extinction followed by increased cladogenesis within the survivors. However, as in parareptiles, the biggest peaks in eureptile Δ_2 values occur during periods of radiation rather than extinction. The two largest peaks coincide with the appearance of eureptiles in the late Moscovian, and with the appearance of archosauromorphs in the Late Permian (Figure 40C). Nevertheless, the fact that the number and magnitude of substantial shifts increases during times of elevated extinction in all three amniote subclades indicates that the selectivity of extinction may be as important as uneven rates of origination in producing tree shape imbalance.

Model	Log Likelihood	AIC	Akaike Weights
Null	-159.1396	332.2791	0.00000218
Extinction	-145.2414	296.4829	0.8719
Origination	-159.6841	325.3683	0.00000047
Extinction and Origination	-146.1597	300.3195	0.1281

Table 7: Results of the comparison between amniote Δ_2 values through time with extinction and origination rates using generalised least squares regression.

The generalised least squares regression analysis produced a surprising result. Based on the Akaike Weights (Table 7), it is overwhelmingly extinction that is found to best fit the Δ_2 curve of amniotes, substantially better than the multivariate model incorporating both origination and extinction. This is indicating that many and large diversification rate shifts are tending to occur during periods of high extinction rate more than high origination rate. This serves to emphasise that one cannot simply assume increased cladogenesis as the driving force behind the diversification rate shifts when carrying out studies of this sort. In early amniotes at least, uneven rates of extinction are an extremely significant influence, perhaps even more so than uneven rates of origination.

Key Innovations Among Amniotes

There are several examples of diversification shifts in early amniotes coinciding with the emergence of key ecological and functional innovations. For instance, the highly significant diversification shift observed in therapsids coincides with several physiological and morphological innovations, which allowed more effective food processing, ventilation and environmental tolerance (Kemp 2006, Hopson 2012). Diversification shifts within Kannemeyeriiformes coincide with the evolution of large body size, and a shift at the very base of Amniota may be related to the amniotic egg, giving reproduction independence from water (although this shift from the very base of the tree should be interpreted with care; the absence of further outgroups makes it difficult to ascertain the precise location of the shift). There are further examples of diversification shifts coinciding with morphological novelties relating to the two case studies examined in more detail here: herbivory and a secondary return to an aquatic environment. The evolution of an aquatic lifestyle coincides with diversification shifts at the base of Sauropterygia and Phytosauria. Cranial and mandibular re-

modelling accompanying increased specializations towards herbivory are marked by shifts in distinct groups, such as dicynodonts (a keratinous beak combined with propalinal lower jaw movements, which evolved earlier in anomodonts) (Reisz and Sues, 2000; Rubidge and Sidor, 2001), Triassic procolophonids (chisel-shaped teeth for processing tough vegetation) (Reisz and Sues, 2000), and plateosaurian sauropodomorph dinosaurs (increase in body size and high browsing) (Sereno, 1999).

It is obviously tempting to view these diversification shifts as representing adaptive radiations: the evolutionary novelty provides a selective advantage and the entry into a new niche and causes increases in the rate of cladogenesis. However the previous analyses do cast doubt on this line of reasoning: one cannot assume increased cladogenesis as the driving force behind diversification rate shifts. Detailed analysis into two case studies (herbivory and an aquatic lifestyle) provided further evidence against this line of reasoning.

Although there were arthropod herbviores in the terrestrial realm before the appearance of amniotes, the vast majority of primary consumers in Carboniferous and earliest Permian terrestrial ecosystems were arthropod detritivores (Shear and Sheldon 2001). Those amniotes which first adopted a high-fibre herbivorous diet were therefore entering an extremely under-filled region of ecospace. However, we see no evidence of an adaptive radiation in these earliest herbivores such as Edaphosauridae, Caseidae and Diadectidae. SymmeTREE identifies no diversification rate shifts in these earliest herbivores. Instead, significant and substantial shifts are found in the later Permian and Triassic herbivore specialists such as Dicynodontia, Plateosauria and Triassic procolophonids. The origination rates of herbivores show that it is not during the Carboniferous and earliest Permian, but during the Middle and Late Permian and across the Permo-Triassic boundary that extinction rates of herbivores are consistently higher than those of other taxa (Figure 42A). This is not only the time when diversification shifts are observed in dicynodonts and Triassic procolophonids, but is also a time of consistently high extinction rates among amniotes (Figure 41). The timing of the shifts is also interesting. Despite dicynodonts and their evolutionary innovations first appearing in the Wordian, the shift in their diversification rate occurs in the late Capitanian. The first members of Plateosauria appear in the Carnian, but this clade does not experience a shift in diversification rate until the Rhaetian. Both the Capitanian and Rhaetian are periods of high extinction rate (Figure 41). One does not see an adaptive radiation of these herbivore specialists coincide with the appearance of their "key innovation". Instead the diversification shift coincides with periods of high extinction rate, as was shown in the earlier analyses. It is therefore here suggested that these key innovations do not alone

cause an increase in the rate of cladogenesis, but instead buffer against extinction. It is the selective extinction of those without the innovation, and only then the subsequent radiation of survivors, that SymmeTREE is detecting.

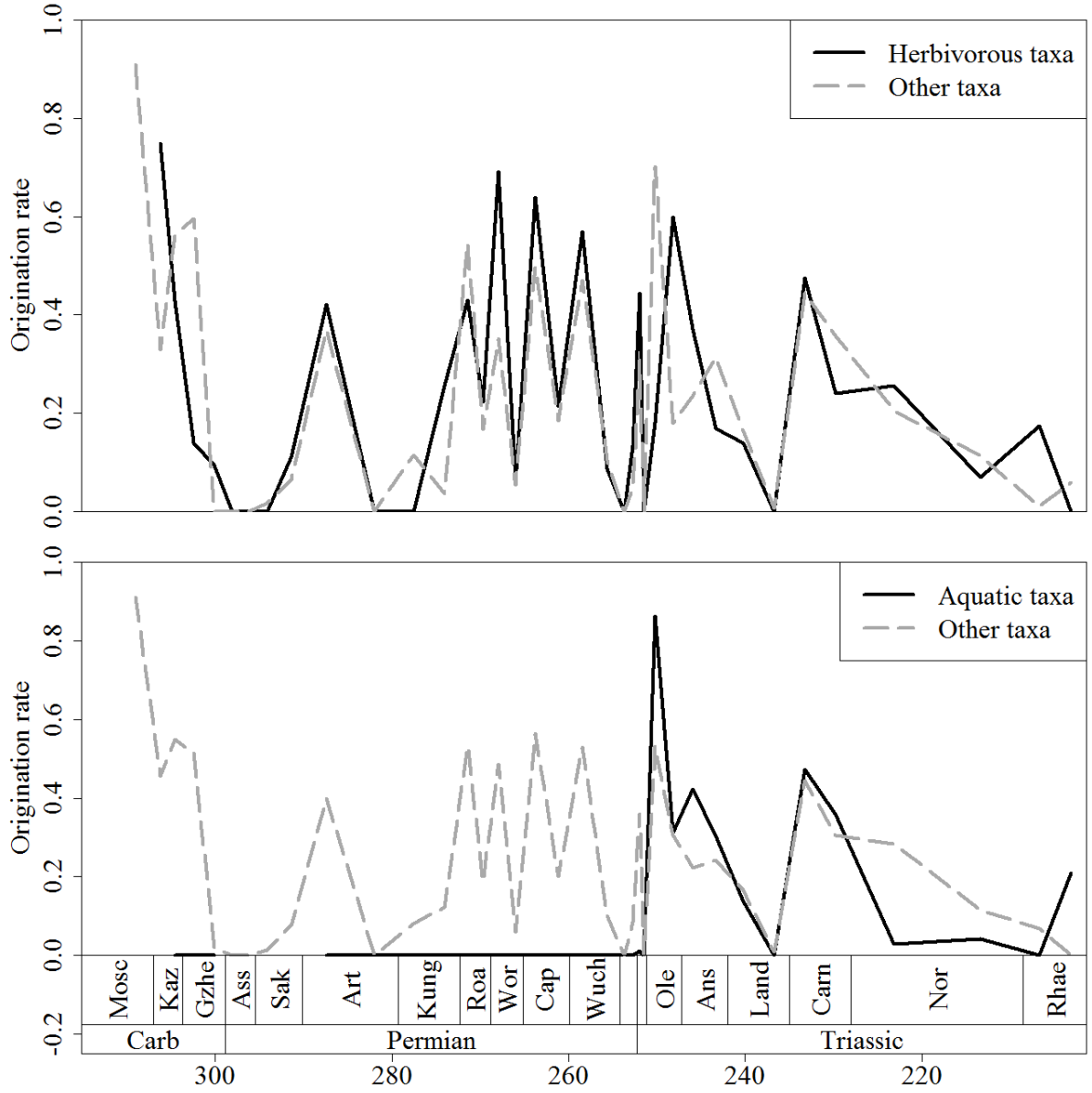

Figure 42: A comparison of per-lineage origination rate of herbivorous (a), aquatic (b) and other lineages through geological time.

Unlike the example of herbivores, amniotes that evolved a secondarily aquatic lifestyle did not colonise under-filled ecospace. Aquatic or semi-aquatic taxa, such as mesosaurid parareptiles and various Late Permian diapsid species, would have faced competition from other medium and large-sized vertebrates (e.g. amphibians; fish). This may explain why those secondarily aquatic lineages show low origination rates during the Carboniferous and Early

Permian (Figure 42B), and no diversification rate increases were identified by Symmetree during this time. It was not until the earliest Triassic that origination rates in aquatic lineages exceeded those in other lineages. It is also not until the Triassic that SymmeTREE identifies diversification rate increases coinciding with the evolution of an aquatic bauplan: at the base of the Sauropterygia and the Phytosauria.

Once again one could infer the influence of extinction on these diversification shifts. The shift observed in sauropterygians, and the increase in origination rate of aquatic amniotes at the same time (Figure 42B), follows immediately after the end-Permian mass extinction, and was perhaps facilitated by the reduced diversity of potential competitors such as fish and marine archegosaurid amphibians (Friedman & Sallan 2012, Koot 2013, Ruta and Benton, 2008). The shift observed in phytosaurs occurs at the end of the Carnian, post-dating their first appearance, but coinciding with a period of high extinction rate and declining diversity not only amongst amniotes (Figure 40, 41) but also among temnospondyl amphibians (Ruta & Benton, 2008). As before we do not see an adaptive radiation of phytosaurs coinciding with the first appearance of their novel bauplan, but instead the diversification shift is deferred to a period of high extinction rate amongst their competitors.

Diversification Rates Within Pelycosaurian-grade Synapsids

As discussed in Chapter 1, pelycosaurian-grade synapsids represent the earliest appearance in terrestrial amniotes of several innovations, including large body size, macro-carnivory, herbivory, and possibly a return to an aquatic environment. Under an adaptive radiation model, such novelties might be expected to lead to great increases in diversification rate within some of the pelycosaurian clades. Indeed, pelycosaurian-grade synapsids were the most diverse amniotes for much of the Early Permian (Figure 40), and the large number of evolutionary novelties could have provided an explanation for this; pelycosaurian-grade synapsids were some of the earliest amniotes to enter these niches, and so would have had empty ecospace in which to diversify.

Curiously, however, SymmeTREE finds no significant or substantial shifts in diversification rate within any families of pelycosaurian-grade synapsids throughout the late Carboniferous and Early Permian, the time at which these evolutionary novelties appeared. There is also no shift found at the base of synapsids at this time, indicating that this highly innovative group is no more diverse compared to contemporary clades than is expected under an equal rates model. Mean Δ_2 values of synapsids show no great peaks prior to the Middle

Permian; a single minor peak appears in the Gzhelian coinciding with a peak in synapsid diversity (see Chapter 5) but is considerably lower than later peaks and coincides with no shifts in diversification rate.

Why is it that the pelycosaurian-grade synapsids experience no great variations in their diversification rate beyond what may be expected from an equal-rates model? A possible explanation may lie in the link between evolutionary innovation, extinction events and diversification rate shifts. During the Late Carboniferous and Early Permian, there are no substantial extinction events. Despite the decline in diversity observed in the Sakmarian (see Chapter 5) the extinction rates of synapsids do not increase far above background rates during the Carboniferous and Early Permian. It is possible that this diversity decrease was driven more by a decrease in origination rate than by an increase in extinction rate. Under the model proposed in this chapter, innovations alone do cause increases in diversification rates during periods of background extinction. It is during the periods of environmental hardship and elevated extinction in which such innovations provide the impetus for an increase in diversification rates. Since pelycosaurian-grade synapsids, during the Late Carbonifeorus and Early Permian, experienced merely a background level of extinction rates, their evolutionary novelties did not translate to increases in diversification rate over those who lacked such innovations. The first mass extinction to occur during the time period occupied by the pelycosaurian-grade synapsids was Olson's extinction, in which therapsids diversified at the expense of basal synapsids.

There are, however, alternative issues that should be discussed, one of which is the comprehensiveness of the supertree. Although the analyses in Chapter 5 show that the synapsid portion of the tree is inclusive enough to infer diversity patterns in synapsids as a whole, there are clearly clades that receive less attention than others, most noticeably Sphenacodontidae and Ophicaodontidae. Both of these clades have undergone very little phylogenetic or taxonomic re-evaluation. The two most diverse pelycosaurian-grade genera, *Ophiacodon* and *Dimetrodon* are only included at genus level in all phylogenetic analyses which are included as source trees in the supertree. Re-evalutation of Sphenacodontidae is a work in progress, and while the work of Brink and Reisz (2014) has increased the taxonomic scope of the phylogenetic analyses, most of the sphenacodontid species currently considered valid have not been examined since the work of Romer and Price (1940). *Ophiacodon*, meanwhile, has received no such revision since Romer and Price's monograph. It is unclear how further examination of these taxa would alter the results presented here. The data presented in Chapter 4 would indicate that an abundance of fragmentary specimens may have

led to oversplitting of the taxa, and it is likely that many of the species in these two families are invalid. Therefore, increasing the scope of phylogenetic analyses would be unlikely to affect results substantially. It is probable that the inferences made from the analyses undertaken herein are still valid, in spite of these issues.

Conclusions

It is tempting to view simultaneously occurring diversification shifts and evolutionary novelties as being causally linked. Indeed a number of studies have made such a connection (Cook and Lessa, 1998; Vences et al., 2002; Rüber et al., 2003; Kozak et al, 2005; Forest et al., 2007; McLeish et al., 2007; Kazancıoğlu et al., 2009). However such analyses often focus on a limited temporal and taxonomic range and do not investigate other possible correlations. The broader scale analysis presented here indicates that the patterns of radiation within early amniotes are heavily connected to the extinction events occurring during this time. The strong correlation of extinction rate and the number of substantial diversification shifts illustrates that uneven extinction rates within amniotes have had just as significant effect on tree topology as the pattern of origination. Some previous studies have suggested that shifts co-occur with extinction events (Ruta et al., 2007) or other extrinsic factors such as climate or geographic changes (Kiessling and Baron-Szabo, 2004; Wiens et al., 2007; Tolley et al., 2008; Steeman et al., 2009). However, the present study indicates that, at least within early amniotes, there is a more complex relationship between the two factors. Extinction selectivity based on morphology and ecology has been documented in a number of clades (Smith and Jeffrey, 1988; Friedman, 2009; Moore and Donoghue, 2009; Roy et al., 2009; Friedman and Sallan, 2012). In early amniotes, the appearance of these novelties such as herbivory and an aquatic bodyplan and even the expansion into almost unoccupied ecospace (as in the earliest herbivores) did not on its own cause significant shifts in diversification rate. Instead, it appears that the diversification shifts identified by SymmeTREE represent selective elimination of taxa and subsequent radiation of survivors, in which those taxa with pre-existing innovations allowing the exploitation of new resources were buffered against extinction and experienced a deferred diversification. Hence, the phylogeny of Palaeozoic amniotes was shaped by the interaction between evolutionary innovation and extinction.

Chapter 7
Conclusions and Future Work

As the most diverse and abundant vertebrate taxa in the terrestrial realm during the Early Permian, understanding the evolution of pelycosaurian-grade synapsids is of vital importance if we are to comprehend the establishment of the earliest terrestrial ecosystems. Many of the ecologies and morphotypes found in terrestrial organisms first appear in the basal synapsids. They provide an ideal model organism for understanding not only macroevolutionary patterns in the earliest terrestrial vertebrates, but an excellent case study into the state of our knowledge and research practices when examining this crucial period in the evolution of life on earth.

Examination of the phylogeny of pelycosaurian-grade synapsids using a variety of methods has produced a consistent set of relationships, at least between higher-level taxa. The position of Caseasauria as the sister to all other synapsids is confirmed by the addition of a basal caseid and postcranial material from eothyridids. Unfortunately there is much work still to be done. Poor support and poor resolution are found in many areas of the tree, and much of this appears to be due to missing data. Simply adding new characters and taxa will not resolve the issue of unscored characters in existing specimens. This requires either more complete specimens of these existing taxa, or detailed re-examinations of the existing specimens. Many of the wildcard taxa have not been examined in the literature since their original descriptions, often from the 1960s and 1970s. In particular, *Echinerpeton intermedium* is in urgent need of re-description. As one of the earliest synapsids it is vital to our understanding of character evolution at the base of the tree, and yet it has not been studied in detail since 1972 and phylogenetic analysis has produced conflicting opinions of its affinities.

The need for taxonomic revision was further highlighted by the analysis of the completeness of the fossil record of the basal synapsids. The negative correlation between the Skeletal Completeness Metric and the number of species named from a particular time bin shows that several species have been named based on very poor material. The most rapid period of discovery was in the three decades between 1940 and 1970, and many of these taxa were defined based on size, locality and stratigraphy. A detailed examination of the amount of morphological variation within speciose genera such as *Dimetrodon*, *Sphenacodon*, *Casea* and *Ophiacodon* is required in order to identify how many species within these genera may still be considered valid.

Despite these issues, and evidence of significant anthropogenic sampling bias, the pattern of species richness identified using multiple methods to correct for sampling is remarkably consistent. Events such as a rapid radiation at the end of the Carboniferous, a mid-Sakmarian trough and an extinction event at the end of the Early Permian are found

independent of which method is used to correct for sampling. This is greatly encouraging; it indicates that a genuine biological signal is visible despite the many issues with the fossil record. Further study is now necessary in order to better understand these events. Examinations of morphological evolution and diversity would supplement the information from species richness. Differences and similarities between diversity and disparity (morphological diversity) would greatly improve our understanding of these events and might provide information as to the causes. Study of Olson's extinction during the Kungurian and Roadian in particular would benefit from such analyses. Patterns of morphological selectivity in the extinction and of morphological evolution during the recovery would be invaluable in understanding the replacement of pelycosaurian-grade synapsids by therapsids. However such an analysis would benefit from a more detailed understanding of early therapsid relationships.

The results observed in the analysis of tree topology provide an interesting insight into the interactions between morphological evolution and lineage diversification. It appears that the many morphological innovations occurring in early amniote clades did not immediately result in massive increases in the rate of cladogenesis in those clades, as would be expected in an adaptive radiation model. Instead, increases in diversification rate appear to occur during periods of high extinction rate, and in particular during mass extinctions. Diversification rate shifts do not temporally coincide with the first appearance of a "key" innovation, but are instead deferred to periods of high extinction rate among plesiomorphic taxa. This realisation would benefit greatly from further analyses, not only to see if such a signal is found in other clades, but also a more detailed examination of the pattern of diversification in the clades examined here. Detailed comparisons of the rates and modes of morphological changes in clades exploring new areas of ecospace, and comparisons with the rates of origination and extinction, both in times of environmental stability and in times of turbulence and mass extinction, would provide confirmation of the patterns observed here as well as a more thorough understanding of macroevolutionary processes.

This thesis provides the first detailed examination of the evolution of pelycosaurian-grade synapsids using a quantitative, and allows a much greater understanding of their period of dominance in Earth's history. The investigation of the completeness of their fossil record also provides much information on the biases that are affecting our interpretations of the fossil record. Information on biases and completeness, as well as richness and diversification patterns, is a necessary starting point into macroevolutionary research, and will hopefully provide a basis for further study into this fascinating group of organisms.

Reference List

Abdala, F., 2007. Redescription of *Platycraniellus elegans* (Therapsida, Cynodontia) from the Lower Triassic of South Africa, and the cladistic relationships of Eutheriodonts. Palaeontology 50, 591-618.

Aho, A. V., Sagiv, Y., Szymanski, T. G. and Ullman, J. D., 1981. Inferring a tree from the lowest common ancestors with an application to the optimization of relational expressions. SIAM Journal on Computing 10, 405-421.

Alroy, J., 1996. Constant extinction, constrained diversification, and uncoordinated stasis in North American mammal. Palaeogeography, Palaeoclimatology, Palaeoecology 127, 285-311.

Alroy, J., 2002. How many named species are valid? Proceedings of the National Academy of Sciences 99, 3706-3711.

Alroy, J., 2010a. Fair sampling of taxonomic richness and unbiased estimation of origination and extinction, in: J. Alroy and G. Hunt (Eds.), Quantitative Methods in Paleobiology. Paleontological Society, pp. 1211-1235.

Alroy, J., 2010b. Geographical, environmental and intrinsic biotic controls on Phanerozoic marine diversification. Palaeontology 53, 1211-1235.

Alroy, J., Aberhan, M., Bottjer, D. J., Foote, M., Fursich, F. T., Harries, P. J., Hendz, A. J. W., Holland, S. M., Ivanz, L. C., Kiessling, W., Kosnik, M. A., Marshall, C. R., McGowan, A. J., Miller, A. I., T.D., O., Patzkowsky, M. E., Peters, S. E., Villier, L., Wagner, P. J., Bonuso, N., Borkow, P. S., Brenneis, B., Clapham, M. E., Fall, L. M., Ferguson, C. A., Hanson, V. L., Krug, A. Z., Layou, K. M., Leckey, E. H., Nurnberg, S., Powers, C. M., Sessa, J. A., Simpson, C., Tomasovych, A. and Visaggi, C. C., 2008. Phanerozoic trends in the global diversity of marine invertebrates. Science 321, 97-100.

Alroy, J., Marshall, C. R., Bambach, R. K., Bezuko, K., Foote, M., Fursich, F. T., Hansen, T. A., Holland, S. M., Ivany, L., Jablonski, D., Jacobs, D. K., Jones, D. C., Kosnik, M. A., Lidgard, S., Low, S., Miller, A. I., Novack-Gottshall, P. M., Oleszewski, T. D., Patzkowsky,

M. E., Raup, D. M., Roy, K., Sepkoski, J. J. Jr., Sommers, M. G., Wagner, P. J. and Webber, A., 2001. Estimates of sampling standardization on estimates of Phanerozoic marine diversification. Proceedings of the National Academy of Sciences 98, 6261-6266.

Amson, E. and Laurin, M., 2011. On the affinities of *Tetraceratops insignis*, an Early Permian synapsid. Acta Palaeontologica Polonica 56, 301-312.

Anderson, J. S. and Reisz, R. R., 2004. *Pyozia mesenensis*, a new, small varanopid (Synapsida, Eupleycosauria) from Russia: "Pelycosaur" diversity in the Middle Permian. Journal of Vertebrate Paleontology 24, 173-179.

Angielczyk, K.D., 2001. Preliminary phylogenetic analysis and stratigraphic congruence of the dicynodont anomodonts (Synapsida: Therapsida). Palaeontologia Africana 37, 53-79.

Angielczyk, K. D., 2002. Redescription, phylogenetic position, and stratigraphic significance of the dicynodont genus *Odontocyclops* (Synapsida: Anomodontia). Journal of Paleontology 76, 1047-1059.

Angielczyk, K. D. and Rubidge, B., 2013. Skeletal morphology, phylogenetic relationships and stratigraphic range of *Eosimops newtoni* Broom, 1921, a pylaecephalid dicynodont (Therapsida, Anomodontia) from the Middle Permian of South Africa. Journal of Systematic Palaeontology 11, 191-231.

Baars, D. L., 1962. Permian system of Colorado Plateau. America Association of Petroleum Geology Bulletin 46, 149-218.

Baars, D. L., 1974. Permian rocks of north-central New Mexico, in: C. T. Siemers (Ed.), Ghost Ranch, New Mexico Geological Society Guide-book. New Mexico Bureau of Mines and Mineral Resources, Socorro, pp. 167-169

Bailey, J. B., 1997. Neural spine elongation in dinosaurs: sailbacks or buffalo-backs? Journal of Paleontology 71, 1124-1146.

Bakker, R. T., 1977. Tetrapod mass extinctions - a model of the regulation of speciation rates and immigration by cycles of topographic diversity, in: A. Hallam (Ed.), Patterns of Evolution as Illustrated by the Fossil Record. Elsevier, Amsterdam, pp. 439-468.

Bakker, R. T., 1986. The Dinosaur Heresies. Kensington, New York.

Bapst, D. W., 2012. paleotree: an R package for paleontological and phylogenetic analyses of evolution. Methods in Ecology and Evolution 3, 803-803.

Bapst, D. W., 2013. When can clades be potentially resolved with morphology. PlosOne 8, e62312.

Barrett, P. M., McGowan, A. J. and Page, V., 2009. Dinosaur diversity and the rock record. Proceedings of the Royal Society B 276, 2667-2674.

Battail, B., 2000. A comparison of Late Permian Gondwanan and Laurasian amniote faunas. Journal of African Earth Sciences 31, 165-174.

Baum, B. R., 1992. Combining trees as a way of combining data sets for phylogenetic inference, and the desirability for combining gene trees. Taxon 41, 1-10.

Bell, M., Upchurch, P., Mannion, P. D. and Lloyd, G. T., 2013. Using the character completeness metric to examine completeness of Mesozoic dinosaurs: a Maastrichtian high and a paleoequatorial low. Journal of Vertebrate Paleontology 5S, 84.

Beninda-Edmonds, O. R., Gittleman, J. L. and Purvis, A., 1999. Building large trees by combining phylogenetic information: a complete phylogeny of the extant carnivora (Mammalia. Biological Reviews 74, 143-175.

Beninda-Edmonds, O. R. and Sanderson, M. J., 2001. Assessment of the accuracy of matrix representation with parsimony supertree construction. Systematic Biology 50, 565-579.

Beninda-Emonds, O. R., 2003. Novel versus unsupported clades: assessing the qualitative support for clades in MRP supertrees. Systematic Biology 52, 839-848.

Beninda-Emonds, O. R., 2004. Trees versus characters and the supertree/supermatrix "paradox". Systematic Biology 53, 356-359.

Beninda-Emonds, O. R. and Bryant, H. N., 1998. Properties of matrix representation with parsimony analyses. Systematic Biology 47, 497-508.

Beninda-Emonds, O. R., Gittleman, J. L. and Steel, M. A., 2002. The (super) Tree of Life: procedures, problems and prospects. Annual Review of Ecology and Systematics 33, 265-289.

Beninda-Emonds, O. R., Jones, K. E., Price, S. A., Cardillo, M., Greyner, R. and Purvis, A., 2004. Garbage in, garbage out. Data issues in supertree construction, in: O. R. Beninda-Emonds (Ed.), Phylogenetic Supertrees: Combining Information to Reveal the Tree of Life. Kluwer Academic Publishers, Netherlands, pp. 267-280.

Bennett, S. C., 1996. Aerodynamics and thermoregulatory function of the dorsal sail of *Edaphosaurus*. Paleobiology 22, 496-506.

Benson, R. B. J., 2012. The global interrelationships of basal synapsids: cranial and postcranial morphological partitions suggest different topologies. Journal of Systematic Palaeontology 10, 601-624.

Benson, R. B. J. and Butler, R. J., 2010. Uncovering the diversification history of marine tetrapods: ecology influences the effect of geological sampling biases, in: A. J. McGowan and A. B. Smith (Eds.), Comparing the Geological and Fossil Records: Implications for Biodiversity Studies. Geological Society, London, pp. 191-208.

Benson, R. B. J., Butler, R. J., Lindgren, J. and Smith, A. S., 2010. Palaeodiversity of Mesozoic marine reptiles: mass extinctions and temporal heterogeneity in geologic megabiases affecting vertebrates. Proceedings of the Royal Society B 277, 829-834.

Benson, R. B. J. and Choiniere, J. N., 2013. Rates of dinosaur limb evolution provide evidence for exceptional radiation in Mesozoic birds. Proceedings of the Royal Society B 280, 20131780.

Benson, R. B. J. and Mannion, P. D., 2012. Multi-variate models are essential for understanding vertebrate diversification in deep time. Biology Letters 8, 127-130.

Benson, R. B. J. and Upchurch, P., 2013. Diversity trends in the establishment of terrestrial vertebrate ecosystems: interactions between spatial and temporal sampling biases. Geology 41, 43-46.

Benton, M. J., 1979. Ectothermy and the success of dinosaurs. Evolution 33, 983-997.

Benton, M. J., 1989. Mass extinction among tetrapods and the quality of the fossil record. Philosophical Transactions of the Royal Society of London. Series B 325, 369-386.

Benton, M. J., 1999. Early origins of modern birds and mammals: molecules vs morphology. BioEssays 21, 1043-1051.

Benton, M. J., 2003. When Life Nearly Dies. Thames & Hudson, London.

Benton, M. J., 2008. How to find a dinosaur, and the role of synonymy in biodiversity studies. Paleobiology 34, 516-533.

Benton, M. J., 2009. The Red Queen and the Court Jester: species diversity and the role of biotic and abiotic factors through time. Science 323, 728-732.

Benton, M. J., 2012. No gap in the Middle Permian record of terrestrial vertebrates. Geology 40, 339-342.

Benton, M. J. and Donoghue, P. C. J., 2007. Paleontological evidence to date the tree of life. Molecular Biology and Evolution 24, 26-53.

Benton, M. J., Dunhill, A. M., Lloyd, G. T. and Marx, F. G., 2011a. Assessing the quality of the fossil record: insights from vertebrates, in: A. J. McGowan and A. B. Smith (Eds.), Comparing the geological and fossil records: implications for biodiversity studies. Geological Society of London, London, pp. 63-94.

Benton, M. J., Dunhill, A. M., Lloyd, G. T. and Marx, F. G., 2011b. Assessing the quality of the fossil record: insights from vertebrates, in: A. J. McGowan and A. B. Smith (Eds.), Comparing the Geological and Fossil Records: Implications for Biodiversity Studies. Geological Society Special Publications, London, pp. 63-94.

Benton, M. J. and Emerson, B. C., 2007. How did life become so diverse? The dynamics of diversification according to the fossil record and molecular phylogenetics. Palaeontology 50, 23-40.

Benton, M. J. and Ruta, M., 2011. Tetrapod evolution through the Permian and Triassic: rock record, supertrees and detecting events, 59th Symposium of Vertebrate Palaeontology and Comparative Anatomy, Lyme Regis, Dorset.

Benton, M. J., Ruta, M., Dunhill, A. M. and Sakamoto, M., 2013. The first half of tetrapod evolution, sampling proxies and fossil record quality. Palaeogeography, Palaeoclimatology, Palaeoecology 372, 18-41.

Benton, M. J. and Storrs, G. W., 1994. Testing the quality of the fossil record: paleontological knowledge is improving. Geology 22, 111-114.

Benton, M. J., Tverdokhlebov, V. P. and Surkov, M. V., 2004. Ecosystem remodelling among vertebrates at the Permian-Triassic boundary in Russia. Nature 432, 97-100.

Benton, M. J., Wills, M. A. and Hitchin, R., 2000. Quality of the fossil record through time. Nature 403, 534-537.

Berman, D. S., Henrici, A. C., Sumida, S. S. and Martens, T., 2004. New materials of *Dimetrodon teutonis* (Synapsida: Sphenacodontidae) from the Lower Permian of Germany. Annals of the Carnegie Museum 73, 48-56.

Berman, D. S., Henrici, A. C., Sumida, S. S., Martens, T. and Pelletier, V., 2014. First European record of a varanodontine (Synapsida: Varanopidae): member of a unique Early Permian upland paleoecosystem, Tambach Basin, Central Germany, in: C. F. Kammerer, K. D. Angielczyk and J. Fröbisch (Eds.), Early Evolutionary History of the Synapsida. Springer, New York, pp. 69-88.

Berman, D. S., Reisz, R. R., Bolt, J. R. and Scott, D., 1995. The cranial anatomy and relationships of the synapsid *Varanosaurus* (Eupelycosauria: Ophiacodontidae) from the Early Permian of Texas and Oklahoma. Annals of the Carnegie Museum 64, 99-133.

Berman, D. S., Reisz, R. R., Martens, T. and Henrici, A. C., 2001. A new species of *Dimetrodon* (Synapsida: Sphenacodontidae) from the Lower Permian of Germany records the first occurence of genus outside of North America. Canadian Journal of Earth Sciences 38, 803-812.

Bernard, E. L., Ruta, M., Tarver, J. E. and Benton, M. J., 2010. The fossil record of early tetrapods: worker effort and the end-Permian mass extinction. Acta Palaeontologica Polonica 55, 229-239.

Borsuk-Bialynicka, M. and Evans, S. E., 2003. A basal archosaruiform from the Early Triassic of Poland. Acta Palaeontologica Polonica 48, 649-652.

Botha-Brink, J. and Modesto, S., 2007. A mixed-age classed 'pelycosaur aggregation from South Africa: earliest evidence of parental care in amniotes?. Proceedings of the Royal Society B 274, 2829-2834.

Botha-Brink, J. and Modesto, S., 2009. Anatomy and relationships of the Middle Permian varanopid *Heleosaurus scholtzi* base on a social aggregation from the Karoo Basin of South Africa. Journal of Vertebrate Paleontology 29, 389-400.

Botha, J., Abdala, F. and Smith, R. M. H., 2007. The oldest cynodont: new clues on the origin and early diversification of the Cynodontia. Zoological Journal of the Linnean Society 149, 477-492.

Brink, K. and Reisz, R. R., 2014. Hidden dental diversity in the oldest terrestrial apex predator *Dimetrodon*. Nature Communication 5, 3269.

Brinkman, D. and Eberth, D. A., 1983. The interrelationships of pelycosaurs. Breviora 473, 1-35.

Brinkman, D., Zhao, X. J. and Nicholls, E. L., 1992. A primitive ichthyosaur from the Lower Triassic of British Columbia. Palaeontology 35, 465-474.

Brocklehurst, N., Upchurch, P., Mannion, P. D. and O'Connor, J., 2012. The completeness of the fossil record of Mesozoic bird: implications for early avian evolution. PlosOne 7, e39056.

Broili, F., 1904. Permische Stegocephalen und Reptilien aus Texas. Palaeontographica 51, 1-120.

Bronzati, M., Montefeltro, F. C. and Langer, M. C., 2012. A species-level supertree of Crocodyliformes. Historical Biology 24, 598-606.

Broom, R., 1903a. On a new reptile (*Proterosuchus fergusi*) from the Karroo beds of Tarkastad, South Africa. Annals of the South African Museum 4.

Broom, R., 1903b. On the skull of a true lizard (*Paliguana whitei*) from the Triassic beds of South Africa. Records fom the Albany Museum 1, 1-3.

Brown, C. M., Evans, D. C., Campione, N. E., O'Brien, L. J. and Eberth, D. A., 2013. Evidence for taphonomic size bias in the Dinosaur Park Formation (Campanian, Alberta), a model Mesozoic terrestrial alluvial-paralic system. Palaeogeography, Palaeoclimatology, Palaeoecology 372, 108-122.

Brusatte, S. L., Benton, M. J., Ruta, M. and Lloyd, G. T., 2008. Superiority, competition and opportunism in the evolutionary radiation of dinosaurs. Science 321, 1485-1488.

Butler, R. J., Barrett, P. M., Nowbath, S. and Upchurch, P., 2009. Estimating the effects of the rock record on pterosaur diversity patterns: implications for hypotheses of bird/pterosaur competitive replacement. Paleobiology 35, 432-446.

Butler, R. J., Benson, R. B. J., Carrano, W. T., Mannion, P. D. and Upchurch, P., 2011a. Sea level, dinosaur diversity and sampling: investigating the 'common cause' hypothesis in the terrestrial realm. Proceedings of the Royal Society B 278, 1165-1170.

Butler, R. J., Brusatte, S. L., Reich, M., Nesbitt, S. J., Schoch, R. R. and Hornung, J. J., 2011b. The sail-backed reptile *Ctenosauriscus* from the latest Early Triassic of Germany and the timing and biogeography of the Early Archosaur radiation. PlosOne 6, e25693.

Cain, S. A., 1938. The species-area cruve. American Midland Naturalist 19, 573-581.

Campione, N. E. and Reisz, R. R., 2010. *Varanops brevirostis* (Eupelycosauria: Varaonpidae) from the Lower Permian of Texas, with discussion of varanopid morphology and interrelationships. Journal of Vertebrate Paleontology 30, 724-746.

Carroll, R. L., 1964. The earliest reptiles. Journal of the Linnean Society (Zoology) 45, 61-83.

Case, E. C., 1907. Revision of the Pelycosauria of North America. Carnegie Institution of Washington 55, 3-176.

Chan, K. M. A. and Moore, B. R., 2002. Whole-tree methods for detecting differential diversification rates. Systematic Biology 51, 855-865.

Chan, K. M. A. and Moore, B. R., 2005. SYMMETREE: whole-tree analysis of differential diversification rates. . Bioinformatics 21, 1709-1710.

Chen, D., Diao, L., Euelnstein, O., Fernandez-Baca, D.-. and Sanderson, M. J., 2003. Flipping: a supertree construction method, in: M. Janoqitz, F.-J. Lapointe, F. R. McMorris, B. Mirkin and F. S. Roberts (Eds.), Bioconsensus. American Mathematical Society, Providence, USA, pp. 135-160.

Cisneros, J. C., Abdala, F., Rubidge, B., Dentzien-Dias, P. C. and Bueno, A. O., 2011. Dental occlusion in a 260-million-year-old therapsid with saber canines from the Permian of Brazil. Science 331, 1603-1605.

Cleary, T. J., Moon, B. C., Dunhill, A. M. and Benton, M. J. 2015. The fossil record of ichthyosaurs, completeness metrics and sampling biases. Palaeontology, in press.

Cluver, M. A., 1978. The skeleton of the mammal-like reptile *Cistecephalus* with evidence for a fossorial mode of life. Annals of the South African Museum 76, 213-246.

Clyde, W. C. and Fisher, D. C., 1997. Comparing the fit of stratigraphic and morphologic data in phylogenetic analysis. Paleobiology 23, 1-19.

Conrad, J., 2008. Phylogeny and systematics of Squamata (Reptilia) based on morphology. Bulletin of the American Museum of Natural History 310, 1-182.

Conrad, J. and Sidor, C. A., 2001. Re-evaluation of *Tetraceratops insignis* (Synapsida: Sphenacodontia). Journal of Vertebrate Paleontology 21, 42A.

Cook, J. A. and Lessa, E. P., 1998. Are rates of diversifiaction in subterranean South American tuco-tucos (genus *Ctenomys*, Rodentia: Octodontidae) unusually high? Evolution 52, 1521-1527.

Cooper, G. A., 1958. The science of paleontology. Journal of Paleontology 32, 1010-1018.

Cope, E. D., 1877a. Descriptions of extinct Vertebrata from the Permian and Triassic formations of the United States. American Philosophical Society 17, 52-63.

Cope, E. D., 1877b. On the Vertebrata of the bone bed in eastern Illinois. American Philosophical Society 17, 52-63.

Cope, E. D., 1878a. Description of extinct Batrachia and Reptilia from the Permian Formation of Texas. Proceedings of the American Philosphical Society 17, 505-530.

Cope, E. D., 1878b. On a new fauna. American Naturalist 12, 327-328.

Cope, E. D., 1878c. The theromorphous Reptilia. American Naturalist 12, 829-830.

Cox, C. B., 1972. A new digging dicynodont from the Upper PErmian of Tanzania, in: K. A. Joysey and T. Kemp (Eds.), Studies in vertebrate evolution. Oliver & Boyd, Edinburgh, pp. 173-189.

Crampton, J. S., Beu, A. G., Cooper, R. A., Jones, C. M., Marshall, B. and Maxwell, P. A., 2003. Estimating the rock volume bias in paleobiodiversity studies. Science 301, 358-360.

Cutbill, J. L. and Funnel, B. M., 1967. Numerical analysis of the fossil record, in: W. B. Harland, C. H. Holand, M. R. House, N. F. Hughes, A. B. Reynolds, M. J. S. Rudwick, G. E. Satterthwaite, L. B. H. Tarlo and E. C. Willey (Eds.), The Fossil Record. Geological Society of London, London.

Damiani, R., Sidor, C. A., Steyer, J. S., Smith, R. M. H., Larsson, H. C. E., Maga, A. and Ide, O., 2006. The vertebrate fauna of the Upper Permian of Niger. V. The primitve temnospondyl *Saharastega moradiensis*. Journal of Vertebrate Paleontology 26, 559-572.

DeBraga, M. and Reisz, R. R., 1995. A new diapsid reptile from the uppermost Carboniferous (Stephanian) of Kansas. Palaeontology 38, 199-212.

DeBraga, M. and Rieppel, O., 1997. Reptile phylogeny and the interrelationships of turtles. Zoological Journal of the Linnean Society 120, 281-354.

DeMar, R., 1970. A primitive pelycosaur from the Pennsylvanian of Illinois. Journal of Paleontology 44, 154-163.

Dilkes, D. W. and Reisz, R. R., 1996. First record of a basal synapsid ('mammal-like reptile') in Gondwana. Proceedings of the Royal Society B 263, 1165-1170.

DiMichele, W. A., Montanez, I. P., Poulsen, C. J. and Tarbor, N., 2009. Climate and vegetational regime shifts in the late Paleozoic ice age earth. Geobiology 7, 200-226.

DiMichele, W. A. and Phillips, T. L., 1996. Climate change, plant extinctions and vegetational recovery during the Middle-Late Pennsylvanian transition: the case of tropical peat-forming environments in North America, in: M. B. Hart (Ed.), Biotic recovery from mass extinction events. Geological Society of London, London, pp. 201-221.

DiMichele, W. A., Tarbor, N., Chaney, D. S. and Nelson, W. J., 2006. From wetlands to wet spots: environmental tracking and the fate of Carboniferous elements in Early Permian tropical floras, in: S. F. Greb and W. A. DiMichele (Eds.), Wetlands Through Time. Geological Society of America, Boulder, Colorado.

Dodson, P., 1990. Counting dinosaurs: how many kinds were there? Proceedings of the National Academy of Sciences 87, 7608-7612.

Dunhill, A. M., 2012. Problems with using rock outcrop area as a paleontological sampling proxy: rock outcrop and exposure area compared with coastal proximity, topography, land use and lithology. Paleobiology 38, 126-143.

Dyke, G. J., Nudds, R. and Benton, M. J., 2007. Modern avian radiation across the Cretaceous-Paleogene boundary. The Auk 124, 339-341.

Efremov, I. A., 1940. Preliminary description of new forms in the Permian and Triassic faunas of terrestrial vertebrates of the USSR. Trudy Paleontologicheskogo Instituta an SSSR 10, 73-81.

Efremov, I. A., 1954. The fauna of terrestrial vertebrates in the Permian copper sandstones of the western Cis-Urals. Transactions of the Paleontological Institute, Academy of Science USSR 56, 146.

Efremov, I. A., 1956. American elements in the fauna of the USSR. Doklady AN SSSR 111.

Ezcurra, M. D., Lecuona, A. and Martinelli, A., 2009. A new basal archosauriform diapsid from the Lower Triassic of Argentina. Journal of Vertebrate Paleontology 30, 1433-1450.

Fara, E. and Benton, M. J., 2000. The fossil record of Cretaceous tetrapods. SEPM 15, 161-165.

Fastovsky, D. E., Huang, Y., Hsu, J., Martin-McNaughton, J., Sheehan, P. M. and Weishampel, D. B., 2004. Shape of Mesozoic dinosaur richness. Geology 32, 877-880.

Felice, R. N. and Angielczyk, K. D., 2014. Was *Ophiacodon* (Synapsida, Eupelycosauria) a swimmer)? A test using vertebral dimensions, in: C. F. Kammerer, K. D. Angielczyk and J. Fröbisch (Eds.), Early Evolution of the Synapsida. Springer, New York, pp. 25-52.

Felsenstein, J., 1978. Cases in which parsimony or compatibility methods will be positively misleading. Systematic Zoology 27, 401-410

Finarelli, J. A. and Clyde, W. C., 2002. Comparing the gap excess ratio and the retention index of stratigraphic character. Systematic Biology 5, 166-176.

Foote, M., 1994. Temporal variation in extinction risk and temporal. Paleobiology 20, 424-444.

Foote, M., 1999. Morphological diversity in the evolutionary radiation of Paleozoic and post-Paleozoic crinoids. Paleobiology 25, 1-115.

Foote, M., 2000. Origination and extinction components of taxonomic diversity: general problems. Paleobiology 26, 74-102.

Forest, F., Chase, M. W., Persoon, C., Crane, P. R. and Hawkins, J. A., 2007. The role of biotic and abiotic factors in evolution of ant dispersal in the milkwort family (Polygalaceae). Evolution 61, 1675-1694.

Fountaine, T., Benton, M. J., Dyke, G. J. and Nudds, R., 2005. The quality of the fossil record of Mesozoic birds. Proceedings of the Royal Society B 272, 289-294.

Fox, D., Fisher, D. C. and Leighton, L. R., 1999. Reconstructing phylogeny with and without temporal data. Science 284, 1816-1819.

Friedman, M., 2009. Ecomorphological selectivity among marine teleost fishes during the end-Cretacous extinction. Proceedings of the National Academy of Sciences 106, 5218-5223.

Friedman, M. and Sallan, L. C., 2012. Five hundred million years of extinction and recovery: a Phanerozoic survey of large-scale diversity patterns in fishes. Palaeontology 55, 707-742.

Fritsch, A., 1895. Über neue Wirbeltiere aus der Permformation Böhmens, nebst einer Übersicht der aus derselben bekannt gewordenen Arten. Sitzungsberichte der Königlich Böhmischen Gesellschaft der Wissenschaften, Mathematisch-Naturwissenschaftliche Klasse 52, 1-17.

Fröbisch, J., 2008. Global taxonomic diversity of anomodonts (Tetrapoda, Therapsida) and the terrestrial rock record across the Permian-Triassic boundary. PlosOne 3, 1-14.

Fröbisch, J., 2009. Composition and similarity of global anomodont-bearing tetrapod faunas. Earth Science Reviws 95, 119-157.

Fröbisch, J., 2013. Vertebrate diversity across the end-Permian mass extinction - separating biological and geological signals. Palaeogeography, Palaeoclimatology, Palaeoecology 372, 50-61.

Fröbisch, J., 2014. Synapsid diversity and the rock record in the Permian-Triassic Beaufort Group (Karoo Supergrou), South Africa, in: C. F. Kammerer, K. D. Angielczyk and J. Fröbisch (Eds.), Early Evolutionary History of the Synapsida. Springer, New York.

Fröbisch, J., Angielczyk, K. D. and Sidor, C. A., 2010. The Triassic dicynodont *Kombuisia* (Synapsida, Anomodontia) from Antarctica, a refuge from the terrestrial Permian-Triassic mass extinction. Naturwissenschaften 97, 187-196.

Fröbisch, J. and Reisz, R. R., 2009. The Late Permian herbivore *Suminia* and the early evolution of arboreality in terrestrial vertebrate ecosystems. Proceedings of the Royal Society B 276, 3611-3618.

Fröbisch, J., Schoch, R. R., Müller, J., Schindler, T. and Schweiss, D., 2011. A new basal sphenacodontid synapsid from the Late Carboniferous of the Saar-Nahe Basin, Germany. Acta Palaeontologica Polonica 56, 113-120.

Funk, D. J. and Omland, K. E., 2003. Species-level paraphyly and polyphyly: frequency, causes and consequences, with insights from animal mitochondrial DNA. Annual Review of Ecology and Systematics 34, 397-423.

Gatesy, J., Baker, R. H. and Hayashi, C., 2004. Inconsistencies in Arguments for the Supertree Approach: Supermatrices versus Supertrees of Crocodylia. Systematic Biology 53, 342-355.

Gatesy, J., Matthee, C., DeSalle, R. and Hayashi, C., 2002. Resolution of a supertree/supermatrix paradox. Systematic Biology 51.

Gatesy, J. and Springer, M., 2004. A critique of matrix representation with parsimony supertrees, in: O. R. Beninda-Edmonds (Ed.), Phylogenetic Supertrees: Combining Information to Reveal the Tree of Life. Kluwer Academic Press, Dordrecht, pp. 369-388.

Gauthier, J. A., Kearney, M., Maisano, J. A., Rieppel, O. and Behlke, A. D. B., 2014. Assembling the squamate tree of life: perspectives from the phentoype and the fossil record. Bulletin of the Peabody Museum of Natural History 53, 3-308.

Gauthier, J. A., Kluge, A. G. and Rowe, T., 1988. Amniote phylogeny and the importance of fossils. Cladistics 4, 105-209.

Germain, D. and Laurin, M., 2005. Microanatomy of the radius and lifestyle in amniotes (Vertebrata, Tetrapoda). Zoologica Scripta 34, 335-350.

Goloboff, P. A., 1993. Estimating character weights during tree search. Cladistics 9, 83-91.

Goloboff, P. A. and Farris, J. S., 2001. Methods for quick concensus estimation. Cladistics 17, S26-S34

Goloboff, P. A., Carpenter, J. M., Salvador Arias, J. and Esquivel, D. R. M., 2008. Weighting against homoplasy improves phylogenetic analysis of morphological data sets. Cladistics 24, 1-16.

Goloboff, P. A., Farris, J. S. and Nixon, K. C., 2008. TNT, a free program for phylogenetic analysis. Cladistics 24, 774-778.

Gould, S. J., Raup, D. M., Sepkoski, J. J. Jr., Schopf, T. J. M. and Simberloff, D. S., 1977. The shape of evolution: a comparison of real and random clades. Paleobiology 3, 23-40.

Gradstein, F. M., Ogg, M. D., Schmitz, M. D. and Ogg, G., 2012. The Geological Time Scale 2012. Elsivier, Boston, USA.

Hammer, O. and Harper, D. A. T., 2006. Palaeontological Data Analysis. Blackwell Publishing, Oxford.

Hammer, O., Harper, D. A. T. and Ryan, P. D., 2001. Past: paleontological statistics software package for education and data analysis. Palaeontologia Electronica 4.

Hannisdal, B. and Peters, S. E., 2011. Phanerozoic Earth system evolution and marine biodiversity. Science 334, 1121-1124.

Haubold, H., 1990. Dinosaurs and fluctuating sea levels during the Mesozoic. Historical Biology 4, 75-106.

Heard, S. B. and Mooers, A. Ø., 2002. Signatures of random and selective mass extinctions in phylogenetic tree balance. Systematic Biology 51, 889-897.

Hendy, A. J. W., 2009. The influence of lithification of Cenozoic marine biodiversity trends. Paleobiology 35, 51-62.

Hill, R. V., 2005. Integration of morphological data sets for phylogenetic analysis of Amniota: the importance of integumentary characters and increased taxonomic sampling. Systematic Biology 54, 530-547.

Hitchin, R. and Benton, M. J., 1997a. Congruence between parsimony and stratigraphy: comparisons of three indices. Paleobiology 23, 20-32.

Hitchin, R. and Benton, M. J., 1997b. Stratigraphic indices and tree balance. Systematic Biology 46, 563-569.

Hone, D. W. E. and Benton, M. J., 2008. Contrasting supertrees and total-evidence methods: pterosaur origins. Zitteliana B 28, 35-60.

Hook, R. W. and Hotton III, N., 1991. A new sphenacodontid pelycosaur (Synapsida) from the Wichita Group, Lower Permian of north-central Texas. Journal of Vertebrate Paleontology 11, 37-44.

Hopson, J. A., 2012. The role of foraging mode in the origin of therapsids: implications for the origin of mammalian endothermy. Fieldiana Life and Earth Sciences 5, 126-148.

Hopson, J. A. and Barghusen, H., 1986. An analysis of therapsid relationships, in: N. Hotton III, P. D. MacLean, J. J. Roth and E. C. Roth (Eds.), The Ecology and Biology of Mammal-Like Reptiles. Smithsonian Institution Press, Washington DC, pp. 83-106.

Huelsenbeck, J. P., 1994. Comparing the stratigraphic record to estimates of phylogeny. Paleobiology 20, 470-483.

Hunt, G. and Carrano, M. T., 2010. Models and methods for analyzing phenotypic evolution in lineages clades, in: J. Alroy and G. Hunt (Eds.), Quantitative Methods in Paleobiology. Paleontological Society, pp. 245-269.

Huttenlocker, A., 2009. An investigation into the cladistic relationships and monophyly of therocephalian therapsids. Zoological Journal of the Linnean Society 157, 865-891.

Huttenlocker, A., Sidor, C. A. and Smith, R. M. H., 2011. A new specimen of *Promoschorhynchus* (Therapsida: Therocephalia: Akidnognathidae) from the Lower Triassic

of South Africa and its implications for theriodont survivorship across the Permo-Triassic boundary. Journal of Vertebrate Paleontology 31, 405-421.

Irmis, R. B., Whiteside, J. H. and Kammerer, C. F., 2013. Non-biotic controls of observed diversity in the paleontologic record: an example from the Permo-Triassic Karoo Basin of South Africa. Palaeogeography, Palaeoclimatology, Palaeoecology 372, 62-77.

Ivakhnenko, M. F., 1995. New primitive Therapsida from the Permian of Eastern Europe. Paleontologicheskii Zhurnal 29, 110-119.

Izart, A., Palhol, F., Gleixner, G., Elie, M., Blaise, T., Suarez-Ruiz, I., Sachsenhofer, R. F., Privalov, V. A. and Panova, E. A., 2012. Palaeoclimate reconstruction from biomarker geochemistry and stable isotopes of n-alkanes from Carboniferous and Early Permian humic coals and limnic sediments in western and eastern Europe. Organic Geochemistry 43, 125-149.

Jaekel, O., 1910. *Naosaurus credneri* im Rotliegenden von Sachsen. Zeitschrift der Deutschen Geologischen Gesellschaft 62, 526-535.

Jalil, N. E., 1999. Continental Permian and Triassic vertebrate localities from Algeria and Morocco and their stratigraphical correlations. Journal of African Earth Sciences 29, 219-302.

Källersjö, M., Albert, V. A. and Farris, J. S. 1999. Homoplasy increases phylogenetic structure. Cladistics 15, 91-93.

Kammerer, C. F., 2011. Systematics of the Anteosauria (Therapsida: Dinocephalia). Journal of Systematic Palaeontology 9, 261-304.

Kammerer, C. F., Angielczyk, K. D. and Fröbisch, J., 2011. A comprehensive taxonmic revivison of *Dicynodon* (Therapsida, Anomodontia) and its implications for dicynodont phylogeny, biogeography and biostratigraphy. Journal of Vertebrate Paleontology 31 (S1), 1-158.

Kammerer, C. F., Jansen, M. and Fröbisch, J., 2013. Therapsid phylogeny revisited. Journal of Vertebrate Paleontology 33 (Program and Abstracts, 2013), 150

Kazancıoğlu, E., Near, T. J., Hanel, R. and Wainwright, P. C., 2009. Influence of sexual selection and feeding functional morphology on diversification rate of parrotfish (Scaridae). Proceedings of the Royal Society B 276, 3439-3446.

Kemp, T., 1978. Stance and gait in the hindlimb of a therocephalian mammal-like reptile. Journal of the Zoological Society of London 186, 143-161.

Kemp, T. S., 1982. Mammal-Like Reptiles and the Origin of Mammals. Academic Press, New York.

Kemp, T. S., 2006. The origin and early radiation of the therapsid mammal-like reptiles: a palaeobiological hypothesis. Journal of Evolutionary Biology 19, 1231-1247.

Kemp, T. S., 2009. Phylogenetic interrelationships and pattern of evolution of the therapsids: testing for polytomy. Palaeontologia Africana 44, 1-12.

Kessler, J. L. P., Soreghan, G. S. and Wacker, H. J., 2001. Equatorial aridity in western Pangaea: Lower Permian Loessite and Dolomitic palaeosols in northeastern New Mexico. Journal of Sedimentary Research 71, 817-832.

Kiessling, W. and Baron-Szabo, R. C., 2004. Extinction and recovery patterns of scleractinian corals at the Cretacous-Tertiary boundary. Palaeogeography, Palaeoclimatology, Palaeoecology 214, 195-223.

King, G. M., 1988. Anomodontia. Gustav Fischer Verlag, Stuttgart, New York.

Kissel, R. A., 2010. Morphology, Phylogeny, and Evolution of the Diadectidae (Cotylosauria: Diadectomorpha). University of Toronto, Toronto.

Kissel, R. A. and Reisz, R. R., 2004. Synapsid fauna of the Upper Pennsylvanian Rock Lake Shale near Garnett, Kansas and the diversity pattern of early amniotes, in: G. Arratia, M. V.

H. Wilson and R. Cloutier (Eds.), Recent Advances in the Origin and Early Radiation of Vertebrates. Verlag Dr. Friedrich Pfeil, Munich, pp. 409-428.

Klein, N. and Albers, P. C. H., 2009. A new species of the sauropsid reptile *Nothosaurus* from the Lower Muschelkalk of the western Germanic Basin, Winterswijk, The Netherlands. Acta Palaeontologica Polonica 54, 589-598.

Kluge, A., 1997a. Testability and the refutation and corroboration of cladistic hypotheses. Cladistics 13, 81-93.

Kluge, A., 1997b. Sophisticated falsification and research cycles: consequences for differential character weighting in phylogenetic systematics. Zoologica Scripta 26, 349-360.

Kluge, A., 2005. What is the rationale for "Ockham's Razor" (a.k.a. parsimony) in phylogenetic inference? In: Albert, V. (ed.), Parsimony, Phylogeny, and Genomics. Oxford University Press, Oxford, pp. 15-42

Kowalewski, M., Kiessling, W., Aberhan, M., Fuersich, F. T., Scarponi, D., Barbour Wood, S. L. and Hoffmeister, A. P., 2006. Ecological, taxonomic, and taphonomic components of the post-Paleozoic increase in sample-level species diversity of marine benthos. Paleobiology 32, 553-561.

Kozak, K. H., Larson, A. A., Bonett, R. M. and Harmon, L. J., 2005. Phylogenetic analysis of ecomorphological divergence, community structure, and diversification rates in dusky salamanders (Plethodontidae: *Desmognathus*). Evolution 59, 2000-2016.

Lane, A., Janis, C. M. and Sepkoski, J. J. Jr., 2005. Estimating paleodiversities: a test of the taxic and phylogenetic methods. Paleobiology 31, 21-34.

Lanave, B., Oreoarata, G., Saccone, C. and Serio, G. 1984. A new method for calculating evolutionary substitution rates. Journal of Molecular Evolution 20, 86-93

Langston, W., jr, 1965. *Oedaleops campi* (Reptilia: Pelycosauria) new genus and species from the Lower Permian of New Mexico and the family Eothyrididae. Bulletin of the Texas Memorial Museum 9, 5-47.

Langston, W., jr and Reisz, R. R., 1981. *Aerosaurus wellesi*, new species, a varanopseid mammal-like reptile from the Lower Permian of New Mexico. Journal of Vertebrate Paleontology 1, 73-96.

Laurin, M., 1993. Anatomy and relationships of *Haptodus garnettensis*, a Pennsylvanian synapsid from Kansas. Journal of Vertebrate Paleontology 13, 200-229.

Laurin, M., 2004. The evolution of body size, Cope's Rule and the origin of amniotes. Systematic Biology 53, 594-622.

Laurin, M. and Reisz, R. R., 1990. *Tetraceratops* is the oldest known therapsid. Nature 345.

Laurin, M. and Reisz, R. R., 1996. The osteology and relationships of *Tetraceratops insignis*, the oldest known therapsid. Journal of Vertebrate Paleontology 16, 95-102.

Lee, M. S. Y. and Worthy, T. H., 2012. Likelihood reinstates *Archaeopteryx* as a primitive bird. Biology Letters 8, 299-303

Lefebvre, B., 2005. Stylophoran supertrees revisited. Acta Palaeontologica Polonica 50, 477-486.

Leidy, J., 1854. On *Bathygnathus borealis*, an extinct saurian of the New Red Sandstone of Prince Edward's Island. Philadelphia Academy of Natural Sciences Proceedings 2, 327-300.

Levasseur, C. and Lapointe, F.-J., 2003. Increasing phylogenetic accuracy with global congruence, in: M. Janowitz, F.-J. Lapointe, F. R. McMorris, B. Mirkin and F. S. Roberts (Eds.), Bioconsensus. American Mathematical Society, Providence, USA, pp. 221-230.

Lewis, P. O., 2001. A likelihood approach to estimating phylogeny from discrete morphological character data. Systematic Biology 50, 913-925.

Lewis, G. E. and Vaughn, P. P., 1965. Early Permian vertebrates from the Cutler Formation of the Placerville Area Colorado. U.S. Geological Survey 503, 1-49.

Liu, J., Rubidge, B. and Li, J., 2009a. New basal synapsid supports Laurasian origin for therapsids. Acta Palaeontologica Polonica 54, 393-400.

Liu, J., Rubidge, B. and Li, J., 2009b. A new specimen of *Biseridens qilianicus* indicates its phylogenetic position as the most basal anomodont. Proceedings of the Royal Society B 277, 285-292.

Lloyd, G. T., 2012. A refined modelling approach to assess the influence of sampling on palaeobiodiversity curves: new support for declining Cretaceous dinosaur richness. Biology Letters 8, 123-126.

Lloyd, G. T., Davis, K. E., Pisani, D., Traver, J. E., Ruta, M., Sakamoto, M., Hone, D. W. E., Jennings, R. and Benton, M. J., 2008. Dinosaurs and the Cretaceous Terrestrial Revolution. Proceedings of the Royal Society B 275, 2483-2490.

Lloyd, G. T. and Friedman, M., 2013. A survey of palaeontological sampling biases in fishes based on the Phanerozoic record of Great Britain. Palaeogeography, Palaeoclimatology, Palaeoecology 372, 5-7.

Lozovsky, V. R., 2003. Correlation of the continental Permian of northern Pangea: a review. Bolletina della Societa Italiano Volume Especiale 2, 239-244.

Lozovsky, V. R., 2005. Olson's gap or Olson's bridge, that is the question, in: S. G. Lucas and K. E. Zeigler (Eds.), The Nonmarine Permian, New Mexico Museum of Natural History and Science Bulletin No. 30. New Mexico Museum of Natural History, Albuquerque, pp. 179-184.

Lucas, S. G., 2004. A global hiatus in the Middle Permian tetrapod fossil record. Stratigraphy 1, 47-64.

Lucas, S. G., 2013. Vertebrate biostratigraphy and biochronology of the upper Paleozoic Dunkard Group, Pennsylvania – West Virginia – Ohio, USA

Lucas, S. G., 2006. Global Permian tetrapod biostratigraphy and biochronology, in: S. G. Lucas, G. Cassinis and J. W. Schneider (Eds.), Non-marine Permian Biostratigraphy and Biochronology: Special Publication 265. Geological Society of London, London.

Lucas, S. G., Cassinis, G. and Schneider, J. W., 2006. Non-marine Permian biostratigraphy and biochronology: an introduction, in: S. G. Lucas, G. Cassinis and J. W. Schneider (Eds.), Non-marine Permian biostratigraphy and biochronology. Geological Society of London, London, pp. 1-14.

Lucas, S. G., Harris, S. K., Speimann, J. A., Berman, D. S., Henrici, A. C., Heckert, S. B., Zeigler, K. E. and Rinehart, L. F., 2005. Early Permian vertebrate assemblage and its biostratigraphic significance, Arroyo del Agua, Rio Arriba County, New Mexico., Geology of the Chama Basin, Field Conference Guidebook. New Mexico Geological Society, pp. 288-296.

Lucas, S. G. and Heckert, S. B., 2001. A global hiatus in the record of Middle Permian tetrapods. Journal of Vertebrate Paleontology 21, 75.

MacDougal, M. J. and Reisz, R. R., 2012. A new parareptile (Parareptilia, Lanthanosuchoidea) from the Early Permian of Oklahoma. Journal of Vertebrate Paleontology 32, 1018-1026.

Maddin, H. C., Evans, D. C. and Reisz, R. R., 2006. An Early Permian varanodontine varanopid (Synapsida: Eupelycosauria) from the Richards Spur Locality, Oklahoma. Journal of Vertebrate Paleontology 26, 957-966.

Maddin, H. C. and Reisz, R. R., 2007. The morphology of the terminal phalanges in Permo-Carboniferous synapsids: and evolutionary perspective. Canadian Journal of Earth Sciences 44, 267-274.

Maddin, H. C., Sidor, C. A. and Reisz, R. R., 2008. Cranial anatomy of *Ennatosaurus tecton* from the Middle Permian of Russia and the evolutionary relationships of Caseidae. Journal of Vertebrate Paleontology 28, 160-180.

Mannion, P. D. and Upchurch, P., 2010. Completeness metrics and the quality of the sauropodomorph fossil record through geological and historical time. Paleobiology 36, 283-302.

Mannion, P. D., Upchurch, P., Carrano, W. T. and Barrett, P. M., 2011. Testing the effect of the rock record on diversity: a multidisciplinary approach to elucidating the generic richness of sauropodomorph dinosaurs through time. Biological Reviews 86, 157-181.

Marjanović, D. and Laurin, M., 2007. Fossils, molecules, divergence times, and the origin of lissamphibians. Systematic Biology 56, 369-388.

Matthew, E. D., 1908. A four horned pelycosaurian from the Permian of Texas. Bulletin of the American Museum of Natural History 24, 183-185.

Maxwell, W. D. and Benton, M. J., 1990. Historical tests of the absolute completeness of the fossil record of tetrapods. Paleobiology 16, 322-335.

Mazierski, D. M. and Reisz, R. R., 2010. Description of a new specimen of *Ianthasaurus hardestiorum* (Eupelycosauria: Edaphosauridae) and a re-evaluation of edaphodaurid phylogeny. Canadian Journal of Earth Sciences 47, 901-912.

McKinney, M. L., 1990. Classifying and analysing evolutionary trends, in: K. J. McNamara (Ed.), Evolutionary Trends. Belhaven, London, pp. 28-58.

McLeish, m. J., Chapman, T. W. and Schwarz, M. P., 2007. Host-driven diversification of gall-inducing Accacia thrips and the aridification of Australia. BMC Biology 5, doi:10.1186/1741-7007-1185-1183.

Miller, A. I. and Foote, M., 1996. Calibrating the Ordovician Radiation of Marine Life: Implications for Phanerozoic Diversity Trends. Paleobiology 22, 304-309.

Modesto, S., 1994. The Lower Permian synapsid *Glaucosaurus* from Texas. Palaeontology 37, 51-60.

Modesto, S., 1995. The skull of the herbivorous *Edaphosaurus boanerges* from the Lower Permian of Texas. Palaeontology 38, 213-239.

Modesto, S., 2006. The cranial skeleton of the Early Permian aquatic reptile *Mesosaurus tenuidens*: implications for relationships and palaeobiology. Zoological Journal of the Linnean Society 146, 345-368.

Modesto, S., 2010. The postcranial skeleton of the aquatic parareptile *Mesosaurus tenuidens* from the Gongwanan Permian. Journal of Vertebrate Paleontology 30, 1378-1395.

Modesto, S. and Reisz, R. R., 1990. Taxonomic status of *Edaphosaurus raymondi* Case. Journal of Paleontology 64, 1049-1051.

Modesto, S., Sidor, C. A., Rubidge, B. and Welman, J., 2001. A second varanopseid skull from the Upper Permian of South Africa: implications for Late Permian 'pelycosaur' evolution. Lethaia 34, 249-259.

Modesto, S., Smith, R. M. H., Campione, N. E. and Reisz, R. R., 2011. The last "pelycosaur": a varanopid synapsid from the *Pristerognathus* Assemblage Zone, Middle Permian of South Africa. Naturwissenschaften 98, 1027-1034.

Montanez, I. P., Tarbor, N., Niemeier, D., DiMichele, W. A., Frank, T. D., Fielding, C. R., Isbell, J. L., Birgenheier, L. P. and Rygel, M. C., 2007. CO2-forced climate and vegetation instability during late Paleozoic deglaciation. Science 315, 87-91.

Moore, B. R., Chan, K. M. A. and Donoghue, M. J., 2004. Detecting Diversification rate variation in supertrees, in: O. R. Beninda-Emonds (Ed.), Phylogenetic Supertrees: Combining Information to Reveal the Tree of Life. Kluwer Academic Publishers, Dordrecht, pp. 487-534.

Moore, B. R. and Donoghue, M. J., 2009. A Bayesian approach from evaluating the impact of historical events on rates of diversification. Proceedings of the National Academy of Sciences 106, 4307-4312.

Müller, J. and Reisz, R. R., 2006. The phylogeny of early eureptiles: comparing parsimony and Bayesian approaches in the investigation of a basal fossil clade. Systematic Biology 55, 503-511.

Nicolas, M. and Rubidge, B. S. 2009. Assessing content and bias in South African Permo-Triassic Karoo tetrapod fossil collections. Palaeontologia Africana 44, 13-20.

Nicolas, M. and Rubidge, B. S., 2010. Changes in Permo-Triassic terrestrial tetrapod ecological representation in the Beaufort Group (Karoo Supergroup) of South Africa. Lethaia 43, 45-59

Norrel, M., 1992. Taxic origin and temporal diversity: the effect of phylogeny, in: M. Novacek and Q. Wheeler (Eds.), Extinction and Phylogeny. Columbia University Press, New York, pp. 89-118.

Norrel, M., 1993. Tree-based approaches to understanding history: comments on ranks, rules and the quality of the fossil record. American Journal of Science 293, 407-417.

Norrel, M. and Novacek, M., 1992. The fossil record and evolution: comparing cladistic and paleontologic evidence for vertebrate history. Science 255, 1690-1693.

O'Keefe, F. R., Sidor, C. A., Larsson, H. C. E., Maga, A. and Ide, O., 2005. The vertebrate fauna of the Upper Permian of Niger - III, morphology and ontogeny of the hindlimb of *Moradisaurus grandis* (Reptilia, Captorhindae). Journal of Vertebrate Paleontology 25, 309-319.

O'Leary, M. A., Bloch, J. I., Flynn, J. J., Gaudin, T. J., Giallombardo, A., Gianni, N. P., Goldberg, S. L., Kraatz, B. P., Luo, Z.-X., Meng, J., Ni, X., Novacek, M., Perini, F. A., Randall, Z. S., Rougier, G. W., Sargis, E. J., Silcox, M. T., Simmons, N. B., Spaulding, M.,

Velazco, P. M., Weksler, M., Wible, J. R. and Cirranello, A. L., 2013. The placental mammal ancestor and the post-K-Pg radiation of placentals. Science 339, 662-667.

Oliveira, T. V. D., Soares, M. B. and Schultz, C. L., 2010. *Trucidocynodon riograndensis* gen. nov. et sp. nov. (Eucynodontia), a new cynodont from the Brazilian Upper Triassic (Santa Maria Formation). Zootaxa 2382, 1-71.

Olson, E. C., 1954. Fauna of the Vale and Choza: 7. Pelycosauria: family Caseidae. Fieldiana: Geology 10, 193-204.

Olson, E. C., 1957. Catalogue of localities of Permian and Triassic terrestrial vertebrates of the territories of the USSR. Journal of Geology 65, 196-226.

Olson, E. C., 1962. Late Permian terrestrial vertebrates, USA and USSR. Transactions of the American Philosophical Society 52, 1-224.

Olson, E. C., 1965. New Permian vertebrates from the Chickasha Formation in Oklahoma. Oklahoma Geological Survey 70, 1-70.

Olson, E. C., 1966. Community evolution and the origin of mammals. Ecology 47, 291-302.

Olson, E. C., 1968. The family Caseidae. Fieldiana: Geology 17, 225-349.

Olson, E. C., 1974. On the source of therapsids. Annals of the South African Museum 64, 27-46.

Olson, E. C. and Barghusen, H., 1962. Permian vertebrates from Oklahoma and Texas. Oklahoma Geological Survey Circular 59, 1-68.

Olson, E. C. and Beerbower, J. R., 1953. The San Angelo formation, Permian of Texas, and its vertebrates. Journal of Geology 61, 389-423.

Osborn, H. F., 1903. On the primary division of the Reptilia into two sub-classes Synapsida and Diapsida. Science 17, 275-276

Williston, S. W., 1912. Primitive reptiles. A review. Journal of Morphology 23, 637-666

Peabody, F. E., 1957. Pennsylvanian reptiles of Garnett, Kansas: *Edaphosaurus*. Journal of Paleontology 31, 947-949.

Pearson, M., Benson, R. B. J., Upchurch, P., Fröbisch, J. and Kammerer, C. F., 2013. Reconstructing the diversity of early terrestrial herbivorous tetrapods. Palaeogeography, Palaeoclimatology, Palaeoecology 372, 41-49.

Peters, S. E., 2006. Macrostratigraphy of North America. Journal of Geology 114, 391-412.

Peters, S. E. and Heim, N. A., 2010. The geological completeness of paleontological sampling in North America. Paleobiology 36, 61-79.

Philips, J., 1860. Life on the Earth. Its origins and succession. Macmillan, Cambridge, UK.

Piaggio-Talice, R., Burleigh, J. G. and Eulenstein, O., 2004. Quartet supertrees, in: O. R. Beninda-Edmonds (Ed.), Phylogenetic Supertrees: Combining Information to Reveal the Tree of Life. Kluwer Academic Press, Dordrecht, pp. 173-191.

Pisani, D., Yates, A. M., Langer, M. C. and Benton, M. J., 2002. A genus-level supertree of the Dinosauria. Proceedings of the Royal Society B 269, 915-921.

Pol, D. and Escapa, I. 2009. Unstable taxa in cladistic analysis: identification and the assessment of relevant characters. Cladistics 25, 515-527

Pol, D., Norrel, M. and Siddall, M. E., 2004. Measures of stratigraphic fit to phylogeny and their sensitivity to tree size, tree shape and scale. Cladistics 20, 64-75.

Pollock, D. D., Zwickl, D. J., McGquire, J. A. and Hillis, D. M., 2002. Increased taxon sampling is advantageous for phylogenetic inference. Systematic Biology 51, 664-671.

Preston, F. W., 1962. The canonical distribution of commonness and rarity: Part I. Ecology 43, 185-215.

Purvis, A., 1995. A modification to Baum and Ragan's method for combining phylogenetic trees. Systematic Biology 44, 251-255.

Purvis, A. and Webster, A. J., 1999. Phylogenetically independent comparisons and primate phylogeny, in: P. C. Lee (Ed.), Comparative Primate Socioecology. Cambridge University Press, Cambridge, pp. 44-70.

Ragan, M. A., 1992. Phylogenetic inference based on matrix representation of trees. Molecular Phylogenetic Evolution 1, 53-58.

Rambaut, A., Harvey, P. H. and Nee, S., 1997. End-Epi: an application for inferring phylogenetic and population dynamical processes from molecular sequences. Computer applications in the Biosciences 13, 303-306.

Raup, D. M., 1972. Taxonomic diversity during the Phanerozoic. Science 177, 1065-1071.

Raup, D. M., 1975. Taxonomic diversity estimates under rarefaction. Paleobiology 1, 333-342.

Raup, D. M., 1991. A kill curve for Phanerozoic marine species. Paleobiology 17, 37-48.

Raup, D. M., Gould, S. J., Schopf, T. J. M. and Simberloff, D. S., 1973. Stochastic models of phylogeny and the evolution of diversity. Journal of Geology 81, 525-542.

Raup, D. M. and Sepkoski, J. J. Jr., 1982. Mass extinctions in the marine fossil record. Science 215, 1501-1503.

Rees, P. M., Ziegler, A. M., Gibbs, M. T., Kutzbach, J. E., Behling, P. J. and Rowley, D. B., 2002. Permian phytogeographic patterns and climate data/model comparisons. Journal of Geology 110, 1-31.

Reisz, R. R., 1972. Pelycosaurian reptiles from the Middle Pennsylvanian of North America. Bulletin of the Museum of Comparitive Zoology 144, 27-60.

Reisz, R. R., 1980. The Pelycosauria: a review of phylogenetic relationships, in: A. L. Panchen (Ed.), The Terrestrial Environmnet and the Origin of Land Vertebrates. Academic Press, London, pp. 553-592.

Reisz, R. R., 1986. Pelycosauria. Gustav Fischer Verlag, Stuttgart, Stuttgart, New York.

Reisz, R. R., 1997. The origin and early evolutionary history of amniotes. Trends in Ecology and Evolution 12, 218-222.

Reisz, R. R., 2005. *Oromycter*, a new caseid from the Lower Permian of Oklahoma. Journal of Vertebrate Paleontology 25, 905-910.

Reisz, R. R. and Berman, D. S., 1986. *Ianthasaurus hardestii* n. sp., a primitive edaphosaur (Reptilia, Pelycosauria) from the Upper Pennsylvanian Rock Lake Shale near Garnett, Kansas. Canadian Journal of Earth Sciences 23, 77-91.

Reisz, R. R., Berman, D. S. and Scott, D., 1992. The cranial anatomy and relationships of *Secodontodaurus*, an unusual mammal-like reptile (Synapsida: Sphenacodontidae) from the early Permian of Texas. Zoological Journal of the Linnean Society 104, 127-184.

Reisz, R. R. and Dilkes, D. W., 2003. *Archaeovenator hamiltonensis*, a new varanopid (Synapsida: Eupelycosauria) from the Upper Carboniferous of Kansas. Canadian Journal of Earth Sciences 40, 667-678.

Reisz, R. R., Dilkes, D. W. and Berman, D. S., 1998. Anatomy and relationships of *Elliotsmithia longiceps* Broom, a small synapsid, not a diapsid reptile. Journal of Vertebrate Paleontology 18, 602-611.

Reisz, R. R. and Fröbisch, J., 2014. The oldest caseid synapsid from the Late Pennsylvanian of Kansas, and the evolution of herbivory in terrestrial vertebrates. PlosOne 9, e94518.

Reisz, R. R., Godfrey, S. J. and Scott, D., 2009. *Eothyris* and *Oedaleops*: Do these Early Permian synapsids from Texas and New Mexico form a clade? Journal of Vertebrate Paleontology 29, 39-47.

Reisz, R. R. and Laurin, M., 2001. The reptile *Macroleter*: First vertebrate evidence for correlation of Upper Permian continental strata of North America and Russia. Geological Society of America Bulletin 113, 1229-1233.

Reisz, R. R. and Laurin, M., 2002. The reptile *Macroleter*: First vertebrate evidence for correlation of Upper Permian continental strata of North America and Russia: Discussion and reply. Geological Society of America Bulletin 114, 1174-1175.

Reisz, R. R. and Laurin, M., 2004. A reevaluation of the enigmatic Permian synapsid *Watongia* and of its stratigraphic significance. Canadian Journal of Earth Sciences 41, 377-386.

Reisz, R. R., Laurin, M. and Marjanović, D., 2010. *Apsisaurus witteri* from the Lower Permian of Texas: yet another small varanopid synapsid, not a Diapsid. Journal of Vertebrate Paleontology 30, 1628-1631.

Reisz, R. R., Maddin, H. C., Fröbisch, J. and Falconnet, J., 2011. A new large caseid (Synapsida, Caseasauria) from the Permian of Rodez (France), including a reappraisal of *"Casea" rutena* Sigogneau-Russell & Russell, 1974. Geodiversitas 33, 227-246.

Reisz, R. R. and Modesto, S., 2007. *Heleosaurus scholtzi* from the Permian of South Africa: varanopid synapsid, not a diapsid reptile. Journal of Vertebrate Paleontology 27, 734-739.

Reisz, R. R. and Sues, H.-D., 2000. Herbivory in late Paleozoic and Triassic terrestrial vertebrates, in: H.-D. Sues (Ed.), Evolution of Herbivory in Terrestrial Vertebrates: Perspectives from the Fossil Record. Cambridge University Press, Cambridge.

Renesto, S., 1994. *Megalancosaurus*, a possibly arboreal archosauromorph (Reptilia) from the Upper Triassic of Northern Italy. Journal of Vertebrate Paleontology 14, 38-52.

Romano, M. and Nicosia, U., 2014. *Alierasaurus ronchii*, gen. et sp. nov., a caseid from the Permian of Sardinia, Italy. Journal of Vertebrate Paleontology 34, 900-913.

Romer, A. S., 1937. New genera and species of pelycosaurian reptiles. Proceedings of the New England Zoological Club 16, 89-96.

Romer, A. S., 1945. The Late Carboniferous vertebrate fauna of Kounova (Bohemia) compared with that of the Texas Redbeds. American Journal of Science 243, 417-442.

Romer, A. S., 1956. Osteology of the Reptiles. University of Chicago Press, Chicago.

Romer, A. S. and Price, L. I., 1940. Review of the Pelycosauria. Geological Society of America Special Publications, Volume 28.

Ronchi, A., Sacchi, E., Romano, M. and Nicosia, U., 2011. A huge caseid pelycosaur from north-western Sardinia and its bearing on European Permian stratigraphy and palaeobiogeography. Acta Palaeontologica Polonica 56, 723-738.

Ronquist, F., 1996. Matrix representation of trees, redundancy and weighting. Systematic Biology 45, 247-253.

Ronquist, F., Teslenko, M., van der Mark, P., Ayres, D. L., Darling, A., Höhna, S., Larget, B., Liu, L., Suchard, M. A. and Huelsenbeck, J. P., 2012. MrBayes 3.2: Efficient Bayesian phylogenetic inference and model choice across a large model space. Systematic Biology 61, 539-542.

Rook, D. L., Heim, N. A. and Marcot, J., 2013. Contrasting patterns and connections of rock and biotic diversity in the marine and non-marine fossil records of North America. Palaeogeography, Palaeoclimatology, Palaeoecology 372, 123-129.

Rowe, T., 1986. Osteological diagnosis of Mammalia, L. 1758, and its relationships to extinct Synapsida. University of California, Berkeley.

Roy, K., Hunt, G. and Jablonski, D., 2009. Phylogenetic conservatism of extinction in marine bivalves. Science 325, 733-737.

Rüber, L., Van Tassell, J. L. and Zardoya, R., 2003. Rapid speciation and ecological divergence in the American seven-spines gobies (Gobiidae, Gobiosomatini) inferred from a molecular phylogeny. Evolution 57, 1584-1598.

Rubidge, B., Erwin, D. H., Remezani, J., Bowring, S. A. and de Klark, W. J., 2013. High-precision temporal calibration of Late Permian vertebrate biostratigraphy: U-Pb zircon constraints from the Karoo Supergroup. Geology 41, 363-366.

Rubidge, B. and Sidor, C. A., 2001. Evolutionary patterns among Permo-Triassic therapsids. Annual Review of Ecology and Systematics 32, 449-480.

Ruta, M. and Benton, M. J., 2008. Calibrated diversity, tree topology and the mother of mass extinctions: the lesson of temnospondyls. Palaeontology 51, 1261-1288.

Ruta, M., Cisneros, J. C., Liebrecht, T., Tsuji, L. A. and Müller, J., 2011. Amniotes through major biological crises: faunal turnover among parareptiles and the end-Permian mass extinction. Palaeontology 54, 1117-1137.

Ruta, M., Jeffery, J. E. and Coates, M. I., 2003. A supertree of early tetrapods. Proceedings of the Royal Society B 270, 2507-2516.

Ruta, M., Pisani, D., Lloyd, G. T. and Benton, M. J., 2007. A supertree of Temnospondyli: cladogenetic patterns in the most species-rich group of early tetrapods. Proceedings of the Royal Society B 274, 3087-3095.

Ruta, M., Wagner, P. J. and Coates, M. I., 2006. Evolutionary patterns in early tetrapods. I. Rapid initial diversification followed by decrease in rates of character change. Proceedings of the Royal Society B 273, 2107-2111.

Sahney, S. and Benton, M. J., 2008. Recovery from the most profound mass extinction of all time. Proceedings of the Royal Society B 275.

Sahney, S., Benton, M. J. and Falcon-Lang, H. J., 2010. Rainforest collapse triggered Carboniferous tetrapod diversification in Euramerica. Geology 38, 1079-1082.

Salamin, N., Hodkinson, T. R. and Savolainen, V., 2002. Building supertrees: an empirical assessment using the grass family (Poaceae). Systematic Biology 51, 134-150.

Sanders, H. L., 1968. Marine benthic diversity: a comparative study. The American Naturalist 102, 243-282.

Sanderson, M. J., Purvis, A. and Henze, C., 1998. Phylogenetic supertrees: assembling the trees of life. Trends in Ecology and Evolution 13, 105-109.

Semple, C. and Steel, M. A., 2000. A supertree method for rooted trees. Discrete Applied Mathematics 105, 501-514.

Sepkoski, J. J. Jr., 1981. A factor analysis description of the Phanerozoic marine fossil record. Paleobiology 7, 3-53.

Sepkoski, J. J. Jr., 1984. A kinetic model of Phanerozoic taxonomic diversity. III. Post-Paleozoic families and mass extinctions. Paleobiology 10, 246-267.

Sepkoski, J. J. Jr., 1993. Ten years in the library: new data confirm paleontological patterns. Paleobiology 19, 43-51.

Sepkoski, J. J. Jr., 1996. Patterns of Phanerozoic extinction: a perspective from global data bases, in: O. H. Walliser (Ed.), Global Events and Event Stratigraphy. Springer, Berlin, pp. 35-51.

Sepkoski, J. J. Jr., 2002. A compendium of fossil marine animal genera. Bulletins of American Paleontology 364, 1-560.

Sepkoski, J. J. Jr., Bambach, R. K., Raup, D. M. and Valentine, J. W., 1981. Phanerozoic marine diversity and the fossil record. Nature 293, 435-437.

Sereno, P. C., 1999. The evolution of dinosaurs. Science 284, 2137-2147.

Sereno, P. C., Dutheil, D. B., Iarochene, M., Larsson, H. C. E., Lyon, G. H., Magwene, P. M., Sidor, C. A., Varricchio, D. J. and Wilson, J. A., 1996. Predatory dinosaurs from the Sahara and Late Cretaceous faunal differentiation. Science 272, 986-991.

Shear, W. A. and Sheldon, P. A., 2001. Rustling in the undergrowth: animals in early terrestrial ecosystems, in: P. G. Gensel and D. Edwards (Eds.), Plants Invade the Land. Columbia University Press, New York.

Shikama, T., Kamei, T. and Murata, M., 1978. Early Triassic ichthyosaurus, *Utatsusaurus hataii* gen . et sp. nov., from the Kitakami Massif, Northeast Japan. Tokyo University Science Reports, Snd Series (Geology) 48, 77-97.

Siddall, M. E., 1996. Stratigraphic consistency and the shape of things. Systematic Biology 45, 111-115.

Siddall, M. E., 1997. Stratigraphic indices in the balance: a reply to Hitchin and Benton. Systematic Biology 46, 569-573.

Siddall, M. E., 1998. Stratigraphic fit to phylogenies: a proposed solution. Cladistics 14, 201-208.

Sidor, C. A., 2001. Simplification as a trend in synapsid cranial evolution. Evolution 55, 1419-1442.

Sidor, C. A., 2003. Evolutionary trends and the origin of the mammalian lower jaw. Paleobiology 29, 605-640.

Sidor, C. A., 2013. The vertebrate fauna of the Upper Permian of Niger - VIII. Nigerpeton ricqlesi (Temnospondyli: Cochleosauridae) and tetrapod biogeographic provinces. Comptes Rendus Pelevol 12, 463-472.

Sidor, C. A., Blackburn, D. C. and Gado, B., 2003. The vertebrate fauna of the Upper Permian of Niger - II, preliminary description of a new pareiasaur. Palaeontologia Africana 39, 45-52.

Sidor, C. A. and Hopson, J. A., 1995. The taxonomic status of the Upper Permian eotheriodont therapssids of the San Angelo Formation (Guadalupian), Texas. Journal of Vertebrate Paleontology 15, 53A.

Sidor, C. A. and Hopson, J. A., 1998. Ghost lineages and "mammalness": assessing the temporal pattern of character aquisition in the Synapsida. Paleobiology 24, 254-273.

Sidor, C. A., O'Brien, L. J., Damiani, R., Steyer, J. S., Smith, R. M. H., Larsson, H. C. E., Sereno, P. C., Ide, O. and Maga, A., 2005. Permian tetrapods from the Sahara show climate-controlled endemism in Pangaea. Nature 434, 886-889.

Sidor, C. A. and Rubidge, B., 2006. *Herpetoskylax hopsoni*, a new biarmosuchian (Therapsida: Biarmosuchia) from the Beaufort Group of South Africa, in: M. T. Carrano (Ed.), Amniote Paleobiology: Perspectives on the Evolution of Mammals, Birds and Reptiles. University of Chicago Press, Chicago, pp. 76-113.

Sidor, C. A. and Smith, R. M. H., 2004. A new galesaurid (Therapsida: Cynodontia) from the Lower Triassic of South Africa. Palaeontology 46, 535-556.

Sidor, C. A. and Welman, J., 2003. A second specimen of *Lemurosaurus pricei* (Therapsida: Burnetiamorpha). Journal of Vertebrate Paleontology 23, 631-642.

Signor, P. W. and Lipps, J. H., 1982. Sampling bias, gradual extinction patterns and catastrophes in the fossil record, in: L. T. Silver and P. H. Schultz (Eds.), Geological Implications of Impacts of Large Asteroids and Comets on the Earth. Geological Society of America, pp. 291-296.

Sigogneau-Russell, D. and Russell, D. E., 1974. Etude du premier caseide (Reptilia: Pelycosauria) d'Europe occidental. Bulletin du Museum National d'Histoire Naturelle 230, 145-216.

Smiley, T. M., Sidor, C. A., Maga, A. and Ide, O., 2008. The vertebrate fauna of the Upper Permian of Niger. VI. First evidence of a gorgonopsian therapsid. Journal of Vertebrate Paleontology 28, 543-547.

Smith, A. B., 1994. Systematics and the fossil record: documenting evolutionary patterns. Blackwell, London.

Smith, A. B., 2001. Large scale heterogeneity of the fossil record: implications for Phanerozoic biodiversity studies. Proceedings of the Royal Society B 356, 351-367.

Smith, A. B., 2007. Intrinsic versus extrinsic biases in the fossil record: contrasting the fossil record of echinoids in the Triassic and early Jurassic using sampling data, phylogenetic analysis and molecular clocks. Paleobiology 33, 310-323.

Smith, A. B. and Jeffrey, C. H., 1988. Selectivity of extinction among sea urchins at the end of the Cretaceous period. Nature 392, 69-71.

Smith, A. B. and Littlewood, D. T. J., 1994. Paleontological data and molecular phylogenetic analysis. Paleobiology 20, 259-273.

Smith, A. B. and McGowan, A. J., 2007. The shape of the Phanerozoic palaeodiversity curve: how much can be predicted from the sedimentary rock record of western Europe. Palaeontology 50, 765-774.

Smith, A. B. and McGowan, A. J., 2008. Temporal patterns of barren intervals in the Phanerozoic. Paleobiology 34, 155-161.

Smith, E. P., Stewart, P. and Cairns, J., 1985. Similarities between rarefaction methods. Hydrobiologia 120, 167-170.

Spencer, M. R. and Wilberg, E. W. 2013. Efficiacy or Convenience? Model-based approaches to phylogeny estimation using morphological data. Cladistics 29, 663-671

Spielmann, J. A., Heckert, A. B. and Lucas, S. G., 2005. The Late Triassic archosauromorph *Trilophosaurus* as an arboreal climber. Revista Italiana di Paleontologia et Stratigrafia 111, 395-412.

Steel, M. A., 1992. The complexity of reconstructing trees from qualitative characters and sub-trees. Journal of Classification 9, 91-116.

Steeman, M. E., Hebesgaard, M. B., Fordyce, R. E., Ho, S. Y. W., Rabosky, D. L., Nielsen, R., Rahbek, C., Glenner, H., Sorensen, M. V. and Willerslev, E., 2009. Radiation of extant cetaceans driven by restructuring of the oceans. Systematic Biology 58, 573-585.

Steyer, J. S., Damiani, R., Sidor, C. A., O'Keefe, F. R., Larsson, H. C. E., Maga, A. and Ide, O., 2006. The vertebrate fauna of the Upper Permian of Niger. IV. *Nigerpeton ricqlesi* (Temnospondyli: Cochleosauridae), and the edopoid colonization of Gondwana. Journal of Vertebrate Paleontology 26, 18-28.

Sues, H.-D. and Reisz, R. R., 1998. Origins and early evolution of herbivory in tetrapods. Trends in Ecology and Evolution 13, 141-145.

Sumida, S. S., 1989. New information on the pectoral girdle and vertebral column in *Lupeosaurus* (Reptilia, Pelycosauria). Canadian Journal of Earth Sciences 26, 1343-1349.

Sumida, S. S., Berman, D. S., Henrici, A. C., Kissel, R. A., Eberth, D. A. and Martens, T., 2002. Origins of the modern terrestrial vertebrate ecosystem documented by an Early Permian assemblage from Germany. Journal of Vertebrate Paleontology 22, 112A-113A.

Sumida, S. S., Pelletier, V. and Berman, D. S., 2014. New information on the basal pelycosaurian-grade synapsid *Oedaleops*, in: C. F. Kammerer, K. D. Angielczyk and J. Fröbisch (Eds.), Early Evolutionary History of the Synapsida. Springer, New York.

Tarbor, N. and Poulsen, C. J., 2008. Palaeoclimate across the Late Pennsylvanian-Early Permian tropical palaeolatitudes: a review of climate indicators, their distribution and relation to palaeophysiographic climate factors. Palaeogeography, Palaeoclimatology, Palaeoecology 268, 293-310.

Tavaré, S. 1986. Some probabilistic and statistical problems on the analysis of DNA sequences. Lectures on Mathematics in the Life Sciences 17. 57-85

Tarver, J. E., Braddy, S. J. and Benton, M. J., 2007. The effects of sampling bias on Palaeozoic faunas and implications for macroevolutionary studies. Palaeontology 50, 117-184.

Tarver, J. E., Donoghue, M. J. and Benton, M. J., 2011. Is evolutionary history repeatedly rewritten in light of new fossil discoveries. Proceedings of the Royal Society B 278, 599-604.

Tarver, J. E. and Donoghue, P. C. J., 2011. The trouble with topology: phylogenies without fossils provide a revisionist perspective of evolutionary history in topological analyses of diversity. Systematic Biology 60, 700-712.

Team, R. C., 2013. R: A language and environment for statistical computing. R Foundation for Satistical Computing, Vienna, Austria.

Thomason, J. J. and Russell, A. P., 1986. Mechanical factors in the evolution of the mammalian secondary palate: a theoretical analysis. Journal of Morphology 189, 199-213.

Tolley, K. A., Chase, b. M. and Forest, F., 2008. Speciation and radiations track climate transitions since the Miocene climatic optimum: a case study of southern African chameleons. Journal of Biogeography 35, 1402-1414.

Tomkins, J. L., LeBas, N. R., Witton, M. P., Martill, D. M. and Humphries, S., 2010. Positive allometry and the prehistory of sexual selection. The American Naturalist 176, 141-148.

Tsuji, L. A., Sidor, C. A., Steyer, J. S., Smith, R. M. H., Tarbor, N. and Ide, O., 2013. The vertebrate fauna of the Upper Permian of Niger - VII. Cranial anatomy and relationships of *Bunostegos akokanensis* (Pareiasauria). Journal of Vertebrate Paleontology 33, 747-763.

Upchurch, P. and Barrett, P. M., 2005. Phylogenetic and taxic perspectives on sauropod diversity, in: R. K.C. and J. A. Wilson (Eds.), The Sauropods: Evolution and Palaeobiology. Univeristy of California Press, Berkley and Los Angeles, California, pp. 104-124.

Upchurch, P., Mannion, P. D., Benson, R. B. J., Butler, R. J. and Carrano, W. T., 2011. Geological and anthropogenic controls on the sampling of the terrestrial fossil record: a case study from the Dinosauria, in: A. J. McGowan and A. B. Smith (Eds.), Comparing the Geological and Fossil Records: Implications for Biodiversity Studies. Geological Society of London, Special Publications, London, pp. 209-240.

Valentine, J. W., 1969. Patterns of taxonomic and ecological structure of the shelf benthos during Phanerozoic time. Palaeontology 12, 684-709.

Vaughn, P. P., 1968. Upper Pennsylvanian vertebrates from the Sangre de Cristo Formation of central Colorado. Los Angeles County Museum Contributions in Science 223, 1-30.

Vaughn, P. P., 1971. A *Platyhistrix*-like amphibian with fused vertebrae, from the Upper Pennsylvanian of Ohio. Journal of Paleontology 45, 464.469.

Vences, M., Andreone, F., F., G., Kosuch, J., Meyer, A., Schaefe, H. C. and Veith, M., 2002. Exploring the potential of life-history key innovation: brook breeding in the radiation of the Malagasy treefrog genus *Boophis*. Molecular Ecology 11, 1453-1463.

Wagner, P. J., 2000. The quality of the fossil record and the accuracy of phylogenetic inferences about sampling and diversity. Systematic Biology 49, 65-86.

Wagner, P. J. and Erwin, D. H., 1995. Phylogenetic tests of speciation hypotheses, in: D. H. Erwin and R. L. Anstey (Eds.), New approaches for studying speciation in the fossil record. Columbia University Press, New York.

Wagner, P. J. and Sidor, C. A., 2000. Age rank/clade rank metrics-sampling, taxonomy, and the meaning of stratigraphic consistency. Systematic Biology 49, 463-479.

Wall, P., Ivany, L. and Wilkinson, B., 2009. Revisiting Raup: exploring the influence of outcrop area on diversity in light of modern sample standardization techniques. Paleobiology 35.

Walther, M. and Fröbisch, J., 2013. The quality of the fossil record of anomodonts. Comptes Rendus Pelevol 12, 495-504.

Weishampel, D. B. and Horner, J. R., 1987. Dinosaurs, habitat bottlenecks and the St. Mary River Formation, in: P. J. Currie and E. H. Koster (Eds.), Fourth international Symposium on Mesozoic Terrestrial Ecosystems and Biota: Short Papers. Royal Tyrell Museum, Drumheller, Canada, pp. 224-229.

Wiens, J. J., Parra-Olea, G., Garcia-Paris, M. and Wake, D. B., 2007. Phylogenetic history underlies elevational patterns of biodiversity in tropical salamanders. Proceedings of the Royal Society B 273, 919-928.

Wilkinson, M., Cotton, J. A., Creevey, C., Eulenstein, O., Harris, S. R., Lapointe, F.-J., Levasseur, C., McInerney, J. O., Pisani, D. and Thorley, J. L., 2005a. The shape of supertrees to come: tree shape related properties of fourteen supertree methods. Systematic Biology 54, 419-431.

Wilkinson, M., Pisani, D., Cotton, J. A. and Corfe, I., 2005b. Measuring support and finding unsupported relationships in supertrees. Systematic Biology 54, 823-831.

Wilkinson, M., Thorley, J. L., Littlewood, D. T. J. and Bray, R. A., 2001. Towards a supertree for the Platyhelminthes?, in: D. T. J. Littlewood and R. A. Bray (Eds.), Interrelationships of the Platyhelminthes. Chapman-Hall, Lonson, pp. 292-301.

Williston, S. W., 1910. New Permian reptiles: Rhachitomous vertebrae. Journal of Geology 18, 585-600.

Williston, S. W., 1911. American Permian Vertebrates. University of Chicago Press, Chicago.

Williston, S. W., 1913. *Ostodolepis brevispinatus*, a new reptile from the Permian of Texas. Journal of Geology 21, 363-366.

Williston, S. W., 1915. New genera of Permian reptiles. American Journal of Science 39, 575-579.

Williston, S. W. and Case, E. C., 1913. Description of a nearly complete skeleton of *Ophiacodon* Marsh. Carnegie Institution of Washington 181, 37-59.

Wills, M. A., 1998. Crustacean disparity through the Phanerozoic: comparing morphological and stratigraphic data. Biological Journal of the Linnean Society 65, 455-500.

Wills, M. A., 1999. Congruence between phylogeny and stratigraphy: randomization tests and the gap excess ratio. Systematic Biology 48, 559-580.

Wills, M. A., Barrett, P. M. and Heathcote, J. F., 2008. The modified gap excess ratio (GER*) and the stratigraphic congruence of dinosaur phylogenies. Systematic Biology 57, 891-904.

Woodhead, J., Reisz, R. R., Fox, D., Drysdale, R., Hellstrom, J., Maas, R., Cheng, H. and Edwards, R. L., 2010. Speleothem climate records from deep time? Exploring the potential with an example from the Permian. Geology 38, 455-458.

Wright, A. M. and Hillis, D. M. 2014. Bayesian analysis using a simple likelihood model outperforms parsimony for estimation of phylogeny from discrete morphological data. PlosOne 9, e109210

Wu, X. C., 1981. The discovery of a new thecodont from north east Shanxi. Vertebrata PalAsiatica 19, 122-132.

Zwickl, D. J. and Hillis, D. M., 2002. Increased taxon sampling greatly reduced phylogenetic error. Systematic Biology 51, 588-598.

Appendix A

Changes made to the character matrix of Benson (2012) for the phylogenetic analysis undertaken herein. With these exceptions, the character scores are unchanged from the nexus file included in the electronic supplement of the original paper.

Scores Changed

Character 17: The specimen BP-1-5678 (?*Elliotsmithia*) was coded, despite the fact that no premaxilla is preserved on this specimen. This coding has been replaced with "?".

Character 51: Both *Eothyris parkeyi* and *Oedaleops campi* both originally scored as state 0 (large contribution of the lacrimal to the orbit), but the observed morphology is no different to that of Sphenacodontidae which were scored as state 1 (contribution of the lacrimal restricted by a descending process of the prefrontal). Eothyrididae have both been re-scored as character state 1.

Character 59: The anterior process of the frontal was originally coded as long in both *Eothyris parkeyi* and *Oedaleops campi* (state 1) despite being shorter than the posterior process (Reisz et al., 2009). Both have been re-scored as state 0.

Character 119: *Mesenosaurus romeri* was originally coded as state 0 (posterolateral orientation of the transverse flange of the pterygoid), but the anterior orientation of the transverse flange was specifically noted by Reisz & Berman (2001). This taxon has been re-scored as state 1 (anterolateral orientation of the transverse flange of the pterygoid).

Character 228: *Stereophallodon ciscoensis* and *Mycterosaurus longiceps* were both originally scored as character state 0 (prominent ventral ridge system on the femur). However, the poorly developed ventral ridge system has been considered characteristic of both these taxa (Brinkman & Eberth 1986, Berman & Reisz 1982). Therefore both have been re-scored as state 1 (ventral ridge system low and feebly developed)

Characters Modified

Character 17 – This character refers to the premaxillary tooth count. Benson (2012) divided it into two character states: state 0 representing 2-4 premaxillary teeth; state 1 representing 5-6 premaxillary teeth. However, these states miss some of the evolutionary variation. Several of the outgroup taxa, as well as some of the more basal members of the clades have four premaxillary teeth. It is possible that four premaxillary teeth is the primitive condition. By including the possession of four premaxiliary teeth in the character state representing fewer teeth, this character does not acknowledge reductions in tooth count from the primitive condition. Therefore the number of character states of character 17 have been increased to three: 0) 2-3 premaxillary teeth; 1) 4 premaxillary teeth; 2) 5-6 premaxillary teeth.

Characters Added

Character 240: Temporal fenestra morphology: 0) narrower dorsally than ventrally; 1) dorsal and ventral margins of similar length, fenestra has an oblong shape; 2) narrower ventrally than dorsally.

Character 241: Webbing under transverse processes of dorsal vertebrae: 0) webbing extensive, extends distally beyond the distal extent of the tips of the transverse processes and anteriorly to the forward edge of the vertebra; 1) webbing slight, does not extend distally beyond the distal extent of the tip of the transverse process; 2) webbing absent.

Character scores for new and modified characters

	Modified Character 17	**New Character 240**	**New Character 241**
Tseajaia campi	1	?	0
Limnoscelis	0	?	0
Captorhinus	0	?	0
Protorothyris archeri	0	?	1
Dimetrodon spp.	1	0	1
Secodontosaurus obtusidens	2	2	?
Ctenorhachis jacksoni	?	?	1
Sphenacodon ferocior	1	0	1
Cryptovenator hirschbergeri	?	?	?
Titanophoneus potens	0	0	1
Biarmosuchus tener	2	0	?
Raranimus dashankouensis	2	0	?
Biseridens qilianicus	2	0	?
Pantelosaurus saxonicus	2	0	?
Cutleria wilmarthi	1	2	?
Ianthodon schultzei	1	0	?
Haptodus garnettensis	2	?	0
Edaphosaurus boanerges	2	0	2
Edaphosaurus novomexicanus	?	?	2
Lupeosaurus kayi	?	?	2
Ianthasaurus hardestii	?	0	1
Glaucosaurus	1	?	?
Echinerpeton intermedium	?	?	0
Archaeothyris florensis	?	?	0
Varanosaurus acutirostris	2	2	0
Ophiacodon spp.	2	2	0
Stereophallodon ciscoensis	2	?	0
Oromycter dolesorum	1	?	?
Ennatosaurus tecton	1	0	2
Eothyris parkeyi	1	1	?
Oedaleops campi	1	0	?
Casea broilii	1	0	2
Cotylorhynchus romeri	1	0	2
Angelosaurus romeri	1	?	2
Angelosaurus dolani	?	?	2
Caseopsis agilis	?	?	?
Trichasaurus texensis	?	?	2
Cotylorhynchus hancocki	?	?	0
Cotylorhynchus bransoni	?	?	2
Euromycter rutenus	1	0	?

	Modified Character 17	**New Character 240**	**New Character 241**
Watongia meieri	?	0	1
Ruthiromia elcobriensis	?	?	1
Varanodon agilis	2	0	1
Varanops brevirostris	2	0	1
Aerosaurus wellesi	1	0	?
Aerosaurus greenleorum	?	?	?
Basicranodon fortsillensis	?	?	?
Archaeovenator hamiltonensis	0	1	1
Mesenosaurus romeri	2	2	?
Mycterosaurus longiceps	1	1	1
Heleosaurus scholtzi	2	1	1
BP 1 5678 Elliotsmithia	?	1	?
Pyozia mesensis	0	?	?
Casea nicholsi	?	?	2
Eocasea martini	?	?	1
"Mycterosaurus" smithae	?	1	?
Apsisaurus witteri	?	?	1

Added Material

Four species have been added to the matrix of Benson (2012): *Casea nicholsi*, *Eocasea martini*, *"Mycterosaurus" smithae* and *Apsisaurus witteri*. New material was also considered for *Oedaleops campi*. Here are presented the character scores for all five of these species:

Eocasea martini -
?????110?010??????????????0?????????????000??????????????????????000?100??000000000001?201010000?12??00??????????????????????????0????000????0?????0?0??1??200000?0000000000000000000??????????????????????????????????0??????1{01}2?01?0?000??0??000?1??0?0

Casea nicholsi -
??0????0?????????0???010??11????????11?0000000001?11?????????????????????????????1001110011??1??1???????0000?0?0000????0?0

“Mycterosaurus” smithae -

?????1000?00??????????????0??3?????????010????????1??00???0?0010000000?20010?01??
??????1????????????????????????????????????0??000??1000???0?????????????10?01?000
????0?00??0001001000011???1?

Apsisaurus witteri -

?????1??0??1????????????????0??0?????????010?00????????????????????????021?00100??1
????????????????2??????001??0????0??00000????????000????0?1?????????????2112?0000?0
0?0000000?001001??0????000?00?0??000?????????????????????11????00110100????????0

Oedaleops campi -

?2000110000001010??1000000?01000100??1010?0??0100100000000100000010??210?0?
0000?011001?1110??????0????????????????????????????0?1???????000?????????????????1????
???00?0?000????0100???000?100000000??0300??????????1000?0?10??0?100?00?000?????
?0?

Appendix B

Autapomorphies included in the Bayesian analysis of pelycosaurian-grade synapsids. Some of these autapomorphies represent specific characteristics within an already existing character. In these cases the relevant character was altered in the Bayesian analysis by adding an extra character state, and the autapomorphous taxon is the only taxon scored with this state. Such characters are noted below. In all other cases, an extra character was added to represent the autapomorphy, with the autapomorphous taxon coded as character state 1 and all others as character state 0, or "?" if the feature is not preserved.

Oedaleops campi – Parietal excludes postparietal from the posterior edge of the skull table (Reisz et al. 2009)

Eothyris parkeyi – No precanine teeth in maxilla (Reisz et al. 2009) (requires modification of character 32)

Ennatosaurus tecton – narrow parasphenoid body (Maddin et al. 2008)
– two large conical premaxillary teeth (Maddin et al. 2008)
– 5-7 apical serrations on marginal teeth arranged longitudinally (Maddin et al. 2008) (requires modification of character 44)

Ianthasaurus hardestiorum – elongate cross-barred dorsal process on axis (Reisz & Berman 1986)
– at least 29 presacral vertebrae (requires modification of character 148) (Reisz & Berman 1986)
– maximum of 8 lateral tubercles on each side of the neural spine (Reisz & Berman 1986)
– proximal tubercles with ventral webbing (Reisz & Berman 1986)
– lateral tubercles lacking on posterior neural spines (or modify character 169) (Reisz & Berman 1986)

Glaucosaurus megalops – prearticular extends to the jaw symphysis (Modesto 1994)
– septomaxilla exposed facially (also in *Haptodus*, *Varanodon* and *Varanosaurus* and therapsids) (Modesto 1994)

Edaphosaurus boanerges – pterygoid tooth plate with 120-150 teeth (Modesto 1995)
– deeply excavated dorsal jaw symphysis (Modesto 1995)
– slender lateral tubercles (Modesto 1995)

Lupeosaurus kayi – transverse processes located high on the centrum (Sumida 1989)

Edaphosaurus novomexicanus – anisodont tooth plate (Modesto & Reisz 1992)
– reduced number of lateral tubercles on anterior presacral neural spines (Modesto & Reisz 1992)

Varanosaurus acutirostris – step-like expansion of the ventral margin of the anterior maxilla (Berman 1995)
– lateral and dorsal surface of snout separated by a sharp ridge (Berman 1995)
– dorsal process of the premaxilla bifurcated (Berman 1995)
– septomaxilla exposed facially (also in *Haptodus*, *Varanodon* and *Glaucosaurus*) (Berman 1995)
– Posterior process of jugal dorsoventrally narrow (also in *Secodontosaurus*) (Berman 1995)
– middorsal margin of the quadratojugal forms the lateral wall of a narrow, shallow, trough-like channel that is bounded medially by the jugal and opens dorsally (Berman 1995)
– up to 56 maxillary teeth (requires modification of character 29) (Berman 1995)
– basipterygoid fits into socket in the posteromedial flange of the quadrate ramus of the pterygoid (Berman 1995)
– cultriform process long and narrow, reaches posterior boarder of the internal naris (Berman 1995)
– cultriform process supported along its length by anterior ramus of pterygoid (Berman 1995)
– dorsal process of stapes projects at right angle from the shaft (Berman 1995)

Haptodus garnettensis – nasal overlaps tongue-like process of lacrimal (Currie 1977)
– notched supratemporal (Laurin 1993)
– robust, chisel-shaped teeth (requires modification of character 40) (Laurin 1993)
– teeth on palatal ramus of the premaxilla (Laurin 1993)
– septomaxilla exposed facially (also in *Varanosaurus*, *Varanodon* and *Glaucosaurus*)

Secodontosaurus obtusidens – skull roof elements thin (Reisz et al. 1992)
– parietal contributes to dorsal margin of the temporal fenestra (Reisz et al. 1992)
– poorly developed supracanine buttress (requires modification of character 37) (Reisz et al. 1992)
– Posterolateral wing of parietal reduced and directed posteriorly (Reisz et al. 1992)
– Postparietal covers large area of supraoccipital (Reisz et al. 1992)
– reduction of dorsal and lateral processes of supraoccipital (Reisz et al. 1992)
– reduction of lateral exposure of prefrontal (Reisz et al. 1992)
– posterior ramus of jugal dorsoventrally narrow (also in *Varanosaurus*) (Reisz et al. 1992)
– transverse flange of pterygoid reduced in width (Reisz et al. 1992)
– Palatal exposure of palatine, vomer and ectopterygoid reduced (Reisz et al. 1992)
– dorsal process of quadrate tilted anterodorsally (Reisz et al. 1992)
– lateral condyle of quadrate extends beyond lateral edge of skull roof (Reisz et al. 1992)
– first dentary tooth directed forwards (Reisz et al. 1992)
– retroarticular process widely separated from reflected lamina of angular (Reisz et al. 1992)

Archaeothyris floresnsis – ectepicondyle angled at 85 degrees to the plane of the distal humerus (Reisz 1972)
– Well developed pubic tubercle (Reisz 1972)

Pyozia mesenensis – contact between quadratojugal and maxilla unexposed laterally (Anderson & Reisz 2004)
– basipterygoid process anteriorly directed (Anderson & Reisz 2004)
– interpterygoid vacuity rounded anteriorly (Anderson & Reisz 2004)

Heleosaurus scholtzi – straight suture between premaxilla and nasal (Botha Brink & Modesto 2009)
– ornamented angular and surangular (Botha Brink & Modesto 2009)

Varanops brevirostris – maxilla dorsal process has anterior and posterior depression of subequal size (Campione & Reisz 2010)
– postorbital with smooth transition from lateral to dorsal surfaces (Campione & Reisz 2010)
– basipterygoid process hypertrophies (Campione & Reisz 2010)
– basipterygoid articular facets elongated mediollaterally (Capione & Reisz 2010)
– posterior dorsal neural spines taper distally in lateral view (Campione & Reisz (2010)
– presence of anterolateral excavation of femur proximal to fourth trochanter (Campione & Reisz 2010)

Archaeovenator hamiltonenesis – medial process of postorbital underlying parietal (Reisz & Dilkes 2003)
– broadly expanded nasal process of premaxilla (Reisz & Dilkes 2003)

Watongia meieri – radius strongly curved (Reisz & Laurin 2004)
– enlarged pisiform (Reisz & Laurin 2004)
– reduced head of clavicle (Reisz & Laurin 2004)

Mesenosaurus romeri – premaxilla slender, forming a narrow rectangular snout in dorsal view (Reisz & Berman 2001)
– long dorsal process of premaxilla forms anterior half of dorsal margin of the external naris (Reisz & Berman 2001)
– lateral surface of premaxilla excavated, narrowing the base of the dorsal process and expanding the narial shelf to extend nearly to the snout tip (Reisz & Berman 2001)
– palatal process of premaxilla with elongated median suture (Reisz & Berman 2001)
– well-developed depression in the lateral surface of the nasal extending from narial border to the anterior end of the prefrontal (Reisz & Berman 2001)
– slight lateral swelling of the maxilla above the canine (also in
– first premaxillary tooth shorter than second and third (Reisz & Berman 2001)
– Vomerine teeth form a single median tooth row (Reisz & Berman 2001)
– Postorbital bar with nearly vertical posterior margin (Reisz & Berman 2001)
– stapes rod-like with expanded quadrate process (requires modification of character 94) (Reisz & Berman 2001)

Varanodon agilis – suspensorium far posterior, well back of occipital condyle (Olson 1965)
– well-developed antorbital fenestra (Olson 1965)
– fourth manual digit elongated and robust (Olson 1965)
– septomaxilla exposed facially (also in *Haptodus*, *Varanosaurus* and *Glaucosaurus*)

Ruthiromia elcobriensis – posterior dorsal centra pinched laterally (hourglass shape in cross section) (Brinkman & Eberth 1983)

Aerosaurus greenleeorum – proximal face of deltopectoral crest on the humerus is a large triangular area (Romer 1937)

Cotylorhynchus hancocki – epicondyle of humerus broad, thin and platelike (Olson & Beerbower 1953)
– attachment of M. pectoralis forms broad concave triangle that flare to form a shelf-like ridge over surface of area of attachment of M. coracobrachialis and M. brachialis (Olson & Beerbower 1953)
– first sacral rib greatly enlarged (Olson 1962)

Cotylorhynchus bransoni – astragulus with large foramen (Olson & Barghusen 1962)

Caseiopsis agilis – deepened acetabulum (Olson 1962)
– thickened pubis (Olson 1962)

Angelosaurus dolani – Femur with internal trochanter and ridge extending to proximal end of intertrochantric fossa (Olson 1962)

Mycterosaurus longiceps – anterior ridge boardering intertrochateric fossa extends proximally nearly to the end of the femur (Berman & Reisz 1982)

Casea broilii – supratemporal and tabular overhang squamosal to form a small but distinct notch (Olson 1968)
– posterior tuber on the parasphenoid (Olson 1968)
– basipterygoid process forms two laterally projecting spurs (Olson 1968)
– basicranial articulation is mobile (Olson 1968)
– palatal teeth separated by deep grooves (Olson 1968)
– absence of stapedial foramen (Olson 1968)
– dorsal processs of stapes positioned more distally (Olson 1968)
– quadrate articulation of the side of the stapes (Olson 1968)

Euromycter rutenus – expanded temporal fenestra (Reisz et al. 2011)
– supernumerary blade-like intranarial bone located posteromedially to the septomaxilla (Olson 1954)

Casea nicholsi – shafts of ribs expanded from the twelfth vertebra to the sacrum (Olson 1954)

Angelosaurus romeri – sacral ribs blade-like (Olson & Barghusen 1962)
– sacral ribs separated at articulation with ilium (Olson & Barghusen 1962)

Lupeosaurus kayi – strong posterior curvature of dorsal blade of scapula (Romer & Price 1940)
– ilium incised to receive sacral ribs (Romer & Price 1940)
– articular surface of sacral ribs concave (Romer & Price 1940)
– Puboischiadic plate broadened dorsoventrally (Romer & Price 1940)

Ianthodon schultzei – lingual fluting on marginal dentition (Kissel & Reisz 2004)
– anterior dorsal bulging of lacrimal (Kissel & Reisz 2004)

Cutleria wilmarthi – jugal-squamosal suture is anteriorly concave

Pantelosaurus saxonicus – Posterior end of the dentary well below posterior edge of the jaw

Ctenorhachis jacksoni – tapering tips of neural spines (requires modification of character 166) (Hook & Hotton 1991)
– posterior neural spines transversely compress posteriorly (Hook & Hotton 1991)

Dimetrodon – Level of jaw articulation below dentary tooth row (Brink & Reisz 2014)

Stereophallodon ciscoensis – labial surface of maxilla extends down almost covering the postcanine dentition (Romer & Price 1940)
– dorsal centra subrectangular in cross section (Brinkman & Eberth 1986)
– lumbar vertebrae trefoil-shaped in cross section (Brinkman & Eberth 1986)
– proximal fibula triangular (Brinkman & Eberth 1986)

Ophiacodon – Canines do not project laterally from the tooth row (Romer & Price 1940)
– Secondary adductor ridge on femur (Romer & Price 1940)

Apsisaurus witteri – anteroposteriorly elongate neural spines (Reisz et al. 2010)
– ovoid suborbital fenestra (Laurin 19991)
– interclavicle head broadened (Laurin 1991)

"Mycterosaurus" smithae – posterior process of the maxilla extends beyond the posterior margin of the temporal fenestra (observed)

Appendix C

List of synapsid taxa used in the diversity estimates, their age ranges and provenance.

Genus	Species	Age range	Age range (localities of uncertain age restricted to two or less time bins)	Country of origin
Ophiacodontidae				
Archaeothyris	*florensis*	Late Moscovian	Late Moscovian	Canada
Baldwinonus	*dunkardensis*	Asselian	Asselian	USA
Baldwinonus	*trux*	Gzhelian-Early Sakmarian	Late Gzhelian-Early Asselian	USA
Clepsydrops	*colletti*	Kasimovian	Kasimovian	USA
Clepsydrops?	*magnus*	Late Kasimovian-Early Gzhelian	Late Kasimovian-Early Gzhelian	USA
Clepsydrops	*vinslovii*	Kasimovian	Kasimovian	USA
Ophiacodon	*navajovicus*	Gzhelian-Early Sakmarian	Late Gzhelian-Early Asselian	USA
Ophiacodon	*hilli*	Early Artinskian	Early Artinskian	USA
Ophiacodon	*major*	Artinskian-Kungurian	Artinskian-Kungurian	USA

Ophiacodon	*mirus*	Gzhelian-Early Sakmarian	Late Gzhelian-Early Sakmarian	USA
Ophiacodon	*retroversus*	Late Sakmarian-Early Kungurian	Late Sakmarian-Early Kungurian	USA
Ophiacodon	*uniformis*	Sakmarian-Kungurian	Sakmarian-Kungurian	USA
Stereophallodon	*ciscoensis*	Late Asselian-Early Sakmarian	Late Asselian-Early Sakmarian	USA
Stereorhachis	*dominans*	Late Gzhelian	Late Gzhelian	France
Varanosaurus	*acutirostris*	Kungurian	Kungurian	USA
Varanosaurus	*wichitaensis*	Kungurian	Kungurian	USA
		Varanopidae		
Aerosaurus	*greenleeorum*	Gzhelian-Early Sakmarian	Late Gzhelian-Early Asselian	USA
Aerosaurus	*wellesi*	Gzhelian-Early Sakmarian	Late Asselian-Early Sakmarian	USA
Apsisaurus	*witteri*	Late Sakmarian-Artinskian	Late Sakmarian-Early Artinskian	USA

Archaeovenator	*hamiltonensis*	Late Kasimovian-Gzhelian	Gzhelian	USA
Basicranodon	*fortsillensis*	Early Artinskian	Early Artinskian	USA
Elliotsmithia	*longiceps*	Capitanian	Capitanian	South Africa
Heleosaurus	*scholtzi*	Capitanian	Capitanian	South Africa
Mesenosaurus	*romeri*	Late Roadian-Wordian	Wordian	Russia
Mycterosaurus	*longiceps*	Kungurian	Kungurian	USA
Mycterosaurus?	*smithae*	Asselian-Early Kungurian	Asselian	USA
Pyozia	*mesenensis*	Late Roadian-Wordian	Wordian	Russia
Ruthiromia	*elcobriensis*	Gzhelian-Early Sakmarian	Late Gzhelian-Early Asselian	USA
Thrausmosaurus	*serratidens*	Early Artinskian	Early Artinskian	USA
Varanodon	*agilis*	Roadian	Roadian	USA
Varanops	*brevirostris*	Artinskian-Kungurian	Artinskian-Kungurian	USA
Watongia	*meieri*	Roadian	Roadian	USA
Sphenacodontidae				
Bathygnathus	*borealis*	Artinskian	Artinskian	Canada
Cryptovenator	*hirschbergeri*	Late Gzhelian	Late Gzhelian	Germany

Ctenorhachis	*jacksoni*	Artinskian-Early Kungurian	Artinskian-Early Kungurian	USA
Ctenospondylus	*casei*	Late Artinskian-Early Kungurian	Late Artinskian-Early Kungurian	USA
Ctenospondylus	*ninevehensis*	Sakmarian	Sakmarian	USA
Macromerion	*schwarzenbergii*	Late Kasimovian-Early Gzhelian	Late Kasimovian-Early Gzhelian	Czech Republic
Neosaurus	*cynodus*	Asselian-Early Sakmarian	Asselian	France
Secodontosaurus	*obtusidens*	Artinskian-Kungurian	Artinskian-Kungurian	USA
Sphenacodon?	*britannicus*	Asselian-Early Sakmarian	Asselian	UK
Sphenacodon	*ferocior*	Gzhelian-Early Kungurian	Late Gzhelian-Artinskian	USA
Sphenacodon	*ferox*	Gzhelian-Early Sakmarian	Late Gzhelian-Early Sakmarian	USA
Dimetrodon	*angelensis*	Early Roadian	Early Roadian	USA
Dimetrodon	*booneorum*	Artinskian-Early Kungurian	Artinskian-Early Kungurian	USA
Dimetrodon	*dollovianus*	Artinskian-Kungurian	Artinskian-Kungurian	USA
Dimetrodon	*giganhomogenes*	Kungurian	Kungurian	USA

Dimetrodon	*grandis*	Kungurian	Kungurian	USA
Dimetrodon	*kempae*	Late Kungurian	Late Kungurian	USA
Dimetrodon	*limbatus*	Artinskian-Kungurian	Artinskian-Kungurian	USA
Dimetrodon	*loomisi*	Kungurian	Kungurian	USA
Dimetrodon	*macrospondylus*	Kungurian	Kungurian	USA
Dimetrodon	*milleri*	Late Sakmarian-Artinskian	Late Sakmarian-Early Artinskian	USA
Dimetrodon	*natalis*	Artinskian-Kungurian	Artinskian-Kungurian	USA
Dimetrodon	*occidentalis*	Asselian-Artinskian	Late Sakmarian-Early Artinskian	USA
Dimetrodon	*teutonis*	Artinskian		Germany
		Edaphosauridae		
Edaphosaurus	*boanerges*	Late Sakmarian-Early Kungurian	Late Sakmarian-Early Kungurian	USA
Edaphosaurus	*colohistion*	Late Gzhelian	Late Gzhelian	USA
Edaphosaurus	*credneri*	Sakmarian	Sakmarian	Germany
Edaphosaurus	*cruciger*	Artinskian-Kungurian	Artinskian-Kungurian	USA
Glaucosaurus	*megalops*	Kungurian	Kungurian	USA

Edaphosaurus	*mirabilis*	Late Kasimovian-Early Gzhelian	Late Kasimovian-Early Gzhelian	USA
Edaphosaurus	*novomexicanus*	Gzhelian-Early Sakmarian	Late Gzhelian-Early Asselian	USA
Edaphosaurus	*pogonias*	Artinskian-Kungurian	Artinskian-Kungurian	USA
Ianthasaurus	*hardestiorum*	Late Kasimovian	Late Kasimovian	USA
Lupeosaurus	*kayi*	Late Sakmarian-Early Kungurian	Late Sakmarian-Early Kungurian	USA
Caseasauria				
Angelosaurus	*dolani*	Early Roadian	Early Roadian	USA
Angelosaurus	*greeni*	Early Roadian	Early Roadian	USA
Angelosaurus	*romeri*	Roadian	Roadian	USA
Casea	*broilii*	Late Kungurian	Late Kungurian	USA
Casea	*halselli*	Late Kungurian	Late Kungurian	USA
Casea	*nicholsi*	Late Kungurian	Late Kungurian	USA
Caseoides	*sanangeloensis*	Early Roadian	Early Roadian	USA
Caseopsis	*agilis*	Early Roadian	Early Roadian	USA
Cotylorhynchus	*bransoni*	Roadian	Roadian	USA

Cotylorhynchus	*hancocki*	Early Roadian	Early Roadian	USA
Cotylorhynchus	*romeri*	Late Kungurian	Late Kungurian	USA
Ennatosaurus	*tecton*	Late Roadian-Wordian	Late Roadian-Wordian	Russia
Eocasea	*martini*	Late Kasimovian-Gzhelian	Gzhelian	USA
Eothyris	*parkeyi*	Early Kungurian	Early Kungurian	USA
Euromycter	*rutenus*	Artinskian-Kungurian	Late Kungurian	France
Oedaleops	*campi*	Gzhelian-Early Sakmarian	Late Asselian-Early Sakmarian	USA
Oromycter	*dolesorum*	Early Artinskian	Early Artinskian	USA
Ruthenosaurus	*russellorum*	Artinskian-Kungurian	Late Kungurian	France
Trichasaurus	*texensis*	Late Kungurian	Late Kungurian	USA

Pelycosaurian-grade synapsids not assigned to the above clades

Cutleria	*wilmarthi*	Asselian-Early Kungurian	Asselian	USA
Echinerpeton	*intermedium*	Late Moscovian	Late Moscovian	Canada

Haptodus	*baylei*	Kasimovian-Early Sakmarian	Gzhelian-Early Sakmarian	France/Poland
Haptodus	*garnettensis*	Late Kasimovian	Late Kasimovian	USA
Haptodus	*grandis*	Asselian-Early Sakmarian	Asselian-Early Sakmarian	UK
Ianthodon	*schultzei*	Late Kasimovian	Late Kasimovian	USA
Milosaurus	*mccordi*	Kasimovian	Kasimovian	USA
Nitosaurus	*jacksonorum*	Gzhelian-Early Sakmarian	Late Gzhelian-Early Asselian	USA
Palaeohatteria	*longicaudata*	Sakmarian	Sakmarian	Germany
Pantelosaurus	*saxonicus*	Asselian	Asselian	Germany
Phreatophasma	*aenigmaticum*	Roadian	Roadian	Russia
Xyrospondylus	*ecordi*	Late Kasimovian	Late Kasimovian	USA

Therapsida

Alopecognathus	*angusticeps*	Capitanian	Capitanian	South Africa
Alrausuchus	*tagax*	Late Roadian-Wordian	Wordian	Russia
Anomocephalus	*africanus*	Capitanian	Capitanian	South Africa
Anteosaurus	*magnificus*	Capitanian	Capitanian	South Africa
Archaeosyodon	*praeventor*	Wordian	Wordian	Russia
Australosyodon	*nyaphuli*	Wordian	Wordian	South Africa

Biarmosuchus	*tchudinovi*	Wordian	Wordian	Russia
Biarmosuchus	*tener*	Wordian	Wordian	Russia
Biseridens	*qilianicus*	Wordian	Wordian	China
Brachyprosopus	*broomi*	Capitanian	Capitanian	South Africa
Bullacephalus	*jacksoni*	Capitanian	Capitanian	South Africa
Chelydontops	*altidentalis*	Capitanian	Capitanian	South Africa
Colobodectes	*cluveri*	Capitanian	Capitanian	South Africa
Criocephalosaurus	*vanderbyli*	Capitanian	Capitanian	South Africa
Deuterosaurus	*biarmicus*	Wordian-Capitanian	Wordian-Early Capitanian	Russia
Diictodon	*feliceps*	Capitanian	Capitanian	South Africa
Emydops	*arctatus*	Capitanian	Capitanian	South Africa
Eodicynodon	*oosthuizeni*	Wordian	Wordian	South Africa
"Eodicynodon"	*oelofseni*	Wordian	Wordian	South Africa
Eosimops	*newtoni*	Capitanian	Capitanian	South Africa
Eriphostoma	*microdon*	Capitanian	Capitanian	South Africa
Estemmenosuchus	*uralensis*	Wordian	Wordian	Russia
Estemmenosuchus	*mirabilis*	Wordian	Wordian	Russia
Galechirus	*scholtzi*	Capitanian	Capitanian	South Africa
Galeops	*whaitsi*	Capitanian	Capitanian	South Africa
Galesuchus	*gracilis*	Capitanian	Capitanian	South Africa
Glanosuchus	*macrops*	Wordian-Capitanian	Wordian-Capitanian	South Africa
Hipposaurus	*boonstrai*	Capitanian	Capitanian	South Africa
Hipposaurus?	*brinki*	Capitanian	Capitanian	South Africa
Ictidosaurus	*angusticeps*	Wordian-Capitanian	Wordian-Capitanian	South Africa
Jonkeria	*truculenta*	Capitanian	Capitanian	South Africa
Kamagorgon	*ulanovi*	Roadian	Roadian	Russia
Lanthanostegus	*mohoii*	Capitanian	Capitanian	South Africa
Lycosuchus	*vanderrieti*	Capitanian	Capitanian	South Africa
Microsyodon	*orlovi*	Roadian	Roadian	Russia

Microurania	*minima*	Late Wordian-Early Capitanian	Late Wordian-Early Capitanian	Russia
"Microurania"	*mikia*	Late Wordian-Early Capitanian	Late Wordian-Early Capitanian	Russia
Mormosaurus	*seeleyi*	Capitanian	Capitanian	South Africa
Moschognathus	*whaitsi*	Capitanian	Capitanian	South Africa
Moschops	*capensis*	Capitanian	Capitanian	South Africa
Niaftasuchus	*zekkeli*	Late Roadian-Wordian	Wordian	Russia
Nikkasaurus	*tatarinovi*	Late Roadian-Wordian	Wordian	Russia
Notosyodon	*gusevi*	Late Wordian-Early Capitanian	Late Wordian-Early Capitanian	Russia
Novocynodon	*kurtogai*	Late Wordian-Capitanian	Late Wordian-Capitanian	Russia
Otsheria	*netzvetajevi*	Wordian	Wordian	Russia
Pachydectes	*elsi*	Capitanian	Capitanian	South Africa
Pampaphoneus	*biccai*	Capitanian	Capitanian	Brazil
"Parabradysaurus"	*silantjevi*	Roadian	Roadian	Russia
Parabradysaurus	*udmurticus*	Wordian-Early Capitanian	Wordian	Russia
Patranomodon	*nyaphulii*	Wordian	Wordian	South Africa
Phreatosaurus	*menneri*	Roadian	Roadian	Russia
Phreatosaurus	*bazhovi*	Wordian-Early Capitanian	Wordian	Russia
Phreatosuchus	*qualeni*	Roadian	Roadian	Russia
Phthinosaurus	*borissiaki*	Late Roadian	Late Roadian	Russia

Phthinosuchus	*discors*	Wordian-Early Capitanian	Late Wordian-Early Capitanian	Russia
Porosteognathus	*efremovi*	Late Wordian-Capitanian	Late Wordian-Capitanian	Russia
Pristerodon	*mackayi*	Capitanian	Capitanian	South Africa
Pristerognathus	*polyodon*	Capitanian	Capitanian	South Africa
Prosictodon	*dubei*	Capitanian	Capitanian	South Africa
Raranimus	*dashankouensis*	Wordian	Wordian	China
Reiszia	*gubini*	Late Roadian-Wordian	Late Roadian-Wordian	Russia
Reiszia	*tippula*	Late Roadian-Wordian	Late Roadian-Wordian	Russia
Rhopalodon	*wangenheimi*	Wordian-Capitanian	Wordian-Capitanian	Russia
Riebeeckosaurus	*longirostris*	Capitanian	Capitanian	South Africa
Robertia	*broomiana*	Capitanian	Capitanian	South Africa
Scylacognathus	*parvus*	Capitanian	Capitanian	South Africa
Sinophoneus	*yumenensis*	Wordian	Wordian	China
Struthiocephaloides	*cavifrons*	Capitanian	Capitanian	South Africa
Struthiocephalus	*whaitsi*	Capitanian	Capitanian	South Africa
Struthionops	*intermedius*	Capitanian	Capitanian	South Africa
Styracocephalus	*platyrhynchus*	Capitanian	Capitanian	South Africa
Syodon	*biarmicum*	Wordian-Capitanian	Wordian-Early Capitanian	Russia
Tapinocaninus	*pamelae*	Wordian	Wordian	South Africa
Tapinocephalus	*atherstonei*	Capitanian	Capitanian	South Africa
Tetraceratops	*insignis*	Late Kungurian	Late Kungurian	USA
Tiarajudens	*eccentricus*	Capitanian	Capitanian	Brazil
Titanophoneus	*adamanteus*	Late Wordian-Early Capitanian	Late Wordian-Early Capitanian	Russia

Titanophoneus	*potens*	Late Wordian-Capitanian	Late Wordian-Early Capitanian	Russia
"*Titanophoneus*"	*rugosus*	Late Wordian-Early Capitanian	Late Wordian-Early Capitanian	Russia
Titanosuchus	*ferox*	Capitanian	Capitanian	South Africa
Ulemica	*efremovi*	Late Wordian-Capitanian	Late Wordian-Early Capitanian	Russia
Ulemica	*invisa*	Late Wordian-Capitanian	Late Wordian-Early Capitanian	Russia
Ulemosaurus	*svijagensis*	Late Wordian-Capitanian	Late Wordian-Early Capitanian	Russia
Venyukovia	*prima*	Wordian	Wordian	Russia

Appendix D

A list of all specimens of pelycosaurian-grade synapsids incorporated into the analysis of the completeness of specimens

Genus	Species	Number	Affinities	Locality	Stage	Material
Archaeothyris	*florensis*	MCZ 4079	Ophiacodontidae	Florence, Nova Soctia	Late Moscovian	Partial skull, several vertebrae, humerus, cervical ribs
Archaeothyris	*florensis*	MCZ 4080	Ophiacodontidae	Florence, Nova Soctia	Late Moscovian	Pelvis, sacral vertebra, axis
Archaeothyris	*florensis*	MCZ 4081	Ophiacodontidae	Florence, Nova Soctia	Late Moscovian	Caudal vertebra
Archaeothyris	*florensis*	MCZ 4082	Ophiacodontidae	Florence, Nova Soctia	Late Moscovian	Anterior dorsal vertebrae
Archaeothyris	*florensis*	MCZ 4083	Ophiacodontidae	Florence, Nova Soctia	Late Moscovian	Postcranial elements
Archaeothyris	*florensis*	MCZ 4084	Ophiacodontidae	Florence, Nova Soctia	Late Moscovian	Articulated caudal vertebrae
Archaeothyris	*florensis*	MCZ 4085	Ophiacodontidae	Florence, Nova Soctia	Late Moscovian	Lower jaw elements, frontal
Archaeothyris	*florensis*	MCZ 4086	Ophiacodontidae	Florence, Nova Soctia	Late Moscovian	Metacarpals
Archaeothyris	*florensis*	MCZ 4087	Ophiacodontidae	Florence, Nova Soctia	Late Moscovian	Presacral vertebrae
Archaeothyris	*florensis*	RM 10056	Ophiacodontidae	Florence, Nova Soctia	Late Moscovian	Maxilla, dentary, presacral and caudal vertebrae, interclacivle, calcaneum
Echinerpeton	*intermedium*	MCZ 4090	Ophiacodontidae (?)	Florence, Nova Soctia	Late Moscovian	Partial skeleton
Echinerpeton	*intermedium*	MCZ 4091	Ophiacodontidae (?)	Florence, Nova Soctia	Late Moscovian	Almost complete interclavicle, vertebral material
Echinerpeton	*intermedium*	MCZ 4092	Ophiacodontidae (?)	Florence, Nova Soctia	Late Moscovian	Complete left maxilla
Echinerpeton	*intermedium*	MCZ 4093	Ophiacodontidae (?)	Florence, Nova Soctia	Late Moscovian	Fragment of a right maxilla
Echinerpeton	*intermedium*	MCZ 4094	Ophiacodontidae (?)	Florence, Nova Soctia	Late Moscovian	Fragments of 3 neural arches
Echinerpeton	*intermedium*	RM 10,057	Ophiacodontidae (?)	Florence, Nova Soctia	Late Moscovian	Almost complete right maxilla, a neural arch, rib and phalanx
Clepsydrops	*colletti*	FMNH 6524	Ophiacodontidae	Danville Locality, Vermillion River, near Danville, Vermillion county Illinois	Kazimovian	Maxillary fragment, many vertebral fragments and isolated elements of the appendicular skeleton

Clepsydrops	*colletti*	FMNH 6530	Ophiacodontidae	Danville Locality, Vermillion River, near Danville, Vermillion county Illinois	Kazimovian	Dorsal vertebra
Clepsydrops	*colletti*	WM 6531	Ophiacodontidae	Danville Locality, Vermillion River, near Danville, Vermillion county Illinois	Kazimovian	Vertebra
Clepsydrops	*colletti*	WM 6534	Ophiacodontidae	Danville Locality, Vermillion River, near Danville, Vermillion county Illinois	Kazimovian	One third cervical, one dorsal vertebra
Clepsydrops	*colletti*	WM 6535	Ophiacodontidae	Danville Locality, Vermillion River, near Danville, Vermillion county Illinois	Kazimovian	Vertebra
Clepsydrops	*colletti*	WM 6540	Ophiacodontidae	Danville Locality, Vermillion River, near Danville, Vermillion county Illinois	Kazimovian	Scapulocoracoid
Clepsydrops	*colletti*	WM 6542	Ophiacodontidae	Danville Locality, Vermillion River, near Danville, Vermillion county Illinois	Kazimovian	Humerus
Clepsydrops	*colletti*	WM 6547	Ophiacodontidae	Danville Locality, Vermillion River, near Danville, Vermillion county Illinois	Kazimovian	Ulna
Clepsydrops	*colletti*	WM 6551	Ophiacodontidae	Danville Locality, Vermillion River, near Danville, Vermillion county Illinois	Kazimovian	Femur

Clepsydrops	*colletti*	WM 6553	Ophiacodontidae	Danville Locality, Vermillion River, near Danville, Vermillion county Illinois	Kazimovian	Radius, fibula
Clepsydrops	*colletti*	WM 6555	Ophiacodontidae	Danville Locality, Vermillion River, near Danville, Vermillion county Illinois	Kazimovian	Tibia
Clepsydrops	*colletti*	WM 6556	Ophiacodontidae	Danville Locality, Vermillion River, near Danville, Vermillion county Illinois	Kazimovian	Pelvic material
Clepsydrops	*colletti*	WM 6557	Ophiacodontidae	Danville Locality, Vermillion River, near Danville, Vermillion county Illinois	Kazimovian	Pelvic material
Clepsydrops	*colletti*	WM 6561	Ophiacodontidae	Danville Locality, Vermillion River, near Danville, Vermillion county Illinois	Kazimovian	Astraguli
Clepsydrops	*colletti*	WM 6573	Ophiacodontidae	Danville Locality, Vermillion River, near Danville, Vermillion county Illinois	Kazimovian	Pelvic material
Clepsydrops	*colletti*	WM 6575	Ophiacodontidae	Danville Locality, Vermillion River, near Danville, Vermillion county Illinois	Kazimovian	Humerus
Clepsydrops	*colletti*	WM 6578	Ophiacodontidae	Danville Locality, Vermillion River, near Danville, Vermillion county Illinois	Kazimovian	Vertebra

Clepsydrops	*vinslovii*	FMNH 6532	Ophiacodontidae	Danville Locality, Vermillion River, near Danville, Vermillion county Illinois	Kazimovian	Third cervical vertebra
Clepsydrops	*vinslovii*	WM 6533	Ophiacodontidae	Danville Locality, Vermillion River, near Danville, Vermillion county Illinois	Kazimovian	Other vertebral elements
Clepsydrops	*vinslovii*	WM 6543	Ophiacodontidae	Danville Locality, Vermillion River, near Danville, Vermillion county Illinois	Kazimovian	Humerus
Clepsydrops	*vinslovii*	WM 6545	Ophiacodontidae	Danville Locality, Vermillion River, near Danville, Vermillion county Illinois	Kazimovian	Humerus
Clepsydrops	*vinslovii*	WM 6547	Ophiacodontidae	Danville Locality, Vermillion River, near Danville, Vermillion county Illinois	Kazimovian	Femur
Clepsydrops	*vinslovii*	WM 6548	Ophiacodontidae	Danville Locality, Vermillion River, near Danville, Vermillion county Illinois	Kazimovian	Femur
Clepsydrops	*vinslovii*	WM 6549	Ophiacodontidae	Danville Locality, Vermillion River, near Danville, Vermillion county Illinois	Kazimovian	Femur
Clepsydrops	*vinslovii*	WM 6550	Ophiacodontidae	Danville Locality, Vermillion River, near Danville, Vermillion county Illinois	Kazimovian	Femur

Clepsydrops	*vinslovii*	WM 6553	Ophiacodontidae	Danville Locality, Vermillion River, near Danville, Vermillion county Illinois	Kazimovian	Partial humerus
Clepsydrops	*vinslovii*	WM 6558	Ophiacodontidae	Danville Locality, Vermillion River, near Danville, Vermillion county Illinois	Kazimovian	Pelvis
Clepsydrops	*vinslovii*	WM 6561	Ophiacodontidae	Danville Locality, Vermillion River, near Danville, Vermillion county Illinois	Kazimovian	Astragulus
Milosaurus	*mccordi*	FM PR 701	Sphenacodontidae (?), Varanopidae (?)	Newton locality, Jasper County, Illinois	Kazimovian	Articulated partial skeleton: pelvis, hind limb, several caudal vertebrae
Milosaurus	*mccordi*	FM PR 702	Sphenacodontidae (?), Varanopidae (?)	Newton locality, Jasper County, Illinois	Kazimovian	Small portion of the maxillary region
Milosaurus	*mccordi*	FM PR 703	Sphenacodontidae (?), Varanopidae (?)	Newton locality, Jasper County, Illinois	Kazimovian	A presacral rib
Milosaurus	*mccordi*	FM PR 704	Sphenacodontidae (?), Varanopidae (?)	Newton locality, Jasper County, Illinois	Kazimovian	A lumbar vertebra
Milosaurus	*mccordi*	FM PR 705	Sphenacodontidae (?), Varanopidae (?)	Newton locality, Jasper County, Illinois	Kazimovian	A lumbar or dorsal nural spine
Haptodus	*baylei*	Geologisches Landesmuseum, Berlin	Sphenacodontia,	Nowa Ruda, Lower Silesia	Kasimovian-Gzhelian	Nearly complete skeleton
Xyrospondylus	*ecordi*	KUVP 9963	Pelycosauria	Garnett Quarry, 10km north of Garnett, Anderson County, Kansas	Late Kazimovian	Posterior cervical vertebra
Haptodus	*garnettensis*	RM 14,156	Sphenacodontia,	Garnett Quarry, 10km north of Garnett, Anderson County, Kansas	Late Kazimovian	Partially articulated skeleton

Haptodus	*garnettensis*	RM 14,157	Sphenacodontia,	Garnett Quarry, 10km north of Garnett, Anderson County, Kansas	Late Kazimovian	Partial skull
Haptodus	*garnettensis*	RM 14,158	Sphenacodontia,	Garnett Quarry, 10km north of Garnett, Anderson County, Kansas	Late Kazimovian	Distal lower jaw
Haptodus	*garnettensis*	RM 14,159	Sphenacodontia,	Garnett Quarry, 10km north of Garnett, Anderson County, Kansas	Late Kazimovian	Femur, tibia, fibula and tarsus
Haptodus	*garnettensis*	RM 14,162	Sphenacodontia,	Garnett Quarry, 10km north of Garnett, Anderson County, Kansas	Late Kazimovian	Quadrate process of the pterygoid
Haptodus	*garnettensis*	RM 14,223	Sphenacodontia,	Garnett Quarry, 10km north of Garnett, Anderson County, Kansas	Late Kazimovian	Ischium, neural arch
Ianthosaurus	*hardestiorum*	KUVP 69035	Edaphosauridae	Garnett Quarry, 10km north of Garnett, Anderson County, Kansas	Late Kazimovian	Portions of the cranial, axial and apendicular skeleton, including a nearly complete articulate series of 27 presacral neural arches
Ianthosaurus	*hardestiorum*	ROM 29940	Edaphosauridae	Garnett Quarry, 10km north of Garnett, Anderson County, Kansas	Late Kazimovian	Partial dorsal neural arch with nearly complete neural spine, 1st sacral, 7 caudal ribs
Ianthosaurus	*hardestiorum*	ROM 29941	Edaphosauridae	Garnett Quarry, 10km north of Garnett, Anderson County, Kansas	Late Kazimovian	1 cervical vertebra, one dorsal vertebra with right rib, 1 lumbar vertebra with attached rib
Ianthosaurus	*hardestiorum*	ROM 29942	Edaphosauridae	Garnett Quarry, 10km north of Garnett, Anderson County, Kansas	Late Kazimovian	Disarticulated and scattered elements of the skull and postcranial skeleton

Ianthosaurus	*hardestiorum*	ROM 37751	Edaphosauridae	Garnett Quarry, 10km north of Garnett, Anderson County, Kansas	Late Kazimovian	Articulated skeleton
Ianthosaurus	*hardestiorum*	ROM 59933	Edaphosauridae	Garnett Quarry, 10km north of Garnett, Anderson County, Kansas	Late Kazimovian	Left maxilla quadrate, postorbital, pterygoid, mandibular ramus, 7 presacral vertebrae, 4 caudal vertebrae, 8 ribs, 7 phalanges
Ianthosaurus	*hardestiorum*	CM 34449	Edaphosauridae	Garnett Quarry, 10km north of Garnett, Anderson County, Kansas	Late Kazimovian	Partial right maxilla
Ianthosaurus	*hardestiorum*	CM 34500	Edaphosauridae	Garnett Quarry, 10km north of Garnett, Anderson County, Kansas	Late Kazimovian	Partial neural spine
Ianthosaurus	*hardestiorum*	CM 34576	Edaphosauridae	Garnett Quarry, 10km north of Garnett, Anderson County, Kansas	Late Kazimovian	Partial neural spine
Ianthosaurus	*hardestiorum*	CM 34577	Edaphosauridae	Garnett Quarry, 10km north of Garnett, Anderson County, Kansas	Late Kazimovian	Dorsal vertebra and base of neural spine
Ianthosaurus	*hardestiorum*	CM 34578	Edaphosauridae	Garnett Quarry, 10km north of Garnett, Anderson County, Kansas	Late Kazimovian	Dorsal portion of right scapula blade
Ianthosaurus	*hardestiorum*	CM 34579	Edaphosauridae	Garnett Quarry, 10km north of Garnett, Anderson County, Kansas	Late Kazimovian	Left femur
Ianthosaurus	*hardestiorum*	CM 34580	Edaphosauridae	Garnett Quarry, 10km north of Garnett, Anderson County, Kansas	Late Kazimovian	Left astragulus

Ianthosaurus	*hardestiorum*	CM 34581	Edaphosauridae	Garnett Quarry, 10km north of Garnett, Anderson County, Kansas	Late Kazimovian	Partial right femur
Ianthosaurus	*hardestiorum*	CM 47700	Edaphosauridae	Garnett Quarry, 10km north of Garnett, Anderson County, Kansas	Late Kazimovian	Centra and neural spines
Ianthodon	*schultzei*	KUVP 133735	Sphenacodontia,	Garnett Quarry, 10km north of Garnett, Anderson County, Kansas	Late Kazimovian	Nearly complete skull roof
Ianthodon	*schultzei*	KUVP 133736	Sphenacodontia,	Garnett Quarry, 10km north of Garnett, Anderson County, Kansas	Late Kazimovian	Left maxilla
Clepsydrops (?)	*magnus*	CMNH 13942	Ophiacodontidae	McKnight Road at junction with Brown	Late Kasimovian - Early Gzhelian	Distal right humerus, proximal right scapula, proximal left ulna
Macromerion (?)	*schwarzenbergii*		Sphenacodontidae	Kounova, 35 miles northwest of Prague	Late Kazimovian-Early Gzhelian	Right maxilla,frontals, fragments of prefrontals and postfrontals, left pelvic girdle
Edaphosaurus (?)	*mirabilis*	Praha Museum	Edaphosauridae	Kounova, 35 miles northwest of Prague	Late Kazimovian-Early Gzhelian	Fragment of a dorsal vertebra, with the centrum and a fragment of the neural spine
Archaeovenator	*hamiltonensis*	KUVP 12483	Varanopidae	Hamilton Quarry, near Hamilton, Greenwood County, Kansas	Late Kasimovian - Gzhelian	Nearly complete articulated specimen
Eocasea	*martini*	KUVP 9616b	Caseidae	Hamilton Quarry, near Hamilton, Greenwood County, Kansas	Late Kasimovian - Gzhelian	Nearly complete articulated specimen
Ophiacodon	*navajovicus*	UCLA VP 1627	Ophiacodontidae	Platyhystrix pocket locality, Halgaito Tongue, San Juan County, Utah	Ghezelian	Dorsal vertebra
Ophiacodon	*navajovicus*	UCLA VP 1628	Ophiacodontidae	Platyhystrix pocket locality, Halgaito Tongue, San Juan County, Utah	Ghezelian	Dorsal vertebra

Ophiacodon	*navajovicus*	UCLA VP 1629	Ophiacodontidae	Platyhystrix pocket locality, Halgaito Tongue, San Juan County, Utah	Ghezelian	Dorsal vertebra
Ophiacodon	*navajovicus*	UCLA VP 1630	Ophiacodontidae	Platyhystrix pocket locality, Halgaito Tongue, San Juan County, Utah	Ghezelian	Dorsal vertebra
Ophiacodon	*navajovicus*	UCLA VP 1631	Ophiacodontidae	Platyhystrix pocket locality, Halgaito Tongue, San Juan County, Utah	Ghezelian	Scapulocoracoid
Ophiacodon	*navajovicus*	UCLA VP 1632	Ophiacodontidae	Platyhystrix pocket locality, Halgaito Tongue, San Juan County, Utah	Ghezelian	Scapulocoracoid
Ophiacodon	*navajovicus*	UCLA VP 1633	Ophiacodontidae	Platyhystrix pocket locality, Halgaito Tongue, San Juan County, Utah	Ghezelian	Scapulocoracoid
Ophiacodon	*navajovicus*	UCLA VP 1634	Ophiacodontidae	Platyhystrix pocket locality, Halgaito Tongue, San Juan County, Utah	Ghezelian	Scapulocoracoid
Ophiacodon	*navajovicus*	UCLA VP 1635	Ophiacodontidae	Platyhystrix pocket locality, Halgaito Tongue, San Juan County, Utah	Ghezelian	Distal left humerus
Aerosaurus	*greenleeorum*	FMNH 464	Varanopidae	El Cobre Canyon, near Abiquiu, Rio Arriba County, New Mexico	Ghezelian-Early Sakmarian	Fragmentary disarticulated postcranial skeleton
Ruthiromia	*elcobriensis*	MCZ 3150	Varanopidae	El Cobre Canyon, near Abiquiu, Rio Arriba County, New Mexico	Ghezelian-Early Sakmarian	Articulated partial vertebral column, pelvis and hind limbs, as well as other fragments
Nitosaurus	*jacksonorum*	AMNH 4782	Edaphosauridae? Nitosauridae? (Romer & Price 1940); Chimera? (Reisz 1986)	El Cobre Canyon, near Abiquiu, Rio Arriba County, New Mexico	Ghezelian-Early Sakmarian	Fragments of limb and pelvic girdle; two proximal caudal centra, incomplete upper and lower jaws

Baldwinonus	*trux*	AMNH 4780	Ophiacodontidae (?)	El Cobre Canyon, near Abiquiu, Rio Arriba County, New Mexico	Ghezelian-Early Sakmarian	Maxilla, articular part of the quadrate, fragments of vertebrae and ribs
Sphenacodon	*ferox*	AM 4778	Sphenacodontidae	El Cobre Canyon, near Abiquiu, Rio Arriba County, New Mexico	Ghezelian-Early Sakmarian	Partial maxilla, quadrate, presacral vertebrae
Ophiacodon	*navajovicus*	MCZ 2007	Ophiacodontidae	El Cobre Canyon, near Abiquiu, Rio Arriba County, New Mexico	Ghezelian-Early Sakmarian	Dorsal (43) and caudal (29) vertebrae without spines , 14 neural spines, Several pahalnges and unguals, Teeth (maxiliary and dentary ?), Proximal and distal radii, Humeri, Proximal and distal femora, 1 scapula, Fibulae (1 whole, one no shaft), Proximal and distal tibiae, Atlas/axis complex with spine
Ophiacodon	*navajovicus*	MCZ 1595	Ophiacodontidae	El Cobre Canyon, near Abiquiu, Rio Arriba County, New Mexico	Ghezelian-Early Sakmarian	Ilium and acetabulum
Ophiacodon	*navajovicus*	MCZ 8079	Ophiacodontidae	El Cobre Canyon, near Abiquiu, Rio Arriba County, New Mexico	Ghezelian-Early Sakmarian	Vertebrae
Ophiacodon	*navajovicus*	AMNH 4776	Ophiacodontidae	El Cobre Canyon, near Abiquiu, Rio Arriba County, New Mexico	Ghezelian-Early Sakmarian	Manus: distal carpals, medial and proximal, metacarpals of digits 1-4, Phalanx 1 of digit 1-3, Phalanx 2 of 1 and 2, Ungula of 1, 2 and 5
Ophiacodon	*navajovicus*	AMNH 2292	Ophiacodontidae	El Cobre Canyon, near Abiquiu, Rio Arriba County, New Mexico	Ghezelian-Early Sakmarian	Partial manus
Ophiacodon	*navajovicus*	AMNH 2299	Ophiacodontidae	El Cobre Canyon, near Abiquiu, Rio Arriba County, New Mexico	Ghezelian-Early Sakmarian	Femur
Ophiacodon	*navajovicus*	AMNH 4777	Ophiacodontidae	El Cobre Canyon, near Abiquiu, Rio Arriba County, New Mexico	Ghezelian-Early Sakmarian	Caudal centrum, cervical centrum Thoracic centrum, humerus, proximal humerus, fragment of proximal ischium

Ophiacodon	*navajovicus*	AMNH 4781	Ophiacodontidae	El Cobre Canyon, near Abiquiu, Rio Arriba County, New Mexico	Ghezelian-Early Sakmarian	
Ophiacodon	*navajovicus*	AMNH 4783	Ophiacodontidae	El Cobre Canyon, near Abiquiu, Rio Arriba County, New Mexico	Ghezelian-Early Sakmarian	
Ophiacodon	*navajovicus*	AMNH 4784	Ophiacodontidae	El Cobre Canyon, near Abiquiu, Rio Arriba County, New Mexico	Ghezelian-Early Sakmarian	
Ophiacodon	*navajovicus*	AMNH 4799	Ophiacodontidae	El Cobre Canyon, near Abiquiu, Rio Arriba County, New Mexico	Ghezelian-Early Sakmarian	
Ophiacodon	*navajovicus*	WM 1101	Ophiacodontidae	El Cobre Canyon, near Abiquiu, Rio Arriba County, New Mexico	Ghezelian-Early Sakmarian	Isolated fragments
Ophiacodon	*navajovicus*	YP 1383	Ophiacodontidae	El Cobre Canyon, near Abiquiu, Rio Arriba County, New Mexico	Ghezelian-Early Sakmarian	Isolated bones
Ophiacodon	*navajovicus*	YP 2837	Ophiacodontidae	El Cobre Canyon, near Abiquiu, Rio Arriba County, New Mexico	Ghezelian-Early Sakmarian	Distal left humerus, calcaneum and astragulus, left carpus, left femur, pubis, axis spine, dorsal spine, right humerus, 2 dorsal vertebrae and spines, distal tibia and fibula
Edaphosaurus	*novomexicus*	UCLA VP 1641 (Transfered to CMNH? Berman et al 1993)	Edaphosauridae	El Cobre Canyon, near Abiquiu, Rio Arriba County, New Mexico	Ghezelian-Early Sakmarian	Several incomplete neural spines

Aerosaurus	*wellesi*	UCMP 35762	Varanopidae	Camp Quarry, 440m south of New Mexico State Highway, 840m southeats of Rio Puerco Bridge at Arroyo del Agua, Rio Arriba County, New Mexico	Ghezelian-Early Sakmarian	Isolated brain case
Aerosaurus	*wellesi*	UCMP 40094	Varanopidae	Camp Quarry, 440m south of New Mexico State Highway, 840m southeats of Rio Puerco Bridge at Arroyo del Agua, Rio Arriba County, New Mexico	Ghezelian-Early Sakmarian	Fragmentary disarticulated remains
Aerosaurus	*wellesi*	UCMP 40095	Varanopidae	Camp Quarry, 440m south of New Mexico State Highway, 840m southeats of Rio Puerco Bridge at Arroyo del Agua, Rio Arriba County, New Mexico	Ghezelian-Early Sakmarian	Fragmentary disarticulated remains
Aerosaurus	*wellesi*	UCMP 40096	Varanopidae	Camp Quarry, 440m south of New Mexico State Highway, 840m southeats of Rio Puerco Bridge at Arroyo del Agua, Rio Arriba County, New Mexico	Ghezelian-Early Sakmarian	Nearly complete articulated specimen

Aerosaurus	*wellesi*	UCMP 40097	Varanopidae	Camp Quarry, 440m south of New Mexico State Highway, 840m southeats of Rio Puerco Bridge at Arroyo del Agua, Rio Arriba County, New Mexico	Ghezelian-Early Sakmarian	Partly articulated but incomplete skeleton
Aerosaurus	*wellesi*	UCMP 40098	Varanopidae	Camp Quarry, 440m south of New Mexico State Highway, 840m southeats of Rio Puerco Bridge at Arroyo del Agua, Rio Arriba County, New Mexico	Ghezelian-Early Sakmarian	Disarticulated elements
Oedaleops	*campi*	UCMP 35758	Eothyrididae	Camp Quarry, 440m south of New Mexico State Highway, 840m southeats of Rio Puerco Bridge at Arroyo del Agua, Rio Arriba County, New Mexico	Ghezelian-Early Sakmarian	Skull, missing palatals, braincase and some facial elements
Oedaleops	*campi*	UCMP 40095	Eothyrididae	Camp Quarry, 440m south of New Mexico State Highway, 840m southeats of Rio Puerco Bridge at Arroyo del Agua, Rio Arriba County, New Mexico	Ghezelian-Early Sakmarian	Isolated dentary bones

Oedaleops	*campi*	UCMP 40281	Eothyrididae	Camp Quarry, 440m south of New Mexico State Highway, 840m southeats of Rio Puerco Bridge at Arroyo del Agua, Rio Arriba County, New Mexico	Ghezelian-Early Sakmarian	Incomplete and distorted skull
Oedaleops	*campi*	UCMP 67222	Eothyrididae	Camp Quarry, 440m south of New Mexico State Highway, 840m southeats of Rio Puerco Bridge at Arroyo del Agua, Rio Arriba County, New Mexico	Ghezelian-Early Sakmarian	Nearly complete maxilla
Oedaleops	*campi*	UCMP 67223	Eothyrididae	Camp Quarry, 440m south of New Mexico State Highway, 840m southeats of Rio Puerco Bridge at Arroyo del Agua, Rio Arriba County, New Mexico	Ghezelian-Early Sakmarian	Incomplete maxilla
Oedaleops	*campi*	UCMP 67224	Eothyrididae	Camp Quarry, 440m south of New Mexico State Highway, 840m southeats of Rio Puerco Bridge at Arroyo del Agua, Rio Arriba County, New Mexico	Ghezelian-Early Sakmarian	Incomplete maxilla

Oedaleops	*campi*	UCMP 67225	Eothyrididae	Camp Quarry, 440m south of New Mexico State Highway, 840m southeats of Rio Puerco Bridge at Arroyo del Agua, Rio Arriba County, New Mexico	Ghezelian-Early Sakmarian	Isolated dentary bones
Ophiacodon	*mirus*		Ophiacodontidae	Camp Quarry, 440m south of New Mexico State Highway, 840m southeats of Rio Puerco Bridge at Arroyo del Agua, Rio Arriba County, New Mexico	Ghezelian-Early Sakmarian	
Edaphosaurus	*novomexicus*	FMNH UC 674	Edaphosauridae	Camp Quarry, 440m south of New Mexico State Highway, 840m southeats of Rio Puerco Bridge at Arroyo del Agua, Rio Arriba County, New Mexico	Ghezelian-Early Sakmarian	Anterior portion of the skeleton, partial skull
Sphenacodon	*ferox*		Sphenacodontidae	Camp Quarry, 440m south of New Mexico State Highway, 840m southeats of Rio Puerco Bridge at Arroyo del Agua, Rio Arriba County, New Mexico	Ghezelian-Early Sakmarian	
Sphenacodon	*ferocior*	CMNH	Sphenacodontidae	Anderson quarry, Rio Arriba County, New Mexico	Ghezelian-Early Sakmarian	35 partial skeletons

Sphenacodon	*ferox*	CMNH	Sphenacodontidae	Cardillo Quarry, Rio Arriba County, New Mexico	Ghezelian-Early Sakmarian	
Sphenacodon	*ferox*		Sphenacodontidae	Quarry Butte, Rio Arriba County, New Mexico	Ghezelian-Early Sakmarian	
Ophiacodon	*mirus*		Ophiacodontidae	Quarry Butte, Rio Arriba County, New Mexico	Ghezelian-Early Sakmarian	
Ophiacodon	*mirus*	CMNH	Ophiacodontidae	VanderHoof quarry, Rio Arriba County, New Mexico	Ghezelian-Early Sakmarian	
Sphenacodon	*ferox*	CMNH	Sphenacodontidae	VanderHoof quarry, Rio Arriba County, New Mexico	Ghezelian-Early Sakmarian	
Ophiacodon	*mirus*		Ophiacodontidae	Welles quarry, Rio Arriba County, New Mexico	Ghezelian-Early Sakmarian	
Sphenacodon	*ferox*		Sphenacodontidae	Welles quarry, Rio Arriba County, New Mexico	Ghezelian-Early Sakmarian	
Ophiacodon	*mirus*	FMNH 671	Ophiacodontidae	Miller Bonebed, Rio Arriba County, New Mexico	Ghezelian-Early Sakmarian	Nearly complete skeleton
Ophiacodon	*mirus*	FMNH 672	Ophiacodontidae	Miller Bonebed, Rio Arriba County, New Mexico	Ghezelian-Early Sakmarian	Partial skeleton
Sphenacodon	*ferox*	FMNH 35	Sphenacodontidae	Poleo Creek	Ghezelian-Early Sakmarian	Mounted skeleton
Ophiacodon	*mirus (?)*	OMNH 55200	Ophiacodontidae	OMNH V1005, North of the Canadian River Seminole County, Oklahoma	Late Gzhelian	Left humerus
Ophiacodon	*mirus (?)*	OMNH 55203	Ophiacodontidae	OMNH V1005, North of the Canadian River Seminole County, Oklahoma	Late Gzhelian	Humerus

Ophiacodon	*mirus (?)*	OMNH 55204	Ophiacodontidae	OMNH V1005, North of the Canadian River Seminole County, Oklahoma	Late Gzhelian	Humerus
Ophiacodon	*mirus (?)*	OMNH 55208	Ophiacodontidae	OMNH V1005, North of the Canadian River Seminole County, Oklahoma	Late Gzhelian	Humerus
Ophiacodon	*mirus (?)*	OMNH 55210	Ophiacodontidae	OMNH V1005, North of the Canadian River Seminole County, Oklahoma	Late Gzhelian	Right radius
Ophiacodon	*mirus (?)*	OMNH 55216	Ophiacodontidae	OMNH V1005, North of the Canadian River Seminole County, Oklahoma	Late Gzhelian	Left Ulna
Ophiacodon	*mirus (?)*	OMNH 55220	Ophiacodontidae	OMNH V1005, North of the Canadian River Seminole County, Oklahoma	Late Gzhelian	Proximal right tibia
Ophiacodon	*mirus (?)*	OMNH 55224	Ophiacodontidae	OMNH V1005, North of the Canadian River Seminole County, Oklahoma	Late Gzhelian	Tibia
Ophiacodon	*mirus (?)*	OMNH 55229	Ophiacodontidae	OMNH V1005, North of the Canadian River Seminole County, Oklahoma	Late Gzhelian	Fibula
Ophiacodon	*mirus (?)*	OMNH 55235	Ophiacodontidae	OMNH V1005, North of the Canadian River Seminole County, Oklahoma	Late Gzhelian	Femur

Ophiacodon	*mirus (?)*	OMNH 55237	Ophiacodontidae	OMNH V1005, North of the Canadian River Seminole County, Oklahoma	Late Gzhelian	Femur
Ophiacodon	*mirus (?)*	OMNH 55238	Ophiacodontidae	OMNH V1005, North of the Canadian River Seminole County, Oklahoma	Late Gzhelian	Femur
Ophiacodon	*mirus (?)*	OMNH 55239	Ophiacodontidae	OMNH V1005, North of the Canadian River Seminole County, Oklahoma	Late Gzhelian	Femur
Ophiacodon	*mirus (?)*	OMNH 55240	Ophiacodontidae	OMNH V1005, North of the Canadian River Seminole County, Oklahoma	Late Gzhelian	Femur
Ophiacodon	*mirus (?)*	OMNH 55241	Ophiacodontidae	OMNH V1005, North of the Canadian River Seminole County, Oklahoma	Late Gzhelian	Left scapulacoracoid, minus posterior coracoid
Ophiacodon	*mirus (?)*	OMNH 55244	Ophiacodontidae	OMNH V1005, North of the Canadian River Seminole County, Oklahoma	Late Gzhelian	Pelvic girdle elements
Ophiacodon	*mirus (?)*	OMNH 55246	Ophiacodontidae	OMNH V1005, North of the Canadian River Seminole County, Oklahoma	Late Gzhelian	Pelvic girdle elements
Ophiacodon	*mirus (?)*	OMNH 55252	Ophiacodontidae	OMNH V1005, North of the Canadian River Seminole County, Oklahoma	Late Gzhelian	Articulated series of 27 distal caudal vertebrae

Ophiacodon	*mirus (?)*	OMNH 55253	Ophiacodontidae	OMNH V1005, North of the Canadian River Seminole County, Oklahoma	Late Gzhelian	Articulated series of 4 lumbar vertebrae, lacking intercentra
Ophiacodon	*mirus (?)*	OMNH 55254	Ophiacodontidae	OMNH V1005, North of the Canadian River Seminole County, Oklahoma	Late Gzhelian	Articulated series of 5 lumbar vertebrae
Ophiacodon	*mirus (?)*	OMNH 55255	Ophiacodontidae	OMNH V1005, North of the Canadian River Seminole County, Oklahoma	Late Gzhelian	Cervical vertebra
Ophiacodon	*mirus (?)*	OMNH 55256	Ophiacodontidae	OMNH V1005, North of the Canadian River Seminole County, Oklahoma	Late Gzhelian	Cervical vertebra
Ophiacodon	*mirus (?)*	OMNH 55257	Ophiacodontidae	OMNH V1005, North of the Canadian River Seminole County, Oklahoma	Late Gzhelian	Dorsal vertebra, incomplete above the level of the transverse process
Ophiacodon	*mirus (?)*	OMNH 55258	Ophiacodontidae	OMNH V1005, North of the Canadian River Seminole County, Oklahoma	Late Gzhelian	Dorsal vertebra, incomplete above the level of the transverse process
Ophiacodon	*mirus (?)*	OMNH 55259	Ophiacodontidae	OMNH V1005, North of the Canadian River Seminole County, Oklahoma	Late Gzhelian	Articulated series of 3 dorsal vertebrae, lacking neural arch above the transverse process
Ophiacodon	*mirus (?)*	OMNH 55274	Ophiacodontidae	OMNH V1005, North of the Canadian River Seminole County, Oklahoma	Late Gzhelian	Centrum of proximal caudal vertebra

Ophiacodon	*mirus (?)*	OMNH 55275	Ophiacodontidae	OMNH V1005, North of the Canadian River Seminole County, Oklahoma	Late Gzhelian	Centrum of proximal caudal vertebra
Ophiacodon	*mirus (?)*	OMNH 55292	Ophiacodontidae	OMNH V1005, North of the Canadian River Seminole County, Oklahoma	Late Gzhelian	Centrum of proximal caudal vertebra
Edaphosaurus	*colohistion*	CM23513	Edaphosauridae	1/2 miles east of Elm Grove, West Virginia	Late Gzhelian	Articulated series of 14 presacral vertebrae, many with ribs, fragments of other vertebrae
Stereorachis	*dominans*	Paris Museum	Ophiacodontidae	Igornay, near Autun, Bourgogne	Late Gzhelian	Disarticulated specimen: partial maxilla, anterior halves of mandibles, 13 vertebrae, clavicle, interclavicale, scapula, humerus and ulna
Cryptovenator	*hirschbergeri*	LFN-PW 2008/5599LS	Sphenacodontidae	Western rim of the Remiguisberg quarry, 1km north of Haschbach in Rhineland Palinate	Late Gzhelian	Anterior right mandible
Baldwinonus (?)	*dunkardensis*	CMNG 8563	Ophiacodontidae (?)	Near Cameron, Monroe County, Ohio	Asselian	Fragmentary right maxilla
Pantelosaurus	*saxonicus*	Säachsisches Geologisches Landsamt, Leipzig	Sphenacodontia,	Königin-Carola-Schacht, Döhlen Basin, near Dresden	Asselian	6 nearly complete skeletons
Sphenacodon (?)	*britannicus*	GSM 22893/4	Sphenacodontidae	Kenilworth	Asselian-early Samarkian	Left maxilla
Haptodus	*grandis*	Gx 1071	Sphenacodontia,	Kenilworth	Asselian-early Samarkian	Part of left maxilla
Neosaurus	*cynodus*	Besancon Museum	Sphenacodontidae	Besancon, Moissey, Department of Jura	Asselian-early Samarkian	Left maxilla
Sphenacodon	*ferox*	CMNH	Sphenacodontidae	Tularosa Locality, Sacramento Mountains, Otero County, New Mexico	Asselian-Early Sakmarian	Nasal, prefrontal, frontal, premaxilla, maxilla and teeth

Edaphosaurus	*novomexicus*	CMNH	Edaphosauridae	Tularosa Locality, Sacramento Mountains, Otero County, New Mexico	Asselian-Early Sakmarian	
Sphenacodon	*ferocior*	MCZ 1489	Sphenacodontidae	Canyon de San Diego, 4 miles south of Jemez Spings, Sandoval County, New Mexico	Asselian-Artinskian	Skull and cervical vertebrae, neural spines
Sphenacodon	*ferocior*	WM 11	Sphenacodontidae	Canyon de San Diego, 4 miles south of Jemez Spings, Sandoval County, New Mexico	Asselian-Artinskian	Fragmentary skeleton
Dimetrodon	*occidentalis*	CM 26565	Sphenacodontidae	Canyon de San Diego, 4 miles south of Jemez Spings, Sandoval County, New Mexico	Asselian-Artinskian	4 mid dorsal vertebrae, 10 neural spines, posterior dentary, anterior coronoid and angular
Sphenacodon	*ferocior*	UM 9649	Sphenacodontidae	Ojo de la Parida, near Socorro, Rio Arribo County, New Mexico	Asselian-Early Kungurain	Femur, neural spine, clavicle
Cutleria	*wilmarthi*	USNM 22099	Sphenacodontia,	Placerville 3+4, 2 miles southeast of Placerville, San Miguel County, Colorado	Asselian-Early Kungurian	Skull and skeleton
Cutleria	*wilmarthi*	MCZ 2987	Sphenacodontia,	Placerville 11-13, 2 miles southeast of Placerville, San Miguel County, Colorado	Asselian-Early Kungurian	Snout
Mycterosaurus (?)	*smithae*	MCZ 2985	Eothyrididae	Placerville 11-13, 2 miles southeast of Placerville, San Miguel County, Colorado	Asselian-Early Kungurian	Partial skull, 5 vertebrae, ribs, fragments of limbs

Stereophallodon	*ciscoensis*	MCZ 1535	Ophiacodontidae	4 miles South of Windthorst, Texas	Late Asselian-Early Sakmarian	Quadrate, articular, skull fragments, 6 centra
Stereophallodon	*ciscoensis*	MCZ 1944	Ophiacodontidae	4 miles South of Windthorst, Texas	Late Asselian-Early Sakmarian	Fragmentary remains
Stereophallodon	*ciscoensis*	MCZ 6618	Ophiacodontidae	4 miles South of Windthorst, Texas	Late Asselian-Early Sakmarian	Fragmentary remains
Stereophallodon	*ciscoensis*	AMNH 4768	Ophiacodontidae	4 miles South of Windthorst, Texas	Late Asselian-Early Sakmarian	Vertebrae, sacral ribs, premaxilla
Stereophallodon	*ciscoensis*	MCZ 6358	Ophiacodontidae	Prideaux Pocket	Late Asselian-Early Sakmarian	3 premaxillae
Stereophallodon	*ciscoensis*	MCZ 6354	Ophiacodontidae	Prideaux Pocket	Late Asselian-Early Sakmarian	5 maxillarz fragments
Stereophallodon	*ciscoensis*	MCZ 6352	Ophiacodontidae	Prideaux Pocket	Late Asselian-Early Sakmarian	2 prefrontals
Stereophallodon	*ciscoensis*	MCZ 6353	Ophiacodontidae	Prideaux Pocket	Late Asselian-Early Sakmarian	Postfrontal
Stereophallodon	*ciscoensis*	MCZ 6348	Ophiacodontidae	Prideaux Pocket	Late Asselian-Early Sakmarian	5 Basioccipitals
Stereophallodon	*ciscoensis*	MCZ 6349	Ophiacodontidae	Prideaux Pocket	Late Asselian-Early Sakmarian	3 parabasisphenoids
Stereophallodon	*ciscoensis*	MCZ 6350	Ophiacodontidae	Prideaux Pocket	Late Asselian-Early Sakmarian	4 quadrates
Stereophallodon	*ciscoensis*	MCZ 6359	Ophiacodontidae	Prideaux Pocket	Late Asselian-Early Sakmarian	8 dentary fragments
Stereophallodon	*ciscoensis*	MCZ 6352	Ophiacodontidae	Prideaux Pocket	Late Asselian-Early Sakmarian	3 articulars
Stereophallodon	*ciscoensis*	MCZ 6371	Ophiacodontidae	Prideaux Pocket	Late Asselian-Early Sakmarian	Axis centrum
Stereophallodon	*ciscoensis*	MCZ 6357	Ophiacodontidae	Prideaux Pocket	Late Asselian-Early Sakmarian	Partial cervical centrum
Stereophallodon	*ciscoensis*	MCZ 6355	Ophiacodontidae	Prideaux Pocket	Late Asselian-Early Sakmarian	20 mid dorsal centra

Stereophallodon	*ciscoensis*	MCZ 6356	Ophiacodontidae	Prideaux Pocket	Late Asselian-Early Sakmarian	22 centra
Stereophallodon	*ciscoensis*	MCZ 6768	Ophiacodontidae	Prideaux Pocket	Late Asselian-Early Sakmarian	3 ilia
Stereophallodon	*ciscoensis*	MCZ 7083	Ophiacodontidae	Prideaux Pocket	Late Asselian-Early Sakmarian	Distal femurs
Stereophallodon	*ciscoensis*	MCZ 6766	Ophiacodontidae	Prideaux Pocket	Late Asselian-Early Sakmarian	Proximal femur
Stereophallodon	*ciscoensis*	MCZ 6765	Ophiacodontidae	Prideaux Pocket	Late Asselian-Early Sakmarian	2 proximal fibulae
Stereophallodon	*ciscoensis*	MCZ 6767	Ophiacodontidae	Prideaux Pocket	Late Asselian-Early Sakmarian	4 proxmial tibiae
Haptodus	*baylei*	Museum d	Sphenacodontia,	Le Télots, Autunois	Early Samarkian	Two poorly preserved skeletons
Haptodus	*baylei*	Museum d	Sphenacodontia,	Margenne, near Autun	Early Samarkian	Immature skeleton
Ophiacodon	*uniformis (?)*	PU 17800	Ophiacodontidae	East side of King	Sakmarian	10 dorsal vertbrae, partial humerus, left limb and foot elements
Ctenospondylus	*ninevehensis*	MCZ 3386	Sphenacodontidae	Clarke Hill, on Couty Route 43 near junction with State Route, Salem Township. Monroe County, Ohio	Sakmarian	Premaxilla, maxilla, right prefrontal, right jugal, left pterygoid, left dentary, axial neural spine, 3 dorsal vertebrae, lumbar vertabra, 4 caudal vertebrae, ribs, part of scapula blade, left humerus, right pelvis
Ctenospondylus	*ninevehensis*	MCZ 8635-42	Sphenacodontidae	Clarke Hill, on Couty Route 43 near junction with State Route, Salem Township. Monroe County, Ohio	Sakmarian	Premaxilla (no teeth), prefrontal, postorbital, squamosal, parietal, nasal, dorsal vertebrae (no spines), causal vertebrae (no spines), scapula blade
Ctenospondylus	*ninevehensis*	MCZ 8665	Sphenacodontidae	Clarke Hill, on Couty Route 43 near junction with State Route, Salem Township. Monroe County, Ohio	Sakmarian	Jugal

Ctenospondylus	*ninevehensis*	MCZ 3353	Sphenacodontidae	Clarke Hill, on Couty Route 43 near junction with State Route, Salem Township. Monroe County, Ohio	Sakmarian	Tooth
Ctenospondylus	*ninevehensis*	MCZ 3102	Sphenacodontidae	Clarke Hill, on Couty Route 43 near junction with State Route, Salem Township. Monroe County, Ohio	Sakmarian	Interclavicle, 18 dorsal vertebrae, 5 neural spines, pelvis (proximal end of all three bones and acetabulum x2), distal pubis, proximal clavicle, maxilla, premaxilla and dentary with teeth, articular, angular, proximal humerus, scapula and proximal coracoid, fibula, proximal ulna, proximal tibia
Palaeohatteria	*longicaudata*	Sächsisches Geologisches Landesamt, Leipzig	Sphenacodontia,	Niederhäslich, near Dresden, Saxony, Germany	Sakmarian	Several well preserved specimens
Edaphosaurus (?)	*credneri (?)*	Geologisches Landesanstalt, Leipzig	Edaphosauridae	Niederhäslich, near Dresden, Saxony, Germany	Sakmarian	Posterior half of presacral region and pelvic region
Dimetrodon (?)	*milleri (?)*	MCZ Iia	Sphenacodontidae	1 mile northwest of Padgett, Young County	Late Sakmarian	Femur
Lupeosaurus	*kayi*	MCZ 1455	Edaphosauridae	Cottonwood Creek, Archer County, Texas	Late Sakmarian	Vertebral collumn
Lupeosaurus	*kayi*	MCZ 1454	Edaphosauridae	Cottonwood Creek, Archer County, Texas	Late Sakmarian	15 dorsal vertebrae, neural spines, scapulacoracoid
Lupeosaurus	*kayi*	MCZ 1264	Edaphosauridae	Cottonwood Creek, Archer County, Texas	Late Sakmarian	Pelvis
Ophiacodon	*retroversus*	MCZ 1120	Ophiacodontidae	Cottonwood Creek, Archer County, Texas	Late Sakmarian	Partial vertebral column
Varanosaurus	*witchitaensis*	MCZ 3424	Ophiacodontidae	Cottonwood Creek, Archer County, Texas	Late Sakmarian	Femur

Lupeosaurus	*kayi*	AMNH 1636	Edaphosauridae	?	Late Sakmarian-Early Artinskian	Incomplete scapulocoracoid
Edaphosaurus	*boanerges*	TMM specimen	Edaphosauridae	Archer City bonebed 3, 2km from Archer City, Archer County, Texas	Late Sakmarian-Artinskian	Skeleton
Edaphosaurus	*boanerges*		Edaphosauridae	Archer City bonebed 3, 2km from Archer City, Archer County, Texas	Late Sakmarian-Artinskian	Neural spines
Apsisaurus	*witteri*	MCZ 1474	Varanopidae	Archer City bonebed 1, 2km from Archer City, Archer County, Texas	Late Sakmarian-Artinskian	Incomplete skull and lower jaw, posterior cervical, dorsal, sacral and anterior caudal vertebrae and ribs, proximal formlimb and hindlimb
Dimetrodon	*milleri*		Sphenacodontidae	Archer City bonebed 1, 2km from Archer City, Archer County, Texas	Late Sakmarian-Artinskian	Pelvis, tail
Dimetrodon	*milleri*	MCZ 1365	Sphenacodontidae	Archer City bonebed 1, 2km from Archer City, Archer County, Texas	Late Sakmarian-Artinskian	Nearly complete skeleton
Ophiacodon	*uniformis*	MCZ 1366	Ophiacodontidae	Archer City bonebed 1, 2km from Archer City, Archer County, Texas	Late Sakmarian-Artinskian	Nearly complete skeleton
Ophiacodon	*uniformis*	MCZ 1413	Ophiacodontidae	Archer City bonebed 1, 2km from Archer City, Archer County, Texas	Late Sakmarian-Artinskian	Partial skeleton
Ophiacodon	*uniformis*	Lost	Ophiacodontidae	Archer City bonebed 1, 2km from Archer City, Archer County, Texas	Late Sakmarian-Artinskian	Dorsal centra of two indeviduals
Ophiacodon	*uniformis*	AMNH 4143	Ophiacodontidae	Archer City bonebed 1, 2km from Archer City, Archer County, Texas	Late Sakmarian-Artinskian	Snout, lower jaw, teeth, 13 vertebrae and ribs
Ophiacodon	*retroversus*	MCZ 1426	Ophiacodontidae	Archer City bonebed 1, 2km from Archer City,	Late Sakmarian-Artinskian	Partial skeleton

				Archer County, Texas		
Sphenacodon	*ferocior*	YP 818	Sphenacodontidae	Rito Puerco, Rio Arriba County, New Mexico	Late Sakmarian-Early Kungurian	Partial skull, nearly complete presacral column, girdles, humerus femur
Sphenacodon	*ferocior*	YP1107	Sphenacodontidae	Rito Puerco, Rio Arriba County, New Mexico	Late Sakmarian-Early Kungurian	Vertebrae, skull fragments
Sphenacodon	*ferocior*	YP 2836	Sphenacodontidae	Rito Puerco, Rio Arriba County, New Mexico	Late Sakmarian-Early Kungurian	Scapulocoracoid
Sphenacodon	*ferocior*	MCZ 4097-99	Sphenacodontidae	Rito Puerco, Rio Arriba County, New Mexico	Late Sakmarian-Early Kungurian	Hundreds of dorsal centra, 39 neural spines from all regions, 3 sacral centra and ribs, 9 anterior caudal centra with one neural spine
Sphenacodon	*ferocior*	MCZ 4872	Sphenacodontidae	Rito Puerco, Rio Arriba County, New Mexico	Late Sakmarian-Early Kungurian	Pterygoid
Sphenacodon	*ferocior*	MCZ 4873	Sphenacodontidae	Rito Puerco, Rio Arriba County, New Mexico	Late Sakmarian-Early Kungurian	Jugal
Sphenacodon	*ferocior*	MCZ 4875	Sphenacodontidae	Rito Puerco, Rio Arriba County, New Mexico	Late Sakmarian-Early Kungurian	Supraoccipital, basioccipital, parasphenoid; occipital region of skull
Sphenacodon	*ferocior*	MCZ 4876	Sphenacodontidae	Rito Puerco, Rio Arriba County, New Mexico	Late Sakmarian-Early Kungurian	Postorbital
Sphenacodon	*ferocior*	MCZ 4882	Sphenacodontidae	Rito Puerco, Rio Arriba County, New Mexico	Late Sakmarian-Early Kungurian	Ptergoids and teeth
Sphenacodon	*ferocior*	MCZ 4931	Sphenacodontidae	Rito Puerco, Rio Arriba County, New Mexico	Late Sakmarian-Early Kungurian	Basisphenoid
Sphenacodon	*ferocior*	MCZ 4932	Sphenacodontidae	Rito Puerco, Rio Arriba County, New Mexico	Late Sakmarian-Early Kungurian	Palatine
Sphenacodon	*ferocior*	MCZ 5736	Sphenacodontidae	Rito Puerco, Rio Arriba County, New Mexico	Late Sakmarian-Early Kungurian	Palatine
Sphenacodon	*ferocior*	MCZ 6652	Sphenacodontidae	Rito Puerco, Rio Arriba County, New Mexico	Late Sakmarian-Early Kungurian	Parietal
Sphenacodon	*ferocior*	MCZ 6653	Sphenacodontidae	Rito Puerco, Rio Arriba County, New Mexico	Late Sakmarian-Early Kungurian	Axis neural spine

Sphenacodon	*ferocior*	MCZ 7052-56	Sphenacodontidae	Rito Puerco, Rio Arriba County, New Mexico	Late Sakmarian-Early Kungurian	Quadrate, squamosal, atlas centrum, prefrontal, articular
Sphenacodon	*ferocior*	MCZ 8091-93	Sphenacodontidae	Rito Puerco, Rio Arriba County, New Mexico	Late Sakmarian-Early Kungurian	Dentary symphysis (no teeth), premaxilla, septomaxilla, postorbital
Sphenacodon	*ferocior*	MCZ 8732	Sphenacodontidae	Rito Puerco, Rio Arriba County, New Mexico	Late Sakmarian-Early Kungurian	Angular
Sphenacodon	*ferox*	MCZ 4877-81	Sphenacodontidae	Rito Puerco, Rio Arriba County, New Mexico	Late Sakmarian-Early Kungurian	Basioccipital, quadrate, dentary fragments, atlas centrum, articulars
Sphenacodon	*ferox*	MCZ 4883-85	Sphenacodontidae	Rito Puerco, Rio Arriba County, New Mexico	Late Sakmarian-Early Kungurian	Scapulocoracoid
Sphenacodon	*ferox*	MCZ 4896	Sphenacodontidae	Rito Puerco, Rio Arriba County, New Mexico	Late Sakmarian-Early Kungurian	Both scapulocoracoids
Sphenacodon	*ferox*	MCZ 4899	Sphenacodontidae	Rito Puerco, Rio Arriba County, New Mexico	Late Sakmarian-Early Kungurian	Interclavicle head
Sphenacodon	*ferox*	MCZ 4902-04	Sphenacodontidae	Rito Puerco, Rio Arriba County, New Mexico	Late Sakmarian-Early Kungurian	Proximal coracoid, clavicles, cleithrum
Sphenacodon	*ferox*	MCZ 4903	Sphenacodontidae	Rito Puerco, Rio Arriba County, New Mexico	Late Sakmarian-Early Kungurian	Clavicles
Sphenacodon	*ferox*	MCZ 4906	Sphenacodontidae	Rito Puerco, Rio Arriba County, New Mexico	Late Sakmarian-Early Kungurian	Humeri
Sphenacodon	*ferox*	MCZ 4916-23	Sphenacodontidae	Rito Puerco, Rio Arriba County, New Mexico	Late Sakmarian-Early Kungurian	1 femur, 1 femur without shaft, pubis, proximal pubis, proximal ilium x 2, acetabulum, ischium, tibia, proximal tibia and shaft, 2 proximal ulnae, astraguli
Sphenacodon	*ferox*	MCZ 4926	Sphenacodontidae	Rito Puerco, Rio Arriba County, New Mexico	Late Sakmarian-Early Kungurian	Angular
Sphenacodon	*ferox*	MCZ 4933	Sphenacodontidae	Rito Puerco, Rio Arriba County, New Mexico	Late Sakmarian-Early Kungurian	Radiale
Sphenacodon	*ferox*	MCZ 5343	Sphenacodontidae	Rito Puerco, Rio Arriba County, New Mexico	Late Sakmarian-Early Kungurian	Prefrontal
Sphenacodon	*ferox*	MCZ 6035	Sphenacodontidae	Rito Puerco, Rio Arriba County, New Mexico	Late Sakmarian-Early Kungurian	Nasal

Sphenacodon	*ferox*	MCZ 6302-05	Sphenacodontidae	Rito Puerco, Rio Arriba County, New Mexico	Late Sakmarian-Early Kungurian	Basisphenoid, basioccipital, frontal, proximal pubis
Sphenacodon	*ferox*	MCZ 6309-11	Sphenacodontidae	Rito Puerco, Rio Arriba County, New Mexico	Late Sakmarian-Early Kungurian	2 x second distal tarsals, 2x thrid distal tarsals, 1x medial centrale
Sphenacodon	*ferox*	MCZ 6315	Sphenacodontidae	Rito Puerco, Rio Arriba County, New Mexico	Late Sakmarian-Early Kungurian	Metapodials, including unguals
Sphenacodon	*ferox*	MCZ 6317	Sphenacodontidae	Rito Puerco, Rio Arriba County, New Mexico	Late Sakmarian-Early Kungurian	Pisiform process
Sphenacodon	*ferox*	MCZ 6321	Sphenacodontidae	Rito Puerco, Rio Arriba County, New Mexico	Late Sakmarian-Early Kungurian	Postorbital
Sphenacodon	*ferox*	MCZ 6654	Sphenacodontidae	Rito Puerco, Rio Arriba County, New Mexico	Late Sakmarian-Early Kungurian	Ulnare
Sphenacodon	*ferox*	MCZ 6655	Sphenacodontidae	Rito Puerco, Rio Arriba County, New Mexico	Late Sakmarian-Early Kungurian	First distal carpal
Sphenacodon	*ferox*	MCZ 7045-51	Sphenacodontidae	Rito Puerco, Rio Arriba County, New Mexico	Late Sakmarian-Early Kungurian	Parietal, exoccipital, jugal, splenial, pterygoid and teeth, epipterygoid, surangular
Sphenacodon	*ferox*	MCZ 7057-62	Sphenacodontidae	Rito Puerco, Rio Arriba County, New Mexico	Late Sakmarian-Early Kungurian	Astragulus, proximal ulna, distal tibia, femur, scapula, humerus
Sphenacodon	*ferox*	MCZ 8082-84	Sphenacodontidae	Rito Puerco, Rio Arriba County, New Mexico	Late Sakmarian-Early Kungurian	Angular, quadrate, parietal
Sphenacodon	*ferox*	MCZ 8097-99	Sphenacodontidae	Rito Puerco, Rio Arriba County, New Mexico	Late Sakmarian-Early Kungurian	Proximal and distal humerus, transvers phlange of pterygoid, proximal corocoid
Sphenacodon	*ferox*	MCZ 8305	Sphenacodontidae	Rito Puerco, Rio Arriba County, New Mexico	Late Sakmarian-Early Kungurian	Phlanges
Sphenacodon	*ferox*	MCZ 8627	Sphenacodontidae	Rito Puerco, Rio Arriba County, New Mexico	Late Sakmarian-Early Kungurian	Pterygoid + teeth, proximal coracoid, distal scapula, proximal and distal fibula and tibia (no shafts); 2 sacral vertebrae, one neural spine, sacral ribs, 7 centra (caudal?), 1 cervical neural spine, dorsal spine fragments
Ophiacodon	*mirus*	MCZ 4810	Ophiacodontidae	Rito Puerco, Rio Arriba County, New Mexico	Late Sakmarian-Early Kungurian	8 dorsal centra, 4 spines

Ophiacodon	*mirus*	MCZ 4856	Ophiacodontidae	Rito Puerco, Rio Arriba County, New Mexico	Late Sakmarian-Early Kungurian	2 femora
Ophiacodon	*mirus*	MCZ 4857	Ophiacodontidae	Rito Puerco, Rio Arriba County, New Mexico	Late Sakmarian-Early Kungurian	Proximal ilia
Ophiacodon	*mirus*	MCZ 4859	Ophiacodontidae	Rito Puerco, Rio Arriba County, New Mexico	Late Sakmarian-Early Kungurian	Humerus shaft
Ophiacodon	*mirus*	MCZ 4860	Ophiacodontidae	Rito Puerco, Rio Arriba County, New Mexico	Late Sakmarian-Early Kungurian	Ischia
Ophiacodon	*mirus*	MCZ 4888	Ophiacodontidae	Rito Puerco, Rio Arriba County, New Mexico	Late Sakmarian-Early Kungurian	Axis centrum and spine
Ophiacodon	*mirus*	MCZ 4900	Ophiacodontidae	Rito Puerco, Rio Arriba County, New Mexico	Late Sakmarian-Early Kungurian	Interclavicle head
Ophiacodon	*mirus*	MCZ 4911-14	Ophiacodontidae	Rito Puerco, Rio Arriba County, New Mexico	Late Sakmarian-Early Kungurian	About a million dorsal vertebrae, one spine, 5 sacral vertebrae with 1 spine, 2 proximal pubes
Ophiacodon	*mirus*	MCZ 4924	Ophiacodontidae	Rito Puerco, Rio Arriba County, New Mexico	Late Sakmarian-Early Kungurian	Astraguli
Ophiacodon	*mirus*	MCZ 4925	Ophiacodontidae	Rito Puerco, Rio Arriba County, New Mexico	Late Sakmarian-Early Kungurian	Calcanea
Ophiacodon	*mirus*	MCZ 4927-30	Ophiacodontidae	Rito Puerco, Rio Arriba County, New Mexico	Late Sakmarian-Early Kungurian	Basioccipital, basisphenoid, quadrate, atlas centrum
Ophiacodon	*mirus*	MCZ 4934	Ophiacodontidae	Rito Puerco, Rio Arriba County, New Mexico	Late Sakmarian-Early Kungurian	Radiale
Ophiacodon	*mirus*	MCZ 4935	Ophiacodontidae	Rito Puerco, Rio Arriba County, New Mexico	Late Sakmarian-Early Kungurian	Articulars
Ophiacodon	*mirus*	MCZ 6285	Ophiacodontidae	Rito Puerco, Rio Arriba County, New Mexico	Late Sakmarian-Early Kungurian	2 tibias
Ophiacodon	*mirus*	MCZ 6286	Ophiacodontidae	Rito Puerco, Rio Arriba County, New Mexico	Late Sakmarian-Early Kungurian	Proximal tibia
Ophiacodon	*mirus*	MCZ 6289	Ophiacodontidae	Rito Puerco, Rio Arriba County, New Mexico	Late Sakmarian-Early Kungurian	Humerus, proximal humerus
Ophiacodon	*mirus*	MCZ 6298	Ophiacodontidae	Rito Puerco, Rio Arriba County, New Mexico	Late Sakmarian-Early Kungurian	Metapodials

Ophiacodon	*mirus*	MCZ 6299	Ophiacodontidae	Rito Puerco, Rio Arriba County, New Mexico	Late Sakmarian-Early Kungurian	1 complete fibula, 1 without shaft
Ophiacodon	*mirus*	MCZ 6300	Ophiacodontidae	Rito Puerco, Rio Arriba County, New Mexico	Late Sakmarian-Early Kungurian	2 sacral ribs
Ophiacodon	*mirus*	MCZ 6301	Ophiacodontidae	Rito Puerco, Rio Arriba County, New Mexico	Late Sakmarian-Early Kungurian	Radius
Ophiacodon	*mirus*	MCZ 6306-6308	Ophiacodontidae	Rito Puerco, Rio Arriba County, New Mexico	Late Sakmarian-Early Kungurian	Distal carpels, tarsals and radiale
Ophiacodon	*mirus*	MCZ 6312-6314	Ophiacodontidae	Rito Puerco, Rio Arriba County, New Mexico	Late Sakmarian-Early Kungurian	Intermedium, ulnare, pisiform
Ophiacodon	*mirus*	MCZ 6319	Ophiacodontidae	Rito Puerco, Rio Arriba County, New Mexico	Late Sakmarian-Early Kungurian	7 posterior caudal vertebrae
Ophiacodon	*mirus*	MCZ 6322	Ophiacodontidae	Rito Puerco, Rio Arriba County, New Mexico	Late Sakmarian-Early Kungurian	Atlas arches
Ophiacodon	*mirus*	MCZ 6656-58	Ophiacodontidae	Rito Puerco, Rio Arriba County, New Mexico	Late Sakmarian-Early Kungurian	Postfrontal, postorbital, prefrontal
Ophiacodon	*mirus*	MCZ 8100	Ophiacodontidae	Rito Puerco, Rio Arriba County, New Mexico	Late Sakmarian-Early Kungurian	Vertebra
Ophiacodon	*mirus*		Ophiacodontidae	Rito Puerco, Rio Arriba County, New Mexico	Late Sakmarian-Early Kungurian	Scapula blade, proximal corocoid
Edaphosaurus	*novomexicus*	MCZ 1383	Edaphosauridae	Rito Puerco, Rio Arriba County, New Mexico	Late Sakmarian-Early Kungurian	2 vertebrae centra, at least 4 mid and posterior dorsal neural spines
Sphenacodon	*ferox*	WM 736	Sphenacodontidae	Baldwin bonebed, Rio Arriba County, New Mexico	Late Sakmarian-Early Kungurian	Fragmentary postcranial remains
Sphenacodon	*ferox*	YP 806	Sphenacodontidae	Baldwin bonebed, Rio Arriba County, New Mexico	Late Sakmarian-Early Kungurian	Dentary
Sphenacodon	*ferox*	WM 10	Sphenacodontidae	Baldwin bonebed, Rio Arriba County, New Mexico	Late Sakmarian-Early Kungurian	Skull, jaws, other bones

Sphenacodon	*ferox*	WM 1218	Sphenacodontidae	Baldwin bonebed, Rio Arriba County, New Mexico	Late Sakmarian-Early Kungurian	Skull, jaws and other bones
Sphenacodon	*ferox*	WM 425	Sphenacodontidae	Baldwin bonebed, Rio Arriba County, New Mexico	Late Sakmarian-Early Kungurian	Skull, shoulder girdle, vertebrae
Sphenacodon	*ferox*	WM 747	Sphenacodontidae	Baldwin bonebed, Rio Arriba County, New Mexico	Late Sakmarian-Early Kungurian	vertebrae and scapulocoracoid
Sphenacodon	*ferox*	WM	Sphenacodontidae	Baldwin bonebed, Rio Arriba County, New Mexico	Late Sakmarian-Early Kungurian	Axis
Sphenacodon	*ferox*	AM 4779	Sphenacodontidae	Baldwin bonebed, Rio Arriba County, New Mexico	Late Sakmarian-Early Kungurian	Partial skull and skeletal fragments
Sphenacodon	*ferox*	UM 9778	Sphenacodontidae	Baldwin bonebed, Rio Arriba County, New Mexico	Late Sakmarian-Early Kungurian	Most of the skull, fragments of ribs
Sphenacodon	*ferox*	WM 672	Sphenacodontidae	Baldwin bonebed, Rio Arriba County, New Mexico	Late Sakmarian-Early Kungurian	Maxilla
Sphenacodon	*ferox*	WM 739	Sphenacodontidae	Baldwin bonebed, Rio Arriba County, New Mexico	Late Sakmarian-Early Kungurian	Maxilla
Sphenacodon	*ferox*	WM 740	Sphenacodontidae	Baldwin bonebed, Rio Arriba County, New Mexico	Late Sakmarian-Early Kungurian	Two maxillae

Sphenacodon	*ferox*	WM 1200	Sphenacodontidae	Baldwin bonebed, Rio Arriba County, New Mexico	Late Sakmarian-Early Kungurian	Dentary
Sphenacodon	*ferox*	WM 168	Sphenacodontidae	Baldwin bonebed, Rio Arriba County, New Mexico	Late Sakmarian-Early Kungurian	Scapulocoracoid
Sphenacodon	*ferox*	UM 3006	Sphenacodontidae	Baldwin bonebed, Rio Arriba County, New Mexico	Late Sakmarian-Early Kungurian	Scapulocoracoid
Sphenacodon	*ferox*	UM 3015	Sphenacodontidae	Baldwin bonebed, Rio Arriba County, New Mexico	Late Sakmarian-Early Kungurian	Scapulocoracoid
Sphenacodon	*ferox*	AM 4798	Sphenacodontidae	Baldwin bonebed, Rio Arriba County, New Mexico	Late Sakmarian-Early Kungurian	Fragmentary material
Sphenacodon	*ferox*	UM 3031	Sphenacodontidae	Baldwin bonebed, Rio Arriba County, New Mexico	Late Sakmarian-Early Kungurian	Axis
Sphenacodon	*ferox*	UM 3588	Sphenacodontidae	Baldwin bonebed, Rio Arriba County, New Mexico	Late Sakmarian-Early Kungurian	Dorsal vertebrae
Sphenacodon	*ferocior*	MCZ 4908	Sphenacodontidae	Baldwin bonebed, Rio Arriba County, New Mexico	Late Sakmarian-Early Kungurian	5 lumbar vertebrae
Sphenacodon	*ferocior*	MCZ 4874	Sphenacodontidae	Baldwin bonebed, Rio Arriba County, New Mexico	Late Sakmarian-Early Kungurian	Dorsal ribs

Sphenacodon	*ferocior*	MCZ 6660	Sphenacodontidae	Baldwin bonebed, Rio Arriba County, New Mexico	Late Sakmarian-Early Kungurian	Loads of vertebrae and spines
Ophiacodon	*mirus*	YP 807	Ophiacodontidae	Baldwin bonebed, Rio Arriba County, New Mexico	Late Sakmarian-Early Kungurian	Incomplete dentary
Ophiacodon	*mirus*	YP 808	Ophiacodontidae	Baldwin bonebed, Rio Arriba County, New Mexico	Late Sakmarian-Early Kungurian	Maxilla
Ophiacodon	*mirus*	WM 157	Ophiacodontidae	Baldwin bonebed, Rio Arriba County, New Mexico	Late Sakmarian-Early Kungurian	Partial skeleton
Ophiacodon	*mirus*	WM 748	Ophiacodontidae	Baldwin bonebed, Rio Arriba County, New Mexico	Late Sakmarian-Early Kungurian	Shoulder girdle
Ophiacodon	*mirus*	UM 3054	Ophiacodontidae	Baldwin bonebed, Rio Arriba County, New Mexico	Late Sakmarian-Early Kungurian	Femur
Ophiacodon	*mirus*	UM 11025	Ophiacodontidae	Baldwin bonebed, Rio Arriba County, New Mexico	Late Sakmarian-Early Kungurian	Isolated bones
Dimetrodon	*limbatus*		Sphenacodontidae	Long Creek, Archer Countzy, Texas	Early Artinskian	
Oromycter	*dolesorum*	FMNH PR 2281	Caseidae	Delose Brothers	Early Artinskian	Left maxilla
Oromycter	*dolesorum*	FMNH PR 2282	Caseidae	Delose Brothers	Early Artinskian	Posterior fragment of right maxilla
Oromycter	*dolesorum*	FMNH PR 2283	Caseidae	Delose Brothers	Early Artinskian	Right premaxilla
Oromycter	*dolesorum*	FMNH PR 2284	Caseidae	Delose Brothers	Early Artinskian	Left premaxilla
Oromycter	*dolesorum*	FMNH PR 2285	Caseidae	Delose Brothers	Early Artinskian	Left lacrimal
Oromycter	*dolesorum*	FMNH PR 2286	Caseidae	Delose Brothers	Early Artinskian	Anterior left dentary
Oromycter	*dolesorum*	FMNH PR 2287	Caseidae	Delose Brothers	Early Artinskian	Posterior left dentary
Oromycter	*dolesorum*	FMNH PR 2288	Caseidae	Delose Brothers	Early Artinskian	Phalanges
Oromycter	*dolesorum*	FMNH PR 2289	Caseidae	Delose Brothers	Early Artinskian	Unguals

Oromycter	*dolesorum*	FMNH PR 2290	Caseidae	Delose Brothers	Early Artinskian	Caudal vertebra
Thrausmosaurus	*serratidens*	KUVP 11122	Sphenacodontidae (?) (Fox 1962), Varanopidae (?) (Modesto & Reisz 2008, Evans et al. 2009)	Delose Brothers	Early Artinskian	Fragment of the left dentary
Thrausmosaurus	*serratidens*	KUVP 11121	Sphenacodontidae (?) (Fox 1962), Varanopidae (?) (Modesto & Reisz 2008, Evans et al. 2009)	Delose Brothers	Early Artinskian	Maxilla
Thrausmosaurus	*serratidens*	KUVP 11120	Sphenacodontidae (?) (Fox 1962), Varanopidae (?) (Modesto & Reisz 2008, Evans et al. 2009)	Delose Brothers	Early Artinskian	Maxilla
Varanops	*brevirostris (?)*	OMNH 73156	Varanopidae	Delose Brothers	Early Artinskian	Maxilla fragment
Varanops	*brevirostris (?)*	OMNH 73157	Varanopidae	Delose Brothers	Early Artinskian	Parabasisphenoid complex
Varanops	*brevirostris (?)*	OMNH 73158	Varanopidae	Delose Brothers	Early Artinskian	Parabasisphenoid complex
Varanops	*brevirostris (?)*	OMNH 73159	Varanopidae	Delose Brothers	Early Artinskian	Axial neural arch
Varanops	*brevirostris (?)*	OMNH 73160	Varanopidae	Delose Brothers	Early Artinskian	Cervical vertebra
Varanops	*brevirostris (?)*	OMNH 73161	Varanopidae	Delose Brothers	Early Artinskian	Cervical vertebra
Varanops	*brevirostris (?)*	OMNH 73162	Varanopidae	Delose Brothers	Early Artinskian	Mid-dorsal vertebra
Varanops	*brevirostris (?)*	OMNH 73163	Varanopidae	Delose Brothers	Early Artinskian	Mid-dorsal vertebra
Varanops	*brevirostris (?)*	OMNH 73164	Varanopidae	Delose Brothers	Early Artinskian	Mid-dorsal vertebra
Varanops	*brevirostris (?)*	OMNH 73165	Varanopidae	Delose Brothers	Early Artinskian	Mid-dorsal vertebra
Varanops	*brevirostris (?)*	OMNH 73166	Varanopidae	Delose Brothers	Early Artinskian	Mid-dorsal vertebra
Varanops	*brevirostris (?)*	OMNH 73167	Varanopidae	Delose Brothers	Early Artinskian	Caudal vertebra
Varanops	*brevirostris (?)*	OMNH 73168	Varanopidae	Delose Brothers	Early Artinskian	Partial humerus
Varanops	*brevirostris (?)*	OMNH 73169	Varanopidae	Delose Brothers	Early Artinskian	Partial humerus
Varanops	*brevirostris (?)*	OMNH 73170	Varanopidae	Delose Brothers	Early Artinskian	Partial humerus
Varanops	*brevirostris (?)*	OMNH 73171	Varanopidae	Delose Brothers	Early Artinskian	Partial ulna
Varanops	*brevirostris (?)*	OMNH 73172	Varanopidae	Delose Brothers	Early Artinskian	Radius
Varanops	*brevirostris (?)*	OMNH 73173	Varanopidae	Delose Brothers	Early Artinskian	Metacarpal IV
Varanops	*brevirostris (?)*	OMNH 73174	Varanopidae	Delose Brothers	Early Artinskian	Ilium

Varanops	*brevirostris (?)*	OMNH 73175	Varanopidae	Delose Brothers	Early Artinskian	Tibia
Varanops	*brevirostris (?)*	OMNH 73176	Varanopidae	Delose Brothers	Early Artinskian	Tibia
Varanops	*brevirostris (?)*	OMNH 73177	Varanopidae	Delose Brothers	Early Artinskian	Sacral rib
Varanops	*brevirostris (?)*	OMNH 73178	Varanopidae	Delose Brothers	Early Artinskian	Metatarsal
Basicranodon	*fortsillensis*	USNM 21859	Varanopidae	Delose Brothers	Early Artinskian	Parasphenoid-basisphenoid complex
Edaphosaurus	*cruciger*		Edaphosauridae	Long Creek, Archer Countzy, Texas	Early Artinskian	
Ophiacodon	*retroversus*	AM 4377	Ophiacodontidae	Three Forks of Little Wichita, Archer County, Texas	Early Artinskian	Associated elements
Dimetrodon	*natalis*	MCZ 1476	Sphenacodontidae	Three Forks of Little Wichita, Archer County, Texas	Early Artinskian	Manus, radius, ulna
Dimetrodon	*natalis*	MCZ 1631	Sphenacodontidae	Three Forks of Little Wichita, Archer County, Texas	Early Artinskian	Cervical vertebrae
Dimetrodon	*limbatus*	AM 4123	Sphenacodontidae	Three Forks of Little Wichita, Archer County, Texas	Early Artinskian	Femur
Dimetrodon	*limbatus*	AM 4125	Sphenacodontidae	Three Forks of Little Wichita, Archer County, Texas	Early Artinskian	Incomplete tibia, fibulae and fragments
Dimetrodon	*limbatus*	AM 4116	Sphenacodontidae	Three Forks of Little Wichita, Archer County, Texas	Early Artinskian	Maxilla, roofing bones of skull
Dimetrodon	*dollovianus*	AM 4057	Sphenacodontidae	Elm Creek, Archer County, Texas	Early Artinskian	Astragulus, Neural spine
Ophiacodon	*major*	AM 4056	Ophiacodontidae	Elm Creek, Archer County, Texas	Early Artinskian	Ilium and vertebrae
Dimetrodon	*milleri*	AMNH 4290	Sphenacodontidae	Fireplace, few miles southwest of Archer City, Archer County, Texas	Early Artinskian	Humerus

Dimetrodon	*natalis*	MCZ 1386	Sphenacodontidae	Table Branch, western headwaters of the South Fork, Souther Archer County, Texas	Early Artinskian	Fragments
Dimetrodon	*milleri*	MCZ 1367	Sphenacodontidae	Table Branch, western headwaters of the South Fork, Souther Archer County, Texas	Early Artinskian	Parts of a skull, coulumn, shoulder girdle
Dimetrodon	*milleri*	MCZ 1374	Sphenacodontidae	Table Branch, western headwaters of the South Fork, Souther Archer County, Texas	Early Artinskian	Fragments of skull, jaw and vertebrae
Edaphosaurus	*boanerges*	MCZ 1372	Edaphosauridae	Table Branch, western headwaters of the South Fork, Souther Archer County, Texas	Early Artinskian	Posterior trunk, sacral and proximal caudal vertebrae and spines
Edaphosaurus	*boanerges*	MCZ 1370	Edaphosauridae	Table Branch, western headwaters of the South Fork, Souther Archer County, Texas	Early Artinskian	Lower jaw
Edaphosaurus	*boanerges*	MCZ 1629	Edaphosauridae	West of Anarene, east of the South Fork, Southern Archer County, Texas	Early Artinskian	Jaw
Ophiacodon	*hilli*	FMNH 454	Ophiacodontidae	Wildcat Canyon, near Winfield, Cowley County, Kansas	Early Artinskian	Nearly complete skeleton
Dimetrodon	*limbatus (?)*	CMNH (?)	Sphenacodontidae	Caballo Mountains Locality, Sierra County, New Mexico	Artinskian	
Ophiacodon	*uniformis*	MCZ 7787	Ophiacodontidae	Geraldine Bonebed, North of Archer City, Archer County, Texas	Artinskian	Astragulus

Ophiacodon	*retroversus*	AM 4195	Ophiacodontidae	Geraldine Bonebed, North of Archer City, Archer County, Texas	Artinskian	Astragulus
Dimetrodon	*natalis*	MCZ 1630	Sphenacodontidae	Geraldine Bonebed, North of Archer City, Archer County, Texas	Artinskian	Neural spine material
Dimetrodon	*natalis*	MCZ 1303	Sphenacodontidae	Geraldine Bonebed, North of Archer City, Archer County, Texas	Artinskian	Fibula
Dimetrodon	*natalis*	MCZ 1630	Sphenacodontidae	Geraldine Bonebed, North of Archer City, Archer County, Texas	Artinskian	Fragments of neural spine
Dimetrodon	*natalis*	MCZ 1756	Sphenacodontidae	Geraldine Bonebed, North of Archer City, Archer County, Texas	Artinskian	
Dimetrodon	*natalis*	MCZ 3429	Sphenacodontidae	Geraldine Bonebed, North of Archer City, Archer County, Texas	Artinskian	
Dimetrodon	*natalis*	MCZ 5530-5555	Sphenacodontidae	Geraldine Bonebed, North of Archer City, Archer County, Texas	Artinskian	
Dimetrodon	*natalis*	MCZ 5631	Sphenacodontidae	Geraldine Bonebed, North of Archer City, Archer County, Texas	Artinskian	
Dimetrodon	*natalis*	MCZ 5632	Sphenacodontidae	Geraldine Bonebed, North of Archer City, Archer County, Texas	Artinskian	
Dimetrodon	*natalis*	MCZ 5633	Sphenacodontidae	Geraldine Bonebed, North of Archer City, Archer County, Texas	Artinskian	

Dimetrodon	*natalis*	MCZ 5864	Sphenacodontidae	Geraldine Bonebed, North of Archer City, Archer County, Texas	Artinskian	
Dimetrodon	*natalis*	MCZ 7724	Sphenacodontidae	Geraldine Bonebed, North of Archer City, Archer County, Texas	Artinskian	
Dimetrodon	*limbatus*	AM 1891	Sphenacodontidae	Geraldine Bonebed, North of Archer City, Archer County, Texas	Artinskian	Part of femur, tibia, vertebrae
Dimetrodon	*limbatus*	MCZ 1908	Sphenacodontidae	Geraldine Bonebed, North of Archer City, Archer County, Texas	Artinskian	Complete lower jaw and teeth, humerus, 11 dorsal vertebrae with spines, neural spine fragments, 8 caudal vertebrae, 1 metapodial, Scapula blade, clavicle shaft, maxilla and teeth
Dimetrodon	*limbatus*	AM 4165	Sphenacodontidae	Geraldine Bonebed, North of Archer City, Archer County, Texas	Artinskian	Pelvis
Dimetrodon	*limbatus*	AM 1891	Sphenacodontidae	Geraldine Bonebed, North of Archer City, Archer County, Texas	Artinskian	Femur
Dimetrodon	*limbatus*	AM 4040	Sphenacodontidae	Geraldine Bonebed, North of Archer City, Archer County, Texas	Artinskian	Fragments of skull and jaw, most of the vertebral collumn
Dimetrodon	*limbatus*	AM 4195	Sphenacodontidae	Geraldine Bonebed, North of Archer City, Archer County, Texas	Artinskian	Vertebrae, humerus, partial humerus and femur
Dimetrodon	*limbatus*	AM 1879	Sphenacodontidae	Geraldine Bonebed, North of Archer City, Archer County, Texas	Artinskian	Femur
Dimetrodon	*limbatus*	AM 4165	Sphenacodontidae	Geraldine Bonebed, North of Archer City, Archer County, Texas	Artinskian	Femur

Dimetrodon	*limbatus*	AM 4039	Sphenacodontidae	Geraldine Bonebed, North of Archer City, Archer County, Texas	Artinskian	Pelvis, sacral and caudal vertebrae, humerus and femur
Dimetrodon	*limbatus*	NM 6723	Sphenacodontidae	Geraldine Bonebed, North of Archer City, Archer County, Texas	Artinskian	Most of a skeleton
Dimetrodon	*limbatus*		Sphenacodontidae	Geraldine Bonebed, North of Archer City, Archer County, Texas	Artinskian	Neural spines
Edaphosaurus	*boanerges*	MCZ 1531	Edaphosauridae	Geraldine Bonebed, North of Archer City, Archer County, Texas	Artinskian	6 individuals, assembled into mounted skeletons at Harvard, Oklahoma and Chicargo
Edaphosaurus	*boanerges*	AMNH 7003	Edaphosauridae	Geraldine Bonebed, North of Archer City, Archer County, Texas	Artinskian	14 speciemens
Dimetrodon	*limbatus*		Sphenacodontidae	Coprolite Bonebed, North of Archer City, Archer County, Texas	Artinskian	Vertebrae
Lupeosaurus (?)	*kayi (?)*		Edaphosauridae	Coprolite Bonebed, North of Archer City, Archer County, Texas	Artinskian	Proximal ulna
Edaphosaurus	*boanerges*		Edaphosauridae	Coprolite Bonebed, North of Archer City, Archer County, Texas	Artinskian	Neural spines
Lupeosaurus	*kayi*	UCLA VP 1651	Edaphosauridae	Lake Kickapoo, Archer County, Texas	Artinskian	Cervical and dorsal vertebrae, first sacral, head of a rib, clavicle, scapulocoracoid
Ctenorhachis	*jacksoni*	USNM 437711	Sphenacodontidae	Lake Kickapoo, Archer County, Texas	Artinskian	12 articulated dorsal vertebrae, 2 more dorsal vertebrae, 2 cervical vertebrae, interclavicle fragment, rib fragment
Secodontosaurus	*obtusidens*	MCZ 2749	Sphenacodontidae	South side of Godwin Creek at the mouth, Archer County, Texas	Artinskian	Distal dentary fragment with teeth, dorsal spine and rib fragments, 13 centra, radius

Dimetrodon	*natalis*	MCZ 1632	Sphenacodontidae	South side of Godwin Creek at the mouth, Archer County, Texas	Artinskian	Fragments of skull and jaw, 2 cervicals
Dimetrodon	*booneorum*	AM 4826	Sphenacodontidae	South side of Godwin Creek at the mouth, Archer County, Texas	Artinskian	Articular, vertebrae and spines
Dimetrodon	*booneorum*	AM 4835	Sphenacodontidae	South side of Godwin Creek at the mouth, Archer County, Texas	Artinskian	Femur, tibia, partial humerus
Dimetrodon	*limbatus*	AM 4636	Sphenacodontidae	South side of Godwin Creek at the mouth, Archer County, Texas	Artinskian	Mounted skeletn
Dimetrodon	*limbatus*	AM 4890	Sphenacodontidae	South side of Godwin Creek at the mouth, Archer County, Texas	Artinskian	Humerus
Dimetrodon	*limbatus*	WM 1178	Sphenacodontidae	South side of Godwin Creek at the mouth, Archer County, Texas	Artinskian	Jaw, Palatine
Dimetrodon	*limbatus*	AM 46722	Sphenacodontidae	South side of Godwin Creek at the mouth, Archer County, Texas	Artinskian	Femur
Dimetrodon	*limbatus*	AM 4619	Sphenacodontidae	South side of Godwin Creek at the mouth, Archer County, Texas	Artinskian	Femur
Dimetrodon	*limbatus*	MCZ 1347	Sphenacodontidae	South side of Godwin Creek at the mouth, Archer County, Texas	Artinskian	Mounted skeleton
Dimetrodon	*limbatus*	WM 1178	Sphenacodontidae	South side of Godwin Creek at the mouth, Archer County, Texas	Artinskian	Jaw fragments, clavicle, other fragments

Dimetrodon	*limbatus*	WM 804	Sphenacodontidae	South side of Godwin Creek at the mouth, Archer County, Texas	Artinskian	Dentary
Dimetrodon	*limbatus*	AM 4622	Sphenacodontidae	South side of Godwin Creek at the mouth, Archer County, Texas	Artinskian	Femur
Dimetrodon	*limbatus*	AM 4826	Sphenacodontidae	South side of Godwin Creek at the mouth, Archer County, Texas	Artinskian	Vertebrae
Dimetrodon	*limbatus*	AM 4883	Sphenacodontidae	South side of Godwin Creek at the mouth, Archer County, Texas	Artinskian	Humerus
Dimetrodon	*limbatus*	AM 4829	Sphenacodontidae	South side of Godwin Creek at the mouth, Archer County, Texas	Artinskian	Pelvis
Ophiacodon	*uniformis*	MCZ 1435	Ophiacodontidae	South side of Godwin Creek at the mouth, Archer County, Texas	Artinskian	Partial skeleton
Ophiacodon	*retroversus*	WM 459	Ophiacodontidae	South side of Godwin Creek at the mouth, Archer County, Texas	Artinskian	Fragmentary skeleton
Ophiacodon	*retroversus*	AM 4620	Ophiacodontidae	South side of Godwin Creek at the mouth, Archer County, Texas	Artinskian	Partial vertebral column
Ophiacodon	*retroversus*	MCZ 1561	Ophiacodontidae	South side of Godwin Creek at the mouth, Archer County, Texas	Artinskian	Several bones
Ophiacodon	*retroversus*	MCZ 1451	Ophiacodontidae	South side of Godwin Creek at the mouth, Archer County, Texas	Artinskian	Several bones

Ophiacodon	*retroversus*	AM 4826	Ophiacodontidae	South side of Godwin Creek at the mouth, Archer County, Texas	Artinskian	Fibula
Varanosaurus	*witchitaensis*	MCZ 5845	Ophiacodontidae	Black Flat, Archer County, Texas	Artinskian	Vertebra
Ophiacodon	*retroversus*	AM 4106	Ophiacodontidae	Middle Fork of the Little Wichita, Archer County, Texas	Artinskian	Associated elements
Dimetrodon	*booneorum*	WM 212	Sphenacodontidae	Middle Fork of the Little Wichita, Archer County, Texas	Artinskian	Femur
Dimetrodon	*booneorum*	WM 202	Sphenacodontidae	Middle Fork of the Little Wichita, Archer County, Texas	Artinskian	Femur
Dimetrodon	*booneorum*	MCZ 1315	Sphenacodontidae	Middle Fork of the Little Wichita, Archer County, Texas	Artinskian	Femur
Dimetrodon	*limbatus*	MCZ 1332	Sphenacodontidae	Middle Fork of the Little Wichita, Archer County, Texas	Artinskian	Femur
Dimetrodon	*limbatus*	MCZ 1319	Sphenacodontidae	Middle Fork of the Little Wichita, Archer County, Texas	Artinskian	Ulnae and pubis
Secodontosaurus	*obtusidens*	AMNH 4007	Sphenacodontidae	Mount Barry, 10 miles west of Wichita Falls, Wichita County, Texas	Artinskian	Partial jaws and occiput
Secodontosaurus	*obtusidens*	AMNH 4021	Sphenacodontidae	Mount Barry, 10 miles west of Wichita Falls, Wichita County, Texas	Artinskian	Maxilla
Lupeosaurus (?)	*kayi (?)*	AMNH 1764	Edaphosauridae	Mount Barry, 10 miles west of Wichita Falls, Wichita County, Texas	Artinskian	Humerus

Ophiacodon	*retroversus*	AMNH 4167	Ophiacodontidae	Mount Barry, 10 miles west of Wichita Falls, Wichita County, Texas	Artinskian	Several isolated vertebrae (dorsal and cervical region)
Ophiacodon	*retroversus*	AM 4026	Ophiacodontidae	Mount Barry, 10 miles west of Wichita Falls, Wichita County, Texas	Artinskian	many bones
Ophiacodon	*retroversus*	AMNH 4166	Ophiacodontidae	Mount Barry, 10 miles west of Wichita Falls, Wichita County, Texas	Artinskian	Vertebrae
Ophiacodon	*retroversus*	AM 4007	Ophiacodontidae	Mount Barry, 10 miles west of Wichita Falls, Wichita County, Texas	Artinskian	many bones
Dimetrodon	*natalis*	AMNH 4110	Sphenacodontidae	Mount Barry, 10 miles west of Wichita Falls, Wichita County, Texas	Artinskian	Crushed skull and other material
Dimetrodon	*limbatus*	AM 4013	Sphenacodontidae	Mount Barry, 10 miles west of Wichita Falls, Wichita County, Texas	Artinskian	Vertebrae
Dimetrodon	*limbatus*	AM 4131	Sphenacodontidae	Mount Barry, 10 miles west of Wichita Falls, Wichita County, Texas	Artinskian	Scapulocoracoid
Dimetrodon	*limbatus*	AM 4026	Sphenacodontidae	Mount Barry, 10 miles west of Wichita Falls, Wichita County, Texas	Artinskian	Vertebrae
Secodontosaurus	*obtusidens*	MCZ 5134	Sphenacodontidae	Briar Creek, Archer County, Texas	Artinskian	Pterygoid, teeth and neural spine
Secodontosaurus	*obtusidens*	MCZ 6382	Sphenacodontidae	Briar Creek, Archer County, Texas	Artinskian	Maxilla fragments and teeth
Secodontosaurus	*obtusidens*	MCZ 6383	Sphenacodontidae	Briar Creek, Archer County, Texas	Artinskian	Distal mandible, dentary and teeth
Secodontosaurus	*obtusidens*	MCZ 6384	Sphenacodontidae	Briar Creek, Archer County, Texas	Artinskian	Maxilla fragments and teeth

Secodontosaurus	*obtusidens*	MCZ 6998	Sphenacodontidae	Briar Creek, Archer County, Texas	Artinskian	Pterygoids and teeth
Secodontosaurus	*obtusidens*	UM 3059	Sphenacodontidae	Briar Creek, Archer County, Texas	Artinskian	Scapulocoracoid
Secodontosaurus	*obtusidens*	UM 9714	Sphenacodontidae	Briar Creek, Archer County, Texas	Artinskian	Two maxillae
Secodontosaurus	*obtusidens*	UM 9698	Sphenacodontidae	Briar Creek, Archer County, Texas	Artinskian	Pterygoid
Dimetrodon	*natalis*	UM 9712	Sphenacodontidae	Briar Creek, Archer County, Texas	Artinskian	Maxilla
Dimetrodon	*natalis*	WM 542	Sphenacodontidae	Briar Creek, Archer County, Texas	Artinskian	Dentary
Dimetrodon	*natalis*	UM 9732	Sphenacodontidae	Briar Creek, Archer County, Texas	Artinskian	Dentary
Dimetrodon	*natalis*	UM 9668	Sphenacodontidae	Briar Creek, Archer County, Texas	Artinskian	Axis
Dimetrodon	*natalis*	UM 9669	Sphenacodontidae	Briar Creek, Archer County, Texas	Artinskian	Axis
Dimetrodon	*natalis*	UM 9670	Sphenacodontidae	Briar Creek, Archer County, Texas	Artinskian	Axis
Dimetrodon	*natalis*	UM 9671	Sphenacodontidae	Briar Creek, Archer County, Texas	Artinskian	Axis
Dimetrodon	*natalis*	UM 3357	Sphenacodontidae	Briar Creek, Archer County, Texas	Artinskian	Axis
Dimetrodon	*natalis*	MCZ 1632	Sphenacodontidae	Briar Creek, Archer County, Texas	Artinskian	Cervical vertebra
Dimetrodon	*natalis*	UM 3678	Sphenacodontidae	Briar Creek, Archer County, Texas	Artinskian	Dorsal vertebra
Dimetrodon	*natalis*	UM 9677	Sphenacodontidae	Briar Creek, Archer County, Texas	Artinskian	Dorsal vertebra
Dimetrodon	*natalis*	UM 16201	Sphenacodontidae	Briar Creek, Archer County, Texas	Artinskian	Dorsal vertebra

Dimetrodon	*natalis*	WM 783	Sphenacodontidae	Briar Creek, Archer County, Texas	Artinskian	neural spine material
Dimetrodon	*natalis*	WM 822	Sphenacodontidae	Briar Creek, Archer County, Texas	Artinskian	Tibiae, radius
Dimetrodon	*natalis*	WM 515	Sphenacodontidae	Briar Creek, Archer County, Texas	Artinskian	Clavicle
Dimetrodon	*natalis*	UM 9757	Sphenacodontidae	Briar Creek, Archer County, Texas	Artinskian	Clavicle
Dimetrodon	*natalis*	MCZ 1305	Sphenacodontidae	Briar Creek, Archer County, Texas	Artinskian	Clavicle
Dimetrodon	*natalis*	UM 3135	Sphenacodontidae	Briar Creek, Archer County, Texas	Artinskian	Scapulocoracoid
Dimetrodon	*natalis*	WM 550	Sphenacodontidae	Briar Creek, Archer County, Texas	Artinskian	Scapulocoracoid
Dimetrodon	*natalis*	WM 825	Sphenacodontidae	Briar Creek, Archer County, Texas	Artinskian	Scapulocoracoid
Dimetrodon	*natalis*	WM 561	Sphenacodontidae	Briar Creek, Archer County, Texas	Artinskian	Scapulocoracoid
Dimetrodon	*natalis*	MCZ 1309	Sphenacodontidae	Briar Creek, Archer County, Texas	Artinskian	Scapulocoracoid
Dimetrodon	*natalis*	MCZ 1330	Sphenacodontidae	Briar Creek, Archer County, Texas	Artinskian	Scapulocoracoid
Dimetrodon	*natalis*	MCZ 1356	Sphenacodontidae	Briar Creek, Archer County, Texas	Artinskian	Scapulocoracoid
Dimetrodon	*natalis*	MCZ 1308	Sphenacodontidae	Briar Creek, Archer County, Texas	Artinskian	Humerus
Dimetrodon	*natalis*	WM 802	Sphenacodontidae	Briar Creek, Archer County, Texas	Artinskian	Humerus
Dimetrodon	*natalis*	WM 248	Sphenacodontidae	Briar Creek, Archer County, Texas	Artinskian	Humerus
Dimetrodon	*natalis*	WM 682	Sphenacodontidae	Briar Creek, Archer County, Texas	Artinskian	Humerus

Dimetrodon	*natalis*	WM 531	Sphenacodontidae	Briar Creek, Archer County, Texas	Artinskian	Humerus
Dimetrodon	*natalis*	WM 545	Sphenacodontidae	Briar Creek, Archer County, Texas	Artinskian	Humerus
Dimetrodon	*natalis*	WM 816	Sphenacodontidae	Briar Creek, Archer County, Texas	Artinskian	Humerus
Dimetrodon	*natalis*	WM 549	Sphenacodontidae	Briar Creek, Archer County, Texas	Artinskian	Humerus
Dimetrodon	*natalis*	UM 9744	Sphenacodontidae	Briar Creek, Archer County, Texas	Artinskian	Humerus
Dimetrodon	*natalis*	UM 3367	Sphenacodontidae	Briar Creek, Archer County, Texas	Artinskian	Humerus
Dimetrodon	*natalis*	UM 3363	Sphenacodontidae	Briar Creek, Archer County, Texas	Artinskian	Humerus
Dimetrodon	*natalis*	UM 3360	Sphenacodontidae	Briar Creek, Archer County, Texas	Artinskian	Humerus
Dimetrodon	*natalis*	UM 3359	Sphenacodontidae	Briar Creek, Archer County, Texas	Artinskian	Humerus
Dimetrodon	*natalis*	WM 79	Sphenacodontidae	Briar Creek, Archer County, Texas	Artinskian	Humerus
Dimetrodon	*natalis*	WM 538	Sphenacodontidae	Briar Creek, Archer County, Texas	Artinskian	Humerus
Dimetrodon	*natalis*	WM 856	Sphenacodontidae	Briar Creek, Archer County, Texas	Artinskian	Humerus
Dimetrodon	*natalis*	WM 683	Sphenacodontidae	Briar Creek, Archer County, Texas	Artinskian	Radius
Dimetrodon	*natalis*	WM 53	Sphenacodontidae	Briar Creek, Archer County, Texas	Artinskian	Radius
Dimetrodon	*natalis*	WM 518	Sphenacodontidae	Briar Creek, Archer County, Texas	Artinskian	Radius
Dimetrodon	*natalis*	WM 819	Sphenacodontidae	Briar Creek, Archer County, Texas	Artinskian	Radius

Dimetrodon	*natalis*	UM 3348	Sphenacodontidae	Briar Creek, Archer County, Texas	Artinskian	Radius
Dimetrodon	*natalis*	WM 108	Sphenacodontidae	Briar Creek, Archer County, Texas	Artinskian	Ulna
Dimetrodon	*natalis*	WM 110	Sphenacodontidae	Briar Creek, Archer County, Texas	Artinskian	Ulna
Dimetrodon	*natalis*	UM 3369	Sphenacodontidae	Briar Creek, Archer County, Texas	Artinskian	Ulna
Dimetrodon	*natalis*	MCZ 1311	Sphenacodontidae	Briar Creek, Archer County, Texas	Artinskian	Ulna
Dimetrodon	*natalis*	WM 834	Sphenacodontidae	Briar Creek, Archer County, Texas	Artinskian	Pelvis
Dimetrodon	*natalis*	WM 881	Sphenacodontidae	Briar Creek, Archer County, Texas	Artinskian	Pelvis
Dimetrodon	*natalis*	WM 557	Sphenacodontidae	Briar Creek, Archer County, Texas	Artinskian	Pelvis
Dimetrodon	*natalis*	WM 823	Sphenacodontidae	Briar Creek, Archer County, Texas	Artinskian	Femur
Dimetrodon	*natalis*	WM 523	Sphenacodontidae	Briar Creek, Archer County, Texas	Artinskian	Femur
Dimetrodon	*natalis*	WM 510	Sphenacodontidae	Briar Creek, Archer County, Texas	Artinskian	Femur
Dimetrodon	*natalis*	WM 58	Sphenacodontidae	Briar Creek, Archer County, Texas	Artinskian	Femur
Dimetrodon	*natalis*	WM 243	Sphenacodontidae	Briar Creek, Archer County, Texas	Artinskian	Femur
Dimetrodon	*natalis*	WM 244	Sphenacodontidae	Briar Creek, Archer County, Texas	Artinskian	Femur
Dimetrodon	*natalis*	WM 245	Sphenacodontidae	Briar Creek, Archer County, Texas	Artinskian	Femur
Dimetrodon	*natalis*	MCZ 1326	Sphenacodontidae	Briar Creek, Archer County, Texas	Artinskian	Femur

Dimetrodon	*natalis*	UM 3389	Sphenacodontidae	Briar Creek, Archer County, Texas	Artinskian	Femur
Dimetrodon	*natalis*	WM 3399	Sphenacodontidae	Briar Creek, Archer County, Texas	Artinskian	Femur
Dimetrodon	*natalis*	WM 525	Sphenacodontidae	Briar Creek, Archer County, Texas	Artinskian	Tibia
Dimetrodon	*natalis*	WM 821	Sphenacodontidae	Briar Creek, Archer County, Texas	Artinskian	Tibia
Dimetrodon	*natalis*	WM 513	Sphenacodontidae	Briar Creek, Archer County, Texas	Artinskian	Tibia
Dimetrodon	*natalis*	MCZ 1322	Sphenacodontidae	Briar Creek, Archer County, Texas	Artinskian	Tibia
Dimetrodon	*natalis*	UM 3353	Sphenacodontidae	Briar Creek, Archer County, Texas	Artinskian	Tibia
Dimetrodon	*natalis*	UM 3377	Sphenacodontidae	Briar Creek, Archer County, Texas	Artinskian	Tibia
Dimetrodon	*natalis*	UM 3365	Sphenacodontidae	Briar Creek, Archer County, Texas	Artinskian	Tibia
Dimetrodon	*natalis*	UM 3376	Sphenacodontidae	Briar Creek, Archer County, Texas	Artinskian	Fibula
Dimetrodon	*natalis*	MCZ 1301	Sphenacodontidae	Briar Creek, Archer County, Texas	Artinskian	Fibula
Dimetrodon	*booneorum*	WM 536	Sphenacodontidae	Briar Creek, Archer County, Texas	Artinskian	Maxilla
Dimetrodon	*booneorum*	WM 812	Sphenacodontidae	Briar Creek, Archer County, Texas	Artinskian	Maxilla
Dimetrodon	*booneorum*	WM 542	Sphenacodontidae	Briar Creek, Archer County, Texas	Artinskian	Dentary
Dimetrodon	*booneorum*	WM 598	Sphenacodontidae	Briar Creek, Archer County, Texas	Artinskian	Dentary
Dimetrodon	*booneorum*	UM 9666	Sphenacodontidae	Briar Creek, Archer County, Texas	Artinskian	Axis

Dimetrodon	*booneorum*	UM 9667	Sphenacodontidae	Briar Creek, Archer County, Texas	Artinskian	Axis
Dimetrodon	*booneorum*	UM 3356	Sphenacodontidae	Briar Creek, Archer County, Texas	Artinskian	Axis
Dimetrodon	*booneorum*	UM 16201	Sphenacodontidae	Briar Creek, Archer County, Texas	Artinskian	Posterior thoracic vertebrae
Dimetrodon	*booneorum*	UM 16145	Sphenacodontidae	Briar Creek, Archer County, Texas	Artinskian	Posterior thoracic vertebrae
Dimetrodon	*booneorum*	UM 3372	Sphenacodontidae	Briar Creek, Archer County, Texas	Artinskian	Vertebra with spine
Dimetrodon	*booneorum*	UM 9679	Sphenacodontidae	Briar Creek, Archer County, Texas	Artinskian	Sacral vertebra
Dimetrodon	*booneorum*	WM 1178	Sphenacodontidae	Briar Creek, Archer County, Texas	Artinskian	Clavicle
Dimetrodon	*booneorum*	UM 3368	Sphenacodontidae	Briar Creek, Archer County, Texas	Artinskian	Interclavicle
Dimetrodon	*booneorum*	WM 553	Sphenacodontidae	Briar Creek, Archer County, Texas	Artinskian	Interclavicle
Dimetrodon	*booneorum*	WM 635	Sphenacodontidae	Briar Creek, Archer County, Texas	Artinskian	Interclavicle
Dimetrodon	*booneorum*	UM 3139	Sphenacodontidae	Briar Creek, Archer County, Texas	Artinskian	Scapulocoracoid
Dimetrodon	*booneorum*	UM 3120	Sphenacodontidae	Briar Creek, Archer County, Texas	Artinskian	Scapulocoracoid
Dimetrodon	*booneorum*	WM 561	Sphenacodontidae	Briar Creek, Archer County, Texas	Artinskian	Scapulocoracoid
Dimetrodon	*booneorum*	WM 845	Sphenacodontidae	Briar Creek, Archer County, Texas	Artinskian	Scapulocoracoid
Dimetrodon	*booneorum*	MCZ 1316	Sphenacodontidae	Briar Creek, Archer County, Texas	Artinskian	Scapulocoracoid
Dimetrodon	*booneorum*	UM 3368	Sphenacodontidae	Briar Creek, Archer County, Texas	Artinskian	Pelvis

Dimetrodon	*booneorum*	UM 9165	Sphenacodontidae	Briar Creek, Archer County, Texas	Artinskian	Humerus
Dimetrodon	*booneorum*	WM 844	Sphenacodontidae	Briar Creek, Archer County, Texas	Artinskian	Humerus
Dimetrodon	*booneorum*	WM 816	Sphenacodontidae	Briar Creek, Archer County, Texas	Artinskian	Humerus
Dimetrodon	*booneorum*	MCZ 1307	Sphenacodontidae	Briar Creek, Archer County, Texas	Artinskian	Radius
Dimetrodon	*booneorum*	WM 819	Sphenacodontidae	Briar Creek, Archer County, Texas	Artinskian	Radius
Dimetrodon	*booneorum*	WM 821	Sphenacodontidae	Briar Creek, Archer County, Texas	Artinskian	Ulna
Dimetrodon	*booneorum*	MCZ 1306	Sphenacodontidae	Briar Creek, Archer County, Texas	Artinskian	Ulna
Dimetrodon	*booneorum*	MCZ 1318	Sphenacodontidae	Briar Creek, Archer County, Texas	Artinskian	Ulna
Dimetrodon	*booneorum*	WM 819	Sphenacodontidae	Briar Creek, Archer County, Texas	Artinskian	Ulna
Dimetrodon	*booneorum*	WM 835	Sphenacodontidae	Briar Creek, Archer County, Texas	Artinskian	Femur
Dimetrodon	*booneorum*	WM 91	Sphenacodontidae	Briar Creek, Archer County, Texas	Artinskian	Femur
Dimetrodon	*booneorum*	WM 131	Sphenacodontidae	Briar Creek, Archer County, Texas	Artinskian	Femur
Dimetrodon	*booneorum*	WM 120	Sphenacodontidae	Briar Creek, Archer County, Texas	Artinskian	Femur
Dimetrodon	*booneorum*	MCZ 1310	Sphenacodontidae	Briar Creek, Archer County, Texas	Artinskian	Femur
Dimetrodon	*booneorum*	UM 3398	Sphenacodontidae	Briar Creek, Archer County, Texas	Artinskian	Femur
Dimetrodon	*booneorum*	UM 3393	Sphenacodontidae	Briar Creek, Archer County, Texas	Artinskian	Femur

Dimetrodon	*booneorum*	WM 61	Sphenacodontidae	Briar Creek, Archer County, Texas	Artinskian	Tibia
Dimetrodon	*booneorum*	WM 126	Sphenacodontidae	Briar Creek, Archer County, Texas	Artinskian	Tibia
Dimetrodon	*booneorum*	WM 514	Sphenacodontidae	Briar Creek, Archer County, Texas	Artinskian	Tibia
Dimetrodon	*booneorum*	WM 68	Sphenacodontidae	Briar Creek, Archer County, Texas	Artinskian	Fibula
Dimetrodon	*limbatus*	WM 841	Sphenacodontidae	Briar Creek, Archer County, Texas	Artinskian	Humerus
Dimetrodon	*limbatus*	NM 6722	Sphenacodontidae	Briar Creek, Archer County, Texas	Artinskian	Skull fragments, jaw, humerus
Dimetrodon	*limbatus*	UM Ivd	Sphenacodontidae	Briar Creek, Archer County, Texas	Artinskian	Mounted skeleton, skull prossibly from different indevidual
Dimetrodon	*limbatus*	WM 460	Sphenacodontidae	Briar Creek, Archer County, Texas	Artinskian	Radius
Dimetrodon	*limbatus*	WM 819	Sphenacodontidae	Briar Creek, Archer County, Texas	Artinskian	Radius
Dimetrodon	*limbatus*	WM 857	Sphenacodontidae	Briar Creek, Archer County, Texas	Artinskian	Femur
Dimetrodon	*limbatus*	UM 9383	Sphenacodontidae	Briar Creek, Archer County, Texas	Artinskian	Femur
Dimetrodon	*limbatus*	WM 819	Sphenacodontidae	Briar Creek, Archer County, Texas	Artinskian	Radius and ulna
Dimetrodon	*limbatus*	WM 850	Sphenacodontidae	Briar Creek, Archer County, Texas	Artinskian	Clavicle
Dimetrodon	*limbatus*	WM 882	Sphenacodontidae	Briar Creek, Archer County, Texas	Artinskian	Scapulocoracoid
Dimetrodon	*limbatus*	WM 874	Sphenacodontidae	Briar Creek, Archer County, Texas	Artinskian	Scapulocoracoid
Dimetrodon	*limbatus*	WM 559	Sphenacodontidae	Briar Creek, Archer County, Texas	Artinskian	Scapulocoracoid

Dimetrodon	*limbatus*	UM 3035	Sphenacodontidae	Briar Creek, Archer County, Texas	Artinskian	Scapulocoracoid
Dimetrodon	*limbatus*	WM 843	Sphenacodontidae	Briar Creek, Archer County, Texas	Artinskian	Humerus
Dimetrodon	*limbatus*	MCZ 1395	Sphenacodontidae	Briar Creek, Archer County, Texas	Artinskian	Humerus
Dimetrodon	*limbatus*	MCZ 1338	Sphenacodontidae	Briar Creek, Archer County, Texas	Artinskian	Humerus
Dimetrodon	*limbatus*	WM 841	Sphenacodontidae	Briar Creek, Archer County, Texas	Artinskian	Humerus
Dimetrodon	*limbatus*	WM 862	Sphenacodontidae	Briar Creek, Archer County, Texas	Artinskian	Pelvis
Dimetrodon	*limbatus*	WM 876	Sphenacodontidae	Briar Creek, Archer County, Texas	Artinskian	Pelvis
Dimetrodon	*limbatus*	WM 847	Sphenacodontidae	Briar Creek, Archer County, Texas	Artinskian	Pelvis
Dimetrodon	*limbatus*	WM 879	Sphenacodontidae	Briar Creek, Archer County, Texas	Artinskian	Pelvis
Dimetrodon	*limbatus*	WM 872	Sphenacodontidae	Briar Creek, Archer County, Texas	Artinskian	Pelvis
Dimetrodon	*limbatus*	WM 520	Sphenacodontidae	Briar Creek, Archer County, Texas	Artinskian	Pelvis
Dimetrodon	*limbatus*	WM 857	Sphenacodontidae	Briar Creek, Archer County, Texas	Artinskian	Femur
Dimetrodon	*limbatus*	WM 815	Sphenacodontidae	Briar Creek, Archer County, Texas	Artinskian	Tibia
Dimetrodon	*limbatus*	UM 9766	Sphenacodontidae	Briar Creek, Archer County, Texas	Artinskian	Tibia
Dimetrodon	*limbatus*	UM 3046	Sphenacodontidae	Briar Creek, Archer County, Texas	Artinskian	Tibia
Dimetrodon	*limbatus*	WM 821	Sphenacodontidae	Briar Creek, Archer County, Texas	Artinskian	Fibula

Dimetrodon	*limbatus*	UM 9767	Sphenacodontidae	Briar Creek, Archer County, Texas	Artinskian	Fibula
Dimetrodon	*limbatus*	UM 3349	Sphenacodontidae	Briar Creek, Archer County, Texas	Artinskian	Fibula
Dimetrodon	*limbatus*	UM 3750	Sphenacodontidae	Briar Creek, Archer County, Texas	Artinskian	Isolated skull elements
Dimetrodon	*limbatus*	UM 9689	Sphenacodontidae	Briar Creek, Archer County, Texas	Artinskian	Isolated skull elements
Dimetrodon	*limbatus*	UM 9690	Sphenacodontidae	Briar Creek, Archer County, Texas	Artinskian	Isolated skull elements
Dimetrodon	*limbatus*	UM 9691	Sphenacodontidae	Briar Creek, Archer County, Texas	Artinskian	Isolated skull elements
Dimetrodon	*limbatus*	UM 9692	Sphenacodontidae	Briar Creek, Archer County, Texas	Artinskian	Isolated skull elements
Dimetrodon	*limbatus*	UM 9721	Sphenacodontidae	Briar Creek, Archer County, Texas	Artinskian	Isolated skull elements
Dimetrodon	*limbatus*	UM 9725	Sphenacodontidae	Briar Creek, Archer County, Texas	Artinskian	Isolated skull elements
Dimetrodon	*limbatus*	UM 9733	Sphenacodontidae	Briar Creek, Archer County, Texas	Artinskian	Isolated skull elements
Dimetrodon	*limbatus*	UM 9743	Sphenacodontidae	Briar Creek, Archer County, Texas	Artinskian	Isolated skull elements
Dimetrodon	*limbatus*	UM 9749	Sphenacodontidae	Briar Creek, Archer County, Texas	Artinskian	Isolated skull elements
Dimetrodon	*limbatus*	UM 1217	Sphenacodontidae	Briar Creek, Archer County, Texas	Artinskian	Braincase
Dimetrodon	*limbatus*	WM 652	Sphenacodontidae	Briar Creek, Archer County, Texas	Artinskian	Interclavicle
Dimetrodon	*limbatus*	WM 504	Sphenacodontidae	Briar Creek, Archer County, Texas	Artinskian	Clavicle
Dimetrodon	*limbatus*	AM 4751	Sphenacodontidae	Briar Creek, Archer County, Texas	Artinskian	Atlas centrum

Dimetrodon	*limbatus*	British Museum *Embolophorus*	Sphenacodontidae	Briar Creek, Archer County, Texas	Artinskian	Vertebra centrum
Dimetrodon	*limbatus*	WM 1080	Sphenacodontidae	Briar Creek, Archer County, Texas	Artinskian	Clavicle
Dimetrodon	*limbatus*	WM 78	Sphenacodontidae	Briar Creek, Archer County, Texas	Artinskian	Maxilla
Dimetrodon	*limbatus*	WM 1016	Sphenacodontidae	Briar Creek, Archer County, Texas	Artinskian	Maxilla
Dimetrodon	*limbatus*	AM 2275	Sphenacodontidae	Briar Creek, Archer County, Texas	Artinskian	Astragulus
Dimetrodon	*limbatus*	WM 1003	Sphenacodontidae	Briar Creek, Archer County, Texas	Artinskian	Carpus
Dimetrodon	*limbatus*	WM 181	Sphenacodontidae	Briar Creek, Archer County, Texas	Artinskian	Partial Pelvis
Ophiacodon	*uniformis*	UM 3423	Ophiacodontidae	Briar Creek, Archer County, Texas	Artinskian	Pelvis
Ophiacodon	*uniformis*	WM 547	Ophiacodontidae	Briar Creek, Archer County, Texas	Artinskian	Femur
Ophiacodon	*uniformis*	WM 130	Ophiacodontidae	Briar Creek, Archer County, Texas	Artinskian	Femur
Ophiacodon	*uniformis*	UM 3360	Ophiacodontidae	Briar Creek, Archer County, Texas	Artinskian	Femur
Ophiacodon	*uniformis*	UM 3361	Ophiacodontidae	Briar Creek, Archer County, Texas	Artinskian	Femur
Ophiacodon	*uniformis*	UM 3366	Ophiacodontidae	Briar Creek, Archer County, Texas	Artinskian	Femur
Ophiacodon	*uniformis*	WM 249	Ophiacodontidae	Briar Creek, Archer County, Texas	Artinskian	Femur
Ophiacodon	*uniformis*	WM 548	Ophiacodontidae	Briar Creek, Archer County, Texas	Artinskian	Femur
Ophiacodon	*uniformis*	WM 840	Ophiacodontidae	Briar Creek, Archer County, Texas	Artinskian	Femur

Ophiacodon	*uniformis*	MCZ 1291	Ophiacodontidae	Briar Creek, Archer County, Texas	Artinskian	Femur
Ophiacodon	*uniformis*	MCY 1292	Ophiacodontidae	Briar Creek, Archer County, Texas	Artinskian	Femur
Ophiacodon	*uniformis*	UM 3352	Ophiacodontidae	Briar Creek, Archer County, Texas	Artinskian	Humerus
Ophiacodon	*uniformis*	WM 143	Ophiacodontidae	Briar Creek, Archer County, Texas	Artinskian	Humerus
Ophiacodon	*uniformis*	UM 3428	Ophiacodontidae	Briar Creek, Archer County, Texas	Artinskian	Ilium
Lupeosaurus	*kayi*	UM IVd	Edaphosauridae	Briar Creek, Archer County, Texas	Artinskian	Scapulocoracoid and partial cleithrum
Edaphosaurus	*cruciger*		Edaphosauridae	Briar Creek, Archer County, Texas	Artinskian	
Edaphosaurus	*boanerges*	UM 3333	Edaphosauridae	Briar Creek, Archer County, Texas	Artinskian	Mounted skeleton
Edaphosaurus	*boanerges*	UM 3446	Edaphosauridae	Briar Creek, Archer County, Texas	Artinskian	Braincase
Edaphosaurus	*boanerges*	WM 819	Edaphosauridae	Briar Creek, Archer County, Texas	Artinskian	Maxilla
Edaphosaurus	*boanerges*	AM 4769	Edaphosauridae	Briar Creek, Archer County, Texas	Artinskian	Vertebrae and spines
Edaphosaurus	*boanerges*	FMNH 814	Edaphosauridae	Briar Creek, Archer County, Texas	Artinskian	Tooth plate
Edaphosaurus	*boanerges*	WM 563	Edaphosauridae	Briar Creek, Archer County, Texas	Artinskian	Vertebrae and spines
Edaphosaurus	*boanerges*	UM 3758	Edaphosauridae	Briar Creek, Archer County, Texas	Artinskian	Axis
Edaphosaurus	*boanerges*	WM 56	Edaphosauridae	Briar Creek, Archer County, Texas	Artinskian	Interclavicle
Edaphosaurus	*boanerges*	WM 534	Edaphosauridae	Briar Creek, Archer County, Texas	Artinskian	Clavicle

Edaphosaurus	*boanerges*	UM 1163	Edaphosauridae	Briar Creek, Archer County, Texas	Artinskian	Scapulocoracoid and humerus
Edaphosaurus	*boanerges*	WM 456	Edaphosauridae	Briar Creek, Archer County, Texas	Artinskian	Humerus
Edaphosaurus	*boanerges*	UM 1166	Edaphosauridae	Briar Creek, Archer County, Texas	Artinskian	Radius and ulna
Edaphosaurus	*boanerges*	UM 1164	Edaphosauridae	Briar Creek, Archer County, Texas	Artinskian	Femur
Edaphosaurus	*boanerges*	UM 1165	Edaphosauridae	Briar Creek, Archer County, Texas	Artinskian	Femur
Edaphosaurus	*boanerges*	WM 703	Edaphosauridae	Briar Creek, Archer County, Texas	Artinskian	Tibia
Edaphosaurus	*boanerges*	UM IVd	Edaphosauridae	Briar Creek, Archer County, Texas	Artinskian	Fibula
Edaphosaurus	*boanerges*	WM 703	Edaphosauridae	Briar Creek, Archer County, Texas	Artinskian	Mounted skeleton
Lupeosaurus	*kayi*	AMNH 4024	Edaphosauridae	?	Artinskian	Posterior dorsal, lumbar and sacral vertebrae
Bathygnathus	*borealis*	Academy of Natural Sciences, Philidelphia 9524	Sphenacodontidae	McLeod Farm well, New London district, Prince Edward Island	Artinskian	Left maxilla, septomaxilla and nasal
Dimetrodon	*teutonis*	MNG 10598	Sphenacodontidae	Bromacker Quarry, Thuringian Forest, near Tambach-Dietharz, 20km south of Cotha	Artinskian	Set of 14 vertebrae, including 5 neural spines and some intercentra
Dimetrodon	*teutonis*	MNG 10654	Sphenacodontidae	Bromacker Quarry, Thuringian Forest, near Tambach-Dietharz, 20km south of Cotha	Artinskian	Partial right scapulocoracoid, left scapula, nearly complete left humerus and partial articulated hindlimbs
Dimetrodon	*teutonis*	MNG 10655	Sphenacodontidae	Bromacker Quarry, Thuringian Forest, near Tambach-Dietharz, 20km south of Cotha	Artinskian	3 articulated posterior dorsal vertebrae and one more

Dimetrodon	*teutonis*	MNG 10693	Sphenacodontidae	Bromacker Quarry, Thuringian Forest, near Tambach-Dietharz, 20km south of Cotha	Artinskian	4 articulated mid-dorsal vertebrae, with 2 neural spines and 3 left ribs, scattered partial vertebrae and ribs
Dimetrodon	*teutonis*	MNG 13433	Sphenacodontidae	Bromacker Quarry, Thuringian Forest, near Tambach-Dietharz, 20km south of Cotha	Artinskian	Right maxilla
Dimetrodon	*limbatus (?)*		Sphenacodontidae	Orlando, Oklahoma	Artinskian-Early Kungurian	
Edaphosaurus	*pogonias*		Edaphosauridae	Orlando, Oklahoma	Artinskian-Early Kungurian	
Ruthenosaurus	*russelorum*	MNHN MCL-1	Caseidae	Colline du Cayla, 1km west of the village of Saint-Christophe-Vallon, commune of Valady, Aveyron	Artinskian-Kungurain	Anterior postcranial skeleton
Euromycter	*rutena*	MNHN MCL-2	Caseidae	Colline du Cayla, 1km west of the village of Saint-Christophe-Vallon, commune of Valady, Aveyron	Artinskian-Kungurain	Complete skull, lower jaw, hyoid apparatus, six cervical vertebrae in articulation, posterior coracoid, clavicle, interclavicle, distal head of right humerus, radius, ulna, manus
Sphenacodon	*ferocior (?)*	UCLA VP 1646	Sphenacodontidae	Organ Rock Shale	Late Artinskian	Axis
Ctenospondylus	*casei (?)*	NTM VP 1001	Sphenacodontidae	Organ Rock Shale	Late Artinskian	Skull roof, posterior lower jaw, basiparasphenoid, presphenoid, quadrates, partial pterygoid, 4 cervical vertebrae, fragments of neural spines, ribs, right cavicle, left distal coracoid
Ctenospondylus	*casei (?)*	NTM VP 1014	Sphenacodontidae	Organ Rock Shale	Late Artinskian	Dorsal vertebra and neural spine
Ctenospondylus	*casei (?)*	NTM VP 1015	Sphenacodontidae	Organ Rock Shale	Late Artinskian	Dorsal vertebra
Ctenospondylus	*casei (?)*	NTM VP 1016	Sphenacodontidae	Organ Rock Shale	Late Artinskian	Parasphenoid and nasal
Ctenospondylus	*casei (?)*	NTM VP 1018	Sphenacodontidae	Organ Rock Shale	Late Artinskian	3 dorsal vertebrae and partial neural spines

Eothyris	*parkeyi*	MCZ 1161	Eothyrididae	Tit Mountain, northeast of Dundee, Archer County, Texas	Early Kungurian	Complete skull and lower jaw
Secodontosaurus	*obtusidens*	AMNH 4091	Sphenacodontidae	Tit Mountain, northeast of Dundee, Archer County, Texas	Early Kungurian	Lower jaw and scapulocoracoid
Secodontosaurus	*obtusidens*	UM 3059	Sphenacodontidae	Tit Mountain, northeast of Dundee, Archer County, Texas	Early Kungurian	Scapulocoracoid
Secodontosaurus	*obtusidens*	UM 9714	Sphenacodontidae	Tit Mountain, northeast of Dundee, Archer County, Texas	Early Kungurian	Two maxillae
Dimetrodon	*macrospondylus*	AMNH 4012	Sphenacodontidae	Tit Mountain, northeast of Dundee, Archer County, Texas	Early Kungurian	Axis, 12 dorsal, 3 lumbar, 2 sacral and 4 caudal vertebrae, part of the ilium, most of the dentary
Dimetrodon	*natalis*	MCZ 1324	Sphenacodontidae	Tit Mountain, northeast of Dundee, Archer County, Texas	Early Kungurian	Femur
Dimetrodon	*limbatus*	MCZ 1448	Sphenacodontidae	Tit Mountain, northeast of Dundee, Archer County, Texas	Early Kungurian	Nearly complete skeleton
Dimetrodon	*limbatus*	AM 4005	Sphenacodontidae	Tit Mountain, northeast of Dundee, Archer County, Texas	Early Kungurian	Vertebrae and spines
Dimetrodon	*limbatus*	MCZ 1449	Sphenacodontidae	Tit Mountain, northeast of Dundee, Archer County, Texas	Early Kungurian	Vertebrae
Dimetrodon	*limbatus*	AM 4273	Sphenacodontidae	Tit Mountain, northeast of Dundee, Archer County, Texas	Early Kungurian	Humerus

Dimetrodon	*limbatus*	AM 4092	Sphenacodontidae	Tit Mountain, northeast of Dundee, Archer County, Texas	Early Kungurian	Postcranial material
Dimetrodon	*limbatus*	AM 4093	Sphenacodontidae	Tit Mountain, northeast of Dundee, Archer County, Texas	Early Kungurian	Postcranial material
Dimetrodon	*limbatus*	WM 843	Sphenacodontidae	Tit Mountain, northeast of Dundee, Archer County, Texas	Early Kungurian	Humerus
Dimetrodon	*dollovianus (?)*	MCZ	Sphenacodontidae	Tit Mountain, northeast of Dundee, Archer County, Texas	Early Kungurian	Fibula
Ophiacodon	*retroversus*	AMNH 4566	Ophiacodontidae	Tit Mountain, northeast of Dundee, Archer County, Texas	Early Kungurian	Pelvic girdle elements
Varanosaurus	*witchitaensis*	MCZ 8260	Ophiacodontidae	Tit Mountain, northeast of Dundee, Archer County, Texas	Early Kungurian	Proximal humerus
Edaphosaurus	*cruciger*	MCZ Vd	Edaphosauridae	Tit Mountain, northeast of Dundee, Archer County, Texas	Early Kungurian	Fibula
Lupeosaurus (?)	*kayi (?)*	MCZ 1652	Edaphosauridae	Tit Mountain, northeast of Dundee, Archer County, Texas	Early Kungurian	Fibula
Secodontosaurus	*obtusidens*	AMNH 4046	Sphenacodontidae	South of Dundee, North of Little Wichita near Slippery Creek	Early Kungurian	Maxilla
Dimetrodon	*natalis*	UM 16201	Sphenacodontidae	South of Dundee, North of Little Wichita near Slippery Creek	Early Kungurian	Dorsal vertebrae

Dimetrodon	*booneorum*	MCZ 1551	Sphenacodontidae	South of Dundee, North of Little Wichita near Slippery Creek	Early Kungurian	Femur
Dimetrodon	*booneorum*	AM 4839	Sphenacodontidae	South of Dundee, North of Little Wichita near Slippery Creek	Early Kungurian	Vertebrae and spines
Dimetrodon	*booneorum*	MCZ 1573	Sphenacodontidae	South of Dundee, North of Little Wichita near Slippery Creek	Early Kungurian	Partial skull
Dimetrodon	*booneorum*	MCZ 1554	Sphenacodontidae	South of Dundee, North of Little Wichita near Slippery Creek	Early Kungurian	Skull fragments
Dimetrodon	*booneorum*	MCZ 1312	Sphenacodontidae	South of Dundee, North of Little Wichita near Slippery Creek	Early Kungurian	Femur
Dimetrodon	*booneorum*	MCZ 1302	Sphenacodontidae	South of Dundee, North of Little Wichita near Slippery Creek	Early Kungurian	Tibia
Dimetrodon	*limbatus*	UM 16148	Sphenacodontidae	South of Dundee, North of Little Wichita near Slippery Creek	Early Kungurian	Humerus
Dimetrodon	*limbatus*	UM 16202	Sphenacodontidae	South of Dundee, North of Little Wichita near Slippery Creek	Early Kungurian	Vertebra
Dimetrodon	*limbatus*	UM 16203	Sphenacodontidae	South of Dundee, North of Little Wichita near Slippery Creek	Early Kungurian	Vertebra
Dimetrodon	*limbatus*	MCZ 1113	Sphenacodontidae	South of Dundee, North of Little Wichita near Slippery Creek	Early Kungurian	Maxilla and Ulna

Dimetrodon	*limbatus*	AM 4811	Sphenacodontidae	South of Dundee, North of Little Wichita near Slippery Creek	Early Kungurian	Femur
Dimetrodon	*limbatus*	AM 4084	Sphenacodontidae	South of Dundee, North of Little Wichita near Slippery Creek	Early Kungurian	Vertebrae
Dimetrodon	*limbatus*	AM 4043	Sphenacodontidae	South of Dundee, North of Little Wichita near Slippery Creek	Early Kungurian	Femur
Dimetrodon	*limbatus*	AM 4044	Sphenacodontidae	South of Dundee, North of Little Wichita near Slippery Creek	Early Kungurian	Partial scapulocoracoid and limb bones
Dimetrodon	*limbatus*	MCZ 1110	Sphenacodontidae	South of Dundee, North of Little Wichita near Slippery Creek	Early Kungurian	Scapulocoracoid
Dimetrodon	*limbatus*	MCZ 1313	Sphenacodontidae	South of Dundee, North of Little Wichita near Slippery Creek	Early Kungurian	Humerus
Dimetrodon	*limbatus*	MCZ 1339	Sphenacodontidae	South of Dundee, North of Little Wichita near Slippery Creek	Early Kungurian	Pelvis
Dimetrodon	*limbatus*	AM 4809	Sphenacodontidae	South of Dundee, North of Little Wichita near Slippery Creek	Early Kungurian	Femur
Dimetrodon	*limbatus*	MCZ 1334	Sphenacodontidae	South of Dundee, North of Little Wichita near Slippery Creek	Early Kungurian	Tibia
Ophiacodon	*uniformis*	MCZ 1297	Ophiacodontidae	South of Dundee, North of Little Wichita near Slippery Creek	Early Kungurian	Femur

Varanosaurus	*witchitaensis*	MCY 6373	Ophiacodontidae	South of Dundee, North of Little Wichita near Slippery Creek	Early Kungurian	Astragulus, femur
Dimetrodon	*limbatus*	WM 1001	Sphenacodontidae	Daggett Creek	Early Kungurian	Skull, jaws, vertebrae, humerus, ulna, tibia
Secodontosaurus	*obtusidens*	AMNH 4062	Sphenacodontidae	Beaver Creek, Wichita County, Texas	Early Kungurian	Occiput and most presacral vertebrae
Dimetrodon	*grandis*	MCZ 1341	Sphenacodontidae	Beaver Creek, Wichita County, Texas	Early Kungurian	Scapulocoracoid
Dimetrodon	*grandis*	AM 4034	Sphenacodontidae	Beaver Creek, Wichita County, Texas	Early Kungurian	Skull, jaws, presacral column and ribs
Dimetrodon	*loomsi*	MCZ 1341	Sphenacodontidae	Beaver Creek, Wichita County, Texas	Early Kungurian	Femur
Edaphosaurus	*cruciger*	AM 4072	Edaphosauridae	Beaver Creek, Wichita County, Texas	Early Kungurian	Neural spine
Secodontosaurus	*obtusidens*	AMNH 4826	Sphenacodontidae	Head of Godwin Creek, Baylor County, Texas	Early Kungurian	Articular
Dimetrodon	*macrospondylus*		Sphenacodontidae	Head of Godwin Creek, Baylor County, Texas	Early Kungurian	
Secodontosaurus	*obtusidens*	MCZ 2944	Sphenacodontidae	South side of Little Wichita River, Texas	Early Kungurian	Part of the axis and third cervical, 4 posterior dorsal and 2 lumbar vertebrae, with fragments of neural spines
Ctenospondylus	*casei*	AMNH 4047	Sphenacodontidae	Slippery Creek, Archer County, Texas	Early Kungurian	Cervical centum, 2 dorsal centra, neural spines
Dimetrodon	*limbatus*		Sphenacodontidae	Slippery Creek, Archer County, Texas	Early Kungurian	
Dimetrodon	*gigashomogenes*		Sphenacodontidae	Slippery Creek, Archer County, Texas	Early Kungurian	
Ophiacodon	*retroversus*	WM 458	Ophiacodontidae	Slippery Creek, Archer County, Texas	Early Kungurian	Nearly complete skeleton
Ophiacodon	*retroversus*	MCZ 1470	Ophiacodontidae	Slippery Creek, Archer County, Texas	Early Kungurian	Nearly complete presacral colum

Ophiacodon	*uniformis*	MCZ 1295	Ophiacodontidae	Slippery Creek, Archer County, Texas	Early Kungurian	Femur
Varanosaurus	*witchitaensis*	MCZ 1353	Ophiacodontidae	Slippery Creek, Archer County, Texas	Early Kungurian	Partial Pelvis
Varanosaurus	*witchitaensis*	UM 3354	Ophiacodontidae	Slippery Creek, Archer County, Texas	Early Kungurian	Several humeri
Varanosaurus	*witchitaensis*	UM 11655	Ophiacodontidae	Slippery Creek, Archer County, Texas	Early Kungurian	Several vertebrae, partial pelvis, femora, partial tibia and fibula
Varanosaurus	*witchitaensis*	UM 15438	Ophiacodontidae	Slippery Creek, Archer County, Texas	Early Kungurian	Several vertebrae
Varanosaurus	*witchitaensis*	MCZ 6374	Ophiacodontidae	Slippery Creek, Archer County, Texas	Early Kungurian	Astragulus, femur
Varanosaurus	*witchitaensis*	MCZ 6375	Ophiacodontidae	Slippery Creek, Archer County, Texas	Early Kungurian	Astragulus, femur
Varanosaurus	*witchitaensis*	MCZ 6341-2	Ophiacodontidae	East of Rendham, Baylor County	Early Kungurian	Tibia (minus shaft), centrum
Ophiacodon	*retroversus*	AMNH 4155	Ophiacodontidae	Big Witchita, northwest of Dundee, Boarder of Archer and Baylor Countz, Texas	Early Kungurian	Nearly complete skeleton
Ophiacodon	*major*	AM 4083	Ophiacodontidae	Big Witchita, northwest of Dundee, Boarder of Archer and Baylor Countz, Texas	Early Kungurian	Femur, pelvis, vertebrae
Ophiacodon	*major*	FMNH	Ophiacodontidae	Big Witchita, northwest of Dundee, Boarder of Archer and Baylor Countz, Texas	Early Kungurian	Pelvis, vertebrae, anterior dentary, partial pelvis
Edaphosaurus	*cruciger*	AM 4060	Edaphosauridae	Big Witchita, northwest of Dundee, Boarder of Archer and Baylor Countz, Texas	Early Kungurian	Complete vertebral column until third caudal
Edaphosaurus	*cruciger*	AM 4039	Edaphosauridae	Big Witchita, northwest of Dundee, Boarder of Archer and Baylor Countz, Texas	Early Kungurian	Incomplete neural spines and vertebrae

Edaphosaurus	*cruciger*	AM 4014	Edaphosauridae	Big Witchita, northwest of Dundee, Boarder of Archer and Baylor Countz, Texas	Early Kungurian	Vertebrae, neural spine fragments, Portion of clavicle, teeth
Varanosaurus	*witchitaensis*	MCZ 6137	Ophiacodontidae	North of Dundee	Early Kungurian	Calcaneum
Varanosaurus	*witchitaensis*	MCZ 6378	Ophiacodontidae	North of Dundee	Early Kungurian	Astragulus, femur
Varanosaurus	*witchitaensis*	MCZ 6377	Ophiacodontidae	?	Early Kungurian	Astragulus, femur
Secodontosaurus	*obtusidens*	MCZ 1124	Sphenacodontidae	Rattlesnake Canyon, Archer County, Texas	Early Kungurian	Skull, left mandible, cervical and anterior dorsal vertebrae, Scapulocoracoids
Dimetrodon	*natalis*	MCZ 1329	Sphenacodontidae	Rattlesnake Canyon, Archer County, Texas	Early Kungurian	Limb bones
Dimetrodon	*natalis*	MCZ 1325	Sphenacodontidae	Rattlesnake Canyon, Archer County, Texas	Early Kungurian	Humerus
Dimetrodon	*natalis*	MCZ 1300	Sphenacodontidae	Rattlesnake Canyon, Archer County, Texas	Early Kungurian	Ulna
Dimetrodon	*natalis*	MCZ 1563	Sphenacodontidae	Rattlesnake Canyon, Archer County, Texas	Early Kungurian	Pelvis
Dimetrodon	*natalis*	MCZ 1328	Sphenacodontidae	Rattlesnake Canyon, Archer County, Texas	Early Kungurian	Femur
Dimetrodon	*natalis*	MCZ 1329	Sphenacodontidae	Rattlesnake Canyon, Archer County, Texas	Early Kungurian	Femur
Dimetrodon	*natalis*	MCZ 1300	Sphenacodontidae	Rattlesnake Canyon, Archer County, Texas	Early Kungurian	Fibula
Dimetrodon	*booneorum*	MCZ 1564	Sphenacodontidae	Rattlesnake Canyon, Archer County, Texas	Early Kungurian	Pelvis
Dimetrodon	*booneorum*	MCZ 1392	Sphenacodontidae	Rattlesnake Canyon, Archer County, Texas	Early Kungurian	Humerus
Dimetrodon	*limbatus*	MCZ 1368	Sphenacodontidae	Rattlesnake Canyon, Archer County, Texas	Early Kungurian	Vertebrae, limb and girdle bones
Dimetrodon	*limbatus*	MCZ 1336	Sphenacodontidae	Rattlesnake Canyon, Archer County, Texas	Early Kungurian	Humerus, ulna
Dimetrodon	*limbatus*	MCZ 1446	Sphenacodontidae	Rattlesnake Canyon, Archer County, Texas	Early Kungurian	Skull

Dimetrodon	*limbatus*	MCZ 1403	Sphenacodontidae	Rattlesnake Canyon, Archer County, Texas	Early Kungurian	Dentary
Dimetrodon	*limbatus*	MCZ 1447	Sphenacodontidae	Rattlesnake Canyon, Archer County, Texas	Early Kungurian	Scapulocoracoid
Dimetrodon	*limbatus*	MCZ 1369	Sphenacodontidae	Rattlesnake Canyon, Archer County, Texas	Early Kungurian	Limbs and girdles
Dimetrodon	*limbatus*	WM 540	Sphenacodontidae	Rattlesnake Canyon, Archer County, Texas	Early Kungurian	Maxilla
Dimetrodon	*limbatus*	MCZ 1390	Sphenacodontidae	Rattlesnake Canyon, Archer County, Texas	Early Kungurian	Humerus
Dimetrodon	*limbatus*	MCZ 1335	Sphenacodontidae	Rattlesnake Canyon, Archer County, Texas	Early Kungurian	Axis
Dimetrodon	*limbatus*	MCZ 1333	Sphenacodontidae	Rattlesnake Canyon, Archer County, Texas	Early Kungurian	Femur
Dimetrodon	*limbatus*	MCZ 1358	Sphenacodontidae	Rattlesnake Canyon, Archer County, Texas	Early Kungurian	Interclavicle
Dimetrodon	*limbatus*	MCZ 1133	Sphenacodontidae	Rattlesnake Canyon, Archer County, Texas	Early Kungurian	Femur
Dimetrodon	*limbatus*	MCZ 2893	Sphenacodontidae	Rattlesnake Canyon, Archer County, Texas	Early Kungurian	Maxilla and teeth, lacrimal, postorbital
Dimetrodon	*limbatus*	MCZ 1108	Sphenacodontidae	Rattlesnake Canyon, Archer County, Texas	Early Kungurian	Femur
Dimetrodon	*limbatus*	AM 4815	Sphenacodontidae	Rattlesnake Canyon, Archer County, Texas	Early Kungurian	Isolated skull elements
Edaphosaurus	*boanerges*	MCZ 1280	Edaphosauridae	Rattlesnake Canyon, Archer County, Texas	Early Kungurian	Clavicle, pelvis
Edaphosaurus	*boanerges*	MCZ 1286	Edaphosauridae	Rattlesnake Canyon, Archer County, Texas	Early Kungurian	Most of the presacral column and spines
Edaphosaurus (?)	*boanerges (?)*		Edaphosauridae	Rattlesnake Canyon, Archer County, Texas	Early Kungurian	Vertebra
Ophiacodon	*retroversus*	MCZ 1121	Ophiacodontidae	Rattlesnake Canyon, Archer County, Texas	Early Kungurian	Most of the skeleton

Ophiacodon	*retroversus*	MCZ 1203	Ophiacodontidae	Rattlesnake Canyon, Archer County, Texas	Early Kungurian	Jaws, braincase, limbs and girdles
Ophiacodon	*retroversus*	MCZ 1103	Ophiacodontidae	Rattlesnake Canyon, Archer County, Texas	Early Kungurian	Fragmentary skeleton
Ophiacodon	*retroversus*	MCZ 1119	Ophiacodontidae	Rattlesnake Canyon, Archer County, Texas	Early Kungurian	Partial vertebral column
Ophiacodon	*retroversus*	MCZ 1484	Ophiacodontidae	Rattlesnake Canyon, Archer County, Texas	Early Kungurian	Partial vertebral column
Ophiacodon	*retroversus*	MCZ 1560	Ophiacodontidae	Rattlesnake Canyon, Archer County, Texas	Early Kungurian	Several bones
Ophiacodon	*retroversus*	MCZ 1200	Ophiacodontidae	Rattlesnake Canyon, Archer County, Texas	Early Kungurian	Atlas centrum
Ophiacodon	*retroversus*	MCZ 1294	Ophiacodontidae	Rattlesnake Canyon, Archer County, Texas	Early Kungurian	Atlas centrum
Ophiacodon	*retroversus*	MCZ 1562	Ophiacodontidae	Rattlesnake Canyon, Archer County, Texas	Early Kungurian	Scapulocoracoid
Ophiacodon	*retroversus*	MCZ 1486	Ophiacodontidae	Rattlesnake Canyon, Archer County, Texas	Early Kungurian	Humerus
Ophiacodon	*retroversus*	MCZ 1450	Ophiacodontidae	Rattlesnake Canyon, Archer County, Texas	Early Kungurian	Pelvic material
Ophiacodon	*retroversus*	MCZ 1296	Ophiacodontidae	Rattlesnake Canyon, Archer County, Texas	Early Kungurian	Pelvic material
Ophiacodon	*retroversus*	MCZ 1299	Ophiacodontidae	Rattlesnake Canyon, Archer County, Texas	Early Kungurian	Femur
Ophiacodon	*retroversus*	MCZ 1205	Ophiacodontidae	Rattlesnake Canyon, Archer County, Texas	Early Kungurian	Femur
Ophiacodon	*retroversus*	MCZ 1206	Ophiacodontidae	Rattlesnake Canyon, Archer County, Texas	Early Kungurian	Femur
Ophiacodon	*retroversus*	MCZ 1298	Ophiacodontidae	Rattlesnake Canyon, Archer County, Texas	Early Kungurian	Fibula
Ophiacodon	*uniformis*	MCZ 1297	Ophiacodontidae	Rattlesnake Canyon, Archer County, Texas	Early Kungurian	Femur

Ophiacodon	*retroversus*	AM 4604	Ophiacodontidae	South of Fulda, north side of Godwin Creek	Early Kungurian	Crushed skull, most of the vertebral column, scapulocoracoid, humerus
Ophiacodon	*retroversus*	WM 790	Ophiacodontidae	South of Fulda, north side of Godwin Creek	Early Kungurian	Femur
Ophiacodon	*retroversus*	WM 709	Ophiacodontidae	South of Fulda, north side of Godwin Creek	Early Kungurian	Many bones
Ophiacodon	*retroversus*	AM4807	Ophiacodontidae	South of Fulda, north side of Godwin Creek	Early Kungurian	Many bones
Ophiacodon	*uniformis*	MCZ 1443	Ophiacodontidae	South of Fulda, north side of Godwin Creek	Early Kungurian	Tibia
Varanosaurus	*witchitaensis*	MCZ 6372	Ophiacodontidae	South of Fulda, north side of Godwin Creek	Early Kungurian	Astragulus, femur
Varanosaurus	*witchitaensis*	MCZ 6070	Ophiacodontidae	South of Fulda, north side of Godwin Creek	Early Kungurian	Proximal tibia
Ctenorhachis	*jacksoni*	USNM 437710	Sphenacodontidae	South of Fulda, north side of Godwin Creek	Early Kungurian	31 artculated vertebrae (4 posterior cerviclas-4 anterior caudals), pelvis, ribs
Dimetrodon	*natalis*	MCZ 1112	Sphenacodontidae	South of Fulda, north side of Godwin Creek	Early Kungurian	Fragments of skeleton
Dimetrodon	*natalis*	MCZ 1443	Sphenacodontidae	South of Fulda, north side of Godwin Creek	Early Kungurian	Fragments of skeleton
Dimetrodon	*natalis*	MCZ 1321	Sphenacodontidae	South of Fulda, north side of Godwin Creek	Early Kungurian	Humerus
Dimetrodon	*natalis*	MCZ 1542	Sphenacodontidae	South of Fulda, north side of Godwin Creek	Early Kungurian	Humerus
Dimetrodon	*natalis*	MCZ 1146	Sphenacodontidae	South of Fulda, north side of Godwin Creek	Early Kungurian	Femur
Dimetrodon	*limbatus*	MCZ 1125	Sphenacodontidae	South of Fulda, north side of Godwin Creek	Early Kungurian	Skull
Dimetrodon	*limbatus*	WM 1	Sphenacodontidae	South of Fulda, north side of Godwin Creek	Early Kungurian	Much of the skull, jaws, vertebral column, humerus, femur, tibia, fibula and scapula
Dimetrodon	*limbatus*	AM 4048	Sphenacodontidae	South of Fulda, north side of Godwin Creek	Early Kungurian	Fragments of skull, jaw, vertebrae, humerus, ulna, tibia

Dimetrodon	*limbatus*	MCZ 1123	Sphenacodontidae	South of Fulda, north side of Godwin Creek	Early Kungurian	Most of the skeleton
Dimetrodon	*limbatus*	KU 705	Sphenacodontidae	South of Fulda, north side of Godwin Creek	Early Kungurian	Column, humerus, skull fragments
Dimetrodon	*limbatus*	MCZ 1547	Sphenacodontidae	South of Fulda, north side of Godwin Creek	Early Kungurian	Pelvis, most of the hind legs, sacrals, and most of the tail
Dimetrodon	*limbatus*	AM 4633	Sphenacodontidae	South of Fulda, north side of Godwin Creek	Early Kungurian	Radius
Dimetrodon	*limbatus*	AM 4818	Sphenacodontidae	South of Fulda, north side of Godwin Creek	Early Kungurian	Quadrate
Dimetrodon	*limbatus*	AM 4821	Sphenacodontidae	South of Fulda, north side of Godwin Creek	Early Kungurian	Scapulocoracoid
Dimetrodon	*limbatus*	MCZ 1314	Sphenacodontidae	South of Fulda, north side of Godwin Creek	Early Kungurian	Humerus
Dimetrodon	*limbatus*	AM 4627	Sphenacodontidae	South of Fulda, north side of Godwin Creek	Early Kungurian	Humerus
Dimetrodon	*limbatus*	MCZ 1115	Sphenacodontidae	South of Fulda, north side of Godwin Creek	Early Kungurian	Pelvis
Dimetrodon	*limbatus*	MCZ 1116	Sphenacodontidae	South of Fulda, north side of Godwin Creek	Early Kungurian	Humerus
Dimetrodon	*limbatus*	AM 4632	Sphenacodontidae	South of Fulda, north side of Godwin Creek	Early Kungurian	Femur
Dimetrodon	*limbatus*	MCZ 1445	Sphenacodontidae	South of Fulda, north side of Godwin Creek	Early Kungurian	Ulna
Dimetrodon	*limbatus*	MCZ 1465	Sphenacodontidae	South of Fulda, north side of Godwin Creek	Early Kungurian	Pelvis
Dimetrodon	*limbatus*	MCZ 1337	Sphenacodontidae	South of Fulda, north side of Godwin Creek	Early Kungurian	Pelvis
Dimetrodon	*limbatus*	AM 4837	Sphenacodontidae	South of Fulda, north side of Godwin Creek	Early Kungurian	Pelvis
Dimetrodon	*limbatus*	WM 787	Sphenacodontidae	South of Fulda, north side of Godwin Creek	Early Kungurian	Femur

Dimetrodon	*limbatus*	UM 3401	Sphenacodontidae	South of Fulda, north side of Godwin Creek	Early Kungurian	Femur
Dimetrodon	*limbatus*	AM 4823	Sphenacodontidae	South of Fulda, north side of Godwin Creek	Early Kungurian	Femur
Dimetrodon	*limbatus*	AM 4621	Sphenacodontidae	South of Fulda, north side of Godwin Creek	Early Kungurian	Tibia
Dimetrodon	*limbatus*	AM 4808	Sphenacodontidae	South of Fulda, north side of Godwin Creek	Early Kungurian	Tibia
Dimetrodon	*booneorum*	MCZ 1537	Sphenacodontidae	South of Fulda, north side of Godwin Creek	Early Kungurian	Jaw fragments, Dorsal and cervical centra and spine fragments, humeri, radius, proximal tibia
Dimetrodon	*booneorum*	MCZ 1443	Sphenacodontidae	South of Fulda, north side of Godwin Creek	Early Kungurian	Limb bones and girdles
Dimetrodon	*booneorum*	WM 1202	Sphenacodontidae	South of Fulda, north side of Godwin Creek	Early Kungurian	Radius
Dimetrodon	*booneorum*	MCZ 1304	Sphenacodontidae	South of Fulda, north side of Godwin Creek	Early Kungurian	Humerus
Dimetrodon	*booneorum*	AM 4806	Sphenacodontidae	South of Fulda, north side of Godwin Creek	Early Kungurian	Femur
Dimetrodon	*booneorum*	WM 788	Sphenacodontidae	South of Fulda, north side of Godwin Creek	Early Kungurian	Femur
Ophiacodon	*uniformis*	MCZ 1443	Ophiacodontidae	Belle Plains, north of Godwin Creek, Baylor County, Texas	Early Kungurian	Tibia
Dimetrodon	*natalis*		Sphenacodontidae	Military Crossing, north of Fulda, Texas	Early Kungurian	
Dimetrodon	*limbatus*		Sphenacodontidae	Military Crossing, north of Fulda, Texas	Early Kungurian	
Dimetrodon	*dollovianus*	WM 152	Sphenacodontidae	North of Fulda, east Baylor County, Texas	Early Kungurian	Scapulocoracoid
Ophiacodon	*retroversus*	MCZ 1204	Ophiacodontidae	North of Fulda, east Baylor County, Texas	Early Kungurian	Partial skeleton

Dimetrodon	*dollovianus*	WM 461	Sphenacodontidae	South of Electra, Western Wichia County, Texas	Early Kungurian	Intrerclavicle
Edaphosaurus	*cruciger (?)*		Edaphosauridae	Elmo, Kansas	Early Kungurian	Fragments
Varanosaurus	*acutirostris*	FMNH PR 1760	Ophiacodontidae	South Pauls Valley Locality, Garvin County, Oklahoma	Early Kungurian	Nearly complete skull with atlas and axis attached
Dimetrodon	*limbatus (?)*		Sphenacodontidae	Waurika, Oklahoma	Early Kungurian	Fragments
Edaphosaurus	*pogonias*		Edaphosauridae	Waurika, Oklahoma	Early Kungurian	
Glaucosaurus	*megalops*		Edaphosauridae	Coal Creek, Baylor County, Texas	Kungurian	
Glaucosaurus	*megalops*	FMNH UC 691	Edaphosauridae	Mitchell Creek, Northeast of Maybelle, Baylor County, Texas	Kungurian	Skull, without roof and lower posterior portion
Varanosaurus	*witchitaensis*	FMNH 651	Ophiacodontidae	Mitchell Creek, Northeast of Maybelle, Baylor County, Texas	Kungurian	Scapula blade, distal humerus, distal femur, proximal tibia and fibula
Mycterosaurus	*longiceps*	AMNH 7002	Varanopidae	Mitchell Creek, Northeast of Maybelle, Baylor County, Texas	Kungurian	Nearly complete skull, scapulae, forelimbs, Pelvis, hindlimbs, vertebrae
Mycterosaurus	*longiceps*	FMNH UC 692	Varanopidae	Mitchell Creek, Northeast of Maybelle, Baylor County, Texas	Kungurian	Nearly complete skull, few postcranial fragments
Mycterosaurus	*longiceps*	FMNH UC 169	Varanopidae	Mitchell Creek, Northeast of Maybelle, Baylor County, Texas	Kungurian	Partial skull and postcranial remains
Mycterosaurus	*longiceps*	WM	Varanopidae	Mitchell Creek, Northeast of Maybelle, Baylor County, Texas	Kungurian	Pelvis, scapulocoracoid
Dimetrodon	*dollovianus*	WM 1201	Sphenacodontidae	Moonshine Creek, Bayor County, Texas	Kungurian	Radius ulna, partial carpus, tarsus
Edaphosaurus	*cruciger*	FMNH UC 658	Edaphosauridae	Moonshine Creek, Bayor County, Texas	Kungurian	Skull

Ophiacodon	*major*	AM	Ophiacodontidae	Military Trail 32, Baylor County, Texas	Kungurian	Ilium
Dimetrodon	*limbatus*	AMNH 4001	Sphenacodontidae	Military Trail 32, Baylor County, Texas	Kungurian	Skull elements, pelvis, femur
Secodontosaurus	*obtusidens*		Sphenacodontidae	Military Trail 32, Baylor County, Texas	Kungurian	
Ophiacodon	*uniformis*	WM 690	Ophiacodontidae	Maybelle, Baylor County, Texas	Kungurian	Skeleton in ventral view
Ophiacodon	*major*	AM 4109	Ophiacodontidae	Maybelle, Baylor County, Texas	Kungurian	10 vertebrae
Dimetrodon	*macrospondylus*	AMNH 4055	Sphenacodontidae	Deep Red Run	Late Kungurian	Axis, humerus
Dimetrodon	*macrospondylus*	AMNH 4065	Sphenacodontidae	Deep Red Run	Late Kungurian	Part of the axis and third cervical, 4 posterior dorsal and 2 lumbar vertebrae, with fragments of neural spines
Dimetrodon	*macrospondylus*	University of Chicargo 1019	Sphenacodontidae	Deep Red Run	Late Kungurian	Dorsal vertebrae
Ophiacodon	*major*	AM 1814	Ophiacodontidae	Deep Red Run	Late Kungurian	Two proximal femurs, one distal
Dimetrodon	*grandis*	AM 4054	Sphenacodontidae	Deep Red Run	Late Kungurian	
Dimetrodon	*dollovianus*	AMNH 4064	Sphenacodontidae	Deep Red Run	Late Kungurian	Fragmentary skeleton
Dimetrodon	*dollovianus*	AM 4282	Sphenacodontidae	Deep Red Run	Late Kungurian	Partial pelvis
Dimetrodon	*dollovianus*	AM 1796	Sphenacodontidae	Deep Red Run	Late Kungurian	Ilium
Dimetrodon	*dollovianus*	AM 1774	Sphenacodontidae	Deep Red Run	Late Kungurian	Spine fragments
Edaphosaurus	*cruciger*		Edaphosauridae	Deep Red Run	Late Kungurian	
Dimetrodon	*gigashomogenes*	MCZ 1342	Sphenacodontidae	Pond Creek, Oklahoma	Late Kungurian	Vertebrae
Dimetrodon	*gigashomogenes*	MCZ 1346	Sphenacodontidae	Pond Creek, Oklahoma	Late Kungurian	Scapulocoracoid
Dimetrodon	*grandis (?)*	UM	Sphenacodontidae	Pond Creek, Oklahoma	Late Kungurian	Fragments
Varanops	*brevirostris*	TMM 43628-1	Varanopidae	Mud Hill Locality, Southwest of Abilene, Taylor County, Texas	Late Kungurian	Partial skull, complete right and partial left rami of lower jaw, nearly complete series of dorsal vertebrae, 1 sacral vertebra, several caudal vertebrae, gastralia, partial pectroal and pelvic gridles and limbs

Varanops	*brevirostris*	FMNH UC 644	Varanopidae	*Cacops* Bonebed, Baylor County, Texas	Late Kungurian	Nearly complete skeleton
Varanops	*brevirostris*	FMNH UR 2423	Varanopidae	*Cacops* Bonebed, Baylor County, Texas	Late Kungurian	Nearly complete skull and lower jaw, atlas and axis
Varanops	*brevirostris*	FMNH P 12841	Varanopidae	*Cacops* Bonebed, Baylor County, Texas	Late Kungurian	Partial skeleton
Varanops	*brevirostris*	MCZ 1926	Varanopidae	*Cacops* Bonebed, Baylor County, Texas	Late Kungurian	Complete skull and lower jaw, girdle and limb bones
Casea	*broilii*	FMNH UC 656	Caseidae	*Cacops* Bonebed, Baylor County, Texas	Late Kungurian	Skull and skeleton
Casea	*broilii*	FMNH UC 657	Caseidae	*Cacops* Bonebed, Baylor County, Texas	Late Kungurian	Ribs (Williston 1911), Skeleton (Romer & Price 1940), Right pes (Olson 1968)
Casea	*broilii*	FMNH UC 698	Caseidae	*Cacops* Bonebed, Baylor County, Texas	Late Kungurian	Skull
Casea	*broilii*	FMNH UC 883	Caseidae	*Cacops* Bonebed, Baylor County, Texas	Late Kungurian	Most of the presacral vertebrae, three sacral and some caudal vertebrae, pelvis, ribs, limb bones
Casea	*broilii*	FMNH UC 901	Caseidae	*Cacops* Bonebed, Baylor County, Texas	Late Kungurian	Manus, radii, himeri, shoulder girdle, some ribs and vertebrae
Casea	*broilii*	FMNH UC 1011	Caseidae	*Cacops* Bonebed, Baylor County, Texas	Late Kungurian	Basal skull and lower jaws
Edaphosaurus	*pogonias*		Edaphosauridae	*Cacops* Bonebed, Baylor County, Texas	Late Kungurian	
Dimetrodon	*gigashomogenes*	AM 4138	Sphenacodontidae	*Cacops* Bonebed, Baylor County, Texas	Late Kungurian	Scapulocoracoid
Dimetrodon	*gigashomogenes*	AM 4173	Sphenacodontidae	*Cacops* Bonebed, Baylor County, Texas	Late Kungurian	Cervical vertebrae
Dimetrodon	*grandis*	AM 4138	Sphenacodontidae	*Cacops* Bonebed, Baylor County, Texas	Late Kungurian	Scapulocoracoid
Dimetrodon	*grandis*	AM 4173	Sphenacodontidae	*Cacops* Bonebed, Baylor County, Texas	Late Kungurian	Cervical vertebrae

Dimetrodon	*loomsi*	WM 411	Sphenacodontidae	Poney Creek, east of the Craddock Region	Late Kungurian	Cervical vertebrae
Dimetrodon	*loomsi*	WM 1140	Sphenacodontidae	Poney Creek, east of the Craddock Region	Late Kungurian	Humerus
Dimetrodon	*kempae*	WM 1139	Sphenacodontidae	Poney Creek, east of the Craddock Region	Late Kungurian	Humerus
Dimetrodon	*gigashomogenes*	WM 411	Sphenacodontidae	Poney Creek, east of the Craddock Region	Late Kungurian	Cervical vertebrae
Dimetrodon	*grandis*	WM 1131	Sphenacodontidae	Crooked Creek	Late Kungurian	Postcranial fragments
Dimetrodon	*grandis*	WM 1197	Sphenacodontidae	Crooked Creek	Late Kungurian	Fragments
Dimetrodon	*grandis*	WM 1158	Sphenacodontidae	Crooked Creek	Late Kungurian	Fragments
Dimetrodon	*loomsi*	WM 214	Sphenacodontidae	Dead Man	Late Kungurian	Partial Skull
Edaphosaurus	*pogonias*	WM 1092	Edaphosauridae	Hog Creek, west of Table Top Mountain, Baylor County, Texas	Late Kungurian	Femur, tibia, fibula
Edaphosaurus	*pogonias*	AM 4015	Edaphosauridae	Hog Creek, west of Table Top Mountain, Baylor County, Texas	Late Kungurian	Presacral column, mounted
Dimetrodon	*grandis*	MCZ 1348	Sphenacodontidae	Hog Creek, west of Table Top Mountain, Baylor County, Texas	Late Kungurian	Jaw
Dimetrodon	*grandis*	MCZ 1345	Sphenacodontidae	Hog Creek, west of Table Top Mountain, Baylor County, Texas	Late Kungurian	Scapulocoracoid
Dimetrodon	*loomsi*	MCZ 1345	Sphenacodontidae	Hog Creek, west of Table Top Mountain, Baylor County, Texas	Late Kungurian	Scapulocoracoid
Varanosaurus	*acutirostris*	BSPHM 1901 XV 20	Ophiacodontidae	Craddock Bonebed, Brush Creek, Craddock Ranch, North of Seymour, Baylor County, Texas	Late Kungurian	Nearly complete skeleton

Varanosaurus	*acutirostris*	NM 15562	Ophiacodontidae	Craddock Bonebed, Brush Creek, Craddock Ranch, North of Seymour, Baylor County, Texas	Late Kungurian	Humerus
Varanosaurus	*acutirostris*	NM 15563	Ophiacodontidae	Craddock Bonebed, Brush Creek, Craddock Ranch, North of Seymour, Baylor County, Texas	Late Kungurian	Femur
Varanosaurus	*acutirostris*	NM 15564	Ophiacodontidae	Craddock Bonebed, Brush Creek, Craddock Ranch, North of Seymour, Baylor County, Texas	Late Kungurian	Pubis
Varanosaurus	*acutirostris*	NM 15565	Ophiacodontidae	Craddock Bonebed, Brush Creek, Craddock Ranch, North of Seymour, Baylor County, Texas	Late Kungurian	Ischium
Varanosaurus	*witchitaensis*	MCZ 6379	Ophiacodontidae	Craddock Bonebed, Brush Creek, Craddock Ranch, North of Seymour, Baylor County, Texas	Late Kungurian	Astragulus, femur
Secodontosaurus	*obtusidens*	FMNH 754	Sphenacodontidae	Craddock Bonebed, Brush Creek, Craddock Ranch, North of Seymour, Baylor County, Texas	Late Kungurian	Maxilla and dentary
Secodontosaurus	*obtusidens*	WM 772	Sphenacodontidae	Craddock Bonebed, Brush Creek, Craddock Ranch, North of Seymour, Baylor County, Texas	Late Kungurian	Clavicle
Secodontosaurus	*obtusidens*	WM 1316	Sphenacodontidae	Craddock Bonebed, Brush Creek, Craddock Ranch, North of Seymour, Baylor County, Texas	Late Kungurian	Scapulocoracoid

Secodontosaurus	*obtusidens*	WM 752	Sphenacodontidae	Craddock Bonebed, Brush Creek, Craddock Ranch, North of Seymour, Baylor County, Texas	Late Kungurian	Partial scapula
Secodontosaurus	*obtusidens*	WM 757	Sphenacodontidae	Craddock Bonebed, Brush Creek, Craddock Ranch, North of Seymour, Baylor County, Texas	Late Kungurian	Proximal scapula
Secodontosaurus	*obtusidens*	WM 433	Sphenacodontidae	Craddock Bonebed, Brush Creek, Craddock Ranch, North of Seymour, Baylor County, Texas	Late Kungurian	Dentary
Dimetrodon	*natalis*		Sphenacodontidae	Craddock Bonebed, Brush Creek, Craddock Ranch, North of Seymour, Baylor County, Texas	Late Kungurian	Femora, humeri
Dimetrodon	*limbatus*		Sphenacodontidae	Craddock Bonebed, Brush Creek, Craddock Ranch, North of Seymour, Baylor County, Texas	Late Kungurian	
Dimetrodon	*gigashomogenes*	WM 1152	Sphenacodontidae	Craddock Bonebed, Brush Creek, Craddock Ranch, North of Seymour, Baylor County, Texas	Late Kungurian	Clavicle
Dimetrodon	*gigashomogenes*	WM 416	Sphenacodontidae	Craddock Bonebed, Brush Creek, Craddock Ranch, North of Seymour, Baylor County, Texas	Late Kungurian	Sacral vertebra
Dimetrodon	*gigashomogenes*	NM 8661	Sphenacodontidae	Craddock Bonebed, Brush Creek, Craddock Ranch, North of Seymour, Baylor County, Texas	Late Kungurian	Vertebrae

Dimetrodon	*grandis*	NM 8635	Sphenacodontidae	Craddock Bonebed, Brush Creek, Craddock Ranch, North of Seymour, Baylor County, Texas	Late Kungurian	Nearly complete skull, lower jaw, vertebrae, ribs, thoracic girdle, humeris, ulna radius, femur tibia and pes
Dimetrodon	*grandis*	NM 8661	Sphenacodontidae	Craddock Bonebed, Brush Creek, Craddock Ranch, North of Seymour, Baylor County, Texas	Late Kungurian	Sacrum
Dimetrodon	*grandis*	WM 765	Sphenacodontidae	Craddock Bonebed, Brush Creek, Craddock Ranch, North of Seymour, Baylor County, Texas	Late Kungurian	Partial dentary
Dimetrodon	*grandis*	WM 764	Sphenacodontidae	Craddock Bonebed, Brush Creek, Craddock Ranch, North of Seymour, Baylor County, Texas	Late Kungurian	Clavicle
Dimetrodon	*grandis*	WM 781	Sphenacodontidae	Craddock Bonebed, Brush Creek, Craddock Ranch, North of Seymour, Baylor County, Texas	Late Kungurian	Interclavicle
Dimetrodon	*grandis*	WM 1136	Sphenacodontidae	Craddock Bonebed, Brush Creek, Craddock Ranch, North of Seymour, Baylor County, Texas	Late Kungurian	Humerus
Dimetrodon	*grandis*	MCZ 1114	Sphenacodontidae	Craddock Bonebed, Brush Creek, Craddock Ranch, North of Seymour, Baylor County, Texas	Late Kungurian	Pelvis
Dimetrodon	*grandis*	MCZ 1118	Sphenacodontidae	Craddock Bonebed, Brush Creek, Craddock Ranch, North of Seymour, Baylor County, Texas	Late Kungurian	Femur

Dimetrodon	*grandis*	WM 857	Sphenacodontidae	Craddock Bonebed, Brush Creek, Craddock Ranch, North of Seymour, Baylor County, Texas	Late Kungurian	Femur
Dimetrodon	*grandis*	WM 779	Sphenacodontidae	Craddock Bonebed, Brush Creek, Craddock Ranch, North of Seymour, Baylor County, Texas	Late Kungurian	Tibia
Dimetrodon	*loomsi*	WM 1322	Sphenacodontidae	Craddock Bonebed, Brush Creek, Craddock Ranch, North of Seymour, Baylor County, Texas	Late Kungurian	Nearly complete skeleton
Dimetrodon	*loomsi*	WM 40	Sphenacodontidae	Craddock Bonebed, Brush Creek, Craddock Ranch, North of Seymour, Baylor County, Texas	Late Kungurian	Skull, jaws, postcranial fragments
Dimetrodon	*loomsi*	NM 8635	Sphenacodontidae	Craddock Bonebed, Brush Creek, Craddock Ranch, North of Seymour, Baylor County, Texas	Late Kungurian	Vertebral column, ribs and maxilla
Dimetrodon	*loomsi*	WM 1207	Sphenacodontidae	Craddock Bonebed, Brush Creek, Craddock Ranch, North of Seymour, Baylor County, Texas	Late Kungurian	Two brain cases
Dimetrodon	*loomsi*	WM 421	Sphenacodontidae	Craddock Bonebed, Brush Creek, Craddock Ranch, North of Seymour, Baylor County, Texas	Late Kungurian	Vertebrae, girdle and limb bones
Dimetrodon	*loomsi*	WM 591	Sphenacodontidae	Craddock Bonebed, Brush Creek, Craddock Ranch, North of Seymour, Baylor County, Texas	Late Kungurian	Maxilla

Dimetrodon	*loomsi*	WM 415	Sphenacodontidae	Craddock Bonebed, Brush Creek, Craddock Ranch, North of Seymour, Baylor County, Texas	Late Kungurian	Dentary
Dimetrodon	*loomsi*	WM 422	Sphenacodontidae	Craddock Bonebed, Brush Creek, Craddock Ranch, North of Seymour, Baylor County, Texas	Late Kungurian	Dentary
Dimetrodon	*loomsi*	WM 592	Sphenacodontidae	Craddock Bonebed, Brush Creek, Craddock Ranch, North of Seymour, Baylor County, Texas	Late Kungurian	Dentary
Dimetrodon	*loomsi*	WM 598	Sphenacodontidae	Craddock Bonebed, Brush Creek, Craddock Ranch, North of Seymour, Baylor County, Texas	Late Kungurian	Dentary
Dimetrodon	*loomsi*	WM 755	Sphenacodontidae	Craddock Bonebed, Brush Creek, Craddock Ranch, North of Seymour, Baylor County, Texas	Late Kungurian	Vertebrae
Dimetrodon	*loomsi*	WM 441	Sphenacodontidae	Craddock Bonebed, Brush Creek, Craddock Ranch, North of Seymour, Baylor County, Texas	Late Kungurian	Axis
Dimetrodon	*loomsi*	WM 596	Sphenacodontidae	Craddock Bonebed, Brush Creek, Craddock Ranch, North of Seymour, Baylor County, Texas	Late Kungurian	Cervical vertebra
Dimetrodon	*loomsi*	WM 757	Sphenacodontidae	Craddock Bonebed, Brush Creek, Craddock Ranch, North of Seymour, Baylor County, Texas	Late Kungurian	Clavicle, scapulocoracoid

Dimetrodon	*loomsi*	WM 149	Sphenacodontidae	Craddock Bonebed, Brush Creek, Craddock Ranch, North of Seymour, Baylor County, Texas	Late Kungurian	Radius, ulna
Dimetrodon	*loomsi*	NM 8862	Sphenacodontidae	Craddock Bonebed, Brush Creek, Craddock Ranch, North of Seymour, Baylor County, Texas	Late Kungurian	Hind limb bones
Dimetrodon	*loomsi*	WM 147	Sphenacodontidae	Craddock Bonebed, Brush Creek, Craddock Ranch, North of Seymour, Baylor County, Texas	Late Kungurian	Hind limb bones
Dimetrodon	*loomsi*	NM 8660	Sphenacodontidae	Craddock Bonebed, Brush Creek, Craddock Ranch, North of Seymour, Baylor County, Texas	Late Kungurian	Femur, tibia
Dimetrodon	*loomsi*	WM 426	Sphenacodontidae	Craddock Bonebed, Brush Creek, Craddock Ranch, North of Seymour, Baylor County, Texas	Late Kungurian	Clavicle
Dimetrodon	*loomsi*	WM 430	Sphenacodontidae	Craddock Bonebed, Brush Creek, Craddock Ranch, North of Seymour, Baylor County, Texas	Late Kungurian	Scapulocoracoid
Dimetrodon	*loomsi*	WM 571	Sphenacodontidae	Craddock Bonebed, Brush Creek, Craddock Ranch, North of Seymour, Baylor County, Texas	Late Kungurian	Scapulocoracoid
Dimetrodon	*loomsi*	WM 578	Sphenacodontidae	Craddock Bonebed, Brush Creek, Craddock Ranch, North of Seymour, Baylor County, Texas	Late Kungurian	Scapulocoracoid

Dimetrodon	*loomsi*	WM 579	Sphenacodontidae	Craddock Bonebed, Brush Creek, Craddock Ranch, North of Seymour, Baylor County, Texas	Late Kungurian	Scapulocoracoid
Dimetrodon	*loomsi*	WM 771	Sphenacodontidae	Craddock Bonebed, Brush Creek, Craddock Ranch, North of Seymour, Baylor County, Texas	Late Kungurian	Humerus
Dimetrodon	*loomsi*	WM 777	Sphenacodontidae	Craddock Bonebed, Brush Creek, Craddock Ranch, North of Seymour, Baylor County, Texas	Late Kungurian	Humerus
Dimetrodon	*loomsi*	WM 585	Sphenacodontidae	Craddock Bonebed, Brush Creek, Craddock Ranch, North of Seymour, Baylor County, Texas	Late Kungurian	Radius
Dimetrodon	*loomsi*	WM 791	Sphenacodontidae	Craddock Bonebed, Brush Creek, Craddock Ranch, North of Seymour, Baylor County, Texas	Late Kungurian	Radius
Dimetrodon	*loomsi*	WM 584	Sphenacodontidae	Craddock Bonebed, Brush Creek, Craddock Ranch, North of Seymour, Baylor County, Texas	Late Kungurian	Ulna
Dimetrodon	*loomsi*	WM 429	Sphenacodontidae	Craddock Bonebed, Brush Creek, Craddock Ranch, North of Seymour, Baylor County, Texas	Late Kungurian	Pelvic material
Dimetrodon	*loomsi*	WM 439	Sphenacodontidae	Craddock Bonebed, Brush Creek, Craddock Ranch, North of Seymour, Baylor County, Texas	Late Kungurian	Pelvic material

Dimetrodon	*loomsi*	WM 759	Sphenacodontidae	Craddock Bonebed, Brush Creek, Craddock Ranch, North of Seymour, Baylor County, Texas	Late Kungurian	Pelvic material
Dimetrodon	*loomsi*	WM 768	Sphenacodontidae	Craddock Bonebed, Brush Creek, Craddock Ranch, North of Seymour, Baylor County, Texas	Late Kungurian	Pelvic material
Dimetrodon	*loomsi*	WM 413	Sphenacodontidae	Craddock Bonebed, Brush Creek, Craddock Ranch, North of Seymour, Baylor County, Texas	Late Kungurian	Pelvic material
Dimetrodon	*loomsi*	WM 589	Sphenacodontidae	Craddock Bonebed, Brush Creek, Craddock Ranch, North of Seymour, Baylor County, Texas	Late Kungurian	Femur
Dimetrodon	*loomsi*	WM 776	Sphenacodontidae	Craddock Bonebed, Brush Creek, Craddock Ranch, North of Seymour, Baylor County, Texas	Late Kungurian	Femur
Dimetrodon	*loomsi*	WM 428	Sphenacodontidae	Craddock Bonebed, Brush Creek, Craddock Ranch, North of Seymour, Baylor County, Texas	Late Kungurian	Tibia
Dimetrodon	*kempae*	MCZ 1361	Sphenacodontidae	Craddock Bonebed, Brush Creek, Craddock Ranch, North of Seymour, Baylor County, Texas	Late Kungurian	Humerus
Trichasaurus	*texensis*	FMNH UC 652	Caseidae (Romer & Price 1940, Benson in press) (?), Edaphosauridae (Olson 1968) (?)	Craddock Bonebed, Brush Creek, Craddock Ranch, North of Seymour, Baylor County, Texas	Late Kungurian	Part of the vertebral column, pelvis, limb and foot elements

Edaphosaurus	*pogonias*	WM 163	Edaphosauridae	Craddock Bonebed, Brush Creek, Craddock Ranch, North of Seymour, Baylor County, Texas	Late Kungurian	Vertebral column
Edaphosaurus	*pogonias*	MCZ 1117	Edaphosauridae	Craddock Bonebed, Brush Creek, Craddock Ranch, North of Seymour, Baylor County, Texas	Late Kungurian	Partial scapulocoracoid
Edaphosaurus	*pogonias*	FMNH 239	Edaphosauridae	Craddock Bonebed, Brush Creek, Craddock Ranch, North of Seymour, Baylor County, Texas	Late Kungurian	Skull, left humerus, scapulocoracoid
Varanosaurus	*acutirostris*	AMNH 4174	Ophiacodontidae	Coffee Creek, Baylor/Willbarger County, Texas	Late Kungurian	Incomplete skeleton, with posterior portion of the skull, thoracic girdle and forelimb missing
Varanosaurus	*acutirostris*	FMNH UR 34	Ophiacodontidae	Coffee Creek, Baylor/Willbarger County, Texas	Late Kungurian	Facial portion of the skull
Edaphosaurus	*pogonias*	AM 4009	Edaphosauridae	Coffee Creek, Baylor/Willbarger County, Texas	Late Kungurian	Skull, jaws and axis
Edaphosaurus	*pogonias*	AM 4002	Edaphosauridae	Coffee Creek, Baylor/Willbarger County, Texas	Late Kungurian	Most of the presacral column, ribs and pelvis
Edaphosaurus	*pogonias*	WM 186	Edaphosauridae	Coffee Creek, Baylor/Willbarger County, Texas	Late Kungurian	Scapulocoracoid
Edaphosaurus	*pogonias*	AM 4037	Edaphosauridae	Coffee Creek, Baylor/Willbarger County, Texas	Late Kungurian	Spine material and clavicle

Edaphosaurus	*pogonias*	WM 16	Edaphosauridae	Coffee Creek, Baylor/Willbarger County, Texas	Late Kungurian	Two pelvic girdles
Edaphosaurus	*pogonias*	AM 4022	Edaphosauridae	Coffee Creek, Baylor/Willbarger County, Texas	Late Kungurian	Partial scapulocoracoid, spine material
Edaphosaurus	*pogonias*	AM 4038	Edaphosauridae	Coffee Creek, Baylor/Willbarger County, Texas	Late Kungurian	Fragments of vertebrae and spines
Edaphosaurus	*pogonias*	WM 1099	Edaphosauridae	Coffee Creek, Baylor/Willbarger County, Texas	Late Kungurian	Tibia
Edaphosaurus	*pogonias*	NM 10461	Edaphosauridae	Coffee Creek, Baylor/Willbarger County, Texas	Late Kungurian	Vertebrae and spines
Secodontosaurus	*obtusidens*	WM 1100	Sphenacodontidae	Coffee Creek, Baylor/Willbarger County, Texas	Late Kungurian	Pelvis and femur
Secodontosaurus	*obtusidens*	WM 25	Sphenacodontidae	Coffee Creek, Baylor/Willbarger County, Texas	Late Kungurian	Pelvis
Dimetrodon	*grandis*	WM 1002	Sphenacodontidae	Coffee Creek, Baylor/Willbarger County, Texas	Late Kungurian	Skull, most of the presacral column and spines, 14 caudals, scapulocoracoid, hind leg bones
Dimetrodon	*grandis*	UM VIIa	Sphenacodontidae	Coffee Creek, Baylor/Willbarger County, Texas	Late Kungurian	Skull
Dimetrodon	*grandis*	AM 4036	Sphenacodontidae	Coffee Creek, Baylor/Willbarger County, Texas	Late Kungurian	Partial skull

Dimetrodon	*grandis*	AM 4033	Sphenacodontidae	Coffee Creek, Baylor/Willbarger County, Texas	Late Kungurian	Jaw
Dimetrodon	*grandis*	WM 1132	Sphenacodontidae	Coffee Creek, Baylor/Willbarger County, Texas	Late Kungurian	Partial skull
Dimetrodon	*grandis*	AM 4169	Sphenacodontidae	Coffee Creek, Baylor/Willbarger County, Texas	Late Kungurian	Dentary and head of ulna
Dimetrodon	*grandis*	MCZ 1491	Sphenacodontidae	Coffee Creek, Baylor/Willbarger County, Texas	Late Kungurian	Skeleton fragments
Dimetrodon	*grandis*	AM 4644	Sphenacodontidae	Coffee Creek, Baylor/Willbarger County, Texas	Late Kungurian	Cervicals, scapulocoracoid, clavice, partial interclavicle
Dimetrodon	*grandis*	AM 4147	Sphenacodontidae	Coffee Creek, Baylor/Willbarger County, Texas	Late Kungurian	Axis
Dimetrodon	*loomsi*	AM 4037	Sphenacodontidae	Coffee Creek, Baylor/Willbarger County, Texas	Late Kungurian	Fragments of skull and dentary
Dimetrodon	*loomsi*	WM 1260	Sphenacodontidae	Coffee Creek, Baylor/Willbarger County, Texas	Late Kungurian	Fragments of skull and dentary
Dimetrodon	*loomsi*	WM 423	Sphenacodontidae	Coffee Creek, Baylor/Willbarger County, Texas	Late Kungurian	Braincase
Dimetrodon	*loomsi*	WM 114	Sphenacodontidae	Coffee Creek, Baylor/Willbarger County, Texas	Late Kungurian	Skeleton

Dimetrodon	*gigashomogenes*	WM 112	Sphenacodontidae	Coffee Creek, Baylor/Willbarger County, Texas	Late Kungurian	Pelvis, 2 cervical vertebrae, most posterior presacral vertebrae, some caudal vertebrae
Dimetrodon	*gigashomogenes*	MCZ 1283	Sphenacodontidae	Coffee Creek, Baylor/Willbarger County, Texas	Late Kungurian	Most of the skeleton
Dimetrodon	*gigashomogenes*	WM 1134	Sphenacodontidae	Coffee Creek, Baylor/Willbarger County, Texas	Late Kungurian	Jaw, braincase and postcranial material
Dimetrodon	*gigashomogenes*	AM 4035	Sphenacodontidae	Coffee Creek, Baylor/Willbarger County, Texas	Late Kungurian	Mounted series of 19 vertebrae with nearly complete neural spines
Dimetrodon	*gigashomogenes*	WM 639	Sphenacodontidae	Coffee Creek, Baylor/Willbarger County, Texas	Late Kungurian	Clavicle and interclavicle
Dimetrodon	*gigashomogenes*	MCZ 1340	Sphenacodontidae	Coffee Creek, Baylor/Willbarger County, Texas	Late Kungurian	Centra, partial shoulder girdle, humerus
Dimetrodon	*gigashomogenes*	MCZ 1109	Sphenacodontidae	Coffee Creek, Baylor/Willbarger County, Texas	Late Kungurian	Coracoid
Dimetrodon	*gigashomogenes*	WM 30	Sphenacodontidae	Coffee Creek, Baylor/Willbarger County, Texas	Late Kungurian	Scapulocoracoid
Dimetrodon	*gigashomogenes*	YP 661	Sphenacodontidae	Coffee Creek, Baylor/Willbarger County, Texas	Late Kungurian	Scapulocoracoid
Dimetrodon	*gigashomogenes*	AM 4149	Sphenacodontidae	Coffee Creek, Baylor/Willbarger County, Texas	Late Kungurian	Humerus

Dimetrodon	*gigashomogenes*	AM 4037	Sphenacodontidae	Coffee Creek, Baylor/Willbarger County, Texas	Late Kungurian	Humerus
Dimetrodon	*gigashomogenes*	UM 3410	Sphenacodontidae	Coffee Creek, Baylor/Willbarger County, Texas	Late Kungurian	Femur
Dimetrodon	*gigashomogenes*	WM 8	Sphenacodontidae	Coffee Creek, Baylor/Willbarger County, Texas	Late Kungurian	Femur
Dimetrodon	*gigashomogenes*	WM 465	Sphenacodontidae	Coffee Creek, Baylor/Willbarger County, Texas	Late Kungurian	Pelvis
Dimetrodon	*gigashomogenes*	WM 1019	Sphenacodontidae	Coffee Creek, Baylor/Willbarger County, Texas	Late Kungurian	3 Lumbar vertebrae
Dimetrodon	*gigashomogenes*	Munich	Sphenacodontidae	Coffee Creek, Baylor/Willbarger County, Texas	Late Kungurian	Pelvis
Dimetrodon	*gigashomogenes*	AM 4103	Sphenacodontidae	Coffee Creek, Baylor/Willbarger County, Texas	Late Kungurian	Interclavicle
Dimetrodon	*loomsi*	FM UR 2333	Sphenacodontidae	South Garfield, Tillman County, Oklahoma	Late Kungurian	Axis
Dimetrodon	*loomsi*	FM UR 2334	Sphenacodontidae	South Garfield, Tillman County, Oklahoma	Late Kungurian	Dorsal vertebra without spine
Dimetrodon	*loomsi*	FM UR 2332	Sphenacodontidae	South Garfield, Tillman County, Oklahoma	Late Kungurian	Spine fragments, teeth, flat pieces of bone
Cotylorhynchus	*romeri*	OUSM 4-0-S1	Caseidae	Ross Farm, 4.75 miles west of Navina, Logan County, Oklahoma	Late Kungurian	Right side of the skull, portion of the interclavicle, one manus
Cotylorhynchus	*romeri*	OUSM 4-0-S2	Caseidae	Pierce Farm, Cleveland County, Oklahoma	Late Kungurian	Caudal vertebrae, pelvis, hindlimb

Cotylorhynchus	*romeri*	OUSM 4-0-S8	Caseidae	Pierce Farm, Cleveland County, Oklahoma	Late Kungurian	Anterior skeleton, first 19 vertebrae, ribs, humeri, scapulae
Cotylorhynchus	*romeri*	OUSM 4-11-S1	Caseidae	Pierce Farm, Cleveland County, Oklahoma	Late Kungurian	3 ribs
Cotylorhynchus	*romeri*	OUSM 4-0-S3	Caseidae	Near Norman, Cleveland County, Oklahoma	Late Kungurian	Partial skeleton
Cotylorhynchus	*romeri*	OUSM 4-0-S13	Caseidae	Near Norman, Cleveland County, Oklahoma	Late Kungurian	Partial skeleton
Cotylorhynchus	*romeri*	OUSM 4-0-S16	Caseidae	Near Norman, Cleveland County, Oklahoma	Late Kungurian	Foot, radius, humerus, tibia, fibula, femur, vertebrae, pelvis
Cotylorhynchus	*romeri*	OUSM 4-1-S2	Caseidae	Near Norman, Cleveland County, Oklahoma	Late Kungurian	Partial skull and lower jaws
Cotylorhynchus	*romeri*	OUSM 4-1-S5	Caseidae	Near Norman, Cleveland County, Oklahoma	Late Kungurian	Skull and jaws
Cotylorhynchus	*romeri*	OUSM 4-1-S10	Caseidae	Near Norman, Cleveland County, Oklahoma	Late Kungurian	Skull and jaws
Cotylorhynchus	*romeri*	OUSM 4-8-S1	Caseidae	Near Norman, Cleveland County, Oklahoma	Late Kungurian	Lumbar vertebrae
Cotylorhynchus	*romeri*	OUSM 4-12-S1	Caseidae	Near Norman, Cleveland County, Oklahoma	Late Kungurian	Scapula, humerus, radius, phalanges, foot
Cotylorhynchus	*romeri*	OUSM 4-32-S1	Caseidae	Near Norman, Cleveland County, Oklahoma	Late Kungurian	Fragments
Cotylorhynchus	*romeri*	Stovall Museum No. 1250	Caseidae	Near Norman, Cleveland County, Oklahoma	Late Kungurian	Skeleton
Cotylorhynchus	*romeri*	FMNH PR 272	Caseidae	Near Norman, Cleveland County, Oklahoma	Late Kungurian	Skeleton lacking skull
Cotylorhynchus	*romeri*	USNM	Caseidae	Near Norman, Cleveland County, Oklahoma	Late Kungurian	Skeleton lacking skull
Cotylorhynchus	*romeri*	AMNH	Caseidae	Near Norman, Cleveland County, Oklahoma	Late Kungurian	Skeleton lacking skull
Cotylorhynchus	*romeri*	MCZ	Caseidae	Near Norman, Cleveland County, Oklahoma	Late Kungurian	Skeleton lacking skull

Cotylorhynchus	*romeri*	OUSM 4-0-S4	Caseidae	Polk Farm, Cleveland County, Oklahoma	Late Kungurian	4 1/2 caudal vertebrae, pelvis
Cotylorhynchus	*romeri*	OUSM 4-0-S5	Caseidae	Polk Farm, Cleveland County, Oklahoma	Late Kungurian	Radius, ulna, front foot, part of second foot
Cotylorhynchus	*romeri*	OUSM 4-0-S21	Caseidae	Polk Farm, Cleveland County, Oklahoma	Late Kungurian	Mounted skeleton (Stovall museum 1251)
Cotylorhynchus	*romeri*	OUSM 4-0-S21	Caseidae	Polk Farm, Cleveland County, Oklahoma	Late Kungurian	Ribs, humerus, right pes and manus, part pelvis
Cotylorhynchus	*romeri*	OUSM 4-0-S23	Caseidae	Polk Farm, Cleveland County, Oklahoma	Late Kungurian	Skull
Cotylorhynchus	*romeri*	OUSM 4-10-S2	Caseidae	Polk Farm, Cleveland County, Oklahoma	Late Kungurian	Vertebral column
Cotylorhynchus	*romeri*	OUSM 4-0-S6	Caseidae	Boggs Farm, Cleveland County, Oklahoma	Late Kungurian	Part of foot
Cotylorhynchus	*romeri*	OUSM 4-0-S10	Caseidae	Boggs Farm, Cleveland County, Oklahoma	Late Kungurian	Skeleton
Cotylorhynchus	*romeri*	OUSM 4-0-S11	Caseidae	Boggs Farm, Cleveland County, Oklahoma	Late Kungurian	Foot, tarsals, metetarsals, phalanges, 10 ribs, fragments of vertebrae pelvis, femur
Cotylorhynchus	*romeri*	OUSM 4-0-S9	Caseidae	SW 1/4 Section 7, Cleveland County, Oklahoma	Late Kungurian	Fragments, ribs
Cotylorhynchus	*romeri*	OUSM 4-0-S14	Caseidae	Burton Farm, Oklahoma	Late Kungurian	Ribs, part of foot
Cotylorhynchus	*romeri*	OUSM 4-0-S17	Caseidae	Burton Farm, Oklahoma	Late Kungurian	Fragments, mostly ribs
Cotylorhynchus	*romeri*	OUSM 4-0-S18	Caseidae	Burgess Farm, Cleveland County, Oklahoma	Late Kungurian	Partial skeleton
Cotylorhynchus	*romeri*	OUSM 4-0-S20	Caseidae	South of Cedar Lane Golf Course, Cleveland County, Oklahoma	Late Kungurian	Skull, shoulder girdle, left forelimb, foot
Cotylorhynchus	*romeri*	OUSM 4-0-S21	Caseidae	South Oklahoma City, Cleveland County, Oklahoma	Late Kungurian	Incomplete skeleton

Cotylorhynchus	*romeri*	OUSM 4-0-S24	Caseidae	3 miles north of Norman on Highway 77, Cleveland County, Oklahoma	Late Kungurian	Partial skeleton
Cotylorhynchus	*romeri*	OUSM 4-0-S26	Caseidae	Richardsom farm, South of Highway 9, Cleveland County, Oklahoma	Late Kungurian	Partial postcranial skeleton
Cotylorhynchus	*romeri*	OUSM 4-0-S28	Caseidae	Noble, Cleveland County, Oklahoma	Late Kungurian	Fragments
Cotylorhynchus	*romeri*	OUSM 4-1-S3	Caseidae	NE 1/4 Section 15	Late Kungurian	Indeterminate bones
Dimetrodon	*gigashomogenes*	CNHM UR 123	Sphenacodontidae	Locality BZ, Knox County, Texas	Late Kungurian	Maxilla and teeth
Dimetrodon	*gigashomogenes*	CNHM UR 30	Sphenacodontidae	Locality KF, Knox County, Texas	Late Kungurian	Maxilla and teeth
Dimetrodon	*gigashomogenes*	CMNH UR 33	Sphenacodontidae	Locality KD, Knox County, Texas	Late Kungurian	Dorsal vertebrae, femur, skull fragments
Dimetrodon	*gigashomogenes*	CMNH UR 34	Sphenacodontidae	Locality KA, Knox County, Texas	Late Kungurian	Partial vertebral column, cervicals 4 and 5, presacrals 20-27, three sacrals and one caudal
Casea	*nicholsi*	CNHM UR 85	Caseidae	KC Locality, Knox County, Texas	Late Kungurian	Posterior portion of skull, pre-caudal vertebral column, partial shoulder girdle, pelvis, femure, proximal fibula
Casea	*nicholsi*	CNHM UR 86	Caseidae	KC Locality, Knox County, Texas	Late Kungurian	Partial basal skull, lower jaw, pre-caudal column, partial pelvis, forelimb, partial pes
Dimetrodon	*gigashomogenes*	CMNH UR 128	Sphenacodontidae	Locality FA, Foard County, Texas	Late Kungurian	14 vertebrae with spines (7-20), partial skull and lower jaw, pelvis, distal femur, other fragments
Dimetrodon	*gigashomogenes*	CMNH UR 122	Sphenacodontidae	Locality FA, Foard County, Texas	Late Kungurian	Dorsal vertebra
Casea	*halselli*	FMNH UR 117	Caseidae	FC Locality, Halsell Ranch, Foard County, Texas	Late Kungurian	Pelvic girdle, partial left femur and tibia, head of right femur, 5 caudal vertebrae lacking arches, fragments of lumbar vertebrae

Caseopsis	*agilis*	FMNH UR 253	Caseidae	Locality KV, MacFayden Ranch, Knox County, Texas	Early Roadian	Partial skull and lower jaw, lumbar vertebra, fragments of other vertebrae, partial left scapula, radius, ulna, pelvis, femur, partial tibia and fibula, parts of the pes
Cotylorhynchus	*hancocki*	CNHM UR 249	Caseidae	Locality KV, MacFayden Ranch, Knox County, Texas	Early Roadian	Humerus and ulna
Cotylorhynchus	*hancocki*	CNHM UR 5250	Caseidae	Locality KV, MacFayden Ranch, Knox County, Texas	Early Roadian	Six vertebrae and ribs
Dimetrodon	*angelensis*	CNHM UR 32	Sphenacodontidae	Locality KV, MacFayden Ranch, Knox County, Texas	Early Roadian	Skull, lower jaw, 4 cervical vertebrae, ulna
Cotylorhynchus	*hancocki*	CNHM UR 144	Caseidae	Locality KN, Little Croton Creek, Knox County, Texas	Early Roadian	Four ribs
Angelosaurus	*dolani*	FMNH UR 149	Caseidae	Locality KN, Little Croton Creek, Knox County, Texas	Early Roadian	Posterior part of the skeleton, some anterior vertebrae, humerus, fragments of skull and jaws
Angelosaurus	*dolani*	FMNH UR 701	Caseidae	Locality KN, Little Croton Creek, Knox County, Texas	Early Roadian	Fragmentary vertebrae
Caseoides	*sanageloensis*	FMNH UR 151	Caseidae	KP Locality, Little Croton Creek, Knox County, Texas	Early Roadian	Right hindlimb, part of foot, left femur, humerus, fragments of vertebra
Caseoides	*sanageloensis*	FMNH UR 152	Caseidae	KP Locality, Little Croton Creek, Knox County, Texas	Early Roadian	Left femur, dorsal ilium, symphysial region of pubish, centrum
Cotylorhynchus	*hancocki*	CNHM UR 480	Caseidae	KY Locality, Driver Ranch, Knox Countz, Texas	Early Roadian	Ischium, parts of the pelvis, ribs, fragments of vertebrae

Cotylorhynchus	*hancocki*	CNHM UR 481	Caseidae	KY Locality, Driver Ranch, Knox Countz, Texas	Early Roadian	Distal humerus, lumbar vertebrae, fragments
Cotylorhynchus	*hancocki*	CNHM UR 563	Caseidae	KY Locality, Driver Ranch, Knox Countz, Texas	Early Roadian	Humerus, ribs, partial pelvis
Dimetrodon	*angelensis*	CMNH UR 482	Sphenacodontidae	KY Locality, Driver Ranch, Knox Countz, Texas	Early Roadian	Vertebrae, scapula, fragments of skull and ribs
Cotylorhynchus	*hancocki*	CNHM UR 487	Caseidae	KAC Locality, Kahn Quarry, Knox County, Texas	Early Roadian	Two scapulocoracoids
Cotylorhynchus	*hancocki*	CNHM UR 488	Caseidae	KAC Locality, Kahn Quarry, Knox County, Texas	Early Roadian	Two humeris, one femur
Cotylorhynchus	*hancocki*	CNHM UR 489	Caseidae	KAC Locality, Kahn Quarry, Knox County, Texas	Early Roadian	Partial skull
Cotylorhynchus	*hancocki*	CNHM UR 490	Caseidae	KAC Locality, Kahn Quarry, Knox County, Texas	Early Roadian	Partial skull and dentition
Cotylorhynchus	*hancocki*	CNHM UR 491	Caseidae	KAC Locality, Kahn Quarry, Knox County, Texas	Early Roadian	Lower jaw and dentition
Cotylorhynchus	*hancocki*	CNHM UR 492	Caseidae	KAC Locality, Kahn Quarry, Knox County, Texas	Early Roadian	Partial lower jaw and dentition
Cotylorhynchus	*hancocki*	CNHM UR 493	Caseidae	KAC Locality, Kahn Quarry, Knox County, Texas	Early Roadian	Lower jaw and dentition

Cotylorhynchus	*hancocki*	CNHM UR 494	Caseidae	KAC Locality, Kahn Quarry, Knox County, Texas	Early Roadian	Partial lower jaw and dentition
Cotylorhynchus	*hancocki*	CNHM UR 500	Caseidae	KAC Locality, Kahn Quarry, Knox County, Texas	Early Roadian	Fragment of jaw
Cotylorhynchus	*hancocki*	CNHM UR 504	Caseidae	KAC Locality, Kahn Quarry, Knox County, Texas	Early Roadian	Caudal vertebrae
Cotylorhynchus	*hancocki*	CNHM UR 506	Caseidae	KAC Locality, Kahn Quarry, Knox County, Texas	Early Roadian	Humerus shaft
Cotylorhynchus	*hancocki*	CNHM UR 564	Caseidae	KAC Locality, Kahn Quarry, Knox County, Texas	Early Roadian	Two dorsal vertebrae
Cotylorhynchus	*hancocki*	CNHM UR 565	Caseidae	KAC Locality, Kahn Quarry, Knox County, Texas	Early Roadian	Five vertebrae, limb bone
Cotylorhynchus	*hancocki*	CNHM UR 567	Caseidae	KAC Locality, Kahn Quarry, Knox County, Texas	Early Roadian	Right ulna
Cotylorhynchus	*hancocki*	CNHM UR 568	Caseidae	KAC Locality, Kahn Quarry, Knox County, Texas	Early Roadian	Caudal vertebrae
Cotylorhynchus	*hancocki*	CNHM UR 569	Caseidae	KAC Locality, Kahn Quarry, Knox County, Texas	Early Roadian	Dorsal vertebrae
Cotylorhynchus	*hancocki*	CNHM UR 571	Caseidae	KAC Locality, Kahn Quarry, Knox County, Texas	Early Roadian	Third or fourth presacral vertebra, one caudal vertebra, ulna, partial femur, ribs

Cotylorhynchus	*hancocki*	CNHM UR 580	Caseidae	KAC Locality, Kahn Quarry, Knox County, Texas	Early Roadian	Sacral vertebrae, four partial posterior presacral vertebrae, sacral rib
Cotylorhynchus	*hancocki*	CNHM UR 581	Caseidae	KAC Locality, Kahn Quarry, Knox County, Texas	Early Roadian	Nearly complete skeleton
Cotylorhynchus	*hancocki*	CNHM UR 585	Caseidae	KAC Locality, Kahn Quarry, Knox County, Texas	Early Roadian	Ulna
Cotylorhynchus	*hancocki*	CNHM UR 586	Caseidae	KAC Locality, Kahn Quarry, Knox County, Texas	Early Roadian	Tibia, partial femur
Cotylorhynchus	*hancocki*	CNHM UR 621	Caseidae	KAC Locality, Kahn Quarry, Knox County, Texas	Early Roadian	Partial skeleton and skull
Cotylorhynchus	*hancocki*	CNHM UR 622	Caseidae	KAC Locality, Kahn Quarry, Knox County, Texas	Early Roadian	Partial skeleton, braincase and palate
Cotylorhynchus	*hancocki*	CNHM UR 623	Caseidae	KAC Locality, Kahn Quarry, Knox County, Texas	Early Roadian	Ulna
Cotylorhynchus	*hancocki*	CNHM UR 624	Caseidae	KAC Locality, Kahn Quarry, Knox County, Texas	Early Roadian	Fragments of skull and teeth
Cotylorhynchus	*hancocki*	CNHM UR 625	Caseidae	KAC Locality, Kahn Quarry, Knox County, Texas	Early Roadian	Unguals
Cotylorhynchus	*hancocki*	CNHM UR 626	Caseidae	KAC Locality, Kahn Quarry, Knox County, Texas	Early Roadian	Caudal vertebrae and limb bones

Cotylorhynchus	*hancocki*	CNHM UR 703	Caseidae	KAC Locality, Kahn Quarry, Knox County, Texas	Early Roadian	Vertebrae, caudal, sacral, lumbar and dorsal vertebrae, pelvis, femur, radius, ulna and ribs
Cotylorhynchus	*hancocki*	CNHM UR 704	Caseidae	KAC Locality, Kahn Quarry, Knox County, Texas	Early Roadian	Phalanx
Cotylorhynchus	*hancocki*	CNHM UR 705	Caseidae	KAC Locality, Kahn Quarry, Knox County, Texas	Early Roadian	Dorsal vertebra
Cotylorhynchus	*hancocki*	CNHM UR 706	Caseidae	KAC Locality, Kahn Quarry, Knox County, Texas	Early Roadian	Dorsal vertebra
Cotylorhynchus	*hancocki*	CNHM UR 707	Caseidae	KAC Locality, Kahn Quarry, Knox County, Texas	Early Roadian	Tibia
Cotylorhynchus	*hancocki*	CNHM UR 708	Caseidae	KAC Locality, Kahn Quarry, Knox County, Texas	Early Roadian	Interclavicle
Cotylorhynchus	*hancocki*	CNHM UR 709	Caseidae	KAC Locality, Kahn Quarry, Knox County, Texas	Early Roadian	Vertebra
Cotylorhynchus	*hancocki*	CNHM UR 710	Caseidae	KAC Locality, Kahn Quarry, Knox County, Texas	Early Roadian	Vertebra
Cotylorhynchus	*hancocki*	CNHM UR 718	Caseidae	KAC Locality, Kahn Quarry, Knox County, Texas	Early Roadian	Vertebrae and pedal phalanges
Cotylorhynchus	*hancocki*	CNHM UR 719	Caseidae	KAC Locality, Kahn Quarry, Knox County, Texas	Early Roadian	Cervical vertebrae and ribs

Cotylorhynchus	*hancocki*	CNHM UR 720	Caseidae	KAC Locality, Kahn Quarry, Knox County, Texas	Early Roadian	Vertebrae, ribs and clavicle
Cotylorhynchus	*hancocki*	CNHM UR 821	Caseidae	KAC Locality, Kahn Quarry, Knox County, Texas	Early Roadian	Vertebrae and ribs
Cotylorhynchus	*hancocki*	CNHM UR 822	Caseidae	KAC Locality, Kahn Quarry, Knox County, Texas	Early Roadian	Humerus and scapulocoracoid
Cotylorhynchus	*hancocki*	CNHM UR 823	Caseidae	KAC Locality, Kahn Quarry, Knox County, Texas	Early Roadian	Humerus
Cotylorhynchus	*hancocki*	FMNH UR 875	Caseidae	KAC Locality, Kahn Quarry, Knox County, Texas	Early Roadian	Pelvis
Cotylorhynchus	*hancocki*	FMNH UR 877	Caseidae	KAC Locality, Kahn Quarry, Knox County, Texas	Early Roadian	Clavicle, rib, cervical vertebrae
Cotylorhynchus	*hancocki*	FMNH UR 878	Caseidae	KAC Locality, Kahn Quarry, Knox County, Texas	Early Roadian	Femur and fibula
Cotylorhynchus	*hancocki*	FMNH UR 879	Caseidae	KAC Locality, Kahn Quarry, Knox County, Texas	Early Roadian	Humerus, clavicle, rib, radiusm 8 vertebrae, chevron
Cotylorhynchus	*hancocki*	FMNH UR 881	Caseidae	KAC Locality, Kahn Quarry, Knox County, Texas	Early Roadian	Tibia
Cotylorhynchus	*hancocki*	FMNH UR 892	Caseidae	KAC Locality, Kahn Quarry, Knox County, Texas	Early Roadian	Scapulocoracoid, 2 vertebrae

Cotylorhynchus	*hancocki*	FMNH UR 893	Caseidae	KAC Locality, Kahn Quarry, Knox County, Texas	Early Roadian	Tibia, sacral vertebrae
Cotylorhynchus	*hancocki*	FMNH UR 894	Caseidae	KAC Locality, Kahn Quarry, Knox County, Texas	Early Roadian	Partial pelvis, 2 sacral vertebrae, one caudal veretbra
Cotylorhynchus	*hancocki*	CNHM UR 582	Caseidae	KAD locality, Driver Ranch, Knox County, Texas	Early Roadian	Partial pelvis
Cotylorhynchus	*hancocki*	CNHM UR 479	Caseidae	KX locality, Driver Ranch, Knox County, Texas	Early Roadian	Third or fourth presacral vertegbra, four dorsal vertebrae, nine caudal vertebrae, parts of ribs, partial femur, clavicle, scapulocoracoid
Cotylorhynchus	*hancocki*	CNHM UR 154	Caseidae	Locality HA, North of the Pease River on the Crowell Quanah highway, Hardeman County, Texas	Early Roadian	Right humerus, proximal radius
Cotylorhynchus	*hancocki*	CNHM UR 483	Caseidae	KAB Locality, Driver Ranch, Knox County, Texas	Early Roadian	Several partial caudal vertebrae
Caseopsis	*agilis (?)*	CNHM UR 255	Caseidae	KR Locality, Alexander Ranch, Knox County, Texas	Early Roadian	Proximal radius, tibia, fibula, distal femur, rib fragments
Cotylorhynchus	*hancocki*	CNHM UR 266	Caseidae	KR Locality, Alexander Ranch, Knox County, Texas	Early Roadian	Ribs, distal humerus
Angelosaurus	*greeni*	CNHM UR 257	Caseidae	KR Locality, Alexander Ranch, Knox County, Texas	Early Roadian	Femur, vertebra, part of rib
Angelosaurus	*greeni*	CNHM UR 258	Caseidae	KR Locality, Alexander Ranch, Knox County, Texas	Early Roadian	Distal Humerus

Angelosaurus	*greeni*	CNHM UR 259	Caseidae	KT Locality, Alexander Ranch, Knox County, Texas	Early Roadian	Humerus
Angelosaurus	*greeni*	CNHM UR 264	Caseidae	KS Locality, Alexander Ranch, Knox County, Texas	Early Roadian	Fragments of Pelvis, distal limb elements
Phreatophasma	*aenigmaticum*	PIN 294-24	Caseidae (?) (Olson 1962), Phreatosuchidae, Dinocephalia (?) (Ivakhnenko 1991)	Santagulov Mine, on the Dema River, Baskir Province, Baskortosan	Roadian	Femur
Varanodon	*agilis*	CNHM UR 986	Varanopidae	Locality BC-8, 3 miles north of Hitchcock, Blaine County, Oklahoma	Roadian	Skull, lower jaws, vertebrae, ribs, shoulder girdles, forelimbs and manus
Cotylorhynchus	*bransoni*	FMNH UR 983	Caseidae	Locality BC-2, Blaine County, Oklahoma	Roadian	Dorsal vertebrae
Cotylorhynchus	*bransoni*	FMNH UR 972	Caseidae	BC-6 Locality, Blaine County, Oklahoma	Roadian	Caudal vertebrae
Watongia	*meieri*	UCMP 143278	Varanopidae	BC-7 Locality, Blaine County, Oklahoma	Roadian	Skull fragments, incomplete forelimbs, shoulder girdle, a few vertebrae, gastralia and ribs
Cotylorhynchus	*bransoni*	FMNH UR 984	Caseidae	BC-7 Locality, Blaine County, Oklahoma	Roadian	Partial humerus
Cotylorhynchus	*bransoni*	FMNH UR 988	Caseidae	BC-7 Locality, Blaine County, Oklahoma	Roadian	Base of pelvis, hind foot
Cotylorhynchus	*bransoni*	FMNH UR 835	Caseidae	KF-1 Locality, Omega Quarry, Kingfisher County, Ohklahoma	Roadian	Left pelvis, left femur, partial sacral rib
Cotylorhynchus	*bransoni*	FMNH UR 836	Caseidae	KF-1 Locality, Omega Quarry, Kingfisher County, Ohklahoma	Roadian	Foot

Cotylorhynchus	*bransoni*	FMNH UR 837	Caseidae	KF-1 Locality, Omega Quarry, Kingfisher County, Ohklahoma	Roadian	Partial forelimb
Cotylorhynchus	*bransoni*	FMNH UR 838	Caseidae	KF-1 Locality, Omega Quarry, Kingfisher County, Ohklahoma	Roadian	Astragulus
Cotylorhynchus	*bransoni*	FMNH UR 839	Caseidae	KF-1 Locality, Omega Quarry, Kingfisher County, Ohklahoma	Roadian	Tibia
Cotylorhynchus	*bransoni*	FMNH UR 840	Caseidae	KF-1 Locality, Omega Quarry, Kingfisher County, Ohklahoma	Roadian	Fibula
Cotylorhynchus	*bransoni*	FMNH UR 841	Caseidae	KF-1 Locality, Omega Quarry, Kingfisher County, Ohklahoma	Roadian	Maxilla and two teeth
Cotylorhynchus	*bransoni*	FMNH UR 842	Caseidae	KF-1 Locality, Omega Quarry, Kingfisher County, Ohklahoma	Roadian	Ungual
Cotylorhynchus	*bransoni*	FMNH UR 843	Caseidae	KF-1 Locality, Omega Quarry, Kingfisher County, Ohklahoma	Roadian	Ungual
Cotylorhynchus	*bransoni*	FMNH UR 910	Caseidae	KF-1 Locality, Omega Quarry, Kingfisher County, Ohklahoma	Roadian	Cervical ribs
Cotylorhynchus	*bransoni*	FMNH UR 912	Caseidae	KF-1 Locality, Omega Quarry, Kingfisher County, Ohklahoma	Roadian	Clavicle

Cotylorhynchus	*bransoni*	FMNH UR 913	Caseidae	KF-1 Locality, Omega Quarry, Kingfisher County, Ohklahoma	Roadian	Chevron
Cotylorhynchus	*bransoni*	FMNH UR 915	Caseidae	KF-1 Locality, Omega Quarry, Kingfisher County, Ohklahoma	Roadian	Series of vertebrae
Cotylorhynchus	*bransoni*	FMNH UR 918	Caseidae	KF-1 Locality, Omega Quarry, Kingfisher County, Ohklahoma	Roadian	Scapulocoracoid
Cotylorhynchus	*bransoni*	FMNH UR 919	Caseidae	KF-1 Locality, Omega Quarry, Kingfisher County, Ohklahoma	Roadian	Scapulocoracoid
Cotylorhynchus	*bransoni*	FMNH UR 923	Caseidae	KF-1 Locality, Omega Quarry, Kingfisher County, Ohklahoma	Roadian	Sacral vertebrae
Cotylorhynchus	*bransoni*	FMNH UR 929	Caseidae	KF-1 Locality, Omega Quarry, Kingfisher County, Ohklahoma	Roadian	Pterygoid
Cotylorhynchus	*bransoni*	FMNH UR 937	Caseidae	KF-1 Locality, Omega Quarry, Kingfisher County, Ohklahoma	Roadian	Caudal vertebrae
Cotylorhynchus	*bransoni*	FMNH UR 982	Caseidae	KF-1 Locality, Omega Quarry, Kingfisher County, Ohklahoma	Roadian	4 dorsal vertebrae
Angelosaurus	*romeri*	FMNH UR 827	Caseidae	KF-1 Locality, Omega Quarry, Kingfisher County, Ohklahoma	Roadian	Pelvis, right femur, 16 presacral vertebrae, 3 sacral vertebrae, 4 caudal vertebrae

Angelosaurus	*romeri*	FMNH UR 828	Caseidae	KF-1 Locality, Omega Quarry, Kingfisher County, Ohklahoma	Roadian	2 sacral, 2 presacral vertebrae
Angelosaurus	*romeri*	FMNH UR 844	Caseidae	KF-1 Locality, Omega Quarry, Kingfisher County, Ohklahoma	Roadian	Partial right pelvis
Angelosaurus	*romeri*	FMNH UR 845	Caseidae	KF-1 Locality, Omega Quarry, Kingfisher County, Ohklahoma	Roadian	Pubis
Angelosaurus	*romeri*	FMNH UR 846	Caseidae	KF-1 Locality, Omega Quarry, Kingfisher County, Ohklahoma	Roadian	Interclavicle
Angelosaurus	*romeri*	FMNH UR 847	Caseidae	KF-1 Locality, Omega Quarry, Kingfisher County, Ohklahoma	Roadian	Dorsal rib
Angelosaurus	*romeri*	FMNH UR 848	Caseidae	KF-1 Locality, Omega Quarry, Kingfisher County, Ohklahoma	Roadian	Dorsal rib
Angelosaurus	*romeri*	FMNH UR 849	Caseidae	KF-1 Locality, Omega Quarry, Kingfisher County, Ohklahoma	Roadian	Dorsal rib
Angelosaurus	*romeri*	FMNH UR 850	Caseidae	KF-1 Locality, Omega Quarry, Kingfisher County, Ohklahoma	Roadian	Dorsal rib
Angelosaurus	*romeri*	FMNH UR 851	Caseidae	KF-1 Locality, Omega Quarry, Kingfisher County, Ohklahoma	Roadian	Dorsal rib

Angelosaurus	*romeri*	FMNH UR 853	Caseidae	KF-1 Locality, Omega Quarry, Kingfisher County, Ohklahoma	Roadian	4 anterior caudal vertebrae
Angelosaurus	*romeri*	FMNH UR 854	Caseidae	KF-1 Locality, Omega Quarry, Kingfisher County, Ohklahoma	Roadian	Fragment of snout, 2 teeth
Angelosaurus	*romeri*	FMNH UR 904	Caseidae	KF-1 Locality, Omega Quarry, Kingfisher County, Ohklahoma	Roadian	Sacrum, 4 sacral vertebrae
Angelosaurus	*romeri*	FMNH UR 907	Caseidae	KF-1 Locality, Omega Quarry, Kingfisher County, Ohklahoma	Roadian	Right scapulocoracoid and humerus
Angelosaurus	*romeri*	FMNH UR 908	Caseidae	KF-1 Locality, Omega Quarry, Kingfisher County, Ohklahoma	Roadian	20 presacral vertebrae
Angelosaurus	*romeri*	FMNH UR 909	Caseidae	KF-1 Locality, Omega Quarry, Kingfisher County, Ohklahoma	Roadian	Left scapulocoracoid
Angelosaurus	*romeri*	FMNH UR 911	Caseidae	KF-1 Locality, Omega Quarry, Kingfisher County, Ohklahoma	Roadian	Tibia
Angelosaurus	*romeri*	FMNH UR 914	Caseidae	KF-1 Locality, Omega Quarry, Kingfisher County, Ohklahoma	Roadian	Pedal phalanges
Angelosaurus	*romeri*	FMNH UR 916	Caseidae	KF-1 Locality, Omega Quarry, Kingfisher County, Ohklahoma	Roadian	3 presacral vertebrae and ribs

Angelosaurus	*romeri*	FMNH UR 917	Caseidae	KF-1 Locality, Omega Quarry, Kingfisher County, Ohklahoma	Roadian	Left femur
Angelosaurus	*romeri*	FMNH UR 926	Caseidae	KF-1 Locality, Omega Quarry, Kingfisher County, Ohklahoma	Roadian	Maxillary, with 2 teeth
Angelosaurus	*romeri*	FMNH UR 927	Caseidae	KF-1 Locality, Omega Quarry, Kingfisher County, Ohklahoma	Roadian	Brain case and partial palate
Angelosaurus	*romeri*	FMNH UR 928	Caseidae	KF-1 Locality, Omega Quarry, Kingfisher County, Ohklahoma	Roadian	Large rib
Angelosaurus	*romeri*	FMNH UR 931	Caseidae	KF-1 Locality, Omega Quarry, Kingfisher County, Ohklahoma	Roadian	Pterygoid
Angelosaurus	*romeri*	FMNH UR 932	Caseidae	KF-1 Locality, Omega Quarry, Kingfisher County, Ohklahoma	Roadian	Anterior dorsal rib
Angelosaurus	*romeri*	FMNH UR 933	Caseidae	KF-1 Locality, Omega Quarry, Kingfisher County, Ohklahoma	Roadian	Clavicle
Angelosaurus	*romeri*	FMNH UR 940	Caseidae	KF-1 Locality, Omega Quarry, Kingfisher County, Ohklahoma	Roadian	3rd presacral rib
Angelosaurus	*romeri*	FMNH UR 941	Caseidae	KF-1 Locality, Omega Quarry, Kingfisher County, Ohklahoma	Roadian	Anterior dorsal rib

Angelosaurus	*romeri*	FMNH UR 942	Caseidae	KF-1 Locality, Omega Quarry, Kingfisher County, Ohklahoma	Roadian	Tooth
Angelosaurus	*romeri*	FMNH UR 943	Caseidae	KF-1 Locality, Omega Quarry, Kingfisher County, Ohklahoma	Roadian	Lower jaws
Angelosaurus	*romeri*	FMNH UR 944	Caseidae	KF-1 Locality, Omega Quarry, Kingfisher County, Ohklahoma	Roadian	2 dorsal ribs
Angelosaurus	*romeri*	FMNH UR 945	Caseidae	KF-1 Locality, Omega Quarry, Kingfisher County, Ohklahoma	Roadian	Anterior dorsal ribs
Angelosaurus	*romeri*	FMNH UR 971	Caseidae	KF-1 Locality, Omega Quarry, Kingfisher County, Ohklahoma	Roadian	20 caudal vertebrae with ribs on anterior ones
Angelosaurus	*romeri*	FMNH UR 978	Caseidae	KF-1 Locality, Omega Quarry, Kingfisher County, Ohklahoma	Roadian	Pubis
Angelosaurus	*romeri*	FMNH UR 979	Caseidae	KF-1 Locality, Omega Quarry, Kingfisher County, Ohklahoma	Roadian	Ilia and ischia
Angelosaurus	*romeri*	FMNH UR 980	Caseidae	KF-1 Locality, Omega Quarry, Kingfisher County, Ohklahoma	Roadian	Pelvis
Mesenosaurus	*romeri*	PIN 4660/7	Varanopidae	Dorogaya Gora	Late Roadian-Wordian	
Mesenosaurus	*romeri*	PIN 4660/10	Varanopidae	Dorogaya Gora	Late Roadian-Wordian	
Mesenosaurus	*romeri*	PIN 4660/12	Varanopidae	Dorogaya Gora	Late Roadian-Wordian	
Mesenosaurus	*romeri*	PIN 4543/19	Varanopidae	Nysogora, Arkangel	Late Roadian-Wordian	
Mesenosaurus	*romeri*	PIN 4543/21	Varanopidae	Nysogora, Arkangel	Late Roadian-Wordian	
Ennatosaurus	*tecton*	PIN 4543/1	Caseidae	Nysogora, Arkangel	Late Roadian-Wordian	

Mesenosaurus	*romeri*	PIN 4653/1	Varanopidae	Karashchelya , Arkangel	Late Roadian-Wordian	Skull
Ennatosaurus	*tecton*	PIN 4653/2	Caseidae	Karashchelya , Arkangel	Late Roadian-Wordian	
Ennatosaurus	*tecton*	PIN 4543	Caseidae	Nyisagora locality, Mezen River near the juction with the Vashka River	Late Roadian-Wordian	Skull, lower jaw, fragment of cheek region and fragment of dentary
Mesenosaurus	*romeri*	PIN 158/1	Varanopidae	Kiselicha, Arkangel	Late Roadian-Wordian	Partial skull, nearly complete right madible
Mesenosaurus	*romeri*	PIN 158/2	Varanopidae	Kiselicha, Arkangel	Late Roadian-Wordian	Orbital region of the skull
Mesenosaurus	*romeri*	PIN 158/3	Varanopidae	Kiselicha, Arkangel	Late Roadian-Wordian	Lower jaw fragments
Mesenosaurus	*romeri*	PIN 158/18	Varanopidae	Kiselicha, Arkangel	Late Roadian-Wordian	Skull fragments and teeth
Mesenosaurus	*romeri*	PIN 158/19	Varanopidae	Kiselicha, Arkangel	Late Roadian-Wordian	Fragmentary skull
Mesenosaurus	*romeri*	PIN 158/20	Varanopidae	Kiselicha, Arkangel	Late Roadian-Wordian	Maxilla fragment
Mesenosaurus	*romeri*	PIN 3706/11	Varanopidae	Peza-1, Arkangel	Late Roadian-Wordian	Partial skull
Mesenosaurus	*romeri*	PIN 3706/15	Varanopidae	Peza-1, Arkangel	Late Roadian-Wordian	Partial skull roof
Mesenosaurus	*romeri*	PIN 3706/28	Varanopidae	Peza-1, Arkangel	Late Roadian-Wordian	Partial skull
Mesenosaurus	*romeri*	PIN 3706/48	Varanopidae	Peza-1, Arkangel	Late Roadian-Wordian	Partial skull
Mesenosaurus	*romeri*	PIN 162/3	Varanopidae	Glyadnaya Schel	Late Roadian-Wordian	Jaw fragments, skull missing snout and occiput
Mesenosaurus	*romeri*	PIN 162/4	Varanopidae	Glyadnaya Schel	Late Roadian-Wordian	Jaw, palate, teeth
Mesenosaurus	*romeri*	PIN 162/38	Varanopidae	Glyadnaya Schel	Late Roadian-Wordian	Skull
Mesenosaurus	*romeri*	PIN 162/56	Varanopidae	Glyadnaya Schel	Late Roadian-Wordian	Skull
Mesenosaurus	*romeri*	PIN 4654/1	Varanopidae	Blignjaa Schleja	Late Roadian-Wordian	
Mesenosaurus	*romeri*	PIN 4541/8	Varanopidae	Ust-Vashka locality, Mezen River Basin, Arkhangel	Late Roadian-Wordian	Skull and jaw fragments
Mesenosaurus	*romeri*	PIN 4541/9	Varanopidae	Ust-Vashka locality, Mezen River Basin, Arkhangel	Late Roadian-Wordian	Maxilla fragment
Mesenosaurus	*romeri*	PIN 4541/15	Varanopidae	Ust-Vashka locality, Mezen River Basin, Arkhangel	Late Roadian-Wordian	
Mesenosaurus	*romeri*	PIN 4541/22	Varanopidae	Ust-Vashka locality, Mezen River Basin,	Late Roadian-Wordian	

				Arkhangel		
Pyozia	*mesenensis*	PIN 3717/33	Varanopidae	Ust-Nyafta, Pyoza River Arkhangelsk Region, Menzen District	Late Roadian-Wordian	Partial skull, anterior cervical vertebrae, pectoral girdal, dorsal vertebrae
Mesenosaurus	*romeri*	PIN 3717/1	Varanopidae	Ust-Nyafta, Pyoza River Arkhangelsk Region, Menzen District	Late Roadian-Wordian	Nearly complete skeleton
Mesenosaurus	*romeri*	PIN 3717/4	Varanopidae	Ust-Nyafta, Pyoza River Arkhangelsk Region, Menzen District	Late Roadian-Wordian	
Mesenosaurus	*romeri*	PIN 3717/10	Varanopidae	Ust-Nyafta, Pyoza River Arkhangelsk Region, Menzen District	Late Roadian-Wordian	Skull fragments
Mesenosaurus	*romeri*	PIN 3717/ 18	Varanopidae	Ust-Nyafta, Pyoza River Arkhangelsk Region, Menzen District	Late Roadian-Wordian	
Mesenosaurus	*romeri*	PIN 3717/19	Varanopidae	Ust-Nyafta, Pyoza River Arkhangelsk Region, Menzen District	Late Roadian-Wordian	Roof of orbital region
Mesenosaurus	*romeri*	PIN 3717/29	Varanopidae	Ust-Nyafta, Pyoza River Arkhangelsk Region, Menzen District	Late Roadian-Wordian	
Mesenosaurus	*romeri*	PIN 3717/34	Varanopidae	Ust-Nyafta, Pyoza River Arkhangelsk Region, Menzen District	Late Roadian-Wordian	
Mesenosaurus	*romeri*	PIN 3717/38	Varanopidae	Ust-Nyafta, Pyoza River Arkhangelsk Region, Menzen District	Late Roadian-Wordian	Palate
Mesenosaurus	*romeri*	PIN 3586/5	Varanopidae	Ust Peza, Arkangelsk	Late Roadian-Wordian	Skull
Mesenosaurus	*romeri*	PIN 3586/8	Varanopidae	Ust Peza, Arkangelsk	Late Roadian-Wordian	Skull fragments
Mesenosaurus	*romeri*	PIN 3586/37	Varanopidae	Ust Peza, Arkangelsk	Late Roadian-Wordian	Jaw fragments

Mesenosaurus	*romeri*	PIN 3586/38	Varanopidae	Ust Peza, Arkangelsk	Late Roadian-Wordian	Anterior skull
Mesenosaurus	*romeri*	PIN 3586/39	Varanopidae	Ust Peza, Arkangelsk	Late Roadian-Wordian	Jaw fragments
Mesenosaurus	*romeri*	PIN 3586/40	Varanopidae	Ust Peza, Arkangelsk	Late Roadian-Wordian	Jaw fragments
Mesenosaurus	*romeri*	PIN 3586/42	Varanopidae	Ust Peza, Arkangelsk	Late Roadian-Wordian	
Mesenosaurus	*romeri*	PIN 3586/49	Varanopidae	Ust Peza, Arkangelsk	Late Roadian-Wordian	
Mesenosaurus	*romeri*	PIN 4609/4	Varanopidae	Leshikanskii, Arkangelsk Province	Late Roadian-Wordian	
Mesenosaurus	*romeri*	PIN 4609/5	Varanopidae	Leshikanskii, Arkangelsk Province	Late Roadian-Wordian	
Mesenosaurus	*romeri*	PIN 4609/6	Varanopidae	Leshikanskii, Arkangelsk Province	Late Roadian-Wordian	
Mesenosaurus	*romeri*	PIN 4609/13	Varanopidae	Leshikanskii, Arkangelsk Province	Late Roadian-Wordian	
Mesenosaurus	*romeri*	PIN 4609/14	Varanopidae	Leshikanskii, Arkangelsk Province	Late Roadian-Wordian	
Mesenosaurus	*romeri*	PIN 4609/16	Varanopidae	Leshikanskii, Arkangelsk Province	Late Roadian-Wordian	
Mesenosaurus	*romeri*	PIN 4609/18	Varanopidae	Leshikanskii, Arkangelsk Province	Late Roadian-Wordian	
Mesenosaurus	*romeri*	PIN 4609/20	Varanopidae	Leshikanskii, Arkangelsk Province	Late Roadian-Wordian	
Mesenosaurus	*romeri*	PIN 4609/23	Varanopidae	Leshikanskii, Arkangelsk Province	Late Roadian-Wordian	
Mesenosaurus	*romeri*	PIN 4609/35	Varanopidae	Leshikanskii, Arkangelsk Province	Late Roadian-Wordian	
Mesenosaurus	*romeri*	PIN 4609/40	Varanopidae	Leshikanskii, Arkangelsk Province	Late Roadian-Wordian	
Mesenosaurus	*romeri*	PIN 4609/49	Varanopidae	Leshikanskii, Arkangelsk Province	Late Roadian-Wordian	Skull
Mesenosaurus	*romeri*	PIN 4659/3	Varanopidae	Kozmogorodskoe, Arkangelsk Province	Late Roadian-Wordian	

Mesenosaurus	*romeri*	PIN 4659/7	Varanopidae	Kozmogorodskoe, Arkangelsk Province	Late Roadian-Wordian	
Mesenosaurus	*romeri*	PIN 4659/13	Varanopidae	Kozmogorodskoe, Arkangelsk Province	Late Roadian-Wordian	
Mesenosaurus	*romeri*	PIN 4659/16	Varanopidae	Kozmogorodskoe, Arkangelsk Province	Late Roadian-Wordian	Partial skull
Mesenosaurus	*romeri*	PIN 4659/17	Varanopidae	Kozmogorodskoe, Arkangelsk Province	Late Roadian-Wordian	
Ennatosaurus	*tecton*	PIN 1580/5	Caseidae	Moroznitsa, near Karpoga, Arkhangelsk	Late Roadian-Wordian	Fibula
Ennatosaurus	*tecton*	PIN 1580/6	Caseidae	Moroznitsa, near Karpoga, Arkhangelsk	Late Roadian-Wordian	Pelvis
Ennatosaurus	*tecton*	PIN 1580/7	Caseidae	Moroznitsa, near Karpoga, Arkhangelsk	Late Roadian-Wordian	Tibia, fibula, pes
Ennatosaurus	*tecton*	PIN 1580/10	Caseidae	Moroznitsa, near Karpoga, Arkhangelsk	Late Roadian-Wordian	Ribs
Ennatosaurus	*tecton*	PIN 1580/11	Caseidae	Moroznitsa, near Karpoga, Arkhangelsk	Late Roadian-Wordian	Distal humerus
Ennatosaurus	*tecton*	PIN 1580/12	Caseidae	Moroznitsa, near Karpoga, Arkhangelsk	Late Roadian-Wordian	Right humerus, part of scapula
Ennatosaurus	*tecton*	PIN 1580/14	Caseidae	Moroznitsa, near Karpoga, Arkhangelsk	Late Roadian-Wordian	Skull and jaws and some cervical vertebrae articulated
Ennatosaurus	*tecton*	PIN 1580/15	Caseidae	Moroznitsa, near Karpoga, Arkhangelsk	Late Roadian-Wordian	Ilium, head of tibia
Ennatosaurus	*tecton*	PIN 1580/16	Caseidae	Moroznitsa, near Karpoga, Arkhangelsk	Late Roadian-Wordian	Lower jaw
Ennatosaurus	*tecton*	PIN 1580/17	Caseidae	Moroznitsa, near Karpoga, Arkhangelsk	Late Roadian-Wordian	Skull and lower jaw
Ennatosaurus	*tecton*	PIN 1580/18	Caseidae	Moroznitsa, near Karpoga, Arkhangelsk	Late Roadian-Wordian	Two dorsal vertebrae
Ennatosaurus	*tecton*	PIN 1580/19	Caseidae	Moroznitsa, near Karpoga, Arkhangelsk	Late Roadian-Wordian	Skull and lower jaw

Ennatosaurus	*tecton*	PIN 1580/22	Caseidae	Moroznitsa, near Karpoga, Arkhangelsk	Late Roadian-Wordian	Dorsal vertebrae
Ennatosaurus	*tecton*	PIN 1580/23	Caseidae	Moroznitsa, near Karpoga, Arkhangelsk	Late Roadian-Wordian	Ilium and sacral ribs
Ennatosaurus	*tecton*	PIN 1580/24	Caseidae	Moroznitsa, near Karpoga, Arkhangelsk	Late Roadian-Wordian	Skull and lower jaw
Ennatosaurus	*tecton*	PIN 1580/101	Caseidae	Moroznitsa, near Karpoga, Arkhangelsk	Late Roadian-Wordian	16 vertebrae and ribs, part of the shoulder girdle, femur, ulna and radius
Ennatosaurus	*tecton*	PIN 1580/102	Caseidae	Moroznitsa, near Karpoga, Arkhangelsk	Late Roadian-Wordian	Radius, ulna, carpus, scapula, part of the coracoid
Ennatosaurus	*tecton*	PIN 1580/103	Caseidae	Moroznitsa, near Karpoga, Arkhangelsk	Late Roadian-Wordian	Ilium and sacral ribs
Ennatosaurus	*tecton*	PIN 1580/104	Caseidae	Moroznitsa, near Karpoga, Arkhangelsk	Late Roadian-Wordian	1 vertebra
Ennatosaurus	*tecton*	PIN 1580/105	Caseidae	Moroznitsa, near Karpoga, Arkhangelsk	Late Roadian-Wordian	4 vertebrae, part of an Indeterminate/ Undescribed limb bone, head of tibia
Ennatosaurus	*tecton*	PIN 1580/106	Caseidae	Moroznitsa, near Karpoga, Arkhangelsk	Late Roadian-Wordian	3 vertebrae
Ennatosaurus	*tecton*	PIN 1580/107	Caseidae	Moroznitsa, near Karpoga, Arkhangelsk	Late Roadian-Wordian	7 presacral and 8 caudal vertebrae, femur, ilium
Ennatosaurus	*tecton*	PIN 1580/108	Caseidae	Moroznitsa, near Karpoga, Arkhangelsk	Late Roadian-Wordian	Humerus, part of radius and ulna, part of scapula, pedal bones
Ennatosaurus	*tecton*	PIN 1580/109	Caseidae	Moroznitsa, near Karpoga, Arkhangelsk	Late Roadian-Wordian	Fragments of vertebrae, part of scapula, radius
Ennatosaurus	*tecton*	PIN 1580/110	Caseidae	Moroznitsa, near Karpoga, Arkhangelsk	Late Roadian-Wordian	2 radii, fibula, centrum, pedal phalanx, sacral rib
Ennatosaurus	*tecton*	PIN 1580/111	Caseidae	Moroznitsa, near Karpoga, Arkhangelsk	Late Roadian-Wordian	5 centra
Ennatosaurus	*tecton*	PIN 1580/112	Caseidae	Moroznitsa, near Karpoga, Arkhangelsk	Late Roadian-Wordian	2 partial maxillae
Ennatosaurus	*tecton*	PIN 1580/113	Caseidae	Moroznitsa, near Karpoga, Arkhangelsk	Late Roadian-Wordian	Interclavicale

Ennatosaurus	*tecton*	PIN 1580/114	Caseidae	Moroznitsa, near Karpoga, Arkhangelsk	Late Roadian-Wordian	Part of ilium
Ennatosaurus	*tecton*	PIN 1580/115	Caseidae	Moroznitsa, near Karpoga, Arkhangelsk	Late Roadian-Wordian	2 anterior dorsal vertebrae
Ennatosaurus	*tecton*	PIN 1580/117	Caseidae	Moroznitsa, near Karpoga, Arkhangelsk	Late Roadian-Wordian	Scapulocoracoid, pterygoid
Ennatosaurus	*tecton*	PIN 1580/118	Caseidae	Moroznitsa, near Karpoga, Arkhangelsk	Late Roadian-Wordian	Part of pelvis, right femur, head of tibia
Ennatosaurus	*tecton*	PIN 1580/119	Caseidae	Moroznitsa, near Karpoga, Arkhangelsk	Late Roadian-Wordian	Fibula
Ennatosaurus	*tecton*	PIN 1580/120	Caseidae	Moroznitsa, near Karpoga, Arkhangelsk	Late Roadian-Wordian	Part of scapula, humerus, radius, ulna, part of clavicle, pedal bones
Ennatosaurus	*tecton*	PIN 1580/121	Caseidae	Moroznitsa, near Karpoga, Arkhangelsk	Late Roadian-Wordian	Ulna and part of humerus
Ennatosaurus	*tecton*	PIN 1580/122	Caseidae	Moroznitsa, near Karpoga, Arkhangelsk	Late Roadian-Wordian	Front part of left side of the skull and lower jaw
Ennatosaurus	*tecton*	PIN 1580/123	Caseidae	Moroznitsa, near Karpoga, Arkhangelsk	Late Roadian-Wordian	Scapula, 2 ribs, part of interclavicle
Ennatosaurus	*tecton*	PIN 1580/124	Caseidae	Moroznitsa, near Karpoga, Arkhangelsk	Late Roadian-Wordian	Ulna and humerus
Ennatosaurus	*tecton*	PIN 1580/125	Caseidae	Moroznitsa, near Karpoga, Arkhangelsk	Late Roadian-Wordian	Scapulocoracoid
Ennatosaurus	*tecton*	PIN 1580/126	Caseidae	Moroznitsa, near Karpoga, Arkhangelsk	Late Roadian-Wordian	Left pes
Ennatosaurus	*tecton*	PIN 1580/127	Caseidae	Moroznitsa, near Karpoga, Arkhangelsk	Late Roadian-Wordian	Right dentary
Mesenosaurus	*romeri*	PIN 1580/1	Varanopidae	Moroznitsa, near Karpoga, Arkhangelsk	Late Roadian-Wordian	
Mesenosaurus	*romeri*	PIN 4657/2	Varanopidae	Petrova Scheya, Arkangelsk	Late Roadian-Wordian	
Heleosaurus	*scholtzi*	SAM-PK-1070	Varanopidae	Victorian West District	Capitanian	Skull, lower jaw, axial skeleton, pectoral and pelvic girdles and femur

Heleosaurus	*scholtzi*	SAM-PK-8305	Varanopidae	Beukesplass (Gannakraal 422), Fraserburg District, Northern Cape Province	Capitanian	Five individuals, with 4 skulls, anterior portions of the vertebral column, articulated ribs, gastralia, osteoderms, forelimbs, anterior caudal vertebrae
Elliotsmithia	*longiceps*	TM 1483	Varanopidae	Abrahamskraal, Prince Albert, Western Cape Province	Capitanian	Postorbital skull and lower jaw, 4 anterior cervical vertebrae, rib fragments, dermal ossifications

Appendix E

A list of all scientific publications containing a phylogenetic analysis of Paleozoic synapsids incorporating at least 3 species from the time period under study. Indicates those which are incorporated into the supertree, and the reason for including those which are not.

Phylogenetic Hypothesis	Status in the supertree
Amson, E. and Laurin, M. 2011. On the affinities of *Tetraceatops insignis*, an early Permian synapsid. Acta Palaeontologica Polonica 56:301-312	Retained
Anderson, J. S. and Reisz, R. R. 2004. *Pyozia mesenensis*, a new, small varanopid (Synapsida, Eupelycosauria) from Russia: "Pelycosaur" diversity in the middle Permian. Journal of Vertebrate Paleontology 24:173-179	Removed; subset of Maddin et al. 2006
Angielczyk, K. D. 2001. Preliminary phylogenetic analysis and stratigraphic congruence of the dicynodont anomodonts (Synapsida: Therapsida). Palaeontologia Africana 37:52-79	Removed; subset of Angielczyk & Rubidge 2012
Angielczyk, K. D. 2002. Redescription, phylogenetic position, and stratigraphic significance of the dicynodont genus *Odontocyclops* (Synapsida: Anomodontia). Journal of Paleontology 76:1047-1059	Removed; subset of Angielczyk & Rubidge 2012
Angielczyk, K. D. 2004. Phylogenetic evidence for and the implications of a dual origin of proaliny in anomodont therapsids (Synapsida). Paleobiology 30:268-296	Forms mini supertree 1 with Modesto et al. 1999, Modesto & Rybczynski 2000 and Rybzynski 2000
Angielczyk, K. D. 2007. New specimens of the Tanzanian dicynodont *"Cryptocynodon" parringtoni* von Huene, 1942 (Therapsida, Anomodontia), with an expanded analysis of Permian dicynodont phylogeny. Journal of Vertebrate Paleontology 27:116-131	Removed; subset of Angielczyk & Rubidge 2012

Angielczyk, K. D. and Kurkin, A. A. 2003. Phylogenetic analysis of Russian Permian dicynodonts (Therapsida: Anomodontia): implications for Permian biostratigraphy and Pangaean biogeography. Zoological Journal of the Linnean Society 139:157-212	Removed; subset of Angielczyk & Rubidge 2012
Angielczyk, K. D. and Rubidge, B. S. 2010. A new pylaecephalid dicynodont (Therapsida, Anomodontia) from the *Tapinocephalus* Assemblage Zone, Karoo Basin, Middle Permian of South Africa	Removed; subset of Angielczyk & Rubidge 2012
Angielcyk, K. D. and Rubidge B. S. 2012. Skeletal morphology, phylogenetic relationships and stratigraphic range of *Eosimops newtoni* Broom, 1921, a pylaecephalid dicynodont (Therapsida, Anomodontia) from the Middle Permian of South Africa. Journal of Systematic Palaeontology (in press)	Retained
Benson, R. B. J. 2012. The global interrelationships of basal synapsids:cranial and postcranial morphology partitions suggest different topologies. Journal of Systematic Palaeontology (in press)	Removed; Subset of analyses presented in this thesis
Berman, D. S., Reisz, R. R., Bolt, J. R. and Scott, D. 1995. The cranial anatomy and relationships of the synapsid *Varanosaurus* (Eupelycosauria: Ophiacodontidae) from the early Permian of Texas and Oklahoma. Annals of Carnegie Museum 64:99-133	Retained
Botha-Brink, J. and Modesto, S. P. 2009. Anatomy and relationships of the middle Permian varanopid *Heleosaurus scholtzi* based on a social aggregation from the Karoo basin of South Africa. Journal of Vertebrate Paleontology 29:389-400	Forms mini supertree 2 with Maddin et al 2006 and Campione & Reisz 2010

Campione, N. E. and Reisz, R. R. 2010. *Varanops brevirostris* (Eupelycosauria: Varanopidae) from the lower Permian of Texas, with discussion of varanopid morphology and interrelationships. Journal of Vertebrate Paleontology 30:724-746	Forms mini supertree 2 with Maddin et al 2006 and Botha Brink & Modesto 2009
Cisneros J. C., Abdala, F., Rubidge, B. S., Dentizien-Dias, P. C. and de Oliveira Bueno, A. 2011. Dental occlusion in a 260 million year old therapsid with saber canines from the Permian of Brazil. Science 331:1603-1605	Retained
Cisneros, J. C., Abdala, F., Atayman-Güven, S., Rubidge, B. S., Celâl Şengör, A. M. and Schultz, C. L. 2012. Carnivorous dinocephalian from the middle Permian of Brazil and tetrapod dispersal in Pangaea. Proceedings of the National Academy of Science 109:1584-1588	Forms mini supertree 3 with Kammerer 2011
Damiani, R., Vasconcelos, C., Renaut, A., Hancox, J. and Yates, A. 2007. *Dolichuranus primaevus* (Therapsida: Anomodontia) from the Middle Triassic of Namibia and its phylogenetic relationships. Palaeontology	Retained
DeBraga, M. & Rieppel, O. 1997. Reptile phylogeny and the interrelationships of turtles. Zoological Journal of the Linnaean Society 120:281-354	Removed; subset of Hill 2005
Fröbisch, J. 2007. The cranial anatomy of *Kombuisia frerensis* Hotton (Synapsida, Dicynodontia) and a new phylogeny of anomodont therapsids. Zoological Journal of the Linnean Society 150:117-144	Removed; subset of Fröbisch et al 2010
Fröbisch, J. and Reisz, R. R. 2008. A new species of *Emydops* (Synapsida, Anomodontia) and a discussion of dental variability and pathology in dicynodonts. Journal of Vertebrate Paleontology 28:770-787	Removed; subset of Fröbisch et al 2010

Fröbisch, J. and Reisz, R. R. 2011. The postcranial anatomy of *Suminia getmanovi* (Synapsida: Anomodontia), the earliest known arboreal tetrapod. Zoological Journal of the Linnean Society 162:661-698	Retained
Fröbisch, J., Angielczyk, K. D. and Sidor, C. A. 2010. The Triassic dicynodont *Kombuisia* (Synapsida, Anomodontia) from Antarctica, a refuge from the terrestrial Permian-Triassic mass extinction. Naturwissenschaften 97:187-196	Retained
Fröbisch, J., Schoch, R. R., Müller, J., Schindler, T. and Schweiss, D. 2011. A new basal sphenacdontid synapsid from the late Carboniferous of the Saar-Nahe Basin, Germany. Acta Palaeontologica Polonica 56:113-120	Retained
Gauthier, J., Kluge, A. G., Rowe, T. 1988. Amniote phylogeny and the importance of fossils. Cladistics 4:105-209	Removed; subset of Hill 2005
Hill, R. V. 2005. Integration of Morphological Data Sets for Phylogenetic Analysis of Amniota: The Importance of Integumentary Characters and Increased Taxonomic Sampling. Sytsematic Biology (54): 530-547	Retained
Huttenlocker, A. 2009. An investigation into the cladistic relationships and monophyly of the therocephalian therapsids (Amniota: Synapsida). Zoological Journal of the Linnean Society 157:865-891	Removed; subset of Huttenlocker et al 2011
Huttenlocker, A., Sidor, C. A. and Smith, R. M. H. 2011. A new specimen of *Promoschorhynchus* (Therapsida: Therocephalia: Akidnognathidae) from the Lower Triassic of South Africa and its implications for theriodont survivorship across the Permo-Triassic boundary. Journal of Vertebrate Paleontology 31:405-421	Retained

Jacobs, L. L., Winkler, D. A., Newman, K. D., Gomani, E. M. and Deino, A. 2005. Therapsids from the Permian Chiweta Beds and the age of the Karoo supergroup in Malawi. Palaeontologia Electronica 8:28A	Removed; subset of Sidor & Welman 2003
Kamerer, C. F. 2011. Systematics of the Anteosauria (Therapsida: Dinocephalia). Journal of Systematic Palaeontology 9:261-304	Forms mini supertree with Cisneros et al 2012
Kammerer, C. F., Angielczyk, K. D. and Fröbisch, J. 2011. A comprehensive taxonomic revision of *Dicynodon* (Therapsida, Anomodontia) and its implications for dicynodont phylogeny, biogeography, and biostratigraphy. Journal of Vertebrate Paleontology 31 (S1):1-158	Retained
Kissel, R. A. and Reisz R. R. 2004. Synapsid fauna of the upper Pennsylvanian Rock Lake Shale near Garnett, Kansas and the diversity pattern of early amniotes. *In* G. Arratia, M. V. H. Wilson and R. Cloutier, eds. Recent Advances in the Origin and Early Radiation of Vertebrates. Verlag Dr. Friedrich Pfeil, München, Germany:pp. 409-428	Retained
Laurin, M. 1993. Anatomy and relationships of *Haptodus garnettensis*, a Pensylvanian synapsid from Kansas. Journal of Vertebrate Paleontology 13:200-229	Removed; subset of Kissel & Reisz 2004
Laurin, M. and Reisz, R. R. 1990. *Tetraceratops* is the oldest known therapsid. Nature 345:249-250	Retained
Lee, M. 2001. Molecules, morphology and the monophyly of diapsid reptiles. Contributions to Zoology 70:http://dpc.uba.uva.nl/ctz/vol70/nr01/art01	Retained
Liu, J., Rubidge, B. S. and Li, J. 2009. New basal synapsid supports Laurasian origin for therapsids. *Acta Palaeontologica Polonica* 54:393-400	Removed; subset of Amson & Laurin 2011

Liu, J., Rubidge, B. S. and Li, J. 2010. A new specimen of *Biseridens qilianicus* indicates ist phylogenetic position as the most basal anomodont. Proceedings of the Royal Society B 277:285-292	Retained
Maddin, H. C., Evans, D. C. and Reisz, R. R. 2006. An early Permian varanodontine varanopid (Synapsida: Eupelycosauria) from the Richards Spur Locality, Oklahoma. Journal of Vertebrate Paleontology 26:957-966	Forms mini supertree 2 with Botha Brink & Modesto 2009 and Campione & Reisz 2010
Maddin, H. C., Sidor, C. A. and Reisz, R. R. 2008. Journal of Vertebrate Paleontology 28:160-180	Retained
Mazierski, D. M. and Reisz, R. R. 2010. Description of a new specimen of *Ianthasaurus hardestiorum* (Eupelycosauria: Edaphosauridae) and a re-evaluation of edaphosaurid phylogeny. Canadian Journal of Earth Sciences 47:901-912	Retained
Modesto, S. P. 1994. The lower Permian synapsid *Glaucosaurus* from Texas. Palaeontology 37:51-60	Retained
Modesto, S. P. 1995. The skull of the herbivorous synapsid *Edaphosaurus boanerges* from the lower Permian of Texas. Palaeontology 38:213-239	Removed; subset of Mazierski & Reisz 2010
Modesto, S. P. and Rybczynski, N. 2000. The amniote faunas of the Russian Permian: implications for Late Permian terrestrial vertebrate biogeography. *In* M. J. Benton, M. A. Shishkin, D. M. Unwin and E. N. Kurochkin, eds. The Age of the Dinosaurs in Russia and Mongolia. Cambridge Univeristy Press, Cambridge:pp. 17-35	Forms mini supertree 1 with Modesto et al 1999, Angielcyzyk 2004 and Rybzynski 2000
Modesto, S. P., Rubidge, B. S. and Welman, J. 1999. The most basal anomodont therapsid and the primacy of Gondwana in the evolution of anomodonts. Proceedings of the Royal Society B 266:331-337	Forms mini supertree 1 with Modesto & Rybczynski 2000, Angielcyzyk 2004 and Rybzynski 2000

Modesto, S. P., Sidor, C. A., Rubidge, B. S. and Welman, J. 2001. A second varanopseid skull from the upper Permian of South Africa: implications for late Permian 'pelycosaur' evolution. Lethaia 34:249-259	Removed; subset of Bother Brink & Modesto 2009
Modesto, S. P., Rubidge, B. S. and Welman, J. 2002. A new dicynodont therapsid from the lowermost Beaufort Group, upper Permian of South Africa. Canadian Journal of Earth Science 39:1755-1765	Removed; subset of Angielczyk & Rubidge 2012
Modesto, S. P., Rubidge, B. S., Visser, I. and Welman, J. 2003. A new basal dicynodont from the upper Permian of South Africa. Palaeontology 46:211-223	Retained
Ray, S. 2006. Functional and Evolutionary aspects of the postcranial anatomy of dicynodonts (Synapsida, Therapsida). Palaeontology 49:1263-1286	Retained
Reisz, R. R. & Dilkes, D. W. 2003. *Archaeovenator hamiltonensis*, a new varanopid (Synapsida: Eupelycosauria) from the upper Carboniferous of Kansas. Canadian Journal of Earth Sciences 40:667-678	Removed; subset of Anderson & Reisz 2004
Reisz, R. R. & Laurin, M. 2004. A reevaluation of the enigmatic Permian synapsid *Watongia* and of ist stratigraphic significance. Canadian Journal of Earth Sciences 41:337-386	Removed; subset of Maddin et al 2006
Reisz, R. R., Berman, D. S. and Scott, D. 1992. The cranial anatomy and relationships of *Secodontosaurus*, an unudual mammal-like reptile(Synapsida: Sphenacodontidae) from the early Permian of Texas. Zoological Journal of the Linnean Society 104:127-184	Retained
Reisz, R. R., Dilkes, D. W. and Berman, D. S. 1998. Anatomy and relationships of *Elliotsmithia longiceps* Broom, a small synapsid (Eupelycosauria: Varanopseidae) from the late Permian of South Africa. Journal of Vertebrate Paleontology 18:602-611	Removed; subset of Modesto et al 2001

Reisz, R. R., Godfrey, S. J. and Cott, D. 2009. *Eothyris* and *Oedaleops*: do these early Permian synapsids from Texas and New Mexico form a clade? Journal of Vertebrate Paleontology 29:39-48	Retained
Reisz, R. R., Laurin, M. and Marjanović, D. 2010. *Apsisaurus witteri* from the lower Permian of Texas: yet another small varanopid synapsid, not a diapsid. Journal of Vertebrate Paleontology 30:1628-1631	Retained
Rieppel, O. & Reisz, R. R. 1999. The origin and early evolution of Turtles. Annual Review of Ecology and Systematics 30:1-22	Removed, subset of Hill 2005
Rubidge, B. S. and van den Heever, J. A. 1997. Morphology and systematic position of the dinocephalian *Styracocephalus platyrhynchus*. Lethaia 30:157-168	Retained
Rubidge, B. S. and Kitching, J. W. 2003. A new burnetiamorph (Therapsida: Biarmosuchia) from the lower Beaufort Group of South Africa. Palaeontology 46:199-210	Retained
Rubidge, B. S., Sidor, C. A. and Modesto, S. P. 2006. A new burnetiamorph (Therapsida: Biarmosuchia) from the middle Permian of South Africa. Journal of Paleontology 80:740-749	Retained
Rybczynski, N. 2000. Cranial anatomy and phylogenetic position of *Suminia getmanovi*, a basal anomodont (Amniota: Therapsida) from the late Permian of Eastern Europe. Zoological Journal of the Linnean Society 130:329-373	Forms mini supertree 1 with Modesto et al 1999, Angielcyzyk 2004 and Modesto & Rybczinski 2000
Sidor, C. A. and Hopson, J. A. 1998. Ghost lineages and "mammalness": assessing the temporal pattern of character acquisition in the Synapsida. Paleobiology 24:254-273	Retained

Sidor, C. A. and Rubidge, B. S. 2006. *Herpetoskylax hopsoni*, a new biarmosuchian (Therapsida: Biarmosuchia) from the Beaufort Group of South Africa). *In* M. T. Carrano, T. J. Gaudin, R. W. Blob and J. R. Wible, eds. Amniote Paleobiology. University of Chicago PRess, Chicago, USA: pp. 76-113	Retained
Sidor C. A. and Smith, R. M. H. 2007. A second burnetiamorph therapsid from the Permian Teekloof Formation of South Africa and its associated fauna. Journal of Vertebrate Paleontology 27:420-430	Forms mini supertree 4 with Smith et al 2006
Sidor, C. A. and Welman, J. 2003. A second specimen of *Lemurosaurus pricei* (Therapsida: Burnetiamorpha). Journal of Vertebrate Paleontology 23:631-642	Retained
Sidor, C. A., Hopson, J. A. and Keyser A. W. 2003. A new burnetiamorph therapsid from the Teekloof Formation, Permian, of South Africa. Journal of Vertebrate Paleontology 24:938-950	Removed; subset of Smith et al 2006
Smith, R. M. H., Rubidge, B. S. and Sidor, C. A. 2006. A new burnetiid (Therapsida: Biarmosuchia) from the upper Permian of South Africa and its biogeographic implications. Journal of Vertebrate Paleontology 26:331-343	Forms mini supertree 4 with Sidor & Smith 2007
Surkov, M. V., Kalandadze, N. N. and Benton, M. J. 2005. *Lystrosaurus georgi*, a dicynodont from the lower Triassic of Russia. Journal of Vertebrate Paleontology 25:402-413	Retained

Appendix F

Character list used in the Character Completeness Metric calculation, and the region of the skeleton required to accept that character as scored

Region of the Skeleton	Other regions required	Character Description
Maxilla	Requires prefrontal	Maxilla-prefrontal contact: absent (0); present (1).
	Requires vomer	Palatal processes of the maxillae are absent (0), form a well-developed crista choanalis with a ridge extending posteriorly onto the palatine (1), contact or nearly contact the ventrally extending vomer with no sutural connection (2); bear a moderately long sutural connection with the lateral margins of the vomer (3), or meet at the midline, sharing a sutural connection and obscuring most of the vomer on the palatal surface (4).
	Requires palatine	Formation of secondary palate occurs such that the posterior portion of the maxillae and palatines approach at the midline, but are slightly open anteriorly, thus creating an incipient incisive fissure or foramen (0), or the anterior portion is more closed than the posterior, leaving no indication of an incisive foramen (1).
	Requires dentary	Maxilla and dentary, medial surface adjacent to alveoli: smooth (0): rugose, striated bone encloses tooth bases (1).
	Requires upper canine	Upper dominant canine in adults large relative to maxillary height (0), medium (1) or extremely reduced (2).
		Maxilla, lateral buttress: absent (0); dorsally oriented buttress on lateral surface (1)
		Maxilla, ascending process, morphology: smoothly curving posterior margin (0); angular emargination in posterior margin so apex of process is located anteriorly (1).
		Maxilla, supracanine buttress on medial surface: absent (0); present, may be expanded into lateral margin of internal naris [choana] (1).
		Maxilla, morphology of dorsal portion of supracanine buttress: anteroposteriorly broad region of thickened bone (0); narrow, strut-like ascending process (1); inapplicable, supracanine buttress absent (?).
		Maxilla, lateral surface orientation: vertical or slopes weakly dorsomedially (0); slopes dorsolaterally, overhanging tooth row (1).

Maxilla		Maxilla, 'lacrimal facet' at base of dorsal process: absent (0); present, distinct dorsoventral ridge present on ascending process divides anterior and posterior depressions (1).
		Maxilla, subnarial foramina: small or absent (0); present and large (1).
		Maxillary facial plate high (0) or low with a height less than 40% its length (1).
		Concave ventral step in maxillary facial plate between caniniform(s) (or anterior-most maxillary teeth) and incisors present (0) or absent (1).
		Broad excavation or pit in the maxilla immediately posterior to the dominant canine absent (0) or present (1).
		Maxilla, ventral surface: straight or weakly convex (0); pronounced convexity (1); strongly convex with prominent 'precanine step' anteriorly (2).
		Posterior region of the maxillary facial plate is folded inward onto the palatal region, so that the maxilla is well exposed ventrally just anterior to the orbit: absent (0) or present (1).
		Maxilla, lateral surface of anterior process bears deep depression dorsally forming narial rim: no (0); yes (1).
Septomaxilla		Septomaxilla, shape: curled in external naris (0); forming a pillar which divides the external naris, septomaxillary foramen subequal in size to anterior part of external naris (1); septomaxilla large and sheet-like (2); anteroposteriorly broad septomaxilla resulting in reduced septomaxillary foramen (3); septomaxillary foramen absent (4).
		Septomaxilla, posterodorsal extension on to lateral surface of skull [facial process]: absent (0); present (1).
		Septomaxilla: contained within external naris (0), escapes to have a short (1) or long facial exposure (2).
		Septomaxilla lateral sheet-like exposure: absent (0); present (1).
Naris		External nares: terminal (0), retracted (1).
		External nares are moderately large and face anterolaterally (0) or are extremely enlarged, close-set and face more anteriorly (1).
		Naris posterodorsal expansion (ordered): absent (0); pinched between nasal and maxilla (1); greatly enlarged, between nasal and lacrimal (2).
Nasal	Requires Frontal	Nasal, length: distinctly shorter than the frontal (0); approximately equal to the frontal (1); longer than frontal (2).
		Median fronto-nasal crest absent (0) or present (1).

Nasal	Requires Lacrimal	Nasal–lacrimal contact absent (0) or present (1).
		Shape of dorsal surface of nasals: flat (0), with median boss (1).
		Nasal, premaxillary process: broad (0); narrow (1)
		V-shaped, posterior border of nasals pointing towards the occiput absent (0) or present (1).
		Nasal, contribution to external naris: forms posterodorsal margin (0); extends anteroventrally as a blade-like process ('external narial shelf') bearing a lateral fossa (1).
Lacrimal	Requires naris	Lacrimal length: participates in margin of external naris (0); does not reach external naris (1).
		Lacrimal lateral surface of anterior process bears deep depression forming narial rim: no (0); yes (1).
		Lacrimal duct (ordered): opens on posterior edge of lacrimal (0); opens laterally near posterior edge of lacrimal (1); opens laterally on concave surface of lacrimal (2).
Frontal	Requires Parietal	Frontal, length: less than 1.5 times parietal length (0); greater than 1.6 times parietal length (1); greater than 2.5 times parietal length (2).
	Requires postfrontal	Frontal, posterolateral process: short (0); long and narrow, matching length of postfrontal, and substantially separating parietal from postfrontal (1); completely absent (2).
		Frontal width:length ratio: <1, frontal narrow (0); >1.5, frontal transversely broad (1).
		Frontal, anterior process length: short (0); longer than posterior process (1); very long, forming at least 2/3 length of bone (2).
		Frontal, anterior process: width equal to that of posterior process (0); narrower than posterior process (1).
		Frontal posterolateral process (ordered): absent, fr-par suture forming right angle to parasagittal plane (0); absent or very short, fr-par suture forming obtuse angle to parasagittal plane (1); long, narrow, forming acute angle with parasagittal plane (2).
Preparietal		Preparietal: absent (0), present (1).
Parietal	Requires nasal	Prefrontal-nasal suture: parasagittal, at least in its caudal third (0); anterolateral (1).
		Size of pineal foramen (ordered): large, more than 25% of mid-parietal length (0); small, less than 25% of mid-parietal length (1); absent (2).

Parietal		Parietal, raised rim around pineal foramen: absent (0); surrounded by raised area forming a pineal 'ridge' or boss (1).
		Position of pineal foramen in dorsal view (ordered): parietal-parietal suture rostral to foramen longer than caudal to it (foramen caudal) (0); equal (foramen in middle) (1); rostral shorter than caudal (foramen rostral) (2); foramen in frontal-parietal suture (3).
		Parietal expanded posteriorly on the midline behind the region of the parietal foramen absent (0) or present (1)
		Parietal (= pineal) opening in adults present (0) or absent/extremely reduced (1).
		Parietal: width/length ratio lower than 0.8 (0); width/length ratio higher than 0.8 (1).
		Parietal, supratemporal notch: shallow (0); deep (1).
		Parietal: in dorsal aspect, the lateral margin is straight or convex (0) or concave (1)
		Parietal ventrolateral flange: absent (0); present (1).
		Parietal crest located posteriorly (0) or extends forwards in adults to include the parietal foramen (1).
		Sagittal crest on parietals: absent (0); present (1).
Prefrontal	Requires jugal	Tuberous ornamentation on prefrontal and/or jugal: absent (0); present (1).
	Requires maxilla	Prefrontal-maxilla contact: absent (0); present anterodorsal to lacrimal (1)
		Prefrontal, ventral process: transversely narrow edge ['tongue-like'] (0); expanded medially forming antorbital buttress (1).
		Prefrontal, lateral surface: approximately flat or convex (0); concave, forming antorbital recess [prefrontal pocket] (1).
Postfrontal	Requires postorbital	Postorbital-postfrontal contact: overall trend approximately straight (0); incised by postorbital (1).
		Adductor musculature originates on lateral surface of postorbital absent (0), present (1), originates on both postorbital and postfrontal (2).
		Postfrontal present (0) or absent (1).
		Postfrontal: without (0) or with (1) posterior extension along its medial contact with the frontal.
		Prefrontal: ventral process tongue-like (0) or expanded medially (1)

Postfrontal		Postfrontal morphology: small, occupies approximately one-third of dorsal orbit rim, not transversely broad, and has approximately flat or convex dorsolateral surface (0); dorsolateral surface concave (recessed between orbit and temporal fenestra) (1); long and broad forming prominent supraorbital shelf (2); strongly recessed posterolateral surface forming anterior part of fossa around temporal fenestra (3).
Squamosal	Requires postorbital	Squamosal anterodorsal process: no or little underlap of posterior process of postorbital (0); extensive underlap of posterior process of postorbital (1). Scored as inapplicable in the absence of a lateral temporal fenestra.
	Requires opisthotic	Mastoid process' absent or poorly developed (0) or squamosal and paroccipital processes of the opisthotic form a distinct, posteriorly projecting 'mastoid process' (1).
	Requires Pro-otic	Medially directed process of the squamosal contacting the pro-otic absent (0) or present, enclosing the pterygoparoccipital foramen (1).
		Squamosal posterodorsal process: absent (0); present (1).
		Posteroventral process of the squamosal absent (0) or present (1).
		Squamosal occipital shelf (ordered): broad, contributes to occipital surface of skull (0); narrow, quadrate exposed in occipital view (1); absent, posterior edge of quadrate exposed in lateral view (2).
		Squamosal external auditory meatus groove: absent (0), present (1)
		Dorsal and lateral surfaces of postorbital: form smooth curve (or dorsal surface absent, postorbital not participating in skull roof) (0); sharply divided (meeting at edge) (1).
Postorbital	Requires supratemporal	Postorbital-supratemporal contact: present (0); absent, (1); inapplicable, supratemporal absent (?).
	Requires temporal	Postorbital, posterior process, length: short (0); long, extending more than half of temporal length (1).
	Requires jugal	Postorbital and jugal, medial orbital process (deep, dorsoventrally tall medial flange): absent (0); present (1).
		Postorbital, posterior process, transverse width: broad (0); narrow (1)
		Postorbital lateral boss at orbital margin: absent (0); present (1).
		Postorbital-squamosal contact: anteroposteriorly short (0); extensive due to long posterior process of the postorbital that obliquely overlaps the squamosal in posterior half of temporal region (1).

Jugal	Requires maxilla and quadratojugal	Jugal, contribution to ventral margin of skull: present (0); absent, jugal excluded from ventral margin by maxilla-quadratojugal contact achieved by a long posterior extension of the maxilla (1); maxilla-quadratojugal contact achieved by long anterior extension of the quadratojugal (2).
	Requires maxilla and lacrimal	Jugal, length and dorsoventral expansion of anterior ramus: intermediate, contacts lacrimal but a distinct anterodorsal projection is absent (0); anterodorsal projection present, anterior process of jugal dorsoventrally deep (1); anterior process of jugal short, terminates ventral to orbital midlength as a tapering splint and maxilla partipates in orbit margin (2).
	Requires squamosal	Jugal-squamosal contact on posterior surface of postorbital bar: absent (0); present (1); inapplicable, temporal fenestra absent (?).
		Jugal-squamosal suture orientation: posteroventral (0); indented (1); anteroventral (2); jugal indented (3).
		Jugal–squamosal ventral contact, perforated by small, elongate fenestra: absent (0); present, upper margin enclosed by anteroventral exension of the squamosal (1); inapplicable, jugal does not contact squamosal ventrally (?).
		Postorbital process of jugal is present (0) or absent (1).
		Jugal, anteroposterior thickness of dorsal ramus (forming postorbital bar): broad, temporal fenestra only weakly emarginates the jugal (0); narrow, jugal strongly emarginated (1); inapplicable, temporal fenestra absent (?).
Quadratojugal	Requires maxilla and squamosal	Anterior extent of quadratojugal (ordered): maxilla-quadratojugal suture (0); extending anterior to ventral portion of squamosal, but not contacting maxilla (1); ≤ anterior extent of ventral portion of squamosal (2); quadratojugal absent (3).
		Quadratojugal superficial anterodorsal process: absent (0); present (1).
Basisphenoid		Basisphenoid, basal tubera: short, broad, with short articular facets facing anterolaterally (0); long and wing-like, with long articular facets facing anteriorly (1); small [?=short and broad], with short articular facets facing anteriorly.
Parasphenoid		Parasphenoid, body shape: transversely broad, width greater than length from basipterygoid processes to posterior end (0); transversely narrow, length greater than width (1).
		Parasphenoid, body [ventral plate] median groove: absent, ventral surface flat (0); or shallow concave region between cristae ventrolaterales (1); deep median sulcus present (2).
		Parasphenoid body, posteroventral emargination [basisphenoid shelf]: absent (0); present (1).

Parasphenoid		Parasphenoid body, median longitudinal ridge on ventral surface: absent (0); present (1)
		Parasphenoid, expansion of body [ventral plate] posterior to basicranial articulation: gradual (0); abrupt (1)
Vomer	Requires palatine	Ventromedian crest between palatines on posterior portion of vomer absent (0) or present (1).
		Vomer, internarial shape: widest posteriorly (0); widest near middle (1).
		Portion of vomer separating the choanae is slightly bulbous, narrowing towards its contact with the premaxilla (0), expands anteriorly and is widest at its contact with the premaxilla (1), or bears specialized transverse processes just behind the contact with the premaxilla overlapping vomerial processes of the crista choanalis (2).
		Interchoanal portion of vomer where it meets the postchoanal portion: broad (0), forms median ridge (1).
		Vomer ventral surface: flat to convex (0), lateral ridges and median trough (1).
		Vomer anterior vault present (0) or absent (1).
		Vomer, width of ventral surface: broad (0); narrow (1).
		Choanal and postchoanal portions of vomer: meet at similar level on palate (0), choanal portion is offset ventrally from postchoanal portion (1).
		Vomers paired (0), fused anteriorly (1) or completely fused (2).
Pterygoid	Requires basipterygoid process	Basal articulation [basicranial joint]: present (0); absent (1)
		Basipterygoid articulation located: high above primary palate (0), just dorsal to basicranial ramus of pterygoid (1), at level basicranial ramus (i.e., suture visible in ventral view) (2).
		Parasagittal ridges running from medial posterior flare of transverse flanges to basioccipital absent (0) or present (1).
		Basal articulation, position: approximately level with transverse flange of pterygoid (0); anterior to transverse flange (1); posterior to transverse flange (2).
		Basicranial rami of pterygoids: broadly separated (0), narrowly separated with median trough formed (1), broadly contacting anterior to basicranium (2).
		Pterygoid bears no median tubercle/crest (0) or a ventromedian tubercle/crest is present anterior to the interpterygoid vacuity (1).
		Medial edge of pterygoid basicranial ramus forms parasagittal ridge on ventral surface: absent (0), present (1).

Pterygoid		Pterygoid, ascending lamina/dorsal flange of the anterior ramus of the pterygoid: low [?poorly ossified] (0); tall (1).
		Interpterygoid vacuity of adults present (0), absent/extremely reduced (1), enlarged and somewhat heart-shaped, with the anterior end positioned between the transverse flanges of the pterygoids (2).
		Pterygoids, interpterygoid vacuity: anteroposteriorly long (0); short (1).
		Pterygoid, distinct transverse flange: present (0); absent (1).
		Pterygoid, transverse flange, orientation of posterior margin: lateral or posterolateral (0); anterolateral (1).
		Pterygoid flange expansion moderate (0), reduced (1) or sharp, posteriorly projecting wings with slight posterolateral expansion (2).
		Ventral rim of pterygoid transverse flanges sweeps posteriorly at the midline vacuity (0) or does not sweep posteriorly at the vacuity (1).
		Pterygoid at level of posterior edge of transverse flange: far from sagittal plane, leaving the interpterygoid vacuity posteriorly opened (0), interpterygoid vacuity closed or constricted posteriorly by median flange (1), or quadrate processes of pterygoid medially appressed (2).
		Interpterygoid vacuity: long (0) or short (1).
		Pterygoid: without (0) or with (1) shelf posterior to its transverse flange.
		Pterygoid, distinct process projects medially from transverse flange: absent (0); present (1).
		Pterygoid, palatal ramus length: two times longer or greater than two times the length of the quadrate ramus (0); palatal ramus less than two times length of quadrate ramus (1).
		Pterygoid, quadrate ramus, medial shelf (‘posteromedian flange’; ‘tympanic flange’): present (0); absent (1).
Epipterygoid	Requires Parietal	Epipterygoid separate from parietal (0) or contacts parietal (1).
	Requires Pro-otic	Posterior apophysis of the epipterygoid contacting or nearly contacting the pro-otic absent (0) or present, enclosing an aperture presumably for the trigeminal nerve (1).
		Trigeminal nerve exit exists between pro-otic incisure and epipterygoid (0), via a foramen between the pro-otic and epipterygoid (1), or via multiple foramina (2).
	Requires Frontal	Epipterygoid–frontal contact absent (0) or present (1).

Epipterygoid		Epipterygoid ascending process appears as a thin rod (0), is slightly expanded anteroposteriorly (1) or is extremely expanded (2).
		Epipterygoid ventral plate: large, part of basicranium (0) or small, excluded from basicranium (1).
Pro-otic		Laterally directed processes of the pro-otic participating in the pterygoparoccipital foramen absent (0) or present (1).
Palatine Palatine		Two palatines: separated by the vomer and pterygoid (0), join in midline (1)
		Palatine, width: broad (0); narrow (1).
Basipterygoid process		Basipterygoid processes (unordered): short, broad, with short articulating facets facing anterolaterally (0); long, wing-like, with long articulating facets facing anteriorly (1); long, with hemispherical articulating facets facing more or less anterolaterally (2).
		Basal articulation, morphology of articular surface of basipterygoid process: single, rounded articular surface (0); flat anterior facet (1); inapplicable, basal articulation absent (?)
Supratemporal		Supratemporal: present (0), absent (1).
		Supratemporal shape: broad, subrectangular, superficial bone that extends onto lateral surface of skull (0); large, elongate (subequal to parietal length), but placed in groove on parietal (1); long, slender, located in groove on parietal (2); supratemporal absent (3).
Tabular	Requires opisthotic	Tabular: contacts paroccipital process of opisthotic (0), restricted dorsally (1).
		Tabular (ordered): large, sheet-like (with ventral expansion) (0); narrow, slender (1); absent (2).
		Tabular, posteromedial process that subdivides posttemporal fenestra and contacts the supratemporal: absent (0); present (1)
		Tabular morphology: subrectangular sheet located dorsal to posttemporal fenestra (0); large, sheet-like, L-shaped bone comprising suborthogonal ventral and medial processes that enclose postemporal fenestra dorsally and laterally (1); reduced, displaced laterally, now located dorsolateral to posttemporal fenestra, medial portion tapering (2); tabular absent (3)
Postparietal		Postparietal size (ordered): sheet-like, both together not much smaller than suproccipital in state 59(1) (0); small, splint-like (1); absent (2).
		Shape of postparietal: wider than tall (0), approximately square (1), or taller than wide (2).
		Postparietals: unfused/paired (0); fused to form a midline element (1).

Quadrate	Requires occipital and squamosal	Quadrate contact: primarily paroccipital process (0), about equal paroccipital process and squamosal (1), mostly squamosal (2)
	Requires quadratojugal	Quadrate and quadratojugal relatively large (0) or reduced in height (1).
		Posteroventral process on quadrate in posterior notch of squamosal absent (0) or present (1).
		Quadrate shape (ordered): straight posteriorly (0); shallowly emarginated (1); with conch (2).
		Quadrate, condyles: distinct, separate (0); confluent, forming a saddle-shaped articular facet (1).
		Occipital margin of quadrate (ordered): anterior slope ≥ 80° (0); 80° > anterior slope > 50° (1); anterior slope ≤ 50° (2).
Occiput		Occiput, slope: approximately vertical (0); inclined anterodorsally by 10-50 degrees (1); strongly inclined anterodorsally by >60 degrees (2); inclined posterodorsally (3)
		Occipital condyle single (0) or double (1).
		Basal tuber small (0) or large, approximately one-third the occipital breadth (1)
		Dorsal surface of the paroccipital process is relatively smooth or straight (0). or deeply hollowed (1) in the floor of the post-temporal fenestra.
		Paroccipital process shape: vertical or nearly vertical sheet, height ≥ 0.5 transverse length (0); elliptical in cross-section, height < 0.5 transverse length (1).
		Paroccipital process orientation: strongly posteroventral and lateral (0), moderately posteroventral and lateral (1), transverse (2)
		Paroccipital process attachment (ordered): ends freely (0); weak contact (1); strong contact (2).
Supraoccipital		Supraoccipital, prominent lateral processes forming dorsal margin of posttemporal fenestra: absent, fenestra bounded dorsally by tabular only (0); present (1)
Exoccipital		Exoccipital, lateral wing: tall and narrow (0); broad, extending ventral to paraoccipital process (1).
Basioccipital		Basioccipital, occipital condyle orientation: posteriorly directed (0); posteroventrally directed (1).

Opisthotic	Requires squamosals and supraoccipital	Opisthotic, paraoccipital process: confined between squamosals, not visible in lateral view, height less than supraoccipital (0); posterolateral flange projecting posterior to squamosals, visible in lateral view and blade-like, taller than supraoccipital (1); short and knob-like (2)
		Opisthotic, morphology and orientation of paraoccipital process: robust, horizontal rod (0); slender rod, extends posteroventrolaterally (1); dorsoventrally broad sheet, extends laterally (2).
Coronoid		Number of coronoids: two (0); one (1).
		The posterodorsal terminal margin of the coronoid process is straight (0), more rounded (1) or comes to a sharp point (2).
		Mandible, shape of coronoid eminence: slightly convex (0); strongly convex (1); subhorizontal/flat (2).
Mandible	Proximal	Mandible, position of coronoid eminence: posteriorly, within posterior 1/3 of total length (0); anteriorly, approximately 2/5 of total length from posterior end (1).
		Mandible, bone forming dorsal margin of coronoid eminence laterally: coronoid or surangular (0); dentary (1).
		Retroarticular process size (ordered): absent (0); small (1); large (2).
		Mandible, retroarticular process: absent (0); present (1).
		Mandible, composition of retroarticular process: formed by articular, angular and surangular (0); formed only by articular, large, and curved ventrally (1); inapplicable, retroarticular process absent (?).
		Postdentary bones' height relative to total dentary height equal (0), between one-half and equal (1) or much less than one-half (2
		Mandibular fenestra absent (0), penetrating the mandible and visible laterally (1), or surangular above and prearticular below a small fenestra on the medial surface of the mandible (2).
		Splenial overlaps angular: along complex suture (0); ventrally (1); dorsally (2); ventrally and dorsally (3).
		Foramen between prearticular and angular (sometimes bordered by splenial as well) on medial surface of lower jaw: absent (0), present (1).
	Distal	Mandibular symphysis: dorsoventrally low, mandible tapers anteriorly (0); doroventrally thick, almost as deep as mandible at midlength of the tooth row (1).

Mandible	Distal	Symphyseal region of the dentary is only moderately expanded mediolaterally with a low mentum angulation in ventral view (0) or is anteroposteriorly thickened (1).
		Splenial exposed laterally near symphysis (0) or obscured by dentary (1).
		Splenial, contribution to mandibular symphysis: present, symphysis formed from dentary and splenial (0); absent, symphysis formed solely by dentary (1)
	Whole	Dentary size: comprises >70% the anteroposterior length of the mandible (0); <65% (1)
		Dentary height increased posteriorly and postdentary bones reduced to form a free standing coronoid process absent (0) or present (1).
		Mandible, size of Meckelian foramen: small, <0.10 of jaw length (0); large, >0.25 of jaw length (1)
		Splenial, exposure on lateral surface of mandible: absent (0); narrow, foming one-fifth or less of the lateral surface (1); broad anteriorly, forming one-third or more of the lateral surface (2).
		Mandible, proportions (not including laminar portion of the angular): intermediate proportions, dorsoventral height 0.20–0.26 total length (0); short and robust, dorsoventral height >0.30 total length (1); very long and dorsoventrally slender, maximum height <0.18 total length (2).
Prearticular	Requires articular	Prearticular and articular, pterygoideus process: formed by articular and prearticular (0); formed by the articular only and sheathed by prearticular (1)
		Prearticular, medial surface: nearly straight (0); twisted posteriorly (1)
Articular		Articular dorsal process: absent (0), present (1).
Angular		Angular, cross-section shape of ventral border of angular: weakly ridged/keeled (0); prominent, sheet-like keel with strongly convex posterior edge (1); reflected lamina separated from mandible by a posterior notch in lateral view (2); ventral surface of angular evenly rounded (3).
		Angular reflected lamina dorsal notch: near articular (0), midway between articular and dentary (1), close to dentary (2)
		Angular, reflected lamina, posterior emargination: short (0); long with free posterodorsal margin (1); inapplicable, reflected lamina absent (?)

Angular		Reflected lamina shape and ventral extent: rounded, projecting below the ventral margin of the dentary at about the level of the second groove (0), slightly anteroposteriorly elongate (spade-shaped) and does not appear to extend below the dentary (1), or is extremely reduced and spoon-shaped (2).
		Reflected lamina of angular (= tympanic) size: large (0) or reduced (1).
		Angular, reflected lamina: shallow (0); deep (1); not applicable, reflected lamina absent (?).
		Angular with pattern of ridges and fossae on its lateral surface: absent (0), present (1).
		Size of lateral exposure of angular: wide (0); narrow (1).
Surangular		Surangular, transverse expansion of dorsal surface: thin, sheet-like surangular, unexpanded (0); transversely expanded dorsally forming broad platform (1)
		Surangular contribution to notch of reflected lamina: absent (0); small (1); large (2).
		Posterior end of surangular: straight (0); strongly curved ventrally (1).
		Dorsal edge of surangular just posterior to dentary with laterally projecting ridge: absent (0), or present (1).
Dentary	Requires angular	Lateral mandibular fenestra between dentary and angular: absent (0); present (1)
		Ventral margins of angular and dentary confluent (0) or angular (= tympanic) positioned dorsal to ventral margin of dentary (1).
		Dentary−angular suture: runs diagonally across lateral surface of mandible (0), posterior margin of dentary deeply incised (1).
		Overall dentary shape is best described as deep/ robust (0), short and banana-shaped (1), or long, slender, and relatively straight with a smooth ventral edge (2)
		Dentary: coronoid eminence (0), coronoid process (1)
		Dentary masseteric fossa in adults absent (0), present high on coronoid process (1) or enlarged, extending to the ventral border of the dentary (2).
		Lateral sulcus along the ramus and coronoid process of the dentary, absent (0) or present (1).
		Area between left and right dentaries widens greatly posteriorly (0) or remains relatively long and narrow (almost slit-like) just posterior to symphyseal region (1).

Dentary		Lateral surface of the dentary is relatively smooth (0) or bears a marked constriction behind the canine (1) in dorsal and ventral views.
		Dentary angle, lateral to the reflected lamina, is absent/rounded (0), moderate/sharp (1) or pronounced, protruding with an angle of < 120° (2).
		Dentary height in canine versus anterior postcanine regions: nearly equivalent (0), shows pronounced difference (1).
Splenial		Splenial, contact with posterior coronoid: absent (0); present (1); inapplicable, posterior coronoid absent (?).
Stapes		Stapes: robust, with thick shaft (0); slender, rod-like shaft (1).
		Dorsal process of stapes present (0) or reduced/ absent (1)
		Stapedial foramen oriented posteroventrally (0), dorsoventrally (1) or reduced/absent (2).
Hyoid		Hyoid: short, directed to quadrate region (0); long, directed posteriorly beyond skull (1).
Vertebrae	Any	Vertebral centra, notochordal canal: present in adults (0); absent in adults (1).
		Neural arches: arches possess lateral excavations (0) or no excavations (1)
Presacral vertebrae	All	Presacral vertebrae, count: 27 or more (0); <27 (1)
	Any	Cervicodorsal centra, ventral surface: low, rounded ridge (0); prominent, transversely narrow, sheet-like keel (1).
Presacral and Sacral Vertebrae	All	Presacral/sacral vertebrae, intercentra: present along entire series (0); present only in parts of series, cartilaginous intercentra may be present in places (1); absent (2).
Cervical vertebrae	Requires a caudal dorsal vertebra	Cervical centra length: no longer than caudal dorsals (0); longer than caudal dorsals (1).
	Requires all	Cervical vertebrae, count: 3 or fewer (0); 5 or more (1)
	Requires anterior	Atlas-axis complex, atlantal and axial intercentra: contact ventrally or in very close proximity (0); widely separated by ventral extension of the atlantal centrum (odontoid) (1).
	Any	Ventral surface of cervical centra: rounded (0); strongly keeled (1).
		Cervical neural arch excavation (ordered): absent (0); shallow (1); deep (2).
Dorsal vertebrae	Any	Dorsal centra (anterior–middle dorsal centra), ventral surface: transversely rounded (0); ventral ridge (1); strongly pinched forming transversely narrow, sheetlike keel (2); ventrally raised platform or keel bearing longitudinal trough (3).

Dorsal vertebrae	Any	Dorsal centra, anteroposterior length: short, subequal to height (0); long, at least 1.5 times as long as high (1).
		Dorsal prezygapophyses: planar, do not contact on midline (0); transversely concave, contact on midline (1); planar and inclined strongly medially, contact on midline (2).
		Dorsal postzygapophyses: widely spaced (0); contact on midline (1).
		Dorsal postzygapophyses, hyposphene: absent (0); present and prominent (1).
		Dorsal neural arches, dorsolateral surfaces: flat or weakly concave, not swollen or buttressed (0); swollen and convex (1); excavated by deep depressions (2).
		Dorsal transverse process, location: approximately at midlength of neural arch, anterior centrodiapophyseal lamina oriented anteroventrally (0); located anteriorly, anterior centrodiapophyseal lamina vertical (1).
		Dorsal transverse processes: prominent but not elongate, a conspicuous lamina extends anteroventrally along lateral surface of neural arch from base of transverse process (0); extend far laterally, lamina weak or absent (1).
Sacral vertebrae	All	Sacral vertebrae, count: two or fewer (0); three or greater (1).
Neural spines	Any Presacral	Presacral neural spines: short (0) or long (more than five times the height of the centrum) (1)
		Presacral neural spines: presacral centrum length to neural spine height ratio is 1:1 to 1:5 (0); ratio is 1:6 to 1:12 (1); ratio is 1:13 to 1:20
		Presacral neural spines: lateral tubercles absent (0); moderately sized lateral tubercles present; large, gall-like lateral tubercles present
		Presacral neural spines: laterally compressed in distal cross section (0) or subcircular
	Anterior cervical	Axial neural spine, anteroposterior length of apex: longer than centrum and extends past anterior surface of centrum (0); shorter than centrum (1); short and spine inclined anterodorsally (2).
		Axial neural spine, height: low, subequal to the centrum height (0); tall, at least 1.5 times the height of the centrum (1); very tall, many times the centrum height (2).
	Cervical	Presacral neural spines: anterior spines exend dorsally (0) or lean anteriorly (1).

Neural spines	Caudal cervical and anterior dorsal	Mammillary processes on caudal cervical and cranial dorsal neural spines: absent (0); present (1).
	Anterior dorsal	Dorsal neural spines, anterior spines: slender, not expanded dorsally (0); expanded dorsally giving club-shaped appearance (1).
	Dorsal	Dorsal neural spines, height: short, approximately 1.5 times centrum height or lower (0); intermediate, 2–3 times centrum height (1); very tall (2).
		Dorsal neural spines, lateral tubercles: absent (0); present (1)
		Dorsal neural spines, longitudinal grooves on anterior and posterior surfaces: absent (0); present (1).
	Dorsal	Dorsal neural spines, when elongate: without 'shoulders' (0); with 'shoulders' (1).
		Dorsal neural spines morphology: consistent along column (0); alternating(1)
	Mid dorsal	Ratio of height of mid-dorsal neural spines from base of zygapophysis: ≤ 1.5 (0); > 1.5 (1).
	Posterior dorsal	Posterior dorsal neural spines, orientation: approximately vertical (0); posteriormost one or two dorsal neural spines anterodorsally inclined (1); several posterior neural spines anterodorsally inclined (2); strongly posterodorsally inclined (3).
	Dorsal or sacral	Dorsal and sacral neural spines, cross section: transversely compressed, subrectangular, blade-like spines (0); subcircular, rod-like for most of spine length [except basally] (1).
	Sacral or caudal	Sacral and caudal neural spines: smooth (0); rugose with longitudinal ridges on lateral surface and tapering apex ['leaf-shaped'] (1)
		Sacral and caudal vertebrae: smooth sided spines (0) or spines with longitudinal ridges (1)
	Caudal	Caudal vertebrae: neural spines are rectangular from the lateral aspect (0) or are wider at the tip (1)
		Caudal vertebrae: neural spines are short and square (0) or tall and pointed (1)
	Any	Neural spines: triangular (0); rectangular (1).
Cervical ribs		Accessory process on craniolateral surface of cranial cervical ribs: absent (0); present (1).
		Cervical ribs: some or all holocephalous (0); all dichocephalous (1).
Thoracic ribs		Trunk ribs: dichocephalous (0); holocephalous (1).

Thoracic ribs		Dorsal ribs, tuberculum (contacts diapophysis) morphology: well-developed and flange-like (0); reduced to low tuberosity (1); low tuberculum with expanded, concave, cup-like articular facet (2)
		Dorsal ribs, curvature: curved proximally, only weakly curved distally (0); strongly arched proximally, curved throughout length enclosing expanded, 'barrelshaped' trunk (1)
Sacral ribs		Sacral ribs (ordered): two unequal (0); two equal (1); three (2).
		Sacral ribs, morphology of first sacral rib: hugely enlarged and braces contact of second sacral rib with ilium (0); subequal to or only slightly larger than more posterior sacral ribs (1).
Sternum		Sternum: not mineralized (0); mineralized (bone or calcified cartilage) (1).
Interclavicle	Shaft	Minimal interclavicle shaft width: ≤ 0.105 tip-to-tip width (0); ≥ 0.137 tip-to-tip width (1).
	Proximal	Interclavicle shape: +-shaped (cranial process present) (0); T-shaped (cranial process absent) (1).
		Interclavicle, shape of posterior margin of head: distinctly offset from shaft by posterolateral emargination (0); grades gradually into shaft (1).
		Interclavicle, angle of head: low angle, interclavicle weakly curved in lateral view (0); head sharply upturned (1)
		Interclavicle, shape of anterior end: triangular, pointed anteriorly with 'diamond-shaped' appearance (0); truncated anteriorly (1); trapezoidal with narrow, straight anterior margin (2).
Clavicle		Clavicle, shape of ventromedial plate: narrow (0); deep (1); intermediate (2); narrow and short, but with additional anterior process (3).
		Clavicle, orientation of long axis of ventromedial plate relative to shaft: highly obtuse angle (0); almost perpendicular (1)
Cleithrum	Requires scapula	Cleithrum, size and contacts: large, approximately two-thirds the height of the scapula and contacts clavicle (0); intermediate, approximately half the height of the scapula and contacts clavicle (1); reduced and does not contact clavicle (2).
		Cleithrum: present (0); absent (1).
Scapula	Proximal	Cranial margin of scapula: straight, at least dorsally (0); convex along entire length (1).
		Scapula, anteroposterior breadth of proximal end (base): broad (0); pinched/narrow (1)
		Scapulocoracoid, glenoid shape: anteroposteriorly elongate and helical (0); short, faces posterolaterally (1)

Scapula		Scapula, posterolateral surface of blade immediately dorsal to glenoid: weakly concave (0); deep, triangular concavity bounded anteriorly by prominent supraglenoid buttress (1); distinct supraglenoid buttress absent (2)
		Supraglenoid foramen: absent (0); present (1).
		Scapula, location of supraglenoid foramen: posterior to supraglenoid buttress (0); anterior to supraglenoid buttress (1); on apex of supraglenoid buttress (2); inapplicable, supraglenoid foramen absent (?) (Figure A6).
	Shaft	Ventral surface of cervical centra: rounded (0); strongly keeled (1).
	Distal	Scapula, anteroposterior breadth of distal end: broad (0); narrow (1).
	Requires corocoid	Scapulocoracoid, notch in anterior margin on scapulocoracoid contact (scapulocoracoid notch): absent (0); present (1).
Corocoid	Proximal	Triceps process on coracoid: small or absent (0); large (1).
		Coracoid, foramen on posterodorsal surface between glenoid and triceps process: absent (0); present (1).
		Coracoids, number: two (0); one (1).
Humerus	Proximal	Humerus, ridge connecting deltopectoral crest to head: double, paired ridge enclosing proximolateral fossa, deltopectoral crest anteroposteriorly expanded and ‘tuberous’ (0); single, fossa absent (1)
		Humerus, anterior surface of deltopectoral crest: weakly concave (0); strongly concave, bounded dorsally by a prominent, proximodistally elongate ridge (1).
		Humerus, morphology of latissimus dorsi attachment: step-like transverse ridge or mound (0); prominent, posteriorly-directed tubercle (1).
		Humerus, ventral surface of proximal end: extends proximally forming a low, anteroposteriorly oriented crest posteroventral to head (0); extends far proximally, forming a prominent crest (1).
	Shaft	Humerus, posterior surface of shaft around exit of entepicondylar foramen: convex (0); exit foramen very large and rimmed by a longitudinal depression, foramen only enclosed by a narrow strip of bone (1).
		Humerus, ‘distinct shaft’: absent (0); present (1).
	Distal end and shaft	Ratio of width of distal head of humerus to shaft length: ≥ 0.3 (0); < 0.3 (1).
	Distal	Entepicondyle: moderately large (0); strongly developed at maturity (1).

Humerus	Distal	Humerus, ectepicondylar (radial epicondylar) foramen: absent, ectepicondylar groove not enclosed and supinator process proximodistally short (0); present (1); long supinator process, but epicondylar foramen not enclosed (2); supinator process very low or absent (3)
		Humerus, entepicondyle (ulnar epicondyle), transverse width: moderate makes up just less than half of transverse width of distal expansion (0); reduced (1); enlarged, makes up more than 2/3 of the distal transverse width (2)
		Humerus, ventral surface (faces anteroventrally) of entepicondyle: flat or weakly convex (0); low, anteroproximally directed ridge on posterior margin (1).
		Ectepicondylar region (ordered): foramen, process bridged (0); supinator process present, groove present (1); process, groove and foramen absent (2).
Radius	Requires humerus	Radius-humerus length ratio (ordered): < 0.68 (0); 0.68 to 0.82 (1); > 0.82 (2).
		Radius shape: straight (0); twisted in lateral view (1).
Ulna	Proximal	Olecranon process (unordered): prominent, extension of ulna (0); absent or low (1); prominent, ossifies separately (2).
		Ulna, broad olecranon (0); narrow, elongate olecranon (1); small (2)
Carpi	Medial	Medial centrale carpi: present (0); absent (1).
		Manus, intermedium size: larger than medial centrale (0); smaller than medial centrale (1).
	Lateral	Lateral centrale: present (0); absent (1).
		Manus, preaxial (lateral) centrale overlaps proximal surface of third distal carpal: no (0); yes (1).
	Ulnare	Manus, ulnare proportions: long (0); short, width >0.6–0.7 times length (1).
	Radiale	Manus, width:length ratio of radiale: subequal or < 1.0 (0); > 1.0 (1).
Metacarpi	Fourth and Fifth	Manus, McV:McIV length ratio: >0.65 (0); <0.65 (1)
	Fourth, requires radius	Manus length, fourth metacarpal:radius length ratio: <0.25 (0); 0.30–0.45 (1); >0.50 (2).
	Any	Manus, metapodial shape: long and slender, two–three times longer than maximal width (0); short and fat with small diaphysis (1).
Manual Phalanges	Digits 2 and 5	Manus, digital formula: X3YZ3 (0); X2YZ2 (1)
	Digit 3	Manus, phalanges in digit III: four (0); three (1)

Manual Phalanges	Digit 4	Manus, phalanges in digit IV: five (0); four or fewer (1)
	Ungual	Manus, ungual phalanges, height:width ratio: low, ratio <1.1 and blood vessel grooves may be visible on the dorsolateral surfaces of the phalanx (0); high, ratio >1.5, strongly recurved and blood vessel grooves are located on the lateral surfaces of the phalanx (1).
		Manus, ungual phalanges, flexor tubercle: single bulbous eminence (0); paired, medial and lateral eminences (1); absent (2)
	Any	Manus, phalanges, distal articular surface orientation: distal (0); ventrodistal (1)
Pelvic girdle	Whole	Pelvic girdle: solid (0); fenestrate (1).
Pubis	Proximal	Pubis, pubic tubercle anteroventral to acetabulum: absent (0); present, projects laterally (1); present, projects dorsally (2); broad, concave region on lateral surface (3); highly striated region bounded by a longitudinal crest dorsally (4)
	Distal and shaft	Lateral and distal pubic tubercles: small or absent (0); large (1)
		Pubis, pectineal ridge: absent (0), present (1).
	Distal	Pubis, midline symphysial contact: enlarged, dorsoventrally broad (0); subequal to height of ischial midline symphysis, restricted to peripheral margin of medial surface (1)
		Pubis, ventral surface of pubic apron: flat or convex, pubes extend ventromedially (0); strongly concave, pubes extend approximately medially (1).
	Requires Acetabulum	Pubis, length relative to acetabulum: >1.5 times (0); 1.0–1.5 times (1).
	Requires Ischium	Obturator foramen size is small (0), moderately enlarged (1) or extremely enlarged (2).
		Pubis and ischium orientation relatively vertical (0) or more horizontal, forming a broad puboischiatic plate (1).
Acetabulum		Acetabulum: elongate (0); circular (1).
Ilium	Dorsal	Ilium, height of dorsal process.
		Ilium, dorsal process morphology: long, tapering posterodorsal blade and anterodorsal blade small or absent (0); marked anterodorsal expansion present, dorsal process tall and plate-like (1)
	Whole	Ilium, medial surface: weakly concave or flat (0); anteroventrally oriented ridge contacts pubic articulation (1).
		Ilium, fossa on dorsal surface [dorsal groove], or external shelf: dorsal groove present (0); external shelf present (1); both absent, ilium plate-like (2).

Ischium	Distal	Ischium: slender, tapering posteriorly (0); expanded posterodorsally (1)
	Shaft	Ischium, dorsal margin of medial surface: smooth (0); longitudinal crest (1).
Hindlimb and trunk		Hindlimb-trunk length ratio: hindlimb much shorter than trunk (0); hindlimb almost as long as trunk or longer (1).
Femur	Proximal	Femur, orientation of head: terminal and anteroposteriorly elongate (0); inflected medially and subspherical (1).
		Femur, proximal articular surface [head] proportions: narrow dorsoventrally (0); broad dorsoventrally (1).
		Femur, ventral ridge system (internal and fourth trochanters): prominent (0); low and feebly developed (1).
		Femur, intertrochanteric fossa: prominent (0); reduced or absent (1).
		Femur, posterior longitudinal ridge located proximally on ventral surface: absent, internal fossa not enclosed posteriorly (0); present, enclosing posterior margin of internal fossa (1).
		Femur, mound-like eminence on dorsal surface of proximal end: extensive, prominent and longitudinally elongate (0); small (1).
		Distinct trochanter minor of the femur absent (0) or present (1).
		Femur, greater trochanter: absent (0); present (1)
	Shaft	Femur, prominent longitudinal ridge extending posterodistally from distal end of internal fossa: absent or low (0); present as a prominent rugose crest (1); present as a prominent angular ridge forming the posteroventral surface of femoral shaft (2); present but low and does not extend far distally, instead forming a distinct fourth trochanter (3).
	Distal	Femur, anterior condyle: dorsoventrally thick (0); dorsoventrally compressed (1).
		Femur, posterior condyle, dorsal surface: convex (0); transversely concave, bearing longitudinal trough (1).
		Femur, condyles: prominent and well-separated, posterior condyle extends slightly further distally than anterior condyle (0); posterior condyle projects far distally (1); condyles both low and indistinctly separated (2)
	Whole	Femur maximum length: distal width ratio: < 4 (0); ≥ 4 (1).
	Reuqires humerus	Femur-humerus length ratio (ordered): > 1.2 (0); 1 to 1.2 (1); < 1 (2).
	Shaft, rquires humerus shaft	Femoral and humeral shaft diameters: femur = 150% humerus (0); more or less equal (up to 120%) (1).

Fibula		Fibula, distal head/shaft diameter: less than 3:1 (0); more than 3:1 (1).
Tibia	Proximal	Tibia, cnemial crest: low (0); prominent and distinct (1)
Lower hindlimb	Tibia, astragulus, fourth digit and metatarsal	(106) Lower leg: foot length ratio: articulated tibia + tibiale/astragalus longer than articulated 4th metatarsal + digit (0); shorter (1).
Astragulus-calcaneum articulation		Astragalus-calcaneum articulation (unordered): flat (0); concave-convex (1); foramen on calcaneum, articulation expanded (2); sutured or fused (3).
		Lepidosauriform ankle joint: absent (0); present (1).
Astragulus		Astragalus: absent (0); present (1).
		Astragalus, proximal neck region: short (0); long (1).
		Astragalus, orientation of tibial articular suface: mediodistal (0); anterodorsal (1
Calcaneum		Lateral tuber on calcaneum: absent (0); present (1).
		Calcaneum (fibulare), proportions: length approximately equal to width (0); length conspicuously greater than width (1).
Tarsals	Lateral centrale, second and third distal	Pes, lateral centrale: no larger than second or third distal tarsals (0); large than second or third distal tarsals (1); absent (2).
	Fifth	Pes, distal tarsal V: present (0); absent (1).
Metatarsals	Fourth, requires digit 4	Fourth metatarsal: short (0); long (at least 40% of digit IV) (1).
	Fifth	Fifth metatarsal: straight (0); hooked (1).
Metapodials	At least two proximal ends from the same limb	Metapodials overlapping proximally: no (0); yes (1).
Fore or Hind limbs	One complete	Appendicular skeleton, limb proportions: short and stout (0); long and slender (1).

Appendix G

Percentages assigned to each region of the skeleton in calculating the Character Completeness Metric

Element	Percentage score assigned
Skull - 69.98%	
Premaxilla	1.99%
Maxilla	2.58%
Septomaxilla	0.80%
Naris	0.60%
Nasal	0.80%
Lacrimal	0.40%
Frontal	0.80%
Preparietal	0.20%
Parietal	2.19%
Postparietal	0.60%
Prefrontal	0.40%
Postfrontal	0.80%
Squamosal	0.99%
Postorbital	0.60%
Jugal	0.40%
Quadratojugal	0.20%
Basisphenoid	0.20%
Parasphenoid	0.99%
Vomer	1.59%
Pterygoid	3.18%
Epipterygoid	0.40%
Pro-otic	0.20%

Palatine	0.40%
Basipterygoid process	0.40%
Supratemporal	0.40%
Tabular	0.60%
Quadrate	0.80%
Supraoccipital	0.20%
Exoccipital	0.20%
Basioccipital	0.20%
Opisthotic	0.20%
Coronoid	0.60%
Prearticular	0.20%
Articular	0.20%
Angular	1.59%
Surangular	0.80%
Dentary	1.79%
Splenial	0.20%
Stapes	0.60%
Hyoid	0.20%
Maxilla and prefrontal	0.40%
Maxilla and vomer	0.20%
Maxilla and palatine	0.20%
Maxilla and dentary	0.20%
Maxilla and upper canine	0.20%
Nasal and frontal	0.40%
Nasal and lacrimal	0.20%
Lacrimal and naris	0.20%
Frontal and parietal	0.20%
Frontal and postfrontal	0.20%
Parietal and nasal	0.20%
Prefrontal and jugal	0.20%
Postfrontal and postorbital	0.40%
Squamosal and postorbital	0.20%
Squamosal and opisthotic	0.20%

Squamosal and pro-otic	0.20%
Postorbital and supratemporal	0.20%
Postorbital and temporal	0.20%
Postorbital and Jugal	0.20%
Jugal, maxilla and quadratojugal	0.20%
Jugal, maxilla and lacrimal	0.20%
Jugal and squamosal	0.60%
Quadratojugal, maxilla and squamosal	0.20%
Vomer and palatine	0.20%
Pterygoid and basipterygoid process	0.80%
Epipterygoid and parietal	0.20%
Epipterygoid and pro-otic	0.40%
Epipterygoid and frontal	0.20%
Tabular and opisthotic	0.20%
Qudrate, occipital and squamosal	0.20%
Quadrate and quadratojugal	0.20%
Opisthotic, squamosal and suporaoccipital	0.20%
Prearticular and articular	0.20%
Dentary and angular	0.40%
Any tooth	0.40%
Any lateral tooth	1.39%
Premaxilliary teeth	0.99%
Premaxilliary or maxilliary teeth	1.59%
Maxilliary teeth	1.79%
Maxilliary or dentary teeth	0.80%
Dentary teeth	0.99%
Coronoid teeth	0.20%
Caniniform teeth	0.99%
Pterygoid teeth	0.80%
Ectopterygoid teeth	0.20%
Vomerine teeth	0.20%
Palatine teeth	0.60%
Parasphenoid teeth	0.60%

Tooth plates	0.20%
Antorbital region of skull	3.78%
Orbital region of skull	2.39%
Postorbital region of skull	6.36%
Whole skull	1.39%
Occiput	1.39%
Whole skull and Mandible	0.20%
Proximal mandible	1.79%
Distal mandible	0.80%
Complete mandible	0.99%

Axial skeleton - 9.58%	
Any vertebral centrum	0.40%
Any presacral vertebral centrum	0.20%
Any anterior cervical vertebral centrum	0.20%
Any cervical vertebral centrum	0.40%
Any dorsal vertebral centrum	1.59%
All Presacral vertebrae	0.20%
All Presacral and sacral vertebrae	0.20%
All cervical vertebrae	0.20%
All sacral vertebrae	0.20%
Any neural spine	0.20%
Any presacral neural spine	0.80%
Any cervical neural spine	0.20%
Any anterior cervical neural spine	0.40%
Any posterior cervical or anterior dorsal neural spine	0.20%
Any anterior dorsal neural spine	0.20%
Any mid-dorsal nueral spine	0.20%
Any posterior dorsal neural spine	0.20%
Any dorsal nueral spine	0.99%

Any dorsal or sacral neural spine	0.20%
Any sacral or caudal neural spine	0.40%
Any caudal neural spine	0.40%
Cervical rib	0.40%
Thoracic rib	0.60%
Sacral rib	0.40%
Any cervical vertebra and any posterior dorsal vertebra	0.20%

Pectoral girdle - 4.37%

Proximal interclavicle	0.80%
Interclacivle shaft	0.20%
Proximal scapula	1.19%
Scapula shaft	0.20%
Distal scapula	0.20%
Corocoid	0.20%
Proximal coracoid	0.40%
Sternum	0.20%
Clavicle	0.40%
Cleithrum	0.20%
Cleithrum and scapula	0.20%
Scapula and corocoid	0.20%

Forelimb - 6.19%

Proximal humerus	0.80%
Humerus shaft	0.40%
Humerus disal end and shaft	0.20%
Distal humerus	0.99%

Medial carpi	0.40%
Lateral carpi	0.40%
Ulnare	0.20%
Radiale	0.20%
Fourth and fifth metacarpus	0.20%
Any metacarpus	0.20%
Manual phalanges from digits 2 or 5	0.20%
Manual phalanges from digit 3	0.20%
Manual phalanges from digit 4	0.20%
Any ungual	0.40%
Any maual phalanx	0.20%
Radius	0.20%
Proximal ulna	0.40%
Fourth metacarpus and radius	0.20%
Humerus and radius	0.20%

Pelvic girdle - 3.2%	
Proximal pubis	0.20%
Pubis shaft and distal end	0.40%
Distal pubis	0.40%
Ischium shaft	0.20%
Distal ischium	0.20%
Dorsal Ilium	0.40%
Complete Ilium	0.40%
Complete pelvic girdle	0.20%
Acetabulum	0.20%
Acetabulum and pubis	0.20%
Pubis and ischium	0.40%

Hindlimb - 5.37%

Proximal femur	1.59%
Femoral shaft	0.20%
Distal femur	0.60%
Whole femur	0.20%
Lateral tarsals and distal tarsals	0.20%
Distal tarsals	0.20%
Distal fibula and shaft	0.20%
Proximal tibia	0.20%
Astragulus	0.60%
Calcaneum	0.40%
Fifth metatarsal	0.20%
Tibia, astragulus, fourth metatarsal and digit	0.20%
Astragulus and calcaneum	0.40%
Fourth metatarsal and pedal digit 4	0.20%

Multiple elements from different regions

Whole skull and single dorsal vertebra	0.20%
Whole skull and complete presacral series	0.20%
Hindlimb and complete dorsal series	0.20%
Femoral shaft and humerus shaft	0.20%
Femur and humerus	0.20%
Two metapodials from the same limb	0.20%
Any complete limb	0.20%

Appendix H

The percentage volume of different regions measured from different skeletons (calculated by treating each region as a geometric shape), and the mean percentages calculated for each region used in calculating the Skeletal Completeness Metric (SCM)

	Varanops brevirostris FMNH 644		*Cotylorhynchus romeri* AMNH 7517		*Ophiacodon uniformis* MCZ 1366		*Dimetrodon milleri* MCZ 1365		
	Volume (mm^3)	Percentage	Volume (mm^3)	Percentage	Volume (mm^3)	Percentage	Volume (mm^3)	Percentage	SCM percentages
Skull (Cone)	81712.56	20.28%	882771.26	4.01%	117672.87	27.53%	38155.24	20.72%	18.13%
Pectoral girdle (Triangular prism)	85045.22	21.11%	677980.80	3.08%	8948.78	2.09%	4560.96	2.48%	7.19%
Humerus (Cylinder)	8825.06	2.19%	2150899.26	9.76%	20401.21	4.77%	5250.53	2.85%	4.89%
Ulna (Cylinder)	5576.35	1.38%	1059676.41	4.81%	12568.60	2.94%	3769.66	2.05%	2.79%
Radius (Cylinder)	5429.76	1.35%	371315.22	1.68%	2712.99	0.63%	1047.04	0.57%	1.06%
Manual Digit 1 (Cylinder)	1998.55	0.50%	149280.93	0.68%	539.94	0.13%	298.65	0.16%	0.37%
Digit 2 (Cylinder)	873.80	0.22%	167111.57	0.76%	650.53	0.15%	286.06	0.16%	0.32%

Digit 3 (Cylinder)	1981.32	0.49%	198164.28	0.90%	1105.85	0.26%	303.00	0.16%	0.45%
Digit 4 (Cylinder)	3896.82	0.97%	132706.67	0.60%	1923.70	0.45%	544.48	0.30%	0.58%
Digit 5 (Cylinder)	1804.89	0.45%	230210.60	1.04%	1280.44	0.30%	204.64	0.11%	0.48%
Pelvic girdle (Triangular prism)	24040.06	5.97%	419586.24	1.90%	14559.98	3.41%	3237.28	1.76%	3.26%
Femur (Cylinder)	18850.47	4.68%	2801037.00	12.71%	38509.62	9.01%	11427.35	6.21%	8.15%
Tibia (Cylinder)	6752.32	1.68%	532070.05	2.41%	16253.70	3.80%	6444.50	3.50%	2.85%
Fibula (Cylinder)	3570.37	0.89%	301496.14	1.37%	9211.02	2.15%	2503.60	1.36%	1.44%
Pelvic Digit 1 (Cylinder)	1638.41	0.41%	712483.16	3.23%	2818.28	0.66%	502.84	0.27%	1.14%
Digit 2 (Cylinder)	1288.76	0.32%	194541.08	0.88%	3115.16	0.73%	557.73	0.30%	0.56%
Digit 3 (Cylinder)	3252.53	0.81%	778638.70	3.53%	8252.71	1.93%	950.18	0.52%	1.70%

Digit 4 (Cylinder)	4609.07	1.14%	372397.20	1.69%	8997.09	2.10%	1453.50	0.79%	1.43%
Digit 5 (Cylinder)	1845.27	0.46%	435729.79	1.98%	6036.06	1.41%	532.63	0.29%	1.03%
Cervical column (Cylinder)	7675.45	1.90%	96971.76	0.44%	7002.64	1.64%	2631.80	1.43%	1.35%
Cervical spines (Cuboid)	2690.35	0.67%	15142.62	0.07%	982.85	0.23%	3734.48	2.03%	0.75%
Dorsal column (Cylinder)	29257.85	7.26%	984560.30	4.47%	24591.76	5.75%	12077.61	6.56%	6.01%
Dorsal spines (Cuboid)	15259.29	3.79%	541339.61	2.46%	6401.56	1.50%	42246.57	22.94%	7.67%
Ribs (Curved cylinder)	46571.66	11.56%	5228967.44	23.72%	67234.4	15.73%	19331.02	10.50%	15.38%
Sacral column (Cylinder)	4564.77	1.13%	351776.55	1.60%	3707.11	0.87%	3021.99	1.64%	1.31%
Sacral spines (Cylinder)	769.24	0.19%	158506.92	0.72%	1443.25	0.34%	2209.68	1.20%	0.61%
Caudal column (Cylinder)	33144.27	8.23%	2095710.56	9.51%	40555.32	9.49%	16873.61	9.16%	9.10%

Appendix I

Substage	Genus	Species	CCM %	Mean	SCM %	Mean
Late Moscovian	*Archaeothyris*	*florensis*	57.36	42.52	36.69	30.35
	Echinerpeton	*intermedium*	27.68		24	
Early Kazimovian	*Haptodus*	*baylei*	25.31	17.94	80.85	35.15
	Milosaurus	*mccordi*	16.94		19.27	
	Clepsydrops	*colletti*	17.93		18.5	
	Clepsydrops	*vinslovii*	11.57		21.98	
Late Kazimovian	*Clepsydrops*	*colletti*	17.93	28.00	18.5	28.94
	Clepsydrops	*vinslovii*	11.57		21.98	
	Clepsydrops	*magnus*	2.58		2.48	
	Archaeovenator	*hamiltonensis*	87.5		57.34	
	Macromerion	*schwarzenbergii*	16.34		6.16	
	Ianthasaurus	*hardestiorum*	56		51.92	
	Edaphosaurus	*mirabilis*	2.19		0.27	
	Milosaurus	*mccordi*	16.94		19.27	
	Haptodus	*baylei*	25.31		80.85	
	Haptodus	*garnettensis*	71.72		83.48	
	Ianthodon	*schultzei*	25.5		4.53	
	Xyrospondylus	*ecordi*	2.4		0.46	
Early Gzhelian	*Clepsydrops*	*magnus*	2.58	35.89	2.48	33.90
	Baldwinonus	*trux*	13.73		14.48	
	Ophiacodon	*navajovicus*	25.71		36.83	
	Ophiacodon	*mirus*	78.12		92.6	
	Archaeovenator	*hamiltonensis*	87.5		57.34	
	Aerosaurus	*greenleeorum*	8.76		6.11	
	Aerosaurus	*wellesi*	83.89		65.69	
	Ruthiromia	*elcobriensis*	24.32		25.48	
	Macromerion	*schwarzenbergii*	16.34		6.16	
	Sphenacodon	*ferox*	72.5		63.86	
	Edaphosaurus	*mirabilis*	2.19		0.27	

Early Gzhelian	*Edaphosaurus*	*novomexicanus*	26.13	35.89	20.89	33.90
	Oedaleops	*campi*	40.03		18.13	
	Haptodus	*baylei*	25.31		80.85	
	Nitosaurus	*jacksonorum*	31.26		17.27	
Late Gzhelian	*Baldwinonus*	*trux*	13.73	36.50	14.48	35.29
	Ophiacodon	*navajovicus*	25.71		36.83	
	Ophiacodon	*mirus*	78.12		92.6	
	Stereorachis	*dominans*	18.91		9.5	
	Archaeovenator	*hamiltonensis*	87.5		57.34	
	Aerosaurus	*greenleeorum*	8.76		6.11	
	Aerosaurus	*wellesi*	83.89		65.69	
	Ruthiromia	*elcobriensis*	24.32		25.48	
	Sphenacodon	*ferox*	72.5		63.86	
	Cryptovenator	*hirschbergeri*	4.98		2.27	
	Edaphosaurus	*novomexicanus*	26.13		20.89	
	Edaphosaurus	*colohistion*	6.38		18.04	
	Oedaleops	*campi*	40.03		18.13	
	Haptodus	*baylei*	25.31		80.85	
	Nitosaurus	*jacksonorum*	31.26		17.27	
Early Asselian	*Baldwinonus*	*trux*	13.73	32.28	14.48	26.77
	Ophiacodon	*navajovicus*	24.91		36.83	
	Ophiacodon	*mirus*	78.12		92.6	
	Baldwinonus	*dunkardensis*	9.74		2.27	
	Aerosaurus	*greenleeorum*	8.76		6.11	
	Aerosaurus	*wellesi*	83.89		65.69	
	Ruthiromia	*elcobriensis*	24.32		25.48	
	Mycterosaurus	*smithae*	34.05		15.77	
	Sphenacodon	*ferox*	72.5		63.86	
	Sphenacodon	*ferocior*	46.39		28.14	
	Neosaurus	*cynodus*	9.74		2.27	
	Sphenacodon	*britannicus*	9.74		2.27	
	Dimetrodon	*occidentalis*	4.19		9.88	

Early Asselian	*Edaphosaurus*	*novomexicanus*	26.13	32.28	20.89	26.77
	Oedaleops	*campi*	40.03		18.13	
	Haptodus	*baylei*	0		0	
	Nitosaurus	*jacksonorum*	31.26		17.27	
	Pantelosaurus	*saxonicus*	69.17		85.12	
	Haptodus	*grandis*	9.74		2.26	
	Cutleria	*wilmarthi*	49.21		26.17	
Late Asselian	*Baldwinonus*	*trux*	13.73	32.44	14.48	26.74
	Ophiacodon	*navajovicus*	24.91		36.83	
	Ophiacodon	*mirus*	78.12		92.6	
	Baldwinonus	*dunkardensis*	9.74		2.27	
	Stereophallodon	*ciscoensis*	35.65		26.07	
	Aerosaurus	*greenleeorum*	8.76		6.11	
	Aerosaurus	*wellesi*	83.89		65.69	
	Ruthiromia	*elcobriensis*	24.32		25.48	
	Mycterosaurus	*smithae*	34.05		15.77	
	Sphenacodon	*ferox*	72.5		63.86	
	Sphenacodon	*ferocior*	46.39		28.14	
	Neosaurus	*cynodus*	9.74		2.27	
	Sphenacodon	*britannicus*	9.74		2.27	
	Dimetrodon	*occidentalis*	4.19		9.88	
	Edaphosaurus	*novomexicanus*	26.13		20.89	
	Oedaleops	*campi*	40.03		18.13	
	Haptodus	*baylei*	0		0	
	Nitosaurus	*jacksonorum*	31.26		17.27	
	Pantelosaurus	*saxonicus*	69.17		85.12	
	Haptodus	*grandis*	9.74		2.26	
	Cutleria	*wilmarthi*	49.21		26.17	
Early Sakmarian	*Baldwinonus*	*trux*	13.73	33.43	14.48	26.11
	Ophiacodon	*navajovicus*	24.91		36.83	
	Ophiacodon	*mirus*	78.12		92.6	

Early Sakmarian	*Stereophallodon*	*ciscoensis*	35.65	33.43	26.07	26.11
	Ophiacodon	*uniformis*	5.98		6.22	
	Aerosaurus	*greenleeorum*	8.76		6.11	
	Aerosaurus	*wellesi*	83.89		65.69	
	Ruthiromia	*elcobriensis*	24.32		25.48	
	Mycterosaurus	*smithae*	34.05		15.77	
	Sphenacodon	*ferox*	72.5		63.86	
	Sphenacodon	*ferocior*	46.39		28.14	
	Neosaurus	*cynodus*	9.74		2.27	
	Sphenacodon	*britannicus*	9.74		2.27	
	Dimetrodon	*occidentalis*	4.19		9.88	
	Ctenospondylus	*ninevehensis*	33.84		27.69	
	Edaphosaurus	*novomexicanus*	26.13		20.89	
	Edaphosaurus	*credneri*	2.99		14.18	
	Oedaleops	*campi*	40.03		18.13	
	Haptodus	*baylei*	41.43		52.22	
	Nitosaurus	*jacksonorum*	31.26		17.27	
	Haptodus	*grandis*	9.74		2.26	
	Cutleria	*wilmarthi*	49.21		26.17	
	Palaeohatteria	*longicaudata*	82.32		52.05	
Late Sakmarian	*Ophiacodon*	*mirus*	25.83	36.12	40.75	30.57
	Ophiacodon	*uniformis*	90.66		67.21	
	Ophiacodon	*retroversus*	0.4		1.2	
	Varanosaurus	*witchitaensis*	2.59		4.08	
	Mycterosaurus	*smithae*	34.05		15.77	
	Apsisaurus	*witteri*	46.22		27.21	
	Sphenacodon	*ferox*	54.99		44.54	
	Sphenacodon	*ferocior*	63.72		57.62	
	Dimetrodon	*occidentalis*	4.19		9.88	
	Ctenospondylus	*ninevehensis*	33.84		27.69	
	Dimetrodon	*milleri*	89.85		77.83	
	Edaphosaurus	*novomexicanus*	1.8		1.46	

Late Sakmarian	*Edaphosaurus*	*credneri*	2.99	36.12	14.18	30.57
	Edaphosaurus	*boanerges*	20.14		33.75	
	Lupeosaurus	*kayi*	11.17		18.27	
	Cutleria	*wilmarthi*	49.21		26.17	
	Palaeohatteria	*longicaudata*	82.32		52.05	
Early Artinskian	*Ophiacodon*	*mirus*	25.83	32.60	40.75	28.26
	Ophiacodon	*uniformis*	90.66		70.65	
	Ophiacodon	*retroversus*	4.79		10.77	
	Ophiacodon	*hilli*	36.84		30.83	
	Ophiacodon	*major*	1.4		0.54	
	Varanosaurus	*witchitaensis*	0.6		0.65	
	Mycterosaurus	*smithae*	34.05		15.77	
	Apsisaurus	*witteri*	46.22		27.21	
	Thrausmosaurus	*serratidens*	12.33		4.533	
	Basicranodon	*fortsillensis*	1.79		2.27	
	Varanops	*brevirostris*	20.71		12.94	
	Sphenacodon	*ferox*	54.99		44.54	
	Sphenacodon	*ferocior*	63.72		57.62	
	Dimetrodon	*occidentalis*	4.19		9.88	
	Dimetrodon	*milleri*	90.65		79.2	
	Bathygnathus	*borealis*	11.94		2.27	
	Dimetrodon	*teutonis*	21.3		23.32	
	Ctenorhachis	*jacksoni*	5.38		7.06	
	Dimetrodon	*booneorum*	29.89		37.18	
	Dimetrodon	*dollovianus*	0.8		0.35	
	Dimetrodon	*limbatus*	89.85		100	
	Dimetrodon	*natalis*	41.84		40.1	
	Secodontosaurus	*obtusidens*	26.66		13.28	
	Edaphosaurus	*novomexicanus*	1.8		1.46	
	Edaphosaurus	*boanerges*	90.07		93.59	
	Lupeosaurus	*kayi*	12.56		21.69	
	Oromycter	*dolesorum*	18.5		4.73	

Early Artinskian	*Euromycter*	*rutena*	72.32	32.60	28.33	28.26
	Ruthenosaurus	*russelorum*	16.96		40.07	
	Cutleria	*wilmarthi*	49.21		26.17	
Late Artinskian	*Ophiacodon*	*mirus*	25.83	33.39	40.75	29.74
	Ophiacodon	*uniformis*	90.66		70.65	
	Ophiacodon	*retroversus*	5.78		10.77	
	Varanosaurus	*witchitaensis*	0.6		0.65	
	Ophiacodon	*major*	0		0	
	Mycterosaurus	*smithae*	34.05		15.77	
	Apsisaurus	*witteri*	46.22		27.21	
	Varanops	*brevirostris*	0		0	
	Sphenacodon	*ferox*	54.99		44.54	
	Sphenacodon	*ferocior*	63.72		57.62	
	Dimetrodon	*occidentalis*	4.19		9.88	
	Dimetrodon	*milleri*	89.85		77.83	
	Bathygnathus	*borealis*	11.94		2.27	
	Dimetrodon	*teutonis*	21.3		23.32	
	Ctenorhachis	*jacksoni*	5.38		7.06	
	Dimetrodon	*booneorum*	29.89		37.18	
	Dimetrodon	*dollovianus*	0		0	
	Dimetrodon	*limbatus*	89.85		100	
	Dimetrodon	*natalis*	39.04		39	
	Secodontosaurus	*obtusidens*	26.66		13.28	
	Ctenospondylus	*casei*	18.94		15.89	
	Edaphosaurus	*novomexicanus*	1.8		1.46	
	Edaphosaurus	*boanerges*	89.87		91.69	
	Lupeosaurus	*kayi*	12.56		21.69	
	Cutleria	*wilmarthi*	49.21		26.17	
	Euromycter	*rutena*	72.32		28.33	
	Ruthenosaurus	*russelorum*	16.96		40.07	
Early Kungurian	*Ophiacodon*	*mirus*	25.83	31.40	40.75	27.21
	Ophiacodon	*uniformis*	16.15		28.73	

Early Kungurian	*Ophiacodon*	*retroversus*	77.69		79.52	
	Varanosaurus	*witchitaensis*	10.98		18.56	
	Ophiacodon	*major*	19.35		53.14	
	Varanosaurus	*acutirostris*	68.13		18.73	
	Mycterosaurus	*smithae*	34.05		15.77	
	Varanops	*brevirostris*	0		0	
	Mycterosaurus	*longiceps*	65.16		43.3	
	Sphenacodon	*ferox*	54.99		44.54	
	Sphenacodon	*ferocior*	38.24		53.01	
	Ctenorhachis	*jacksoni*	10.38		20.37	
	Dimetrodon	*booneorum*	27.08		21.55	
	Dimetrodon	*dollovianus*	4.19		6.24	
	Dimetrodon	*limbatus*	52.9		61.57	
	Dimetrodon	*natalis*	12.16		21.99	
	Secodontosaurus	*obtusidens*	64.01		31.67	
	Ctenospondylus	*casei*	4.98		1.7	
	Dimetrodon	*grandis*	25.46		49.29	
	Dimetrodon	*loomsi*	2.59		4.08	
	Dimetrodon	*macrospondylus*	4.58		12.58	
	Edaphosaurus	*novomexicanus*	1.8		1.46	
	Edaphosaurus	*boanerges*	9.98		19.64	
	Lupeosaurus	*kayi*	0.2		0.72	
	Edaphosaurus	*cruciger*	66.33		36.43	
	Glaucosaurus	*megalops*	44.25		18.13	
	Euromycter	*rutena*	72.32		28.33	
	Ruthenosaurus	*russelorum*	16.96		40.07	
	Cutleria	*wilmarthi*	49.21		26.17	
	Eothyris	*parkeyi*	62.13		18.13	
Late Kungurian	*Varanosaurus*	*witchitaensis*	6.58	45.79	8.16	39.96
	Ophiacodon	*major*	4.78		7.62	
	Varanosaurus	*acutirostris*	87.48		71.57	
	Varanops	*brevirostris*	91.67		87.09	

Late Kungurian	*Mycterosaurus*	*longiceps*	65.16	45.79	43.3	39.96
	Dimetrodon	*dollovianus*	64.75		45.47	
	Dimetrodon	*limbatus*	14.54		7.97	
	Dimetrodon	*natalis*	5.38		13.04	
	Secodontosaurus	*obtusidens*	20.51		18.33	
	Dimetrodon	*gigashomogenes*	40.64		54.61	
	Dimetrodon	*grandis*	93.31		87.66	
	Dimetrodon	*loomsi*	83.89		71.29	
	Dimetrodon	*macrospondylus*	7.79		6.63	
	Dimetrodon	*kempae*	2.39		4.89	
	Edaphosaurus	*cruciger*	57.75		18.13	
	Edaphosaurus	*pogonias*	88.33		55.3	
	Glaucosaurus	*megalops*	44.25		18.13	
	Euromycter	*rutena*	72.32		28.33	
	Ruthenosaurus	*russelorum*	16.96		40.07	
	Trichasaurus	*texensis*	11.77		39.86	
	Casea	*broilii*	100		97.98	
	Casea	*nicholsi*	19.76		24.65	
	Casea	*halselli*	4.39		9.06	
	Cotylorhynchus	*romeri*	94.46		100	
Early Roadian	*Varanodon*	*agilis*	67.94	29.05	71.28	29.11
	Watongia	*meieri*	27.1		12.56	
	Dimetrodon	*angelensis*	39.02		15.16	
	Angelosaurus	*dolani*	30.1		33.66	
	Angelosaurus	*greeni*	9.17		5.91	
	Caseoides	*sanageloensis*	5.39		13.91	
	Caseopsis	*agilis*	21.71		24.05	
	Cotylorhynchus	*hancocki*	42.96		61.32	
	Angelosaurus	*romeri*	43.23		48.41	
	Cotylorhynchus	*bransoni*	30.29		29.91	
	Phreatophasma	*aenigmaticum*	2.59		4.08	
Late Roadian	*Varanodon*	*agilis*	67.94	46.58	71.28	44.08

Late Roadian	*Watongia*	*meieri*	27.1	46.58	12.56	44.08
	Mesenosaurus	*romeri*	91.87		83.57	
	Pyozia	*mesenensis*	37.84		16.74	
	Angelosaurus	*romeri*	43.23		48.41	
	Cotylorhynchus	*bransoni*	30.29		29.91	
	Ennatosaurus	*tecton*	71.77		86.1	
	Phreatophasma	*aenigmaticum*	2.59		4.08	
Early Wordian	*Mesenosaurus*	*romeri*	91.87	67.16	83.57	62.14
	Pyozia	*mesenensis*	37.84		16.74	
	Ennatosaurus	*tecton*	71.77		86.1	
Late Wordian	*Mesenosaurus*	*romeri*	91.87	67.16	83.57	62.14
	Pyozia	*mesenensis*	37.84		16.74	
	Ennatosaurus	*tecton*	71.77		86.1	
Early Capitanian	*Elliotsmithia*	*longiceps*	37.06	60.38	10.25	41.27
	Heleosaurus	*scholtzi*	83.69		72.28	
Early Capitanian	*Elliotsmithia*	*longiceps*	37.06	60.38	10.25	41.27
	Heleosaurus	*scholtzi*	83.69		72.28	

Appendix J

List of source trees used in the formation of the expanded supertree. For references in which more than one dataset was analysed, the tree used in the study is identified by the figure in which the results were presented.

Archosauromorpha

Andres B, Clark JM, Xing X (2010) A new rhamphorhynchid pterosaur from the Upper Jurassic of Xingjiang, China, and the phylogenetic relationships of basal pterosaurs. *J.Vert. Paleontol.* 30: 163-187

Bennett CS (2012) The phylogenetic position of the Pterosauria within the Archosauromorpha re-examined. *Historical Biol.* 25: 1-19
Figure 2 and 3

Benton MJ (1999) *Scleromochlus taylori* and the origin of dinosaurus and pterosaurs. *Philos. T. Roy. Soc. B*. 354: 1423-1446

Benton MJ, Allen JL (1997) *Boreopricea* from the Lower Triassic of Russia, and the relationships of the prolacertiform reptiles. *Palaeontology* 40: 931-953

Benton MJ, Walker AD (2002) *Erpetosuchus*, a crocodile-like basal archosaur from the Late Triassic of Elgin, Scotland. *Zool. J. Linn. Soc.* 136: 25-47

Butler RJ, Brusatte SL, Reich M, Nesbitt SJ, Schoch RR, Homung JJ (2011) The sail-backed reptile *Ctenosauriscus* from the latest Early Triassic of Germany and the timing and biogeography of the early archosaur radiation. *PlosOne* 6: e25693
Figures 14 and 15

Clark JM, Sues H-D (2002) Two new basal crocodylomorph archosaurs from the Lower Jurassic and the monophyly of the Sphenosuchia. *Zool. J. Linn. Soc.* 136: 77-95

Clark JM, Xu X, Forster CA, Wang Y (2004) A Middle Jurassic sphenosuchian from China and the origin of the crocodilian skull. *Nature* 430: 1021-2024

Desojo JB, Ezcurra MD, Schultz CL (2011) An unusual new archosauriform from the Middle-Late Triassic of southern Brazil and the monophyly of Doswelliidae. *Zool. J. Linn. Soc.* 161: 839-871

Dilkes DW (1995) The rhynchosaur *Howesia browni* from the Lower Triassic of South Africa. *Palaeontology* 38: 665-685

Dilkes DW (1998) The Early Triassic rhynchosaur *Mesosuchus browni* and the interrelationships of basal archosauromorph reptiles. *Philos. T. Roy. Soc. B.* 353: 501-541

Dilkes DW, Arcucci A (2012) *Proterochampsa barrionuevoi* (Archosauriformes: Proterochampsia) from the Late Triassic (Carnian) of Argentina and a phylogenetic analysis of Proterochampsia. *Palaeontology* 55: 853-885

Ezcurra MD (2006) A review of the systematic position of the dinosauriform archosaur *Eucoelophysis baldwini* Sullivan & Lucas, 1999 from the Upper Triassic of New Mexico, USA. *Geodiversitas* 28: 649-684

Ezcurra MD (2010) A new early dinosaur (Saurischia: Sauropodomorpha) from the Late Triassic of Argentina: a reassessment of dinosaur origin and phylogeny. *J. Syst. Palaeontol.* 8: 371-425

Ezcurra MD, Novas, FE (2007) Phylogenetic relationships of the Triassic theropod *Zupaysaurus rougieri* from NW Argentina. *Historical Biol.* 19: 35-72

Ezcurra MD, Lecuoina A, Martinelli A (2010) A new basal archosauriform diapsid from the Lower Triassic of Argentina. *J.Vert. Paleontol.* 30: 1433-1450

Franca MAG, Ferigolo J, Langer MC (2011) Associated skeletons of a new Middle Triassic "Rauisuchia" from Brazil. *Naturwissenschaften* 98: 389-395

Gower DJ, Sennikov AG (1997) *Sarmatosuchus* and the early history of the Archosauria. *J.Vert. Paleontol.* 17: 60-73

Harris SR, Gower DJ, Wilkinson M (2003) Intraorganismal homology, character construction, and the phylogeny of aetosaurian archosaurs (Reptilia, Diapsida). *Syst. Biol.* 52: 239-252

Hone DW, Benton MJ (2008) A new genus of rhynchosaur from the Middle Triassic of South-West England. *Palaeontology* 51: 95-115

Jalil NE (1997) A new prolacertiform diapsid from the Triassic of North Africa and the interrelationships of the Prolacertiformes. *J.Vert. Paleontol.* 17: 506-525

Langer MC, Schultz CL (2000) A new species of the Late Triassic rhynchosaur *Hyperodapedon* from the Santa Maria formation of South Brazil. *Palaeontology* 43: 633-652

Li C, Wi X-C, Zhao L-J, Sato T, Wang L-T (2012) A new archosaur (Diapsida, Archosauriformes) from the marine Triassic of China. *J.Vert. Paleontol.* 32: 1064-1081

Lü J, Ji Q (2006) Preliminary results of a phylogenetic analysis of the pterosaurs from western Liaoning and surrounding areas. *J. Paleontol. Soc. Korea* 22: 239-261

Martinez RN, Alcobar OA (2009) A basal sauropodomorph (Dinosauria: Saurischia) from the Ischigualasto Formation (Triassic, Carnian) and the Early Evolution of Sauropodomorpha. *PlosOne* 4: e4397

Martinez RN, Sereno PC, Acobar OA, Colombi CE, Renne PR, Montanez, Currie BS (2011) A basal dinosaur from the dawn of the dinosaur era in southwestern Pangaea. *Science* 331: 206-210

Modesto SP, Sues H-D (2004) The skull of the Early Triassic archosauromorph reptile *Prolacerta broomi* and its phylogenetic significance. *Zool. J. Linn. Soc.* 140: 335-351

Montefeltro FC, Bittencourt JS, Langer MC, Schultz CL (2013) Postcranial anatomy of the hyperodapedontine rhynchosaur *Teyumbaita sulcognathus* (Azevedo and Schulty, 1987) from the Late Triassic of Southern Brazil. *J. Vert. Paleontol.* 33: 67-84

Nesbitt SJ (2003) *Arizonasaurus* and its implications for archosaur divergence. *P. Roy Soc. B.* 270: 234-237

Nesbitt SJ (2007) The anatomy of *Effigia okeeffeae* (Archosauria, Suchia), theropod-like convergence, and the distribution of related taxa. *B. Am. Mus. Nat. Hist.* 302: 1-84

Nesbitt SJ, Irmis RB, Parker WG, Smith ND, Turner AH, Rowe T (2009a) Hindlimb osteology and distribution of basal dinosauromorphs from the Late Triassic of North America. *J.Vert. Paleontol.* 29: 498-516

Nesbitt SJ, Smith ND, Irmis RB, Turner AH, Downs A, Norell MA (2009b) A complete skeleton of a Late Triassic saurischian and the early evolution of dinosaurs. *Science* 326: 1530-1533

Olson PE, Sues H-D, Norell MA (2000) First record of *Erpetosuchus* (Reptilia: Archosauria) from the Late Triassic of North America. *J.Vert. Paleontol.* 20: 633-636

Parker WG (2007) Reassessment of the aetosaur *Desmatosuchus chamaensis* with a reanalysis of the phylogeny of the Aetosauria (Archosauria: Pseudosuchia). *J. Syst. Palaeontol.* 5: 41-68

Parker WG (2006) A new species of the Late Triassic phytosaur *Pseudopalatus* (Archosauria: Pseudosuchia) from Petrified Forest National Park, Arizona. In *A Century of Research at Petrified Forest National Park: Geology and Paleontology*, eds Parker, WG, Ash, SR, Irmis, RB (Museum of Northern Arizona Bulletin 62, Flagstaff, Arizona), pp 126-143

Parrish JM (1993) Phylogeny of the Crocodylotarsi, with reference to archosaurian and crurotarsan monophyly. *J.Vert. Paleontol.* 13: 287-308

Renesto S, Binelli G (2006) *Vallesaurus cenensis* Wild, 1991, a drepanosaurid (Reptilia, Diapsida) from the Late Triassic of Northern Italy. *Riv. Ital. Paleontol. S.* 112: 77-94

Sereno PC (1991) Basal archosaurs: phylogenetic relationships and functional implications. *J.Vert. Paleontol.* 11: 1-53

Sereno PC (1999) The evolution of dinosaurs. *Science* 284: 2137-2147

Stocker MR (2012) A new phytosaur (Archosauriformes, Phytosauria) from the Lot's Wife Beds (Sonslea Member) within the Chinle Formation (Upper Triassic) of Petrified Forest National Park, Arizona. *J.Vert. Paleontol.* 32: 573-586

Wang X, Kellner AWA, Zhou Z, de Almeida Campos D (2005) Pterosaur diversity and faunal turnover in Cretaceous terrestrial ecosystems in China. *Nature* 437: 875-879

Weinbaum JC & Hungerbühler A (2007) A revision of *Poposaurus gracilis* (Archosauria: Suchia) based on two new specimens from the Late Triassic of the southwestern USA. *Palaeontol. Z.* 81: 131-145

Yates AM (2003) A new species of the primitive dinosaur *Thecodontosaurus* (Saurischia: Sauropodomorpha) and its implications for the systematics of early dinosaurs. *J. Syst. Palaeontol.* 1: 1-42

Figures 22 and 26

Yates AM, Kitching JW (2003) The earliest known sauropod dinosaur and the first steps towards sauropod locomotion. *P. Roy Soc. B.* 270: 1753-1758

Ichthyopterygia

Jiang D-Y, Schmitz L, Hao W-C, Sun Y-L (2006) A new mixosaurid ichthyosaur from the Middle Triassic of China. *J.Vert. Paleontol.* 26: 60-69

Maisch MW, Matzke AT (2003a) Observations on Triassic ichthyosaurs. Part X: The Lower Triassic *Merriamosaurus* from Spitzbergen – additional data on its anatomy and phylogenetic position. *Neues Jahrb. Geol. P-A.* 227: 93–137

Maisch MW, Matzke AT (2003b). Observations on Triassic ichthyosaurs. Part XII. A new Lower Triassic ichthyosaur genus from Spitzbergen. *Neues Jahrb. Geol. P-A.* 229: 317–338

Maisch MW, Matzke AT (2005) Observations on Triassic ichthyosaurs. Part XIV: The Middle Triassic mixosaurid *Phalarodon major* (V. HUENE, 1916) from Switzerland and a reconsideration of mixosaurid phylogeny. *Neues Jahrb. Geol. P-M*: 597–613

Motani R (1999) Phylogeny of the Ichthyopterygia. *J.Vert. Paleontol.* 19: 473-496

Sander PM (2000) Ichthyosauria: their diversity, distribution and phylogeny. *Palaeontol. Z.* 74: 1-35

Thorne PM, Ruta M, Benton MJ (2011) Resetting the evolution of marine reptiles at the Triassic-Jurassic boundary. *Proc. Natl. Acad. Sci.* 108: 8339-8344

Mini-supertree 3 is formed from Motani (1999) and Thorne et al. (2011)

Lepidosauriformes

Apesteguia S, Novas FE (2003) Large Cretaceous spehondontian from Patagonia provides insight into lepidosaur evolution in Gondwana. *Nature* 425: 609-612

Apesteguia S, Gomez RO, Rougier GW (2012) A basal sphenodontian (Lepidosauria) from the Jurassic of Patagonia: new insights on the phylogeny and biogeography of Gondwanan rhynchocephalians. *Zool. J. Linn. Soc.* 166: 342-360

Dupret V (2004) The pleurosaurs: anatomy and phylogeny. Revue de Paléobiologie 9: 61-80

Evans SE, Borsuk-Bialyncka M (2009) A small lepidosauromorph reptile from the Early Triassic of Poland. *Palaeontol. Pol.* 65: 179-202

Gauthier J, Estes R, de Queiroz K (1988) A phylogenetic analysis of Lepidosauromorpha. In *Phylogenetic Relationships of the Lizard Families*, eds Estes, RJ, Pregill, GK (Stanford University Press: Stanford, California), pp. 16-98.

Rauhut OWM, Heyng AM, López-Arbarello A, Hecker A (2012) A new rhynchocephalian from the Late Jurassic of Germany with a dentition that is unique amongst tetrapods. *PlosOne* 7: e46739

Reynoso VH (2000) An unusual aquatic sphenodontian (Reptilia: Diapsida) from the Tlayua Formation (Albian), Central Mexico. *J. Paleontol.* 74: 133-148

Sues, H-D, Shubin, NH & Olsen, PE (1994) A new sphenodontian (Lepidosauria: Rhynchocephalia) from the McCoy Brook formation (Lower Jurassic) of Nova Scotia, Canada. *J.Vert. Paleontol.* 14: 327-340

Parareptilia

Cisneros JC, Damiani R, Schultz C, de Rosa Á, Schwanke C, Neto LW, Aurélio PLP (2004) A procolophonoid reptile with temporal fenestration from the Middle Triassic of Brazil. *P. Roy Soc. B.* 271: 1541-1546

Jalil NE, Janvier P (2005) Les pareiasaures (Amniota, Parareptilia) du permien supérieur du Bassin d'Argana, Maroc. *Geodiversitas* 27: 35-132

Lee M (1995) Historical burden in systematics and the interrelationships of 'Parareptiles'. *Biol. Rev.* 70: 459-547

Lee M (1997) Pareiasaur phylogeny and the origin of turtles. *Zool. J. Linn. Soc.* 120: 197-280

Lyson TR, Bever GS, Bhullar B-AS, Joyce WG, Gauthier J (2010) Transitional fossils and the origin of turtles. *Biol. Lett.* 6: 830-833

MacDougall MJ, Reisz RR (2012) A new parareptile (Parareptilia, Lanthanosuchoidea) from the Early Permian of Oklahoma. *J.Vert. Paleontol.* 32: 1018-1026

Modesto SP, Damiani R. (2007) The procolophonoid reptile *Sauropareion anoplus* from the lowermost Triassic of South Africa. *J.Vert. Paleontol.* 27: 337-349
Figures 7 A,B, 8

Modesto SP, Reisz RR (2009) New material of *Colobomycter pholeter*, a small parareptile from the Lower Permian of Oklahoma. *J.Vert. Paleontol.* 28: 677-684

Modesto S, Sues H-D, Damiani R (2001) A new Triassic procolophonid reptile and its implications for procolophonoid survivorship during the Permo-Triassic extinction event. *P. Roy Soc. B.* 268: 2047-2052

Modesto S, Damiani RJ & Sues H-D (2002) A reappraisal of *Coletta seca*, a basal procolophonoid reptile from the Lower Triassic of South Africa. *Palaeontology* 45: 883-895

Modesto SP, Damiani RJ, Neveling J, Yates AM (2003) A new Triassic owenettid parareptile of the Mother of Mass Extinctions. *J.Vert. Paleontol.* 23: 715-719

Müller J, Li J-L, Reisz RR (2009) A new bolosaurid parareptile, *Belebey chengi* sp. nov., from the Middle Permian of China and its paleogeographic significance. *Naturwissenschaften* 95: 1169-1174

Reisz RR, Scott D (2002) *Owenetta kitchingorum*, sp. nov. a small parareptile (Procolophonia: Owenettidae) from the Lower Triassic of South Africa. *J.Vert. Paleontol.* 22: 244-256

Reisz RR, Müller J, Tsuji L, Scott, D (2007) The cranial osteology of *Belebey vegrandis* (Parareptilia: Bolosauridae) from the Middle Permian of Russia, and its bearing on reptilian evolution. *Zool. J. Linn. Soc.* 151: 191-214

Säilä LK (2008) The osteology and affinities of *Anomoiodon liliensterni*, a procolophonid reptile from the Lower Triassic Bundsandstein of Germany. *J.Vert. Paleontol.* 28: 1199-1205

Sues H-D, Reisz, RR (2008) Anatomy and phylogenetic relationships of *Sclerosaurus armatus* (Amniota: Parareptilia) from the Buntsandstein (Triassic) of Europe. *J.Vert. Paleontol.* 28: 1031-1042

Tsuji LA (2006) Cranial anatomy and phylogenetic affinities of the Permian parareptile *Macroleter poezicus*. *J.Vert. Paleontol.* 26: 849-865

Tsuji LA, Müller J (2008) A re-evaluation of *Parasaurus geinitzi*, the first named pareiasaur (Amniota, Parareptilia). *Can. J. Earth. Sci.* 45: 1111-1121

Mini-supertree 4 is formed from Jalil & Janvier 2005 and Tsuji & Müller 2008

Mini-supertree 5 is formed from Lyson et al 2010, MacDougal & Reisz 2012 and Modesto & Reisz 2009

Sauropterygia

Holmes R, Cheng Y-N, Wu X-C (2008) New information on the skull of *Keichousaurus hui* (Reptilia: Sauropterygia) with comments on sauropterygian interrelationships. *J.Vert. Paleontol.* 28: 76-84

Figure 7

Klein N, Albers PCH (2009) A new species of the sauropsid reptile *Nothosaurus* from the Lower Muschelkalk of the western Germanic Basin, Winterswijk, The Netherlands. *Acta Palaeontol. Pol.* 54: 589-598

O'Keefe FR (2004) Preliminary description and phylogenetic position of a new plesiosaur (Reptilia: Sauropterygia) from the Toacian of Holzmaden, Germany. *J. Paleontol.* 78: 973-988

Rieppel O (2000a) *Paraplacodus* and the phylogeny of Placodontia (Reptilia:Sauropterygia). *Zool. J. Linn. Soc.* 130: 635-659

Rieppel O (2000b) The cranial anatomy of Plancochelys placodonta Jaekel, 1902, and a review of the Cyamodontoidea (Reptilia, Placodonta). *Fieldiana* 45: 1-104

Rieppel, O, Zannon, RT (1997) The interrelationships of Placodontia. *Historical Biol.* 12: 211-227

Rieppel O, Jinling L, Jun L (2003) *Lariosaurus xingyiensis* (Reptilia: Sauropterygia) from the Triassic of China. *Can. J. Earth. Sci.* 40: 621-634

Sato T, Cheng Y-N, Wu X-C, Li C (2010) Osteology of *Yunguisaurus* (Reptilia; Sauropterygia), a Triassic pistosauroid from China. *Paleontol. Res.* 14: 179-195

Storrs GW (1993) The systematic position of *Silvestrosaurus* and a classification of Triassic sauropterygians (Neodiapsida). *Palaeontol. Z.* 67: 178-191

Synapsida

Abdala F (2007) Redescription of *Platycraniellus elegans* (Therapsida, Cynodontia) from the lower Triassic of South Africa, and the cladistic relationships of eutheriodonts. *Palaeontology* 59: 591-618

Abdala F, Neveling J, Welman, J (2006) A new trirachodontid cynodont from the lower levels of the Burgersdorp Fromation (Lower Triassic) of the Beaufort Group, South Africa and the cladistics relationships of Gondwanan gomphodonts. *Zool. J. Linn. Soc.* 147: 383-413

Amson E, Laurin M (2011) On the affinityies of *Tetraceatops insignis*, an Early Permian synapsid. *Acta Palaeontol. Pol.* 56: 301-312

Angielczyk KD (2004) Phylogenetic evidence for and the implications of a dual origin of propaliny in anomodont therapsids (Synapsida). *Paleobiology* 30: 268-296

Angielczyk KD, Rubidge BS (2012) Skeletal morphology, phylogenetic relationships and stratigraphic range of *Eosimops newtoni* Broom, 1921, a pylaecephalid dicynodont (Therapsida, Anomodontia) from the Middle Permian of South Africa. *J. Syst. Palaeontol.* 11: 191-231

Benson RBJ (2012) The global interrelationships of basal synapsids: cranial and postcranial morphology partitions suggest different topologies. *J. Syst. Palaeontol.* 10: 601-624

Berman DS, Reisz RR, Bolt JR, Scott D (1995) The cranial anatomy and relationships of the synapsid *Varanosaurus* (Eupelycosauria: Ophiacodontidae) from the Early Permian of Texas and Oklahoma. *Ann. Carnegie Mus.* 64: 99-133

Bonaparte JF, Martinelli AG, Schultz CL (2005) New information on *Brasilodon* and *Brasilitherium* (Cnodontia, Probainognathia) from the Late Triassic of southern Brazil. *Rev. Bras. Palaeontol.* 8: 25-46

Botha J, Abdala F, Smith R (2007) The oldest cynodont: new clues on the origin and early diversification of the Cynodontia. *Zool. J. Linn. Soc.* 149: 477-492

Botha-Brink J, Modesto SP (2009) Anatomy and relationships of the Middle Permian varanopid *Heleosaurus scholtzi* based on a social aggregation from the Karoo Basin of South Africa. *J.Vert. Paleontol.* 29: 389-400

Campione NE, Reisz RR (2010) *Varanops brevirostris* (Eupelycosauria: Varanopidae) from the Lower Permian of Texas, with discussion of varanopid morphology and interrelationships. *J.Vert. Paleontol.* 30, 724-746

Cisneros JC, Abdala F, Rubidge BS, Dentizien-Dias PC, de Oliveira Bueno A (2011) Dental occlusion in a 260 million year old therapsid with saber canines from the Permian of Brazil. *Science* 331: 1603-1605

Cisneros JC, Abdala F, Atayman-Güven S, Rubidge BS, Celâl Şengör AM, Schultz CL (2012) Carnivorous dinocephalian from the Middle Permian of Brazil and tetrapod dispersal in Pangaea. *Proc. Natl. Acad. Sci.* 109: 1584-1588

Damiani R, Vasconcelos C, Renaut A, Hancox J, Yates A (2007) *Dolichuranus primaevus* (Therapsida: Anomodontia) from the Middle Triassic of Namibia and its phylogenetic relationships. *Palaeontology* 50: 1531-1546

Fröbisch J, Reisz RR (2011) The postcranial anatomy of *Suminia getmanovi* (Synapsida: Anomodontia), the earliest known arboreal tetrapod. *Zool. J. Linn. Soc.* 162: 661-698

Fröbisch J, Angielczyk KD, Sidor CA (2010) The Triassic dicynodont *Kombuisia* (Synapsida, Anomodontia) from Antarctica, a refuge from the terrestrial Permian-Triassic mass extinction. *Naturwissenschaften* 97: 187-196

Fröbisch J, Schoch RR, Müller J, Schindler T, Schweiss D (2011) A new basal sphenacodontid synapsid from the Late Carboniferous of the Saar-Nahe Basin, Germany. *Acta Palaeontol. Pol.* 56: 113-120

Gebauer EVI (2007) *Phylogeny and Evolution of the Gorgonopsia with a Special reference to the Skull and Skeleton of GPIT/RE/7113 (*'Aelurognathus*?'* parringtoni*)* (Eberhard-Karls Universität, Tübingen)

Govender R, Yates A (2009) Dicynodont postcrania from the Triassic of Namibia and their implication for the systematics of kannemeyeriiform dicynodonts. *Paleontol. Afr.* 44: 41-57

Hopson JA, Kitching JW (2001) A probainognathian cynodont from South Africa and the phylogeny of nonmammalian cynodonts. *Bull. Mus. Comp. Zool.* 156: 5-35

Kamerer CF (2011) Systematics of the Anteosauria (Therapsida: Dinocephalia). *J. Syst. Palaeontol.* 9: 261-304

Kammerer CF, Angielczyk KD, Fröbisch J (2011) A comprehensive taxonomic revision of *Dicynodon* (Therapsida, Anomodontia) and its implications for dicynodont phylogeny, biogeography, and biostratigraphy. *J.Vert. Paleontol.* 31 (S1):1-158

Kissel RA, Reisz RR (2004) Synapsid fauna of the upper Pennsylvanian Rock Lake Shale near Garnett, Kansas and the diversity pattern of early amniotes. In *Recent Advances in the Origin and Early Radiation of Vertebrates*, eds Arratia G, Wilson MVH, Cloutier, R (Verlag Dr. Friedrich Pfeil: München, Germany), pp 409-428.

Liu J, Li J-L (2003) A new material of kannemeyeriid from Xinjiang and the restudy of *Parakannemeyeria brevirostris*. *Vertebrat. PalAsiatic.* 41: 147–156

Liu J, Olsen P (2010) The phylogenetic relationships of Eucynodontia (Amniota: Synapsida). *J. Mamm. Evol.* 17: 151-176

Liu J, Li J-L, Cheng Z (2002) The *Lystrosaurus* fossils from Xinjiang and their bearing on the terrestrial Permo-Triassic boundary. *Vertebrat. PalAsiatic.* 40: 267–275

Liu J, Rubidge BS, Li J (2010) A new specimen of *Biseridens qilianicus* indicates its phylogenetic position as the most basal anomodont. *P. Roy Soc. B.* 277: 285-292

Lucas SG & Luo Z (1993) *Adelobasileus* from the Upper Triassic of West Texas: the oldest mammal. *J.Vert. Paleontol.* 13: 209-334

Luo Z-X (1994) Sister taxon relationships of mammals and the transformations of the diagnostic mammalian characters. In *In the Shadow of the Dinosaurs – Early Mesozoic Tetrapods,* eds Fraser NC, Sues, H-D (Cambridge University Press: Cambridge), pp. 98-128.

Luo Z-X, Crompton AW, Sun A-L (2001) A new mammaliaform from the Early Jurassic of China and evolution of mammalian characteristics. *Science* 292: 1535-1540

Maddin HC, Evans DC, Reisz, RR (2006) An Early Permian varanodontine varanopid (Synapsida: Eupelycosauria) from the Richards Spur Locality, Oklahoma. *J.Vert. Paleontol*. 26: 957-966

Maddin HC, Sidor CA, Reisz RR (2008) Cranial anatomy of *Ennatosaurus tecton* (Synapsida: Caseidae) from the Middle Permian of Russia and the evolutionary relationships of Caseidae. *J.Vert. Paleontol.* 28: 160-180

Maisch MW (2001) Observations on Karoo and Gondwana vertebrates. Part 2: A new skull-reconstruction of *Stahleckeria potens* von Huene, 1935 (Dicynodontia, Middle Triassic) and a reconsideration of kannemeyeriiform phylogeny. *Neues Jahrb. Geol. P-A*. 220: 127-152

Maisch MW, Gebauer EVI (2005) Reappraisal of *Geikia locusticeps* (Therapsida: Dicynodontia) from the Upper Permian of Tanzania. *Palaeontology* 48: 309-324

Martinez RN, May CL, Forster CA (1996) A new carnivorous cynodont from the Ischigualasto Formation (Late Triassic, Argentina) with comments on eucynodont phylogeny. *J.Vert. Paleontol.* 16: 271-284

Mazierski DM, Reisz RR (2010) Description of a new specimen of *Ianthasaurus hardestiorum* (Eupelycosauria: Edaphosauridae) and a re-evaluation of edaphosaurid phylogeny. *Can. J. Earth. Sci.* 47: 901-912

Modesto SP (1994) The Lower Permian synapsid *Glaucosaurus* from Texas. *Palaeontology* 37: 51-60

Modesto SP & Rybczynski, N (2000) The amniote faunas of the Russian Permian: implications for Late Permian terrestrial vertebrate biogeography. In *The Age of the Dinosaurs in Russia and Mongolia*, eds Benton MJ, Shishkin MA, Unwin DM, Kurochkin EN (Cambridge Univeristy Press: Cambridge), pp. 17-35.

Modesto SP, Rubidge BS & Welman J (1999) The most basal anomodont therapsid and the primacy of Gondwana in the evolution of anomodonts. *P. Roy Soc. B.* 266: 331-337

Modesto SP, Rubidge BS, Visser I, Welman J (2003) A new basal dicynodont from the Upper Permian of South Africa. *Palaeontology* 46: 211-223

Oliveira EV (2006) Reevaluation of *Therioherpeton cargnini* Bonaparte & Barberena, 1975 (Probainognathia, Therioherpetidae) from the Upper Triassic of Brazil. *Geodiversitas* 28: 447-465

Oliveira EV, Soares MB, Schultz CL (2010) *Trucidocynodon riograndensis* gen. nov et sp. noc. (Eucynodontia), a new cynodont from the Brazilian Upper Triassic (Santa Maria Formation). *Zootaxa* 2382: 1-71

Ray S (2006) Functional and Evolutionary aspects of the postcranial anatomy of dicynodonts (Synapsida, Therapsida). *Palaeontology* 49: 1263-1286

Reisz RR, Berman DS, Scott D (1992) The cranial anatomy and relationships of *Secodontosaurus*, an unusual mammal-like reptile (Synapsida: Sphenacodontidae) from the Early Permian of Texas. *Zool. J. Linn. Soc.* 104: 127-184

Reisz RR, Godfrey SJ, Cott D (2009) *Eothyris* and *Oedaleops*: do these Early Permian synapsids from Texas and New Mexico form a clade? *J.Vert. Paleontol.* 29: 39-48

Reisz RR, Laurin M, Marjanović D (2010) *Apsisaurus witteri* from the Lower Permian of Texas: yet another small varanopid synapsid, not a diapsid. *J.Vert. Paleontol.* 30: 1628-1631

Rowe T (1993) Phylogenetic systematics and the early history of mammals. In *Mammal phylogeny* (Springer: New York), 129-145

Rubidge BS, van den Heever JA (1997) Morphology and systematic position of the dinocephalian *Styracocephalus platyrhynchus*. *Lethaia* 30: 157-168

Rubidge BS, Kitching, JW (2003) A new burnetiamorph (Therapsida: Biarmosuchia) from the lower Beaufort Group of South Africa. *Palaeontology* 46: 199-210

Rubidge BS, Sidor CA, Modesto SP (2006) A new burnetiamorph (Therapsida: Biarmosuchia) from the Middle Permian of South Africa. *J. Paleontol.* 80: 740-749

Rybczynski N (2000) Cranial anatomy and phylogenetic position of *Suminia getmanovi*, a basal anomodont (Amniota: Therapsida) from the Late Permian of eastern Europe. *Zool. J. Linn. Soc.* 130: 329-373

Sidor CA Hancox JA (2006) *Elliotherium kersteni*, a new tritheledontid from the lower Elliot Formation (Upper Triassic of South Africa). *J. Paleontol.* 80: 333-342

Sidor CA, Hopson JA (1998) Ghost lineages and "mammalness": assessing the temporal pattern of character acquisition in the Synapsida. *Paleobiology* 24: 254-273

Sidor CA, Rubidge BS (2006) *Herpetoskylax hopsoni*, a new biarmosuchian (Therapsida: Biarmosuchia) from the Beaufort Group of South Africa). In *Amniote Paleobiology* eds Carrano MT, Gaudin TJ, Blob RW, Wible JR (University of Chicago Press: Chicago, USA), pp. 76-113.

Sidor CA, Smith RMH (2004) A new galesaurid (Therapsida: Cynodontia) from the Lower Triassic of South Africa. *Palaeontology* 47: 535-556

Sidor CA, Smith, RMH (2007) A second burnetiamorph therapsid from the Permian Teekloof Formation of South Africa and its associated fauna. *J.Vert. Paleontol.* 27: 420-430

Sidor CA, Welman J (2003) A second specimen of *Lemurosaurus pricei* (Therapsida: Burnetiamorpha). *J.Vert. Paleontol.* 23: 631-642

Sigurdsen T, Huttenlocker AK, Modesto SP, Rowe TB, Damiani R (2012) Reassessment of the morphology and paleobiology of therocephalian *Tetracynodon darti* (Therapsida), and the phylogenetic relationships of the Baurioidea. *J.Vert. Paleontol.* 32: 1112-1134

Smith RMH, Rubidge BS, Sidor CA (2006) A new burnetiid (Therapsida: Biarmosuchia) from the Upper Permian of South Africa and its biogeographic implications. *J.Vert. Paleontol.* 26: 331-343

Sues H-D, Hopson JA (2010) Anatomy and phylogenetic relationships of *Boreogomphodon jeffersoni* (Cynodontia: Gomphodontia) from the Upper Triassic of Virginia. *J.Vert. Paleontol.* 30: 1202-1220

Surkov MV, Kalandadze NN, Benton MJ (2005) *Lystrosaurus georgi*, a dicynodont from the Lower Triassic of Russia. *J.Vert. Paleontol*, 25: 402-413

Vega-Dias C, Maisch MW, Schultz CL (2004) A new phylogenetic analysis of Triassic dicynodonts (Therapsida) and the systematic position of *Jachaleria candelariensis* from the Upper Triassic of Brazil. *Neues Jahrb. Geol. P-A.* 231: 145–166

Wible JR (1991) Origin of Mammalia: the craniodental evidence re-examined. *J.Vert. Paleontol.* 11: 1-28

Mini-supertree 6 is formed from Angielczyk 2004, Modesto et al 1999, Modesto & Rybzynski 2000 and Rybzynski 2000

Mini-supertree 7 is formed from Botha Brink & Modesto 2009, Campione & Reisz 2010 and Maddin et al 2006

Mini-supertree 8 is formed from Cisneros et al. 2012 and Kammerer 2011

Mini-supertree 9 is formed from Sidor & Smith 2007 and Smith et al. 2006

Chelonia

Anquetin J (2012) Reassessment of the phyloegentic interrelationships of basal turtles (Testudinata). *J. Syst. Palaeontol.* 10: 3-45

Anquetin J, Barrett PM, Jones MH, Moore-Fay S, Evans SE (2009) A new stem turtle from the Middle Jurassic of Scotland: new insights into the evolution and palaeoecology of basal turtles. *Proc. R. Soc. B.* 276: 879-886.

Gaffney ES, Rich TH, Vickers-Rich P, Constantine A, Vacca R, Kool L (2007) *Chubutemys*, a new eucryptodiran turtle from the Early Cretaceous of Argentina and the relationships of the Meiolaniidae. *Am. Mus. Novit.* 3599: 1-35

Li C, Wu X-C, Rieppel O, Wang L-T, Zhao L-J (2008) An ancestral turtle from the Late Triassic of southwestern China. *Nature* 456: 497-501

Rougier GW, de la Fuente MS, Arcucci AB (1995) Late Triassic turtles from South America. *Science* 268: 855-858

Sterli J (2010) Phylogenetic relationships among extinct and extant turtles: the position of Pleurodira and the effects of the fossils on rooting crown-group turtles. *Contrib. Zool.* 79: 93-106

Mini-supertree 10 is formed from Li et al. 2008 and Sterli 2010

Basal

Bickelmann C, Müller J, Reisz RR (2009) The enigmatic diapsid *Acerosodontosaurus piveteaui* (Reptilia: Neodiapsida) from the Upper Permian of Madagascar and the paraphyly of "younginiform" reptiles. *Can. J. Earth. Sci*. 46: 651-661

DeBraga M, Reisz RR (1995) A new diapsid reptile from the uppermost Carboniferous (Stephanian) of Kansas. *Palaeontology* 38: 199-212

Evans SE (2009) An early kuehneosaurid reptile from the Early Triassic of Poland. *Palaeontol. Pol.* 65: 145-178

Hill RV (2005) Integration of morphological data sets for phylogenetic analysis of Amniota: the importance of integumentary characters and increased taxonomic sampling. *Syst. Biol.* 54: 530-547

Jiang D-Y, Maisch M-W, Sun Y-L, Matzke AT, Hao W-C (2004) A new species of *Xinpusaurus* (Thalattosauria) from the Upper Triassic of China. *J.Vert. Paleontol*. 24: 80-88

Kissel R (2010) *Morphology, Phylogeny and Evolution of Diadectidae (Cotylosauria: Diadectomorpha)* (University of Toronto: Toronto).

Laurin M, Reisz RR (1997) A new perspective on tetrapod phylogeny. In *Amniote Origins: Completing the Transition to Land*, eds Sumida S, Martin KLM (San Diego Academic Press: San Diego California), pp. 9

Lee M (2001) Molecules, morphology, and the monophyly of diapsid reptiles. *Contrib. Zool.* 70: 1-22

Li C, Wu X-C, Rieppel O, Wang L-T, Zhao L-J (2008) An ancestral turtle from the Late Triassic of southwestern China. *Nature* 456: 497-501

Liu J, Rieppel O (2005) Restudy of *Anshunsaurus huangguoshuensis* (Reptilia: Thalattosauria) from the Middle Triassic of Guizhou, China. *Am. Mus. Novit.* 3488: 1-34

Modesto SP, Reisz RR (2002) An enigmatic new diapsid reptile from the upper Permian of Eastern Europe. *J.Vert. Paleontol.* 22: 851-855

Müller J (2003) Early loss and multiple return of the lower temporal arcade in diapsid reptiles. *Naturwissenschaften* 90: 473-476

Müller J (2005) The anatomy of *Askeptosaurus italicus* from the Middle Triassic of Monte San Giorgio and the interrelationships of thalattosaurs (Reptilia, Diapsida). *Can. J. Earth. Sci.* 42: 1347-1367

Müller J, Reisz RR (2006) The phylogeny of early eureptiles: comparing parsimony and Bayesian approaches in the investigation of a basal fossil clade. *Syst. Biol.* 55: 503-511

Reisz RR, Liu J, Li JL, Müller J (2011) A new captorhinid reptile, *Gansurhinus qingtozshanensis*, gen. et sp. nov., from the Permian of China. *Naturwissenschaften* 98: 435-441

Reisz RR, Modesto SP, Scott DM (2011) A new Early Permian reptile and its significance in early diapsid evolution. *P. Roy Soc. B.* 278: 3731-3737

Rieppel O, DeBraga M Turtles as diapsid reptiles. *Nature* 384: 453-455

Sumida SS, Dodick J, Metcalf A, Albright G (2010) *Reiszorhinus olsoni*, a new single-tooth-rowed captorhinid reptile from the Lower Permian of Texas. *J.Vert. Paleontol.* 30: 704-714

Wu XC, Cheng YN, Sato T, Shan HY (2009) *Miodentosaurus brevis* Cheng et al., 2007 (Diapsida: Thalattosauria): its postcranial skeleton and phylogenetic relationships. Vertebrat. *PalAsiatic.* 47: 1-20

Mini-supertree 1 formed from Bickelmann et al. 2009, Evans 2009 and Reisz et al. 2011

Mini-supertree 2 formed from Hill 2005 and Li et al. 2009

Appendix K

List of taxa removed from the expanded supertree due to the inability to resolve their phylogenetic position

"Basal" taxa

Anthracodromeus longiceps
Protorothyris archeri
Cephalerpeton ventriarmatum
Hylonomus lyelli
Hovasaurus boulei
Thadeosaurus colcanapi
Galesphyrus capensis
Kenyasaurus mariakaniensis

Synapsida

Traversodon stahleckeri
Propelanomodon devilliersi
Dicynodon trigonocephalus
Uralokannemeyeria vjuschkovi
Xiyukannemeyeria brevirostris
Zambiasaurus submersus
Prorubidgea spp.
Lystrosaurus youngi
Cteniosaurus platyceps
Mirotenthes digitipes
Ictidostoma hemburyi
Hofmeyria atavus
Euchambersia mirabilis

Parareptilia

Bunostegos akokanensis
Koiloskiosaurus cogburgensis
Nanoparia luckhoffi

Sauropterygia

ELASMOSAURIDAE

Neusticosaurus peyeri

Neusticosaurus.toeplitschi

Neusticosaurus edwardsi

Microcleidus homalospondylus

Saurosphargis volzi

Hanosaurus hupehensis

Wumengosaurus delicatomandibularis

Qianxisaurus chajiangsensis

Dianopachysaurus dingi

Diandongosaurus acutidentatus

Chicenia sungi

Kwangsisaurus orientalis

Sanchiaosaurus dengi

Sinosaurosphargis yunguiensis

Nothosaurus haasi

Nothosaurus giganteus

Nothosaurus jagisteus

Nothosaurus edingerae

Nothosaurus marchicus

Nothosaurus winterswijkensis

Nothosaurus youngi

Nothosaurus juvenilis

Nothosaurus tchernovi

Nothosaurus winkelhorsti

Nothosaurus yangiuanensis

Ceresiosaurus spp.

Lepidosauromorpha

Polysphenodon muelleri

Clevosaurus wangi

Archosauromorpha

Nicrosaurus kapffi

Nicrosaurus meyeri

Eocursor parvus

Mystriosuchus planirostris

Ebrachosuchus neukami

Boreopricea funerea

Jesairosaurus lehmani

Malerisaurus robinsonae

Pseudohesperosuchus jachaleri

Turfanosuchus dabensis

Yonghesuchus sangbiensis

Procompsognathus triassicus

Gojirasaurus quayi

Segisaurus halli

Saltoposuchus connectens

Preondactylus buffarinii

Chilenosuchus forttae

Jingshanosaurus xinwaensis

Yunnanosaurus spp.

Ichthyopterygia

Thaisaurus chonglakmanii

Guizhouichthyosaurus tangae

Appendix L

The expanded supertree, containing 686 amniotes from the late Carboniferous until the end of the Triassic. Nodes with negative support according the V support metric (Wilkinson et al. 2005)

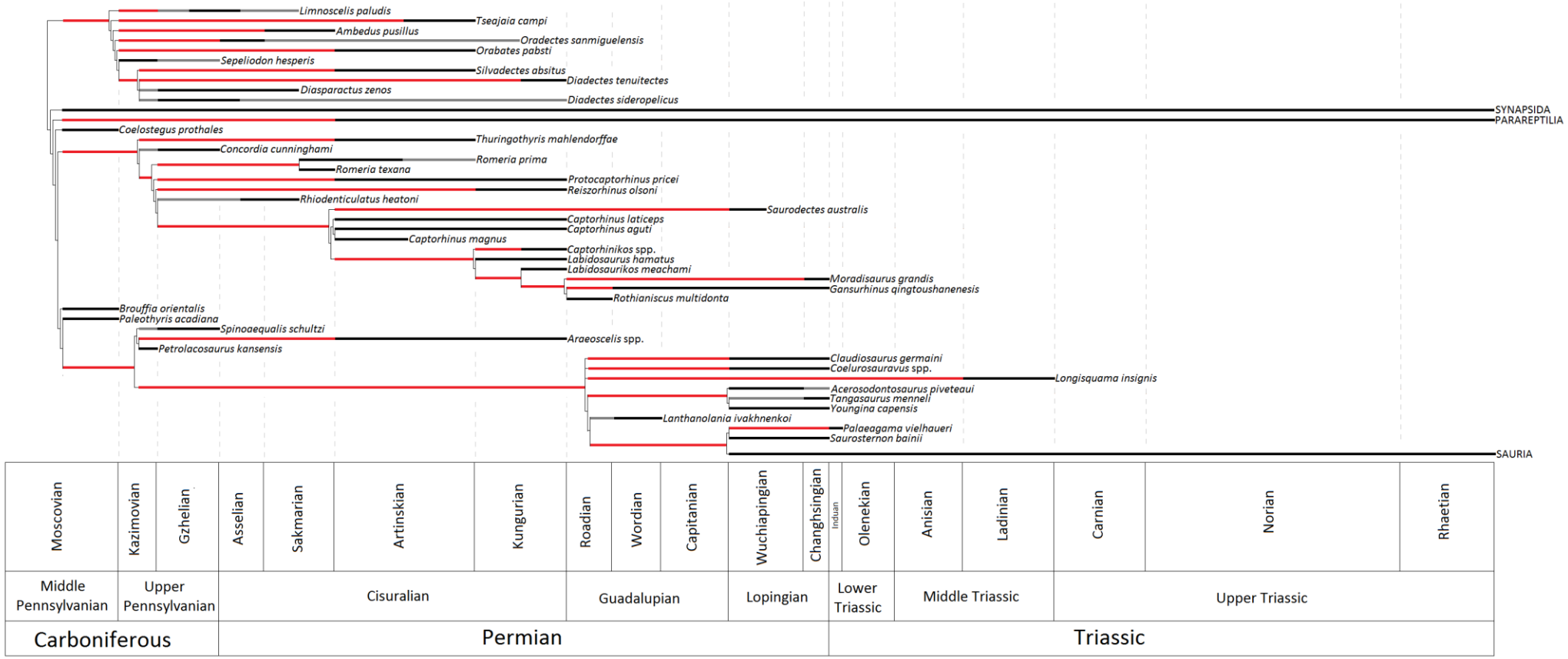

Figure L1: Portion of the time calibrated expanded supertree showing the relationships of diadectomorphs and basal eureptiles

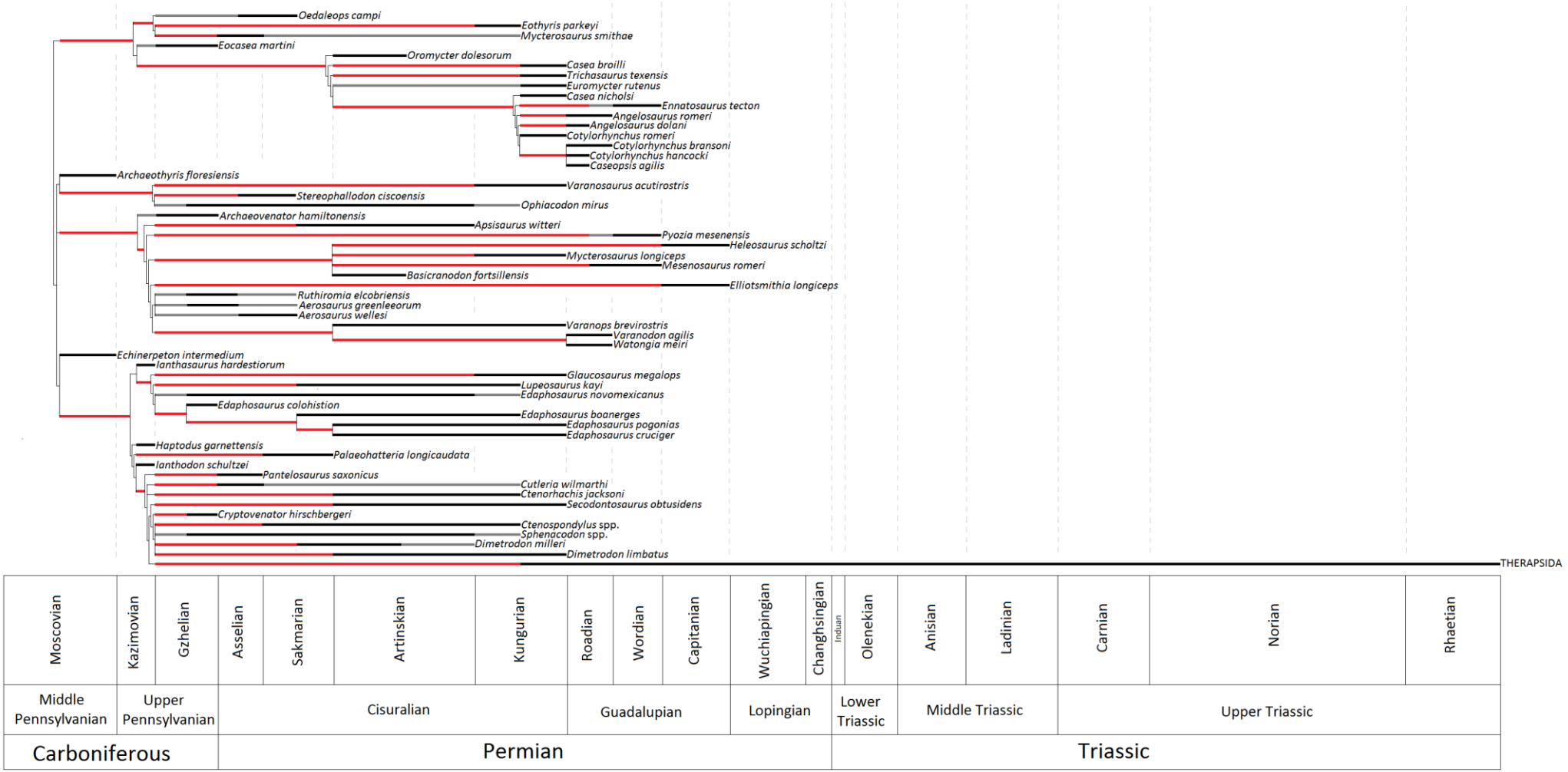

Figure L2: Portion of the time calibrated expanded supertree showing the relationships of pelycosaurian-grade synapsids

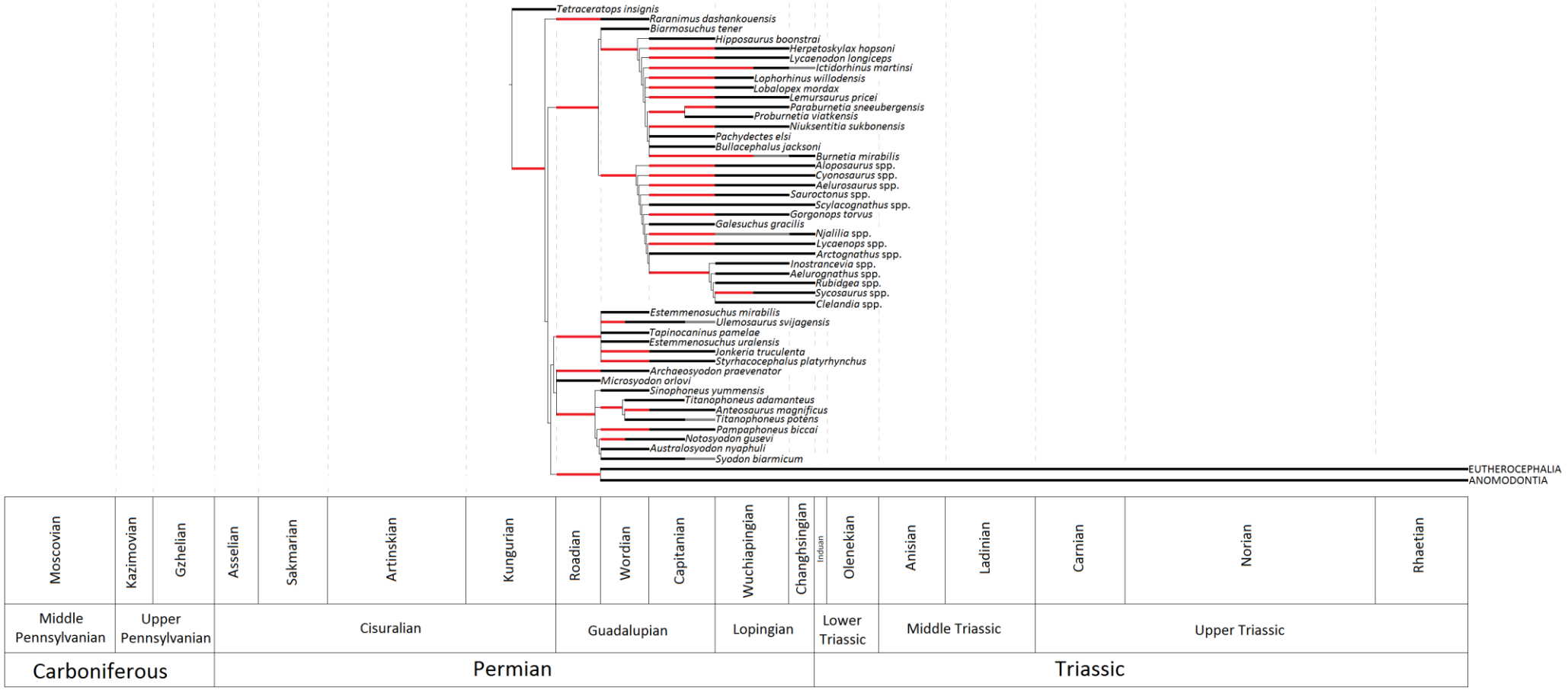

Figure L3: Portion of the time calibrated expanded supertree showing the relationships of basal therapsids, including biarmosuhcians and dinocephalians

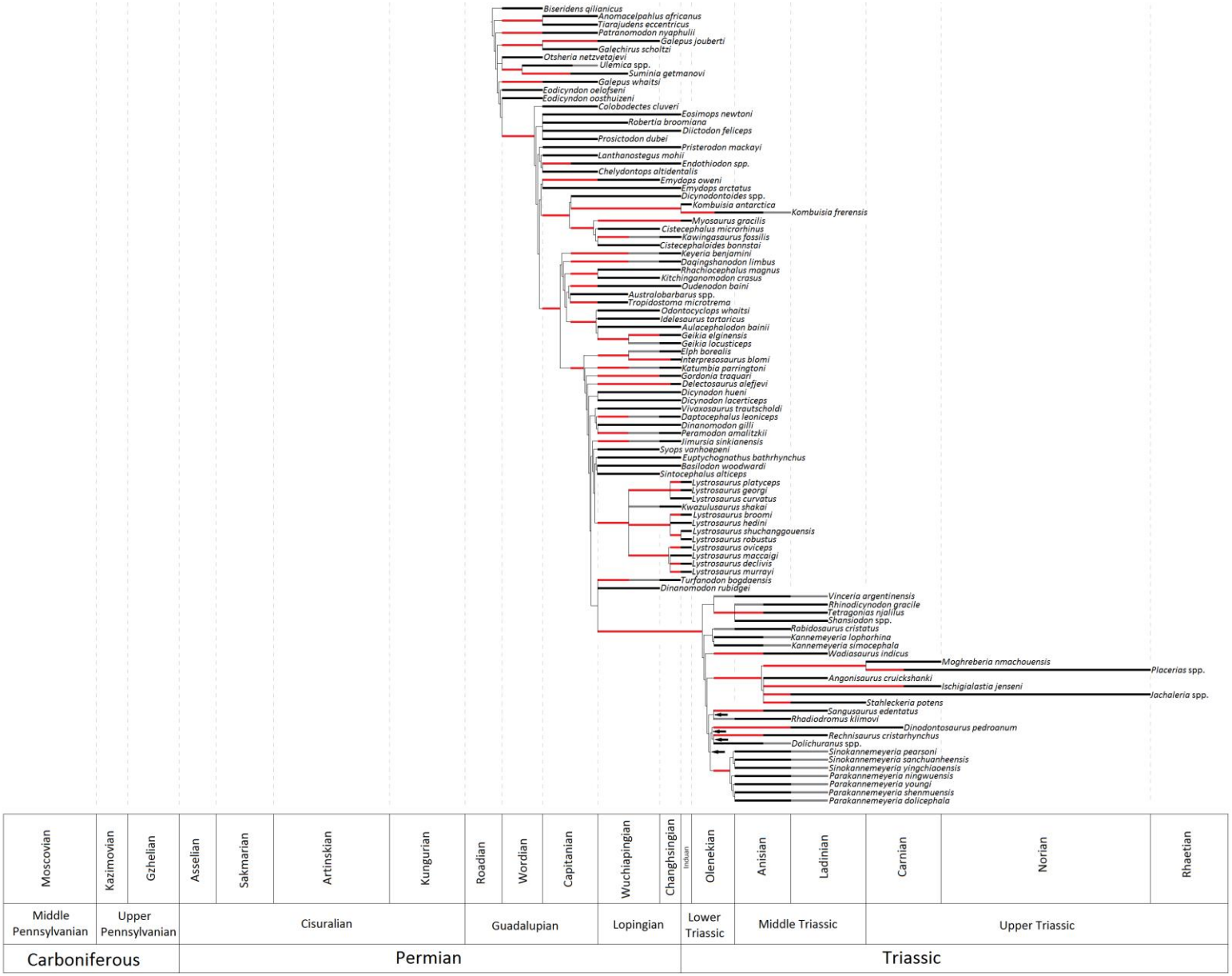

Figure L4: Portion of the time calibrated expanded supertree showing the relationships of anomodont therapsids. Black arrows indicate nodes with negative support.

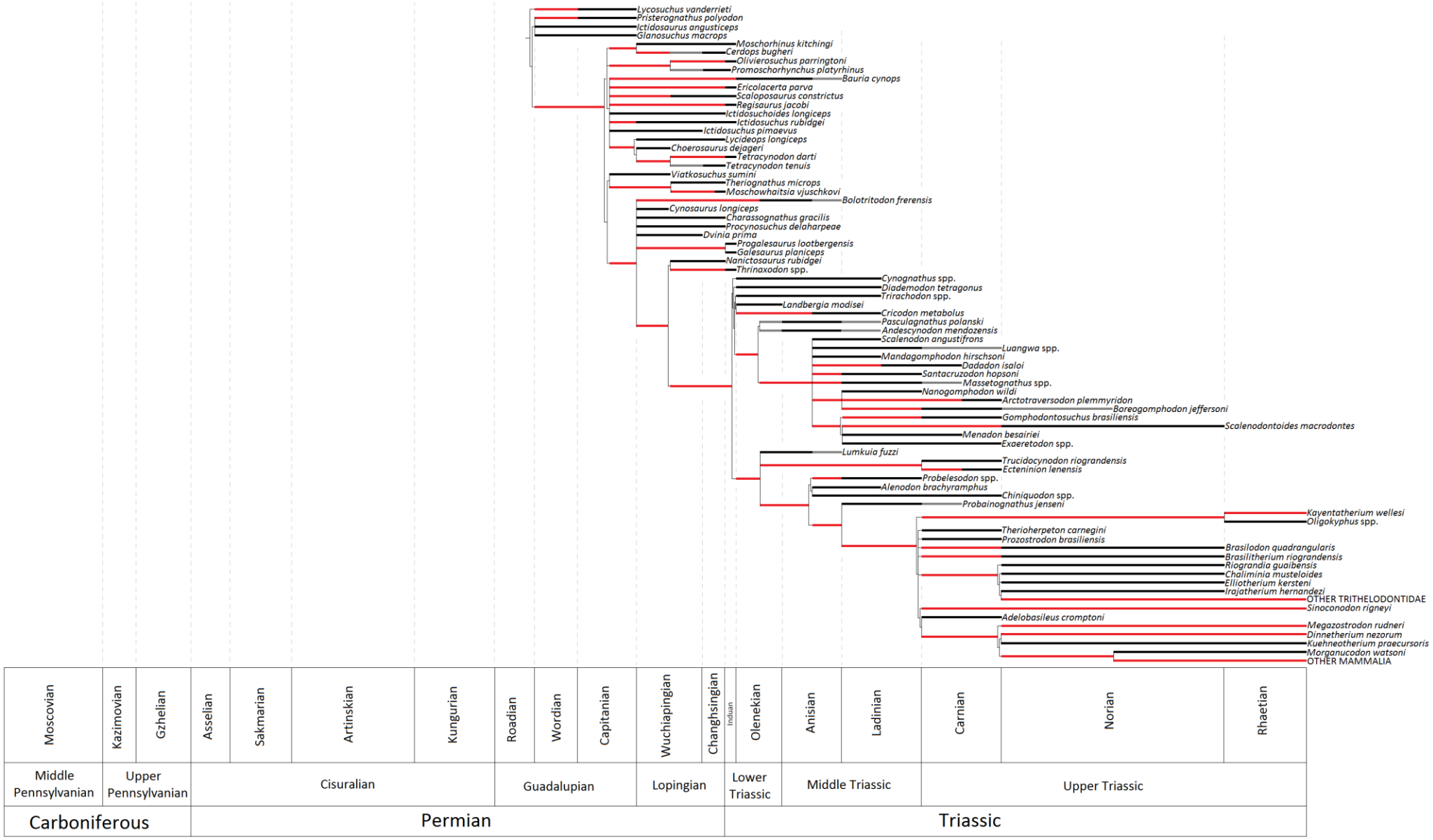

Figure L5: Portion of the time calibrated expanded supertree showing the relationships of eutheriodont therapsids

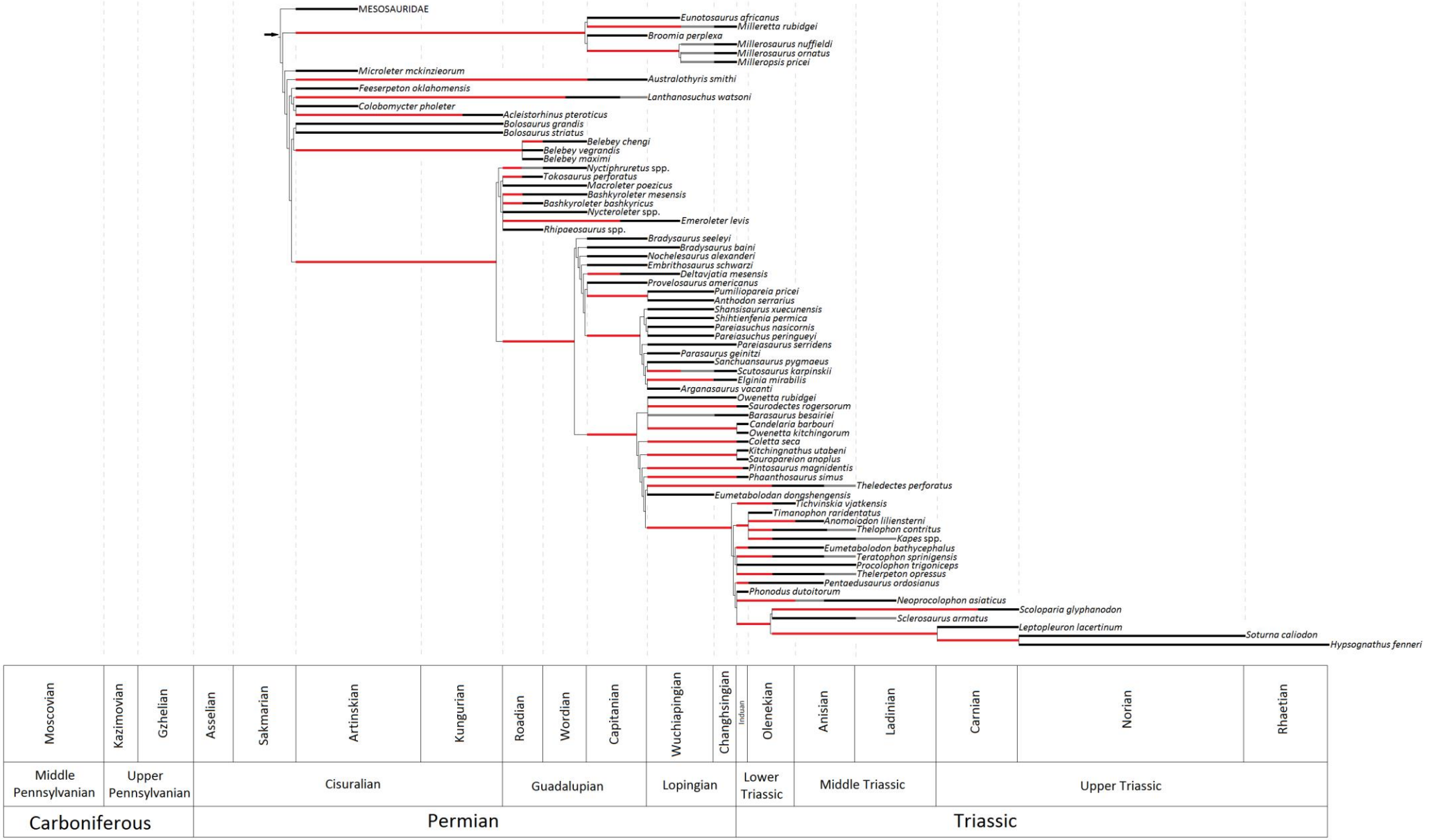

Figure L6: Portion of the time calibrated expanded supertree showing the relationships of parareptiles

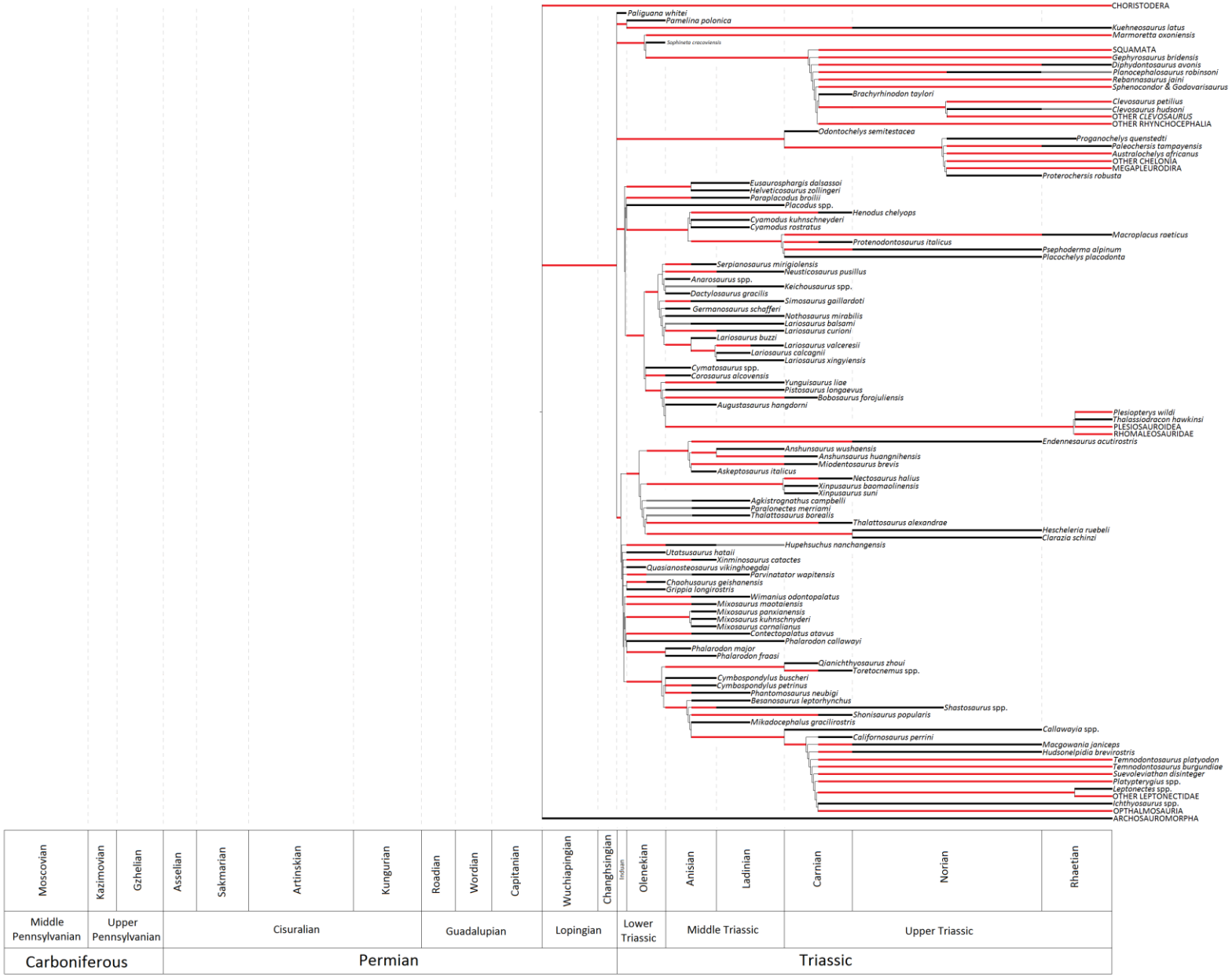

Figure L7: Portion of the time calibrated expanded supertree showing the relationships of lepidosauriform saurians

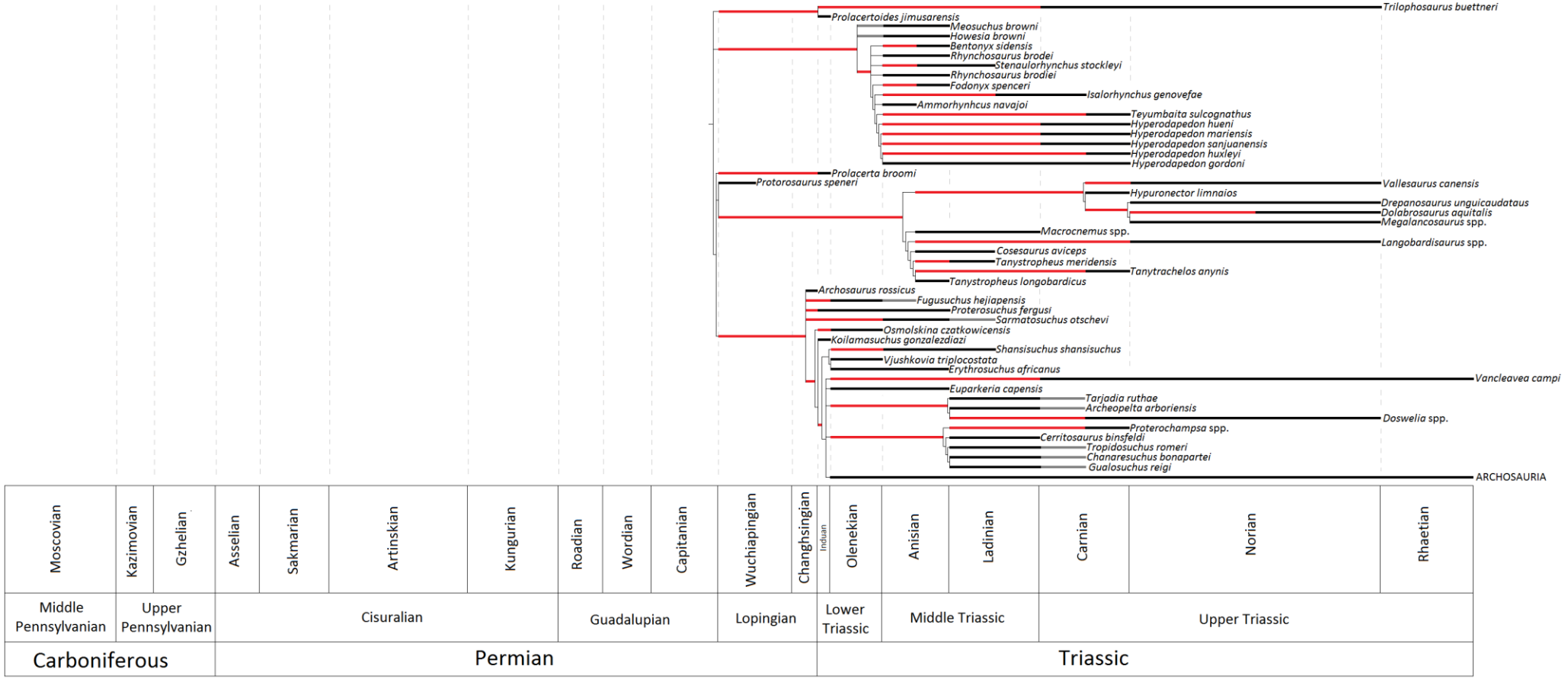

Figure L7: Portion of the time calibrated expanded supertree showing the relationships of basal archosauriformes.

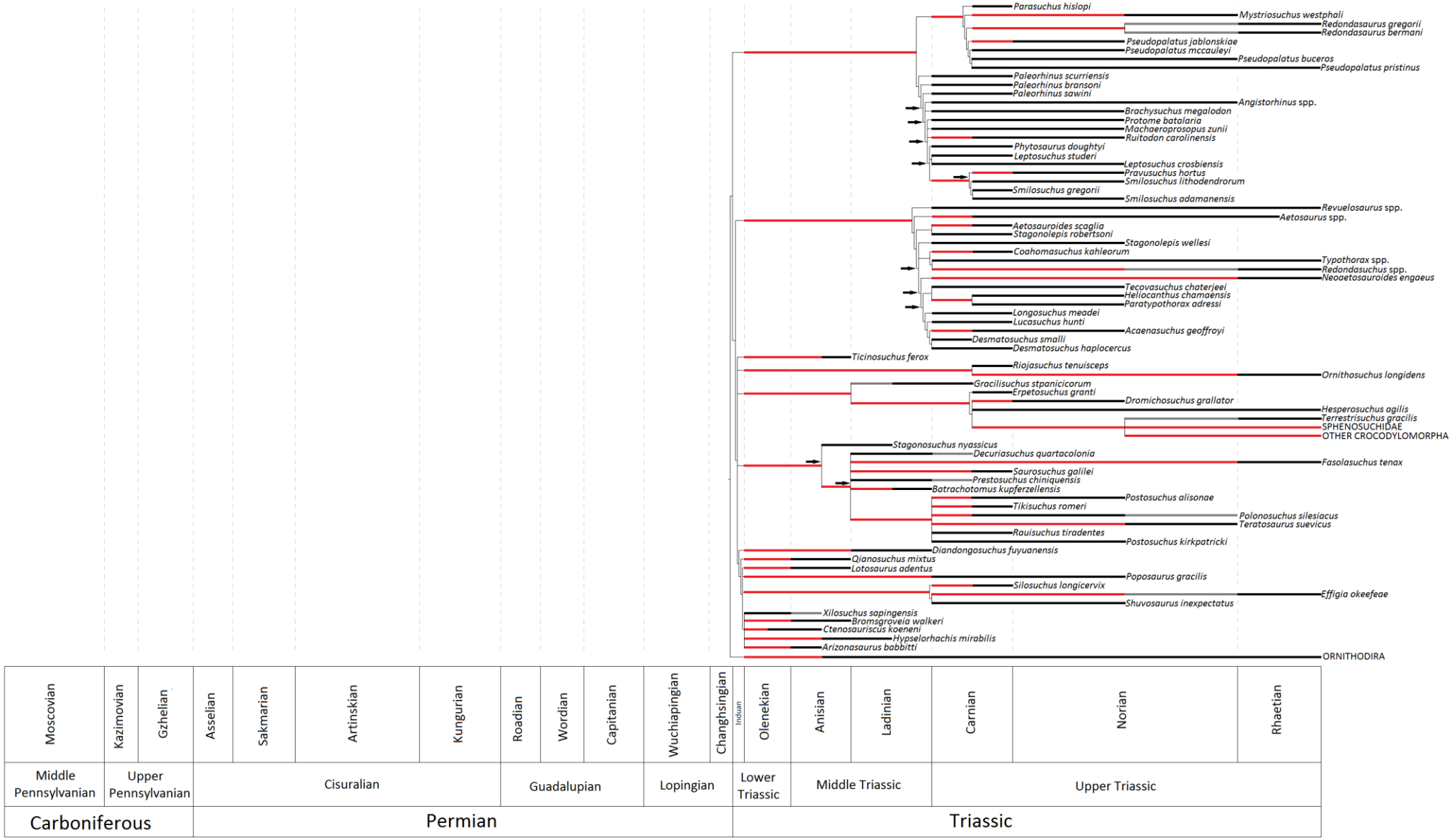

Figure L9: Portion of the time calibrated expanded supertree showing the relationships of crurotarsan archosaurs. Black arrows indicate nodes with negative support

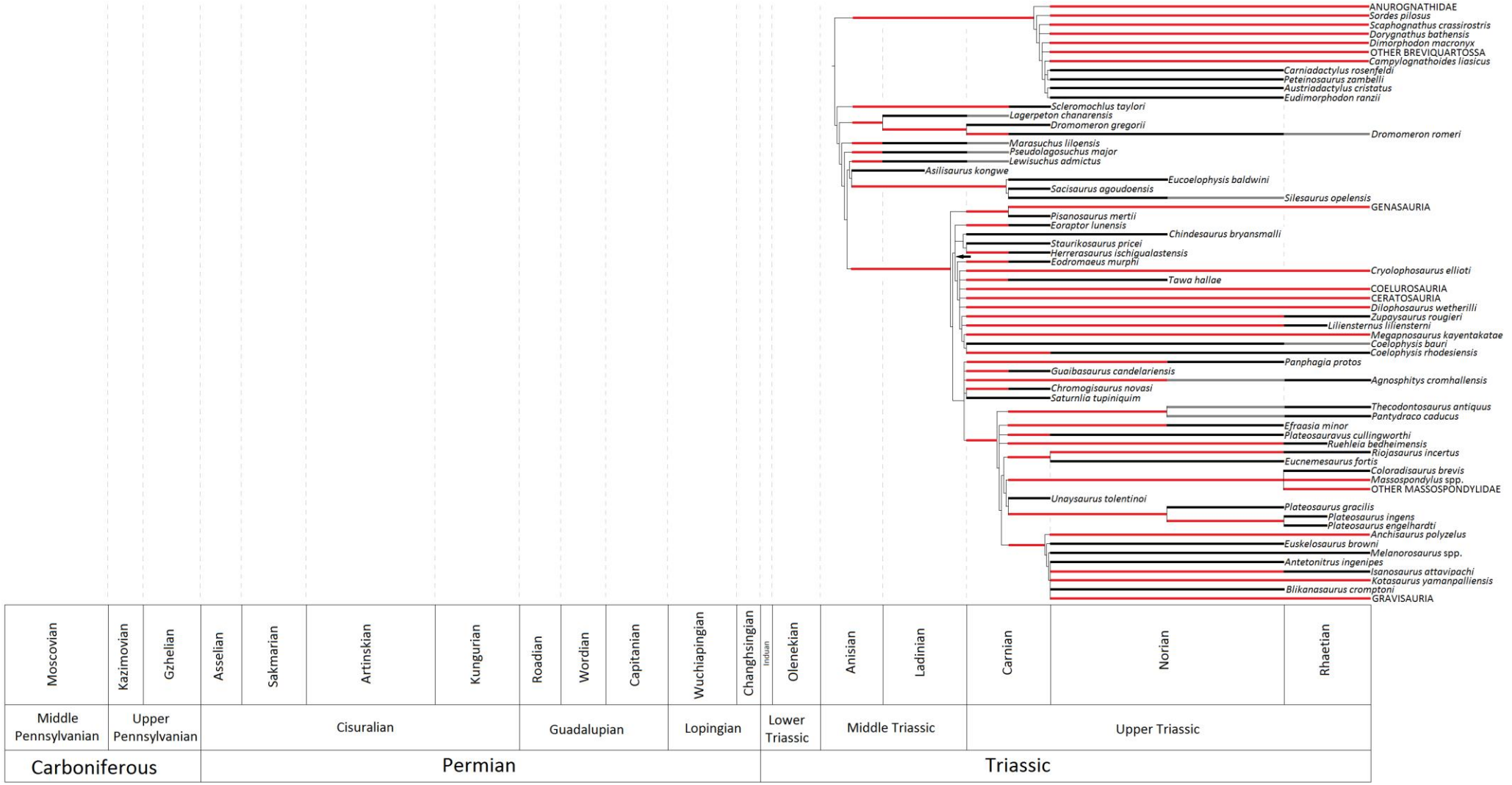

Figure L10: Portion of the time calibrated expanded supertree showing the relationships of ornithodiran archosaurs. Black arrow indicates a node with negative support.

Appendix M

All species included in the expanded supertree, and their age ranges.

Genus	*Species*	Age range (where uncertainty exists, species are assigned to the full range of possible dates	Age range (localities of uncertain age restricted to two or less time bins)
		Diadectomorpha	
Ambedus	*pusillus*	Sakmarian	Sakmarian
Diadectes	*tenuitectes*	Late Kungurian	Late Kungurian
Diadectes	*sideropelicus*	Late Kazimovian-Kungurian	Gzhelian-Kungurian
Diasparactus	*zenos*	Late Kazimovian-Early Sakmarian	Gzhelian-Early Asselian
Limnoscelis	*paludis*	Gzhelian-Early Sakmarian	Late Gzhelian-Early Asselian
Oradectes	*sanmiguelensis*	Asselian-Early Kungurian	Asselian
Orobates	*pabsti*	Artinskian	Artinskian
Sepeliodon	*hesperis*	Kazimovian-Gzhelian	Kazimovian
Silvadectes	*absitus*	Artinskian	Artinskian
Tseajaia	*campi*	Late Artinskian	Late Artinskian

Synapsida

Adelobasileus	*cromptoni*	Carnian	Carnian
Aelurognathus	*spp*	Wuchapingian	Wuchapingian
Aelurosaurus	*spp*	Wuchapingian-Changsingian	Wuchapingian-Changsingian
Aerosaurus	*greenleeorum*	Gzhelian-Early Sakmarian	Late Gzhelian-Early Asselian
Aerosaurus	*wellesi*	Gzhelian-Early Sakmarian	Late Asselian-Early Sakmarian
Aleodon	*brachyrhamphus*	Late Anisian-Early Ladinian	Late Anisian-Early Ladinian
Aloposaurus	*spp*	Wuchapingian-Changsingian	Wuchapingian-Changsingian
Andescynodon	*mendoyensis*	Late Olenekian-Early Ladinian	Anisian
Angelosaurus	*dolani*	Early Roadian	Early Roadian
Angelosaurus	*romeri*	Roadian	Roadian
Angonisaurus	*cruickshanki*	Late Anisian-Early Ladinian	Late Anisian-Early Ladinian
Anomocephalus	*africanus*	Capitanian	Capitanian
Anteosaurus	*magnificus*	Capitanian	Capitanian
Apsisaurus	*witteri*	Late Sakmarian-Artinskian	Late Sakmarian-Early Artinskian
Archaeosyodon	*praeventor*	Wordian	Wordian
Archaeothyris	*florensis*	Late Moscovian	Late Moscovian
Archaeovenator	*hamiltonensis*	Late Kasimovian-Gzhelian	Gzhelian
Arctognathus	*spp*	Capitanian-Changsingian	Capitanian-Changsingian
Arctotraversodon	*plemmyridon*	Late Carnian	Late Carnian

Aulacephalodon	*bainii*	Wuchapingian-Changsingian	Wuchapingian-Changsingian
Australobarbarus	*spp*	Late Capitanian-Early Wuchapingian	Late Capitanian-Early Wuchapingian
Australosyodon	*nyaphuli*	Wordian	Wordian
Basilodon	*woodwardi*	Wuchapingian-Changsingian	Wuchapingian-Changsingian
Bauria	*cynops*	Olenekian-Anisian	Olenekian-Early Anisian
Biarmosuchus	*tener*	Wordian	Wordian
Biseridens	*qilianicus*	Wordian	Wordian
Bolotridon	*frerensis*	Late Olenekian-Anisian	Late Olenekian-Early Anisian
Boreogomphodon	*jeffersoni*	Carnian-Early Norian	Carnian
Brasilitherium	*riograndensis*	Norian	Norian
Brasilodon	*quadrangularis*	Norian	Norian
Bullacephalus	*jacksoni*	Capitanian	Capitanian
Burnetia	*mirabilis*	Late Wuchapingian-Changsingian	Changsingian
Casea	*broilii*	Late Kungurian	Late Kungurian
Cerdops	*burgheri*	Late Wuchapingian-Changsingian	Changsingian
Chaliminia	*musteloides*	Norian	Norian
Charassognathus	*gracilis*	Early Wuchapingian	Early Wuchapingian
Chelydontops	*altidentalis*	Capitanian	Capitanian
Chiniquodon	*spp*	Late Anisian-Carnian	Late Anisian-Carnian
Choerosaurus	*dejageri*	Early Wuchapingian	Early Wuchapingian
Cistecephaloides	*boonstrai*	Wuchapingian	Wuchapingian
Cistecephalus	*microrhinus*	Wuchapingian	Wuchapingian
Clelandia	*spp*	Wuchapingian-Changsingian	Wuchapingian-Changsingian

Colobodectes	*cluveri*	Capitanian	Capitanian
Cotylorhynchus	*bransoni*	Roadian	Roadian
Cotylorhynchus	*hancocki*	Early Roadian	Early Roadian
Cotylorhynchus	*romeri*	Late Kungurian	Late Kungurian
Cricodon	*metabolus*	Late Anisian-Early Ladinian	Late Anisian-Early Ladinian
Cryptovenator	*hirschbergeri*	Late Gzhelian	Late Gzhelian
Ctenospondylus	*spp*	Sakmarian-Early Kungurian	Sakmarian-Early Kungurian
Cutleria	*wilmarthi*	Asselian-Early Kungurian	Asselian
Cynognathus	*spp*	Olenekian-Early Ladinian	Olenekian-Early Ladinian
Cynosaurus	*longiceps*	Wuchapingian-Changsingian	Wuchapingian-Changsingian
Cyonosaurus	*spp*	Wuchapingian-Changsingian	Wuchapingian-Changsingian
Dadadon	*isaloi*	Late Ladinian-Early Carnian	Late Ladinian-Early Carnian
Daptocephalus	*leoniceps*	Late Wuchapingian-Changsingian	Changsingian
Daqingshanodon	*limbus*	Late Wuchapingian-Changsingian	Changsingian
Delectosaurus	*arefjevi*	Late Changsingian	Late Changsingian
Diademodon	*tetragonus*	Olenekian-Early Ladinian	Olenekian-Early Ladinian
Dicynodon	*hueni*	Wuchapingian-Changsingian	Wuchapingian-Changsingian
Dicynodon	*lacerticeps*	Wuchapingian-Changsingian	Wuchapingian-Changsingian
Dicynodontoides	*spp*	Late Capitanian-Changsingian	Late Capitanian-Changsingian

Diictodon	*feliceps*	Capitanian-Changsingian	Capitanian-Changsingian
Dimetrodon	*limbatus*	Artinskian-Kungurian	Artinskian-Kungurian
Dimetrodon	*milleri*	Late Sakmarian-Artinskian	Late Sakmarian-Early Artinskian
Dinanomodon	*gilli*	Wuchapingian-Changsingian	Wuchapingian-Changsingian
Dinanomodon	*rubidgei*	Wuchapingian	Wuchapingian
Dinodontosaurus	*pedroanum*	Ladinian-early Carnian	Ladinian
Dolichuranus	*spp*	Late Olenekian-Anisian	Late Olenekian-Early Anisian
Dvinia	*prima*	Wuchapingian	Wuchapingian
Ecteninion	*lunensis*	Late Carnian	Late Carnian
Edaphosaurus	*boanerges*	Late Sakmarian-Early Kungurian	Late Sakmarian-Early Kungurian
Edaphosaurus	*colohistion*	Late Gzhelian	Late Gzhelian
Edaphosaurus	*cruciger*	Artinskian-Kungurian	Artinskian-Kungurian
Edaphosaurus	*novomexicanus*	Gzhelian-Early Kungurian	Late Gzhelian-Artinskian
Edaphosaurus	*pogonias*	Artinskian-Kungurian	Artinskian-Kungurian
Elliotherium	*kersteni*	Norian	Norian
Elliotsmithia	*longiceps*	Capitanian	Capitanian
Elph	*borealis*	Late Wuchapingian-Changsingian	Changsingian
Emydops	*arctatus*	Capitanian-Changsingian	Capitanian-Changsingian
Emydops	*oweni*	Wuchapingian	Wuchapingian
Endothiodon	*spp*	Late Capitanian-Changsingian	Late Capitanian-Changsingian

Ennatosaurus	*tecton*	Late Roadian-Wordian	Wordian
Eodicynodon	*oelofseni*	Wordian	Wordian
Eodicynodon	*oosthuizeni*	Wordian	Wordian
Eosimops	*newtoni*	Capitanian-Changsingian	Capitanian-Changsingian
Eothyris	*parkeyi*	Early Kungurian	Early Kungurian
Ericiolacerta	*parva*	Induan	Induan
Estemmenosuchus	*uralensis*	Wordian	Wordian
Estemmenosuchus	*mirabilis*	Wordian	Wordian
Euptychognathus	*bathyrhynchus*	Wuchapingian-Changsingian	Wuchapingian-Changsingian
Euromycter	*rutenus*	Artinskian-Kungurian	Late Kungurian
Exaeretodon	*spp*	Ladinian-Carnian	Ladinian-Carnian
Galechirus	*scholtzi*	Capitanian	Capitanian
Galeops	*whaitsi*	Capitanian	Capitanian
Galepus	*jouberti*	Wuchapingian	Wuchapingian
Galesaurus	*planiceps*	Induan	Induan
Galesuchus	*gracilis*	Capitanian	Capitanian
Geikia	*elginensis*	Changsingian	Changsingian
Geikia	*locusticeps*	Late Wuchapingian-Changsingian	Changsingian
Glanosuchus	*macrops*	Wordian-Capitanian	Wordian-Capitanian
Glaucosaurus	*megalops*	Kungurian	Kungurian
Gomphodontosuchus	*brasiliensis*	Carnian	Carnian
Gordonia	*traquairi*	Changsingian	Changsingian
Gorgonops	*torvus*	Wuchapingian	Wuchapingian
Haptodus	*garnettensis*	Late Kasimovian	Late Kasimovian
Heleosaurus	*scholtzi*	Capitanian	Capitanian
Herpetoskylax	*hopsoni*	Wuchiapingian	Wuchiapingian
Hipposaurus	*boonstrai*	Capitanian	Capitanian
Ianthasaurus	*hardestiorum*	Late Kasimovian	Late Kasimovian

Ianthodon	*schultzei*	Late Kasimovian	Late Kasimovian
Ictidorhinus	*martinsi*	Late Wuchapingian-Changsingian	Changsingian
Ictidosaurus	*angusticeps*	Wordian-Capitanian	Wordian-Capitanian
Ictidosuchoides	*longiceps*	Late Capitanian-Changsingian	Late Capitanian-Changsingian
Ictidosuchops	*rubidgei*	Wuchapingian-Induan	Wuchapingian-Induan
Ictidosuchus	*primaevus*	Late Capitanian-Early Wuchapingian	Late Capitanian-Early Wuchapingian
Idelesaurus	*tartaricus*	Wuchapingian	Wuchapingian
Inostrancevia	*spp*	Wuchapingian	Wuchapingian
Interpresosaurus	*blomi*	Late Changsingian	Late Changsingian
Irajatherium	*hernandezei*	Norian	Norian
Ischigualastia	*jenseni*	Late Carnian	Late Carnian
Jachaleria	*spp*	Ladinian-Norian	Ladinian-Norian
Jimusaria	*sinkianensis*	Late Wuchapingian-Changsingian	Changsingian
Jonkeria	*truculenta*	Capitanian	Capitanian
Kannemeyeria	*lophorhina*	Late Olenekian-Anisian	Late Olenekian-Early Anisian
Kannemeyeria	*simocephala*	Late Olenekian-Anisian	Late Olenekian-Early Anisian
Katumbia	*parringtoni*	Late Wuchapingian-Changsingian	Changsingian
Kawingasaurus	*fossilis*	Late Wuchapingian-Changsingian	Changsingian
Keyseria	*benjamini*	Late Wuchapingian-Changsingian	Changsingian
Kitchinganomodon	*crassus*	Wuchapingian	Wuchapingian
Kombuisia	*antarctica*	Induan	Induan
Kombuisia	*frerensis*	Late Olenekian-Anisian	Late Olenekian-Early Anisian

Kuehneotherium	*praecursoris*	Norian-Rhaetian	Norian-Rhaetian
Kwazulusaurus	*shakai*	Late Wuchapingian-Changsingian	Changsingian
Langbergia	*modisei*	Olenekian	Olenekian
Lanthanostegus	*mohoii*	Capitanian	Capitanian
Lemurosaurus	*pricei*	Wuchiapingian	Wuchiapingian
Lobalopex	*mordax*	Early Wuchapingian	Early Wuchapingian
Lophorhinus	*willodensis*	Early Wuchapingian	Early Wuchapingian
Luangwa	*spp*	Late Anisian-Carnian	Late Anisian-Ladinian
Lumkuia	*fuzzi*	Late Olenekian-Anisian	Late Olenekian-Early Anisian
Lupeosaurus	*kayi*	Late Sakmarian-Early Kungurian	Late Sakmarian-Early Kungurian
Lycaenodon	*longiceps*	Wuchiapingian	Wuchiapingian
Lycaenops	*spp*	Wuchapingian-Changsingian	Wuchapingian-Changsingian
Lycideops	*longiceps*	Wuchapingian-Changsingian	Wuchapingian-Changsingian
Lycosuchus	*vanderrieti*	Capitanian	Capitanian
Lystrosaurus	*broomi*	Induan	Induan
Lystrosaurus	*curvatus*	Late Changsingian-Induan	Late Changsingian-Induan
Lystrosaurus	*declivis*	Induan	Induan
Lystrosaurus	*georgi*	Induan	Induan
Lystrosaurus	*hedini*	Late Changsingian-Induan	Late Changsingian-Induan
Lystrosaurus	*maccaigi*	Late Changsingian-Induan	Late Changsingian-Induan
Lystrosaurus	*murrayi*	Induan	Induan
Lystrosaurus	*oviceps*	Induan	Induan
Lystrosaurus	*platyceps*	Induan	Induan
Lystrosaurus	*robustus*	Induan	Induan

Lystrosaurus	*shichanggouensis*	Induan	Induan
Massetognathus	*spp*	Ladinian-Early Carnian	Ladinian
Menadon	*besairei*	Ladinian-Early Carnian	Ladinian-Early Carnian
Mesenosaurus	*romeri*	Late Roadian-Wordian	Wordian
Microsyodon	*orlovi*	Roadian	Roadian
Moghreberia	*nmachouensis*	Carnian	Carnian
Morganucodon	*watsoni*	Late Norian-Rhaetian	Late Norian-Rhaetian
Moschorhinus	*kitchingi*	Wuchapingian-Induan	Wuchapingian-Induan
Moschowhaitsia	*vjushkovi*	Late Changsingian	Late Changsingian
Mycterosaurus	*longiceps*	Kungurian	Kungurian
Myosaurus	*gracilis*	Induan	Induan
Nanictosaurus	*rubidgei*	Late Wuchapingian-Changsingian	Late Wuchapingian-Changsingian
Nanogomphodon	*wildi*	Ladinian	Ladinian
Niuksenitia	*sikbonensis*	Wuchiapingian	Wuchiapingian
Njalila	*spp*	Wuchapingian-Changsingian	Late Changsingian
Notosyodon	*gusevi*	Late Wordian-Early Capitanian	Late Wordian-Early Capitanian
Odontocyclops	*whaitsi*	Wuchapingian	Wuchapingian
Oedaleops	*campi*	Gzhelian-Early Sakmarian	Late Asselian-Early Sakmarian
Oligokyphus	*spp.*	Rhaetian	Rhaetian
Olivierosuchus	*parringtoni*	Induan	Induan
Ophiacodon	*mirus*	Gzhelian-Early Kungurian	Late Gzhelian-Artinskian
Ophiacodon	*retroversus*	Late Sakmarian-Early Kungurian	Late Sakmarian-Early Kungurian

Oromycter	*dolesorum*	Early Artinskian	Early Artinskian
Otsheria	*netzvetajevi*	Wordian	Wordian
Oudenodon	*bainii*	Wuchapingian-Changsingian	Wuchapingian-Changsingian
Pachydectes	*elsi*	Capitanian	Capitanian
Palaeohatteria	*longicaudata*	Sakmarian	Sakmarian
Pampaphoneus	*biccai*	Capitanian	Capitanian
Pantelosaurus	*saxonicus*	Asselian	Asselian
Paraburnetia	*sneeubergensis*	Wuchiapingian	Wuchiapingian
Parakannemeyeria	*dolichocephala*	Anisian-Early Ladinian	Anisian
Parakannemeyeria	*ningwuensis*	Anisian-Early Ladinian	Anisian
Parakannemeyeria	*youngi*	Anisian-Early Ladinian	Anisian
Parakannemeyeria	*shenmuensis*	Anisian-Early Ladinian	Anisian
Pascualgnathus	*polanskii*	Late Olenekian-Early Ladinian	Anisian
Patranomodon	*nyaphulii*	Wordian	Wordian
Peramodon	*amaltzkii*	Late Wuchapingian-Changsingian	Changsingian
Placerias	*spp*	Late Carnian-Norian	Late Carnian-Norian
Platycraniellus	*elegens*	Induan	Induan
Pristerodon	*mackayi*	Capitanian-Changsingian	Capitanian-Changsingian
Pristerognathus	*polyodon*	Capitanian-Early Wuchapingian	Capitanian-Early Wuchapingian
Probainognathus	*jenseni*	Ladinian-Early Carnian	Ladinian
Probelesodon	*spp*	Ladinian	Ladinian
Proburnetia	*viatkensis*	Late Capitanian-Early Wuchapingian	Late Capitanian-Early Wuchapingian

Procynosuchus	*delaharpeae*	Wuchapingian-Changsingian	Wuchapingian-Changsingian
Progalesaurus	*lootbergensis*	Induan	Induan
Promoschorhynchus	*platyrhinus*	Late Wuchapingian-Early Induan	Changsingian-Early Induan
Prosictodon	*dubei*	Capitanian	Capitanian
Prozostrodon	*brasiliensis*	Carnian	Carnian
Pyozia	*mesenensis*	Late Roadian-Wordian	Wordian
Rabidosaurus	*cristatus*	Late Olenekian-Anisian	Anisian
Raranimus	*dashankouensis*	Wordian	Wordian
Rechnisaurus	*cristarhynchus*	Late Anisian-Early Ladinian	Late Anisian-Early Ladinian
Regisaurus	*jacobi*	Induan	Induan
Rhachiocephalus	*magnus*	Wuchapingian-Changsingian	Wuchapingian-Changsingian
Rhadiodromus	*klimovi*	Late Olenekian-Anisian	Anisian
Rhinodicynodon	*gracile*	Anisian-Early Ladinian	Late Anisian-Early Ladinian
Riograndia	*guaibensis*	Norian	Norian
Robertia	*broomiana*	Capitanian-Early Wuchapingian	Capitanian-Early Wuchapingian
Rubidgea	*spp*	Wuchapingian-Changsingian	Wuchapingian-Changsingian
Ruthiromia	*elcobriensis*	Gzhelian-Early Sakmarian	Late Gzhelian-Early Asselian
Sangusaurus	*edentus*	Late Anisian-Early Ladinian	Late Anisian-Early Ladinian
Santacruzodon	*hopsoni*	Ladinian	Ladinian
Sauroctonus	*progressus*	Wuchapingian	Wuchapingian

Scalenodon	*angustifrons*	Late Anisian-Early Ladinian	Late Anisian-Early Ladinian
Scalenodon	*hirschsoni*	Late Anisian-Early Ladinian	Late Anisian-Early Ladinian
Scalenodontoides	*macrodontes*	Norian	Norian
Scaloposaurus	*constricus*	Late Wuchapingian-Induan	Late Wuchapingian-Induan
Scylacognathus	*spp*	Capitanian-Changsingian	Capitanian-Changsingian
Secodontosaurus	*obtusidens*	Artinskian-Kungurian	Artinskian-Kungurian
Shansiodon	*spp*	Anisian-Early Ladinian	Anisian
Sinokannemeyeria	*pearsoni*	Anisian-Early Ladinian	Anisian
Sinokannemeyeria	*yingchiaoensis*	Anisian-Early Ladinian	Anisian
Sinokannemeyeria	*sanchuanheensi*	Anisian-Early Ladinian	Anisian
Sinophoneus	*yumenensis*	Wordian	Wordian
Sintocephalus	*alticeps*	Wuchapingian	Wuchapingian
Sphenacodon	*spp*	Gzhelian-Early Kungurian	Late Gzhelian-Artinskian
Stahleckeria	*potens*	Ladinian	Ladinian
Stereophallodon	*ciscoensis*	Late Asselian-Early Sakmarian	Late Asselian-Early Sakmarian
Styracocephalus	*platyrhynchus*	Capitanian	Capitanian
Suminia	*getmanovi*	Late Capitanian-Early Wuchapingian	Late Capitanian-Early Wuchapingian
Sycosaurus	*spp*	Late Wuchapingian-Changsingian	Changsingian
Syodon	*biarmicum*	Wordian-Capitanian	Wordian-Early Capitanian

Syops	*vanhoepeni*	Wuchapingian	Wuchapingian
Tapinocaninus	*pamelae*	Wordian	Wordian
Tetraceratops	*insignis*	Late Kungurian	Late Kungurian
Tetracynodon	*tenuis*	Late Wuchapingian-Changsingian	Late Wuchapingian-Changsingian
Tetracynodon	*darti*	Induan	Induan
Tetragonias	*njalilus*	Late Anisian-early Ladinian	Late Anisian-early Ladinian
Theriognathus	*microps*	Late Wuchapingian-Changsingian	Changsingian
Therioherpeton	*carnegini*	Carnian	Carnian
Thinaxodon	*spp*	Induan	Induan
Tiarajudens	*eccentricus*	Capitanian	Capitanian
Titanophoneus	*adamanteus*	Late Wordian-Early Capitanian	Late Wordian-Early Capitanian
Titanophoneus	*potens*	Late Wordian-Capitanian	Late Wordian-Early Capitanian
Trichasaurus	*texensis*	Late Kungurian	Late Kungurian
Trirachodon	*spp*	Olenekian-Early Ladinian	Olenekian-Early Ladinian
Tropidosoma	*microtrema*	Early Wuchapingian	Early Wuchapingian
Trucidocynodon	*riograndensis*	Carnian	Carnian
Turfanodon	*bogdaensis*	Late Wuchapingian-Changsingian	Changsingian
Ulemica	*spp*	Late Wordian-Capitanian	Late Wordian-Early Capitanian
Ulemosaurus	*svijagensis*	Late Wordian-Capitanian	Late Wordian-Early Capitanian
Varanodon	*agilis*	Roadian	Roadian
Varanops	*brevirostris*	Artinskian-Kungurian	Artinskian-Kungurian
Varanosaurus	*acutirostris*	Kungurian	Kungurian

Viatkosaurus	*sumini*	Late Capitanian-Early Wuchapingian	Late Capitanian-Early Wuchapingian
Vinceria	*argentinensis*	Late Olenekian-Early Ladinian	Anisian
Vivaxosaurus	*trautscholdi*	Wuchapingian-Changsingian	Wuchapingian-Changsingian
Wadiasaurus	*indicus*	Late Anisian-Early Ladinian	Late Anisian-Early Ladinian
Watongia	*meieri*	Roadian	Roadian

Parareptilia			
Acleistorhinus	*pteroticus*	Late Kungurian	Late Kungurian
Anomoiodon	*liliensterni*	Early Anisian	Early Anisian
Anthodon	*serrarius*	Wuchapingian	Wuchapingian
Arganaceras	*vacanti*	Early Wuchapingian	Early Wuchapingian
Australothyris	*smithi*	Capitanian	Capitanian
Barasaurus	*besairiei*	Wuchapingian-Iduan	Changsingian-Induan
Bashkyroleter	*mesensis*	Late Roadian-Wordian	Wordian
Bashkyroleter	*bashkyricus*	Late Roadian	Late Roadian
Belebey	*chengi*	Wordian	Wordian
Belebey	*vegrandis*	Late Roadian	Late Roadian
Belebey	*maximi*	Late Roadian	Late Roadian
Bolosaurus	*grandis*	Artinskian-Kungurian	Artinskian-Kungurian
Bolosaurus	*striatus*	Artinskian-Kungurian	Artinskian-Kungurian
Bradysaurus	*seeleyi*	Capitanian	Capitanian

Bradysaurus	*baini*	Capitanian-early Wuchupingian	Capitanian-early Wuchupingian
Broomia	*perplexa*	Capitanian	Capitanian
Candelaria	*barbouri*	Early Ladinian	Early Ladinian
Coletta	*seca*	Induan	Induan
Colobomycter	*pholeter*	Early Artinskian	Early Artinskian
Deltavjatia	*mesensis*	Late Capitanian-Early Wuchapingian	Late Capitanian-Early Wuchapingian
Elginia	*mirabilis*	Changsingian	Changsingian
Embrithosaurus	*schwarzi*	Capitanian	Capitanian
Emeroleter	*levis*	Late Capitanian-Early Wuchapingian	Late Capitanian-Early Wuchapingian
Eudibamus	*cursoris*	Artinskian	Artinskian
Eumetabolodan	*dongshengensis*	Wuchapingian	Wuchapingian
Eumetabolodon	*bathycephalus*	Olenekian-Early Anisian	Late Olenekian-Early Anisian
Eunotosaurus	*africanus*	Capitanian-early Wuchupingian	Capitanian-early Wuchupingian
Feeserpeton	*oklahomensis*	Early Artinskian	Early Artinskian
Hypsognathus	*fenneri*	Norian-Rhaetian	Norian-Rhaetian
Kapes	spp	Late Olenekian-Early Ladinian	Late Olenekian-Anisian
Kitchingnathus	*utabeni*	Induan	Induan
Lanthanosuchus	*watsoni*	Late Wordian-Capitanian	Late Wordian-Early Capitanian
Leptopleuron	*lacertinum*	Carnian	Carnian
Macroleter	*poezicus*	Roadian-Wordian	Roadian-Wordian
Mesosauridae	*spp*	Early Artinskian	Early Artinskian
Microleter	*mckinzueorum*	Early Artinskian	Early Artinskian
Milleretta	*rubidgei*	Late Wuchapingian-Changsingian	Changsingian
Milleropsis	*pricei*	Late Wuchapingian-Changsingian	Changsingian

Millerosaurus	*nuffieldi*	Late Wuchapingian-Changsingian	Changsingian
Millerosaurus	*ornatus*	Late Wuchapingian-Changsingian	Changsingian
Neoprocolophon	*asiaticus*	Anisian-Early Ladinian	Late Anisian-Early Ladinian
Nochelesaurus	*alexanderi*	Capitanian	Capitanian
Nycteroleter	*spp*	Roadian-Wordian	Roadian-Wordian
Nyctiphruretus	*spp*	Late Roadian-Wordian	Wordian
Owenetta	*rubidgei*	Wuchapingian-Changsingian	Wuchapingian-Changsingian
Owenetta	*kitchingorum*	Induan	Induan
Parasaurus	*geinitzi*	Early Wuchapingian	Early Wuchapingian
Pareiasaurus	*serridens*	Wuchapingian-Changsingian	Wuchapingian-Changsingian
Pareiasuchus	*peringueyi*	Wuchapingian	Wuchapingian
Pareiasuchus	*nasicornis*	Wuchapingian	Wuchapingian
Pentaedrusaurus	*ordosianus*	Olenekian-Early Anisian	Olenekian
Phaantosaurus	*simus*	Induan	Induan
Phonodus	*dutoitorum*	Induan	Induan
Pintosaurus	*magnidentes*	Late Induan	Late Induan
Procolophon	*trigoniceps*	Induan-Anisian	Induan-Anisian
Provelosaurus	*americanus*	Capitanian	Capitanian
Pumiliopareia	*pricei*	Wuchapingian	Wuchapingian
Rhipaeosaurus	*spp*	Roadian	Roadian
Sanchuansaurus	*pygmaeus*	Wuchapingian	Wuchapingian
Saurodectes	*rogersorum*	Induan	Induan
Sauropareion	*anoplus*	Induan	Induan
Scleorsaurus	*armatus*	Late Olenekian-Early Ladinian	Late Olenekian-Anisian
Scoloparia	*glyphanodon*	Late Carnian	Late Carnian

Scutosaurus	*kapinskii*	Late Wuchapingian-Changsingian	Changsingian
Shansisaurus	*xuecunensis*	Wuchapingian	Wuchapingian
Shihtienfenia	*permica*	Wuchapingian	Wuchapingian
Soturnia	*caliodon*	Norian	Norian
Teratophon	*sprinigensis*	Late Olenekian-Anisian	Late Olenekian-Early Anisian
Theledectes	*perforatus*	Late Olenekian-Anisian	Late Olenekian-Early Anisian
Thelerpeton	*opressus*	Late Olenekian-Anisian	Late Olenekian-Early Anisian
Thelophon	*contritus*	Late Olenekian-Anisian	Late Olenekian-Early Anisian
Tichvinskia	*vjatkensis*	Late Olenekian	Late Olenekian
Timanophon	*raridentatus*	Early Olenekian	Early Olenekian
Tokosaurus	*perforatus*	Late Roadian	Late Roadian
Basal Eureptiles			
Acrosodontosaurus	*piveteaui*	Wuchapingian-Changsingian	Wuchapingian
Agkistrognathus	*campbelli*	Late Olenekian-Early Ladinian	Late Anisian-Early Ladinian
Anshunsaurus	*wushaensis*	Ladinian	Ladinian
Anshunsaurus	*huangguosuensis*	Early Carnian	Early Carnian
Araeoscelis	*spp*	Artinskian-Kungurian	Artinskian-Kungurian
Askeptosaurus	*italicus*	Late Anisian	Late Anisian
Brouffia	*orientalia*	Late Moscovian	Late Moscovian

Captorhinikos	*spp*	Late Kungurian	Late Kungurian
Captorhinus	*aguti*	Artinskian-Kungurian	Artinskian-Kungurian
Captorhinus	*laticeps*	Artinskian-Kungurian	Artinskian-Kungurian
Captorhinus	*magnus*	Early Artinskian	Early Artinskian
Clarazia	*schinzi*	Norian	Norian
Claudiosaurus	*germaini*	Wuchapingian-Changsingian	Changsingian
Coelostegus	*prothales*	Late Moscovian	Late Moscovian
Coelurosauravus	*spp*	Wuchapingian-Changsingian	Wuchapingian
Concordia	*cunninghami*	Late Kasimovian-Gzhelian	Gzhelian
Endennesaurus	*acutirostris*	Norian	Norian
Gasurhinus	*quingtoushanensis*	Wordian-Changsingian	Wordian-Changsingian
Hecheleria	*rubeli*	Norian	Norian
Labidosaurikos	*meachami*	Late Kungurian	Late Kungurian
Labidosaurus	*hamatus*	Kungurian	Kungurian
Lanthanolania	*ivakhnenkoi*	Late Roadian-Wordian	Wordian
Longisquama	*insignis*	Ladinian	Ladinian
Miodentosaurus	*brevis*	Early Carnian	Early Carnian
Moradisaurus	*grandis*	Changsingian	Changsingian
Nectosaurus	*halius*	Late Carnian	Late Carnian
Palaeagama	*vielhaueri*	Induan	Induan
Paleothyris	*acadiana*	Late Moscovian	Late Moscovian
Paralonectes	*merriami*	Late Olenekian-Early Ladinian	Late Anisian-Early Ladinian
Petrolacosaurus	*kansensis*	Late Kazimovian	Late Kazimovian
Protocaptorhinus	*pricei*	Artinskian-Kungurian	Artinskian-Kungurian

Reiszorhinus	*olsoni*	Kungurian	Kungurian
Rhiodenticulatus	*heatoni*	Gzhelian-Early Sakmarian	Late Asselian-Early Sakmarian
Romeria	*prima*	Late Sakmarian	Late Sakmarian
Romeria	*texana*	Late Sakmarian-Artinskian	Late Sakmarian-Early Artinskian
Rothianiscus	*multidonta*	Roadian	Roadian
Saurorictus	*australis*	Early Wuchapingian	Early Wuchapingian
Saurosternon	*bainii*	Wuchapingian-Changsingian	Wuchapingian-Changsingian
Spinoaequalis	*schultzei*	Late Kazimovian-Gzhelian	Gzhelian
Tangasaurus	*mennelli*	Wuchapingian-Changsingian	Late Changsingian
Thalattosaurus	*borealis*	Late Olenekian-Early Ladinian	Late Anisian-Early Ladinian
Thalattosaurus	*alexandreae*	Late Carnian	Late Carnian
Thuringothyris	*mahlendorffae*	Artinskian	Artinskian
Xinpusaurus	*suni*	Early Carnian	Early Carnian
Xinpusaurus	*baomaolinensis*	Early Carnian	Early Carnian
Youngina	*capensis*	Wuchapingian-Changsingian	Wuchapingian-Changsingian
Lepidosauriformes			
Brachyrhinodon	*taylori*	Late Carnian	Late Carnian
Clevosaurus	*hudsoni*	Late Norian-Rhaetian	Rhaetian
Diphydontosarus	*avonis*	Rhaetian	Rhaetian
Kuehneosaurus	*latus*	Norian-Rhaetian	Norian-Rhaetian

Paliguana	*whitei*	Induan	Induan
Pamelina	*polonica*	Olenekian	Olenekian
Planocephalosaurus	*robinsonae*	Late Norian-Rhaetian	Rhaetian
Sophineta	*cracoviensis*	Late Olenekian	Late Olenekian
Chelonia			
Odontochelys	*semitestacea*	Early Carnian	Early Carnian
Palaeochersis	*talampayensis*	Rhaetian	Rhaetian
Proganochelys	*quenstedti*	Late Norian-Early Rhaetian	Late Norian-Early Rhaetian
Proterochersis	*intermedia*	Late Norian	Late Norian
Archosauromorpha			
Acaenasuchus	*geoffroyi*	Late Carnian-Early Norian	Late Carnian-Early Norian
Aetosauroides	*scagliai*	Carnian	Carnian
Aetosaurus	*spp*	Late Carnian-Early Rhaetian	Late Carnian-Early Rhaetian
Agnosphitys	*cromhallensis*	Late Norian-Rhaetian	Rhaetian
Ammorhynchus	*navajoi*	Early Anisian	Early Anisian
Angistorhinus	*spp*	Carnian-Norian	Carnian-Norian
Antetonitrus	*ingeniceps*	Norian	Norian
Archeopelta	*arborensis*	Ladinian-Early	Ladinian

		Carnian	
Archosaurus	*rossicus*	Late Changsingian	Late Changsingian
Arizonasaurus	*babbitti*	Early Anisian	Early Anisian
Asilisaurus	*kongwe*	Late Anisian-Early Ladinian	Late Anisian-Early Ladinian
Austriadactylus	*cristatus*	Norian	Norian
Batrachotomus	*kupferzellensis*	Late Ladinian	Late Ladinian
Bentonyx	*sidensis*	Late Anisian	Late Anisian
Blikanasaurus	*cromptoni*	Norian	Norian
Brachysuchus	*megalodon*	Carnian-Early Norian	Carnian-Early Norian
Bromsgroveia	*walkeri*	Anisian	Anisian
Carniadactylus	*rosenfeldi*	Norian	Norian
Cerritosaurus	*binsfeldi*	Ladinian	Ladinian
Chanaresuchus	*bonapartei*	Ladinian-Early Carnian	Ladinian
Chindesaurus	*bryansmalli*	Carnian-Early Norian	Carnian-Early Norian
Chromogisaurus	*novasi*	Late Carnian	Late Carnian
Coahomasuchus	*kahleorum*	Late Carnian	Late Carnian
Coelophysis	*bauri*	Late Carnian-Rhaetian	Late Carnian-Norian
Coelophysis	*rhodesiensis*	Norian-Rhaetian	Norian-Rhaetian
Coloradisaurus	*brevis*	Rhaetian	Rhaetian
Cosesaurus	*aviceps*	Late Anisian-Early Ladinian	Late Anisian-Early Ladinian
Ctenosauriscus	*koeneni*	Late Olenekian-Early Anisian	Late Olenekian-Early Anisian
Decuriasuchus	*quartacolonia*	Ladinian-Early Carnian	Ladinian
Desmatosuchus	*haploceras*	Carnian	Carnian
Desmatosuchus	*smalli*	Early Carnian	Early Carnian
Diandongosuchus	*fuyuanensis*	Ladinian	Ladinian

Dolabrosaurus	*aquatilis*	Late Norian	Late Norian
Doswellia	*spp*	Late Carnian-Norian	Late Carnian-Norian
Drepanosaurus	*unguicaudatus*	Norian	Norian
Dromicosuchus	*grallator*	Early Norian	Early Norian
Dromomeron	*gregorii*	Carnian	Carnian
Dromomeron	*romeri*	Late Carnian-Rhaetian	Late Carnian-Norian
Effigia	*okeeffeae*	Late Norian-Rhaetian	Rhaetian
Efraasia	*minor*	Late Norian	Late Norian
Eodromaeus	*murphi*	Late Carnian	Late Carnian
Eoraptor	*lunensis*	Late Carnian	Late Carnian
Erpetosuchus	*granti*	Late Carnian	Late Carnian
Erythrosuchus	*africanus*	Olenekian-Anisian	Olenekian-Anisian
Eucnemesaurus	*fortis*	Norian	Norian
Eucoelophysis	*baldwini*	Late Carnian-Early Norian	Late Carnian-Early Norian
Eudimorphodon	*ranzii*	Norian	Norian
Euparkeria	*capensis*	Olenekian-Anisian	Olenekian-Anisian
Euskelosaurus	*brownii*	Norian	Norian
Fasolasuchus	*tenax*	Rhaetian	Rhaetian
Fodonyx	*spenceri*	Late Anisian	Late Anisian
Fugusuchus	*hejiapensis*	Olenekian-Early Anisian	Olenekian
Gracilisuchus	*stipanicicorum*	Ladinian-Early Carnian	Late Ladinian-Early Carnian
Guaibasaurus	*candelariensis*	Late Carnian	Late Carnian
Gualosuchus	*reigi*	Ladinian-Early Carnian	Ladinian
Heliocanthus	*chamaensis*	Late Carnian-Norian	Late Carnian-Norian
Herrerasaurus	*ischigualastensis*	Late Carnian	Late Carnian

Hesperosuchus	*agilis*	Late Carnian-Rhaetian	Late Carnian-Rhaetian
Howesia	*browni*	Late Olenekian-Anisian	Anisian
Hyperodapedon	*huenei*	Carnian	Carnian
Hyperodapedon	*mariensis*	Carnian	Carnian
Hyperodapedon	*sanjuanensis*	Carnian	Carnian
Hyperodapedon	*huxleyi*	Late Carnian	Late Carnian
Hyperodapedon	*gordoni*	Anisian-Carnian	Anisian-Carnian
Hypselorhachis	*mirabilis*	Late Anisian-Early Ladinian	Late Anisian-Early Ladinian
Hypuronecter	*limnaios*	Late Carnian	Late Carnian
Isalorhynchus	*genovefae*	Late Ladinian-Early Carnian	Late Ladinian-Early Carnian
Isanosaurus	*attavipachi*	Rhaetian	Rhaetian
Koilamasuchus	*gonzalezdiazi*	Induan-Olenekian	Olenekian
Lagerpeton	*chanarensis*	Ladinian-Early Carnian	Ladinian
Langobardisaurus	*spp*	Norian	Norian
Leptosuchus	*studeri*	Carnian	Carnian
Leptosuchus	*crosbiensis*	Carnian-Early Norian	Carnian-Early Norian
Lewisuchus	*admixtus*	Ladinian-Early Carnian	Ladinian
Liliensternus	*liliensterni*	Early Rhaetian	Early Rhaetian
Longosuchus	*meadei*	Carnian	Carnian
Lotosaurus	*adentus*	Anisian	Anisian
Lucasuchus	*hunti*	Carnian	Carnian
Machaeroprosopus	*zunni*	Carnian-Early Norian	Carnian-Early Norian
Macrocnemus	*spp*	Late Anisian-Ladinian	Late Anisian-Ladinian

Marasuchus	*lilloensis*	Ladinian-Early Carnian	Ladinian
Megalancosaurus	*spp*	Norian	Norian
Melanorosaurus	*spp*	Norian-Rhaetian	Norian-Rhaetian
Mesosuchus	*browni*	Late Olenekian-Anisian	Anisian
Mystriosuchus	*westphali*	Late Norian	Late Norian
Neoaetosauroides	*engaeus*	Rhaetian	Rhaetian
Ornithosuchus	*longidens*	Late Carnian	Late Carnian
Osmolskina	*czatkowicensis*	Olenekian	Olenekian
Paleorhinus	*scurriensis*	Carnian	Carnian
Paleorhinus	*bransoni*	Carnian	Carnian
Paleorhinus	*sawini*	Carnian	Carnian
Panphagia	*protos*	Late Carnian	Late Carnian
Pantydraco	*caducus*	Late Norian-Rhaetian	Rhaetian
Parasuchus	*hislopi*	Late Carnian	Late Carnian
Paratypothorax	*andressorum*	Late Carnian-Norian	Late Carnian-Norian
Peteinosaurus	*zambelli*	Norian	Norian
Phytosaurus	*doughtyi*	Carnian	Carnian
Pisanosaurus	*mertii*	Late Carnian	Late Carnian
Plateosauravus	*cullingworthi*	Norian	Norian
Plateosaurus	*engelhardti*	Early Rhaetian	Early Rhaetian
Plateosaurus	*gracilis*	Late Norian	Late Norian
Plateosaurus	*ingens*	Early Rhaetian	Early Rhaetian
Polonosuchus	*silesiacus*	Late Carnian-Norian	Late Carnian-Early Norian
Poposaurus	*gracilis*	Carnian-Early Norian	Carnian-Early Norian
Postosuchus	*alisonae*	Early Norian	Early Norian
Postosuchus	*kirkpatricki*	Carnian-early Norian	Carnian-early Norian
Pravusuchsus	*hortus*	Early Norian	Early Norian

Prestosuchus	*chiniquensis*	Ladinian-Early Carnian	Ladinian
Prolacerta	*broomi*	Induan	Induan
Prolacertoides	*jimusarensis*	Induan	Induan
Proterochampsa	*spp*	Late Carnian	Late Carnian
Proterosaurus	*speneri*	Early Wuchapingian	Early Wuchapingian
Proterosuchus	*spp*	Induan-Anisian	Induan-Anisian
Protome	*batalaria*	Early Norian	Early Norian
Pseudolagosuchus	*major*	Ladinian-Early Carnian	Ladinian
Pseudopalatus	*jablonskiae*	Early Norian	Early Norian
Pseudopalatus	*mccauleyi*	Late Carnian-Early Norian	Late Carnian-Early Norian
Pseudopalatus	*buceros*	Late Carnian-Norian	Late Carnian-Norian
Pseudopalatus	*pristinus*	Late Carnian-Rhaetian	Late Carnian-Rhaetian
Qianosuchus	*mixtus*	Anisian	Anisian
Rauisuchus	*tridentes*	Carnian	Carnian
Redondasaurus	*bermani*	Late Norian-Rhaetian	Rhaetian
Redondasaurus	*gregorii*	Late Norian-Rhaetian	Rhaetian
Redondasuchus	*spp*	Late Norian-Rhaetian	Rhaetian
Revueltosaurus	*spp*	Carnian-Rhaetian	Carnian-Rhaetian
Rhynchosaurus	*brodei*	Anisian	Anisian
Rhynchosaurus	*articeps*	Anisian	Anisian
Riojasaurus	*incertus*	Rhaetian	Rhaetian
Riojasuchus	*tenuisceps*	Rhaetian	Rhaetian
Ruehleia	*bedheimensis*	Early Rhaetian	Early Rhaetian
Rutiodon	*caronlinensis*	Late Carnian-Early Norian	Late Carnian-Early Norian
Sacisaurus	*agoudoensis*	Late Carnian	Late Carnian

Sarmatosuchus	*otschevi*	Anisian-Early Ladinian	Late Anisian-Early Ladinian
Saturnalia	*tupiniquim*	Carnian	Carnian
Saurosuchus	*galilei*	Late Carnian	Late Carnian
Scleromochlus	*taylori*	Late Carnian	Late Carnian
Shansisuchus	*shansisuchus*	Anisian-Early Ladinian	Anisian
Shuvosaurus	*inexpectatus*	Carnian-Early Norian	Carnian-Early Norian
Silesaurus	*opelensis*	Late Carnian-Norian	Late Carnian-Early Norian
Sillosuchus	*longicervix*	Late Carnian	Late Carnian
Smilosuchus	*lithodendrorum*	Late Carnian-Early Norian	Late Carnian-Early Norian
Smilosuchus	*gregorii*	Late Carnian	Late Carnian
Smilosuchus	*adamanensis*	Late Carnian-Early Norian	Late Carnian-Early Norian
Stagonolepis	*robertsoni*	Late Carnian	Late Carnian
Stagonolepis	*wellesi*	Carnian-Early Norian	Carnian-Early Norian
Stagonosuchus	*nyassicus*	Late Anisian-Early Ladinian	Late Anisian-Early Ladinian
Staurikosaurus	*pricei*	Carnian	Carnian
Stenaulorhynchus	*stockleyi*	Late Anisian-Early Ladinian	Late Anisian-Early Ladinian
Tanystropheus	*longobardicus*	Late Anisian	Late Anisian
Tanystropheus	*meridensis*	Early Ladinian	Early Ladinian
Tanytrachelos	*ahynis*	Late Carnian	Late Carnian
Tarjadia	*ruthae*	Ladinian-Early Carnian	Ladinian
Tawa	*hallae*	Late Carnian-Early Norian	Late Carnian-Early Norian

Tecovasuchus	*chatterjeei*	Carnian-Early Norian	Carnian-Early Norian
Teratosaurus	*suevicus*	Late Norian	Late Norian
Terrestrisuchus	*gracilis*	Late Norian-Rhaetian	Rhaetian
Teyumbaita	*sulcognathus*	Late Carnian	Late Carnian
Thecodontosaurus	*antiquus*	Late Norian-Rhaetian	Rhaetian
Ticinosuchus	*ferox*	Late Anisian	Late Anisian
Tikisuchus	*romeri*	Late Carnian	Late Carnian
Trilophosaurus	*buettneri*	Carnian-Norian	Carnian-Norian
Tropidosuchus	*romeri*	Ladinian-Early Carnian	Ladinian
Typothorax	*spp*	Carnian-Rhaetian	Carnian-Rhaetian
Unaysaurus	*tolentinoi*	Late Carnian	Late Carnian
Vallesaurus	*cenensis*	Norian	Norian
Vancleavea	*campi*	Carnian-Rhaetian	Carnian-Rhaetian
Vjushkovia	*triplocostata*	Olenekian	Olenekian
Xilousuchus	*sapingensis*	Olenekian-Early Anisian	Olenekian
Zupaysaurus	*rougieri*	Rhaetian	Rhaetian

Ichthyopterygia

Besanosaurus	*leptorhynchus*	Late Anisian-Early Ladinian	Late Anisian-Early Ladinian
Californisaurus	*perrini*	Late Carnian	Late Carnian
Callaywayia	*spp*	Carnian-Norian	Carnian-Norian
Chaohusaurus	*geishanensis*	Late Olenekian	Late Olenekian

Contectopalatus	*atavus*	Late Anisian-Early Ladinian	Late Anisian-Early Ladinian
Cymbospondylus	*buchseri*	Late Anisian	Late Anisian
Cymbospondylus	*petrinus*	Anisian	Anisian
Grippia	*longirostris*	Olenekian	Olenekian
Hudsonelpidia	*brevirostris*	Norian	Norian
Hupehsuchus	*nanchangensis*	Anisian-Ladinian	Anisian
Ichthyosaurus	*spp*	Late Carnian-Rhaetian	Late Carnian-Rhaetian
Leptonectes	*spp*	Late Rhaetian	Late Rhaetian
Macgowania	*janiceps*	Norian	Norian
Mikadocephalus	*gracilirostris*	Late Anisian-Early Ladinian	Late Anisian-Early Ladinian
Mixosaurus	*maotaiensis*	Late Anisian	Late Anisian
Mixosaurus	*panxianensis*	Late Anisian	Late Anisian
Mixosaurus	*kuhnschnyderi*	Late Anisian	Late Anisian
Mixosaurus	*cornalianus*	Late Anisian	Late Anisian
Parvinatator	*wapitensis*	Late Olenekian-Early Ladinian	Late Anisian-Early Ladinian
Phalarodon	*callawayi*	Olenekian-Ladinian	Olenekian-Ladinian
Phalarodon	*major*	Early Anisian	Early Anisian
Phalarodon	*fraasi*	Anisian	Anisian
Phantomosaurus	*neubigi*	Late Anisian-Early Ladinian	Late Anisian-Early Ladinian
Qianichthyosaurus	*zhoui*	Early Carnian	Early Carnian
Quasianosteosaurus	*vikinghoegdai*	Early Olenekian	Early Olenekian
Shastosaurus	*spp*	Ladinian-Early Norian	Ladinian-Early Norian
Shonisaurus	*polularis*	Late Carnian	Late Carnian
Toretocnemus	*spp*	Late Carnian	Late Carnian
Utatsusaurus	*hatai*	Olenekian	Olenekian
Wimanius	*odontopalatus*	Late Anisian-Early Ladinian	Late Anisian-Early Ladinian

Xinminosaurus	*cactates*	Late Anisian	Late Anisian
Sauropterygia			
Anarosaurus	*spp*	Early Anisian	Early Anisian
Augustasaurus	*hangdornii*	Anisian	Anisian
Bobosaurus	*forojuliensis*	Early Carnian	Early Carnian
Chinchenia	*sungi*	Ladinian	Ladinian
Corosaurus	*alcovensis*	Late Olenekian-Early Anisian	Late Olenekian-Early Anisian
Cyamodus	*kuhnschnyderi*	Late Anisian-Early Ladinian	Late Anisian-Early Ladinian
Cyamodus	*rostratus*	Late Anisian-Early Ladinian	Late Anisian-Early Ladinian
Cymatosaurus	*spp*	Early Anisian	Early Anisian
Dactylossaurus	*gracilis*	Early Anisian	Early Anisian
Diandongosaurus	*acutidentatus*	Anisian	Anisian
Dianopachysaurus	*dingi*	Anisian	Anisian
Eusaurosphargis	*dalsassoi*	Late Anisian-Early Ladinian	Late Anisian-Early Ladinian
Germanosaurus	*schafferi*	Early Anisian	Early Anisian
Hanosaurus	*hupehensis*	Early Olenekian	Early Olenekian
Helveticosaurus	*zollingeri*	Late Anisian-Early Ladinian	Late Anisian-Early Ladinian
Henodus	*chelyops*	Early Carnian	Early Carnian
Keichousaurus	*spp*	Anisian-Ladinian	Anisian
Kwangsisaurus	*orientalis*	Olenekian	Olenekian
Lariosaurus	*balsami*	Anisian-Ladinian	Late Anisian-Ladinian
Lariosaurus	*curionii*	Ladinian	Ladinian

Lariosaurus	*buzzi*	Late Anisian	Late Anisian
Lariosaurus	*valceresii*	Late Ladinian	Late Ladinian
Lariosaurus	*calcagnii*	Early Ladinian	Early Ladinian
Lariosaurus	*xingyiensis*	Ladinian	Ladinian
Macroplacus	*raeticus*	Rhaetian	Rhaetian
Neusticosaurus	*pusillus*	Ladinian	Ladinian
Nothosaurus	*mirabilis*	Anisian-Ladinian	Anisian-Ladinian
Paraplacodus	*broilii*	Anisian-Early Ladinian	Anisian-Early Ladinian
Pistosaurus	*longaevus*	Anisian-Ladinian	Anisian-Ladinian
Placochelys	*placodonta*	Carnian-Norian	Carnian-Norian
Placodus	*spp*	Olenekian-Ladinian	Olenekian-Ladinian
Protenodontosaurus	*italicus*	Late Carnian	Late Carnian
Psephoderma	*alpinum*	Norian-Rhaetian	Norian-Rhaetian
Qianxisaurus	*chajiangsensis*	Ladinian	Ladinian
Sanchiaosaurus	*dengi*	Anisian	Anisian
Serpianosaurus	*mirigiolensis*	Late Anisian	Late Anisian
Simosaurus	*gaillardoti*	Late Anisian-Ladinian	Late Anisian-Ladinian
Thalassiodracon	*hawkinsi*	Late Rhaetian	Late Rhaetian
Wumengosaurus	*delicatomandibularis*	Anisian	Anisian
Yunguisaurus	*liae*	Ladinian	Ladinian

Appendix N

The clades in the expanded supertree which are found to have experienced substantial ($p<0.1$) and significant ($p<0.05$) diversification rate shifts relative to their sister. Method of time slicing, ages used in dating the tree, and the treatment of poorly supported nodes indicated at the top of the tables

	Ruta method of time slicing; ages of taxa taking uncertainty of dating into account; poorly supported nodes retained.	
	$p<0.05$	$p<0.1$
Late Moscovian	Amniota	Amniota
Early Kazimovian		
Late Kazimovian		
Early Gzhelian		
Late Gzhelian		
Early Asselian		
Late Asselian		
Early Sakmarian		
Late Sakmarian		
Early Artinskian		Ankyromorpha
Late Artinskian		
Early Kungurian		Amniota
Late Kungurian		Amniota
Early Roadian		
Late Roadian		

Early Wordian		Therapsida
Late Wordian		Therapsida
Early Capitanian	Therapsida	Therapsida Clade containing Pylaecephalidae and all anomodonts more derived
Early Wuchiapingian	Eutherocephalia Clade containing Pareiasauridae and Procolophonoidea	Eutherocephalia Clade containing Pareiasauridae and Procolophonoidea
Late Wuchiapingian		
Early Changsingian		
Late Changsingian		
Early Induan		Clade containing Leptopleurinae and Procolophoninae Sauria
Late Induan		Clade containing Leptopleurinae and Procolophoninae Sauria
Early Olenekian	Sauria	Clade containing Erythrosuchidae and all archosauromorphs more derived Sauria

Late Olenekian	Sauria	Clade containing Erythrosuchidae and all archosauromorphs more derived
		Archosauromorpha
		Sauria
Early Anisian	Sauria	Kannemeyeriiformes
		Sauropterygia
	Archosauromorpha	Sauria
		Archosauromorpha
Late Anisian	Sauria	Eucynodontia
		Anomodonts more derived than *Wadiasaurus*.
		Kannemeyeriiformes
	Archosauromorpha	Sauria
		Archosauromorpha
Early Landinian	Archosauromorpha	Anomodonts more derived than *Wadiasaurus*
	Sauria	Paracrocodylomorpha
		Archosauria
		Archosauromorpha
Late Landinian	Sauria	Sauria
	Archosauromorpha	Archosauromorpha

Early Carnian	Saurischia	Saurischia
		Dinosauromorpha
	Archosauromorpha	Archosauromorpha
		Archosauria
Late Carnian	Archosauria	Phytosauria
		Saurischia
	Sauria	Archosauria
		Sauria
	Saurischia	Archosauromorpha
Early Norian	Clade containing Kayentatheridae and all cynodonts more derived	Clade containing Kayentatheridae and all cynodonts more derived
	Saurischia	Saurischia
	Archosauria	Archosauria
	Clade containing Protorosauria and all archosauromophs more derived	Clade containing Protorosauria and all archosauromophs more derived
	Sauria	Sauria
	Archosauromorpha	Archosauromorpha

Late Norian	Saurischia	Clade containing Kayentatheridae and all cynodonts more derived
	Archosauria	Saurischia
	Archosauromorpha	Archosauria
	Sauria	Clade containing Protorosauria and all archosauromophs more derived
	Clade containing Protorosauria and all archosauromophs more derived	Sauria
		Archosauromorpha
Early Rhaetian	Saurischia	Saurischia
	Archosauria	Archosauria
	Plateosauria	Plateosauria
	Sauria	Sauria
	Archosauromorpha	Archosauromorpha
Late Rhaetian	Saurischia	Saurischia
	Archosauria	Archosauria
	Sauria	Archosauromorpha
		Sauria

	Ruta method of time slicing; ages of uncertainly dated formations are restricted to at most two substages; poorly supported nodes retained.	
	p<0.05	p<0.1
Late Moscovian	Amniota	Amniota
Early Kazimovian		
Late Kazimovian		
Early Gzhelian		
Late Gzhelian		
Early Asselian		
Late Asselian		
Early Sakmarian		
Late Sakmarian		
Early Artinskian		Ankyromorpha
Late Artinskian		
Early Kungurian	Amniota	Amniota
Late Kungurian	Amniota	Amniota
Early Roadian		
Late Roadian		
Early Wordian		Therapsida
Late Wordian		Therapsida
Early Capitanian	Therapsida	Therapsida Clade containing Pylaecephalidae and all anomodonts more derived

Early Wuchiapingian	Eutherocephalia Clade containing Pareiasauridae and Procolophonoidea	Eutherocephalia Clade containing Pareiasauridae and Procolophonoidea
Late Wuchiapingian		Clade containing Pareiasauridae and Procolophonoidea
Early Changsingian		
Late Changsingian		
Early Induan		Clade containing Leptopleurinae and Procolophoninae Sauria
Late Induan		Clade containing Leptopleurinae and Procolophoninae Sauria
Early Olenekian	Sauria	Clade containing Erythrosuchidae and all archosauromorphs more derived Sauria
Late Olenekian	Sauria	Clade containing Erythrosuchidae and all archosauromorphs more derived Archosauromorpha Sauria

Early Anisian	Sauria Archosauromorpha	Kannemeyeriiformes Sauropterygia Sauria Archosauromorpha
Late Anisian	Sauria Archosauromorpha	Eucynodontia Anomodonts more derived than *Wadiasaurus*. Sauria Archosauromorpha
Early Landinian	Archosauromorpha Sauria	Paracrocodylomorpha Archosauria Archosauromorpha
Late Landinian	Sauria Archosauromorpha	Sauria Archosauromorpha
Early Carnian	Saurischia Archosauromorpha	Saurischia Dinosauromorpha Archosauromorpha Archosauria

		Phytosauria
	Archosauria	
		Saurischia
Late Carnian	Sauria	Archosauria
		Sauria
	Saurischia	
		Archosauromorpha
	Clade containing Kayentatheridae and all cynodonts more derived	Clade containing Kayentatheridae and all cynodonts more derived
	Saurischia	Saurischia
	Archosauria	Archosauria
Early Norian	Clade containing Protorosauria and all archosauromophs more derived	Clade containing Protorosauria and all archosauromophs more derived
	Sauria	Sauria
	Archosauromorpha	Archosauromorpha
	Saurischia	Clade containing Kayentatheridae and all cynodonts more derived
	Archosauria	Saurischia
	Archosauromorpha	Archosauria
Late Norian	Sauria	Clade containing Protorosauria and all archosauromophs more derived
		Sauria
	Clade containing Protorosauria and all archosauromophs more derived	Archosauromorpha

Early Rhaetian	Saurischia	Saurischia
	Archosauria	Archosauria
	Plateosauria	Plateosauria
	Sauria	Sauria
	Archosauromorpha	Archosauromorpha
Late Rhaetian	Saurischia	Saurischia
	Archosauria	Archosauria
	Sauria	Archosauromorpha
		Sauria

	Ruta method of time slicing; ages of taxa taking uncertainty of dating into account; Nodes with negative support collaped into a polytomy.	
	p<0.05	p<0.1
Late Moscovian	Amniota	Amniota
Early Kazimovian		
Late Kazimovian		
Early Gzhelian		
Late Gzhelian		
Early Asselian		
Late Asselian		
Early Sakmarian		
Late Sakmarian		
Early Artinskian		Ankyromorpha
Late Artinskian		
Early Kungurian		Amniota
Late Kungurian		Amniota
Early Roadian		
Late Roadian		
Early Wordian		Therapsida
Late Wordian		Therapsida
Early Capitanian	Therapsida	Therapsida Clade containing Pylaecephalidae and all anomodonts more derived

Early Wuchiapingian	Eutherocephalia Clade containing Pareiasauridae and Procolophonoidea	Eutherocephalia Clade containing Pareiasauridae and Procolophonoidea
Late Wuchiapingian		
Early Changsingian		
Late Changsingian		
Early Induan		Clade containing Leptopleurinae and Procolophoninae Sauria
Late Induan		Clade containing Leptopleurinae and Procolophoninae Sauria
Early Olenekian	Sauria	Clade containing Erythrosuchidae and all archosauromorphs more derived Sauria
Late Olenekian	Sauria	Clade containing Erythrosuchidae and all archosauromorphs more derived Archosauromorpha Sauria

Early Anisian	Sauria Archosauromorpha	Kannemeyeriiformes Sauropterygia Sauria Archosauromorpha
Late Anisian	Sauria Archosauromorpha	Eucynodontia Anomodonts more derived than *Wadiasaurus*. Kannemeyeriiformes Sauria Archosauromorpha
Early Landinian	Archosauromorpha Sauria	Anomodonts more derived than *Wadiasaurus* Paracrocodylomorpha Archosauria Archosauromorpha
Late Landinian	Sauria Archosauromorpha	Sauria Archosauromorpha
Early Carnian	Saurischia Archosauromorpha	Saurischia Dinosauromorpha Archosauromorpha Archosauria

Late Carnian	Archosauria Sauria Saurischia	Phytosauria Saurischia Archosauria Sauria Archosauromorpha
Early Norian	Clade containing Kayentatheridae and all cynodonts more derived Saurischia Archosauria Clade containing Protorosauria and all archosauromophs more derived Sauria Archosauromorpha	Clade containing Kayentatheridae and all cynodonts more derived Saurischia Archosauria Clade containing Protorosauria and all archosauromophs more derived Sauria Archosauromorpha
Late Norian	Saurischia Archosauria Archosauromorpha Sauria Clade containing Protorosauria and all archosauromophs more derived	Clade containing Kayentatheridae and all cynodonts more derived Saurischia Archosauria Clade containing Protorosauria and all archosauromophs more derived Sauria Archosauromorpha
Early Rhaetian	Saurischia Archosauria Plateosauria Sauria Archosauromorpha	Saurischia Archosauria Plateosauria Sauria Archosauromorpha

Late Rhaetian	Saurischia	Saurischia
	Archosauria	Archosauria
	Sauria	Archosauromorpha
		Sauria

	Tarver method of time slicing, ages taking uncertainty of dating into account, poorly supported nodes retained	
	p<0.05	p<0.1
Late Moscovian	Amniota	Amniota
Early Kazimovian		
Late Kazimovian		Clade containing Captorhinidae and Diapsida
Early Gzhelian	Clade containing Captorhinidae and Diapsida	Clade containing Captorhinidae and Diapsida
Late Gzhelian	Clade containing Captorhinidae and Diapsida	Clade containing Captorhinidae and Diapsida
Early Asselian	Clade containing Captorhinidae and Diapsida	Clade containing Captorhinidae and Diapsida
Late Asselian	Clade containing Captorhinidae and Diapsida	Clade containing Captorhinidae and Diapsida
Early Sakmarian	Clade containing Captorhinidae and Diapsida	Clade containing Captorhinidae and Diapsida
Late Sakmarian	Clade containing Captorhinidae and Diapsida	Clade containing Captorhinidae and Diapsida
Early Artinskian		Clade containing Captorhinidae and Diapsida Ankyromorpha
Late Artinskian		Clade containing Captorhinidae and Diapsida Ankyromorpha
Early Kungurian		Clade containing Captorhinidae and Diapsida Ankyromorpha

Late Kungurian		Clade containing Captorhinidae and Diapsida Ankyromorpha
Early Roadian	Sphenacodontia	Sphenacodontia Ankyromorpha Clade containing Captorhinidae and Diapsida
Late Roadian	Sphenacodontia	Sphenacodontia Ankyromorpha Clade containing Captorhinidae and Diapsida
Early Wordian	Sphenacodontia Clade containing Captorhinidae and Diapsida	Therapsida Sphenacodontia Ankyromorpha Clade containing Captorhinidae and Diapsida
Late Wordian	Sphenacodontia Clade containing Captorhinidae and Diapsida	Therapsida Clade containing Dinocephalia, Therocephalia and Annomodontia Sphenacodontia Ankyromorpha Clade containing Captorhinidae and Diapsida

Early Capitanian	Therapsida	Clade containing Venjukkovoidea and all anomodonts more derived
		Therapsida
	Sphenacodontia	Sphenacodontia
		Ankyromorpha
		Clade containing Milleretidae and all parareptiles more derived
	Clade containing Captorhinidae and Diapsida	Clade containing Captorhinidae and Diapsida
		Amniota
Late Capitanian	Therapsida	Clade containing Pylaecephalidae and all anomodonts more derived
		Clade containing Venjukkovoidea and all anomodonts more derived
	Sphenacodontia	Therapsida
		Sphenacodontia
		Ankyromorpha
	Clade containing Captorhinidae and Diapsida	Clade containing Milleretidae and all parareptiles more derived
		Clade containing Captorhinidae and Diapsida
		Amniota

		Clade containing Eutherocephalia and Scylacosauridae
	Therapsida	Clade containing Venjukkovoidea and all anomodonts more derived
		Therapsida
		Sphenacodontia
		Ankyromorpha
Early Wuchiapingian	Sphenacodontia	
		Diapsida
		Amniota
		Clade containing Captorhinidae and Diapsida
	Clade containing Captorhinidae and Diapsida	Clade containing Milleretidae and all parareptiles more derived
		Clade containing Pylaecephalidae and all anomodonts more derived

		Clade containing Eutherocephalia and Scylacosauridae
	Therapsida	Clade containing Pylaecephalidae and all anomodonts more derived
		Clade containing Venjukkovoidea and all anomodonts more derived
		Therapsida
	Sphenacodontia	Sphenacodontia
		Ankyromorpha
Late Wuchiapingian		Clade containing Milleretidae and all parareptiles more derived
	Clade containing Milleretidae and all parareptiles more derived	
		Diapsida
		Clade containing Captorhinidae and Diapsida
	Clade containing Captorhinidae and Diapsida	
		Amniota

		Clade containing Eutherocephalia and Scylacosauridae
	Therapsida	
		Clade containing Pylaecephalidae and all anomodonts more derived
		Clade containing Venjukkovoidea and all anomodonts more derived
	Sphenacodontia	
		Therapsida
		Sphenacodontia
Early Changsingian		
	Clade containing Milleretidae and all parareptiles more derived	Ankyromorpha
		Clade containing Milleretidae and all parareptiles more derived
		Diapsida
	Clade containing Captorhinidae and Diapsida	Clade containing Captorhinidae and Diapsida
		Amniota

		Clade containing Eutherocephalia and Scylacosauridae
	Therapsida	Clade containing Pylaecephalidae and all anomodonts more derived
		Clade containing Venjukkovoidea and all anomodonts more derived
		Therapsida
Late Changsingian	Sphenacodontia	Sphenacodontia
		Ankyromorpha
	Clade containing Milleretidae and all parareptiles more derived	Clade containing Milleretidae and all parareptiles more derived
		Diapsida
	Clade containing Captorhinidae and Diapsida	Clade containing Captorhinidae and Diapsida
		Amniota

		Clade containing Eutherocephalia and Scylacosauridae
	Therapsida	
		Clade containing Pylaecephalidae and all anomodonts more derived
	Clade containing Milleretidae and all parareptiles more derived	Clade containing Venjukkovoidea and all anomodonts more derived
	Clade containing Sauria, *Saurosternon* and *Palaeagama*	Therapsida
		Sphenacodontia
Early Induan	Sphenacodontia	Clade containing Leptopleurinae and Procolophoninae
		Ankyromorpha
		Clade containing Milleretidae and all parareptiles more derived
	Diapsida	
		Sauria
	Clade containing Captorhinidae and Diapsida	Clade containing Captorhinidae and Diapsida
		Amniota
	Amniota	
		Diapsida

		Clade containing Eutherocephalia and Scylacosauridae
	Therapsida	
		Clade containing Pylaecephalidae and all anomodonts more derived
	Clade containing Milleretidae and all parareptiles more derived	Clade containing Venjukkovoidea and all anomodonts more derived
	Clade containing Sauria, *Saurosternon* and *Palaeagama*	Therapsida
		Sphenacodontia
Late Induan	Sphenacodontia	Clade containing Leptopleurinae and Procolophoninae
		Ankyromorpha
		Clade containing Milleretidae and all parareptiles more derived
	Diapsida	
		Sauria
	Clade containing Captorhinidae and Diapsida	Clade containing Captorhinidae and Diapsida
		Amniota
	Amniota	
		Diapsida

Early Olenekian	Therapsida	Clade containing Eutherocephalia and Scylacosauridae
		Clade containing Pylaecephalidae and all anomodonts more derived
	Sphenacodontia	Clade containing Venjukkovoidea and all anomodonts more derived
		Therapsida
	Sauria	Ankyromorpha
		Clade containing Milleretidae and all parareptiles more derived
	Clade containing Captorhinidae and Diapsida	Clade containing Erythrosuchidae and all archosauromorphs more derived
		Archosauromorpha
		Sauria
	Clade containing Milleretidae and all parareptiles more derived	Diapsida
		Clade containing Leptopleurinae and Procolophoninae
	Amniota	Clade containing Captorhinidae and Diapsida
		Amniota
		Sphenacodontia

Late Olenekian	Therapsida	Clade containing Eutherocephalia and Scylacosauridae
		Clade containing Pylaecephalidae and all anomodonts more derived
	Clade containing Milleretidae and all parareptiles more derived	Clade containing Venjukkovoidea and all anomodonts more derived
		Therapsida
		Sphenacodontia
	Archosauromorpha	Clade containing Leptopleurinae and Procolophoninae
		Ankyromorpha
	Sauria	Clade containing Milleretidae and all parareptiles more derived
	Clade containing Captorhinidae and Diapsida	Clade containing Erythrosuchidae and all archosauromorphs more derived
		Archosauromorpha
	Sphenacodontia	Sauria
		Diapsida
	Amniota	Clade containing Captorhinidae and Diapsida
		Amniota

Early Anisian	Therapsida	Clade containing Eutherocephalia and Scylacosauridae
		Clade containing Pylaecephalidae and all anomodonts more derived
	Sphenacodontia	Clade containing Venjukkovoidea and all anomodonts more derived
		Therapsida
		Sphenacodontia
	Clade containing Milleretidae and all parareptiles more derived	Clade containing Leptopleurinae and Procolophoninae
		Ankyromorpha
	Archosauromorpha	Clade containing Milleretidae and all parareptiles more derived
		Sauropterygia
	Sauria	Clade containing Erythrosuchidae and all archosauromorphs more derived
		Archosauromorpha
	Clade containing Captorhinidae and Diapsida	Sauria
		Diapsida
	Amniota	Clade containing Captorhinidae and Diapsida
		Amniota

Late Anisian	Therapsida	Eucynodontia
		Eutherocephalia
	Sphenacodontia	Therapsida
		Sphenacodontia
	Clade containing Milleretidae and all parareptiles more derived	Clade containing Pylaecephalidae and all anomodonts more derived
		Clade containing Venjukkovoidea and all anomodonts more derived
		Clade containing Eutherocephalia and Scylacosauridae
	Archosauromorpha	Anomodonts more derived than *Wadiasaurus*
		Clade containing Leptopleurinae and Procolophoninae
	Sauria	Ankyromorpha
		Clade containing Milleretidae and all parareptiles more derived
	Clade containing Captorhinidae and Diapsida	Clade containing Erythrosuchidae and all archosauromorphs more derived
		Archosauromorpha
		Sauria
		Diapsida
	Amniota	Clade containing Captorhinidae and Diapsida
		Amniota

Early Landinian	Therapsida	Ankyromorpha
		Eucynodontia
		Eutherocephalia
	Sphenacodontia	Therapsida
		Sphenacodontia
	Clade containing Milleretidae and all parareptiles more derived	Clade containing Traversodontidae and Trirachodontidae
		Clade containing Venjukkovoidea and all anomodonts more derived
	Archosauromorpha	Clade containing Eutherocephalia and Scylacosauridae
		Anomodonts more derived than *Wadiasaurus*
	Sauria	Clade containing Leptopleurinae and Procolophoninae
		Clade containing Pylaecephalidae and all anomodonts more derived
		Clade containing Milleretidae and all parareptiles more derived
	Clade containing Captorhinidae and Diapsida	Paracrocodylomorpha
		Clade containing Erythrosuchidae and all archosauromorphs more derived Archosauromorpha
		Sauria
		Diapsida
	Amniota	Clade containing Captorhinidae and Diapsida
		Amniota

		Clade containing Traversodontidae and Trirachodontidae
	Therapsida	Eucynodontia
		Eutherocephalia
		Clade containing Eutherocephalia and Scylacosauridae
	Sphenacodontia	Anomodonts more derived than *Wadiasaurus*
		Clade containing Pylaecephalidae and all anomodonts more derived
	Clade containing Milleretidae and all parareptiles more derived	Clade containing Venjukkovoidea and all anomodonts more derived
Late Landinian		Therapsida
		Sphenacodontia
	Archosauromorpha	Ankyromorpha
		Clade containing Leptopleurinae and Procolophoninae
		Clade containing Milleretidae and all parareptiles more derived
	Sauria	Paracrocodylomorpha
		Clade containing Erythrosuchidae and all archosauromorphs more derived
	Clade containing Captorhinidae and Diapsida	Archosauromorpha
		Sauria
		Diapsida
	Amniota	Clade containing Captorhinidae and Diapsida
		Amniota

	Therapsida	Clade containing Traversodontidae and Trirachodontidae
	Sphenacodontia	Eucynodontia Eutherocephalia Clade containing Eutherocephalia and Scylacosauridae
	Clade containing Milleretidae and all parareptiles more derived	Anomodonts more derived than *Wadiasaurus* Clade containing Pylaecephalidae and all anomodonts more derived Clade containing Venjukkovoidea and all anomodonts more derived
Early Carnian	Archosauromorpha	Therapsida Phytosauria Dinosauromorpha Sphenacodontia
	Sauria	Clade containing Leptopleurinae and Procolophoninae Ankyromorpha
	Clade containing Captorhinidae and Diapsida	Clade containing Milleretidae and all parareptiles more derived Clade containing Erythrosuchidae and all archosauromorphs more derived Archosauromorpha Sauria Diapsida
	Amniota	Clade containing Captorhinidae and Diapsida Amniota

Late Carnian	Therapsida	Eutherocephalia
		Eucynodontia
	Eucynodontia	Therapsida
		Phytosauria
	Sphenacodontia	Dinosauromorpha
		Sphenacodontia
	Dinosauriformes	Ankyromorpha
		Archosauromorpha
		Sauria
	Clade containing Milleretidae and all parareptiles more derived	Diapsida
		Clade containing Pylaecephalidae and all anomodonts more derived
	Archosauromorpha	Clade containing Leptopleurinae and Procolophoninae
		Clade containing Venjukkovoidea and all anomodonts more derived
		Clade containing Milleretidae and all parareptiles more derived
	Sauria	Clade containing Erythrosuchidae and all archosauromorphs more derived
		Clade containing Traversodontidae and Trirachodontidae
		Clade containing Eutherocephalia and Scylacosauridae
	Clade containing Captorhinidae and Diapsida	Anomodonts more derived than *Wadiasaurus*
		Clade containing Captorhinidae and Diapsida
	Amniota	Amniota
		Phytosauria
		Dinosauriformes

	Eucynodontia	Clade containing Traversodontidae and Trirachodontidae
	Therapsida	Eucynodontia
	Sphenacodontia	Eutherocephalia
		Clade containing Eutherocephalia and Scylacosauridae
	Clade containing Milleretidae and all parareptiles more derived	
		Anomodonts more derived than *Wadiasaurus*
	Protorosauria	Clade containing Pylaecephalidae and all anomodonts more derived
		Clade containing Venjukkovoidea and all anomodonts more derived
		Therapsida
		Sphenacodontia
	Dinosauriformes	Clade containing Leptopleurinae and Procolophoninae
Early Norian		
		Ankyromorpha
	Archosauromorpha	Clade containing Milleretidae and all parareptiles more derived
		Sauropterygia
		Protorosauria
		Phytosauria
	Sauria	Saurischia
		Dinosauriformes
		Dinosauromorpha
	Clade containing Captorhinidae and Diapsida	Clade containing Erythrosuchidae and all archosauromorphs more derived
		Archosauromorpha
		Sauria
		Diapsida
	Amniota	Clade containing Captorhinidae and Diapsida
		Amniota

	Eucynodontia	Clade containing Traversodontidae and Trirachodontidae
	Therapsida	Eucynodontia Eutherocephalia Clade containing Eutherocephalia and Scylacosauridae
	Sphenacodontia	Anomodonts more derived than *Wadiasaurus* Clade containing Pylaecephalidae and all anomodonts more derived
	Clade containing Milleretidae and all parareptiles more derived	Clade containing Venjukkovoidea and all anomodonts more derived Therapsida Sphenacodontia
Late Norian	Protorosauria	Clade containing Leptopleurinae and Procolophoninae
	Dinosauriformes	Ankyromorpha Clade containing Milleretidae and all parareptiles more derived
	Archosauromorpha	Sauropterygia Protorosauria Phytosauria Saurischia Dinosauriformes Dinosauromorpha
	Sauria	Clade containing Erythrosuchidae and all archosauromorphs more derived
	Clade containing Captorhinidae and Diapsida	Archosauromorpha Sauria Diapsida
	Amniota	Clade containing Captorhinidae and Diapsida Amniota

Early Rhaetian	Eucynodontia	Clade containing Traversodontidae and Trirachodontidae
	Therapsida	Eucynodontia
		Eutherocephalia
		Clade containing Eutherocephalia and Scylacosauridae
	Sphenacodontia	Anomodonts more derived than *Wadiasaurus*
		Clade containing Pylaecephalidae and all anomodonts more derived
	Clade containing Milleretidae and all parareptiles more derived	Clade containing Venjukkovoidea and all anomodonts more derived
		Therapsida
		Sphenacodontia
	Protorosauria	Clade containing Leptopleurinae and Procolophoninae
		Ankyromorpha
	Dinosauriformes	Clade containing Milleretidae and all parareptiles more derived
	Archosauromorpha	Sauropterygia
		Protorosauria
		Phytosauria
		Saurischia
		Dinosauriformes
	Sauria	Dinosauromorpha
		Clade containing Erythrosuchidae and all archosauromorphs more derived
	Clade containing Captorhinidae and Diapsida	Archosauromorpha
		Sauria
		Diapsida
	Amniota	Clade containing Captorhinidae and Diapsida
		Amniota

		Clade containing Traversodontidae and Trirachodontidae
	Eucynodontia	
		Eucynodontia
		Eutherocephalia
		Clade containing Eutherocephalia and Scylacosauridae
	Therapsida	
		Anomodonts more derived than *Wadiasaurus*
		Clade containing Pylaecephalidae and all anomodonts more derived
	Sphenacodontia	
		Clade containing Venjukkovoidea and all anomodonts more derived
		Therapsida
		Sphenacodontia
	Clade containing Milleretidae and all parareptiles more derived	Clade containing Leptopleurinae and Procolophoninae
Late Rhaetian		
		Ankyromorpha
	Protorosauria	Clade containing Milleretidae and all parareptiles more derived
		Sauropterygia
	Dinosauriformes	Protorosauria
		Phytosauria
		Saurischia
	Archosauromorpha	Dinosauriformes
		Dinosauromorpha
		Clade containing Erythrosuchidae and all archosauromorphs more derived
	Sauria	
		Archosauromorpha
	Clade containing Captorhinidae and Diapsida	Sauria
		Diapsida
		Clade containing Captorhinidae and Diapsida
	Amniota	
		Amniota